

Raphael M. Ottenbrite
Editor-in-Chief
Kinam Park
Teruo Okano
Editors

Biomedical Applications of Hydrogels Handbook

Biomedical Applications of Hydrogels Handbook

Editor-in-Chief

Raphael M. Ottenbrite

Editors

Kinam Park

Teruo Okano

Biomedical Applications of Hydrogels Handbook

 Springer

Editor-in-Chief

Raphael M. Ottenbrite
Professor Emeritus
Virginia Commonwealth University
Richmond, VA, USA
ottenbrite@vcu.org

Editors

Kinam Park
Biomedical Engineering and Pharmaceutics
Purdue University
West Lafayette, IN, USA
kpark@purdue.edu

Teruo Okano
Institute of Biomedical Engineering
Tokyo Women's Medical University
Shinjuku-ku, Tokyo, Japan
tokano@abmes.twmu.ac.jp

Associate Editors

Rolando Barbucci
Interuniversity Research Centre for Advanced
Medical Systems
University of Siena
Siena, Italy
barbucci@unisi.it

Arthur J. Coury
Vice President
Biomaterials Research
Genzyme Corporation
Cambridge, MA, USA
art.coury@genzyme.com

Haruma Kawaguchi
Graduate School of Science and Technology
Keio University
Yokohama, Japan
haruma@aplc.keio.ac.jp

Advisory Board Chair
Nicholas A. Peppas
Department of Chemical Engineering
The University of Texas at Austin
Austin, TX, USA
peppas@che.utexas.edu

ISBN 978-1-4419-5918-8 e-ISBN 978-1-4419-5919-5

DOI 10.1007/978-1-4419-5919-5

Springer New York Dordrecht Heidelberg London

Library of Congress Control Number: 2010929391

© Springer Science+Business Media, LLC 2010

All rights reserved. This work may not be translated or copied in whole or in part without the written permission of the publisher (Springer Science+Business Media, LLC, 233 Spring Street, New York, NY 10013, USA), except for brief excerpts in connection with reviews or scholarly analysis. Use in connection with any form of information storage and retrieval, electronic adaptation, computer software, or by similar or dissimilar methodology now known or hereafter developed is forbidden.

The use in this publication of trade names, trademarks, service marks, and similar terms, even if they are not identified as such, is not to be taken as an expression of opinion as to whether or not they are subject to proprietary rights.

Printed on acid-free paper

Springer is part of Springer Science+Business Media (www.springer.com)

Advisory Board

Nicholas A. Peppas, Chair

Department of Chemical Engineering
The University of Texas at Austin
Austin, TX, USA

Allan Hoffman

University of Washington Engineered Biomaterials
University of Washington
Seattle, WA, USA

Emo Chiellini

Chemistry & Industrial Chemistry
University of Pisa
Pisa, Italy

Fu-Zhai Cui

Director of Biomaterials
Tsinghua University
Beijing, China

Karel Dusek

Institute of Macromolecular Chemistry
Academy of Sciences of the Czech Republic
Prague, CHEK

Jindrich Kopecek

Department of Bioengineering and of Pharmaceutics
and Pharmaceutical Chemistry, University of Utah
Salt Lake City, Utah, USA

Claudio Migliaresi

Department of Materials Engineering
University of Trento
Trento - Italy

Yoshihito Osada

Division of Biological Sciences
Hokkaido University
Sapporo, Japan

Buddy D. Ratner

Director, University of Washington Engineered Biomaterials
University of Washington
Seattle, WA USA

Nathan Ravi

Department of Ophthalmology
Washington University

Etienne Schacht

Polymer Material
Ghent University
Ghent, Belgium

Tianwei Tan

College of Life Science and Technology
Beijing University of Chemical Technology

Preface

Substances that absorb significant quantities of water are called gels or hydrogels. Naturally occurring materials with these properties play a very important role in all forms of life. In this Handbook, the biomedical applications of hydrogels are addressed by experts in the field from around the world. The phenomenal properties of hydrogels continue to stimulate scientists to seek new insights into the development of novel biomaterials and bioapplications.

Composed of three-dimensional polymer networks, hydrogels can absorb large quantities of water. Consequently, they are soft, pliable, wet materials with a wide range of potential biomedical applications. Hydrogels are currently widely used in bioapplications and play a crucial role in modern strategies to remedy malfunctions in and injuries to living systems.

The high water content of hydrogels renders them compatible with most living tissue and their viscoelastic nature minimizes damage to the surrounding tissue when implanted in the host. In addition, their mechanical properties parallel those of soft tissue, which makes them particularly appealing to tissue engineers. These novel, bioactive materials are capable of interacting with the host tissues, assisting and improving the healing process, and mimicking functional and morphological characteristics of organ tissue.

Biomaterials play a crucial role in modern strategies of tissue replacement and restoration because they provide the biophysical and biochemical surroundings that are able to direct cellular behavior and functions. The concept of designing hydrogels as temporary or permanent devices for regeneration and restoration of tissues is being vigorously pursued in many laboratories, that often involve international cooperative endeavors. Both natural and synthetic hydrogels are used for repairing and regenerating a wide variety of tissues and organs. The ability to engineer composite hydrogels has generated new opportunities in addressing challenges in tissue engineering as well as in tissue function restoration.

Most hydrogels have biological traits, such as high tissue-like water content and permeability for influx of nutrients and excretion of metabolites. Cells encapsulated in a 3-D hydrogels environment are surrounded by a gels matrix that does not promote attachment or potential phenotype differentiation, thus making hydrogels especially suitable for engineered scaffolds. These hydrophilic composite structures are being designed to mimic the transport and mechanical properties of natural soft tissue. Hydrogels can homogeneously incorporate and suspend cells as well as growth factors and other bioactive reagents while allowing rapid diffusion of hydrophilic nutrients and metabolites to the incorporated cells or surrounding tissue.

One of the essentials for an effective tissue scaffold is that it degrades in a controlled manner so that when the bioreplacement is complete and functional in vivo none of the scaffolding materials remain. Biodegradable hydrogels are derived from fibrin, hyaluronic acid, collagen, chitosan, and poly(lactic acid) components to create hybrid hydrogels that are biocompatible and can provide appropriate signals to regulate cell behavior. Degradation of hydrogels leads to a loss in mechanical strength and finally disintegration. Therefore, the degradation rate of the gels needs to be carefully controlled to match the rate of new tissue formation.

There are a number of hydrogels that behave as smart materials and offer natural adaptations, such as sensing devices, actuating and regulating functions, and feedback control systems. These stimuli-responsive polymer gels react to changes in their surroundings, such

as surrounding composition, temperature, and pH. They are of interest as intelligent, or smart, biomimetic materials that can function as biosensors, processors, and activators of an electrical response. The applications of electroconductive hydrogels as biorecognition membranes for implantable biosensors, as electro-stimulated drug-eluting devices and as a low interfacial impedance layer on neuronal prostheses present new horizons for biodetection devices. Both biomolecular recognition and responsive functions that perceive a biomolecule target and induce structural changes can be introduced into the hydrogels network.

Hydrogels-based drug delivery systems with integrated smart systems and biomolecular imaging capability open many opportunities for effective therapeutic delivery and monitoring as well as molecular imaging probes in noninvasive procedures for early detection and treatment of disease. This multifunctionality makes it possible to self-regulate and control hydrogels-based devices to maintain physiological variables for applications such as drug delivery and cell cultures.

Hydrogels implants for drug delivery can be preformed or injected. The preformed hydrogels are processed with the active reagent *in vitro* prior to *in vivo* implantation. Injectable hydrogels are implanted as a liquid that gels *in situ* with the reagent incorporated and suspended in the gels precursor prior to gelation, enabling homogenous and facile implantation. *In situ* gelling of stimuli-sensitive block copolymer hydrogels has many advantages, such as simple drug formulation, site-specificity, sustained drug release behavior, less systemic toxicity, and the ability to deliver both hydrophilic and hydrophobic drugs. For example, PEG-based amphiphilic copolymers are extensively used for biomedical applications due to their unique self-assembly and biocompatibility properties. The PEG-based amphiphilic copolymers exhibit unique changes in micellar architecture and aggregation number in response to changes near physiological temperature and/or pH. Therefore, *in situ* gelling systems made with PEG-based amphiphilic copolymers are being investigated worldwide.

These topics as well as several other biomedical applications of hydrogels are covered in the ensuing chapters by the most highly qualified experts in the field. I wish to thank them and the many others who have contributed to this publication.

Richmond, VA

Raphael M. Ottenbrite

Contents

Preface	vii
List of Contributors	xvii
Introduction to Hydrogels	1
<i>Hossein Omidian and Kinam Park</i>	
Crosslinked Polymers	1
Hydrogels Synthesis	2
Expansion of a Hydrogels Structure	3
Swelling Forces in Hydrogels	4
Swelling Mechanism	6
Water in Hydrogels	6
Hydrogels Properties	8
Hydrogels Characterization	8
Hydrogels Applications.	12
Summary	15
References	15
Part I Stimuli-Sensitive Hydrogels	17
Stimuli-Responsive Hydrogels and Their Application to Functional Materials	19
<i>Ryo Yoshida and Teruo Okano</i>	
Introduction.	19
Stimuli-Responsive Gels as Functional Materials	19
Function of Mechanical Motion	20
Function of Information Transmission and Transformation	20
Function of Mass Transport	21
Cell-Sheet Engineering Using an Intelligent Surface	24
Cell-Sheet Engineering.	24
Intelligent Surfaces	26
Design of Network Structure for Functional Gels	29
Topological Gels, Double Network Structure Gels, Nanocomposite Gels	29
Graft Gels.	30
Microfabrication of Gels	30
Self-Oscillating Gels as Novel Biomimetic Materials	31
Design of Self-Oscillating Gels	32
Self-Oscillating Behaviors of the Gels	33
Self-Oscillation of the Miniature Bulk Gels	33
Control of Oscillation Period and Amplitude	34
On–Off Regulation of Self-Beating Motion	34
Peristaltic Motion of Gels with Propagation of Chemical Wave	34

Design of Biomimetic Micro-/Nanoactuator Using Self-Oscillating Polymer and Gels	34
Self-Walking Gels	34
Microfabrication of the Gels by Lithography	37
Control of Chemical Wave Propagation in Self-Oscillating Gels Array	37
Self-Oscillating Polymer Chains as “Nanooscillator”	38
Self-Flocculating/Dispersing Oscillation of Microgels	38
Fabrication of Microgel Beads Monolayer	40
Self-Oscillation Under Physiological Conditions	41
References	41
Feedback Control Systems Using Environmentally and Enzymatically Sensitive Hydrogels	45
<i>Irma Y. Sanchez and Nicholas A. Peppas</i>	
Hydrogels as Basic Functional Elements of a Control System.	45
Hydrogels in Sensors	47
Optical Transduction	47
Mechanical Transduction.	48
Electric Transduction.	48
Limitation of Enzyme Secondary Substrate	48
Preservation of Enzyme Activity.	50
Hydrogels as Actuators	50
Magnetically Controlled Systems	51
Ultrasonically Controlled Systems	51
Electronically Controlled Systems	51
Photo-Controlled Systems	51
Thermally Controlled Systems	53
Chemically Controlled Systems	53
Protein-Responsive and Controlled Systems	54
Self-Regulated Hydrogel-Based Systems	55
pH Feedback Systems	55
Temperature Feedback Systems	57
Protein Concentration Feedback Systems	57
Enzyme Cofactor Feedback System	57
Glucose Concentration Feedback Systems	58
Hydrogel-Based Feedforward and Cascade Systems	60
Summary	62
References	63
Biomolecule-Responsive Hydrogels	65
<i>Takashi Miyata</i>	
Introduction.	65
Glucose-Responsive Hydrogels	66
Glucose-Responsive Hydrogels Using Glucose Oxidase.	66
Glucose-Responsive Hydrogels Using Phenylboronic Acid	67
Glucose-Responsive Hydrogels Using Lectin	69
Protein-Responsive Hydrogels	72
Enzyme-Responsive Hydrogels	72
Antigen-Responsive Hydrogels.	74

Contents	xi
Other Biomolecule-Responsive Hydrogels	77
Molecularly Imprinted Hydrogels	77
Other Biomolecule-Responsive Hydrogels	80
Summary	84
References	84
Stimuli-Responsive PEGylated Nanogels for Smart Nanomedicine	87
<i>Motoi Oishi and Yukio Nagasaki</i>	
Introduction	87
Synthesis and Characterization of Stimuli-Responsive PEGylated Nanogels	88
Tumor-Specific Smart ¹⁹ F MRI Nanoprobes Based on pH-Responsive PEGylated Nanogels	90
pH-Responsive PEGylated Nanogels for Intracellular Drug Delivery Systems	94
Smart Apoptosis Nanoprobe Based on the PEGylated Nanogels Containing GNPs for Monitoring the Cancer Response to Therapy	98
Summary	104
References	104
Stimuli-Sensitive Microhydrogels	107
<i>Haruma Kawaguchi</i>	
Introduction	107
Stimuli-Sensitive Microgels	107
Preparation of Microhydrogels	107
Stimuli Responsiveness of Microhydrogels	109
Preparation of Inorganic Nanoparticles/Polymer Composite Microgels	112
Polymer Composite Microgel Functions	114
Metal Oxide Nanoparticles/Thermosensitive Polymer Composite Microgels	114
Miscellaneous Nanoparticles/Thermosensitive Composite Microgels	116
Summary	117
References	117
Part II Hydrogels For Drug Delivery	121
In-Situ Gelling Stimuli-Sensitive PEG-Based Amphiphilic Copolymer Hydrogels	123
<i>Doo Sung Lee and Chaoliang He</i>	
Introduction	123
Thermogelling PEG–PNIPAM Block Copolymers	124
Pluronic-Based In-Situ Forming Hydrogels	126
Thermogelling PEG/PLGA Amphiphilic Block Copolymers	127
Thermogelling Star-Shaped and Graft PEG/PLGA Amphiphilic Copolymers	131
Thermogelling PEG–PCL Amphiphilic Copolymers	132
Thermogelling PEG-Based Amphiphilic Multiblock Copolymers	134
pH- and Thermo-Sensitive PEG–Polyester Amphiphilic Copolymer Hydrogels	134
PEG-Based Amphiphilic Copolymers Modified by Anionic Weak Polyelectrolytes	135
PEG-Based Amphiphilic Copolymers Modified by Cationic Weak Polyelectrolytes	138

Summary	141
Acknowledgments	142
References	142
Biodegradable Hydrogels for Controlled Drug Release.	147
<i>Luis García, María Rosa Aguilar, and Julio San Román</i>	
Introduction.	147
The Nature of Biodegradable Hydrogels.	148
Physical Hydrogels	149
Hydrophobic Interactions Hydrogels	150
Ionic Interaction Hydrogels	152
Hydrogen Bonded Hydrogels.	153
Chemically Bonded Hydrogels	153
Summary	154
References	154
Thermo-Responsive Biodegradable Hydrogels from Stereocomplexed Poly(lactide)s	157
<i>Tomoko Fujiwara, Tetsuji Yamaoka, and Yoshiharu Kimura</i>	
Introduction.	157
Micelles and Hydrogels with Various Block, Graft, and Armed PLA Copolymers	158
Stereocomplexation of Enantiomeric PLAs, and the Hydrogels Applications	159
Hydrogels Study on Enantiomeric PLA–PEG Linear Block Copolymers	162
Motivation of the Study on Stereocomplexed Micellar Hydrogels	162
Copolymer Synthesis and Gels Formation	163
Hydrogels from Micellar Solutions of ABA Triblock Copolymers	163
Hydrogels from BAB Triblock Copolymers	167
Hydrogels from AB Diblock Copolymers	168
Hydrogels Properties and Applications	173
Summary	173
References	173
Hydrogels-Based Drug Delivery System with Molecular Imaging	179
<i>Keun Sang Oh and Soon Hong Yuk</i>	
Introduction.	179
Hydrogels Polymers for Imaging Probes	180
Poly(Ethylene Glycol) (PEG) and Its Copolymers	183
Poly(<i>N</i> -isopropylacrylamide) (PNIPAM).	183
Molecular Probes for Imaging	184
Gold Nanoparticles	184
Magnetic Nanoparticles	184
Fluorescence Dyes	185
Microbubbles	187
Quantum Dots	187
Molecular Probe/Polymer Composite Systems.	187
Iron Oxide Nanoparticles/Polymer Composite Systems	189

Contents	xiii
Quantum Dot/Polymer Composite Systems	190
Microbubble/Polymer Composite Systems	191
Drug Delivery System with Molecular Imaging Capability	191
Summary	193
References	193
Part III Hydrogels for Tissue Engineering	201
Hydrogels for Tissue Engineering Applications.	203
<i>Rong Jin and Pieter J. Dijkstra</i>	
Introduction.	203
Hydrogels Designs for Tissue Engineering.	204
Crosslinking Methods to Form Hydrogels	206
Chemical Crosslinking by Radical Polymerization	206
Crosslinking Functional Groups	207
Crosslinking by Enzymatic Reactions	210
Crosslinking by Stereocomplexation	211
Hydrogels by Thermo-Gelation	212
Crosslinking by Self Assembly.	212
Crosslinking by Inclusion Complexation.	213
Combining Physical and Chemical Crosslinking.	214
Naturally Derived Hydrogels	215
Protein-Based Polymers	215
Polysaccharides.	216
Synthetic Hydrogels	217
Hydrogels Based on PEG–PLA and PEG–PGA Copolymers	217
Fumaric Acid-Based Hydrogels	217
Hybrid Hydrogels.	217
Tissue Engineering Applications.	219
Bone Graft Substitutes	219
Cartilage Regeneration	220
Conclusions.	221
References	221
Composite Hydrogels for Scaffold Design, Tissue Engineering, and Prostheses.	227
<i>V. Guarino, A. Gloria, R. De Santis, and L. Ambrosio</i>	
Introduction.	227
Basic Concepts and Properties	228
Scaffolds for Tissue Regeneration	235
Summary	242
References	242
Hydrogels for Cartilage Tissue Engineering.	247
<i>Pierre Weiss, Ahmed Fatimi, Jerome Guicheux, and Claire Vinatier</i>	
Introduction.	247
Characterization of Hydrogels	248
Theory of Viscoelastic Behavior	248

Cartilage Morphology, Properties and Diseases	250
Composition of Articular Cartilage	250
Chondrocyte	250
Histological Organization of Articular Cartilage.	251
Extracellular Matrix (ECM)	253
Pathology of Articular Cartilage	253
Cartilage Repair	254
Cartilage Regeneration	255
Tissue Engineering (TE)	255
Hydrogels Polymers	257
In Situ Crosslinkable Hydrogels	261
Polymer Associations.	262
Physical and Mechanical Behavior	262
Summary	264
References	264
Gelatin-Based Hydrogels for Controlled Cell Assembly	269
<i>Xiaohong Wang, Yongnian Yan, and Renji Zhang</i>	
Introduction.	269
Gelatin-Based Hydrogels for the Controlled Hepatocyte Assembly	274
Establishing a Multicellular Model by 3D Cell Assembly for Metabolic Syndrome	278
Cryopreservation of 3D Constructs Based on Controlled Cell Assembly	280
Conclusions.	282
References	283
Double Network Hydrogels as Tough, Durable Tissue Substitutes	285
<i>Takayuki Murosaki and Jian Ping Gong</i>	
Introduction.	285
Robust Gels with High Elasticity.	286
DN Gels from Synthetic Polymers	286
Necking Phenomenon of DN Gels	288
Local Damage Zone Model for the Toughening Mechanism of DN Gels	290
Robust Gels from Bacterial Cellulose	290
Sliding Friction of Gels.	292
Frictional Behavior of Gels.	292
Dependence on Load	292
Sample Area Dependence	293
Substrate Effect.	294
Extremely Low Friction Gels.	295
Template Effect on Gels Surface Structure and Its Friction	295
Robust Hydrogels with Low Friction as Candidates for Artificial Cartilage.	296
Wear Properties of Robust DN Gels	298
Biocompatibility of Robust DN Hydrogels.	298
Evaluation of Robust Gels	298
Summary	300
References	301

Hydrogels Contact Lenses	303
<i>Jiri Michalek, Radka Hobzova, Martin Pradny, and Miroslava Duskova</i>	
Introduction	303
Contact Lens Terminology	306
Materials Used for Hydrogels Contact Lenses	307
HEMA	307
Other Glycol Methacrylates	307
Dihydroxy Methacrylates	308
Methacrylic Acid	308
Acrylamides	309
1-Vinyl-2-Pyrrolidone	310
FDA Contact Classification	310
Selected Types of Hydrogels Contact Lens Materials	311
Silicone Hydrogels	312
Current Trends in Silicone-Hydrogels Lenses	313
Summary	313
References	314
Part IV Hydrogels With Unique Properties	317
Electroconductive Hydrogels	319
<i>Ann M. Wilson, Gusphyl Justin, and Anthony Guiseppi-Elie</i>	
Introduction	319
Inherently Conductive Electroactive Polymers	320
Hydrogels	323
Electroconductive Hydrogels	325
Synthesis of Electroconductive Hydrogels	326
Conclusions	333
Acknowledgments	333
References	333
Self-assembled Nanogel Engineering	339
<i>Nobuyuki Morimoto and Kazunari Akiyoshi</i>	
Introduction	339
Self-Assembled Polysaccharide Nanogels	339
Stimuli-Responsive Self-Assembled Nanogels	341
Thermoresponsive Nanogels	342
Dual Stimuli (Heat-Redox)-Responsive Nanogels	343
Photoresponsive Nanogels	344
Biomedical Applications of Polysaccharide Nanogels	345
Design and Function of Nanogel-Based Hydrogels Materials	346
Hybrid Gels Crosslinked by Polymerizable Nanogels	346
Rapid Shrinking Hydrogels Using Nanogel Crosslinker	347
Biodegradable Nanogel-Crosslinked Hydrogels and Application in Regenerative Medicine	347
Summary	348
References	348

Engineered High Swelling Hydrogels	351
<i>Hossein Omidian and Kinam Park</i>	
Introduction.	351
Engineered Hydrogels	352
Purity of HSHs	358
Hydrogels Characterization	360
Hydrogels Stability	364
Engineered HSH Polymers	365
Summary	369
References	369
Superabsorbent Hydrogels	375
<i>Grigoriy Mun, Ibragim Suleimenov, Kinam Park, and Hossein Omidian</i>	
Introduction.	375
Hydrogels Swelling.	376
Mechanism of Hydrogels Swelling.	378
The Effect of Neutralization and Acidity on the Swelling Capacity of Polycarbonic Acids	380
Donnan's Equilibrium and Potential in a Hydrogels Solution System	380
Effect of Concentration Redistribution	384
Kinetics of Hydrogels Swelling	387
Summary	390
References	390
Name Index	393
Subject Index	423

List of Contributors

- María Rosa Aguilar**, Institute of Polymer Science and Technology, CSIC and CIBER-BBN, Juan de la Cierva 3, 28006 – Madrid, Spain
- Kazunari Akiyoshi**, Institute of Biomaterials and Bioengineering, Tokyo Medical and Dental University, 2-3-10 Kanda-surugadai, Chiyoda-ku, Tokyo 101-0062, Japan
- L. Ambrosio**, Institute of Composite and Biomedical Materials, National Research Council, P.le Tecchio 80, Naples 80125, Italy
- R. De Santis**, Institute of Composite and Biomedical Materials, National Research Council, P.le Tecchio 80, Naples 80125, Italy
- Pieter J. Dijkstra**, Polymer Chemistry and Biomaterials, Faculty of Science and Technology, University of Twente, The Netherlands
- Miroslava Duskova**, Institute of Macromolecular Chemistry, Academy of Sciences of the Czech Republic, Heyrovsky sq. 2, 162 06, Prague 6, Czech Republic
- Ahmed Fatimi**, Laboratoire d'ingénierie Ostéo-articulaire et dentaire, LIOAD Faculté de chirurgie dentaire, Université de Nantes, IFR 26, 1 place A. Ricordeau, F-44042, Nantes, France
- Tomoko Fujiwara**, Department of Chemistry, University of Memphis, Memphis, TN 38152, USA
- Luis García**, Institute of Polymer Science and Technology, CSIC and CIBER-BBN, Juan de la Cierva 3, 28006 – Madrid, Spain
- A. Gloria**, Institute of Composite and Biomedical Materials, National Research Council, P. le Tecchio 80, Naples 80125, Italy
- Jian Ping Gong**, Faculty of Advanced Life Science, Hokkaido University, Sapporo 060-0810, Japan
- V. Guarino**, Institute of Composite and Biomedical Materials, National Research Council, P.le Tecchio 80, Naples 80125, Italy
- Jerome Guicheux**, Inserm, UMR_S 791, Laboratoire d'ingénierie Ostéo-articulaire et dentaire, LIOAD, 1 place A. Ricordeau, F-44042, Nantes, France; Laboratoire d'ingénierie Ostéo-articulaire et dentaire, LIOAD Faculté de chirurgie dentaire, Université de Nantes, IFR 26, 1 place A. Ricordeau, F-44042, Nantes, France
- Chaoliang He**, Department of Polymer Science and Engineering, Sungkyunkwan University, Suwon, Gyeonggi 440-746, Republic of Korea
- Anthony Guiseppi-Elie**, ABTECH Scientific, Inc., Biotechnology Research Park, 800 East Leigh Street, 23219, Richmond, VA, USA; Center for Bioelectronics, Biosensors and Biochips (C3B), Clemson University Advanced Materials Center, 100 Technology Drive, 29625, Anderson, SC, USA
- Radka Hobzova**, Institute of Macromolecular Chemistry, Academy of Sciences of the Czech Republic, Heyrovsky sq. 2, 162 06, Prague 6, Czech Republic
- Rong Jin**, Polymer Chemistry and Biomaterials, Faculty of Science and Technology, University of Twente, The Netherlands
- Gusphyl Justin**, Center for Bioelectronics, Biosensors and Biochips (C3B), Clemson University Advanced Materials Center, 100 Technology Drive, 29625, Anderson, SC, USA
- Haruma Kawaguchi**, Department of Chemistry, Kanagawa University, Yokohama, Japan

- Yoshiharu Kimura**, Department of Polymer Science and Engineering, Kyoto Institute of Technology, Kyoto, Japan
- Doo Sung Lee**, Department of Polymer Science and Engineering, Sungkyunkwan University, Suwon, Gyeonggi 440-746, Republic of Korea
- Jiri Michalek**, Institute of Macromolecular Chemistry, Academy of Sciences of the Czech Republic, Heyrovsky sq. 2, 162 06, Prague 6, Czech Republic
- Takashi Miyata**, Department of Chemistry and Materials Engineering, Kansai University, Suita, Osaka 564-8680, Japan
- Nobuyuki Morimoto**, Department of Materials Processing, Graduate School of Engineering, Tohoku University, 6-6-02 Aramaki-aza Aoba, Aoba-ku, Sendai, 980-8579 Japan
- Grigoriy Mun**, Department of Chemical Physics and Macromolecular Chemistry, Kazakh National University, Almaty, Republic of Kazakhstan
- Takayuki Murosaki**, Faculty of Advanced Life Science, Hokkaido University, Sapporo 060-0810, Japan
- Yukio Nagasaki**, Tsukuba Interdisciplinary Materials Science (TIMS), University of Tsukuba, 1-1-1 Tennoudai, Tsukuba, Ibaraki 305-8573, Japan
- Keun Sang Oh**, Department of Advanced Materials, Hannam University, 461-6 Jeonmin Dong, Yusung Gu, Daejeon, Korea 305-811
- Motoi Oishi**, Tsukuba Interdisciplinary Materials Science (TIMS), University of Tsukuba, 1-1-1 Tennoudai, Tsukuba, Ibaraki 305-8573, Japan
- Teruo Okano**, Institute of Advanced Biomedical Engineering and Science, TWIns., Tokyo Women's Medical University, 8-1 Kawada-cho, Shinjuku-ku, Tokyo 162-8666, Japan
- Hossein Omidian**, College of Pharmacy, Nova Southeastern University, Fort Lauderdale, FL, USA
- Kinam Park**, Departments of Biomedical Engineering and Pharmaceutics, Purdue University, West Lafayette, IN, USA
- Kinam Park**, Departments of Biomedical Engineering and Pharmaceutics, Purdue University, West Lafayette, IN, USA
- Nicholas A. Peppas**, Pratt Chair of Engineering, Department of Biomedical Engineering, The University of Texas at Austin, TX 78712, USA
- Martin Pradny**, Institute of Macromolecular Chemistry, Academy of Sciences of the Czech Republic, Heyrovsky sq. 2, 162 06, Prague 6, Czech Republic
- Julio San Román**, Institute of Polymer Science and Technology, CSIC and CIBER-BBN, Juan de la Cierva 3, 28006 – Madrid, Spain
- Irma Y. Sanchez**, Department of Mechatronics and Automation, Tecnologico de Monterrey, Monterrey, Nuevo León 64849, Mexico
- Ibragim Suleimenov**, Almaty Institute of Power Engineering and Telecommunications, Almaty, Republic of Kazakhstan
- Claire Vinatier**, Inserm, UMR_S 791, Laboratoire d'ingénierie Ostéo-articulaire et dentaire, LIOAD, 1 place A. Ricordeau, F-44042, Nantes, France; Laboratoire d'ingénierie Ostéo-articulaire et dentaire, LIOAD Faculté de chirurgie dentaire Université de Nantes IFR 26, 1 place A. Ricordeau, F-44042, Nantes, France; GRAFTYS SA, 415 rue Claude Ledoux, 13854 Aix en Provence, France
- Xiaohong Wang**, Key Laboratory for Advanced Materials Processing Technology, Ministry of Education & Center of Organ Manufacturing, Department of Mechanical Engineering, Tsinghua University, 100084, Beijing, China; Institute of Life Science and Medicine, Tsinghua University, 100084, Beijing, China
- Ann M. Wilson**, ABTECH Scientific, Inc., Biotechnology Research Park, 800 East Leigh Street, 23219, Richmond, VA, USA

- Pierre Weisse**, Inserm, UMR_S 791, Laboratoire d'ingénierie Ostéo-articulaire et dentaire, LIOAD, 1 place A. Ricordeau, F-44042, Nantes, France; Laboratoire d'ingénierie Ostéo-articulaire et dentaire, LIOAD Faculté de chirurgie dentaire, Université de Nantes, IFR 26, 1 place A. Ricordeau, F-44042, Nantes, France
- Yongnian Yan**, Key Laboratory for Advanced Materials Processing Technology, Ministry of Education & Center of Organ Manufacturing, Department of Mechanical Engineering, Tsinghua University, 100084, Beijing, China; Institute of Life Science and Medicine, Tsinghua University, 100084, Beijing, China
- Tetsuji Yamaoka**, Advanced Medical Engineering Center, National Cardiovascular Center Research Institute, Osaka, Japan
- Ryo Yoshida**, Department of Materials Engineering, Graduate School of Engineering, The University of Tokyo, 7-3-1 Hongo, Bunkyo-ku, Tokyo 113-8656, Japan
- Soon Hong Yuk**, Department of Advanced Materials, Hannam University, 461-6 Jeonmin Dong, Yusung Gu, Daejeon, Korea 305-811
- Renji Zhang**, Laboratory for Advanced Materials Processing Technology, Ministry of Education & Center of Organ Manufacturing, Department of Mechanical Engineering, Tsinghua University, 100084, Beijing, China; Institute of Life Science and Medicine, Tsinghua University, 100084, Beijing, China

Introduction to Hydrogels

Hossein Omidian and Kinam Park

Abstract Hydrogels are a class of crosslinked polymers that, due to their hydrophilic nature, can absorb large quantities of water. These materials uniquely offer moderate-to-high physical, chemical, and mechanical stability in their swollen state. The structure of a hydrogel can be designed for a specific application by selecting proper starting materials and processing techniques. Since the equilibrium swelling capacity of a hydrogel is a balance between swelling and elastic forces, hydrogels with different swelling capacities can be designed by modulating the contribution of individual forces. Certain hydrogels respond to the changes in environmental factors by altering their swelling behavior. This chapter explains the evolution of hydrogels as a new class of the crosslinked polymers, the hydrogel structures, swelling forces, swelling kinetics, types of water in a swollen hydrogel, and composite properties of hydrogel materials.

Crosslinked Polymers

Compared with metals, glass, and ceramic, polymers are unique as their molecular weight can be regulated from low to ultra high to provide different properties. For example, polyethylene is supplied as wax and also as a very durable packaging material; these are made based on low and high molecular weight polyethylene, respectively. Poly(ethylene oxide) can be made as low and very high molecular weight materials with applications such as plasticizer and flocculent, respectively. Usually, high molecular weights promote intermolecular interactions between the polymer chains and have better chemical, physical, and mechanical properties. For example, increased melting temperature, stability, and mechanical resistance are generally provided by high molecular weight polymers. Polymers have enormous applications as general commodities where environmental factors, such as temperature and mechanical forces, exist at low-to-moderate levels. However, such polymers fail when the magnitude of these factors increases substantially. For instance, extreme pHs, high temperatures, high mechanical forces, or strong solvents can either degrade the polymers or weaken the intermolecular forces. For these applications, the magnitude of intermolecular forces needs to be supplemented with other auxiliary forces. Crosslinked rubbers are the first generation of such polymers which benefited from this concept. Without crosslinking, the rubber in tires could not fulfill their task. The idea of crosslinking as a tool to form permanent intermolecular bonds quickly spread into other areas, such as the contact lens industry where poly(methyl methacrylate) and poly(hydroxyethyl methacrylate) are crosslinked with ethylene glycol dimethacrylate (see Chap. 16).

H. Omidian • College of Pharmacy,
Nova Southeastern University, Fort Lauderdale, FL, USA
e-mail: omidian@nova.edu

K. Park • Departments of Biomedical Engineering and Pharmaceutics,
Purdue University, West Lafayette, IN, USA

Hydrogels Synthesis

By definition, a hydrogel is a crosslinked polymer network having hydrophilic properties. While hydrogels are generally prepared based on hydrophilic monomers, hydrophobic monomers are sometimes used in hydrogels preparation in order to regulate the properties for specific applications. In general, the three integral parts of the hydrogels synthesis are monomer, initiator, and crosslinker. To control the heat of polymerization and the final hydrogels properties, diluents can be used, such as water or other aqueous solutions. After the synthesis, the hydrogels mass needs to be washed to remove impurities left from the synthesis process. These include non-reacted monomers, initiators, crosslinkers, as well as unwanted products produced via side reactions (Fig. 1). The hydrogels properties can be modulated by varying the synthetic factors, such as reaction vessel, reaction time, reaction temperature, monomer type, type of crosslinker, crosslinker-to-monomer ratio, monomer concentration, and type and amount of initiator.

Synthetic hydrogels are generally produced via bulk, solution, and inverse dispersion techniques. While the first two reactions are homogeneous, the inverse dispersion method is conducted in the dispersed and continuous phases. Among the homogeneous polymerizations, the solution reaction is preferred due to better control of the heat of polymerization, and hence the polymer properties. Most of the high-swelling hydrogels are produced in this way. Generally, monomer(s), initiator, and crosslinker(s) are freely soluble in water, or have good solubility in water. The product of this reaction can be dried out and pulverized for various applications. Particles of various sizes are used for different applications. For example, particles in the size range of 150–300 μm are preferred for hygiene products. In agriculture, very small particles are used for seed germination, while larger particles are used to moisten the soil. Hydrogels can also be prepared in micron sizes via an inverse dispersion technique based on the dispersed and continuous phases. The former is aqueous and the latter is organic. The monomer is usually dissolved in the dispersed phase, and a surfactant is dissolved in the organic phase to help the monomer and other aqueous reagents to be effectively dispersed throughout the continuous phase. Although particles with desirable sizes can be obtained by this technique, removal of the organic solvents, such as

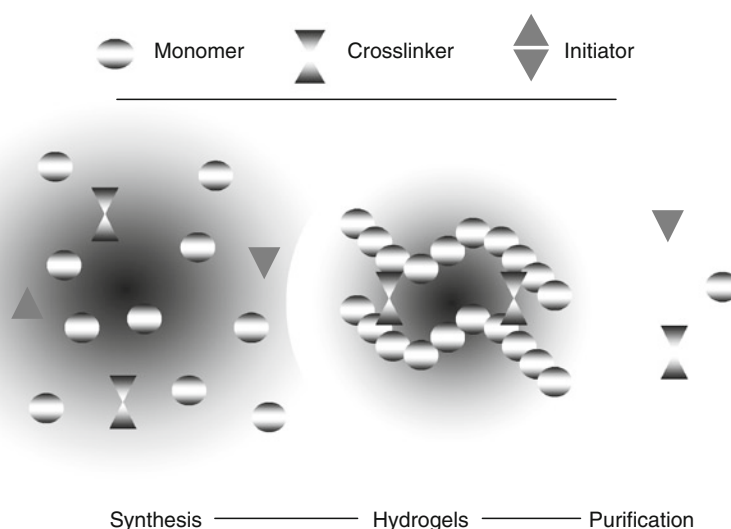


Fig. 1. Hydrogels synthesis.

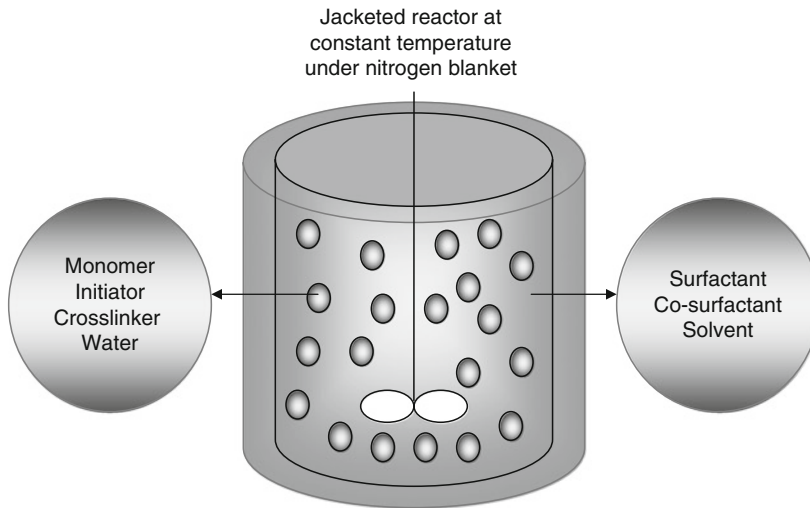


Fig. 2. Inverse dispersion polymerization.

n-hexane and toluene, is a very challenging problem. A typical inverse suspension polymerization to produce hydrogels with high swelling capacity is shown in Fig. 2. The technique is appropriate for highly hydrophilic monomers, such as salts of acrylic and methacrylic acids, as well as acrylamide.

Expansion of a Hydrogels Structure

The hydrophilic polymers without crosslinking are called hydrosol (soluble in water) when they are dissolved in aqueous solution. Hydrosols display liquid behavior and hydrogels display solid behavior, respectively. A hydrosol cannot retain a shape; the hydrogels counterpart does because of the restricted movement of polymer chains due to the intermolecular crosslinks. The method of crosslinking polymer chains depends on the type of monomer and the final application. Hydrophilic monomers containing double bonds, such as acrylic acid, acrylamide, and hydroxyethyl methacrylate, can be polymerized and can form chemical bonds with crosslinkers that have double bonds. A chemical-bonded hydrogels has permanent properties due to the covalent nature of the crosslink entity.

Less common, hydrophilic monomers that contain interactive functional groups, such as $-\text{OH}$, $-\text{COOH}$ or $-\text{COO}^-$, are used to crosslink hydrogels, for example, via hydroxyl–carboxyl interactions. In addition, crosslinking can be performed by physical means. Monomers, such as *N*-isopropylacrylamide, that contain hydrophobic groups, in aqueous solutions, aggregate at certain temperatures, displaying a hydrosol/hydrogels transition. Hydrogen bonding can also function as a crosslinking tool in polymers containing a multitude of hydroxyl groups, such as in poly(vinyl alcohol). Hydrogen bonding provides crosslinks to polymers that contain the same or different functional groups. For example, poly(acrylic acid) and polyacrylamide are both highly soluble in water, but their blend display partial insolubility as a result of hydrogen bonding between the respective carboxyl and amide groups. Solid–liquid behavior of hydrosol and hydrogels polymers as well as approaches to convert a hydrosol to a hydrogels are shown in Fig. 3.

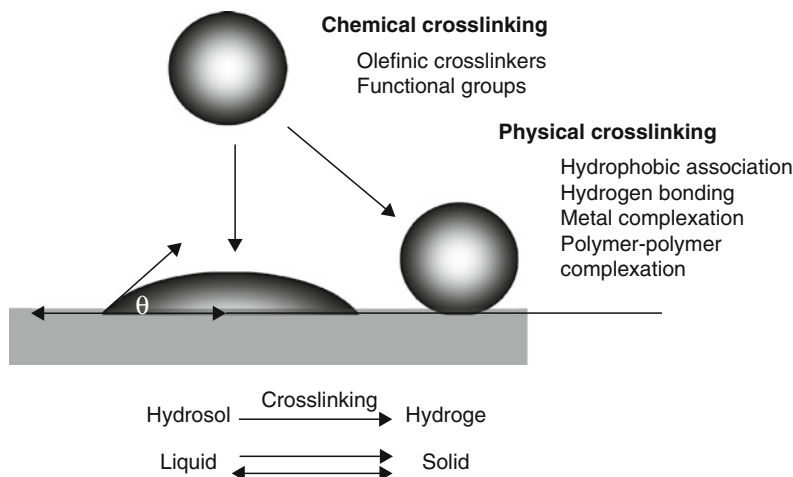


Fig. 3. Chemical and physical gels.

Hydrocol polymers, such as poly(acrylic acid) or its derivatives, can also be crosslinked with metal ions. The magnitude of the crosslink depends on the metal ion type and its valence. Natural hydrocol polymers, such as alginic acid and chitosan, readily form hydrogels in the presence of calcium and phosphate ion, respectively. Similarly, electrolytic crosslinking interactions occur between macromolecules with cations and anions. For example, alginic acid, with $-\text{COO}^-$ groups, and chitosan, with $-\text{NH}_2$ groups, interact in aqueous solutions to form an insoluble hydrogels complex. Furthermore, hydrogels can also be formed by polymer chain aggregation. Hydrocolloids, such as agar and gelatin display hydrocol/hydrogels transition in the aqueous solution with changes in temperature. Crosslinks are formed via chain aggregation, which results in stronger chain–chain interactions than chain–water interactions.

Swelling Forces in Hydrogels

Hydrogels are usually defined by their degree of swelling. The swelling capacity of a hydrogels can be determined by the amount of space inside the hydrogels network available to accommodate water. However, the underlying foundation that determines hydrogels swelling starts with the polymer–water interactive forces. Basically, the more hydrophilic the polymer structure is, the stronger the polymer–water interaction becomes. Hydrogels with hydrophilic functional groups swell in water exclusively as a result of polymer–water interaction forces. If the hydrogels structure contains ionic groups, osmosis is generated by the counter ions due to the difference in ion concentration within the gels and the outside solution. The greater the difference in the ion concentration is, the larger the osmotic pressure becomes. The source of ions in hydrogels is the ionization of the concomitant pendant ionic groups; whereby, the polymer backbone assumes either a negative or a positive charge and the hydrogels is defined as an anionic or cationic, respectively. The ionic charges in the polymer backbone repel each other in an aqueous solution and generate significant expansions in space for water absorption.

Overall, the three forces; polymer–water interactions, electrostatic, and osmosis expand the hydrogels network. Hydrogels swelling, by definition, is the restricted solubility. In other words, infinite solubility of a hydrogels is prevented by elastic forces, which originate from the network crosslinking. The balance of these two different forces determines the equilibrium hydrogels swelling, as shown in Fig. 4.

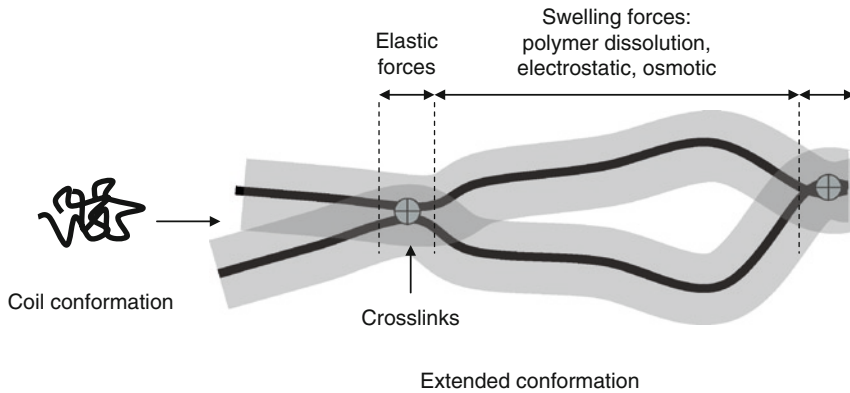


Fig. 4. Swelling forces in hydrogels.

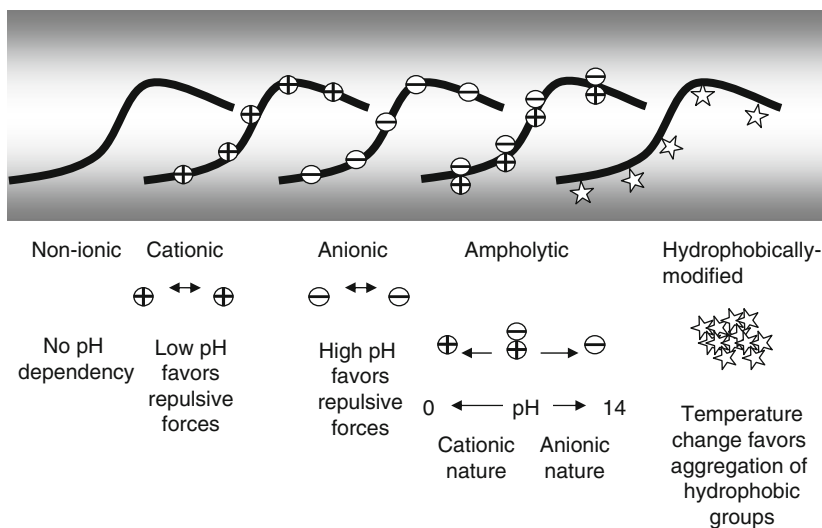


Fig. 5. Different hydrogels structures.

Hydrogels are classified as non-ionic, ionic (anionic, cationic, and ampholytic) as well as those with hydrophilic backbones that contain hydrophobic groups. Non-ionic hydrogels, such as poly(*N*-vinyl pyrrolidone) and poly(ethylene oxide), swell in aqueous medium solely due to water–polymer interactions. The cationic hydrogels swelling is dependent on the pH of the aqueous medium, which determines the degree of dissociation of the ionic chains. Cationic hydrogels display superior swelling at acidic media since their chain dissociation is favored at low pHs. Similarly, anionic hydrogels dissociate more in higher pH media, and hence, display superior swelling in neutral to basic solutions.

Ampholytic hydrogels possess both positive and negative charges that are balanced at a certain pH (their iso-electric point). A change in pH can change the overall ionic (cationic or anionic) properties. For example, ampholytic gelatin dissolves in water at low pHs due to its cationic nature in an acidic medium. The hydrophobic modified hydrogels contain a hydrophilic backbone with pendant hydrophobic groups. In an aqueous solution, the balance between the hydrophilic and hydrophobic interactions changes with temperature. Therefore, depending on the nature of these groups, hydrophobic association occurs at a specific temperature, which results in gelation as depicted in Fig. 5.

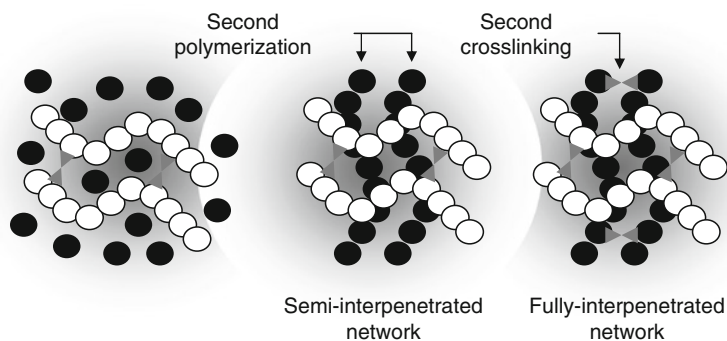


Fig. 6. Multiple hydrogels systems.

For certain applications, a hydrogels based on a single polymer system may not meet the requirements of the intended applications. For example, a very high-swelling hydrogels can offer greater swelling but may have inferior mechanical properties. In these circumstances, a multiple hydrogels process, as shown in Fig. 6, can be used. These systems can be prepared by performing a second polymerization or a second crosslinking process on the original hydrogels platform.

Swelling Mechanism

The water absorption in hydrogels is dependent on many factors, such as; network parameters, nature of the solution, hydrogels structure (porous or poreless), and drying techniques. The most important factor is the crosslink density, which is determined by the effective concentration of the crosslinker used in the crosslinking process. This, in turn, determines the distance (molecular weight) between the two crosslinks on the same polymer chain. The shorter the distance, the higher the crosslink density. Nevertheless, the magnitude of the crosslink density determines the swelling feature of a given hydrogels. At the lower extreme, the swelling process can be seen as a diffusion process followed by a relaxation process. In other words, the rate at which water itself can diffuse into the network structure is rate-determining at the beginning of the swelling process. This mostly depends on the molecular weight of the solvent, solution temperature and the extent of porosity within the hydrogels structure. The second step in the hydrogels swelling is determined by how fast polymer chains can relax which is a slower absorption process. As shown in Fig. 7, the absorption mechanism in highly crosslinked hydrogels potentially changes toward a single diffusion process as polymer chain movement is limited by the high crosslink density. In other words, a highly crosslinked hydrogels behaves like a metal mesh which allows a constant amount of water to continuously pass.

Water in Hydrogels

The water accommodated by a hydrogels structure can be classified into four types as shown in Fig. 8. The water in the outermost layer is called free and can be easily removed from the hydrogels under mild conditions. The interstitial water is the type of water which is not attached to the hydrogels network, but physically trapped in between the hydrated polymer chains. The bound water is directly attached to the polymer chain through hydration

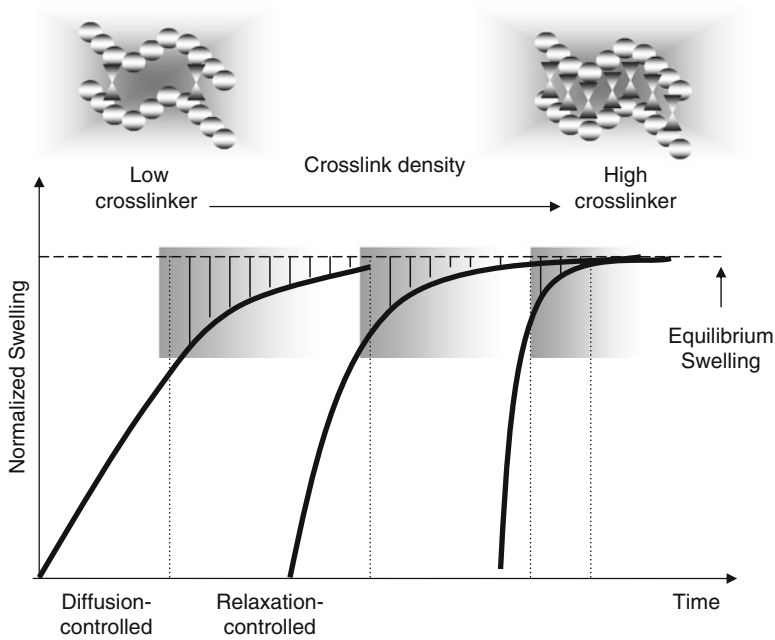


Fig. 7. Swelling kinetics.

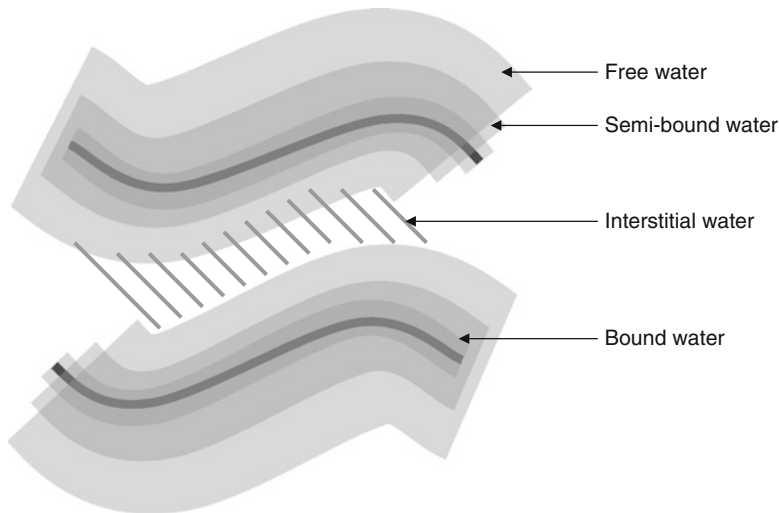


Fig. 8. Different types of water in hydrogels.

of functional groups or ions. The bound water remains as an integral part of the hydrogels structure and can only be separated at very high temperatures. Semi-bound water is a type of water with intermediate properties of a bound water and free water. Although other layers of water can be accommodated into the hydrogels structure, these have much weaker interactions with functional groups and ions as they are farther away from the functional cores. The free and interstitial water can potentially be removed from the hydrogels by centrifugation and mechanical compression. All water types in a hydrogels can be identified and characterized in a simple differential scanning calorimeter thermogram.

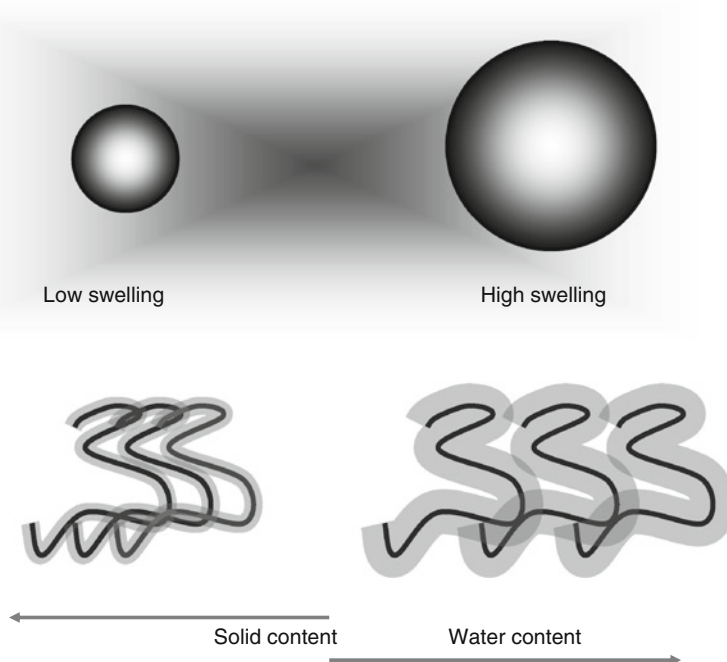


Fig. 9. Composite properties of hydrogels.

Hydrogels Properties

A hydrogels is a composite of a solid (a polymer) and a liquid (water). The final properties of a hydrogels are also determined by the composition of the composite (the polymer-to-water ratio). As shown in Fig. 9, a low- or a high-swelling hydrogels is characterized by a high- or low-polymer/water ratio, respectively. Hydrogels, with superior stability in their swollen state (hydrogels for contact lens), require a high solid content; while a low-solid-content hydrogels (superabsorbent in baby diapers) is desirable when superior swelling capacity is a major requirement. The solid/liquid content of a hydrogels is determined by the crosslinker/monomer ratio during the hydrogels synthesis or post-synthesis.

Hydrogels Characterization

Structural characterization: A hydrogels has chemical and physical structures; for example, when two or more monomers are used in the reaction, or when a monomer is grafted onto a polymer backbone, analytical techniques, such as FTIR and NMR, are used to monitor the degree of copolymerization or grafting processes. On the other hand, the physical structure of a hydrogels is related to its composite nature. A non-porous hydrogels is a two-phase composite of solid polymer and water while a porous hydrogels is a three-phase composite of a solid polymer, water, and air. Each of these phases affects the physical properties of a hydrogels, such as density, refractive index, mechanical property, and porosity. Since air has no mechanical properties, its presence in hydrogels severely affects the mechanical properties. However, due to its gaseous properties, air can provide a very effective path for water absorption, if pores are interconnected. The unique swelling properties of superporous hydrogels are due to the great proportion of air (~30%) in the composite structure. The extent of

the porosity, pore size, and size distribution can significantly affect swelling and mechanical properties of a hydrogels. Scanning electron microscopy, mercury porosimetry, liquid intrusion, and image analysis are used for pore characterization within a porous hydrogels.

In liquid extrusion technique, a liquid is used to fill the pores of the hydrogels in dry state. The liquid–hydrogels system should have a lower surface free energy than that of air–hydrogels system. Pores are occupied spontaneously as the free energy of the system decreases. A non-reactive gas is then used to extrude the liquid out of the hydrogels. To determine the displaced volume “dV” of liquid in a porous system, the (1) is used:

$$p dV = (\gamma_{sg} - \gamma_{sl}) dS, \quad (1)$$

where “ p ” is the differential pressure, γ_{sg} is the free energy of the hydrogels–gas interface, γ_{sl} is the free energy of the hydrogels–liquid interface, and “ dS ” is the increase in hydrogels–gas surface area. Assuming that surface energies are equilibrated and pores are circular, the diameter of the hydrogels pores, D , can be calculated by (2)

$$p = 4\gamma \cos \theta / D, \quad (2)$$

where “ θ ” is the contact angle of the wetting liquid [1, 2].

Swelling: Since the weight, volume, and dimension values of a hydrogels change during the swelling process (Fig. 10), any of these factors can be used to characterize swelling behavior of a hydrogels. The most commonly used method is the weight-swelling ratio, which can be expressed in weight unit or in percentage as shown in (3)

$$Q_t = (m_{st} - m_d) / m_d \text{ (as g/g)} \text{ or } Q_t = [(m_{st} - m_d) / m_d] \times 100 \text{ (as\%)}, \quad (3)$$

where Q_t is the swelling at time “ t ”, m_{st} is the weight of the swollen hydrogels at time “ t ”, and m_d is the weight of the dry hydrogels. When $m_{st} \gg m_d$, the weight-swelling ratio can simply be expressed as in (4)

$$Q_t = m_{st} / m_d \quad (4)$$

For superabsorbent hydrogels with very high swelling capacities, the above equation is acceptable. When $t \rightarrow \infty$, the Q_t becomes Q_∞ , the equilibrium swelling capacity, or swelling at equilibrium. The Q_∞ is also called a “power factor” in hydrogels, which can be used to

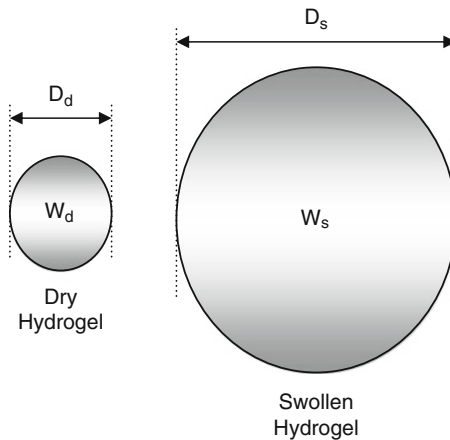


Fig. 10. Swelling measurement.

compare the equilibrium swelling capacity of hydrogels. The higher the power factor is, the greater the swelling capacity becomes.

To measure the swelling kinetics in hydrogels, several values of Q_t are measured at their corresponding swelling time. For comparative purposes, hydrogels can be characterized by their “rate factor,” which is the time for the hydrogels swelling to reach certain percentage of the equilibrium swelling capacity. The lower the “rate factor”, the faster the swelling kinetics.

Swelling in hydrogels can also be expressed in other ways. The volume-swelling ratio is one when the ultimate volume of the swollen gels is the goal for a given application. For example, if the hydrogels is intended to occupy the largest space possible, the volume ratio is more meaningful than the weight ratio. On the other hand, if the absorption of ions from a corresponding solution is intended, the weight ratio is more applicable. The dimensional swelling ratio is straightforward and very useful for the fast comparative purposes. Since the opacity of a hydrogels also changes during the swelling process, the turbidity measurements may be used.

In addition, since the swelling in hydrogels is driven by swelling pressure, pressure sensors can be utilized to characterize swelling in hydrogels. However, for many applications, the swelling pressure in a hydrogels is not the only source of stress on the hydrogels mass. Any external pressure tends to reduce the swelling pressure of hydrogels and has to be taken into account in swelling measurements. For example, an effective diaper absorbent must be able to swell under the external pressure of baby’s weight. For an agricultural absorbent hydrogels, the swelling pressure depends on the depth and the density of the soil, as different pressures are experienced due to the soil weight. For these applications, a loaded swelling measurement is more meaningful than a free swelling determination, in which no external pressure is present (Fig. 11).

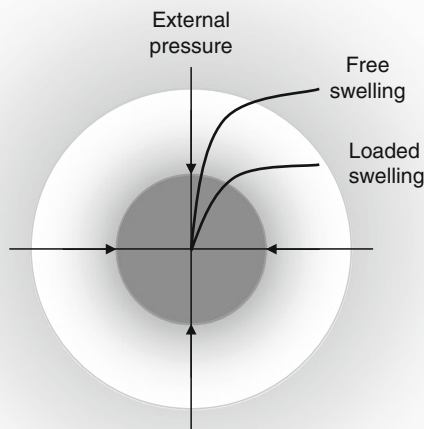


Fig. 11. Free and loaded swelling.

Mechanical strength: For most applications, the most important requirement is how well a hydrogels can maintain its shape in the swollen or wet state; this is called the wet-state stability. Crosslinking the polymer chains is usually necessary to improve the hydrogels mechanical properties. With increases in the crosslinking density, the mechanical properties are increased at the expense of swelling. Crosslinking in hydrogels can be homogeneous (bulk crosslinking) or heterogeneous (surface crosslinking). The former occurs when the crosslinker is soluble in the monomer. Surface crosslinking is generally incorporated either after the hydrogels are formed or during the hydrogels synthesis using a water-insoluble crosslinker. A hydrophobic crosslinker can provide surface crosslinking if it is dissolved in the continuous phase of an inverse dispersion system. Generally, in the swollen state, a bulk-crosslinked hydrogels with a high crosslinking density is brittle, while a surface-crosslinked hydrogels is tough. Either method, improves the stability of a hydrogels in wet state.

Deswelling in hydrogels is also related to the mechanical properties. Water absorbed into a weak hydrogels is desorbed to a greater extent. For example, an important requirement for a diaper absorbent is a dry feeling in the swollen state. If a mechanically weak hydrogels is used in diaper, then the fluid absorbed into the hydrogels can partially leak from the hydrogels, which is not desirable in this application. A weak hydrogels in its fully swollen state under mild stress can also break apart into smaller swollen particles. These smaller particles increase the contact area of the swollen hydrogels with the surrounding dry environment and causing faster desorption.

The desorption in hydrogels is dependent on many factors. Desorption similar to the absorption process is a diffusion process. Therefore, depending on how wet the surrounding environment is, the desorption process takes place at a slow or fast rate. The wetter the surrounding environment are, the slower the desorption process. Desorption processes generally happen at a liquid–air, liquid–liquid, and liquid–solid interface depending on the application. For each given application, a proper desorption or deswelling measurement can be devised. There are a number of ways that the hydrogels desorption can be evaluated. A fully swollen hydrogels is placed in an oven at a certain temperature, and its weight reduction is monitored over time. Alternatively, the fully swollen hydrogels is placed in contact with a dry solid and the weight loss is monitored over time. Depending on the environment temperature, the dryness, the porosity, the texture of the dry environment and the environment pressure, the desorption process may range from a linear to an exponential trend as shown in Fig. 12.

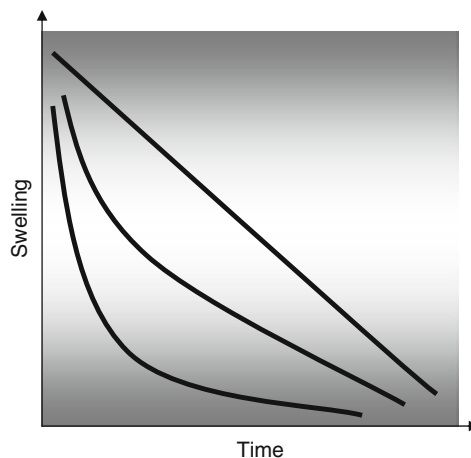


Fig. 12. Hydrogels deswelling.

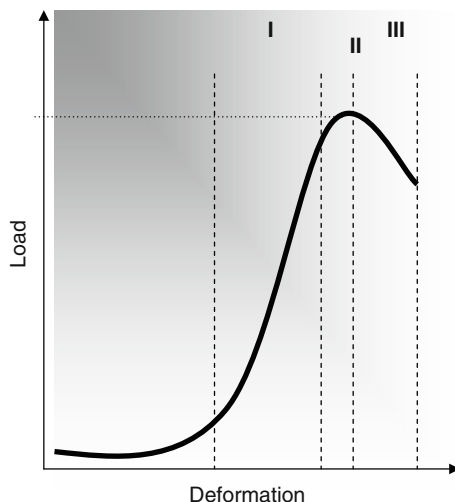


Fig. 13. Hydrogels strength.

To measure the mechanical properties, a hydrogel is deformed under a static compressive loading using a simple mechanical tester, such as a texture analyzer. The hydrogel in its swollen state is placed under the probe of the instrument, and then a specific load is applied at a constant rate. The hydrogel resists the continuous load by deforming itself up to a point where the applied load becomes stronger than the resistance of the hydrogel. At this point, or so-called breaking point, the hydrogel reaches its maximum deformation and then fails. Depending on the hydrogel structure, the hydrogel deforms itself at a slow or fast rate, followed by the breaking point. On the load-deformation graph, as shown in Fig. 13, hydrogel resistance to the applied load is shown by the slope of the load-deformation curve (I). The sharper the slope, the higher the hydrogel resistance is, and hence, the higher the hydrogel modulus. At point II, the hydrogel starts to break, which is expressed as hydrogel maximum strength. The slope of the load-deformation at the region III indicates the rate at which the hydrogel breaks apart, fast or slow. If the slope is mild, the breaking or failing process occurs slowly and the hydrogel breaks in a ductile mode. On the other hand, a hydrogel breaks apart quickly in a brittle fracture mode if the slope is sharp.

Hydrogels like polymers are viscoelastic materials. Therefore, they have elastic and viscous components. These two are characterized by storage modulus and loss modulus, respectively. Viscoelastic properties of swollen hydrogels can be measured by a rheometer, as shown in Fig. 14. The hydrogel structure can be correlated to its elastic modulus, as shown in the graph [3, 4] using the following equation

$$G' = \rho RT / M_c, \quad (5)$$

where G' is the elastic modulus, ρ is density, R is gas constant, T is absolute temperature, and M_c is the molecular weight between two crosslinks. As M_c decreases, the elastic modulus, or elastic nature of the swollen hydrogels increases. This can be accounted for by an increase in crosslink density of the hydrogels.

Hydrogels Applications

As shown in Fig. 15, hydrogels can be used as a swelling agent or as a delivery platform for active compounds. Hydrogels with higher swelling capacity are mostly used in hygiene and agriculture fields where retention of water and aqueous solutions, of say urine and tap

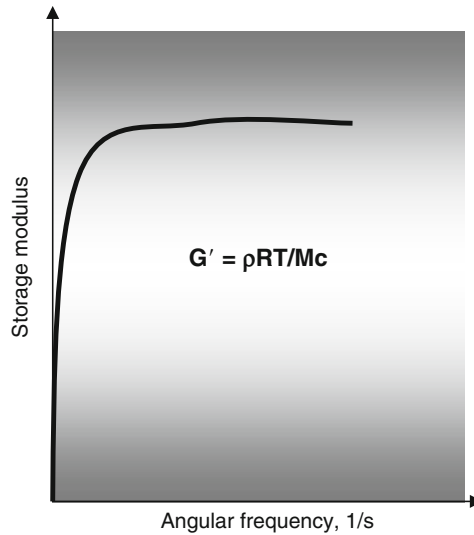


Fig. 14. Hydrogels viscoelasticity.

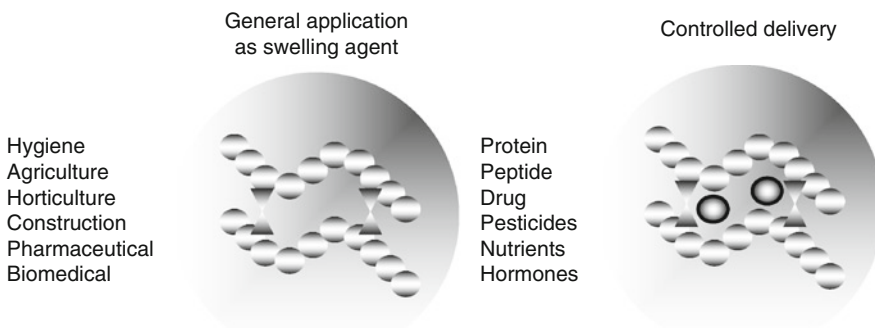


Fig. 15. Hydrogels applications.

water, is expected, respectively. For the delivery of drugs, pesticides, proteins, colorants, for example, hydrogels with lower swelling capacity are generally used. Nevertheless, for each application, the hydrogels is usually specifically designed and manufactured to meet that particular need.

Hydrogels for hygiene products, such as baby diapers, are disposable short-term products; therefore, they are required to offer high and fast swelling properties as well as moderate stability. These should be safe, non-toxic and be able to function in solutions containing urine and salts while loaded. As far as the purity is concerned, hygiene hydrogels must have very limited amounts of residual monomers and other reagents. In agriculture, while high swelling capacity is very desirable, the fast swelling rate is not needed in most applications. Agricultural hydrogels should absorb ion-containing aqueous solutions, while being stable to UV irradiation, oxygen, ozone, acidic rains, temperature variation, microorganisms, and soil composition. Crosslinked hydrophilic polymers are used in the pharmaceutical industry as superdisintegrant and as controlled delivery platforms. For these applications, the hydrogels has to meet specific requirements, such as; medium swelling capacity, fast swelling rate, drug compatibility, safety, non-toxicity, shelf stability, and high purity. They also must function in the stomach under variable pH values, forces, and food contents.

For hygiene products, the goal is to make thinner hydrogels pads with higher absorbency under load, increased swelling pressure and increased suction power [5]. The absorbency limit for the hydrogels used in baby diapers under load is 35–40 mL/g [6]. Although the hydrogels absorbent can keep the skin area dry, there is a serious concern that these synthetic materials can increase the incidence of diaper dermatitis. Their non-biodegradability, toxicity, and environmental pollution are also of concern [7–9].

In the agriculture and horticulture fields, a major challenge is to maintain the hydrogels stability under harsh and long-term environmental conditions. Ions and ultraviolet irradiation can degrade the hydrogels swelling properties via complexation or breaking the crosslinks. For example, an acrylic-based super water-absorbent hydrogels will be dissolved in the swelling medium in a few days when directly exposed to UV irradiation. An agricultural concern is the variable quality of the water used for irrigation. Hydrogels display significantly different swelling behavior from one location to another due to the changes in water quality and environmental factors.

There are numerous studies that show the advantages and disadvantages of hydrogels in agricultural field. Superabsorbent hydrogels for use in soil to promote plant growth has been reviewed by Kazanskii et al. [10]. Crosslinked poly(acrylamide-co-sodium acrylate) microgels as well as polyacrylamide, poly(acrylic acid), poly(vinyl alcohol), and potassium polyacrylate have been produced via electron beam irradiation [11]. The average plant height, leaf width, total dry weight and wilting time increased when these hydrogels were added to the soil [12]. The germination of seeds and the growth of young plants were also better with hydrogels based on starch grafted with acrylic acid and acrylamide [13]. Hydrogels with better resistance against salts were prepared by incorporating potassium humate into acrylic acid/acrylamide hydrogels. The hydrogels swelling was found to be highest in saline containing monovalent cations and also independent of the cation type, (ammonium, potassium, or sodium) [14]. Corn growth is promoted when hydrogels based on acrylic acid and sodium humate are added into the soil [15].

The effects of water quality, type of fertilizer, soil pH, and the surrounding temperature have been evaluated for acrylamide-co-potassium acrylate hydrogels in [16]. The growth of rice is enhanced in soils containing superabsorbent hydrogels based on crosslinked carboxymethylcellulose and acrylamide [17]. Hydrogels have also been used to reduce the environmental problem of polyphenols and organic contents in olive mill wastewater. Hydrogels help the wastewater to be immobilized, so that it can be used as plant fertilizer [18]. Methacrylated cashew gum copolymerized with acrylamide has been claimed as soil conditioner. The swelling capacity of the hydrogels was significantly enhanced via alkaline hydrolysis of the hydrogels [19]. Semi-interpenetrated hydrogels network of sodium acrylate and poly(vinyl alcohol) are used in soils containing high salt content [20]. A starch-based hydrogels of acrylamide and acrylic acid has improved water retention capacity of the soil [21].

Agricultural hydrogels have also been used for controlled delivery applications. Generally, hydrogels for this application are biodegradable. Starch-grafted lactide has been studied as a biodegradable carrier to release urea fertilizer at a slow pace. The urea release can be adjusted by the grafting level as hydrophobic lactide can reduce the starch swellability in water [22]. Crosslinked poly(acrylic acid)/organo-attapulgitic clay has been prepared and used to release urea fertilizer in a controlled manner. In this study, the effect of the urea concentration, the amounts of crosslinker and kaolin, the neutralization degree of the acrylic acid, the temperature, pH and ionic strength of the solutions were evaluated [23]. In a similar study using acrylic acid and maleic anhydride hydrogels, the slow release and improved water retention properties claimed by crosslinking the hydrogels surface [24]. Slow release nitrogen fertilizers have also been prepared using crosslinked poly(acrylic acid) [25] and its clay composite [26].

Hydrogels in biomedical applications are generally non-thrombogenic, so they can be used in blood contact, for example, in wound dressing products. Hydrogels can be designed to

be responsive to specific molecules, such as glucose, so they can be used as biosensors or in drug delivery applications. Biodegradable hydrogels based on lightly crosslinked high molecular weight polyaspartate were prepared for personal care and biomedical applications as an alternative to synthetic poly(acrylic acid) hydrogels [27]. The semi-interpenetrated hydrogels based on poly(aspartic acid) and poly(acrylic acid) are sensitive to salts, pH, and temperature; therefore, they have potential applications in many biomedical areas [28]. Hydrogels based on sodium carboxymethylcellulose and hydroxyethylcellulose crosslinked with divinyl sulfone have been suggested as an alternative for diuretic therapy in cases of edema [29]. Chitosan crosslinked with periodate-oxidized sucrose is being used as a delivery platform of bioactive agents for wound dressing application [30].

For pharmaceutical applications, superdisintegrants are used to help with proper disintegration of tablet and capsule dosage forms. These are crosslinked carboxymethylcellulose, poly(*N*-vinylpyrrolidone), and starch glycolate. In drug delivery area, hydrogels with interconnected pore structure and unique swelling and mechanical properties are suggested as drug delivery platform for drugs with narrow absorption window [31–33]. Gelatin crosslinked with genipin has been introduced as a controlled release carrier of bioactive compounds [34]. Drug release rates are decreased with increase in drug molecular weight [35]. The release kinetics of antimicrobial agents, such as lysozyme, nisin, and sodium benzoate, have been studied with crosslinked poly(vinyl alcohol) hydrogels [36].

Biocompatible and an environmentally safe hydrogels products are prepared from aqueous solutions of hydroxyethyl cellulose, sodium carboxymethylcellulose and hyaluronic acid crosslinked by carbodiimide [37]. Similar eco-friendly water management materials based on guar gum-g-polyacrylic acid and attapulgitte clay are used for agricultural and horticultural applications [38]. There are several new high performance superabsorbent hydrogels, which have potential applications in different fields [39].

Summary

Crosslinked hydrophilic polymers provide superior physical, chemical, and environmental properties in their wet state. These features has made hydrogels invaluable in numerous disciplines including; hygiene, agriculture, biomedical, and pharmaceutical. Successful design of a hydrogels for a specific application requires careful understanding of the application and environment that the hydrogels is intended to serve. Although challenging, a hydrogels can be tailored to address some special need in almost any discipline due to the wide spectrum of synthetic and natural hydrogels structures and processing technologies available.

References

1. Jena AK, Gupta KM (1999) In-plane compression porometry of battery separators. *J Power Sources* 80:46–52
2. Adamson AW (1967) *Physical chemistry of surfaces*. Interscience, New York
3. Sperling LH (2001) *Introduction to physical polymer science*. Wiley, New York, 3rd edition, p. 370
4. Jiang H et al (1999) Rheology of highly swollen chitosan/polyacrylate hydrogels. *Polymer* 40:4593–4602
5. Nagorski H (1994) Characterization of a new superabsorbent polymer generation. *Superabsorbent Polym* 573:99–111
6. Masuda F (1994) Trends in the development of superabsorbent polymers for diapers. *Superabsorbent Polym* 573:88–98
7. Prasad HRY, Srivastava P, Verma KK (2003) Diaper dermatitis: an overview. *Indian J Pediatr* 70(8):635–637
8. Prasad HRY, Srivastava P, Verma KK (2004) Diapers and skin care: merits and demerits. *Indian J Pediatr* 71(10):907–908
9. Wong DL et al (1992) Diapering choices: a critical review of the issues. *Pediatr Nurs* 18(1):41–54

10. Kazanskii KS, Dubrovskii SA (1992) Chemistry and physics of agricultural hydrogels. *Adv Polym Sci* 104:97–133
11. Abd El-Rehim HA (2005) Swelling of radiation crosslinked acrylamide-based microgels and their potential applications. *Radiat Phys Chem* 74(2):111–117
12. Abd El-Rehim HA, Hegazy ESA, Abd El-Mohdy HL (2004) Radiation synthesis of hydrogels to enhance sandy soils water retention and increase plant performance. *J Appl Polymer Sci* 93(3):1360–1371
13. Chen P et al (2004) Synthesis of superabsorbent polymers by irradiation and their applications in agriculture. *J Appl Polym Sci* 93(4):1748–1755
14. Chu M et al (2008) Influence of potassium humate on the swelling properties of a poly(acrylic acid-co-acrylamide)/potassium humate superabsorbent composite. *J Appl Polym Sci* 107(6):3727–3733
15. Chu M et al (2006) Synthesis of poly(acrylic acid)/sodium humate superabsorbent composite for agricultural use. *J Appl Polym Sci* 102(6):5137–5143
16. El-Rehim HAA, Hegazy ES, El-Mohdy HLA (2006) Effect of various environmental conditions on the swelling property of PAAm/PAAcK superabsorbent hydrogel prepared by ionizing radiation. *J Appl Polym Sci* 101(6):3955–3962
17. Ibrahim SM, El Salmawi KM, Zahran AH (2007) Synthesis of crosslinked superabsorbent carboxymethyl cellulose/acrylamide hydrogels through electron-beam irradiation. *J Appl Polym Sci* 104(3):2003–2008
18. Davies LC, Novais JM, Martins-Dias S (2004) Detoxification of olive mill wastewater using superabsorbent polymers. *Environ Technol* 25(1):89–100
19. Guilherme MR et al (2005) Synthesis of a novel superabsorbent hydrogel by copolymerization of acrylamide and cashew gum modified with glycidyl methacrylate. *Carbohydr Polym* 61(4):464–471
20. Li YF et al (2004) Study on the synthesis and application of salt-resisting polymeric hydrogels. *Polym Adv Technol* 15(1–2):34–38
21. Luo W et al (2005) Synthesis and properties of starch grafted poly[acrylamide-co-(acrylic acid)]/montmorillonite nanosuperabsorbent via gamma-ray irradiation technique. *J Appl Polym Sci* 96(4):1341–1346
22. Chen L et al (2008) Controlled release of urea encapsulated by starch-g-poly(L-lactide). *Carbohydr Polym* 72(2):342–348
23. Liang R, Liu MZ (2007) Preparation of poly(acrylic acid-co-acrylamide)/kaolin and release kinetics of urea from it. *J Appl Polym Sci* 106:3007–3015
24. Liu MZ et al (2006) Synthesis of a slow-release and superabsorbent nitrogen fertilizer and its properties. *Polym Adv Technol* 17(6):430–438
25. Liu MZ et al (2007) Preparation of superabsorbent slow release nitrogen fertilizer by inverse suspension polymerization. *Polym Int* 56(6):729–737
26. Liang R, Liu MZ (2006) Preparation and properties of coated nitrogen fertilizer with slow release and water retention. *Ind Eng Chem Res* 45(25):8610–8616
27. Chang CJ, Swift G (1999) Poly(aspartic acid) hydrogel. *J Macromol Sci – Pure Appl Chem* A36(7–8):963–970
28. Zhao Y, Kang J, Tan TW (2006) Salt-, pH- and temperature-responsive semi-interpenetrating polymer network hydrogel based on poly(aspartic acid) and poly(acrylic acid). *Polymer* 47(22):7702–7710
29. Sannino A et al (2003) Biomedical application of a superabsorbent hydrogel for body water elimination in the treatment of edemas. *J Biomed Mater Res A* 67A(3):1016–1024
30. Pourjavadi A, Aghajani V, Ghasemzadeh H (2008) Synthesis, characterization and swelling behavior of chitosan–sucrose as a novel full-polysaccharide superabsorbent hydrogel. *J Appl Polym Sci* 109(4):2648–2655
31. Omidian H, Park K (2008) Swelling agents and devices in oral drug delivery. *J Drug Deliv Sci Technol* 18(2):83–93
32. Omidian H, Park K, Rocca JG (2007) Recent developments in superporous hydrogels. *J Pharm Pharmacol* 59(3):317–327
33. Omidian H, Rocca JG, Park K (2005) Advances in superporous hydrogels. *J Control Release* 102(1):3–12
34. Abbasi A, Eslamian M, Rousseau D (2008) Modeling of caffeine release from crosslinked water-swellaable gelatin and gelatin–maltodextrin hydrogels. *Drug Deliv* 15(7):455–463
35. Brazel CS, Peppas NA (1999) Mechanisms of solute and drug transport in relaxing, swellaable, hydrophilic glassy polymers. *Polymer* 40(12):3383–3398
36. Buonocore GG et al (2003) A general approach to describe the antimicrobial agent release from highly swellaable films intended for food packaging applications. *J Control Release* 90(1):97–107
37. Sannino A et al (2005) Crosslinking of cellulose derivatives and hyaluronic acid with water-soluble carbodiimide. *Polymer* 46(25):11206–11212
38. Wang WB, Zheng YA, Wang AQ (2008) Synthesis and properties of superabsorbent composites based on natural guar gum and attapulgit. *Polym Adv Technol* 19(12):1852–1859
39. Shimomura T, Namba T (1994) Preparation and application of high-performance superabsorbent polymers. *Superabsorbent Polym* 573:112–127

Part I

Stimuli-Sensitive Hydrogels

Stimuli-Responsive Hydrogels and Their Application to Functional Materials

Ryo Yoshida and Teruo Okano

Abstract Many kinds of stimuli-responsive polymer gels that respond to the change in their surroundings such as solvent composition, temperature, pH, and supply of electric field have been developed. They are of interest as intelligent (or smart, biomimetic) materials which have sensor, processor, and actuator functions. This article is related to stimuli-responsive gels and their application for bio- or biomimetic materials designed as self-oscillating gels.

Introduction

With the discovery of “volume phase transition” phenomena by Tanaka in 1978 [1], research using gels as functional materials was activated. Many stimuli-responsive polymer gels, that change volume abruptly in response to a change in their surroundings, such as solvent composition, temperature, pH, and supply of electric field, light, have been developed. Their ability to swell and deswell according to conditions makes them interesting for use as new intelligent materials. Applications for biomedical fields have three functions; (a) sensing an external signal (sensor function), (b) evaluation (processor function), and (c) action (actuator function) which were developed as “intelligent gels” or “smart gels.”

Stimuli-responsive gels and their application to functional materials, mainly to biomaterials and biomimetic materials are very important. Particularly, intelligent material systems that use temperature-responsive poly(*N*-isopropylacrylamide) (poly(NIPAAm) or PNIPAAm). Several intelligent systems have been created using the bulk properties and the surface properties of PNIPAAm gels, such as intelligent drug delivery systems (DDS), temperature-responsive chromatography and cell-sheet engineering. In addition, biomimetic materials exhibiting self-oscillating behavior have been developed based on the PNIPAAm gels.

Stimuli-Responsive Gels as Functional Materials

The functions of stimuli-responsive gels can be roughly classified into three categories; (a) mechanical motion, (b) mass transport, and (c) conversion and transmission of information.

R. Yoshida • Department of Materials Engineering, Graduate School of Engineering, The University of Tokyo, 7-3-1 Hongo, Bunkyo-ku, Tokyo 113-8656, Japan

T. Okano • Institute of Advanced Biomedical Engineering and Science, TWIns., Tokyo Women's Medical University, 8-1 Kawada-cho, Shinjuku-ku, Tokyo 162-8666, Japan
e-mail: tokano@abmes.twmu.ac.jp

Function of Mechanical Motion

In the 1980s and 1990s, several mechanical devices using gels were devised and developed. These devices were controlled by changing temperature or an electric field (artificial muscles, robot hands to lift or grasp objects, and as artificial fish that swim by a repeating flexing motion) [2]. In addition, several chemo-mechanical gels (biochemo-mechanical gels) that can connect when glucose was added to an external solution were demonstrated [3]. Recently, more interest is shown in electrically stimulated systems using polyelectrolyte gels, organogels [4], gels consisting of carbon nanotube, and ionic liquid [5]. For example, an ion conductive polymer actuator obtained by plating gold to both sides of a perfluoro carboxylic acid film causes a bending motion and biomimetic motion in an electric field [6]. Another actuating system, driven by a magnetic field using a PVA gels-containing film magnetite (Fe_3O_4) particles (ferrogel) provides dynamic motion in response to magnetic field [7].

Function of Information Transmission and Transformation

The function to memorize or convert information is key for stimuli devices. The molecular designs to memorize structure at the molecular level in a polymer network have the following important characteristics:

Shape Memory

Osada et al. [8] pioneered the “shape memory gels” that consisted of acrylic acid and steryl acrylate with long hydrophobic side chains. The gels return to their original shape by heating. Several potential applications including artificial valves, artificial anus and medical implements, sporting goods, are being pursued.

Optical Function

Materials that change color reversibly are important for displays, recorders and sensors that lead to gels with optical conversion functions have been prepared [9–11]. New sensor materials that determine analyte concentrations by wavelength changes of diffracted light and “gels opals” that exhibit color changes with temperature by covalently bonding self-assembled PNIPAAm gels particles using divinyl sulfone [12] and porous PNIPAAm gels with “structural color” with reversible opal structure [13, 14]. The periodically ordered interconnecting porous structures were created in these gels by using a closest-packing silica colloidal crystal as a template. The porous gels changes “structural color” corresponding to temperature, which can be tuned by changing the amount of the crosslinker. Porous glucose-responsive gels that change the structural color in response to glucose concentration were prepared using glucose-responsive gels with phenyl boronic acid groups to be applied as a sensor for blood sugar levels [15].

Dimmer materials using PNIPAAm gels with high pigment concentrations were made by arranging the gels particulates containing carbon black on a glass substrate. The glass transmitted light changes reversibly with temperature [16]. To diffuse and condense pigment by volume change is similar to the function of pigments in cells of living organisms.

Molecular Recognition

Gels that recognize specific chemical substances, like a catalyst or an enzyme, have been prepared by molecular imprinting [17]. Target molecules are mixed into the solution containing the monomer with a recognition site, then polymerized so that a complex is formed by the interaction between the target molecule and the monomer. After polymerization, the target molecules are removed since the information for the target molecules is memorized in the polymer network. For example, to target theophylline, it was crosslinked in a methacrylic acid polymer network using a high concentration of crosslinker (>70%) to produce a rigid network [18].

Several hydrogels were developed to recognize environmental stimuli, such as gels that captured metal ions at different temperatures [19]. Biomolecule-responsive gels were developed that are glucose-responsive and antigen-responsive by utilizing biomolecular interactions to establish reversible crosslinking [20, 21].

Function of Mass Transport

Pulsatile Drug Release Control Using Hydrogels

Several gels that function to capture or release a chemical or biological substance and to separate or purify substances are used for biomedical applications [22, 23]. A major use is drug delivery (DDS) by stimuli-responsive gels, intelligent DDS with auto-feedback mechanism that release the drug only when it is needed and stops the release at normal state. An example is the release of antipyretics only when the body temperature rises; another senses an increase in glucose in the blood and releases insulin automatically. The on-off control for drug release by small temperature changes in the body can be realized using temperature-responsive NIPAAm copolymer gels (Fig. 1) [24].

Several regulating systems for insulin release have been developed [25–29]. An on-off regulation for insulin release is effective in response to external glucose concentration by utilizing the reversible complex formation between glucose and the phenylboronic acid group (Fig. 2).

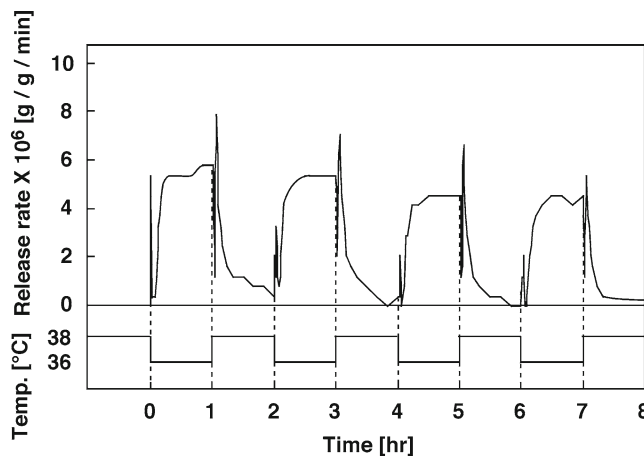


Fig. 1. Indomethacin release from poly(NIPAAm-co-dimethylacrylamide-co-butyl methacrylate) gels in response to stepwise temperature changes between 36 and 38°C in PBS (pH 7.4).



Fig. 3. Temperature-dependent wettability changes for PIPAAm-grafted surfaces at 10 and 37°C.

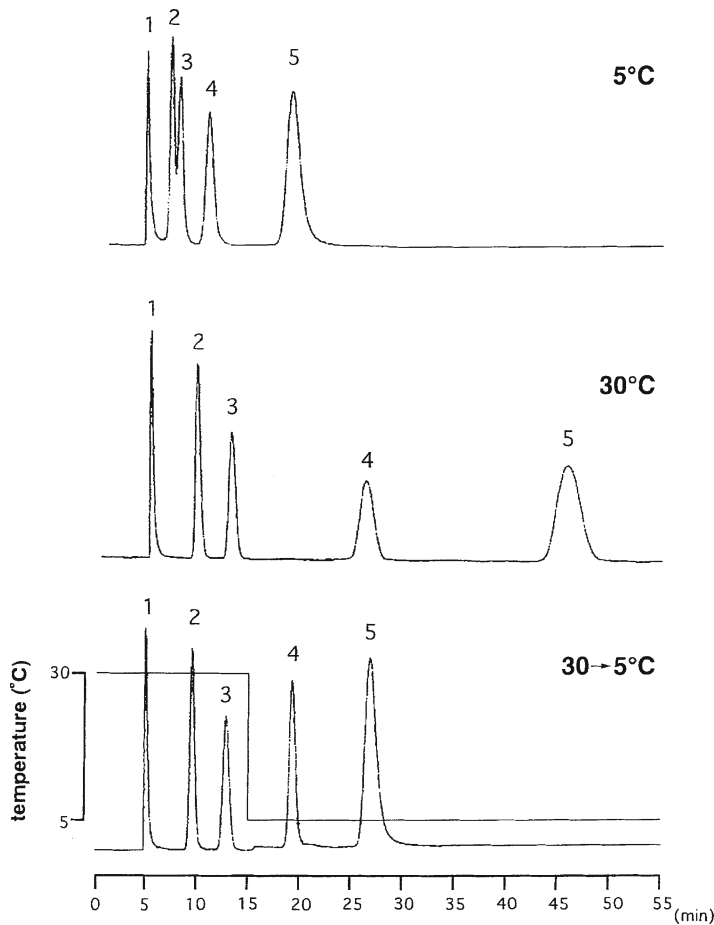


Fig. 4. Chromatograms of a mixture of four steroids and benzene with step gradient by changing column temperature. Peaks: 1, benzene; 2, cortisone; 3, prednisolone; 4, hydrocortisone acetate; and 5, testosterone. Column, NIPAAm-BMA copolymer-modified silica; eluent, water; flow rate, 1.0 ml/min; detection, UV 254 nm.

These surface characteristic changes are used for aqueous separations of bioactive compounds, including; steroid hormones [36, 37], polypeptides and proteins [38–41], and nucleic acids [42].

NIPAAm copolymer on the surface of silica gels can act as a temperature-responsive chromatograph enabling high-speed separation of mixtures by controlling the interaction between the carrier surface and substance by the temperature (Fig. 4) [36, 37]. By applying stepwise temperature changes from higher temperature to lower temperature, the retention time

for hydrophobic component is controllable. Since the mobile phase is water, an organic solvent is not used for the separation and analysis of physiologically active substances or cells.

Cell-Sheet Engineering Using an Intelligent Surface

The development of tissue engineering has progressed significantly from the original concepts [43, 44]. The current paradigm involves constructing scaffolds from biodegradable polymers with seeded cells that proliferate and deposit extracellular matrix (ECM) molecules, such as collagen and fibronectin, eventually regaining their native structure and tissue morphology as the scaffold degrades [45].

Some success was achieved for cell-sparse tissues (using large amounts of ECM and relatively few cells) such as heart valves [46], bone [47], and cartilage [48], as well as the reconstruct of human ears on the backs of mice [49]. However, these polymer scaffolds have undesirable consequences; inflammatory reactions due to the implantation of nonnatural materials with scaffold degradation, the space formerly occupied by the polymer is usually filled by cells and deposits of ECM, that can lead to pathological fibrosis which poorly resembles the native tissue structure. It is also commonly seen that cells on the periphery of the scaffolds are maintained and closely resemble native tissues, whereas there is significant cell necrosis at the interior due to restricted passive diffusion to delivery of nutrients and the removal of metabolic wastes. Therefore, current technologies are still severely lacking in terms of achieving successful tissue reconstruction.

Cell-Sheet Engineering

The architecture of many tissues, such as the heart or liver, mainly consist of associated and with comparatively little associated ECM. To recreate these tissues, cell-dense structures that mimic normal structure and function need to be engineered. To meet this purpose, a new approach using cell-sheet engineering with temperature-responsive culture dishes (Fig. 5)

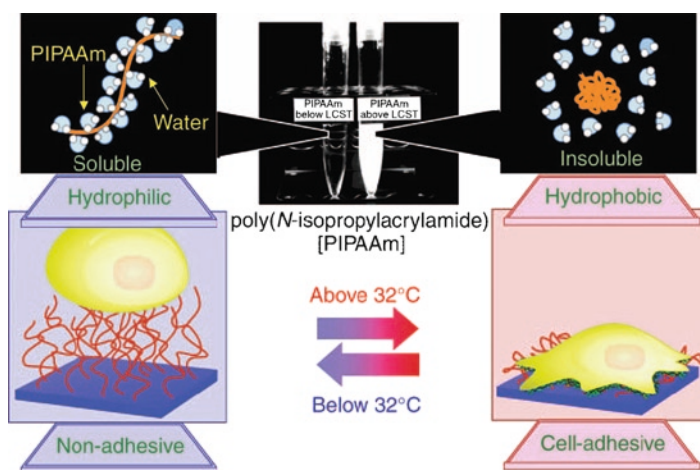


Fig. 5. Temperature-responsive culture dishes. The temperature-responsive polymer poly(*N*-isopropylacrylamide) (PIPAAm) exhibits a transition from hydrophobic to hydrophilic across its lower critical solution temperature (LCST) of 32°C. After electron-beam polymerization and grafting to normal tissue-culture polystyrene (TCPS) dishes, temperature-responsive culture surfaces can be produced. The noninvasive harvest of various cell types as intact sheets, along with deposited extracellular matrix, can be achieved by reducing the culture temperature.

[50, 51] must be followed. To create these surfaces, the temperature-responsive polymer, poly(*N*-isopropylacrylamide) (PIPAAm), is covalently grafted onto normal tissue-culture polystyrene (TCPS) dishes with radical polymerization. The PIPAAm-grafted culture surfaces provide controlled cell adhesion with simple temperature changes by exploiting the property changes of the polymer at the lower critical solution temperature (LCST) of 32°C. In culture conditions at 37°C, the surface is slightly hydrophobic, allowing cells to adhere and grow similarly to normal TCPS dishes. After the necessary culture period, the temperature is lowered to 20°C, causing the polymer to become hydrophilic. Under these conditions, the polymer swells and a hydration layer is created at the surface-cell interface and the cells are detached spontaneously, enabling them to be harvested as intact sheets [52] (Fig. 6). During cell harvesting, PIPAAm remains on the culture dish surface because the temperature-responsive polymer is covalently bonded to the dish. Normally in cell-based therapies, including tissue engineering, cells are grown in TCPS dishes and harvested using proteolytic enzymes, such as trypsin or dispase to degrade the adhesive molecules and ECM that the cells are attached to. However, treatment with these enzymes also degrades the surface-cell molecules, including growth factor receptors, ion channels, and cell-to-cell junction proteins that are vital for the differentiated functions of the cells. Using temperature-responsive surfaces, the need for proteolytic enzymes is avoided and crucial cell-to-cell and cell-to-ECM interactions are preserved [52].

Using this noninvasive cell-harvesting method, intact cell sheets can be recovered along with their deposited ECM on the basal surface. Cells harvested in this fashion can also be transferred to other surfaces, such as new cultural dishes [53, 54], other cell sheets [55] and even directly to host tissue [56–59]. The deposited ECM acts as a “molecular glue,” providing direct contact and adhesion to these surfaces without the need for additional mediators, such as carrier substrates or sutures.

Tissue reconstruction in the body can be accomplished in many ways using cell-sheet engineering. It can be transplanted as single cell sheets, for use as corneal surfaces [57, 58] (Fig. 7) and periodontal ligament tissue [60], as well as in the reconstruction of the bladder [59] and skin [61], using two-dimensional manipulation. It can be used to recreate three-dimensional structures by homotypic layering of cell sheets, as in the case of cardiac

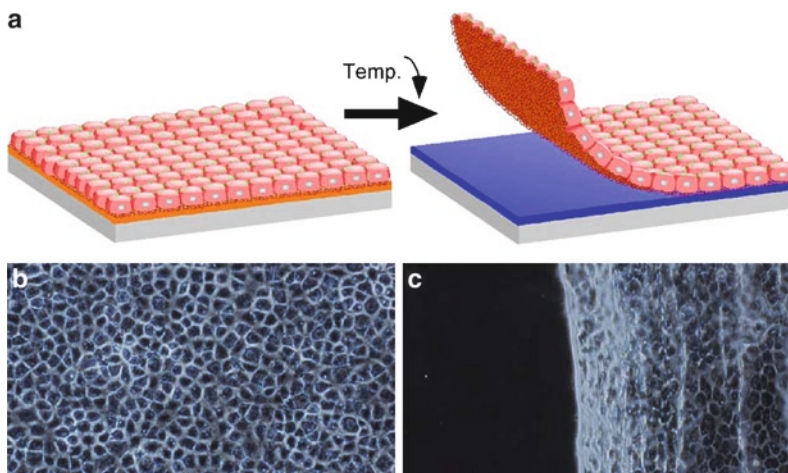


Fig. 6. Cell-sheet engineering using PIPAAm-grafted surfaces. (a) Schematic illustration for temperature-induced recovery of intact monolayer cultures. (b) Confluent culture of endothelial cells on PIPAAm-grafted dishes at 37°C. (c) Detaching endothelial cell sheet by lowering culture temperature to 20°C.

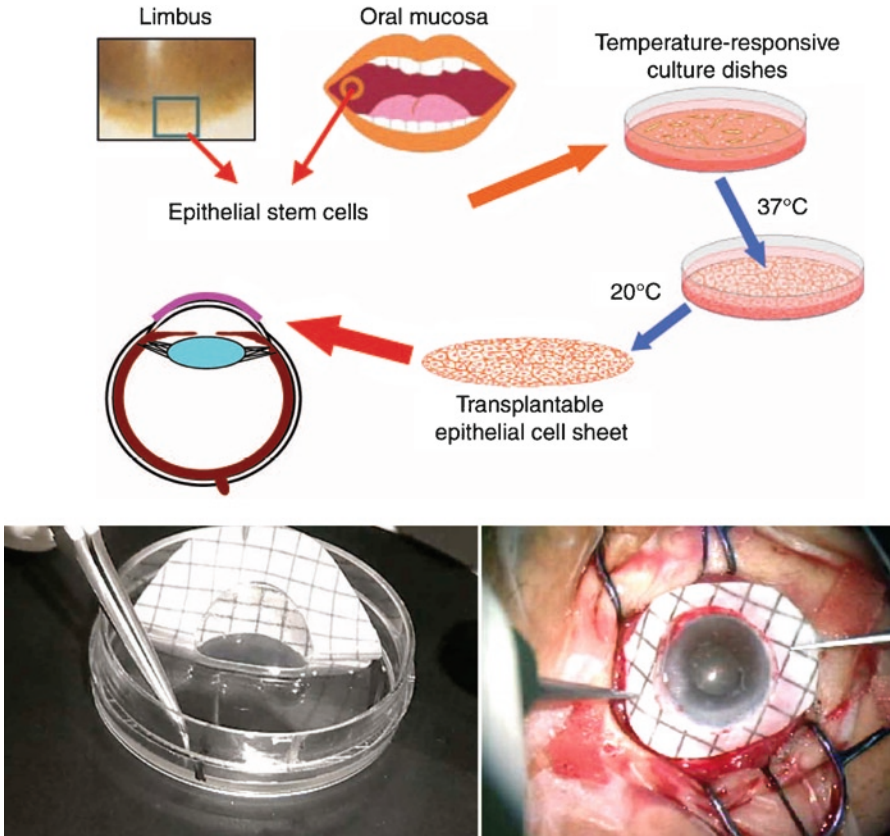


Fig. 7. Corneal surface reconstruction. Small biopsies from the limbus (the border between the cornea and neighboring conjunctiva) or from oral mucosa provide for the isolation of epithelial stem cells. Cell sheets fabricated on temperature-responsive culture dishes are harvested and transplanted directly to the ocular surface without the need for carrier substrates or sutures.

muscle [56] (Fig. 8), and it can be formed into laminar structures to recreate liver lobules [55] or kidney glomeruli by using heterotypic stratification of different cell sheets.

Using cell sheets, various cell-dense tissues that demonstrate differentiated functions while avoiding the need for biodegradable scaffolds, whose applicability is strictly limited can be engineered.

Intelligent Surfaces

Based on the intelligent surface properties of temperature-responsive culture dishes, cell-sheet engineering has been used to reconstruct various tissues without the need for biodegradable scaffolds. These temperature-responsive surfaces can be expanded for other applications.

Immobilization of Cell-Adhesive Peptides

Currently, cell culturing methods generally use animal-derived products, such as fetal bovine serum or mouse 3T3 feeder cells, to enhance cell attachment and growth. However, due to safety issues attributed to the risk of pathogen transmission, the use of these products is best avoided.

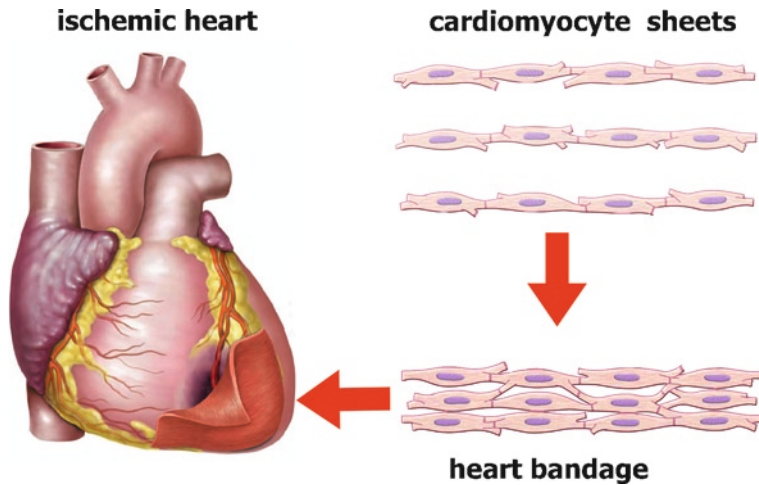


Fig. 8. Myocardial cell-sheet engineering. Cardiomyocyte sheets harvested from temperature-responsive culture surfaces and layered to form three-dimensional tissues that beat synchronously and simultaneously. The layered cardiomyocyte sheets can act as a “heart bandage” for the recovery of ischemic cardiac tissue.

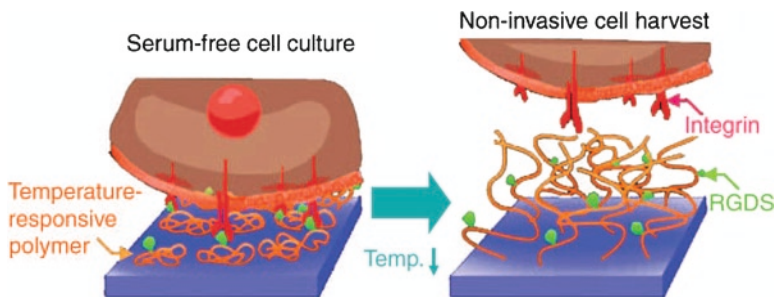


Fig. 9. Immobilization of Arg-Gly-Asp-Ser (RGDS) peptides to temperature-responsive surfaces. Cells can be cultured in serum-free conditions by immobilizing the synthetic cell-adhesive RGDS peptide to temperature-responsive culture dishes. By decreasing the culture temperature, the cells can still be noninvasively harvested, while the RGDS peptides remain attached to the temperature-responsive polymer surface.

Additionally, the US Food and Drug Administration classifies tissue-engineered constructs cocultured with animal cells, such as mouse 3T3 cells as xenografts, thus delaying their clinical application.

To overcome the need for serum, we immobilized the synthetic adhesive peptide Arg-Gly-Asp-Ser (RGDS) onto temperature-responsive dishes. The temperature-responsive PIPAAm surfaces were functionalized by copolymerization with a reactive comonomer containing a free carboxyl group, after which the synthetic RGDS peptide is immobilized on the temperature-responsive surface [62, 63]. Cells attach, spread, and grow to confluency at 37°C, even in serum-free conditions supplemented with recombinant growth factors. After reaching confluency, cells can be harvested as intact sheets by simple temperature changes, in the same manner as normal PIPAAm dishes. Cells cultured on these dishes in serum-free conditions resemble cells cultured in a medium containing 10% fetal bovine serum. In addition, cell harvest from these surfaces is achieved by controlling the binding affinity between the RGDS ligand and cell-surface integrin proteins, with the RGDS ligand remaining on the culture surface after cell sheet removal (Fig. 9).

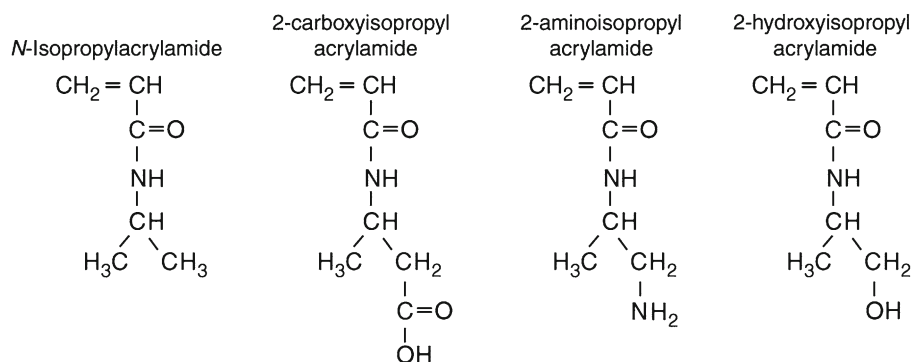


Fig. 10. Synthesis of functionalized temperature-responsive copolymers with various functionalized comonomers, such as 2-carboxyisopropyl acrylamide, 2-aminoisopropyl acrylamide, and 2-hydroxyisopropyl acrylamide. These comonomers contain the isopropylacrylamide backbone chain of poly(*N*-isopropylacrylamide) (PIPAAm) and reactive pendant groups. These functionalized PIPAAm derivatives show sensitive phase transitions in response to temperature change similar to PIPAAm, enabling the immobilization of various ligands to the temperature-responsive surfaces.

Currently, work is under way on immobilizing other growth factors onto temperature-responsive surfaces. The copolymerization with other functionalized comonomers containing amino or hydroxyl groups enable the attachment of various ligands (Fig. 10). This eliminates the need for other animal-derived products, such as feeder cells to increase cell growth, such that, the length of culture can be dramatically decreased.

Micropatterned Surfaces

To mimic normal function, it is necessary to recreate a 3D tissue architecture with the integration of multiple cell types. As shown with liver reconstruction, interactions between various cell types are needed to preserve differentiated cell functions. Layering of various patterned cell sheets is thought to be able to create structures that resemble normal tissues. However, the creation of micropatterned surfaces is generally very complex and must exploit differences in cell adhesion for coculture, thus significantly limiting applicability. Therefore, a novel method was created for micropatterned cell seeding [64, 65].

Using metal micropatterned masks, PIPAAm was selectively grafted onto TCPS dishes to create surfaces controlled by localized temperature-responsive regions. Hepatocytes seeded at 20°C, a temperature at which PIPAAm-grafted portions are hydrophilic, attached only to ungrafted TCPS portions and conform to the pattern. After 5 h, the culture temperature is raised to 37°C, and fibroblasts seeded at this time are only attached to the PIPAAm-grafted regions, creating and maintaining a micropatterned coculture system. This technique conceivably enables the facile design and creation of micropatterned cell sheets that can be manipulated to create 3D structures that mimic normal tissues, if the surfaces are grafted with different temperature-responsive polymers (Fig. 11).

It was shown that by incorporating a hydrophobic monomer, *n*-butyl methacrylate, into the PIPAAm feed, the LCST of the copolymers can be systematically lowered [66]. Using this technique, it is possible to create micropatterned surfaces with different temperature-responsive domains across the entire culture surface to provide the intact harvest of cell sheets with various cell types. This approach can be used to create cell sheets consisting of cardiomyocytes or hepatocytes cocultured with endothelial cells that mimic microvascular networks within the tissues.

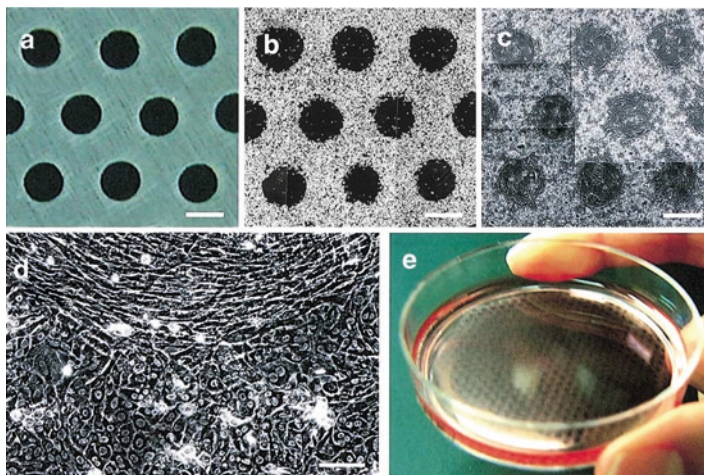


Fig. 11. Patterned co-culture of hepatocytes and fibroblasts. (a) Metal patterned mask having circular holes (1 mm in diameter). (b) Hepatocytes are seeded and cultured on PIPAAm-pattern-grafted dishes for 5 h at 20°C, then spread at 37°C only on nongrafted TCPS domains. (c) The second cell type, fibroblasts, are seeded at 37°C, and cocultured in an organized pattern. (d) Magnified image of the border of two domains after a 7-day culture at 37°C. Note the fibroblast orientation around the circumferences of nongrafted domains. Bar 1 mm in (a)–(c), 100 μm in (d). (e) Macroscopic view of pattern-seeded hepatocytes before the second cell seeding. Circular domains spread all over the 60-mm dish surfaces.

Although the field of tissue engineering has made significant advances during the past 20 years, there still remains considerable difficulty in recreating tissues and organs because of the limitations of traditional scaffold-based methods. Cell-sheet engineering, which utilizes temperature-responsive intelligent surfaces, should overcome many of the problems that have limited conventional approaches in the past and establish a new basis for regenerative medicine.

Design of Network Structure for Functional Gels

To design gels with unique property and function, several attempts to create unique network structure in nanoorder scale by molecular and supramolecular design have been done.

Topological Gels, Double Network Structure Gels, Nanocomposite Gels

Polyrotaxane has a supramolecular structure in which many cyclic molecules, α -cyclodextrin (α -CD), are threaded on a single polymer chain, poly(ethylene glycol) (PEG), and are trapped by capping the chain with bulky end group. Ito et al. [67] chemically crosslinked α -CDs contained in a polyrotaxane and developed a gels with the polymer topologically interlocked by figure-of-eight crosslinks. The figure-of-eight crosslinks can pass the polymer chains freely to equalize the tension of the threading polymer chains just like pulleys. Therefore, stress may be automatically relaxed in the gels. As a result, transparent gels with good tensility, low viscosity, and large swelling ability in water are obtained. Considering these properties, application to biomaterials, such as a soft contact lens and an artificial joint, should be possible.

Since gels are generally weak and fragile, the application area is restricted. To solve this disadvantage, Osada et al. [68] developed gels with extremely high mechanical strength

by preparing interpenetrating polymer network (IPN, or double network (DN)) structures. The DN gels consisting of PAMPS and PAAm showed very high mechanical strength to compression or cutting. Haraguchi et al. [69] have found out that physical properties are improvable by constructing an organic-inorganic network at nanolevels. Nanocomposite hydrogels (NC gels) composed of PNIPAAm in which inorganic clay (Na-hectrite) forms physical crosslinking points was synthesized. In the NC gels, the distance between crosslinking points are long and uniform, as a result that the polymer behaves like a linear polymer and the gels has extraordinary mechanical, optical, and swelling/deswelling properties.

Graft Gels

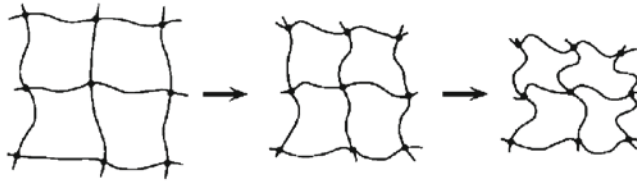
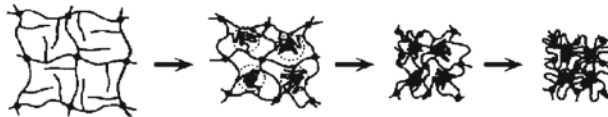
Several potential applications of stimuli-responsive gels, such as smart actuators, when a fast response is needed. The kinetics of swelling and deswelling in these gels are typically governed by diffusion-limited transport of the polymeric components of the network in water, the rate of which is inversely proportional to the square of the smallest dimension of the gels. Several strategies have been explored to increase the response dynamics, such as controlling the size and shape of gels or introducing porosity to control macroscopic structure.

On the other hand, molecular designs for rapid response by tailoring the gels architecture at the molecular level attract is attracting attention. We prepared a thermosensitive gels with a comb structure by grafting PNIPAAm chains onto the crosslinked networks of the same PNIPAAm (Fig. 12) [70, 71]. Within the gels, terminally grafted chains have freely mobile ends, distinct from the typical network structure in which both ends of the PNIPAAm chains are crosslinked and relatively immobile. With increasing temperature, grafted PNIPAAm chains begin to collapse from their expanded (hydrated) form to compact (dehydrated) forms. This collapse occurs before the PNIPAAm network begins to shrink, because of the mobility of the grafted chains. The grafted polymer chains dehydrate to create hydrophobic nuclei which enhance aggregation of the crosslinked chains. Whereas similar gels lacking the grafted side chains take more than a month to undergo full deswelling; the graft gels collapse in about 20 min (Fig. 12). As the grafted chains are lengthened the deswelling rate becomes faster. To control the response, the introduction of other grafted polymer chains, such as PEG or the copolymer of NIPAAm and dimethylacrylamide, to change the hydrophilicity and the phase transition temperature of grafted chains [72].

Microfabrication of Gels

Application to micromachines, μ -TAS: Microfabrication technology, such as photolithography or X-ray lithography, can be employed in the preparation of microgels. Since any shape of gels can be created by these methods, applications to micromachines and μ -TAS such as soft microactuator, microgel valve, and gels displays [73], can be made. Ito et al. synthesized thermosensitive polymer with photo-reactive groups by introducing azidoaniline into the -COOH site in the copolymer of NIPAAm and acrylic acid (AAc) [74]. After coating the polymer on a glass plate, it was irradiated with UV Light through a photo-mask. By removing the unreacted polymer, a micropatterned microgel was obtained. By this method, the lattice-shaped PNIPAAm gels with a quick response was prepared with a specific surface area. Beebe et al. [75, 76] coated the pH-sensitive gels (AAc/HEMA copolymer gels) around a post in microchannel by photolithography, and designed the microgel valve to change the direction of flow in the microchannel in response to the pH of the fluid. At higher pH, the gels swells and stops the flow to the right direction, but allows the flow by deswelling at lower pH.

The structures made by photolithography are two-dimensional, using microfabrications of gels with three-dimensional structure are being attempted. Two-photon initiated

Homopolymer gel**Comb-type graft polymer gel**

○ : Hydrophobic cluster

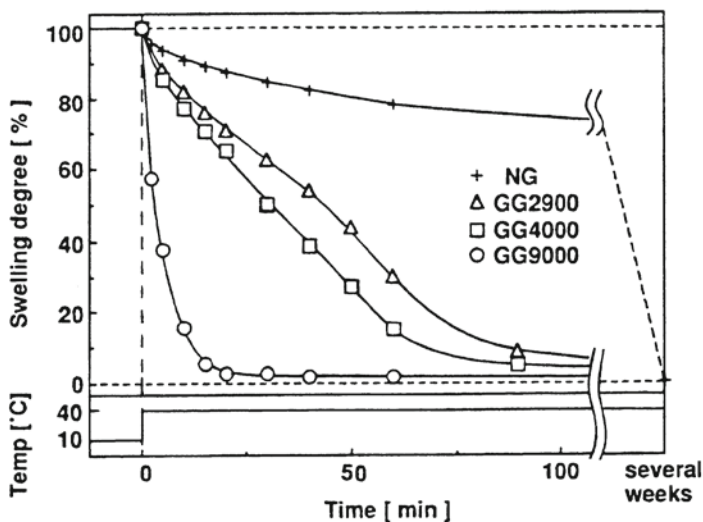


Fig. 12. (Top) Structure and shrinking mechanisms for conventional homopolymer and comb-type grafted PNI-PAAm gels undergoing temperature-induced collapse in aqueous media (bottom). The time course of deswelling of the hydrogels undergoing shrinking, at 40°C, in response to stepwise temperature changes from 10°C.

polymerization was applied to prepare micromachines and integrated circuits for chemical operation with 3D-structure. This method was used to fabrication of microgels and microcantilevers made of photo-responsive gels to deflect under illumination [77].

Self-Oscillating Gels as Novel Biomimetic Materials

Autonomous oscillation is one of the characteristic behaviors in living systems that spontaneously changes with temporal periodicity (called “temporal structure”) such as heartbeat, brain waves, pulsatile secretion of hormone, cell cycle, biorhythm, and so forth, are examples. From the standpoint of biomimetics, several stimuli-responsive polymer systems have been studied, but the polymer systems undergoing self-oscillation under constant condition without any on–off switching of external stimuli are not available. If such autonomous

polymer systems like a living organism could be realized, by using completely synthetic polymers, then unprecedented biomimetic materials will be created.

In order to realize the autonomous polymer system by tailor made molecular design, we focused on the Belousov–Zhabotinsky (BZ) reaction [78–80], which is well-known for exhibiting temporal and spatiotemporal oscillating phenomena. The BZ reaction is often analogically compared with the TCA cycle (Krebs cycle), which is a key metabolic process taking place in the living body. The overall process of the BZ reaction is the oxidation of an organic substrate, such as malonic acid (MA) or citric acid, by an oxidizing agent (bromate ion) in the presence of a strong acid and a metal catalyst. In the course of the reaction, the catalyst undergoes spontaneous redox oscillation. When the solution is homogeneously stirred, the color of the solution periodically changes, like a neon sign, based on the redox changes of the metal catalyst. When the solution is cast as a thin film in stationary conditions, concentric or spiral wave patterns develop. The oxidation wave propagates in the medium at a constant speed and is called a “chemical wave.”

Design of Self-Oscillating Gels

We attempted to convert the chemical oscillation of the BZ reaction to the mechanical changes of gels and generate an autonomic swelling–deswelling oscillation under nonoscillatory outer conditions. A copolymer gels which consists of NIPAAm and ruthenium tris(2,2'-bipyridine) ($\text{Ru}(\text{bpy})_3^{2+}$) was prepared. $\text{Ru}(\text{bpy})_3^{2+}$, acting as a catalyst for the BZ reaction, was appended to the polymer chains of NIPAAm (Fig. 13). The poly(NIPAAm-co- $\text{Ru}(\text{bpy})_3^{2+}$)

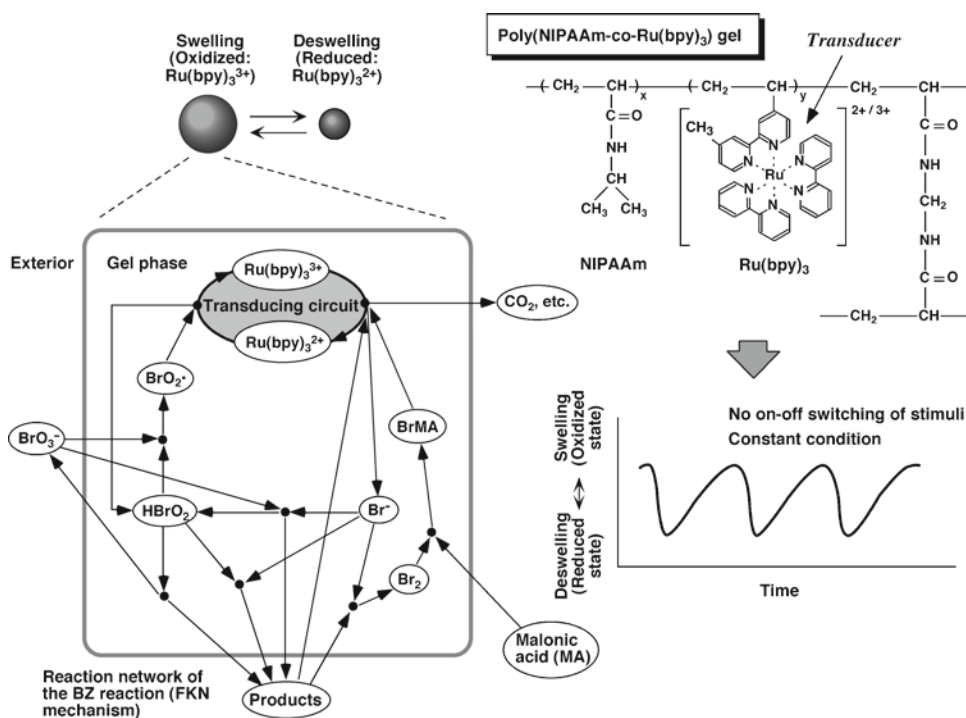


Fig. 13. Mechanism of self-oscillation for poly(NIPAAm-co- $\text{Ru}(\text{bpy})_3^{2+}$) gels coupled with the Belousov–Zhabotinsky reaction.

gels has a phase transition temperature due to the themosensitive constituent NIPAAm. The oxidation of the $\text{Ru}(\text{bpy})_3^{2+}$ moiety caused not only an increase in the swelling degree of the gels, but also a rise in the transition temperature. These characteristics may be interpreted by considering an increase in hydrophilicity of the polymer chains due to the oxidation of Ru(II) to Ru(III) in the $\text{Ru}(\text{bpy})_3$ moiety. As a result, it is expected that the gels undergoes a cyclic swelling–deswelling alteration when the $\text{Ru}(\text{bpy})_3$ moiety is periodically oxidized and reduced under constant temperature. When the gels is immersed in an aqueous solution containing the substrates of the BZ reaction (MA, acid, and oxidant) except for the catalyst, the substrates penetrates into the polymer network and the BZ reaction occurs in the gels. Consequently, periodical redox changes induced by the BZ reaction produce periodical swelling–deswelling changes of the gels (Fig. 13). Since first being reported in 1996 as a “self-oscillating gels” [81, 82], we have been systematically studying the self-oscillating polymer and gels as well as their applications to novel biomimetic materials [83].

Self-Oscillating Behavior of the Gels

Self-Oscillation of the Miniature Bulk Gels

Shown in Fig. 14 is the observed oscillating behavior under a microscope for the miniature cubic poly(NIPAAm-co- $\text{Ru}(\text{bpy})_3^{2+}$) gels (each length of about 0.5 mm). In miniature gels sufficiently smaller than the wavelength of the chemical wave (typically several millimeter), the redox change of ruthenium catalyst can be regarded to occur homogeneously without pattern formation [84]. Due to the redox oscillation of the immobilized $\text{Ru}(\text{bpy})_3^{2+}$, mechanical swelling–deswelling oscillation of the gels autonomously occurs with the same period as for the redox oscillation. The volume change is isotropic and the gels beats as a whole, like a heart muscle cell. The chemical and mechanical oscillations are synchronized without a phase difference (the gels exhibits swelling during the oxidized state and deswelling during the reduced state).

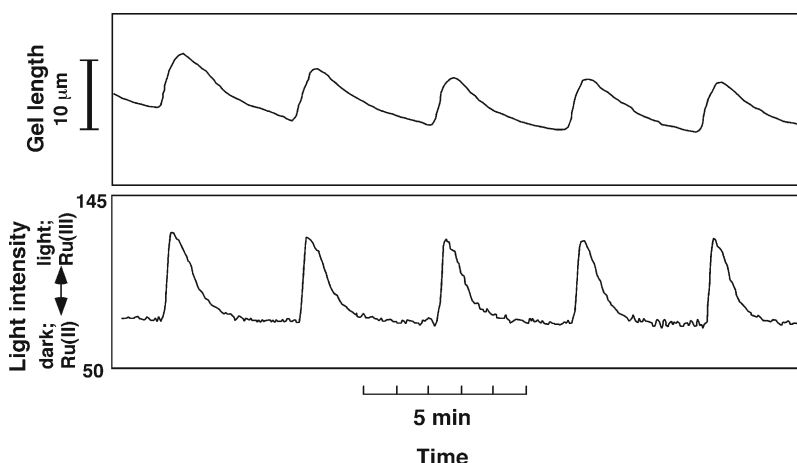


Fig. 14. Periodic redox changes of the miniature cubic poly(NIPAAm-co- $\text{Ru}(\text{bpy})_3^{2+}$) gels (*lower*) and the swelling–deswelling oscillation (*upper*) at 20°C. Color changes of the gels accompanied by redox oscillations (orange: reduced state, light green: the oxidized state) were converted to 8-bit grayscale changes (dark: reduced, light: oxidized) by image processing. Transmitted light intensity is expressed as an 8-bit grayscale value. Outer solution: $[\text{MA}] = 62.5 \text{ mM}$; $[\text{NaBrO}_3] = 84 \text{ mM}$; $[\text{HNO}_3] = 0.6 \text{ M}$.

Control of Oscillation Period and Amplitude

Typically, the oscillation period increases with a decrease in the initial concentration of substrates. The swelling–deswelling amplitude of the gels increases with an increase in the period and amplitude of the redox changes. Therefore, the swelling–deswelling amplitude of the gels is controllable by changing the initial concentration of substrates.

On–Off Regulation of Self-Beating Motion

Inherently, in a BZ reaction there is an abrupt transition from steady state (nonoscillating state) to oscillating state with a change in any controlling parameter, such as chemical composition or light. Utilizing this characteristic, reversible on–off regulation of self-beating triggered by the addition and removal of MA was successfully achieved [85]. Also, since the NIPAAm gels is thermosensitive and so the beating rhythm can be also controlled by temperature [86].

Peristaltic Motion of Gels with Propagation of Chemical Wave

When the gels size is larger than chemical wavelength, the chemical wave propagates in the gels by coupling with diffusion of intermediates. Then peristaltic motion of the gels is created. Shown in Fig. 15 is a cylindrical gels immersed in an aqueous solution containing the BZ reactants. The chemical waves propagate in the gels at a constant speed in the direction of the gels length [87]. Considering the orange (Ru(II)) and green (Ru(III)) zones represent the shrunken and swollen parts, respectively, the locally swollen and shrunken parts move with the chemical wave, like the peristaltic motion of living worms. The tensile force of the cylindrical gels with oscillation was also measured [88].

It is well known that the period of oscillation is affected by light illumination for the Ru(bpy)₃²⁺-catalyzed BZ reaction [89]. Therefore, we make a pacemaker with a desired period (or wavelength) by local illumination of laser beam to the gels. The period (or wavelength) can be changed by local illumination to a pacemaker that already exists in the gels. Chemical and optical control of the self-sustaining peristaltic motion of the porous structural gels are possible [90–93].

Design of Biomimetic Micro-/Nanoactuator Using Self-Oscillating Polymers and Gels

Self-Walking Gels

Further, we successfully developed a novel biomimetic walking-gels actuator made of self-oscillating gels [94]. To produce directional movement gels, asymmetrical swelling–deswelling is desired. For these purposes, as a third component, hydrophilic 2-acrylamido-2-methyl-propanesulfonic acid (AMPS) was copolymerized into the polymer to lubricate the gels and to cause anisotropic contraction. During polymerization, the monomer solution faces two different hydrophilic glass surface and a hydrophobic Teflon surface; since Ru(bpy)₃²⁺ monomer is hydrophobic, it easily migrates to the Teflon surface. As a result, a nonuniform distribution along the height is formed by the components, and the resulting gels gradient distribution component in the polymer network.

To convert the bending and stretching changes in one-directional, we fabricated a ratchet with an asymmetrical surface structure. The gels was repeatedly bent and stretch autonomously on the ratchet base, resulting in the forward motion of the gels, while backward

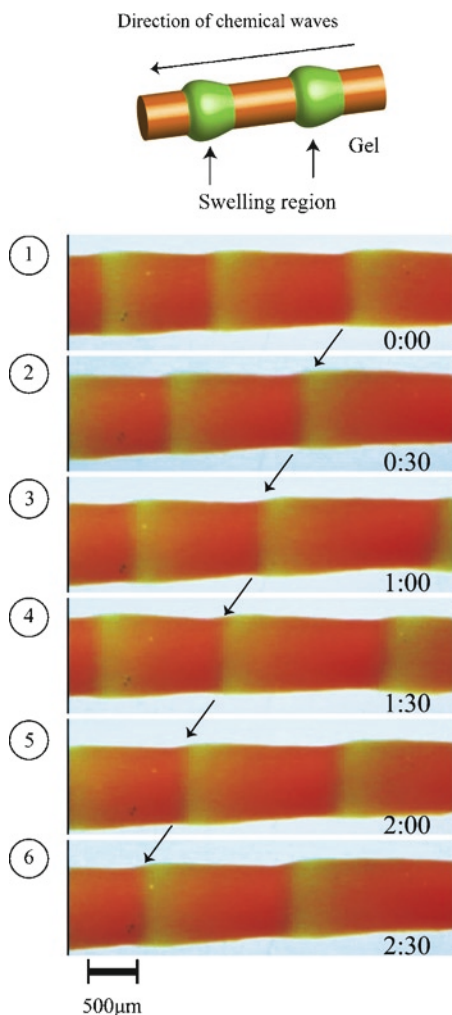


Fig. 15. Time course of peristaltic motion of poly(NIPAAm-co-Ru(bpy)₃²⁺-co-AMPS) gels in a solution of the BZ substrates (MA, sodium bromate, and nitric acid, 18°C). The green and orange colors correspond to the oxidized and reduced states of the Ru moiety in the gels, respectively.

movement was prevented by the teeth of the ratchet. Successive profiles of the “self-walking” motion of the gels is shown in Fig. 16. The walking velocity of the gels actuator was approximately 170 μm/min. Since the oscillating period and the propagating velocity of the chemical wave changes with substrate concentration in the outer solution, the walking velocity of the gels can be controlled. By using the gels with a gradient structure, another type of actuator that generates a pendulum motion was also developed [95].

Design of mass transport surface utilizing peristaltic motion of gels: An attempt was made to transport an object by utilizing the peristaltic motion of poly(NIPAAm-co-Ru(bpy)₃-co-AMPS) gels. As a model object, a cylindrical poly(acrylamide) (PAAm) gels was put on the gels surface. It was observed that the PAAm gels was transported on the gels surface with the propagation of the chemical wave as it rolled (Fig. 17) [96]. A model was proposed to describe the mass transport phenomena based on the Hertz contact theory, based on the relation between the transportability and the peristaltic motion. The functional gels surface

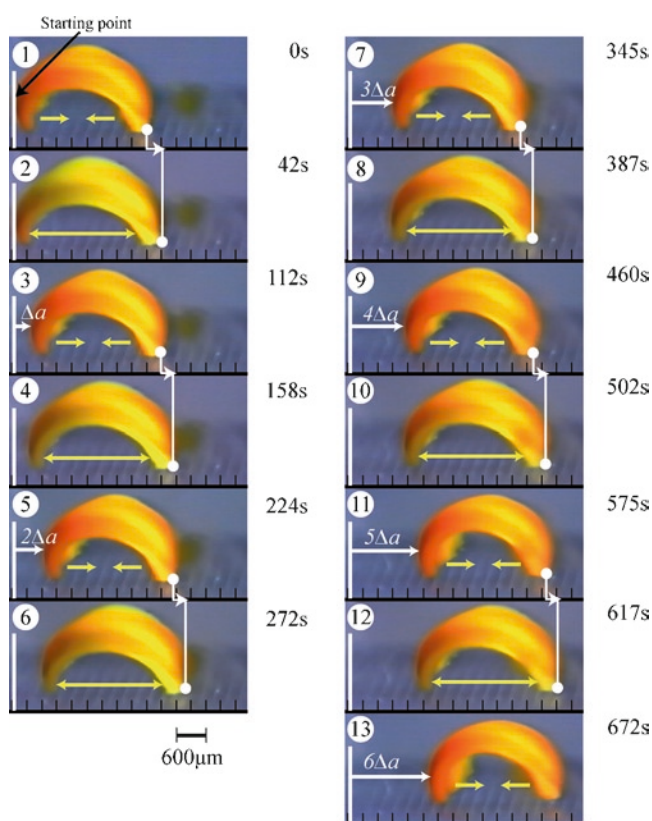


Fig. 16. Time course of self-walking motion of the gels actuator. During stretching, the front edge can slide forward on the base, but the rear edge is prevented from sliding backwards. Oppositely, during bending, the front edge is prevented from sliding backwards while the rear edge can slide forward. This action is repeated, and as a result, the gels walks forward. Outer solution: $[MA]=62.5$ mM, $[NaBrO_3]=84$ mM, $[HNO_3]=0.894$ M, $18^\circ C$.

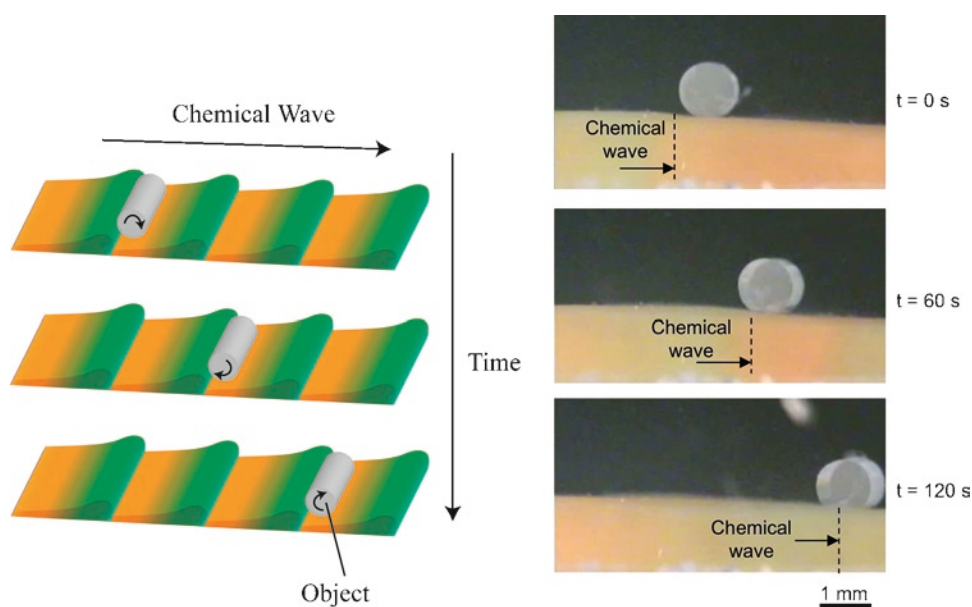


Fig. 17. Schematic illustration of mass transport on the peristaltic surface (*left*) and observed transport of cylindrical PAAm gels on the poly(NIPAAm-co-Ru(bpy)₃²⁺-co-AMPS) gels sheet.

generating autonomous and periodic peristaltic motion has potential for several applications such as to transport soft materials, formation of ordered structures of micro- and/or nanomaterials and a self-cleaning surface.

Microfabrication of the Gels by Lithography

Microfabrication of self-oscillating gels by lithography for application to ciliary motion actuator (artificial cilia) [97]. The gels membrane with micro projection array on the surface was fabricated by utilizing X-ray lithography (LIGA) method. With the propagation of chemical wave, the micro projection array exhibits dynamic rhythmic motion like cilia. The actuator may also serve as a microconveyer.

Control of Chemical Wave Propagation in Self-Oscillating Gels Array

A chemo-mechanical actuator utilizing a reaction-diffusion wave across the gap junction was constructed to make a new microconveyer by micropatterned self-oscillating gels array [98]. Unidirectional propagation of the chemical wave the BZ reaction was induced on gels arrays. Using a triangle-shaped gels as an element of the array, the chemical wave is propagated from the corner side of the triangle gels to the plane side of the other gels (C-to-P) across the gap junction, whereas, it propagated from the plane side to the corner side (P-to-C) in the case of the pentagonal gels array (Fig. 18). By fabricating different shapes of gels arrays, control of the direction is possible. The swelling and deswelling changes of the gels follow a unidirectional propagation of the chemical wave.

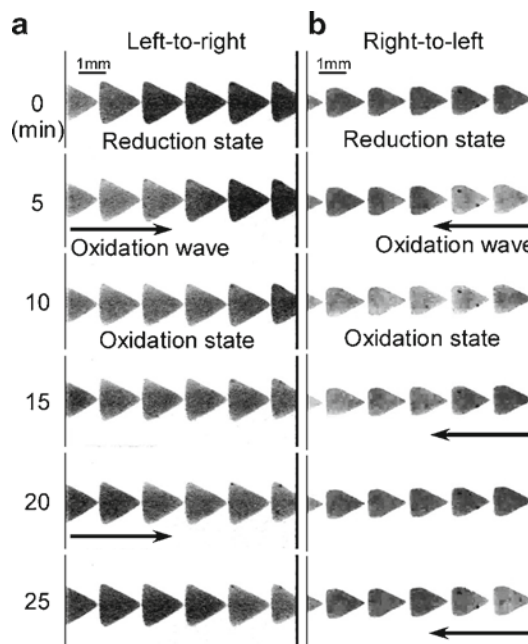


Fig. 18. Propagating behavior of the chemical wave on the (a) triangle gels array and (b) pentagonal gels array.

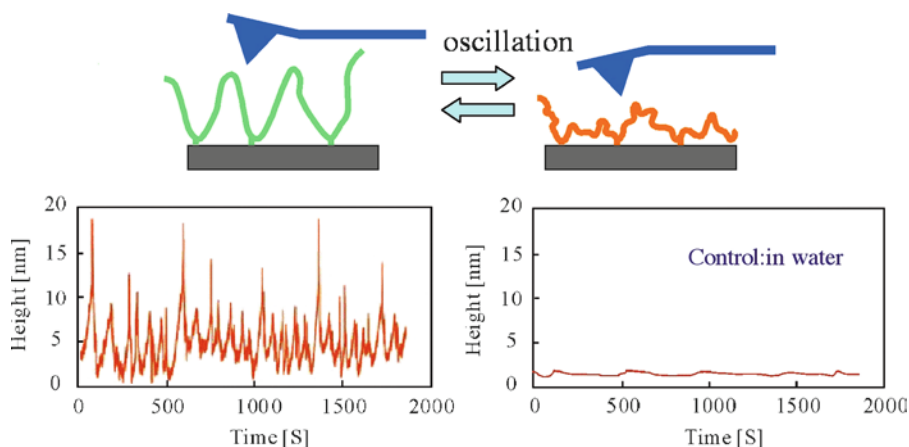


Fig. 19. Self-oscillating behavior of immobilized polymer in the BZ substrate solution ($[MA]=0.1$ M, $[NaBrO_3]=0.3$ M, $[HNO_3]=0.3$ M) measured by AFM.

Self-Oscillating Polymer Chains as a “Nano-oscillator”

The periodic changes of linear and uncrosslinked polymer chains can be easily observed as cyclic transparent and opaque changes for the polymer solution with color changes due to the redox oscillation of the catalyst [99]. Synchronized with the periodical changes between Ru(II) and Ru(III) states of the $Ru(bpy)_3^{2+}$ site, the polymer becomes hydrophobic and hydrophilic, and exhibits cyclic soluble–insoluble changes. Further, by grafting the polymers or arraying the gels beads on the surface of substrates, self-oscillating surfaces as nanoconveyers were designed. The self-oscillating polymer was covalently immobilized on a glass surface and self-oscillation was directly observed at a molecular level by AFM [100]. The self-oscillating polymer with *N*-succinimidyl group was immobilized on an aminosilane-coupled glass plate. While no oscillation was observed in pure water, nanoscale oscillation was observed in an aqueous solution containing the BZ substrates (Fig. 19). The amplitude was about 10–15 nm and the period was about 70 s, although some irregular behavior was observed due to no stirring. The amplitude was less than that in solution, as observed by DLS (23.9 and 59.6 nm). This smaller amplitude may be due to the structure of the immobilized polymer that was a loop-train-tail: the moving regions were shorter than the soluble polymer, as illustrated in Fig. 19. The amplitude and frequency were controlled by the concentration of reactant in the solution. The oscillation polymer chain may be used as a component for nanoclocks or nanomachines.

Self-Flocculating/Dispersing Oscillation of Microgels

A submicron-sized poly(NIPAAm-co- $Ru(bpy)_3^{2+}$) gels beads were prepared by surfactant-free aqueous precipitation polymerization, and the oscillating behavior analyzed [100–104]. Shown in Fig. 20, the oscillation profiles of transmittance for the microgel dispersions. At low temperatures (20–26.5°C), on raising the temperature, the amplitude of the oscillation became larger. The increase in amplitude is due to increased deviation of the hydrodynamic diameter between the Ru(II) and Ru(III) states. Furthermore, a remarkable change in waveform was observed between 26.5 and 27°C. The amplitude of the oscillations dramatically decreased at 27.5°C, and the periodic transmittance changes

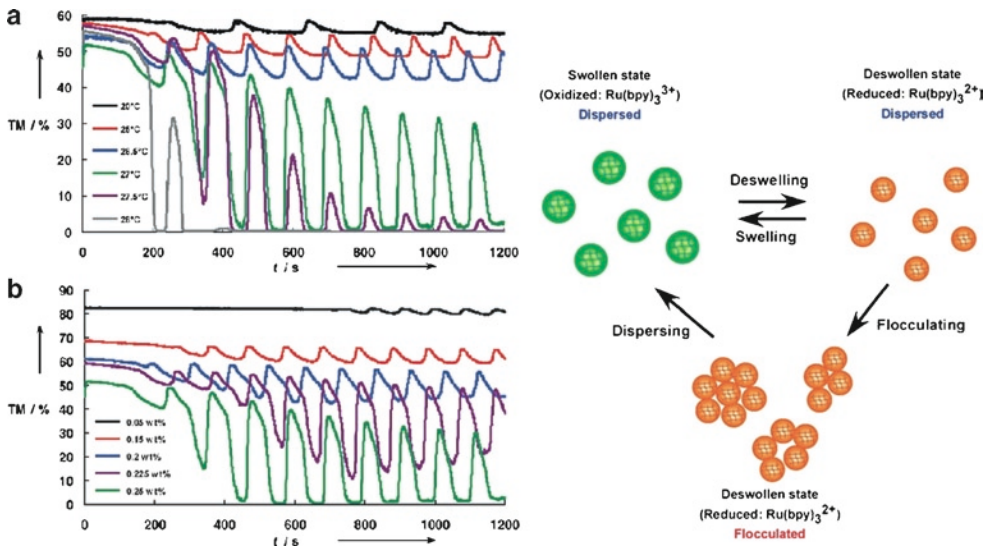


Fig. 20. Self-oscillating profiles of optical transmittance for microgel dispersions. The microgels were dispersed in aqueous solutions containing MA (62.5 mM), NaBrO_3 (84 mM), and HNO_3 (0.3 M). Microgel concentration was 0.25 wt%. (a) Profiles measured at different temperatures. (b) Profiles measured at different microgel dispersion concentrations at 27°C.

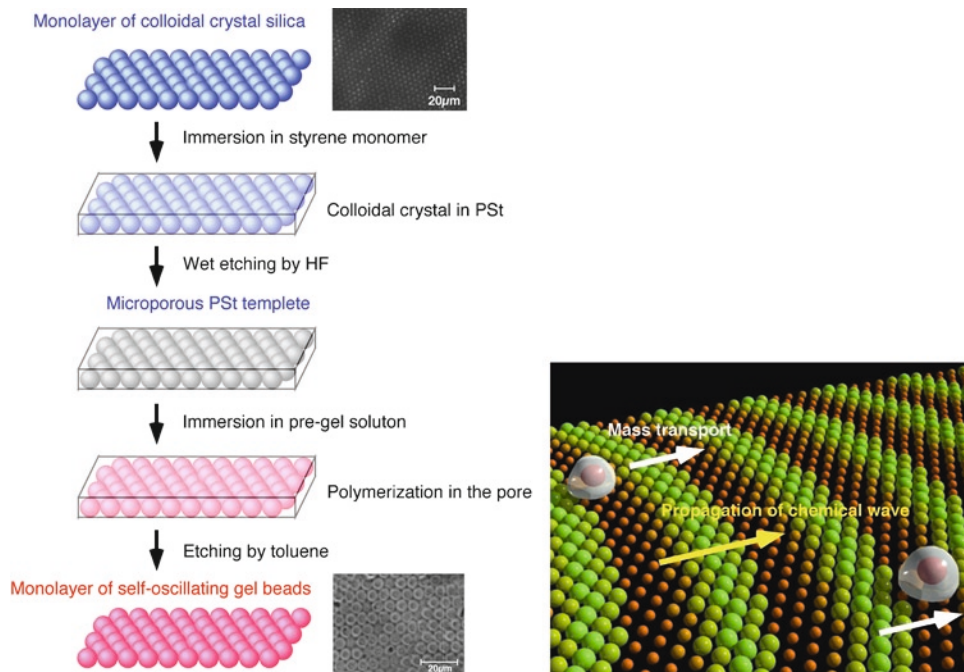


Fig. 21. Preparation of self-oscillating gels beads monolayer by two-step template polymerization and schematic illustration of functional surface (nanoconveyor) using self-oscillating gels beads array. The operating conditions of self-oscillating polymer systems are limited to the nonphysiological environment where the strong acid and the oxidant coexist.

could no longer be observed at 28°C. The sudden change in oscillation waveform should be related to the difference in colloidal stability between the Ru(II) and Ru(III) states. The microgels should fluctuate due to the lack of electrostatic repulsion when the microgels were deswollen. The remarkable change in waveform was only observed at higher dispersion concentrations (greater than 0.225 wt%). The self-oscillating property makes microgels more attractive for future developments such as microgel assembly, optical and rheological applications.

Fabrication of Microgel Beads Monolayer

The construction of micro/nanoconveyers by grafting or arraying self-oscillating polymer or gels beads by fabrication method for organized monolayers of microgel beads was investigated (Fig. 21) [105]. A 2D close-packed array of thermosensitive microgel beads was prepared by double template polymerization. A 2D colloidal crystal of silica beads with 10 μm diameter was obtained by solvent evaporation. This monolayer of colloidal crystal serves as the first template for preparation of macroporous polystyrene. The macroporous polystyrene trapping the crystalline order can be used as a negative template for fabricating a gels bead array. By this double template polymerization method, functional surfaces using thermosensitive PNIPAAm gels beads were fabricated. It was observed that topography

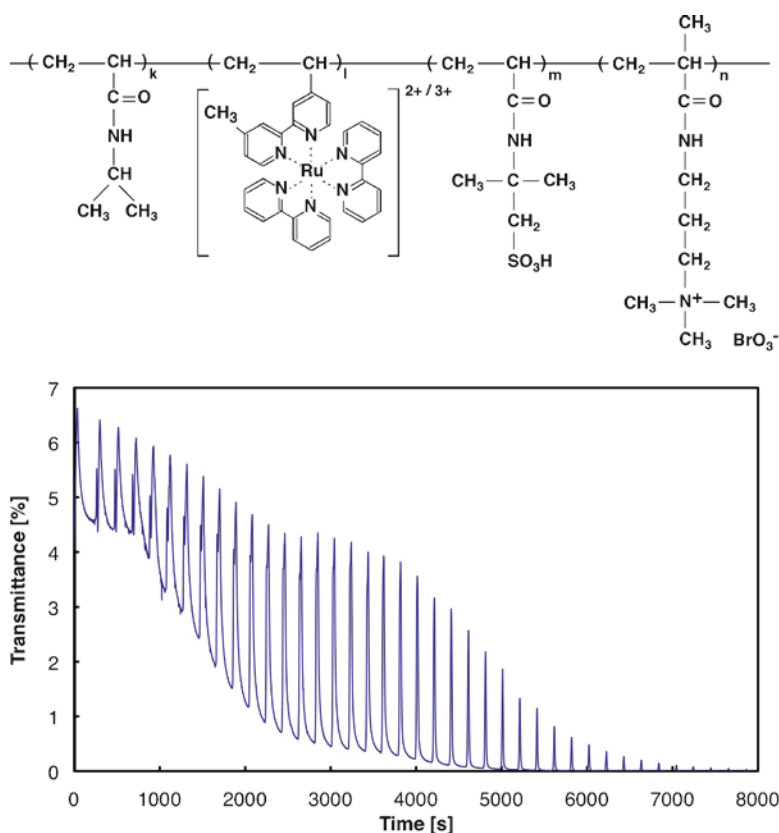


Fig. 22. Chemical structure of poly(NIPAAm-co-Ru(bpy)₃²⁺-co-AMPS-co-MAPTAC) (upper) and the oscillating profiles of the optical transmittance for the polymer solution at 12°C when only MA (0.7 M) is added to the solution (lower).

of the surface changed with temperature. The fabrication method demonstrated here was so versatile that many kinds of gels beads could be obtained. This method may be a key technology to create new functional surface.

Self-Oscillation Under Physiological Conditions

To extend the application field to biomaterials, more sophisticated molecular designs for self-oscillation under physiological condition are needed. The integrated polymer system was constructed so that all of the BZ substrates, other than biorelated organic substrate, were incorporated into the polymer chain [106–109]. The quarternary copolymer was synthesized that includes both of the pH-control and oxidant-supplying sites in the poly(NIPAAm-co-Ru(bpy)₃) chain at the same time. As a pH-control site, 2-acrylamido-2-methyl-propanesulfonic acid (AMPS) was incorporated for pH-control; methacrylamidopropyltrimethylammonium chloride (MAPTAC) with a positively charged group was incorporated as a capture site for the anionic oxidizing agent (bromate ion). By using this polymer, self-oscillation under biological conditions where only the organic acid (malonic acid) exists was achieved (Fig. 22).

References

1. Tanaka T (1978) *Phys Rev Lett* 4:820; Tanaka T (1981) *Sci Am* 244:124
2. Osada Y, Okuzaki H, Hori H (1992) *Nature* 355:242
3. Kokufuta E, Zhang YQ, Tanaka T (1994) *J Biomater Sci Polym Ed* 6:35
4. Hirai T, Nemoto H, Hirai M, Hayashi S (1994) *J Appl Polym Sci* 53:79
5. Fukushima T, Asaka K, Kosaka A, Aida T (2005) *Angew Chem Int Ed* 44:2410
6. Asaka K, Oguro K (2000) *J Electroanal Chem* 480:186
7. Zrinyi M, Szabo D, Filipcsei G, Feher J (2002) In: Osada Y, Khokhlov AR (eds) *Polymer gels and networks*. Marcel Dekker, New York, pp 309–355
8. Osada Y, Matsuda A (1995) *Nature* 376:219
9. Weissman JM, Sunkara HB, Tse AS, Asher SA (1996) *Science* 274:959
10. Holtz JH, Asher SA (1997) *Nature* 389:829
11. Holtz JH, Holtz JSW, Munro CH, Asher SA (1998) *Anal Chem* 70:780
12. Hu ZB, Lu XH, Gao J (2001) *Adv Mater* 13:1708
13. Takeoka Y, Watanabe M (2003) *Adv Mater* 15:199
14. Takeoka Y, Watanabe M (2002) *Langmuir* 18:5977
15. Nakayama D, Takeoka Y, Watanabe M, Kataoka K (2003) *Angew Chem Int Ed* 42:4197
16. Akashi R, Tsutsui H, Komura A (2002) *Adv Mater* 14:1808
17. Komiyama M, Takeuchi T, Mukawa T, Asanuma H (2003) *Molecular imprinting – from fundamentals to applications*. Wiley-VCH, Weinheim
18. Vlatakis G, Andersson LI, Muller R, Mosbach K (1993) *Nature* 361:645
19. Oya T, Enoki T, Grosberg AY, Masamune S, Sakiyama T, Takeoka Y, Tanaka K, Wang G, Yilmaz Y, Feld MS, Dasari R, Tanaka T (1999) *Science* 286:1543
20. Miyata T, Asami N, Urugami T (1999) *Nature* 399:766
21. Miyata T, Jige M, Nakaminami T, Urugami T (2006) *Proc Natl Acad Sci USA* 103:1190
22. Hoffman AS (2002) *Adv Drug Deliv Rev* 43:3
23. Okano T (ed) (1998) *Biorelated polymers and gels – controlled release and applications in biomedical engineering*. Academic Press, San Diego
24. Yoshida R, Okano T, Sakurai Y, Sakai K (1994) *J Biomater Sci Polym Ed* 6:585
25. Makino K, Mack EJ, Okano T, Kim SW (1990) *J Control Release* 12:235
26. Kost J, Horbett TA, Ratner BD, Singh MJ (1985) *Biomed Mater Res* 19:1117
27. Ishihara K, Kobayashi M, Shinohara J (1983) *Makromol Chem Rapid Commun* 4:327
28. Ito Y, Casolaro M, Kono K, Imanishi Y (1989) *J Control Release* 10:195
29. Kataoka K, Miyazaki H, Bunya M, Okano T, Sakurai Y (1998) *J Am Chem Soc* 120:12694
30. Matsumoto A, Yoshida R, Kataoka K (2004) *Biomacromolecules* 5:1038
31. Yoshida R, Sakai K, Okano T, Sakurai Y (1993) *Adv Drug Deliv Rev* 11:85

32. Kikuchi A, Okano T (2002) *Adv Drug Deliv Rev* 54:53
33. Kiser RF, Wilson G, Needham D (1998) *Nature* 394:459
34. Takei YG, Aoki T, Sanui K, Ogata N, Sakurai Y, Okano T (1994) *Macromolecules* 27:6163
35. Yakushiji T, Sakai K, Kikuchi A, Aoyagi T, Sakurai Y, Okano T (1998) *Langmuir* 14:4657
36. Kanazawa H, Yamamoto K, Matsushima Y, Takai N, Kikuchi A, Sakurai Y, Okano T (1996) *Anal Chem* 68:100; *ibid* 69:823
37. Kanazawa H, Matsushima Y, Okano T (1998) *Trends Anal Chem* 17:435
38. Kanazawa H, Yamamoto K, Kashiwase Y, Matsushima Y, Takai N, Kikuchi A, Sakurai Y, Okano T (1997) *J Pharm Biomed Anal* 15:1545
39. Yoshizako K, Akiyama Y, Yamanaka H, Shinohara Y, Hasegawa Y, Carredano E, Kikuchi A, Okano T (2002) *Anal Chem* 74:4160
40. Yamanaka H, Yoshizako K, Akiyama Y, Sota H, Hasegawa Y, Shinohara Y, Kikuchi A, Okano T (2003) *Anal Chem* 75:1658
41. Kobayashi J, Kikuchi A, Sakai K, Okano T (2003) *Anal Chem* 73:2027
42. Sakamaoto C, Okada Y, Kanazawa H, Ayano E, Nishimura T, Ando M, Kikuchi A, Okano T (2004) *J Chromatogr A* 103:247
43. Vacanti JP (1988) *Arch Surg* 123:545
44. Langer R, Vacanti JP (1993) *Science* 260:920
45. Vacanti JP, Langer R (1999) *Lancet* 354(Suppl 1):S132
46. Shinoka T, Breuer CK, Tanel RE, Zund G, Miura T, Ma PX, Langer R, Vacanti JP, Mayer JE Jr (1995) *Ann Thorac Surg* 60:S513
47. Puelacher WC, Vacanti JP, Ferraro NF, Schloo B, Vacanti CA (1996) *Int J Oral Maxillofac Surg* 25:223
48. Vacanti CA, Langer R, Schloo B, Vacanti JP (1991) *Plast Reconstr Surg* 88:753
49. Cao Y, Vacanti JP, Paige KT, Upton J, Vacanti CA (1997) *Plast Reconstr Surg* 100:297
50. Yamada N, Okano T, Sakai H, Karikusa F, Sawasaki Y, Sakurai Y (1990) *Makromol Chem Rapid Commun* 11:571
51. Okano T, Yamada N, Sakai H, Sakurai Y (1993) *J Biomed Mater Res* 27:1243
52. Kushida A, Yamato M, Konno C, Kikuchi A, Sakurai Y, Okano T (1999) *J Biomed Mater Res* 45:355
53. Hirose M, Kwon OH, Yamato M, Kikuchi A, Okano T (2000) *Biomacromolecules* 1:377
54. Nandkumar MA, Yamato M, Kushida A, Konno C, Hirose M, Kikuchi A, Okano T (2002) *Biomaterials* 23:1121
55. Harimoto M, Yamato M, Hirose M, Takahashi C, Isoi Y, Kikuchi A, Okano T (2002) *J Biomed Mater Res* 62:464
56. Shimizu T, Yamato M, Isoi Y, Akutsu T, Setomaru T, Abe K, Kikuchi A, Umezumi M, Okano T (2002) *Circ Res* 90:e40
57. Nishida K, Yamato M, Hayashida Y, Watanabe K, Maeda N, Watanabe H, Yamamoto K, Nagai S, Kikuchi A, Tano Y, Okano T (2004) *Transplantation* 77:379
58. Nishida K, Yamato M, Hayashida Y, Watanabe K, Yamamoto K, Adachi E, Nagai S, Kikuchi A, Maeda N, Watanabe H, Okano T, Tano Y (2004) *N Engl J Med* 351:1187
59. Shiroyanagi Y, Yamato M, Yamazaki Y, Toma H, Okano T (2004) *BJU Int* 93:1069
60. Hasegawa M, Yamato M, Kikuchi A, Okano T, Ishikawa I (2005) *Tissue Eng* 11:469
61. Yamato M, Utsumi M, Kushida A, Konno C, Kikuchi A, Okano T (2001) *Tissue Eng* 7:473
62. Ebara M, Yamato M, Aoyagi T, Kikuchi A, Sakai K, Okano T (2004) *Biomacromolecules* 5:505
63. Ebara M, Yamato M, Aoyagi T, Kikuchi A, Sakai K, Okano T (2004) *Tissue Eng* 10:1125
64. Yamato M, Konno C, Utsumi M, Kikuchi A, Okano T (2002) *Biomaterials* 23:561
65. Yamato M, Kwon OH, Hirose M, Kikuchi A, Okano T (2001) *J Biomed Mater Res* 55:137
66. Tsuda Y, Kikuchi A, Yamato M, Sakurai Y, Umezumi M, Okano T (2004) *J Biomed Mater Res* 69A:70
67. Okumura Y, Ito K (2001) *Adv Mater Des* 13:485
68. Gong JP, Katsuyama Y, Kurokawa T, Osada Y (2003) *Adv Mater* 15:1155
69. Haraguchi K, Takehisa T (2002) *Adv Mater* 14:1120
70. Yoshida R, Uchida K, Kaneko Y, Sakai K, Kikuchi A, Sakurai Y, Okano T (1995) *Nature* 374:240
71. Kaneko Y, Sakai K, Kikuchi A, Yoshida R, Sakurai Y, Okano T (1995) *Macromolecules* 28:7717
72. Kaneko Y, Nakamura S, Sakai K, Aoyagi T, Kikuchi A, Sakurai Y, Okano T (1998) *Macromolecules* 31:6099
73. Hu Z, Chen Y, Wang C, Zheng Y, Li Y (1998) *Nature* 393:149
74. Chen G, Imanishi Y, Ito Y (1998) *Macromolecules* 31:4379
75. Beebe DJ, Moore JS, Bauer JM, Yu Q, Liu RH, Devadoss C, Jo BH (2000) *Nature* 404:588
76. Eddington DT, Beebe DJ (2004) *Adv Drug Deliv Rev* 56:199
77. Watanabe T, Akiyama M, Totani K, Kuebler SM, Stellacci F, Wenseleers W, Braun K, Marder SR, Perry JW (2002) *Adv Funct Mater* 12:611

78. Zaikin AN, Zhabotinsky AM (1970) *Nature* 225:535
79. Field RJ, Burger M (eds) (1985) *Oscillations and traveling waves in chemical systems*. Wiley, New York
80. Epstein IR, Pojman JA (1998) *An introduction to nonlinear chemical dynamics: oscillations, waves, patterns, and chaos*. Oxford University Press, New York
81. Yoshida R, Takahashi T, Yamaguchi T, Ichijo H (1996) *J Am Chem Soc* 118:5134
82. Yoshida R, Takahashi T, Yamaguchi T, Ichijo H (1997) *Adv Mater* 9:175
83. Yoshida R (2008) *Bull Chem Soc Jpn* 81:676
84. Yoshida R, Tanaka M, Onodera S, Yamaguchi T, Kokufuta E (2000) *J Phys Chem A* 104:7549
85. Yoshida R, Takei K, Yamaguchi T (2003) *Macromolecules* 36:1759
86. Ito Y, Nogawa M, Yoshida R (2003) *Langmuir* 19:9577
87. Maeda S, Hara Y, Yoshida R, Hashimoto S (2008) *Angew Chem Int Ed* 47:6690
88. Sasaki S, Koga S, Yoshida R, Yamaguchi T (2003) *Langmuir* 19:5595
89. Amemiya T, Ohmori T, Yamaguchi T (2000) *J Phys Chem* 104:336
90. Yoshida R, Sakai T, Tabata O, Yamaguchi T (2002) *Sci Technol Adv Mater* 3:95
91. Takeoka Y, Watanabe M, Yoshida R (2003) *J Am Chem Soc* 125:13320
92. Shinohara S, Seki T, Sakai T, Yoshida R, Takeoka Y (2008) *Chem Commun* 39:4735
93. Shinohara S, Seki T, Sakai T, Yoshida R, Takeoka Y (2008) *Angew Chem Int Ed* 47:9039
94. Maeda S, Hara Y, Sakai T, Yoshida R, Hashimoto S (2007) *Adv Mater* 19:3480
95. Maeda S, Hara Y, Yoshida R, Hashimoto S (2008) *Macromol Rapid Commun* 29:401
96. Murase Y, Maeda S, Hashimoto S, Yoshida R (2009) *Langmuir* 25:483
97. Tabata O, Hirasawa H, Aoki S, Yoshida R, Kokufuta E (2002) *Sens Actuators A* 95:234
98. Tateyama S, Shibuta Y, Yoshida R (2008) *J Phys Chem B* 112:1777
99. Yoshida R, Sakai T, Ito S, Yamaguchi T (2002) *J Am Chem Soc* 124:8095
100. Ito Y, Hara Y, Uetsuka H, Hasuda H, Onishi H, Arakawa H, Ikai A, Yoshida R (2006) *J Phys Chem B* 110:5170
101. Suzuki D, Sakai T, Yoshida R (2008) *Angew Chem Int Ed* 47:917
102. Suzuki D, Yoshida R (2008) *Macromolecules* 41:5830
103. Suzuki D, Yoshida R (2008) *J Phys Chem B* 112:12618
104. Sakai T, Yoshida R (2004) *Langmuir* 20:1036
105. Sakai T, Takeoka Y, Seki T, Yoshida R (2007) *Langmuir* 23:8651
106. Hara Y, Yoshida R (2005) *J Phys Chem B* 109:9451
107. Hara Y, Yoshida R (2005) *Langmuir* 21:9773
108. Hara Y, Sakai T, Maeda S, Hashimoto S, Yoshida R (2005) *J Phys Chem B* 109:23316
109. Hara Y, Yoshida R (2008) *J Phys Chem B* 112:8427

Feedback Control Systems Using Environmentally and Enzymatically Sensitive Hydrogels

Irma Y. Sanchez and Nicholas A. Peppas

Abstract A large number of hydrogels can be classified as smart materials that offer a natural integration of sensing, actuating, and regulating functions applicable to feedback control systems. This multifunctionality added to biocompatibility and enzyme-based selectivity characteristics enables self-regulation or implicit control in hydrogels-based devices to maintain physiological variables at a desired level or range by appropriate drug release. Therefore, hydrogels can enhance the performance of individual actuator and sensing units. Applications of hydrogels in explicit and implicit controller systems are presented based on recent experimental and theoretical research studies. Integration of cascade and feedforward control types of functionalities in hydrogels systems is suggested from their capability to respond to more than one stimulus. Enzymatic glucose sensing and insulin delivery are often used as references for the discussion of hydrogels in the development of sensor, actuator, and control technology due to the relevance of the diabetes disease.

Hydrogels as Basic Functional Elements of a Control System

Hydrogels material properties enable the necessary functions for an automatic system: sensing a key environmental variable whose value must be maintained at a desired level or range, providing a means for a corrective action to eliminate a deviation in such variable, and correlating appropriately the sensed environmental condition with the active interference in the environment. These functions may be implemented individually in separate devices or integrated in a single device. Hydrogels can be applied in both cases. Their responsive nature makes them suitable to design effective sensors and actuators as well as to perform as self-regulated systems.

When the hydrogels volume change is stimulated by a signal external to the process or the close environment, the hydrogels system constitutes an actuator. The volume change of the hydrogels may cause an event by itself or by activating and allowing the intervention of additional elements frequently of different material and structure. The aforementioned event will lead to a change in an environmental condition that may be detected by another device or component of the external source that manipulates or triggers the hydrogels swelling behavior. In this case, the hydrogels system is an actuator that can be part of a regulation system.

I.Y. Sanchez • Department of Mechatronics and Automation, Tecnológico de Monterrey, Monterrey, NL 64849, Mexico
e-mail: isanchez@itesm.mx

N.A. Peppas • Pratt Chair of Engineering, Department of Biomedical Engineering, The University of Texas Austin, TX, 78712, USA

Hydrogels may be used as components of sensor devices. A sensor is composed of a sensing element and a transducing element or transducer. The sensing element is exposed to the process and changes with a particular variable. The transducer converts the response of the sensing element into an output signal, which can be used in a monitoring system to report the measurement or in a control system as a feedback signal. Electrochemical action is a typical transduction principle for analytical measurements. Electrodes covered with an enzyme containing hydrogels layer are manufactured for substrate concentration measurements. In such sensors, nonswelling hydrogels are used. Hydrogels with swelling behavior have been widely characterized showing an effective primary sensing function. However, transducing systems for their swelling response have not been investigated to the same extent.

Feedback is essential for an automatic system, since it allows a reactive response to a change in the environment or process to be controlled regardless of the cause of such variation. Environmentally responsive hydrogels may function as feedback systems for the delivery of therapeutic or other beneficial agents either contained in the hydrogels material or in a reservoir with a hydrogels cap. The interaction of hydrogels with the environment is based on a reciprocal effect: (a) a particular condition of the environment can produce a volume change of the hydrogels; (b) its inter- and intramolecular spaces change in size, thus modulating the resistance for the outward diffusion of the contained drug; and (c) the released drug changes the environmental condition in question, which is detected again by the same hydrogels, closing a loop. The *controller* element of the system is implicit in this interaction. Since all the basic control functions are assumed by the hydrogels, the resulting systems are called self-regulated (Fig. 1).

Specific body analytes reflect different physiological conditions which need to be controlled for the effective treatment of a disease. Hydrogels can be pH and the ionic strength. Concentrations of acids and bases are reflected by the pH, while those of salts by the ionic strength of the medium. Hydrogels responsiveness to other species can be achieved by the incorporation of enzymes that allow their transformation into any of the previously mentioned compounds. A typical example is the oxidation of glucose upon interaction with glucose oxidase that produces gluconolactone and hydrogen peroxide; the first product hydrolyses immediately giving gluconic acid. Hydrogels can also exhibit temperature sensitivity. Moreover, hydrogels are viable for the preservation of biological components and for *in vivo* implantations. Therefore, they can act as feedback systems for a wide variety of medical purposes.

It should be noted that all the basic functional elements for process control could be implemented by either on/off or continuous devices. Both categories include hydrogels-based sensors and actuators as well as self-regulated hydrogels systems. When the hydrogels response shows a sharp transition with respect to time and stimulation or input-environmental variable, an on/off behavior can be obtained. A balance between the width of the transition range and the time response is necessary for continuous operation of the hydrogels systems.

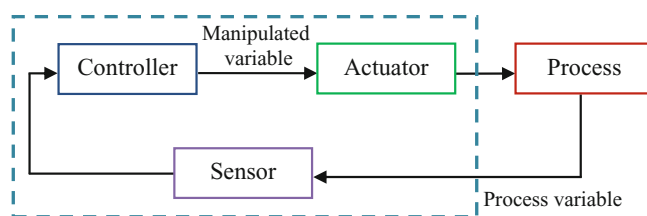


Fig. 1. Configuration of a feedback control system. Elements of control systems (*continuous rectangles*) and integration of sensor, controller and actuator in a self-regulated or implicit controller system (*dashed rectangle*).

Hydrogels in Sensors

The sensor implements the essential feedback for automatic regulation. Feedback control systems have been applied to different medical systems. Some of them are based on the sensing of physical variables (like in the case of an automatic defibrillator that responds to an abnormal heart beat with an electrical discharge to the heart) while others on the sensing of chemical variables (like the adjustment of the frequency of a pace maker according to the oxygen consumption rate) [1]. Further applications of feedback systems depend on their ability to sense different chemical and biochemical variables continuously in the body. Miniaturization and proper communication are necessary for their integration with the controller and actuator components for implantable and high compliance applications. Hydrogels are suitable materials for implicit control of diverse variables since enzymes, antibodies or mimics can be incorporated to provide selectivity for different species. However, the application of hydrogels for monitoring purposes and implementing feedback signals to external controllers requires a transduction system. Transduction methods for hydrogels-based sensors, besides methods to improve their sensitivity and stability, are the subject of current investigations. Frequently, enzymatic glucose sensing is a context for proof-of-concept and development of sensor technology due to the relevance of the diabetes disease.

Optical Transduction

Fluorescence and refraction are common transduction principles adapted to hydrogels systems [2]. Hydrogels color variations resulting from their volume changes allow the use of optical transduction principles for sensor applications such as contact lenses or intraocular lenses for glucose sensing from tears. Polystyrene nanospheres with attached glucose oxidase are imbedded in a hydrogels membrane by carrying out the polymerization process from a reaction solution containing the nanoparticles. The glucose-dependant swelling of the hydrogels causes the wavelength of the diffracted light to shift as the distance between the nanoparticles change, producing an observable color variation (Fig. 2a) [3]. Similarly, glucose binding to boronic acid derivatives in a polyacrylamide gels [4] and binding of avidin or antibiotin to a biotinylated poly(*N*-isopropyl acrylamide-co-acrylic acid) hydrogels [5] produce crosslinking and volume reduction leading to a change in the refractive index and the observed color. Fluorescence detection of calcium levels in T-cells has been used to monitor the activity triggered by an antigen in a poly(ethylene glycol) hydrogels platform for clinical diagnostics or biodefense [6].

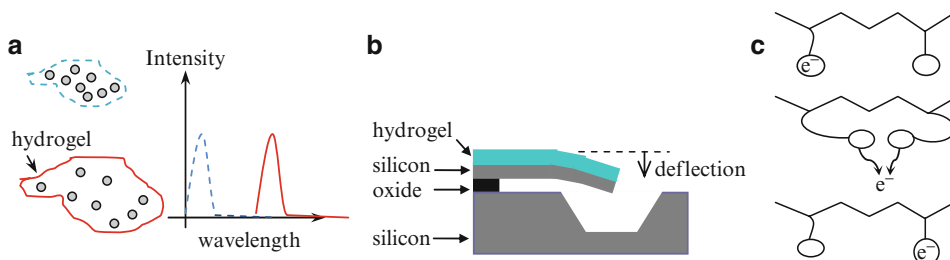


Fig. 2. Transduction mechanisms for hydrogels-based sensors. (a) wavelength shift of diffracted light from hydrogels with polystyrene particles (b) microcantilever deflection and (c) enzyme wiring through tethers of redox centers for electron, e^- , transfer. Adapted from [2], [7], and [1], respectively.

Mechanical Transduction

Cantilevers have been proposed as transduction systems for hydrogels volume transitions. A hydrogels deposited on the surface of a cantilever may cause a displacement of the free end of this structure or a decrement in the natural frequency of vibration upon swelling (Fig. 2b). A pH microsensor has been developed, achieving high sensitivity and repeatability [7]. A poly(methacrylic acid-g-ethylene glycol) was covalently attached to a silicon surface. Synthesis and patterning of the hydrogels was carried out by UV lithography, a common procedure in planar technologies in the integrated circuit industry. The deflection of the hydrogels covered microcantilever showed a pH sensitivity two orders of magnitude greater than those of pH microsensors based on electrochemical principles (ion selective field-effect transistors (ISFET), metal oxide electrodes). The incorporation of an enzyme in the hydrogels can enhance the sensitivity of cantilever sensors for the quantification of a substrate or analyte in comparison with other enzyme immobilization techniques. The mass increment due to the enzyme–substrate coupling is accompanied by the absorption of water onto the hydrogels patterned surface. In the case of glucose oxidase, the conversion of glucose into gluconic acid causes a pH drop and the cationic hydrogels to swell, and produces a deflection which can be correlated with the environmental glucose concentration. The combination of hydrogels and silicon microstructures can also be used for the development of ultrasensitive immunosensors.

Electric Transduction

Electron transport from a selective electrochemical reaction suggests the use of electrode transducers. The glucose oxidase enzyme, GOx, catalyzes the redox reaction of glucose with oxygen producing an electron exchange. The active site of the enzyme is surrounded by electrically insulating protein, which hinders the charge transfer on the surface of an electrode-based transducer. To overcome this difficulty, the enzyme is “wired” or connected through an electron conductive hydrogels to the electrode [1]. The wiring of the enzyme GOx consists in its immobilization in a hydrogels with fast redox centers at the ends of tethers of the polymer structure (Fig. 2c). Electrons are transferred when the pendant redox centers approximate to each other. In this way, the flavin adenine dinucleotide (FAD) centers of the active site of the enzyme are reduced (to FADH₂) by the glucose substrate, and reoxidized on the surface of the electrode. The hydrogels layer on the electrode allows for a high density of wired enzymes per unit area favoring electrode kinetics and limiting glucose diffusion. The high current density achieved makes this electrode configuration suitable for miniaturization [1] and its integration in a closed loop system.

Limitation of Enzyme Secondary Substrate

The specificity and the reversibility of enzymatic reactions impart desirable characteristics for hydrogels-based sensors. Therefore, proper conditions for these reactions must be controlled, such as the presence of a secondary substrate. The glucose sensitivity of a hydrogels-based system through the incorporation of GOx depends on oxygen availability. The catalase enzyme is often added to the system to regenerate oxygen from the hydrogen peroxide produced by the enzymatic glucose oxidation. The catalase reaction serves the double purpose of replenishing a reactant (oxygen) and eliminating a toxic inhibiting substance (hydrogen peroxide). In spite of the use of catalase, oxygen may still limit the response of the glucose-sensitive hydrogels system due to the low solubility of oxygen in aqueous solutions and blood. In order to enhance oxygen transport to the system, the use of macroporous

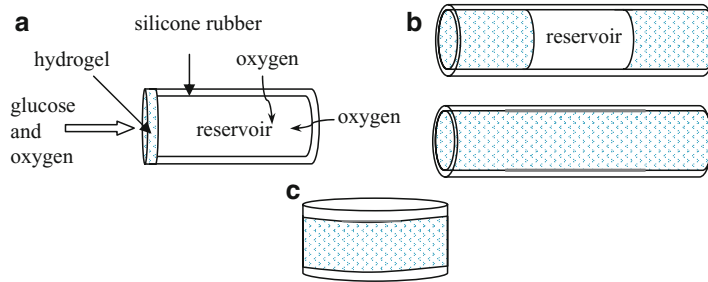


Fig. 3. Membrane (a), tube (b), and sandwich (c) configuration of enzymatic hydrogels devices with silicone rubber-covered surfaces for oxygen transport. Glucose oxidase is contained in the hydrogels. Reservoirs may contain an insulin solution or a gas (air or tissue gases). Adapted from [8].

hydrogels and silicone rubber components has been proposed. The latter are intended to create exclusive pathways for oxygen penetration into a hydrogels material that may contain insulin or cap an insulin reservoir [8].

Different configurations favor oxygen diffusion over glucose diffusion to solve oxygen limitation for the GOx reaction inside the hydrogels (Fig. 3), as discussed in [8]. Silicone rubber-covered surfaces impede glucose diffusion but are permeable to oxygen. Those devices based on a hydrogels membrane cap and a reservoir encased by silicone rubber allow glucose and oxygen to transport through the membrane and only oxygen to diffuse through the reservoir walls. In this work, a silicone rubber “tube” with hydrogels-filled sections and a hydrogels material sandwiched by silicone rubber disks offer adjustable two-dimensional diffusion systems. In the tube design, glucose and oxygen diffuse in the axial direction and only oxygen diffuses also in the radial direction. In the “sandwich” configuration, glucose and oxygen diffuse radially and only oxygen permeates through the silicone rubber disks. The oxygen concentration within the hydrogels can be increased by changing the length of the tube or the radius of the sandwich.

Studies on oxygen limitations in the GOx reaction within the hydrogels membrane, tube and sandwich delivery systems have been reported disregarding the swelling of the hydrogels, which would be less restricted in the sandwich design [8]. The authors developed mathematical models that produced the same qualitative results as the experimental systems. Their analysis was based on the square of the Thiele modulus, φ^2 , the Biot number, Bi, and the relative consumption rates of oxygen and glucose, O/G. The square of the Thiele modulus is the ratio of the internal diffusion time ($L_i^2/\alpha_i D_i$, where L_i is the diffusional distance inside the gels, α_i is the equilibrium partition coefficient or ratio of the concentration inside the gels over the concentration in the solution, and D_i is the diffusivity in the membrane for the species i) to the reaction time (c_i/v , where c_i is the concentration in solution and v is the velocity of the enzymatic reaction). The Biot number expresses the ratio of the internal diffusion time over the external diffusion time or characteristic time for the diffusion through the hydrogels-medium interface (L_i/k_i , where k_i is the mass transfer coefficient). The analysis of the consumption ratio O/G revealed an optimal value for glucose response indicated by the pH of the hydrogels.

The following trends were observed in a hydrogels membrane system [8]. A considerable increase in oxygen availability, without a corresponding noticeable decrease in glucose concentration or in the hydrogels pH, indicated either an excess of glucose or a process limited by glucose oxidation kinetics. When the same area was available for both oxygen and glucose transport through the membrane, a pH plateau was reached near 50 mg/dL. Excess of oxygen, attained with a gas reservoir, produced lower pH values in the gels, high O/G values and a wider range of response, from 0 to 500 mg/dL.

The two-dimensional designs outperformed the membrane system. Changes in pH were greater than those with the membrane. The sandwich system reached a plateau at 200 mg/dL. The tube design filled with hydrogels was sensitive to glucose concentrations up to 350 mg/dL. The pH for the case of the tube design with a gas reservoir could still be reduced at glucose concentrations beyond 500 mg/dL. The tube designs, compared to the sandwich design, were more effective to enhance oxygen delivery to the hydrogels because of the higher oxygen transfer area. The tube with central gas reservoir achieved O/G ratios 33% greater than those for the tube completely filled with hydrogels due to the high diffusivity of oxygen through a gas. Under similar conditions of glucose limited diffusion, Biot number and gels volume but different geometric proportions, membrane systems only achieved two-thirds of the maximum response (total conversion of glucose in the hydrogels), while the tube and sandwich designs approximated much closer to the maximum response.

Regarding the dynamic behavior, the tube and sandwich systems showed greater response times than the membrane system. Settling times for the response before glucose concentration step changes were greater at higher concentration values. The larger sizes and geometric factors resulted also in increased response times.

Both the Biot and Thiele numbers determine the system dynamics. When the Biot number of the system is high, as in the tube and sandwich designs, internal diffusion is expected to dominate over external transport conditions such as the convective transport of glucose from the body. Enzyme loading directly affects the Thiele modulus. A high enzyme loading will not significantly reduce the response time since the system would be diffusion limited. However, when the Thiele modulus is low, the time response of the system will depend on enzyme loading.

Preservation of Enzyme Activity

The duration of the activity of the enzymes is an important determining factor for the useful life of enzymatic sensors. The hydrophilicity of hydrogels produces a proper environment for the preservation of enzyme activity and the diffusion of the analyte or substrate. Therefore, enzyme immobilization in hydrogels improves the performance of diverse composite sensors. Silicon sensor platforms can be used taking advantage of the compatibility of photopolymerization procedures with microfabrication techniques. For example, ISFET have been used as transduction systems for urea measurements based on the basic nature of products from urease interactions and the pH sensitivity of silicon semiconductors [9].

Immobilization procedures often include the difunctional component of glutaraldehyde, which acts as a crosslinking agent between enzymes. Glutaraldehyde can provide better retention of enzymes within a system as well as longer preservation of their activity [9]. Incorporation of poly(ethylene glycol) in the enzyme containing material helps to preserve enzyme activity and prevent immunoreactions to implanted systems [10, 11]. However, pegylation and glutaraldehyde crosslinking increase the density of the system and the diffusion limitations for the detection of substrate concentrations.

The limited activity of natural enzymes can be overcome by the use of mimics. Hydrogels have been used as a support polymer for imprinting cavities with catalytic activity. A chymotrypsin mimetic has been produced with a hydrogels (the volume changes switch the enzymatic activity on and off by altering the diffusivity of the substrate) with enhanced activity and stability [12].

Hydrogels as Actuators

Actuators respond to an external signal intended to cause a change in the process. The external signal comes from a device or controller that may be operated either in an open loop or in a closed loop. The controller of an automatic drug delivery system, for instance, uses

the information of the state of the patient (fed back through a sensor device) and an algorithm to determine the control signal to be sent to the actuator to deliver the proper amount of drug. In the manual mode, the application time and magnitude of the dose is decided by the patient who directly determines the control signal or manipulation of the actuator (on-demand function of the actuator). Hydrogels-based actuators can be manipulated through a continuous or an on/off control signal. This signal or manipulation can be of different nature [13, 14]: magnetic, ultrasonic, electric, optic, thermal, chemical, or biochemical.

Magnetically Controlled Systems

The responsiveness to a magnetic field can be achieved through the incorporation of magnetic beads into the hydrogels material. Copolymer matrices of ethylene with vinyl acetate and crosslinked alginate matrices with imbedded magnets have achieved enhanced drug release rates with increasing frequency of the oscillating magnetic field [15]. Repeated magnetic pulsatile or on/off stimulations required a higher frequency to compensate gradual drug depletion.

Ultrasonically Controlled Systems

Ultrasound increases diffusion and erosion controlled drug delivery rates [14]. The response to ultrasound does not require any modification in the synthesis of the polymeric material. Poly(ethylene-co-vinyl acetate) matrices have also been studied under ultrasound excitation. Solid drug particles in the dry material absorb ultrasound energy impeding stimulation for drug release. In the swollen state, the drug particles dissolve and ultrasound energy produces a higher increment in release rates than in the nonswollen state. Reversible increments in drug release were observed at low ultrasound frequencies from swollen systems [16]. Self-assembled monolayers responsive to ultrasound energy were used as coatings for drug-containing polymeric systems. The ultrasound energy disassembles the coating, which is rebuilt when ultrasound applications ceases [17]. This system has been used to deliver an anti-biofilm formation agent [18].

Electronically Controlled Systems

Electric fields can be applied on a membrane or in the solution to control the solute transport. A switching electrical field has been used to direct the binding of charged surfactant molecules to one or other side of an ionic hydrogels strip producing a controlled “worm-like motion” [19], illustrating an actuation mechanism with possible application for an artificial muscle or a drug delivery system. Hydrogels volume changes controlled by pulse width modulation have been experimented for the electric manipulation of hydrogels-based valves or pumps [20, 21]. The electric stimulated swelling dynamics was improved due to the added electrostatic effects by using the hydrogels as an electrolyte material in an electrolysis cell where protons are produced at one electrode and attracted to the other.

Photo-Controlled Systems

Photo-sensitive gels experience volume transition or chemical degradation when exposed to light [14]. These changes can be produced by the isomerization of chromophores in the excited photoreceptors in some materials [22, 23]. Azobenzene transition from the *trans* to the *cis* form by exposure to UV radiation causes dipole interactions that strip water from hydrogels materials [12]. Ophthalmic drug delivery systems have been designed using azobenzene copolymers whose molecular openings are regulated by changing the polarization of

laser irradiation [24]. Visible light has also been investigated as a safe and available stimulus source for rapid hydrogels phase transition based on light heating [25]. Other compounds such as cinnamic acid derivatives and fumaric amide have also been used in the fabrication of photo-sensitive hydrogels [26, 27].

Fumaric amide can give photosensitivity to biomaterials shown through gels–sol phase transitions [27]. The motion of F_1 -ATPase (enzyme-based molecular motor) tethered with beads has been manipulated by the *trans–cis* isomerization of fumaric amide inside a self-assembled supramolecular hydrogels. Supramolecular hydrogels, in contrast to polymeric hydrogels, are built from supramolecular units or gelating agents which bond noncovalently (through hydrogen bonds, π – π stacking and van der Waals interactions) to produce fibers and crosslinking among fibers [27, 43]. The gelating agents consist of a hydrophilic sugar head, a hydrophobic lipid tail, and a hydrogen bonding spacer (Fig. 4). Fumaric amide was inserted in the spacer. Upon UV radiation, the entangled fibers in the gels state turned into spherical aggregates in the sol state. The recovery of the gels state was possible under visible light and in the presence of bromine. The phase transition was effective for the release of preloaded vitamin B12, concanavalin A and 100-nm beads. Moreover, Brownian motion of beads could be stopped at a specific bead size and gelating agents concentration. These materials were designed for on/off control of the Brownian motion of bacteria and enzymes whose activity depend on their mobility. The same motion control was achieved with hydrogels without fumaric amide or any covalent insertion of a “switching” unit by changing the environment temperature around the gels–sol transition temperature [28]. Localized stimulation allowed the gels–sol transition in specific parts in contrast with a bulk response of the material.

Gold nanoshells covered with a temperature-sensitive poly(*N*-isopropyl acrylamide-co-acrylic acid) hydrogels have been studied for potential drug delivery application [29]. Silicon dioxide particles with a seed-grown gold layer can be fabricated with the proper dimensions to absorb light in the near-infrared range from 800 to 1,200 nm. Radiation within this range can penetrate through skin, tissue, and water. Light absorption in these systems causes an increase in temperature and subsequent shrinking of the hydrogels (Fig. 5). Changes in the composition of acrylic acid adjust the lower critical solution temperature

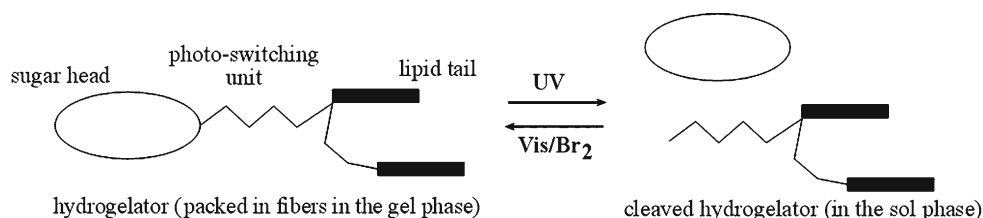


Fig. 4. Supramolecular hydrogels with fumaric amide photo isomerizable unit for a photo-actuated system. The material experiences a reversible phase transition in response to light stimuli. Adapted from [27].

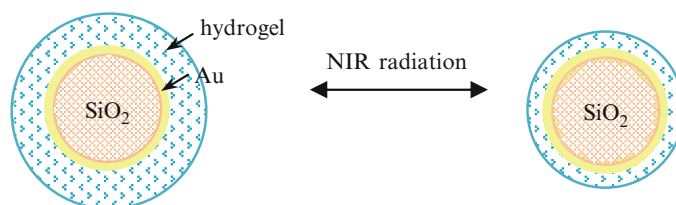


Fig. 5. Gold nanoshells with silica cores covered by a poly(*N*-isopropyl acrylamide-co-acrylic acid) hydrogels (photothermally controlled actuator system). Heating by NIR excitation of gold plasmon resonance results in hydrogels shrinking. Adapted from [29].

and enhance the reversibility of volume changes. Drug loaded hydrogels can also release the drug by collapsing the gels upon external photo-excitation.

Thermally Controlled Systems

Thermal energy can produce hydrogels swelling or contraction. Polymer networks of acrylic acid (AA) and acrylamide (AAM) show a direct swelling response with respect to an increment in temperature. The formation of hydrogen bonds between carboxylic and amide groups at low temperature causes the collapse of the polymeric structure. On the other hand, the disruption of hydrogen bonds at a high environmental temperature allows the expansion of the material. Interpenetrating networks with an equimolar composition of AA and AAM and low crosslinking agent content (0.1 mol%) to produce more abrupt volume transition and higher temperature sensitivity than the corresponding homopolymers and random copolymers [30], both traits are convenient for drug delivery applications. Temperature responsiveness of interpenetrating networks has been employed as the actuation mechanism of gold composite systems for drug delivery [31].

A temperature change can provoke not only a volume variation but an optical response of a hydrogels system. The volume of poly(acrylic acid-co-acrylamide) hydrogels determines the level of optical transparency. Dal et al. found that changes in hydrogels optical properties were more reversible when the temperature range for the transmittance transition narrows and the temperature in the inflection point is lower for smaller monomer concentrations [32]. A monomer ratio (AA/AAM) of 0.5 maximizes the number of bonds, widens the optical transition range and shifts this range to higher temperature values. High crosslinking agent concentration and high initiator concentrations lead to denser materials and wide transition ranges at higher temperature values. Release kinetics studies showed consistent higher decay rates of exponential profiles at higher temperature and less diffusion resistance. If the temperature forcing input is produced within the hydrogels system, for example, by the heat from an enzymatic reaction, an optical transducer could be used to produce an analyte measurement and, simultaneously, the volume transitions would allow self-regulated drug delivery.

Thermally actuated enzymatic hydrogels systems have been used in bioreactors. The swollen state of the hydrogels promotes absorption of the substrate while the collapse of the hydrogels may help to expulse enzymatic products, both effects can be achieved by cycling the hydrogels stimulation in order to favor the conversion of the substrate. The conversion in a packed-bed reactor and in a continuous stirred-tank reactor was investigated using poly(*N*-isopropyl acrylamide-co-acrylamide) hydrogels beads with immobilized β -galactosidase enzyme [33]. Temperature oscillation just below the hydrogels transition temperature (lowest critical solution temperature, LCST) outperformed isothermal conversion of the enzymatic reaction. Fast heating and cooling rates could lead to higher conversions as long as reversible volume changes were produced. However, several factors provoked the restricted reversibility of the swelling of the beads and affected the conversion in the reactors. Heating and cooling rates were limited by the viscoelastic dynamics of the hydrogels systems. In addition, the expansion at a temperature above the LCST was slower than below the LCST, and thermal heating from the exterior of the hydrogels beads approaching the LCST may have caused the formation of a "skin" that reduced the squeezing effect of the hydrogels syneresis. Optimization of temperature cycles was recommended for packed columns to reduce or avoid reactant tunneling among collapsing beads.

Chemically Controlled Systems

Chemical species can also stimulate actuator systems. The response of enzymatic materials can be triggered by the availability of an activating agent. For example, calcium addition can be used as a control signal to produce the conformational changes of calmodulin

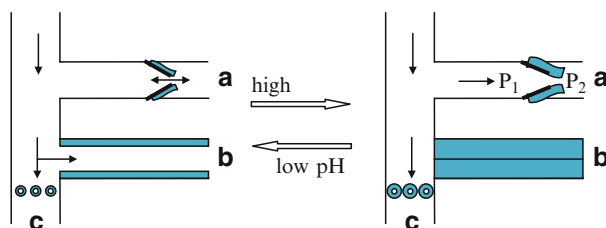


Fig. 6. Chemically controlled actuators based on an anionic hydrogels. The check valve (a) is activated at high pH and flow is allowed when pressure P_1 is greater than pressure P_2 ; channel covered with hydrogels strips (b) and hydrogels jackets on rigid posts (c) restrict flow area as pH increases. Adapted from [39], [38] and [37], respectively.

protein molecules contained in a hydrogels drug delivery system [34]. Fibrous hydrogels materials used for the regeneration of dental tissues are crosslinked at high calcium concentrations and can be deformed by the action of a collagenase enzyme [35]. A chemically controlled system has been made of a micellar dithiol crosslinked N-isopropyl acrylamide gels [36]. The presence of glutathione degrades the material by breaking the disulfide bonds. A preloaded drug release could therefore be controlled by the induced degradation.

Microfluidic devices can be controlled chemically. Hydrogels have been used to manipulate microflows in response to pH changes (Fig. 6) [20]. A poly(2-hydroxyethyl methacrylate-co-acrylic acid) hydrogels on the walls of a microchannel was observed to regulate the flow resistance by varying the cross section area for the flow according to the pH with diffusion limitations along the channel [37]. Faster regulation was achieved by the application of a hydrogels coating on posts at the entrance of a channel [38]. Nonresponsive materials have been used for different supporting structures, such as two close nonparallel flexible walls for a check valve. Strips made out of a pH-sensitive hydrogels attached to these walls reduced the space allowing opening or complete closure with a positive or negative pressure differential, respectively. The check valve was pH activated, since it required a swollen hydrogels to close [39].

Protein Responsive and Controlled Systems

Specific ligands can be incorporated in the hydrogels to affect the cell behavior [2]. Arg-Gly-Asp (RGD) peptides in a hydrogels system for tissue regeneration allow cell adhesion by the interaction with integrin proteins on the cell surface [40, 41]. Hydrogels with Ile-Lys-Val-Ala-Val (IKVAV) peptides have been applied to direct stem cell differentiation into neuronal cells [42].

Drug delivery systems activated by the presence of enzymes in the environment have been proposed [43]. This activation mechanism allows targeted drug delivery as in the case of tumors where specific proteases are found. For example, polyacrylamide hydrogels have been synthesized with enzyme cleavable peptides [44]; the enzymes in the medium degrade the material and can produce gradual release of the drug content.

An esterase sensitive system consisting of a self-assembled supramolecular hydrogels has been studied. The gelating agent can incorporate a prodrug (inactive drug precursor) with an ester bond susceptible of cleavage by the hydrolysis reaction catalyzed by esterases. A second drug can be encapsulated in the material for simultaneous release of two possibly complementary drugs upon degradation of the material (Fig. 7). Gelating agents of an acetaminophen (analgesic)-based prodrug were used to fabricate these materials to encapsulate curcumin (antioxidant). The amphiphilic properties of gelating agents effectively incorporated the hydrophobic curcumin and provided the necessary hydration for lipase-induced degradation. The release rates increased with enzyme concentration and temperature. The acetaminophen-based gelating agents were not cytotoxic. Gel-sol reversible transition was not intended to

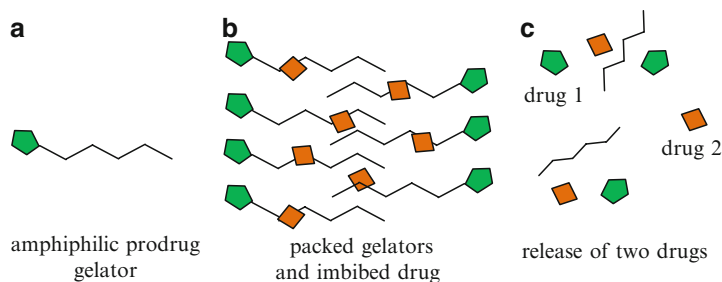


Fig. 7. Supramolecular hydrogels from prodrug gelators as a protein-controlled actuator system. Amphiphilic prodrug gelator from a well known therapeutic (a), packing of prodrug gelator and encapsulation of a second therapeutic (b), release of therapeutics upon esterase degradation (c). Adapted from [43].

control drug delivery in the described lipase responsive system. Nevertheless, the effect of temperature on phase transition and the effect of enzymes on degradation can be combined. A temperature range may ease enzyme diffusion toward cleavable links in a two step mechanism [45–47] for drug release.

Self-Regulated Hydrogels-Based Systems

In self-regulated systems, the controller function is implicit in the hydrogels material structure as well as on the device design. The static and dynamic characteristics of a self-regulated system correlate the input feedback variable with an output variable [48]. The input variable drives the hydrogels response or the output variable change. These variables represent the main interactions with the surroundings. The autonomous systems presented here are based on feedback variables that allow hydrogels actuation by the environment for controlling a particular condition.

Miniaturized systems offer the possibility of painless, economic, continuous, and optimal drug infusion since they allow the management of small quantities of samples, reactants, and drugs. Low costs and easier operation are also possible for diagnostics systems when scaled down. The reduction of response times of small systems facilitates taking advantage of the integration of multiple functions in a hydrogels material. Some characteristics may be lost by miniaturization, such as the drug storage capacity within a hydrogels, but can be compensated by combining elements of different structures and materials. However, the complexity of such hybrid systems is reduced by the elimination of processing circuits (transducers, control algorithms), energy sources, wires and separate sensors and actuators due to hydrogels multifunctionality. *In situ* photopolymerization of hydrogels is easily incorporated in the manufacturing procedure of microfluidic platforms [20]. This technique is also convenient as part of an implantation procedure of monolithic drug delivery devices or tissue engineering applications.

pH Feedback Systems

The pH sensitivity of anionic hydrogels provides temporal release control in systems proposed for oral drug administration [49]. The hydrogels-based system prevents drug delivery in the stomach where the acidic pH causes the polymeric matrix to contract. When the hydrogels reaches the upper small intestine, where the pH is higher, the polymeric structure swells and eases drug diffusion. This on/off self-regulated system is active during its digestion process.

The incorporation of enzymes in ionic hydrogels can transform the pH sensitivity into responsiveness to the concentration of the enzyme substrate in the environment. The enzymatic reactions that produce acid or basic compounds modify the pH of the system leading to a volume change and inherent diffusivity variations. Since the pH changes are a function of the substrate concentration, continuous (as opposed to on/off) drug release regulation can be achieved for periods of time that are limited by enzyme activity, drug depletion, polymer degradation or body elimination [10, 50]. Urease-containing anionic hydrogels deliver drug in response to high concentrations of urea because of the swelling driven by the increment in the pH from the production of ammonium hydroxide (NH_4OH). While a cationic hydrogel with glucose oxidase can open its mesh structure for insulin delivery as glucose concentration increases due to its transformation into gluconic acid and the consequent pH decrement.

Autonomous pH regulation in a microfluidic system has been designed based on the sensing and actuating functions of a hydrogels component [51]. The objective was to achieve a neutral pH in the output flow from a T-junction where an acid input was mixed with a compensating basic input. A poly(acrylic acid-co-2-hydroxyethyl methacrylate) hydrogels postpressing on a poly(dimethyl siloxane) membrane (PDMS) on top of the orifice influenced the input of the basic solution. The orifice sealing increased at high pH of the output by tensing the PDMS membrane upon radial swelling of the post. The occluded area of the orifice decreased when the output pH was very acidic due to the radial shrinking of the anionic hydrogels post and the raising of the PDMS membrane (Fig. 8). The geometry of the orifice determined the type of regulation for the basic input: a circular orifice caused an on/off action and an oscillatory pH of the output flow, while a star geometry provided a stable output pH by gradual adjustments of the compensating basic flow. The pH regulation was limited by saturation effects due to pressure conditions in the channels. The proposed valve mechanism responsive to the environmental pH could be applied to drug delivery systems.

Anionic and cationic hydrogels (with opposite responses to pH) have been combined in a microfluidic sorter system by placing valves on each side of the T-junction of two microchannels. At the T-connection, the course of an input flow could be directed to one or another side depending on which valve was opened at the pH of the flow [38]. This type of combination allows the manipulation of flows according to their chemical characteristics.

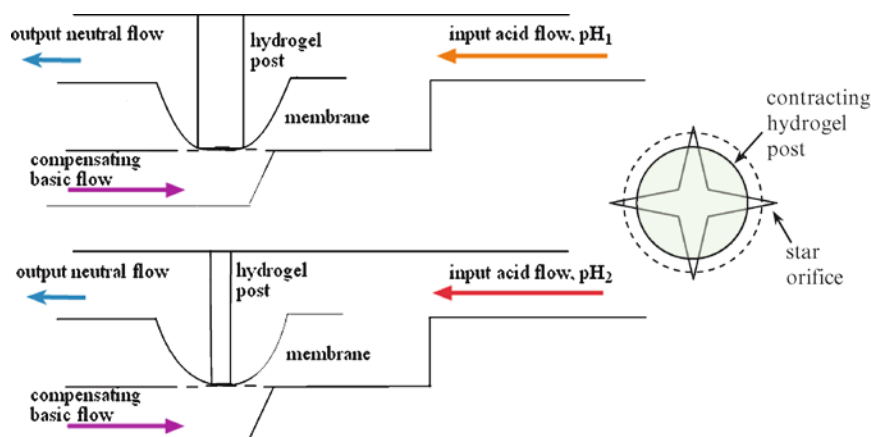


Fig. 8. Self-regulated system for pH control of the output flow. If the input flow has lower pH ($\text{pH}_2 < \text{pH}_1$), the hydrogels contracts radially allowing more free area for the pass of the compensating basic flow. A star orifice is obstructed by the hydrogels post. Adapted from [51].

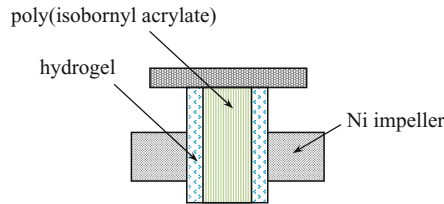


Fig. 9. Self-regulated system for temperature control. A hydrogels with negative swelling sensitivity with respect to temperature on the surface of the shaft of a magnetically impulsed propeller allows cooling flow above the LCST. Adapted from [52].

Temperature Feedback Systems

A temperature-sensitive hydrogels has been used for an autonomous cooling system in a lab-on-a-chip device (Fig. 9) [52]. The hydrogels formed around the axis of a nickel propeller for cooling water recirculation exerted on/off control of the rotation. The propeller was driven by an external magnetic stirrer, whose rotation speed determined the cooling flow rate. The hydrogels was a crosslinked copolymer of N-isopropyl acrylamide (NIPAAm) and 3-methacrylamido-propyltrimethylammonium chloride (MAPTAC), the latter was included to raise the LCST or onset operation temperature for the propeller. The hydrogels ring around the propeller was fabricated by the liquid-phase photopolymerization technique. When the temperature reached the LCST, the hydrogels collapsed allowing free movement of the propeller. At lower temperatures, the swollen hydrogels clutched the propeller. Temperature responsive systems may be also applied for closed loop drug delivery for the management of fever or infections.

Protein Concentration Feedback Systems

Proteins attached to hydrogels materials increase the possibilities for self-regulated systems. Hydrogels have been grafted with antigen and antibodies to create crosslinks that can be undone by the competitive binding with free antigen in the environment. The number of undone noncovalent crosslinks depends on the exogeneous antigen concentration which determines the degree of hydrogels swelling that enables controlled drug delivery [53, 54]. Hydrogels may also be designed as enzyme-sensitive systems, for example, biodegradable hydrogels for delivery of anti-inflammatory drugs. The gels degradation is promoted by enzymes as well as hydroxyl radicals that are produced at inflamed sites. This system could provide osteoarthritis treatment in a closed loop mode [14].

Enzyme Cofactor Feedback System

Enzymatic reactions offer different possibilities for drug delivery control by an immobilized oxidase enzyme that depends on the availability of an oxidizing cofactor or secondary substrate [2]. The concentration of the latter mediates the regulation of drug release. The constant presence of glucose in blood and the oxygen limitations do not favor reversible changes in ionic hydrogels for insulin delivery in diabetes treatment. However, the glucose composition of the blood as well as the possibility of other oxidizing agents make the glucose oxidase enzyme useful for the delivery of other drugs in the context of different pathologies. Oxidizing agents concentrate in inflammation sites and tumors and can induce drug release from the swelling of hydrogels through gluconic acid enzymatic production [2]. As a secondary substrate for glucose oxidase, polysulfide nanoparticle systems with glucose oxidase oxidize sulfides in the presence of glucose to produce swelling and drug release [55].

Glucose Concentration Feedback Systems

Research on closed loop control of glucose levels in a diabetic patient highlights important aspects for the application of autonomous systems. The feasibility of an insulin self-regulated delivery system based on injectable hydrogels microparticles with glucose sensitivity has been evaluated for the purpose of blood glucose regulation [56]. Synthesis parameters determine the capacity of hydrogels microparticles to: (a) respond to glucose concentration, (b) store enough insulin to reduce frequency of injections (3 days sparse at least), (c) circulate in blood capillaries, and (d) degrade at a rate that allows diffusion-controlled insulin depletion. Particles of 30 μm in size exhibit instantaneous response to pH changes [10]. This observation was used to simplify the analysis by neglecting the viscoelastic behavior of the hydrogels. The analysis considered the kinetics of the glucose oxidation and constant diffusivities for glucose, gluconic acid and insulin. Results showed the direct effect of the crosslinking ratio (number of moles of crosslinking agent per mol of monomer) on the maximum swelling and the degradation rate. The number of injected particles as well as the insulin loading determined the release rate but did not affect the release duration. The size of the collapsed hydrogels particles was directly correlated to the duration of the release. However, the swelling of hydrogels particles before high glucose concentrations produced an incremental change in the mesh size that increased the diffusion path for insulin delivery. A low crosslinking ratio produced higher delivery rates and shorter release durations. For higher transition pH values, the cationic particles tended to have higher volume and lower internal pH values making hydrogels contraction improbable. Higher content of basic functional groups led to an increase in the initial pH value of the microparticles and lower rates of gluconic acid production or decreased sensitivity of the system. The large size of the hydrogels particles to achieve acceptable release duration would inhibit them to circulate through capillaries. The simulation with a physiological model at a basal state produced wide oscillations in glucose levels.

Some disadvantages of hydrogels microparticles for injectable systems could be avoided by using implantable membranes. Limitations of size for release duration and for stable glucose control are clearly solved in macrosystems because of their longer response times. However, the effects of the buffer physiological medium, the continuous presence of glucose and the Donnan equilibrium suggest restricted volume changes for the hydrogels system regardless of its size. A simulation study of glucose responsive hydrogels membranes for insulin delivery in a diabetic patient with a diet of three meals per day showed they could be useful for days, but insulin release profiles decreased monotonically in spite of the elevated glucose levels during the meals (Fig. 10) [50]. Specific viscoelastic effects of the hydrogels membrane and GOx-catalase reaction kinetics in the hydrogels medium were based on experiments with poly(methacrylic acid-g-ethylene glycol). The Sorensen model was used for the simulation of the glucose-insulin physiologic process for an adult male of 70 kg. The initial interaction of the implanted hydrogels membrane with the glucose containing physiological fluids dominated the volume response of the membrane over the pH changes caused by the meals. The small variations in the pH of the membrane during the meals were due to a combination of the glucose composition and the buffer effect of the blood. Even at fasting glucose levels, glucose would tend to diffuse into the gels causing a sustained production of gluconic acid that would oppose the recovery of the higher physiological pH. Furthermore, the Donnan equilibrium inside the gels would determine the conservation of a local pH different from the pH of the physiological environment.

Apart from the particular diabetes application characteristics, those of the hydrogels in a self-regulated system can be improved in order to produce flexible delivery profiles similar to those that can be obtained with an explicit controller [57–59]. A hydrogels-based insulin delivery system should achieve mesh size variations around the size of insulin at a physiological pH. Mesh size and transition pH can be adjusted by modifying the number, the type and the

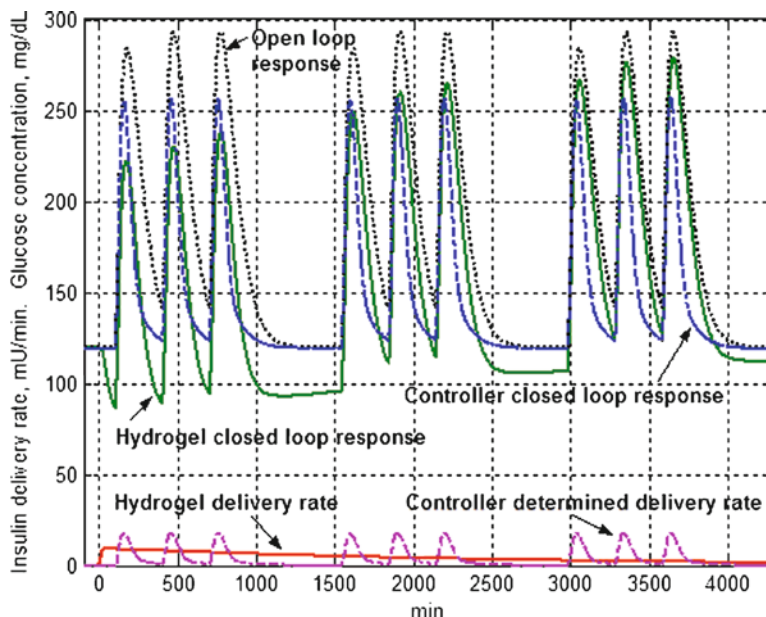


Fig. 10. Hydrogels membrane as a self-regulated control system of blood glucose levels in a diabetic patient. Simulation results are shown using a hydrogels membrane insulin delivery system and an explicit controller during 3 days with three meals per day. Reprinted with authorization from [50], © AIChE Journal.

concentration of monomers. Even if the critical pH of an ionic hydrogels was adjusted closer to a neutral value, the buffer characteristic of physiological fluids would offer a resistance to the volume changes of the membrane. Hydrogels materials with temperature and glucose sensitivity can be suggested from the possibility to couple the energy produced by the enzymatic reaction of glucose to the modulation of molecular openings and drug delivery. Hydrogels without pH sensitivity would eliminate the limitations due to the buffer environment and the Donnan equilibrium effect. However, they would also be subjected to the saturation of the glucose oxidase enzyme due to the constant presence of glucose in the physiological environment. Limitations of hydrogels monolithic systems for continuous blood glucose regulation may be overcome by hydrogels-based devices. Hydrogels may be used in hybrid systems for a more effective insulin delivery.

Alternative insulin delivery systems have been suggested by combining membrane and particle structures and using non-covalent enzyme immobilization. Covalent attachment requires exposure to fabrication steps involving high temperatures and violent mixing that may diminish the activity of the enzyme. Physical attachment may be less aggressive to the enzyme although the possibility for enzyme leakage is higher. Researchers have proposed a self-regulatory system consisting of poly(*N*-isopropyl acrylamide-co-methacrylic acid) hydrogels nanoparticles supported in a hydrophobic enzymatic membrane (Fig. 11) [60]. Glucose oxidase and catalase were mixed with dissolved ethyl cellulose and hydrogels nanoparticles. The membrane was formed after evaporation of the solvent. The analysis of washing water showed no loss of enzymes in spite of their physical immobilization. The activity of the physically immobilized enzymes was 80% of the enzymes in solution. Optimal values for the ratio of glucose oxidase units to catalase units (1:11) and the amounts of each enzyme in the system were determined by comparing the pH behavior at different glucose concentrations. The permeability values, obtained through diffusion cell experiments, were not higher for the maximum enzyme content but only the determined optimal quantities. Insulin transport was dependent on glucose concentration as shown by varying the glucose concentration in the

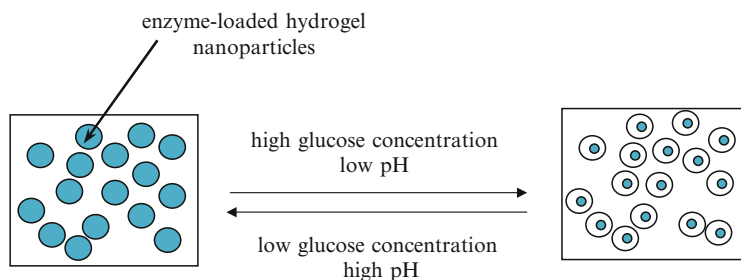


Fig. 11. Hydrophobic membrane with hydrogels nanoparticles for a self-regulated system. Nanoparticles contain glucose oxidase and catalase. The composite membrane increases insulin permeability before high glucose concentrations. Adapted from [60].

receptor cell. The small thickness of the membrane and diameter of the hydrogels particles favored fast and reversible responses compared to hydrogels membranes [50]. The membrane structure would ease implantation in specific parts of the body (avoiding problems of an injectable system) and the microparticles would contribute to the fast response necessary for appropriate action before glucose levels.

Drug availability can limit the use of self-regulated systems. The drug is usually imbedded in the responsive material or contained in an attached reservoir. In order to overcome the disadvantage of drug depletion from these systems, the production of the drug may be added. Insulin-secreting cells, for instance, can be sustained in a proper reservoir or compartment that allows flux of cell metabolites through the reservoir walls and controlled insulin release through the responsive material cap. Fibroblasts, myoblasts, and hepatocytes from the same patient have been genetically engineered to express insulin and used as an insulin source for a self-regulated delivery system [61]. These non- β cells have better immunological acceptance than transplanted human corpse β cells, but show a slow reaction to physiological conditions. Insulin accumulated in a compartment can be dosed through the dynamic diffusion barrier provided by the responsive material. A possible insulin feedback inhibition effect on the cells might be useful to prevent excessive insulin accumulation.

A cell-material hybrid device for controlled insulin release that incorporates the insulin-secreting autologous non- β cells mentioned and a concanavalin A-glycogen hydrogels has been proposed [61]. This material changes from a gels to a sol state when exposed to high glucose concentrations. The concanavalin A acts as a crosslinking agent in a material with glycogen pendant groups. At high concentrations, glucose from the environment competitively binds to concanavalin A destroying the crosslinks of the material. If the exterior glucose concentration is low, internal crosslinks are reestablished. The device was constructed as a 6 cm in diameter disk, 1 cm thick. Silicon sheets and polycarbonate plates were used as structural materials to support the cell layer and the hydrogels layer separated by a 0.02 μm AnodiscTM membrane. In vitro tests showed induced insulin release at glucose concentrations above physiological levels. Oxygen limitation diminished cell viability. Accumulated death cells also caused less cell viability. Toxicity and leakage of concavalin A toward the cell layer affected cell viability and glucose sensitivity. The responsive material can be redesigned to show sol-gel transitions in the physiological range.

Hydrogels-Based Feedforward and Cascade Systems

In many processes, feedback control is not enough to keep the process variable within the control limits, especially in presence of disturbances. When an external variable to the control system changes, the time and difficulty to correct the deviation caused in the process

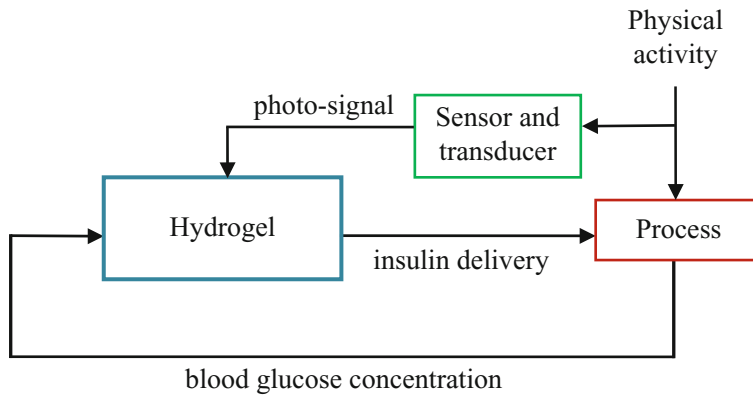


Fig. 12. Feedforward scheme applied by double responsiveness to the environment. The system is based on a single hydrogels component. If physical activity increases, the increment of the heart rate can be detected and used to produce a photo-signal to cause the hydrogels to decrease insulin delivery before blood glucose level drops. Heart rate external detection would help to prevent a hypoglycemic event due to the increment in physical activity by anticipating its effect. The basic glucose sensitivity of the hydrogels-based insulin delivery systems allows a reactive response before other disturbances like meals.

variable increases. To improve the performance of the feedback systems, the control system is modified to attenuate or compensate for effects. The variety of environmental stimuli on hydrogels systems as well as possible combinations of materials and physical structures could be used to take advantage of control schemes, such as feedforward and cascade.

In a feedforward system, the detection of a disturbance before it affects the process variable or controlled variable is used to apply an additional manipulation in order to compensate the disturbance effect. This strategy could be applied, for example, in an enzymatic hydrogels-based insulin delivery system to adjust release based on the heart frequency. The heart frequency reflects the level of physical activity of the patient. If the heart rate increases, as detected by an extensometric gauge or pulsoxymeter, a transduction system could generate a radiation signal that would decrease hydrogels swelling [29] and insulin release before glucose levels decreased to avoid a hypoglycemic episode (Fig. 12). The glucose-oxidase reaction that determines the pH of the microenvironment of the hydrogels would implement the glucose concentration feedback, the pH responsiveness of the hydrogels would implement a basic control function, and the responsiveness to near-infrared radiation determined from the external variable would produce the feedforward control function. The resultant hydrogels action would come from the net effect of the driving inputs: pH and irradiated energy.

The cascade control strategy consists in the attenuation of the effect of a disturbance by controlling an auxiliary variable that manifests the presence of the disturbance before it causes a variation of the main variable. If the secondary variable is returned to its normal value quickly enough, then the effect on the main variable will be reduced or even eliminated. This scheme tries to interfere in the cascade or domino sequence of effects from a disturbance source to the main controlled variable through nested control loops. In the sense of a cascade propagation of effects and corrective actions, a cascade arrangement could correspond to concentric hydrogels systems imbedded with different drugs. When the physiological condition that activates the response of the external hydrogels allows extreme swelling such that the interior hydrogels gets exposed to another physiological condition, the response of the inner system may deliver drug before a complex symptom. For example, an external glucose oxidase containing hydrogels may be kept swollen at persistent high glucose levels. This situation leads to malfunction of kidneys, which can be manifested by high urea concentrations

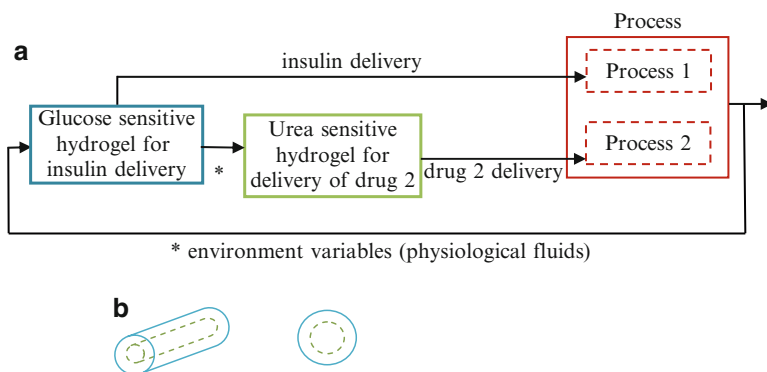


Fig. 13. Cascade scheme applied by concentric hydrogels materials. Conceptual diagram (a) and possible physical structures (b) are shown for sequential activation from the external hydrogels component in direct contact with physiological environment.

detected by an internal urease-containing hydrogels that may allow the release of a drug to decrease urea levels (Fig. 13). In this case, the nested systems produce independent actions on the environment instead of reinforcing actions for the control of a single variable.

Summary

Monolithic hydrogels systems have several limitations regarding drug-loading capacity, velocity, and reversibility of response and mechanical strength. Hybrid systems compensate for these limitations and take advantage of the responsiveness of hydrogels to varied environmental conditions. The hydrogels materials used for sensors and actuators in a multicomponent control system require special transduction means for continuous feedback systems.

Physical and biochemical hydrogels stimuli may not exclusively correspond to one type of feedback system, but can be related mainly to explicit controller and implicit controller biomedical feedback systems, respectively. Ultrasound, magnetic, light, electrical and thermal signals with high energy content are not appropriate for biological environments; typically, they require an external source or controller. The flexibility of explicit controllers encourages the use of hydrogels in the development of separate sensor and actuator units. External physical stimulation by ultrasound, magnetism, electric fields, or temperature can enhance drug diffusion delivery by increasing the mobility of the drug molecules. Therefore, physical external stimulation may also augment drug delivery rates from hydrogels, even if there is no interference with the swelling behavior. Ultrasound provides a mechanical actuation mechanism for drug delivery systems that do not require special hydrogels synthesis procedures and are expected to have less impact on the integrity of the drug. Continuous external stimulation and hydrogels reversible response may mediate the regulation of variable drug release profiles in a continuous closed loop treatment with an explicit controller. A system chemically stimulated may act irreversibly and, therefore, not be suitable for continuous control. The same applies for any kind of stimulated degradation based drug delivery system. However, a scheme of on/off activation of multiple drug hydrogels compartments may allow modifications in the release profile for temporal closed loop control in these cases. Even when research on hydrogels systems aim to achieve implantable applications, the concepts related to their operation may be a reference for the development of diverse advanced products for health care.

References

- Heller A (2005) Integrated medical feedback systems for drug delivery. *AIChE J* 51(4):1054–1066
- Ulijn RV, Bibi N, Jayawarna V, Thornton PD, Todd SJ, Mart RJ, Smith AM, Gough JE (2007) Bioresponsive hydrogels. *Mater Today* 10(4):40–48
- Holtz JH, Asher SA (1997) Polymerized colloidal crystal hydrogel films as intelligent chemical sensing materials. *Nature* 389(6653):829–832
- Ben-Moshe M, Alexeev VL, Asher SA (2006) Fast responsive crystalline colloidal array photonic crystal glucose sensors. *Anal Chem* 78(14):5149–5157
- Kim J, Nayak S, Lyon LA (2005) Bioresponsive hydrogel microlenses. *J Am Chem Soc* 127(26):9588–9592
- Kim H, Cohen RE, Hammond PT, Irvine DJ (2006) Live lymphocyte array for biosensing. *Adv Funct Mater* 16(10):1313–1323
- Hilt JZ, Gupta AK, Bashir R, Peppas NA (2003) Ultrasensitive biomems sensors based on microcantilevers patterned with environmentally responsive hydrogels. *Biomed Microdevices* 5(3):177–184
- Klumb LA, Horbett TA (1991) Design of insulin delivery devices based on glucose sensitive membranes. *J Control Release* 18:59–80
- Jiménez C, Bartrol J, de Rooij NF, Koudelka-Hep M (1997) Use of photopolymerizable membranes based on polyacrylamide hydrogels for enzymatic microsensor construction. *Anal Chim Acta* 351(1):169–176
- Podual K, Doyle FJ III, Peppas NA (2000) Dynamic behavior of glucose oxidase-containing microparticles of poly(ethylene glycol)-grafted cationic hydrogels in an environment of changing pH. *Biomaterials* 21:1439–1450
- Owens DE, Peppas NA (2006) Opsonization, biodistribution, and pharmacokinetics of polymeric nanoparticles. *Int J Pharm* 307(1):93–102
- Karmalkar RN, Premnath V, Kulkarni MG, Mashelkar RA (2000) Switching biomimetic hydrogels. *Proc R Soc Lond, Ser A* 456(1998):1305–1320
- Kost J, Langer R (1992) Responsive polymer systems for controlled delivery of therapeutics. *Trends Biotechnol* 10(4):127–131
- Traitel T, Goldbart R, Kost J (2008) Smart polymers for responsive drug-delivery systems. *J Biomater Sci Polym Ed* 19(6):755–767
- Saslavski O, Couvreur P, Peppas NA (1998) In: Heller J, Harris F, Lohmann H, Merkle H, Robinson J (eds) *Controlled release of bioactive materials*, vol 1. Controlled Release Society, Basel, p 26
- Aschkenasy C, Kost J (2005) On-demand release by ultrasound from osmotically swollen hydrophobic matrices. *J Control Release* 110(1):58–66
- Kwok C, Mourad P, Crum L, Ratner B (2001) Self-assembled molecular structures as ultrasonically-responsive barrier membranes for pulsatile drug delivery. *J Biomed Mater Res* 57:151–164
- Norris P, Noble M, Francolini I, Vinogradov AM, Stewart PS, Ratner BD, Costerton JW, Stoodley P (2005) Ultrasonically controlled release of ciprofloxacin from self-assembled coatings on poly(2-hydroxyethyl methacrylate) hydrogels for *Pseudomonas aeruginosa* biofilm prevention. *Antimicrob Agents Chemother* 49:4272–4279
- Osada Y, Okuzaki H, Hori H (1992) A polymer gel with electrically driven motility. *Nature* 355:242–244
- Eddington DT, Beebe DJ (2004) Flow control with hydrogels. *Adv Drug Deliv Rev* 56(2):199–210
- Basseti MJ, Chatterjee AN, De SK, Aluru NR, Beebe DJ (2005) Development and modeling of electrically triggered hydrogels for microfluidic applications. *J Microelectromech Syst* 14(5):1198–1207
- West J (2003) Drug delivery – pulsed polymers. *Nat Mater* 2(11):709–710
- Mamada A, Tanaka T, Kungwachakun D, Irie M (1990) Photoinduced phase transition of gels. *Macromolecules* 23(5):1517–1519
- Lee JK, Lee H, Jang E, Lee SD, Kim SJ (2005) Photo-triggering of the membrane gates in photo-responsive polymer for drug release. In: *Engineering in medicine and biology society. 27th Annual International Conference of the IEEE-EMBS. Shanghai, China*, pp 5069–5072
- Suzuki A, Tanaka T (1990) Phase transition in polymer gels induced by visible light. *Nature* 346:345–347
- Lendlein A, Jiang H, Junger O, Langer R (2005) Light-induced shape-memory polymers. *Nature* 434(7035):879–882
- Matsumoto S, Yamaguchi S, Ueno S, Komatsu H, Ikeda M, Ishizuka K, Iko Y, Tabata KV, Aoki H, Ito S, Noji H, Hamachi I (2008) Photo gel-sol/sol-gel transition and its patterning of a supramolecular hydrogel as stimulus-responsive biomaterials. *Chem Eur J* 14(13):3977–3986
- Yamaguchi S, Matsumoto S, Ishizuka K, Iko Y, Tabata KV, Arata HF, Fujita H, Noji H, Hamachi I (2008) Thermally responsive supramolecular nanomeshes for on/off switching of the rotary motion of F_1 -ATPase at the single-molecule level. *Chem Eur J* 14:1891–1896
- Kim JH, Lee TR (2008) Thermo-responsive hydrogel-coated gold nanoshells for in vivo drug delivery. *J Biomed Pharm Eng* 2(1):29–35
- Owens DE, Jian YC, Fang JE, Slaughter BV, Chen YH, Peppas NA (2007) Thermally responsive swelling properties of polyacrylamide/poly(acrylic acid) interpenetrating polymer network nanoparticles. *Macromolecules* 40:7306–7310

31. Owens DE, Eby JK, Jian Y, Peppas NA (2007) Temperature-responsive polymer-gold nanocomposites as intelligent therapeutic systems. *J Biomed Mater Res* 83A:692–695
32. Dai H, Chen Q, Qin H, Guan Y, Shen D, Hua Y, Tang Y, Xu J (2006) A temperature-responsive copolymer hydrogel in controlled drug delivery. *Macromolecules* 39(19):6584–6589
33. Park TG, Hoffman AS (1993) Thermal cycling effects on the bioreactor performances of immobilized beta-galactosidase in temperature-sensitive hydrogel beads. *Enzyme Microb Technol* 15(6):476–482
34. Ehrick J, Deo S, Browning T, Bachas L, Madou M, Daunert S (2005) Genetically engineered protein in hydrogels tailors stimuli-responsive characteristics. *Nat Mater* 4(4):298–302
35. Jun HW, Yuwono V, Paramonov SE, Hartgerink JD (2005) Enzyme-mediated degradation of peptide-amphiphile nanofiber networks. *Adv Mater* 17(21):2612–2617
36. Li CM, Madsen J, Armes SP, Lewis AL (2006) A new class of biochemically degradable, stimulus-responsive triblock copolymer gelators. *Angew Chem Int Ed* 45(21):3510–3513
37. Liu RH, Yu Q, Beebe DJ (2001) Fabrication and characterization of hydrogel based microvalves. *J Microelectromech Syst* 11:45–53
38. Beebe DJ, Moore J, Bauer J, Yu Q, Liu RH, Devadoss C, Jo BH (2000) Functional hydrogel structures for autonomous flow control inside microfluidic channels. *Nature* 404:588–590
39. Yu Q, Bauer JM, Moore JS, Beebe DJ (2001) Responsive biomimetic hydrogel valve for microfluidics. *Appl Phys Lett* 78:2589–2591
40. Zourob M, Gough JE, Ulijn RV (2006) A micropatterned hydrogel platform for chemical synthesis and biological analysis. *Adv Mater* 18(5):655–659
41. Hall H, Hubbell JA (2005) Modified fibrin hydrogels stimulate angiogenesis in vivo: potential application to increase perfusion of ischemic tissues. *Materwiss Werksttech* 36(12):768–774
42. Silva GA, Silva GA, Czeisler C, Niece KL, Beniash E, Harrington DA, Kessler JA, Stupp SI (2004) Selective differentiation of neural progenitor cells by high-epitope density nanofibers. *Science* 303:1352–1355
43. Vemula PK, Cruikshank GA, Karp JF, John G (2009) Self-assembled prodrugs: an enzymatically triggered-drug delivery platform. *Biomaterials* 30:383–393
44. Plunkett KN, Berkowski KL, Moore JS (2005) Chymotrypsin responsive hydrogel: application of a disulfide exchange protocol for the preparation of methacrylamide containing peptides. *Biomacromolecules* 6(2):632–637
45. Lee MR, Baek KH, Jin HJ, Jung YG, Shin I (2004) Targeted enzyme-responsive drug carriers: studies on the delivery of a combination of drugs. *Angew Chem Int Ed* 43(13):1675–1678
46. van Bommel KJC, Stuart MCA, Feringa BL, van Esch J (2005) Two-stage enzyme mediated drug release from LMWG hydrogels. *Org Biomol Chem* 3(16):2917–2920
47. Kumashiro T, Ooya T, Yui N (2004) Dextran hydrogels containing poly(*N*-isopropyl acrylamide) as grafts and cross-linkers exhibiting enzymatic regulation in a specific temperature range. *Macromol Rapid Commun* 25:867
48. Gupta P, Vermani K, Garg S (2002) Hydrogels: from controlled release to pH-responsive drug delivery. *Drug Discov Today* 7(10):569–579
49. Peppas NA, Wood KM, Blanchette JO (2004) Hydrogels for oral delivery of therapeutic proteins. *Expert Opin Biol Ther* 4(6):881–887
50. Sánchez-Chávez IY, Martínez-Chapa SO, Peppas NA (2008) Computer evaluation of hydrogel-based systems for diabetes closed Loop treatment. *AIChE J* 54(7):1901–1911
51. Lee SH, Eddington DT, Kim YM, Kim W, Beebe DJ (2003) Control mechanism of an organic self-regulating microfluidic system. *J Electromech Syst* 12(6):848–854
52. Agarwal AK, Dong L, Beebe DJ, Jiang H (2007) Autonomously-triggered microfluidic cooling using thermo-responsive hydrogels. *Lab Chip* 7(3):310–315
53. Miyata T, Asami N, Uragami T (1999) A reversibly antigen-responsive hydrogel. *Nature* 399:766–769
54. Nakayama G, Roskos K, Fritzing B, Heller J (1995) A study of reversibly inactivated lipases for use in a morphine-triggered naltrexone delivery system. *J Biomed Mater Res* 29:1389–1396
55. Duncan R (2003) The dawning era of polymer therapeutics. *Nat Rev Drug Discov* 2(5):347–360
56. Farmer TG, Edgar TF, Peppas NA (2008) In vivo simulations of the intravenous dynamics of submicrometer particles of pH-responsive cationic hydrogels in diabetic patients. *Ind Eng Chem Res* 47(24):10053–10063
57. Sanchez-Chávez IY, Morales-Menéndez R, Martínez-Chapa SO (2009) Glucose optimal control system in diabetes treatment. *Appl Math Comput* 209(1):19–30
58. Parker RS, Doyle FJ III, Ward JH, Peppas NA (2000) Robust H_{∞} glucose control in diabetes using a physiological model. *AIChE J* 46:2537–2549
59. Parker R, Doyle F III, Peppas NA (1999) Model-based algorithm for blood glucose control in type I diabetic patients. *IEEE Trans Biomed Eng* 46(2):148–157
60. Zhang K, Wu X (2002) Modulated insulin permeation across a glucose-sensitive polymeric composite membrane. *J Control Release* 80:169–178
61. Cheng SY, Constantinidis I, Sambanis A (2006) Use of glucose-responsive material to regulate insulin release from constitutively secreting cells. *Biotechnol Bioeng* 93(6):1079–1088

Biomolecule-Responsive Hydrogels

Takashi Miyata

Abstract Biomolecule-responsive hydrogels that exhibit volume changes in response to target biomolecules have become increasingly important because of their potential applications as smart biomaterials. Researchers are developing novel biomedical systems using glucose, proteins and other biomolecule-responsive hydrogels as biosensing systems for applications such as drug delivery and cell culture systems. In the synthesis of biomolecule-responsive hydrogels, both biomolecular recognition and responsive functions that perceive a target biomolecule and induce structural changes must be introduced into the hydrogels network. Many biomolecule-responsive hydrogels are prepared by combining structural designs of hydrogels networks with molecular recognition events of biomolecules, such as enzymes, lectins and antibodies. Most important is the need to synthesize and develop more biomolecule-responsive hydrogels in tandem with their biomedical applications so that the field continues to evolve.

Introduction

Hydrogels are attractive soft materials consisting of physically or chemically cross-linked polymer networks and large amounts of aqueous solutions. Since hydrogels have a variety of fascinating properties; swelling properties, mechanical properties, permeation properties, surface properties, and optical properties. They have been already utilized as adsorbents, chromatography columns, contact lenses, foods, and industrial materials [1–3]. In addition, some hydrogels have a unique property in that they undergo abrupt changes in their volume in response to environmental changes, such as pH and temperature [4–7]. Such unique hydrogels are named stimuli-responsive hydrogels, intelligent hydrogels or smart hydrogels. Stimuli-responsive hydrogels are fascinating materials for mimicking natural feedback systems because they can sense a stimulus as a signal and induce volume changes. Therefore, stimuli-responsive hydrogels are very suitable materials for designing smart systems in the biochemical and biomedical fields; they can be utilized as switches, sensors, actuators, bio-reactors, separation systems, drug delivery systems, and cell culture systems.

Many researchers have prepared various types of stimuli-responsive hydrogels that undergo volume changes in response to environmental changes such as pH [8, 9], temperature [10–14], electric field [15, 16], and light [17, 18]. The pH-responsive hydrogels are usually formed from polymers with carboxyl or amino groups that can carry charge in response to pH changes [19–24]. Some polymers have lower critical solution temperature (LCST), such as poly(*N*-alkylacrylamide), poly(vinyl methyl ether), poly(ethylene oxide)-poly(propylene oxide)-poly(ethylene oxide); they are unique polymers whose solubility in water changes drastically at their LCST. Hydrogels with these polymers as main chains exhibit abrupt volume changes in response to temperature [25–29]. These pH- and temperature-responsive hydrogels

T. Miyata • Department of Chemistry and Materials Engineering, Kansai University,
Suita, Osaka, 564-8680 Japan
e-mail: tmiyata@kansai-u.ac.jp

are effective biomaterials for constructing self-regulating drug delivery systems, cell culture systems, and diagnostic signals for monitoring physiological changes.

Most biosystems are closely associated with a natural feedback system, such as homeostasis. These natural feedback systems perceive specific ions or biological molecules like enzymes and hormones, and induce conformational changes that rearrange their constitutional biomolecules to elicit biological responses. For example, they respond to the presence of specific molecules as well as physicochemical and environmental changes like pH and temperature. Therefore, stimuli-responsive hydrogels that respond to specific biomolecules (biomolecule-responsive hydrogels) are required to develop self-regulating systems by mimicking natural feedback signals. Specific biomolecules, such as a tumor marker, give important signals for monitoring living biological systems and stimuli-responsive hydrogels that can recognize these target biomolecules are very useful for fabricating molecular diagnostics systems and self-regulating drug delivery systems. For example, the stimuli-responsive hydrogels that undergo volume changes in response to blood glucose concentrations can self-regulate insulin delivery in the amount of insulin necessary. There are several biomolecule-responsive hydrogels that exhibit swelling/shrinking changes in response to target biomolecules and so provide the potential for many bioapplications, such as smart devices in sensing systems and molecular diagnostics [30, 31].

Glucose-Responsive Hydrogels

Insulin, which is secreted from the Islets of Langerhans of the pancreas, controls glucose metabolism. The inability of the pancreas to control blood glucose concentrations is the cause of diabetes. To treat diabetes, specific amounts of insulin are administered along with close monitoring of the blood glucose concentration. Consequently, glucose-responsive hydrogels are attractive candidates as an artificial pancreas to control the administration of insulin in response to the blood glucose levels. A typical glucose-responsive insulin release system is illustrated in Fig. 1. Currently, there are three different types of strategies used for glucose-responsive hydrogels to self-regulate insulin release.

Glucose-Responsive Hydrogels Using Glucose Oxidase

The combination of an enzymatic reaction of glucose oxidase with the pH-responsive swelling/shrinking behavior of polyelectrolyte hydrogels is the most common approach. The glucose-responsive hydrogels regulate insulin release by changing the pH environment in response to the

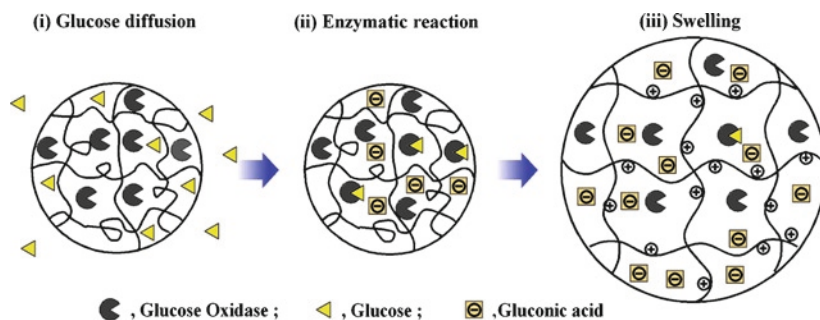


Fig. 1. Schematic representation of the glucose-responsive hydrogels consisting of pH-responsive networks and glucose oxidase.

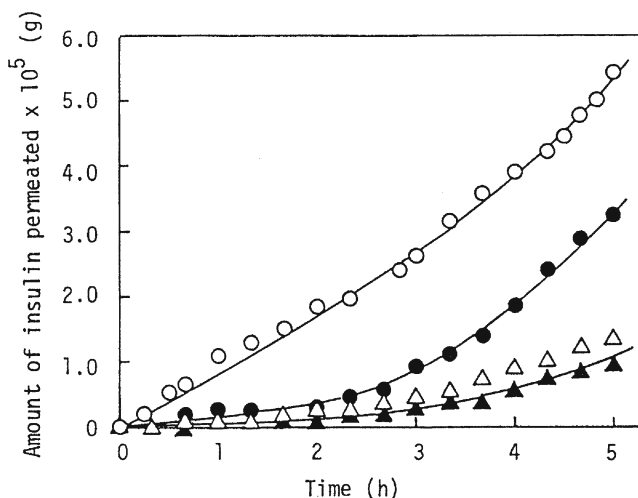


Fig. 2. Permeation profile of insulin through a glucose-responsive polymer membrane consisting of a poly(amine) and glucose oxidase-immobilized hydrogels. Glucose concentration: (filled triangle) 0 M; (filled circle) 0.1 M; (open circle) 0.2 M; (open triangle) 0.2M without glucose oxidase [32].

glucose levels in the blood; the pH-responsive hydrogels respond to the environmental changes, followed by swelling or shrinking accordingly to control the rate of insulin release.

Basically, the glucose oxidase-loaded hydrogels convert glucose to gluconic acid which lowers the pH within the hydrogel. The lower pH causes the pH-responsive hydrogels networks to be expanded and allow insulin to permeate into the blood through the networks; thus enabling self-regulated insulin release in response to the glucose concentration.

A glucose-responsive insulin release system using a copolymer of *N,N*-diethylaminoethyl methacrylate (DEA) and 2-hydroxypropyl methacrylate (HPMA) as the pH-responsive polymer was reported, in which glucose oxidase was loaded in a DEA-HPMA composite membrane to sense glucose [32]. The presence of glucose enhanced the insulin permeability through the glucose oxidase-loaded DEA-HPMA copolymer membranes (Fig. 2). As the glucose diffuses into the copolymer membranes, it is converted to gluconic acid by the glucose oxidase; the gluconic acid decreases the pH and induces the copolymer membranes to swell and to release insulin. In addition, glucose-responsive polymer capsules containing insulin were prepared by a conventional interfacial precipitation [33]. The steady-state behavior of the glucose-responsive hydrogels membrane prepared by entrapping the glucose oxidase within the DEA-hydroxyethyl methacrylate copolymer matrix was investigated from both theoretical and experimental view points [34–36].

The complex formed between methacrylic acid (MAAc) and ethylene glycol (EG) was utilized to form a pH-responsive hydrogels network to prepare glucose-responsive hydrogels [37, 38]. The poly(MAAc-EG) hydrogel's pH-responsive swelling/shrinking behavior responded to the pH changes elicited by the gluconic acid generated based on the amount of glucose converted by the glucose oxidase. The swelling of the glucose oxidase-loaded hydrogels at high glucose (hyperglycemic conditions) was greater than at low glucose concentrations.

Glucose-Responsive Hydrogels Using Phenylboronic Acid

Phenylboronic acid and its derivatives recognize glucose as they form complexes with polyol compounds. These complexes are dissociated in the presence of competing polyol compounds that have a stronger affinity for phenylboronic acid. Totally synthetic hydrogels

with glucose-responsivity were prepared based on the complex that forms between phenylboronic acid and a polyol compound. For example, a complex readily forms between poly(vinyl alcohol) (PVA) and a copolymer of *N*-vinyl-2-pyrrolidone (NVP) and 3-(acrylamide) phenylboronic acid (PBA). A glucose-responsive insulin delivery system was derived by using the complex formation between PVA and poly(NVP-co-PBA), which dissociates in the presence of free glucose [39, 40].

The strategy involved combining the glucose recognition function of phenylboronic acid with temperature-responsive PNIPAAm to form glucose-responsive hydrogels. The dissociation of phenylboronic acid moiety is in equilibrium between the uncharged (nonionic) and the charged (ionic) form (Fig. 3); since glucose forms a complex with the charged phenylboronic acid more readily than with the uncharged form, the presence of glucose leads to an increase in charged form and a decrease in uncharged form due to a shift in the dissociation equilibrium of the phenylboronic acid. Therefore, the solubility of PNIPAAm copolymers with phenylboronic acid groups is greatly enhanced by the presence of glucose due to a shift in the LCST by increasing number of charges. For example, LCST of the copolymer of NIPAAm and 3-(acrylamido)phenylboronic acid (APBA) is shifted to a higher temperature in the presence of free glucose, based on the shift in the dissociation equilibrium of phenylboronic acid due to complex formations with glucose [41].

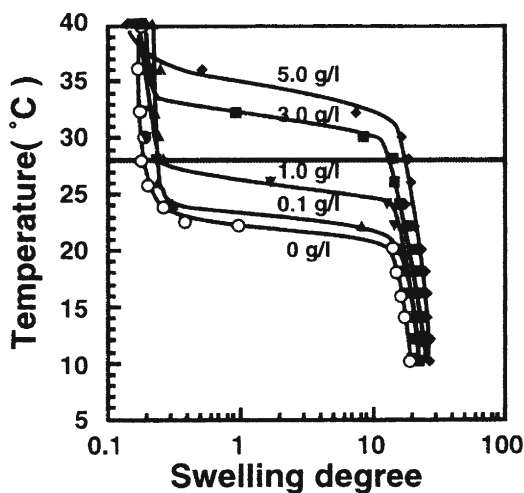
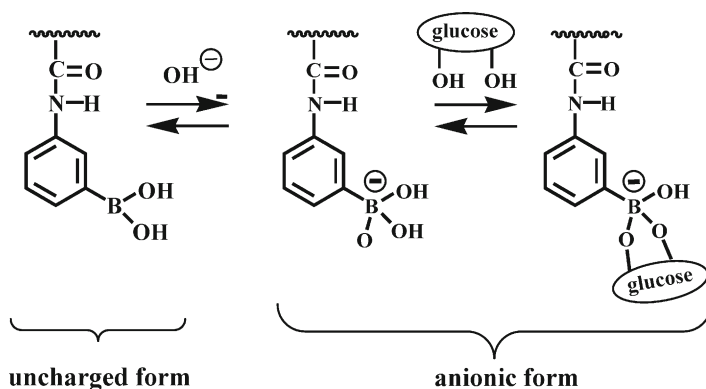


Fig. 3. Temperature dependence of swelling curves for PNIPAAm copolymer hydrogels with phenylboronic acid moieties at different glucose concentrations [42].

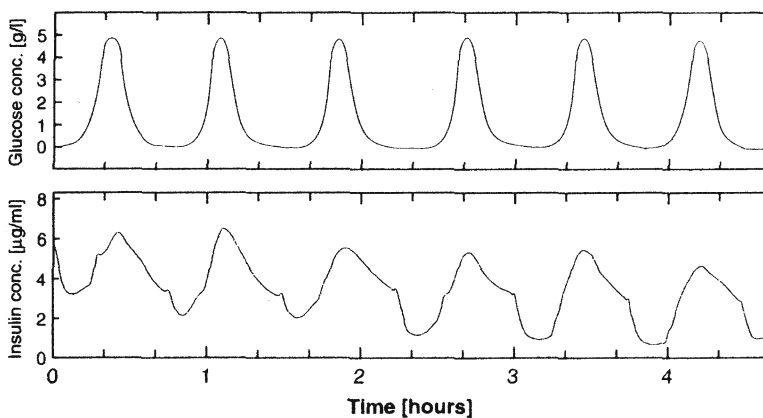


Fig. 4. Repeated on–off release of FITC-insulin from the glucose-responsive hydrogels at 28°C, pH 9.0, in response to external glucose concentration [42].

Some glucose-responsive insulin release systems focus on glucose-responsive LCST changes of PNIPAAm copolymer with phenylboronic acid. Totally synthetic hydrogels showing glucose-responsive volume changes were prepared by copolymerization of NIPAAm and monomeric phenylboronic acid [42, 43]. The LCST of these NIPAAm–APBA hydrogels in the presence of free glucose was higher than that in its absence (Fig. 3). Therefore, the NIPAAm–APBA hydrogels swell in response to free glucose at a constant temperature between LCSTs in the presence and absence of glucose. Insulin was not released from the hydrogels in a buffer solution without glucose but a remarkable insulin release took place for the hydrogels immersed in a solution with glucose. Repeated on–off release of insulin on changing the concentration of external glucose was achieved by using the NIPAAm–APBA hydrogels (Fig. 4). In addition, the hydrogels that exhibit glucose-responsive swelling/shrinking changes under physiological conditions (pH and temperature) were prepared by copolymerizing an APBA derivative with a low pKa and a monomer with a higher LCST than that of PNIPAAm [44]. These results indicate that glucose-responsive hydrogels can be developed by combining the glucose recognition features of phenylboronic acid with the temperature-responsive behavior of PNIPAAm derivatives without any biological components, such as glucose oxidase.

Glucose-Responsive Hydrogels Using Lectin

Lectins are carbohydrate-binding proteins that form complexes with carbohydrate chains of glycoproteins and glycolipids on the cell surface. Lectins are used to fabricate sensing systems based on this unique property of carbohydrate recognition. For example, glucose-responsive insulin systems control the release of glycosylated insulin by lectin-binding in response to free glucose using the competitive and complementary binding properties of glycosylated insulin and glucose to lectins [45–48].

Saccharide-responsive hydrogels are prepared by combining the carbohydrate-binding ability of concanavalin A (Con.A), which is a lectin that recognizes glucose and mannose, with temperature-responsive PNIPAAm [49]. The LCST of the Con.A-loaded PNIPAAm hydrogels is shifted by complex formation between Con.A and the ionic saccharide, dextran sulfate. The Con.A-loaded PNIPAAm hydrogels swells dramatically in the presence of the ionic saccharide dextran sulfate because the LCST is increased by incorporating ionized

saccharide in the hydrogels. The hydrogels collapse to its native volume by replacing the ionic saccharide dextran sulfate with the nonionic saccharide. Thus, the Con.A-loaded PNIPAAm hydrogels can undergo abrupt volume changes in response to ionized saccharide based on the combination of carbohydrate-binding property of Con.A with the temperature-responsive property of PNIPAAm.

Some polymers modified with pendant saccharides have been synthesized as potential biomaterials for biochemical and biomedical applications [50]. These pendant-saccharide polymers form complexes with lectins but the complexes are inhibited by the presence of saccharide which has a stronger affinity for lectin. For example, the competitive and complementary binding properties of poly(2-glucosyloxyethyl methacrylate) (PGEMA) as a pendant glucose polymer was investigated using Con.A as a lectin [51]. PGEMA formed a complex with Con.A but the resulting PGEMA–Con.A complex dissociated in the presence of free glucose and mannose. Since Con.A forms a complex with glucose and mannose but not with galactose, the PGEMA–Con.A complex does not dissociate in the presence of free galactose. This monosaccharide-responsive behavior of the PGEMA–Con.A complex is useful in fabricating glucose-responsive hydrogels.

Researchers have developed glucose-responsive hydrogels that undergo volume changes in response to glucose concentration by using complexes between lectins and polymer with pendant glucose as reversible crosslinks in their networks. For example, glucose-responsive hydrogels were prepared by copolymerization of a monomer with a pendant glucose (GEMA) and *N,N'*-methylenebisacrylamide (MBAA) after the formation of GEMA–Con.A complex that acted as reversible crosslinks in the networks [52]. The Con.A-entrapped PGEMA hydrogels swelled immediately in a buffer solution containing free glucose and mannose, but did not change volume in a solution containing galactose (Fig. 5). The compressive modulus measurements demonstrated that crosslinking density of the Con.A-entrapped PGEMA hydrogels decreased with increasing glucose concentration in a buffer solution. Therefore, the glucose-responsive swelling behavior of the Con.A-entrapped PGEMA hydrogels is attributed to the dissociation of the complex between Con.A and pendant glucose on GEMA that played an

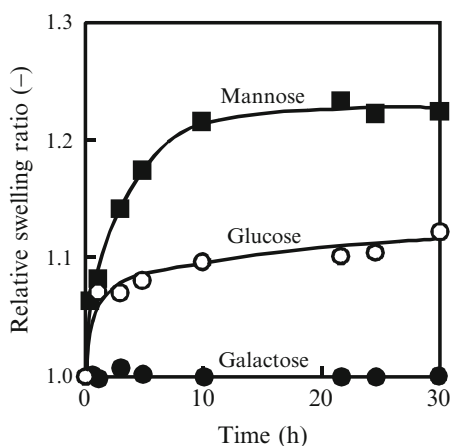


Fig. 5. Swelling ratio changes of PGEMA–Con.A hydrogels as a function of time, when the hydrogels was immersed in a buffer solution containing 1 wt% of monosaccharide: (open circle), glucose; (filled square), mannose; (filled circle) galactose [52].

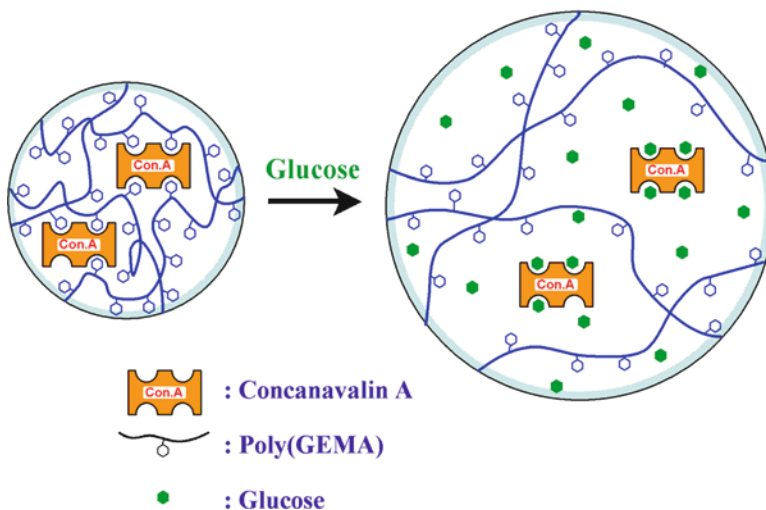


Fig. 6. Schematic representation of glucose-responsive swelling changes of the PGEMA–Con.A hydrogels [52].

important role as reversible crosslinks (Fig. 6). Con.A has a stronger affinity for mannose than glucose and does not have any for galactose. Therefore, the presence of free mannose and glucose induced the dissociation of PGEMA–Con.A complex by competitive complex exchange, while free galactose does not. As a result, the Con.A-entrapped PGEMA hydrogels swell remarkably more in the presence of mannose and glucose as they decrease the crosslinking density, but do not change in the presence of galactose.

To obtain reversible glucose-responsive hydrogels that swell in the presence of free glucose and shrink in its absence, Con.A-copolymerized PGEMA hydrogels were prepared by copolymerizing GEMA with chemically vinyl-modified Con.A [53]. The Con.A-copolymerized PGEMA hydrogels exhibited reversible volume changes in response to stepwise changes in glucose concentration but the Con.A-entrapped hydrogels did not change. The Con.A-entrapped hydrogels did not shrink in the absence of free glucose because the Con.A had leaked out of the hydrogels during the swelling in the presence of free glucose. However, since Con.A in the Con.A-copolymerized PGEMA hydrogels was covalently immobilized in the hydrogels networks, the hydrogels shrank in the absence of glucose due to repeated complex formation between Con.A and pendant glucose on PGEMA.

Sol–gel phase transitions responding to changes in the environmental glucose concentrations were also achieved based on the complex formation between a polymer with pendant glucose and Con.A [54, 55]. The addition of Con.A induced the gelation of aqueous solutions containing a polymer with pendant glucose, such as vinylpyrrolidinone-allylglucose or acrylamide-allylglucose copolymers, and the sol–gel phase transition obtained was strongly dependent upon glucose concentration in the solution. The releases of lysozyme and insulin as model protein drugs were controlled by sol–gel phase transition based on the complex formation between the polymer with pendant glucose and Con.A [56]. The glucose-responsive hydrogels regulated the release of model drugs in response to the glucose concentration. Thus, smart systems, such as self-regulated drug release systems that regulate insulin release in response to environmental glucose concentration, can be fabricated by using the complex formation and dissociation between Con.A and polymers with pendant glucose groups.

Protein-Responsive Hydrogels

Enzyme-Responsive Hydrogels

Some enzymes give important diagnostic signals for several physiological changes. Enzymes located in specific areas of the body can also provide signals for site-specific drug delivery. Therefore, enzyme-responsive hydrogels that undergo changes triggered by selective enzyme catalysis can be utilized as smart materials to monitor physiological changes or direct drugs to a specific site. In order to develop enzyme-responsive hydrogels, some researchers have focused on enzymatic activity followed by structural changes of hydrogels networks [57]. Biodegradable polymers are promising candidates for preparing enzyme-responsive hydrogels since they are degraded by specific enzymes.

The microbial enzymes localized predominantly in the colon have been used as promising markers for drug delivery to the colon. Colon-specific drug is conjugated via azoaromatic bonds to construct the delivery systems since these bonds are degraded by azoreductase, an enzyme produced by the microbial flora of the colon, to release the drug [58–63]. The copolymer hydrogels, prepared with acrylamide derivatives, acrylic acid and crosslinker with azoaromatic bonds, swell at high pH and shrink at low pH; protein drugs loaded in this hydrogels are protected against digestion by proteolytic enzymes in the stomach (low pH). In the colon, azoreductase is accessible to the azoaromatic crosslinks due to swelling of the hydrogels and to degrade the hydrogels networks to release drug release.

Dextranases are microbial enzymes that exist in the colon; as smart biomaterials for achieving colon-specific drug delivery, dextranase-responsive hydrogels were prepared by crosslinking of dextran with diisocyanate [64]. These dextran hydrogels were degraded *in vitro* (in a human colonic fermentation model) and *in vivo* (in rats).

Tetrapeptide sequence, Cys-Tyr-Lys-Cys, as a crosslinker was used to create poly(acrylamide) hydrogels that degrade when subjected to α -chymotrypsin [65]. The chemoselective conjugations of methacrylamide containing peptides were made for more advanced protease-responsive hydrogels applications. A new type of disulfide-based thermo-responsive triblock copolymer was also synthesized by atom transfer radical polymerization (ATRP) of 2-(methacryloyloxy)ethyl phosphorylcholine (MPC) and NIPAAm using the disulfide-based initiator [66]. The cleavage of the central disulfide bond induced irreversible dissolution of the micellar gels.

Monitoring two or more enzymes simultaneously to sense physiological changes would allow clinical screening for several diseases at the same time. Dual-stimuli-responsive hydrogels, which degrade in the presence of two enzymes, papain and dextranase, were prepared as an interpenetrating polymer network (IPN) hydrogels of oligopeptide-terminated poly(ethylene glycol) (PEG) and dextran that can be degraded by papain and dextranase, respectively [67, 68]. The presence of both papain and dextranase induced the degradation of the PEG/dextran IPN hydrogels, but the presence of one of the two enzymes did not result in degradation (Fig. 7). Furthermore, the gelatin/dextran IPN hydrogels released lipid microspheres in the presence of both α -chymotrypsin and dextranase but did not in the presence of either enzyme alone (Fig. 8). Dual-stimuli-responsive hydrogels that degrade in the presence of a specific enzyme within a certain temperature range were also prepared by combining PNIPAAm temperature responsiveness with enzymatic biodegradation [69, 70]. The temperature-responsive biodegradation of the hydrogels was based on the effect of network structural changes, caused by PNIPAAm temperature responsiveness, on the formation of the enzyme-substrate complex.

A enzyme-responsive hydrogels formation was achieved by crosslinking functionalized PEG and a lysine-containing polypeptide through the action of transglutaminase (TGase) that

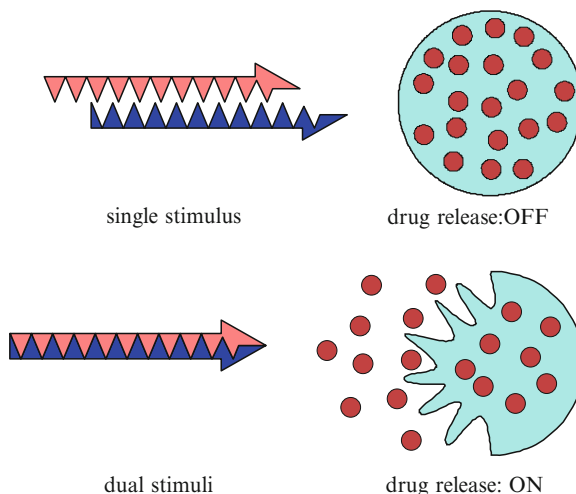


Fig. 7. Concept of dual-stimuli-responsive drug release by IPN-structured hydrogels [68].

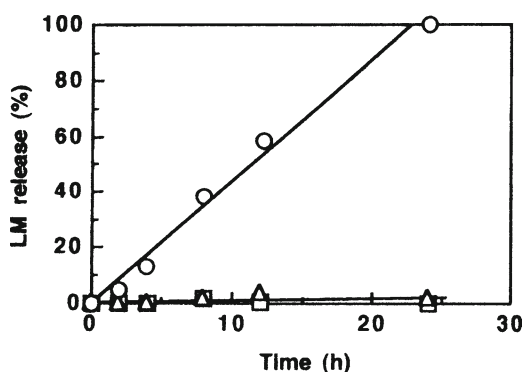


Fig. 8. Lipid microsphere release from gelatin/dextran IPN hydrogels in phosphate buffer at 37°C. *Open circle*, 5 U/ml α -chymotrypsin+0.5 U/ml dextranase; *open triangle*, 5 U/ml α -chymotrypsin; *open square*, 0.5 U/ml dextranase [68].

catalyzes an acyl-transfer reaction between the γ -carboxamide of protein-bound glutamyl residues and the ϵ -amino group of Lys residues [71, 72]. Short peptide substrates of TGase provide enzyme-responsive gelation of polymer-peptide conjugates within the few minutes, which is for many medical applications.

Chemically crosslinked polyethylene glycol acrylamide hydrogels that are enzyme-responsive and swell/collapse in response to specific proteases are very interesting [73]. These enzyme-responsive hydrogels are programmable to respond uniquely to target enzymes by selection of appropriate enzyme cleavable linkers. Enzyme-responsive hydrogels that exhibited selective, enzyme-triggered, charge-induced polymer swelling were prepared to release dextran and protein from the hydrogels [74] (Fig. 9). The enzyme-responsive hydrogels, with the zwitterionic peptide linkers that are hydrolyzed by specific enzyme, swelled due to doubly charged peptide fragments produced by the enzymatic hydrolysis. These enzyme-responsive hydrogels have applications in selective therapeutic release at specifically targeted enzyme locations.

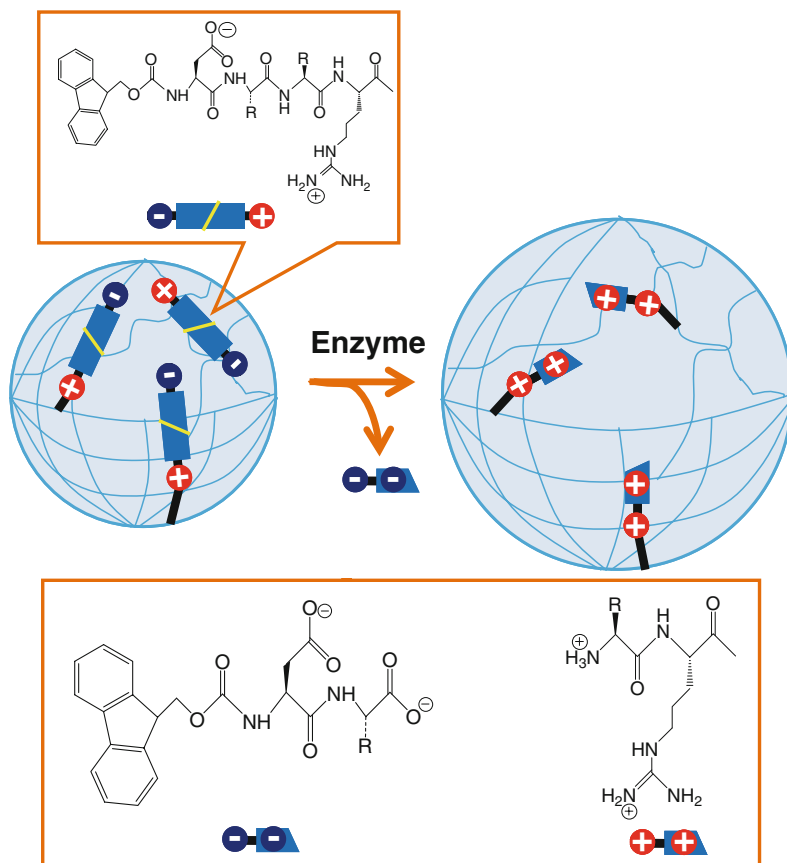


Fig. 9. Schematic representation of selective enzyme-triggered charge-induced swelling of the enzyme-responsive hydrogels with the zwitterionic peptide linkers that are hydrolyzed by specific enzyme [74].

Antigen-Responsive Hydrogels

An antibody recognizes a specific antigen and forms an antigen–antibody binding through multiple noncovalent bonds, such as electrostatic, hydrogen, hydrophobic, and van der Waals interactions. The specificity and versatility of antibodies provide the basis for immunological assays to detect and signal physiological changes to specific biomolecules [75]. Antigen-responsive hydrogels were prepared to recognize a target antigen and induce the volume changes of the hydrogels.

The first antigen-responsive hydrogels were designed to swell in response to a target antigen. Using rabbit IgG as the antigen and goat anti-rabbit IgG (GAR IgG) as the antibody, an antigen–antibody binding hydrogels network was constructed with reversible crosslinks. The antigen–antibody entrapped hydrogels were prepared by copolymerizing rabbit IgG with polymerizable groups, acrylamide (AAM) and *N,N'*-methylenebisacrylamide (MBAA) in the presence of GAR IgG, whose antigen–antibody binding form crosslinks [76]. The antigen–antibody entrapped hydrogels swell in a buffer solution containing rabbit IgG as a target antigen and the swelling ratio is directly dependent upon the antigen concentration of the buffer solution.

The application of stimuli-responsive hydrogels requires reversible behavior in response to environmental stimuli changes. Therefore, reversibly antigen-responsive hydrogels that undergo reversible swelling/shrinking changes in response to a target antigen were developed by forming a semi-interpenetrating polymer network (semi-IPN) composed of linear PAAm grafted with antibodies (GAR IgG) and PAAm networks grafted with antigen (rabbit IgG). The complexes that form between the grafted antibodies and grafted antigens act as reversible crosslinks (Fig. 10) [77]. The antigen-antibody semi-IPN hydrogels, in the presence of rabbit IgG as a target antigen in a buffer solution, drastically increase their swelling ratio but do not change their swelling ratio in the presence of goat IgG. Furthermore, the antigen-antibody semi-IPN hydrogels swell immediately in the presence of rabbit IgG and shrank in its absence, when their hydrogels were immersed in a buffer solution with and without

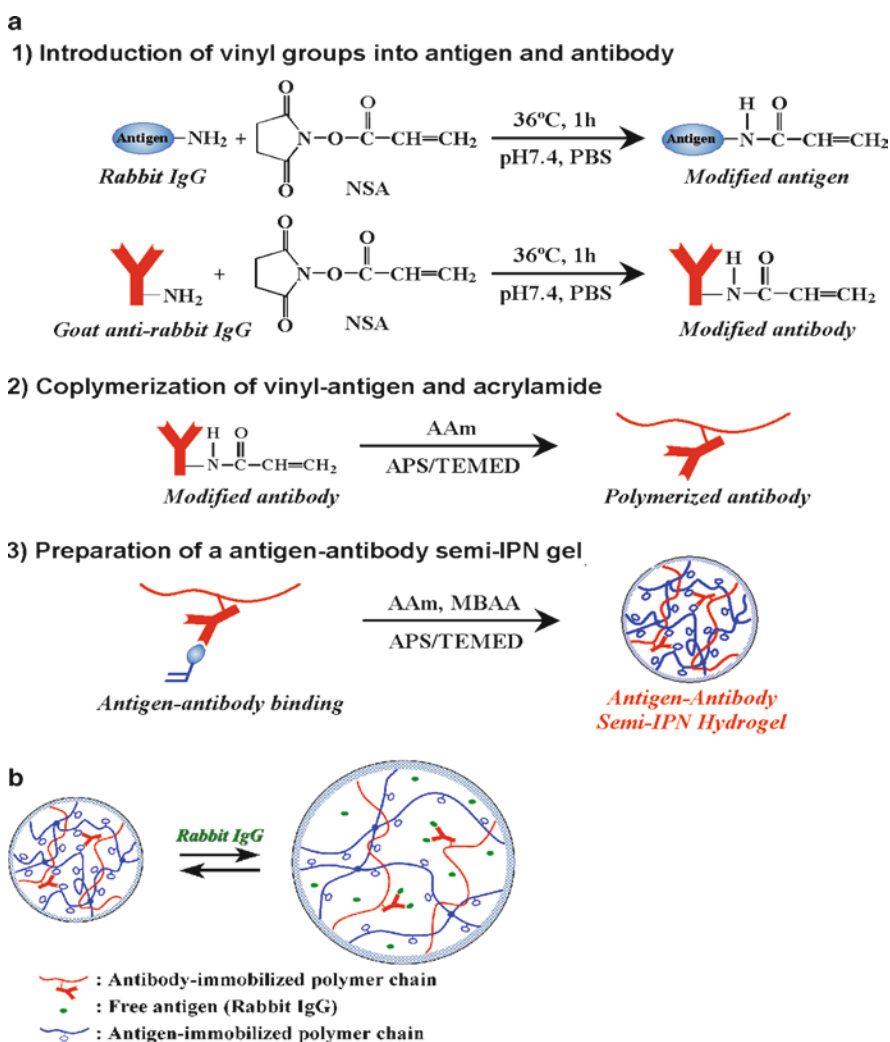


Fig. 10. Schematic representation of the preparation (a) and responsive behavior (b) of an antigen-responsive hydrogels with a semi-IPN structure [77].

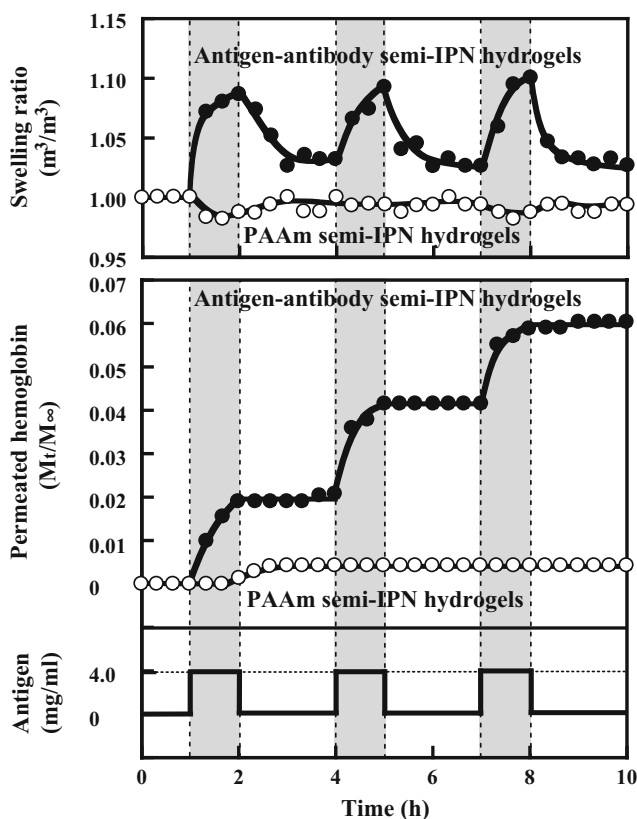


Fig. 11. Reversible swelling changes and antigen-responsive permeation profiles of hemoglobin, through the PAAm semi-IPN hydrogels (*open circle*) and the antigen-antibody semi-IPN hydrogels (*filled circle*) in response to stepwise changes in the antigen concentration between 0 and 4 mg/ml [77].

rabbit IgG (Fig. 11). These reversible antigen-responsive volume changes are due to reversible changes in the crosslinking density caused by the formation and dissociation of the binding between grafted antigen and grafted antibody in the absence and presence of a free antigen, respectively (Fig. 10b). These results suggest that the antigen-antibody semi-IPN hydrogels can recognize only rabbit IgG and induce reversibly responsive volume change.

Biomolecule-responsive hydrogels are used for self-regulated drug delivery systems in which drugs are administered in response to specific physiological changes. Antigen-responsive drug release systems were constructed using antigen-antibody semi-IPN hydrogels as smart devices for self-regulated drug delivery [77]. The drug permeates through the antigen-antibody semi-IPN hydrogels in the presence of a target antigen but not in its absence (Fig. 11). The antigen-antibody semi-IPN hydrogels controls drug permeation in response to changes in the target antigen concentration. Thus, reversibly antigen-responsive hydrogels are effective as smart devices to modulate drug release in response to a specific antigen and physiological changes.

Antigen-responsive hydrogels were prepared by the copolymerization of functionalized antibody Fab' fragments with NIPAAm and MBAA [78]. The PNIPAAm hydrogels with Fab' fragments undergo reversible volume changes in alternative incubations with hydrophobic fluorescein and hydrophilic dendrimer-modified fluorescein as target antigens in a buffer solution.

The antigen-responsive swelling/shrinking behavior of the PNIPAAm hydrogels with Fab' fragments was attributed to drastic changes in hydrophilicity of PNIPAAm-based networks by the exchange of Fab' fragment binding between hydrophobic and hydrophilic antigen.

Stimuli-responsive hydrogels microparticles were fabricated as dynamically tunable microlens array using antigen-responsive microlenses, prepared from antigen-antibody bonded microparticles [79–82]. A coulombic assembly of the NIPAAm-AAc hydrogels microparticles was fabricated on a glass substrate after being conjugated with biotin to bind antigen and aminobenzophenone. The antigen-responsive hydrogels microlenses, constructed by using a simple bright field optical microscopic technique, exhibit a difference in appearance in the differential interference contrast (DIC) images in response to a target antigen. These antigen-responsive hydrogels microlens constructs may have applications as a label-free biosensing/bioassay of protein and small molecules.

Other Biomolecule-Responsive Hydrogels

Molecularly Imprinted Hydrogels

Enzymes and antibodies can recognize specific substrate based on fitting guest molecules into molecular cavity. Molecular imprinting is a technique to make biomimetic polymers with molecular cavity as recognition sites [83–89]. After monomers are prearranged around a print molecule by noncovalent interactions and then polymerized, the print molecule is removed from the resulting polymer for leaving a molecular cavity as a recognition site (Fig. 12). The molecularly imprinted polymer can recognize the guest molecule (print molecule) on the basis of a combination of reversible binding and shape complementarity of the cavity. Molecular imprinting is also used to create molecular recognition sites in stimuli-responsive hydrogels.

Temperature-responsive hydrogels consisting of NIPAAm and AAc were prepared in the presence of norephedrine as the print molecule by molecular imprinting [90]. These norephedrine-imprinted hydrogels do not change in the presence of norephedrine when the hydrogels are in the swollen state at a low temperature. However, in the collapsed state at a high temperature, the hydrogels swell gradually with increasing norephedrine concentration but do not with increasing adrenaline concentration (Fig. 13). The norephedrine-responsive swelling behavior of the norephedrine-imprinted hydrogels is due to a shift of LCST by the binding of norephedrine with its recognition site created by molecular imprinting. Other studies revealed that temperature-responsive hydrogels prepared by molecular imprinting can memorize the print molecule in their collapsed states and that undergo their specific volume change in response to the guest molecule [91, 92].

In molecular imprinting, low-molecular-weight monomers with a functional group, such as acrylic acid, are used as ligand monomers for the print molecule. Most molecular imprinting requires a large amount of crosslinkers to fix the structure of the molecular cavity for the print molecule. However, biomolecules such as lectin and antibody can be utilized as

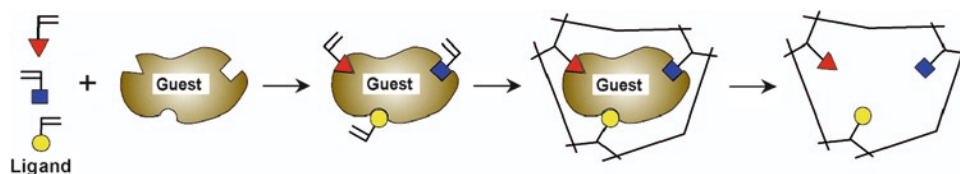


Fig. 12. Schematic illustration of molecular imprinting in a hydrogels.

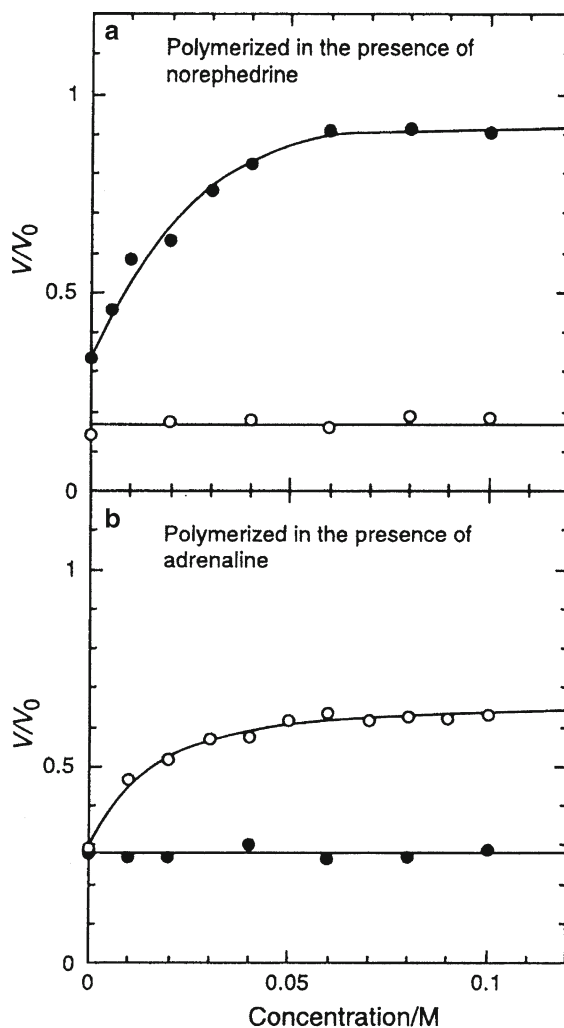


Fig. 13. Equilibrium swelling ratios at 50°C as a function of concentration of either norephedrine (*filled circle*) or adrenaline (*open circle*) in water for molecular recognition hydrogels prepared in the presence of norephedrine (a) and adrenaline (b) [90].

ligands for a print biomolecule with minute amounts of crosslinkers that enable structural changes in response to a target biomolecule.

α -Fetoprotein (AFP) is a tumor-specific marker glycoprotein widely used for the serum diagnosis of primary hepatoma. To prepare tumor marker-responsive hydrogels in biomolecular imprinting, lectins and antibodies were used as ligands for saccharide and peptide chains of AFP as a print biomolecule, respectively (Fig. 14) [93]. After synthesis of poly(acrylamide) (PAAm)-grafted lectins and acryloyl-antibody, AAm as a main monomer was copolymerized with MBAA as a chemical crosslinker and acryloyl-antibody in the presence of print AFP and PAAm-grafted lectins to form lectin–AFP–antibody complexes. The AFP-imprinted hydrogels were then prepared by removing the print AFP from the resultant networks having lectin–AFP–antibody complexes. The AFP-imprinted hydrogels began to shrink as soon as they were

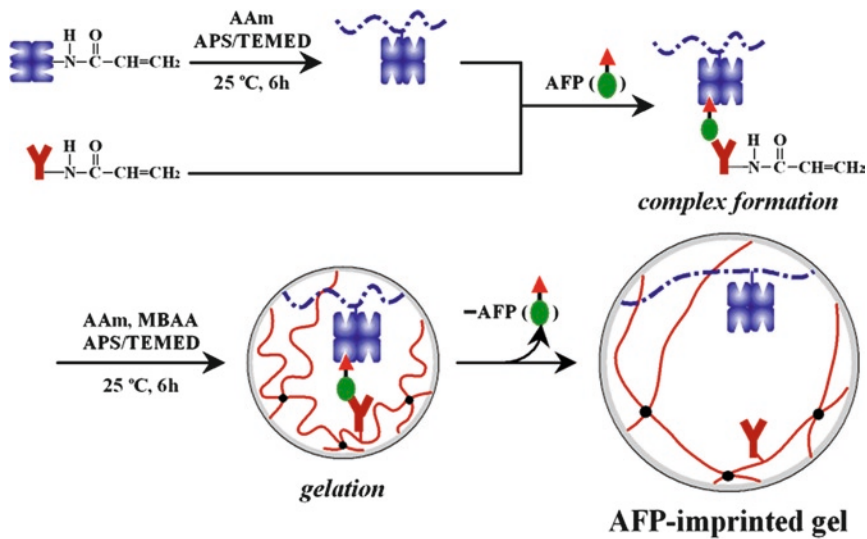


Fig. 14. Synthesis of tumor marker-responsive hydrogels using lectins and antibodies as ligands for print glycoprotein molecules (tumor-specific marker AFP) in biomolecular imprinting [93].

immersed in a phosphate buffer solution containing AFP, but nonimprinted hydrogels prepared without using molecular imprinting experienced slight swelling and PAAm hydrogels exhibited no volume change. The fact that the swelling ratio of AFP-imprinted hydrogels depended on the AFP concentration in a buffer solution means that the hydrogels were tumor marker-responsive hydrogels. The compressive modulus measurements demonstrated that crosslinking density of the AFP-imprinted hydrogels increased gradually with increasing AFP concentration in a buffer solution, but those of the nonimprinted and PAAm hydrogels did not change at all. Biomolecular imprinting enabled the lectins and antibodies as ligands to be organized at optimal positions for the simultaneous recognition of AFP saccharide and peptide chains. Therefore, AFP-responsive shrinking of the AFP-imprinted hydrogels is due to the formation of the sandwich-like lectin–AFP–antibody complexes that played an important role as crosslinks.

Glycoprotein recognition behavior by AFP-imprinted and nonimprinted hydrogels were investigated by measuring their swelling ratios in the presence of AFP or ovalbumin (Fig. 15). Ovalbumin has a saccharide chain similar to AFP, but has a peptide chain different from AFP. The swelling ratio of the nonimprinted hydrogels increased slightly in the presence of AFP and ovalbumin, but immediately shrank in the presence of AFP while swelling slightly in the presence of ovalbumin. These demonstrate that AFP-imprinted hydrogels only shrink when both lectins and antibodies in the hydrogels simultaneously recognize the saccharide and peptide chains of the target glycoprotein. Therefore, swelling or shrinking behaviors of AFP-imprinted hydrogels in the presence of glycoproteins enable the accurate detection and recognition of glycoproteins with a double-lock function. This fascinating behavior of biomolecule-imprinted hydrogels with the accurate detection and recognition of a tumor-specific marker glycoprotein indicates many future opportunities as smart biomaterials for fabricating novel sensor systems and molecular diagnostics.

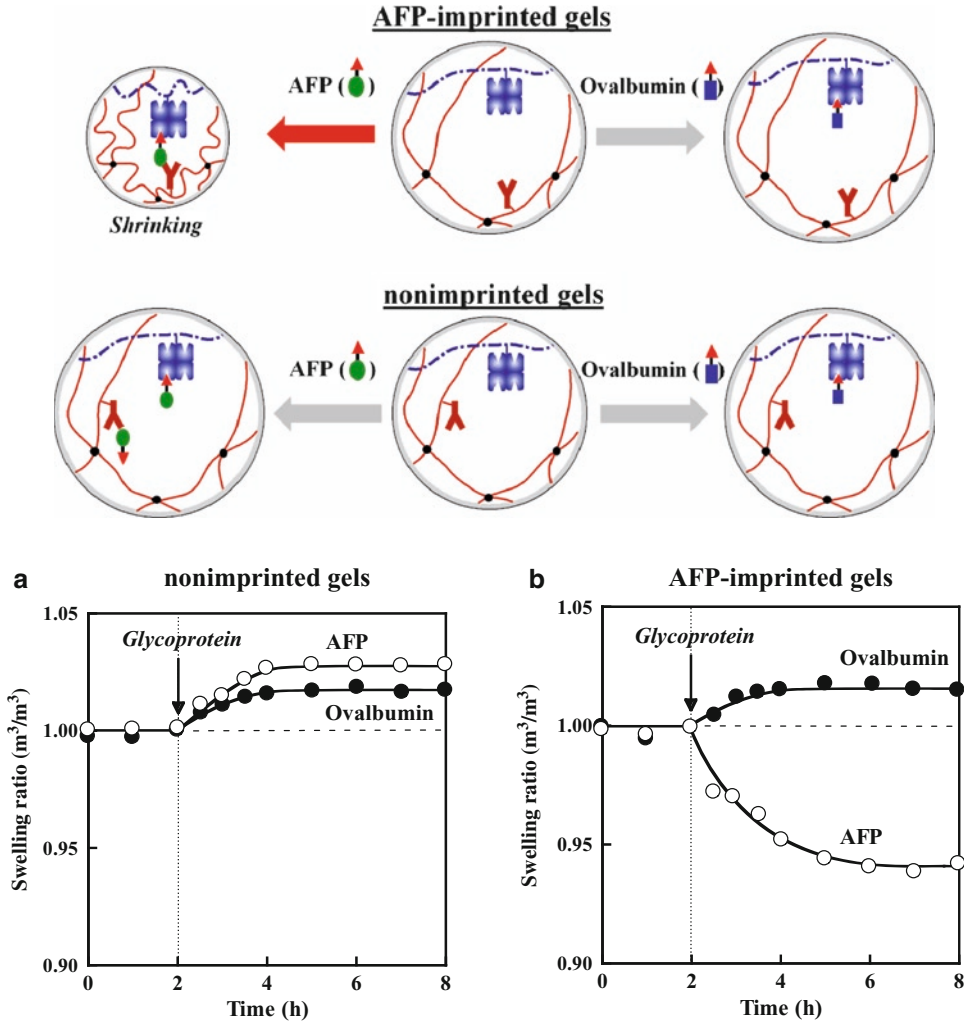


Fig. 15. Swelling ratio changes of nonimprinted hydrogels (a) and AFP-imprinted hydrogels (b) following the addition of AFP (open circle) and ovalbumin (filled circle) after their swelling had attained equilibrium in a phosphate buffer solution at 25°C [93].

Other Biomolecule-Responsive Hydrogels

In addition to glucose-responsive hydrogels and protein-responsive hydrogels, biomolecule-responsive hydrogels undergo structural changes in response to biomolecules such as cell surface receptors and antibiotic drugs as well as DNA. Assembly and erosion profiles of noncovalently associated hydrogels were produced by the interaction of a low-molecular-weight heparin-modified polyethylene glycol star polymer (PEG-LMWH) and a dimeric heparin-binding growth factor (VEGF) (Fig. 16) [94]. The addition of VEGF, which played a key role as a crosslinker, into a phosphate-buffered saline (PBS) of PEG-LMWH immediately formed hydrogels by the complex formation of PEG-LMWH and VEGF. However, selective removal of VEGF crosslinks in the presence of VEGF receptors induced receptor-mediated erosion of the PEG-LMWH/VEGF hydrogels. The VEGF release in response to cell surface receptors

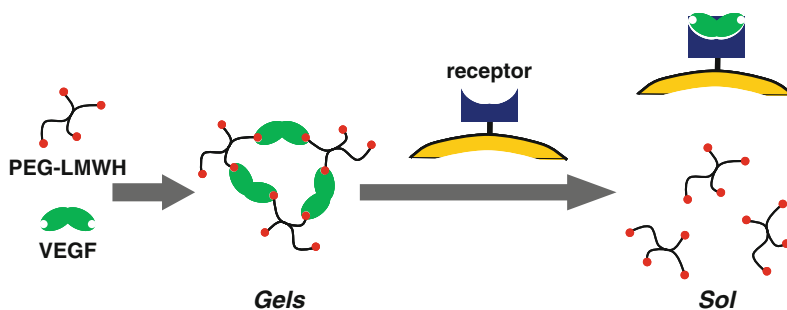


Fig. 16. Schematic representation of hydrogels formation by the crosslinking of heparin-modified star polymer by dimeric, heparin-binding growth factors, followed by receptor-mediated erosion [94].

was achieved by the receptor-mediated erosion of the PEG-LMWH/VEGF hydrogels. Selective release of such growth factors from cell receptor-responsive hydrogels showed potential for use in vascular therapy.

Cell-responsive sol–gel transition systems, made by gelation of multiarmed PEG with an adhesion receptor-binding motif (an adhesion ligand based on the RGD peptide) by the addition of the bis-cysteine peptide crosslinker, are sequence sensitive to matrix metalloproteinases (MMPs), a protease family extensively involved in tissue development and remodeling (Fig. 17) [95, 96]. A Michael-type addition reaction between vinyl sulfone-functionalized multiarmed PEGs and mono-cysteine adhesion peptides or bis-cysteine MMP substrate peptides was used to form the cell-responsive hydrogels that were designed to locally respond to local protease activity such as MMP at the cell surface. The MMP-responsive hydrogels were proteolytically invaded by primary human fibroblasts and the invasion process depended on MMP substrate activity, adhesion ligand concentration, and network crosslinking density. When the MMP-responsive hydrogels were used to deliver recombinant human bone morphogenetic protein-2 to the site of critical defects in rat cranium, bone regeneration was dependent on the proteolytic responsive behavior of the hydrogels. These results indicate potential applications of the cell-responsive hydrogels in tissue engineering and regenerative medicine.

Some proteins undergo a substantial conformational change in response to a given stimulus. This conformational change of proteins has provided useful tools in engineering smart hydrogels with specified responses to particular stimuli. For example, smart hydrogels that undergo volume changes or sol–gel transition in response to pH and temperature were prepared by bioconjugation of well-defined folding motifs of proteins and synthetic polymers [97, 98]. Similarly, hybrid hydrogels are capable of producing a stimuli-responsive action mechanism caused by an induced conformational change and binding affinities of genetically engineered proteins in response to a stimulus [99]. As a biological recognition element to prepare the stimuli-responsive hydrogels, calmodulin (CaM), which is a calcium-binding protein exhibiting two conformational changes; one in the presence of Ca^{2+} and the other in the presence of phenothiazines, was used. The hybrid hydrogels demonstrated three-stage active swelling characteristics achieved by coupling ligand sensing with the conformational change of the site-specifically immobilized CaM. The hybrid hydrogels controlled transport of small molecules in response to Ca^{2+} by their reversible swelling/shrinking cycles. They act as a gate controlling the flow from a reservoir in microfluidics.

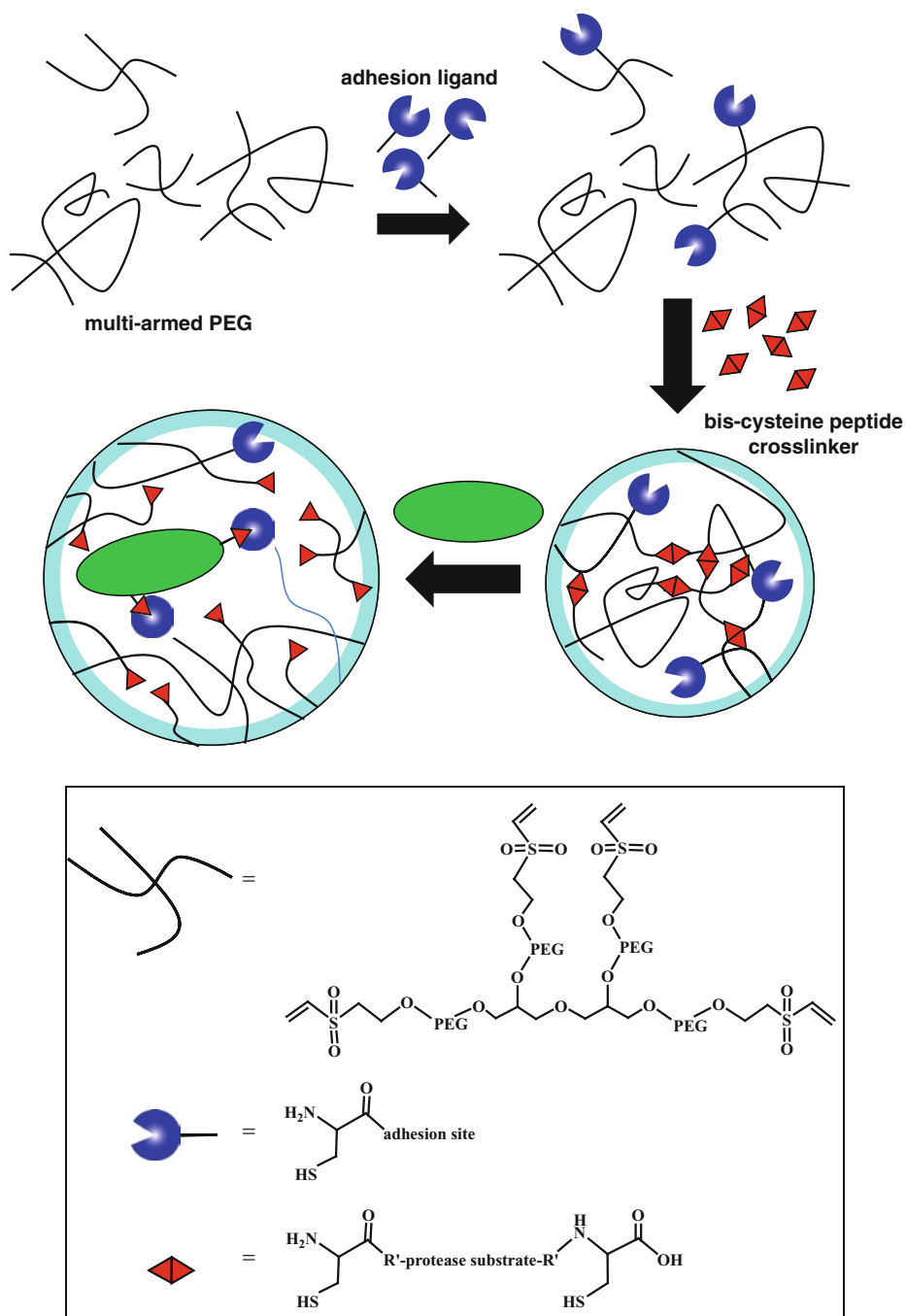


Fig. 17. Cell-responsive sol-gel transition systems by gelation of multiarmed PEG with an adhesion receptor-binding motif by the addition of the bis-cysteine peptide crosslinker [95].

Drug-responsive hydrogels can be designed for trigger-inducible release of human vascular endothelial growth factor [100]. Polyacrylamide conjugated with genetically engineered bacterial gyrase subunit B (GyrB) forms a hydrogels by the addition of

the aminocoumarin antibiotic coumermycin because of the dimerization of GyrB through coumermycin. The addition of increasing concentrations of clinically validated novobiocin (albamycin) resulted in dissociation of the hydrogels by the dissociation of the GyrB subunits, followed by the release of the human vascular endothelial growth factors 121 (VEGF₁₂₁) entrapped within the hydrogels networks. Such antibiotic-inducible release using drug-responsive hydrogels enables optimal administration of the rapidly growing number of protein-based biopharmaceuticals.

Most of the biomolecule-responsive hydrogels made to exploit molecular recognition events of proteins, such as enzyme, lectin, and antibody. Since DNAs form duplexes with complementary DNAs or DNA aptamers, the mutated sequence and the folded structure bind to specific targets, their molecular recognition functions can provide the useful tools for creating biomolecule-responsive hydrogels with a wide variety of uses. The concept of reversibly DNA-responsive sol–gel transition systems using DNA-strand displacement by base pairing provided the possibility of cyclically manipulating sol–gel transitions by the addition of DNA strands that acted as crosslinkers at constant temperature and under unchanged buffer conditions [101]. Controllable macroscopic rheological properties of DNA-responsive sol–gel transition, trapping, and DNA-triggered release from DNA-responsive hydrogels were visualized using fluorescent semi-conductor quantum dots (QDs) [102]. The DNA-responsive sol–gel transition system was combined with a specific thrombin-binding aptamer, which was able to form a double-stacked G quadruplex with a high affinity to α -thrombin, in order to capture and release the thrombin [103]. These results point to the potential of the DNA-responsive sol–gel transition as a controlled release system.

DNA-responsive hydrogels that are capable of shrinking or swelling in response to DNA were prepared with a stem-loop structured DNA on the basis of the binding with its complementary target DNA [104, 105]. Highly selective target-responsive hydrogels were engineered with DNA aptamers as the crosslinks that selectively recognize a variety of target molecules (Fig. 18) [106]. The hydrogels formed by hybridization of the DNA aptamer and two kinds of single-stranded DNAs conjugated with polyacrylamide was dissolved by the addition of adenosine, which was the target molecule to competitively bind the DNA aptamer. Thus, biomolecule-responsive hydrogels conjugated with DNA have many advantages in sensing systems and the selective release of therapeutic agents in response to the target molecule demonstrating physiological changes.

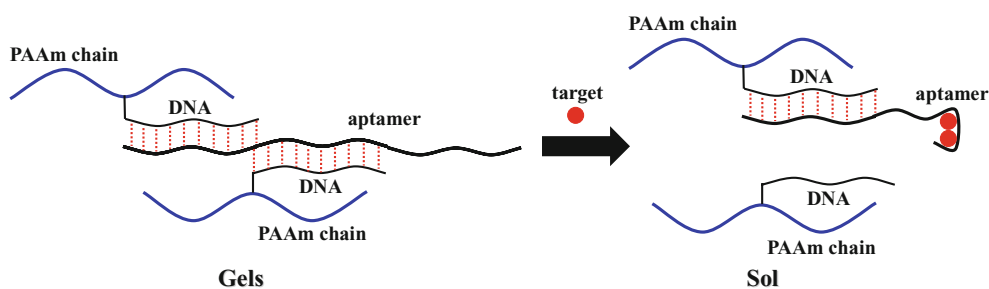


Fig. 18. Schematic representation of target molecule-responsive sol–gel transition by hybridization of the DNA aptamer and DNA-polyacrylamide conjugates [106].

Summary

Biomolecule-responsive hydrogels that undergo volume changes in response to a variety of target biomolecules are useful in many bioapplications. The properties of the biomolecule-responsive hydrogels can provide the useful tools for creating intelligent biomaterials with a wide variety of uses. The design of the biomolecule-responsive hydrogels requires detailed understanding of the structural factors that control their molecular recognition and responsive behavior. The knowledge gained from successful designs provides the basis for the development of smart biomaterials as well as more insight into the biological functions of biomolecules, cells and other biosystems. Bioconjugation of polymers with biomolecular recognition is directing research to better strategies for developing biomolecule-responsive biomaterials that have the high potential as smart biomaterials for spatiotemporally controlled drug delivery, cell culture, and tissue engineering.

References

1. Peppas NA (1987) *Hydrogels in medicine and pharmacy*. CRC, Boca Raton
2. DeRossi D, Kajiwara K, Osada Y, Yamauchi A (1991) *Polymer gels, fundamentals and biomedical applications*. Plenum, New York
3. Miyata T (2002) Gels and interpenetrating polymer networks. In: Yui N (ed) *Supramolecular design for biological applications*. CRC, Boca Raton, FL, pp 95–136, Chapter 6
4. Dusek K (1993) Responsive gels: volume transitions I, *Adv Polym Sci*, vol 109. Springer, Berlin
5. Dusek K (1993) Responsive gels: volume transitions II, *Adv Polym Sci*, vol 110. Springer, Berlin
6. Okano T (1998) *Biorelated polymers and gels*. Academic, Boston
7. Miyata T (2002) Stimuli-responsive polymers and gels. In: Yui N (ed) *Supramolecular design for biological applications*. CRC, Boca Raton, FL, pp 191–225, Chapter 9
8. Tanaka T, Fillmore D, Sun S-T, Nishio I, Swislow G, Shah A (1980) *Phys Rev Lett* 45:1636–1639
9. Annaka M, Tanaka T (1992) *Nature* 355:430–432
10. Tanaka T (1978) *Phys Rev Lett* 40:820823
11. Hirokawa Y, Tanaka T (1984) *J Chem Phys* 81:6379–6380
12. Amiya T, Hirokawa Y, Hirose Y, Li Y, Tanaka T (1987) *J Chem Phys* 86:2375–2379
13. Chen G, Hoffman AS (1995) *Nature* 373:49–52
14. Yoshida R, Uchida K, Kaneko T, Sakai K, Kikuchi A, Sakurai Y, Okano T (1995) *Nature* 374:240–242
15. Tanaka T, Nishio I, Sun S-T, Ueno-Nishio S (1982) *Science* 218:467–469
16. Osada Y, Okuzaki H, Hori H (1992) *Nature* 355:242–244
17. Irie M (1993) *Adv Polym Sci* 110:49–65
18. Suzuki A, Tanaka T (1990) *Nature* 346:345–347
19. Siegel RA (1993) *Adv Polym Sci* 109:233–267
20. Peppas LB, Peppas NA (1989) *J Control Release* 8:267–274
21. Brazel CS, Peppas NA (1995) *Macromolecules* 28:8016–8020
22. Dong L-C, Hoffman AS (1991) *J Control Release* 15:141–152
23. Miyata T, Nakamae K, Hoffman AS, Kanzaki Y (1994) *Macromol Chem Phys* 195:1111–1120
24. Nakamae K, Nizuka T, Miyata T, Furukawa M, Nishino T, Kato K, Inoue T, Hoffman AS, Kanzaki Y (1997) *J Biomater Sci Polym Ed* 9:43–53
25. Hoffman AS (1987) *J Control Release* 6:297–305
26. Okano T (1993) *Adv Polym Sci* 110:179–197
27. Dong L-C, Hoffman AS (1990) *J Control Release* 13:21–31
28. Okano T, Bae YH, Jacobs H, Kim SW (1990) *J Control Release* 11:255–265
29. Katono H, Maruyama A, Sanui K, Ogata N, Okano T, Sakurai Y (1991) *J Control Release* 16:215–227
30. Miyata T, Urugami T, Nakamae K (2002) *Adv Drug Deliv Rev* 54:79–98
31. Miyata T, Urugami T (2002) Biological stimuli-responsive hydrogels. In: Dumitriu S (ed) *Polymeric biomaterials*. Marcel Dekker, New York, pp 959–974, Chapter 36
32. Ishihara K, Kobayashi M, Ishimaru N, Shinohara I (1984) *Polym J* 16:625–631
33. Ishihara K, Matsui K (1986) *J Polym Sci Polym Lett Ed* 24:413–417

34. Albin G, Horbett TA, Ratner BD (1985) *J Control Release* 2:153–164
35. Albin GW, Horbett TA, Miller SR, Ricker NL (1987) *J Control Release* 6:267–291
36. Cartier S, Horbett TA, Ratner BD (1995) *J Membr Sci* 106:17–24
37. Hassan CM, Doyle FJ III, Peppas NA (1997) *Macromolecules* 30:6166–6173
38. Parker RS, Doyle FJ III, Peppas NA (1999) *IEEE Trans Biomed Eng* 46:148–157
39. Kataoka K, Miyazaki H, Okano T, Sakurai Y (1994) *Macromolecules* 27:1061–1062
40. Shiino D, Murata Y, Kubo A, Kim YJ, Kataoka K, Koyama Y, Kikuchi A, Yokoyama M, Sakurai Y, Okano T (1995) *J Control Release* 37:269–276
41. Aoki T, Nagao Y, Sanui K, Ogata N, Kikuchi A, Sakurai Y, Kataoka K, Okano T (1996) *Polym J* 28:371–374
42. Kataoka K, Miyazaki H, Bunya M, Okano T, Sakurai Y (1998) *J Am Chem Soc* 120:12694–12695
43. Matsumoto A, Kurata T, Shiino D, Kataoka K (2004) *Macromolecules* 37:1502–1510
44. Matsumoto A, Yoshida R, Kataoka K (2004) *Biomacromolecules* 5:1038–1045
45. Brownlee M, Cerami A (1979) *Science* 206:1190–1191
46. Seminoff LA, Olsen GB, Kim SW (1989) *Int J Pharm* 54:241–249
47. Kim SW, Pai CM, Makino K, Seminoff LA, Holmberg DL, Gleeson JM, Wilson DE, Mack EJ (1990) *J Control Release* 11:193–201
48. Makino K, Mack EJ, Okano T, Kim SW (1990) *J Control Release* 12:235–239
49. Kokufuta E, Zhang Y-Q, Tanaka T (1991) *Nature* 351:302–304
50. Miyata T, Nakamae K (1997) *Trend Polym Sci* 5:198–206
51. Nakamae K, Miyata T, Jikihara A, Hoffman AS (1994) *J Biomater Sci Polym Ed* 6:79–90
52. Miyata T, Jikihara A, Nakamae K, Hoffman AS (1996) *Macromol Chem Phys* 197:1135–1146
53. Miyata T, Jikihara A, Nakamae K, Hoffman AS (2004) *J Biomater Sci Polym Ed* 15:1085–1098
54. Lee SJ, Park K (1996) *J Mol Recognit* 9:549–557
55. Obaidat AA, Park K (1996) *Pharm Res* 13:989–995
56. Obaidat AA, Park K (1997) *Biomaterials* 18:801–806
57. Ulijn RV (2006) *J Mater Chem* 16:2217–2225
58. Saffran M, Kumar GS, Savariar C, Burnham JC, Williams F, Neckers DC (1986) *Science* 233:1081–1086
59. Yeh P-Y, Kopeckova P, Kopecek J (1994) *J Polm Sci A Polym Chem* 32:1627–1637
60. Yeh P-Y, Kopeckova P, Kopecek J (1995) *Macromol Chem Phys* 196:2183–2202
61. Ghandehari H, Kopeckova P, Yeh P-Y, Kopecek J (1996) *Macromol Chem Phys* 197:965–980
62. Ghandehari H, Kopeckova P, Kopecek J (1997) *Biomaterials* 18:861–872
63. Akala EO, Kopeckova P, Kopecek J (1998) *Biomaterials* 19:1037–1047
64. Hovgaard L, Brøndsted H (1995) *J Control Release* 36:159–166
65. Plunkett KN, Berkowski KL, Moore JS (2005) *Biomacromolecules* 6:632–637
66. Li C, Madsen J, Armes SP, Lewis AL (2006) *Angew Chem Int Ed* 45:3510–3513
67. Yamamoto N, Kurisawa M, Yui N (1996) *Macromol Rapid Commun* 17:313–318
68. Kurisawa M, Yui N (1998) *J Control Release* 54:191–200
69. Kurisawa M, Matsuo Y, Yui N (1998) *Macromol Chem Phys* 199:705–709
70. Huh KM, Hashi J, Ooya T, Yui N (2000) *Macromol Chem Phys* 201:613–619
71. Sperinde JJ, Griffith LG (1997) *Macromolecules* 30:5255–5264
72. Hu B-H, Messersmith PB (2003) *J Am Chem Soc* 125:14298–14299
73. Thornton PD, McConnell G, Ulijn RV (2005) *Chem Commun* 47:5913–5915
74. Thornton PD, Mart RJ, Ulijn RV (2007) *Adv Mater* 19:1252–1256
75. Diamandis EP, Christopoulos TK (1996) *Immunoassay*. Academic, New York
76. Miyata T, Asami N, Uragami T (1999) *Macromolecules* 32:2082–2084
77. Miyata T, Asami N, Uragami T (1999) *Nature* 399:766–769
78. Lu Z-R, Kopeckova P, Kopecek J (2003) *Macromol Biosci* 3:296–300
79. Nayak S, Lyon LA (2005) *Angew Chem Int Ed* 44:7686–7708
80. Kim J, Nayak S, Lyon LA (2005) *J Am Chem Soc* 127:9588–9592
81. Kim J, Singh N, Lyon LA (2006) *Angew Chem Int Ed* 45:1446–1449
82. Kim J, Singh N, Lyon LA (2007) *Chem Mater* 19:2527–2532
83. Wulff G, Sarhan A, Zabrocki K (1973) *Tetrahedron Lett* 44:4329–4332
84. Sellergren B, Lepisto M, Mosbach K, Am J (1988) *Chem Soc* 110:5853–5860
85. Mosbach K (1994) *Trends Biochem Sci* 19:9–14
86. Shea K (1994) *Trends Polym Sci* 2:166–173
87. Wulff G (1995) *Angew Chem Int Ed Engl* 34:1812–1832
88. Byrne M, Park K, Peppas NA (2002) *Adv Drug Deliv Rev* 54:149–161
89. Bergmann NM, Peppas NA (2008) *Prog Polym Sci* 33:271–288
90. Watanabe M, Akahoshi T, Tabata Y, Nakayama D (1998) *J Am Chem Soc* 120:5577–5578

91. Wang GQ, Kuroda K, Enoki T, Grosberg A, Masamune S, Oya T, Takeoka Y, Tanaka T (2000) *Proc Natl Acad Sci USA* 97:9861–9864
92. Oya T, Enoki T, Grosberg AY, Masamune S, Sakiyama T, Takeoka Y, Tanaka K, Wang GQ, Yilmaz Y, Feld MS, Dasari R, Tanaka T (1999) *Science* 286:1543–1545
93. Miyata T, Jige M, Nakaminami T, Uragami T (2006) *Proc Natl Acad Sci USA* 103:1190–1193
94. Yamaguchi N, Zhang L, Chae B-S, Palla CS, Furst EM, Kiick KL (2007) *J Am Chem Soc* 129:3040–3041
95. Lutolf MP, Raeber GP, Zisch AH, Tirelli N, Hubbell JA (2003) *Adv Mater* 15:888–892
96. Lutolf MP, Lauer-Fields JL, Schmoekel HG, Metters AT, Weber FE, Fields GB, Hubbell JA (2003) *Proc Natl Acad Sci USA* 100:5413–5418
97. Petka WA, Harden JL, McGrath KP, Wirtz D, Tirrell DA (1998) *Science* 281:389–392
98. Wang C, Stewart RJ, Kopecek J (1999) *Nature* 397:417–420
99. Ehrick JD, Deo SK, Browning TW, Bachas LG, Madou MJ, Daunert S (2005) *Nat Mater* 4:298–302
100. Ehrbar M, Schoenmakers R, Christen EH, Fussenegger M, Weber W (2008) *Nat Mater* 7:800–804
101. Lin DC, Yurke B, Langrana NA (2004) *J Biomech Eng* 126:104–110
102. Liedl T, Dietz H, Yurke B, Simmel F (2007) *Small* 3:1688–1693
103. Wei B, Cheng I, Luo KQ, Mi Y (2008) *Angew Chem Int Ed* 47:331–333
104. Murakami Y, Maeda M (2005) *Macromolecules* 38:1535–1537
105. Murakami Y, Maeda M (2005) *Biomacromolecules* 6:2927–2929
106. Yang H, Liu H, Kang H, Tan W (2008) *J Am Chem Soc* 130:6320–6321

Stimuli-Responsive PEGylated Nanogels for Smart Nanomedicine

Motoi Oishi and Yukio Nagasaki

Abstract PEGylated nanogels are composed of cross-linked polyamine gels core with tethered PEG chains. The stimuli-responsive PEGylated nanogels have significant volume phase transitions in response to the extracellular pH (7–6.5) of a tumor environment as well as endosomal/lysosomal pH (6.5–5.5). The pH-responsive PEGylated nanogels containing ^{19}F compounds in the polyamine gels core have remarkable on–off ^{19}F FMR signals (T_2 values of ^{19}F) and signal-to-noise (S/N) ratio in response to the extracellular of tumor environment, making these nanogels effective as tumor-specific smart ^{19}F MRI (magnetic resonance imaging) nanoprobes. The doxorubicin (DOX)-loaded pH-responsive PEGylated nanogels release DOX intracellular in response to endosomal/lysosomal pH, thereby conferring more antitumor activity than free DOX against naturally drug-resistant human hepatoma cells. The PEGylated nanogel with gold nanoparticles as the fluorescence quencher in the core and fluorescence dye-labeled DEVD (Asp-Glu-Val-Asp) peptide at the tethered PEG chain end provide pronounced fluorescence signals in response to apoptotic cells. Thus, stimuli-responsive PEGylated nanogels can be utilized as smart nanomedicines for cancer diagnosis and therapy.

Introduction

Nanochemistry and biomimetic chemistry are concerned with the creation of nanosized gels (“nanogels”) with well-defined shapes and functions [1–3]. Nanogels that contain poly(ethylene glycol) (PEG) tethered chains (PEGylated nanogels) have attracted considerable attention in the fields of biotechnological, pharmaceutical, and medical applications, including biological analysis, cosmetics, diagnostics, and drug delivery systems (DDS) due to their excellent biocompatible and nontoxic characteristics of PEG [4–7]. Thus, the PEG corona of the PEGylated nanogels is believed to prevent recognition by a group of scavenger cells in the reticuloendothelial system that mainly involves the liver, spleen, and lungs, resulting in prolonged blood circulation. A variety of drug and/or probe-loaded PEGylated nanogels (nanomedicines) have been developed to precisely and safely deliver the appropriate concentrations of anticancer drugs and/or probes to tumor tissue that preferentially accumulate in the tumor by the enhanced permeability and retention (EPR) effect [8].

Recently, stimuli-responsive and PEGylated nanogels have been intensively studied for nanomedicine applications, such as bioinspired mechanisms to create artificial virus. A key factor in the development of the stimuli-responsive PEGylated nanogels has been the incorporation of a smart polymeric gels that can be triggered to induce a significant change in the characteristics of the nanoparticles in response to stimulus. The PEGylated nanogels

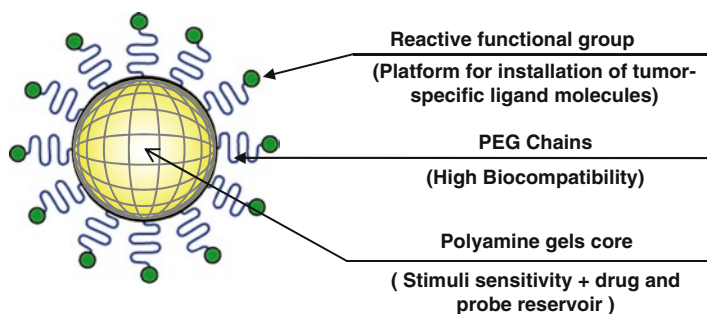
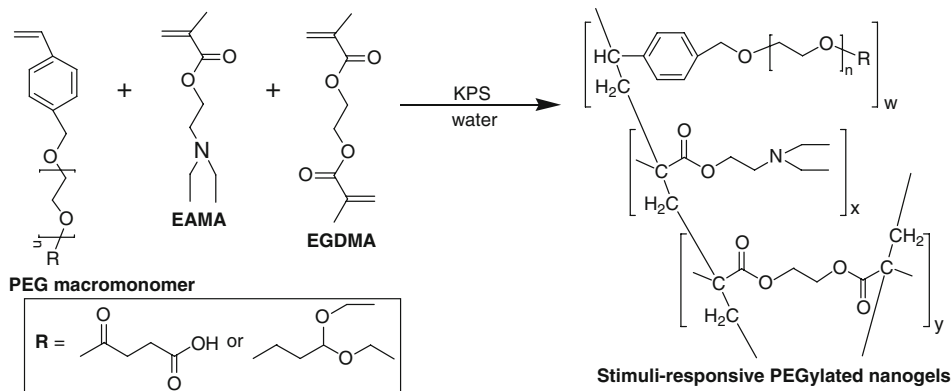
M. Oishi and Y. Nagasaki • Tsukuba Interdisciplinary Materials Science (TIMS),
University of Tsukuba, 1-1-1 Tennoudai, Tsukuba, Ibaraki 305-8573, Japan
e-mail: nagasaki@nagalabo.jp

exhibit extremely high dispersion stability as well as reversible volume phase transition (swelling) in response to pH, temperature, and ionic strength due to the protonation of the polyamine gels core surrounded by the tethered PEG chains [9–12]. For example, pH-responsive PEGylated nanogels are being used to address biomedical applications, such as the extracellular environment of tumor tissues (pH=6.5–7.0) [13, 14] and endosomes/lysosomes (pH=5.0–6.5) [15–17] that are known to be slightly more acidic than normal tissues (pH=7.4).

A new class of nanosized (<100 nm), stimuli-responsive, PEGylated nanogels that are constructed from a cross-linked core of stimuli-responsive poly[2-(*N,N*-diethylamino)ethyl methacrylate] (PEAMA) gels and tethered PEG chains, which have a carboxylic acid group or acetal group as a platform moiety for the installation of a tumor-specific ligand. For instance, the pH-responsive PEGylated nanogels containing ^{19}F compounds in the PEAMA gels core showed remarkable on–off regulation of ^{19}F MR (magnetic resonance) signals in response to extracellular pH of tumor environments, demonstrating the utility of these nanogels as tumor-specific smart ^{19}F MRI (magnetic resonance imaging) nanoprobe [18]. Additionally, antitumor activity of doxorubicin (DOX)-loaded pH-responsive PEGylated nanogels against the human hepatoma cell line HuH-7, which is a natural drug-resistance tumor cell line, is superior to that of free DOX due to the subsequent release of DOX in response to endosomal/lysosomal pH [19]. Furthermore, PEGylated nanogels containing gold nanoparticles (GNPs) (fluorescence quencher) in the PEAMA gels core and fluorescence dye-labeled DEVD peptide at the tethered PEG chain end have pronounced fluorescence signals in apoptotic cells, due to the release of fluorescence dyes through the cleavage of the DEVD peptide by the activated caspase-3 [20]. Thus, PEGylated nanogels represent a promising strategy as smart nanomedicines for cancer diagnosis and therapy.

Synthesis and Characterization of Stimuli-Responsive PEGylated Nanogels

The synthesis of stimuli-responsive PEGylated nanogels via an emulsion polymerization technique is a well-established and widely utilized technique in industrial fields [21]. PEG macromonomers are often used to stabilize the monomer droplets during polymerization [22, 23]. In this case, heterobifunctional PEG macromonomer bearing a 4-vinylbenzyl group and carboxylic acid group at the chain end ($\text{CH}_2=\text{CH}-\text{Ph}-\text{PEG}-\text{COOK}$) functions as a stabilizer for the monomer droplets as well as comonomers that are incorporated into the particle. The 2-(*N,N*-diethylamino) ethyl methacrylate (EAMA) was chosen as the comonomer because it is hydrophobic at basic pH's and becomes hydrophilic as the pH is lowered. The copolymerization of $\text{CH}_2=\text{CH}-\text{Ph}-\text{PEG}-\text{COOK}$ (M_n 8,000) and EAMA was conducted with potassium persulfate (KPS) as the initiator and ethylene glycol dimethacrylate (EGDMA) as the crosslinker (1.0 mol%), as shown in Scheme 1. Since PEAMA undergoes a volume phase transition as a function of pH [24], the effects of the environmental pH on the sizes of the PEGylated nanogels were assessed (Fig. 1). A sharp pH sensitivity was observed between pH 7.0 and 7.5 with a unimodal size distribution ($\mu_2/\Gamma^2 < 0.15$); the PEGylated nanogels in acid pH's have a 6.6-fold larger hydrodynamic volume than the PEGylated nanogels in basic conditions. This behavior is similar to the α/pH curve for the PEGylated nanogels. This finding indicates that protonation of the amino groups in the PEAMA gels core triggers swelling of the PEAMA gels core due to an increase in the ion osmotic pressure coupled with polymer solvation. The zeta (ζ)-potentials of the PEGylated nanogels, obtained by changing the environmental pH, are shown in Fig. 2. The ζ -potential in the acidic region was positively



Scheme 1. Synthesis of stimuli-responsive PEGylated nanogels via emulsion polymerization.

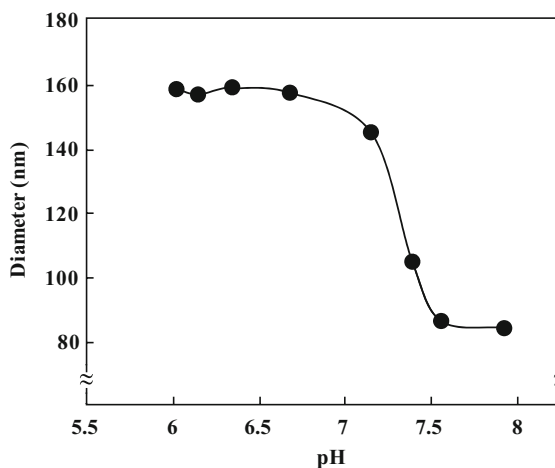


Fig. 1. Effects of pH on the size of the stimuli-responsive PEGylated nanogels.

charged due to existence of the amino groups in the PEAMA gels core. There was a significant decrease in the ξ -potential around pH 7, reflecting the pK_a of PEAMA ($pK_a = 7.5$) [25]. Neither coagulation nor precipitation of the PEGylated nanogels was observed over the entire pH range, indicating high dispersion stability due to the PEG tethered chains.

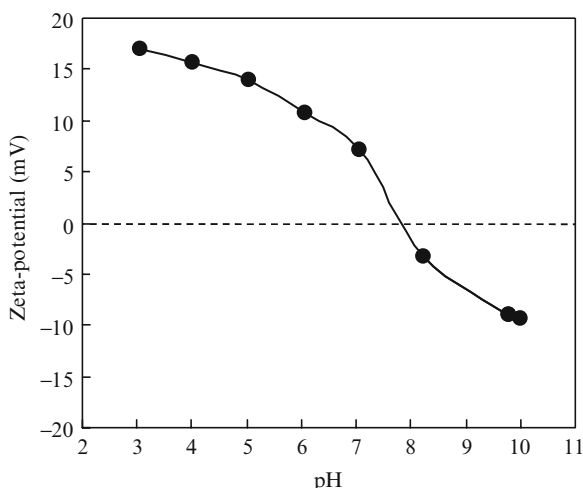


Fig. 2. Effects of pH on the zeta-potentials of the stimuli-responsive PEGylated nanogels.

Tumor-Specific Smart ^{19}F MRI Nanoprobes Based on pH-Responsive PEGylated Nanogels

MRI based on ^1H has been recognized as a powerful and noninvasive method for cancer diagnosis [26, 27]. However, the intense proton background causes insufficient discrimination of tumor tissue from normal tissue. An important advancement in this field is the ^{19}F MRI technique [28], which is capable of producing high-contrast in vivo images, since there is no endogenous ^{19}F in the body as a source of background noise. ^{19}F is 100% naturally abundant and has an MR sensitivity nearly as high as protons. Since long circulating nanosized (<100 nm) and PEGylated species have been reported to accumulate in solid tumors through the EPR effect [8], an important goal in tumor imaging is to develop PEGylated ^{19}F -nanoprobes. The extracellular pH of tumor environment is usually 0.4–1.0 pH units lower than the physiological pH 7.4 [13, 14]; therefore, the MRI of tumors can be improved by designing pH-responsive ^{19}F -nanoprobes that attenuate the ^{19}F MR signal outside of the tumor and switch on the signal inside the tumor. In this regard, the synthesis of smart ^{19}F MRI nanoprobes based on pH-responsive PEGylated nanogels consisting of a cross-linked poly[2-(*N,N*-diethylamino)ethyl methacrylate]-co-poly(2,2,2-trifluoroethyl methacrylate) (PEAMA-co-PTFEMA) gels core and tethered PEG chains that bear an acetal group as a platform for installation of tumor-specific ligand molecules was reported (Fig. 3) [18].

The pH-responsive PEGylated nanogels as smart ^{19}F MRI nanoprobes were synthesized by emulsion copolymerization of EAMA and 2,2,2-trifluoroethyl methacrylate (TFEMA) at various molar ratios in the presence of heterobifunctional PEG macromonomer bearing an acetal group at the α -end and a 4-vinylbenzyl group at the ω -end (acetal-PEG-Ph-CH=CH₂), KPS, and 1.0 mol% of EGDMA. The pH dependency of the diameters of the PEGylated nanogels containing various amounts of TFEMA is shown in Fig. 4. As the TFEMA mol% increased in the nanogel, the size of the PEGylated nanogels decreased due to the increase in hydrophobic and nonionizable PTFEMA segment, leading to decrease in the ion osmotic pressure of the PEAMA-co-PTFEMA gels core. PEGylated nanogels, containing TFEMA, show volume phase transition points in the pH range of 6.8–7.3, strongly indicating that

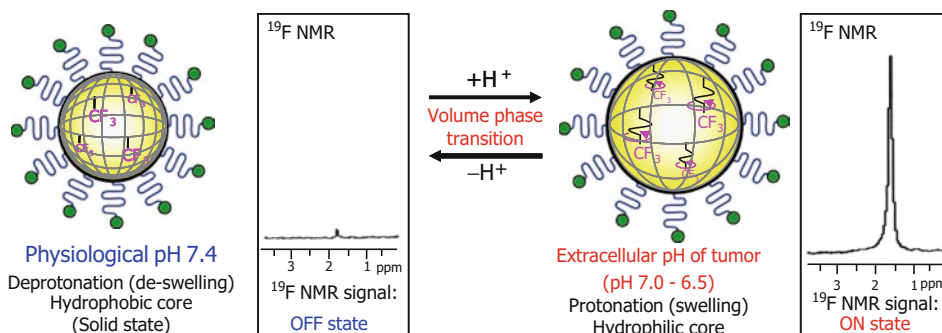


Fig. 3. Schematic illustration of the ^{19}F MRI nanoprobe based on the pH-responsive PEGylated nanogel.

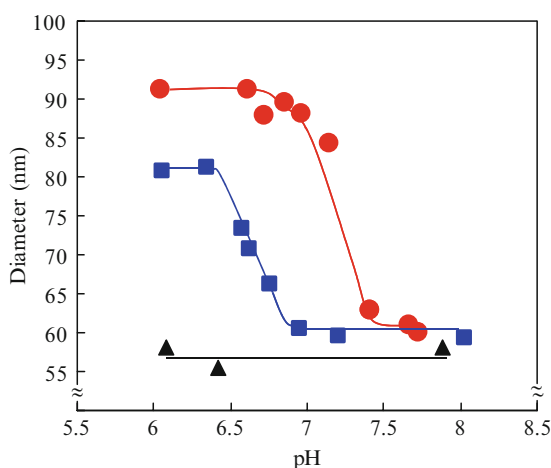


Fig. 4. Effects of pH on the size of the pH-responsive PEGylated nanogels containing 10 (red), 30 (blue), and 50 mol% (black) of TFEMA in PEAMA gels core.

the swelling of PEGylated nanogels only occurs at the extracellular pH of tumor tissue (pH 6.5–7.0). In addition, there was a negligible change in the diameter (~ 58 nm) of the PEGylated nanogels due to the highly hydrophobic core that contains >50 mol% TFEMA. The $V_{\text{swelling}}/V_{\text{shrinking}}$ ratio denotes the extent of hydrodynamic volume change at the volume phase transition point. For PEGylated nanogels containing the TFEMA the $V_{\text{swelling}}/V_{\text{shrinking}}$ ratio in the gels core was smaller than that of PEGylated nanogels without the TFEMA ($V_{\text{swelling}}/V_{\text{shrinking}} = 3.9$), as shown in Fig. 5.

The intensity of the ^{19}F NMR signal (-73 ppm) for the PEGylated nanogels ($450 \mu\text{g/mL}$) was measured by ^{19}F NMR spectroscopy at both the physiological pH ($=7.4$) and the extracellular pH ($=6.5$) of tumor environments (Fig. 6). Almost no ^{19}F NMR signal background was observed at physiological pH ($=7.4$), where the PEAMA-co-PTFEMA gels core is hydrophobic due to the deprotonation of the amino groups; the absence of any ^{19}F NMR signals is likely due to the broadening effect caused by the limited molecular motion of the ^{19}F compounds in the hydrophobic (solid-state) gels core [29]. In sharp contrast, the PEGylated nanogels in the TFEMA range of 5–40 mol% showed clear ^{19}F NMR signals at the extracellular pH ($=6.5$) of tumor environments. The signal intensity of the PEGylated nanogels in the TFEMA range of 10–50 mol% is consistent with the $V_{\text{swelling}}/V_{\text{shrinking}}$ ratio of the PEGylated

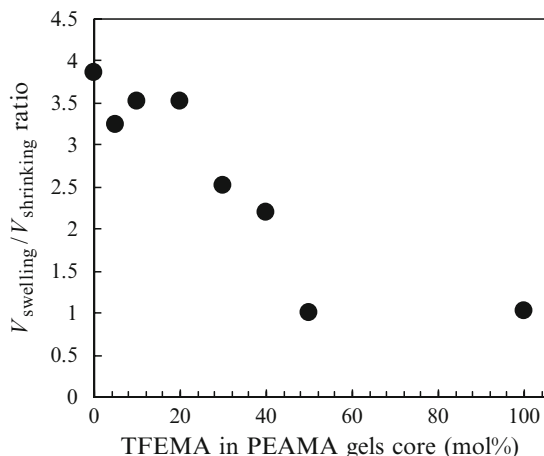


Fig. 5. $V_{\text{swelling}}/V_{\text{shrinking}}$ ratio of the PEGylated nanogels containing various amounts of TFEMA in PEAMA gels core.

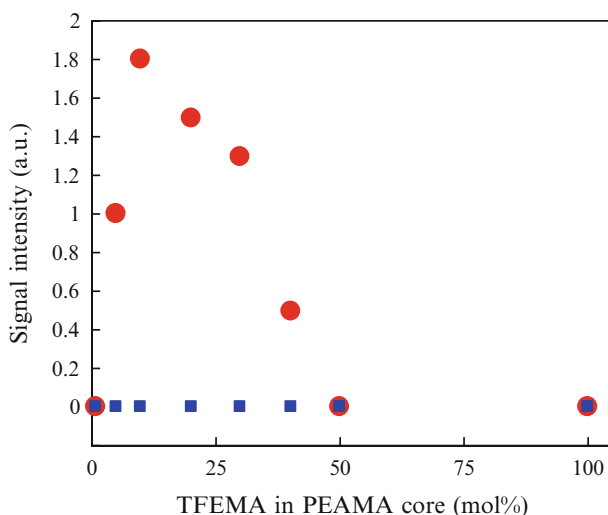


Fig. 6. Intensity of the ^{19}F MR signals of the PEGylated nanogels containing various amounts of TFEMA in PEAMA gels core at pH 6.5 (red circle) and 7.4 (blue square).

nanogels shown in Fig. 5. The intensity of the ^{19}F NMR signals of the PEGylated nanogels increased with decreasing TFEMA; the highest intensity of the ^{19}F NMR signal was observed at 10 mol% TFEMA. These findings indicate that the PEGylated nanogels with a high $V_{\text{swelling}}/V_{\text{shrinking}}$ ratio have a more hydrophilic core and higher mobility than those with a low $V_{\text{swelling}}/V_{\text{shrinking}}$ ratio. However, the intensity of the ^{19}F NMR signal of the PEGylated nanogels containing less than 5 mol% TFEMA significantly decreased even though the $V_{\text{swelling}}/V_{\text{shrinking}}$ ratio was almost similar to that of PEGylated nanogels containing 10 mol% TFEMA. This is likely due to lower ^{19}F concentration ($[^{19}\text{F}] = 250 \mu\text{M}$) than that of PEGylated nanogel containing 10 mol% TFEMA ($[^{19}\text{F}] = 500 \mu\text{M}$), because the amount of all PEGylated nanogels was constant (450 $\mu\text{g}/\text{mL}$). The pH-responsive PEGylated nanogel containing 10 mol% TFEMA showed an increase in the intensity of the ^{19}F NMR signal in synchronization with the decreasing

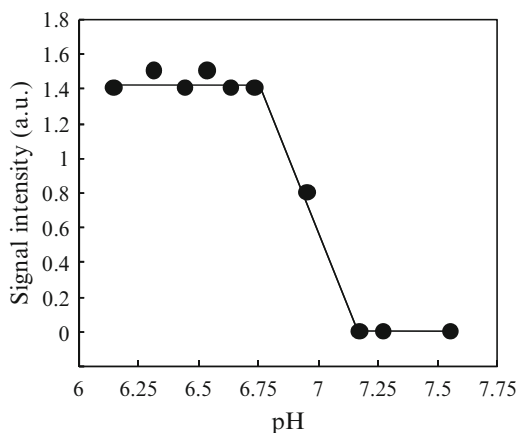


Fig. 7. Effect of pH on the intensity of the ^{19}F NMR signal from the PEGylated nanogel containing 10 mol% of TFEMA in PEAMA gels core ($[^{19}\text{F}] = 500 \mu\text{M}$).

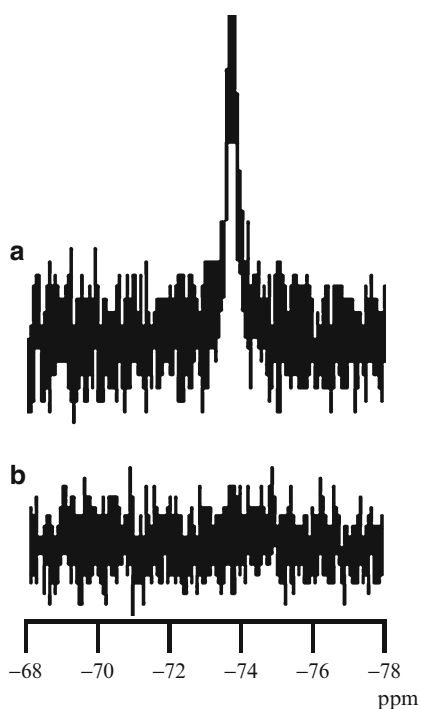
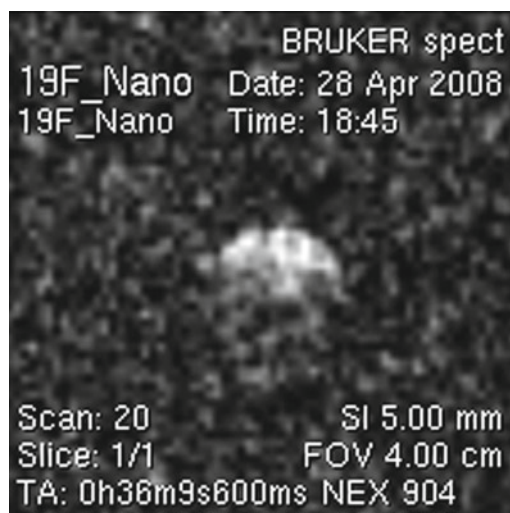


Fig. 8. ^{19}F NMR spectra of the pH-responsive PEGylated nanogels containing 10 mol% of TFEMA in the presence of 90% fetal bovine serum (FBS) at (a) pH 6.5 and (b) pH 7.4.

pH as shown in Fig. 7. This behavior is consistent with both the pH-dependent volume phase transition (Fig. 4) and the α/pH curve of the PEGylated nanogels. Additionally, the pH-responsive PEGylated nanogel containing 10 mol% TFEMA retained the on-off regulation of the ^{19}F NMR signal even in the presence of 90% fetal bovine serum (FBS) (Fig. 8a, b), which means that it can be used for in vivo applications. The T_1 and T_2 relaxation times for ^{19}F for the PEGylated nanogels containing 10 mol% TFEMA, as measured by ^{19}F MRI (7.0 T) at the

Table 1. T_1 and T_2 relaxation times of ^{19}F for the pH-responsive PEGylated nanogels at pH=7.4 and 6.5

pH	T_1 (ms)	T_2 (ms)	S/N ratio ^a
7.4	<30	<1	~0
6.5	280	56.8	7.63

^aCalculated from phantom images**Fig. 9.** ^{19}F MRI of the phantom containing the pH-responsive PEGylated nanogels at pH=6.5 ($[^{19}\text{F}] = 500 \mu\text{M}$).

physiological pH=7.4 and extracellular pH=6.5 of tumor environment, are listed in Table 1. The T_2 value at pH=7.4 was found to be too small (T_2 was estimated to be 100 μs based on signal line width); the absence of ^{19}F MRI signals is due to the broadening effect caused by the limited molecular motion of the ^{19}F compounds in the hydrophobic (solid-state) core. In sharp contrast, the T_2 values for the PEGylated nanogels at pH6.5 were significantly larger than at pH7.4. This is in accordance with the size variation of the PEGylated nanogels as function of pH. This complete on–off regulation of the T_2 values (^{19}F MRI signal intensity) by the pH-responsive PEGylated nanogels is a remarkable characteristic for tumor-specific ^{19}F MRI nanoprobe. The phantom image of ^{19}F MRI for the PEGylated nanogels at pH6.5 using the surface coil receive system is shown in Fig. 9. Since the signal at the top surface is stronger than that at the bottom for the ^{19}F phantom image arising from the reception profile of the surface coil, the signal-to-noise (S/N) ratios at the top surface of the images for the PEGylated nanogels at pH=7.4 and 6.5 were measured to be ~0 and 7.63, respectively (Table 1). The increases in the S/N ratios, in response to extracellular pH (=6.5) of tumor environment, are so remarkable that the PEGylated nanogels can be used as a tumor-specific smart ^{19}F MRI nanoprobe.

pH-Responsive PEGylated Nanogels for Intracellular Drug Delivery Systems

Anticancer drugs have been widely approved for clinical use against many malignancies. Nevertheless, the therapeutic effects of many anticancer drugs are limited due to their low water solubility and serious side effects. Therefore, selective augmentation of anticancer drug

concentrations within tumor tissues is a major challenge not only in reducing the severity of side-effects but also in improving therapeutic efficacy [30–32]. Consequently, several nanosized drug carriers, including water-soluble polymer–drug conjugate [33, 34], long-circulating liposomes [35–37], and polymeric micelles [38, 39], have been developed to deliver precise and safe concentrations of anticancer drugs to the tumor tissues. Since they show extended bioavailability with reduced nonspecific accumulation in normal tissues and preferential accumulation in tumor tissues due to the EPR effect [8], some of these carriers have been approved for clinical use [40] or are currently in clinical trials [41]. However, even though these carriers reach the tumor tissue, the concentrations of the active anticancer drugs within the cancer cells are often insufficient due to inefficient release of the drugs from the carriers into the cytoplasm, thus, higher dosages of the anticancer drugs are required. A promising approach to improving the efficacy of cancer chemotherapy is the development of carrier systems that can be triggered to release the anticancer drug in response to intracellular chemical stimuli, such as pH, glutathione, and enzymes. Recently, the achievement of remarkably enhanced antitumor activity in cultured cancer cells through the use of DOX-loaded pH-responsive PEGylated nanogels was reported that have pH-triggered release (Fig. 10) [19]. Thus, pH-responsive PEGylated nanogels represent a promising strategy for the intracellular delivery of anticancer drug in vivo.

The pH-responsive PEGylated nanogel was synthesized by emulsion copolymerization of EAMA with heterobifunctional PEG macromonomer with a 4-vinylbenzyl group at the α -end and a carboxylic acid group at the ω -end ($\text{CH}_2=\text{CH}-\text{Ph}-\text{PEG}-\text{COOK}$; M_n 8,000), and 1.0 mol% EGDMA, as described earlier [15–17]. As a control, a non-pH-responsive PEGylated nanogel with a polystyrene-co-PEAMA gels core was also synthesized by emulsion polymerization with styrene (St) and EAMA (1.8:1 ratio). By decreasing the pH from 8.0 to 6.0, the diameter of the pH-responsive PEGylated nanogel increased proportionally with a unimodal distribution ($\mu_2/\Gamma^2=0.08\text{--}0.13$), reaching a 6.6-fold larger hydrodynamic volume ($d=156$ nm) at the endosomal pH compared with that at the physiological pH ($d=83$ nm) as stated above. In contrast, there was a negligible change in the diameter (82 nm) of the non-pH-responsive PEGylated nanogel as the pH decreased from 8.0 to 6.0, probably due to the fact that its highly hydrophobic core was 50% PSt.

The loading of DOX, as both an anticancer drug and a fluorescence probe, into the PEAMA gels core of the PEGylated nanogel was achieved using solvent evaporation [42]. The diameter of the DOX-loaded PEGylated nanogels was found to be slightly increased, with

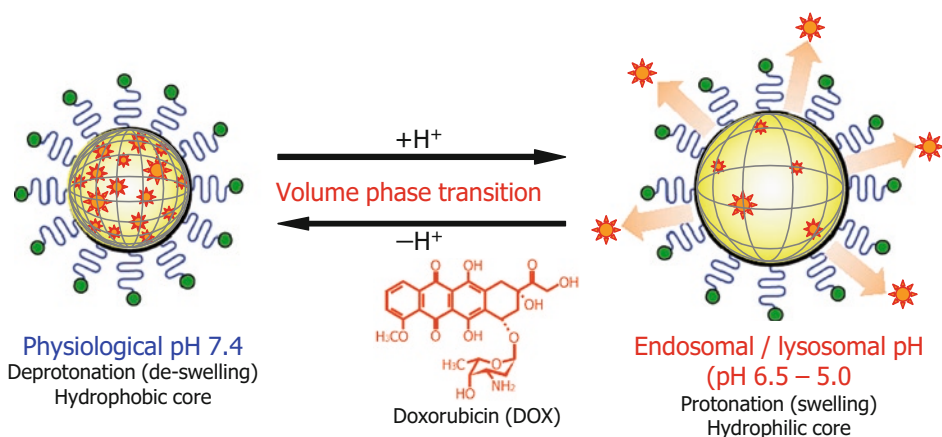


Fig. 10. Schematic illustration of endosomal/lysosomal release of DOX using pH-responsive PEGylated nanogel.

unimodal distribution ($\mu_2/\Gamma^2 < 0.11$). The loading efficiency and loading capacity of DOX into the PEGylated nanogel was 80%, based on the initial amount of DOX and 26 wt%, respectively, as determined by the UV absorption at 485 nm. Compared with the same amount of free DOX, the fluorescence intensity of the DOX-loaded PEGylated nanogel was very weak (Fig. 11), indicates that a high amount of DOX was trapped in the PEAMA gels core of the PEGylated nanogel, leading to fluorescence quenching [43, 44].

The release of DOX from the DOX-loaded PEGylated nanogel was evaluated with time and pH-dependent profiles (pH 7.4–5.3), as shown in Fig. 12. Only 13% release of the DOX was observed for the DOX-loaded PEGylated nanogel under physiological conditions (pH 7.4). On the other hand, the release of the DOX from the DOX-loaded PEGylated nanogel gradually increased and reached a plateau after 24 h as the pH decreased. A significant DOX release (39%) was observed at pH 5.3. The observed DOX release profile

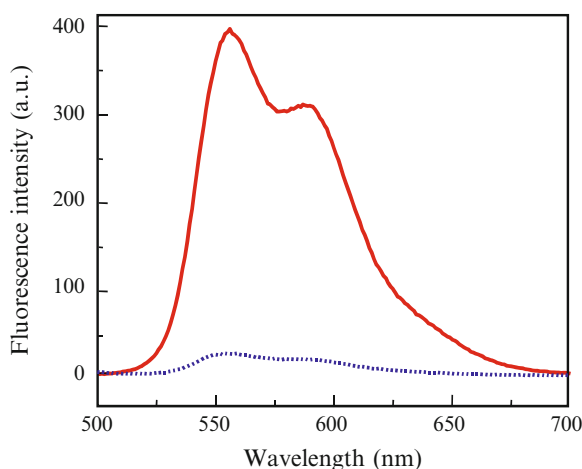


Fig. 11. Fluorescence spectra of the DOX-loaded pH-responsive PEGylated nanogel (blue line) and free DOX (red line) ([DOX] = 10 $\mu\text{g}/\text{mL}$, Excitation = 485 nm).

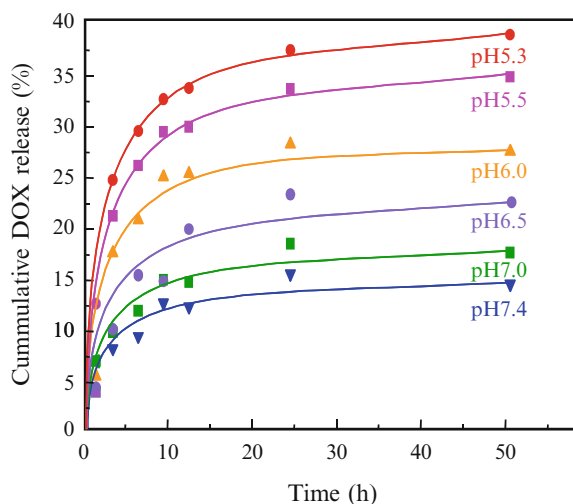


Fig. 12. Time-dependent and pH-dependent DOX release profiles of the DOX-loaded pH-responsive PEGylated nanogels.

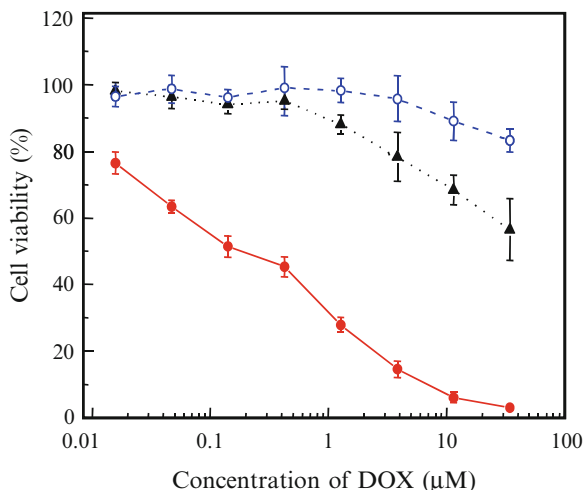


Fig. 13. Antitumor activities of the free DOX (*black triangle*), DOX-loaded pH-responsive PEGylated nanogel (*red circle*), and DOX-loaded non-pH-responsive PEGylated nanogel (*blue circle*) HuH-7 cells (human hepatoma cells). The plotted data represent the average \pm S.E.M. of six experiments \pm S.E.M.

at lower pH values is noteworthy considering that the pH values in the endosome and lysosome are in the range of 5–6, where cellular compartments of the PEAMA gels core of the DOX-loaded PEGylated nanogel swell the most and effectively activate the pH-triggered release of the loaded DOX.

To estimate the antitumor activity of the DOX-loaded PEGylated nanogels, the MTT assay was used with HuH-7 cells that belong to the group of naturally drug-resistant tumors [45]. The DOX-loaded non-pH-responsive PEGylated nanogel (82 nm) was evaluated as a control. As shown in Fig. 13, the DOX-loaded pH-responsive PEGylated nanogel displayed higher antitumor activity than either free DOX or the DOX-loaded non-pH-responsive PEGylated nanogel. The IC_{50} of the DOX-loaded pH-responsive PEGylated nanogel was 0.14 μ M, whereas the IC_{50} values of free DOX and the DOX-loaded non-pH-responsive PEGylated nanogel could not be determined even at DOX concentrations of up to 34 μ M. This indicates that loaded DOX is released from the pH-responsive PEGylated nanogel in response to the endosomal and lysosomal pH levels, whereas the DOX-loaded non-pH-responsive PEGylated nanogel does not, presumably due to the absence of swelling of the PSt-co-PEAMA gels core in the endosomal/lysosomal compartments. Furthermore, the lower antitumor activity of the free DOX compared with the pH-responsive DOX-loaded PEGylated nanogel against HuH-7 cells may be due to efflux mediated by the P-glycoprotein pump, which would decrease the intracellular drug concentration [46]. In contrast, the DOX released from the PEGylated nanogel may reach the nuclei before it can be pumped out, since the DOX-loaded pH-responsive PEGylated nanogel traveling the endocytic pathway may release the DOX at a distance from the P-glycoprotein pump [47].

Fluorescence microscopy was used to examine the internalization of the DOX-loaded PEGylated nanogels, the release of DOX from the nanogel in the endosome and/or lysosome, and the subsequent transport of DOX through the cytoplasm into the nucleus. As shown in Fig. 14, an increase in nuclear fluorescence intensity was observed for the free DOX after only 1 h (Fig. 14a) due to the binding of DOX to the nuclear DNA. Both DOX-loaded non-pH-responsive PEGylated nanogel and the DOX-loaded pH-responsive PEGylated nanogel showed fluorescence exclusively in the cytoplasm after 1 and 12 h (no nuclear fluorescence), which confirms the intracellular distribution of the nanogels and/or the

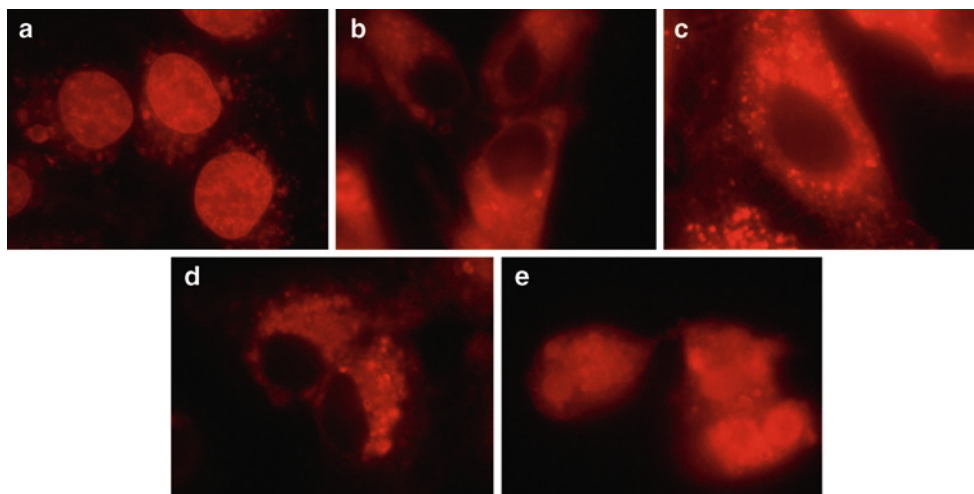


Fig. 14. Fluorescence microscope images of the HuH-7 cells incubated with free DOX, DOX-loaded non-pH-responsive PEGylated nanogel, and DOX-loaded pH-responsive PEGylated nanogel (12.5 $\mu\text{g}/\text{mL}$). (a) free DOX after 1 h of exposure; (b) DOX-loaded non-pH-responsive PEGylated nanogel after 1 h exposure and (c) 36 h exposure; (d) DOX-loaded pH-responsive PEGylated nanogel after 1 h exposure and (e) 36 h exposure.

released DOX. After 36 h of exposure, an increase in nuclear fluorescence intensity was observed for the DOX-loaded pH-responsive PEGylated nanogel (Fig. 14e), whereas the DOX-loaded non-pH-responsive PEGylated nanogel still showed fluorescence only in the cytoplasm (Fig. 14c).

These results indicate that both the DOX-loaded non-pH-responsive PEGylated nanogel and the DOX-loaded pH-responsive PEGylated nanogel are taken up by cells via the endocytic pathway and are transported into the endosomal/lysosomal compartments. In these acidic compartments, protonation of the amino groups causes swelling and solvation of the PEAMA gels core, with consequent release of DOX from the pH-responsive PEGylated nanogel. Ultimately, the released DOX diffuses via the cytoplasm into the cell nucleus. On the other hand, efficient release of DOX from the non-pH-responsive PEGylated nanogel did not occur. Therefore, the pH-responsive PEGylated nanogel described here appears to be an effective chemotherapy with enhanced therapeutic efficacy.

Smart Apoptosis Nanoprobe Based on the PEGylated Nanogels Containing GNPs for Monitoring the Cancer Response to Therapy

Monitoring cancer responses to therapy is one of the important issues to minimize the duration of treatment with ineffective regimens in cancer patients. One of the current efforts for monitoring cancer responses is to measure the tumor volume changes using MRI [48]. Nevertheless, the MRI technique cannot detect early cancer response because the change in tumor volume is typically delayed for about a month after initiation of the therapy.

An important advance in this field is apoptosis imaging techniques, since most anticancer drugs generally kill cells by activating apoptosis within several days. One of the most frequently activated cysteine proteases during the apoptosis process is caspase-3 [49, 50], which cleaves specific proteins that contain the Asp-Glu-Val-Asp (DEVD) peptide sequence [51]. A promising approach to monitoring the cancer response *in vivo* is the development of nanosized (<100 nm) and nonfouling probes with complete on-off regulation of the signal in response

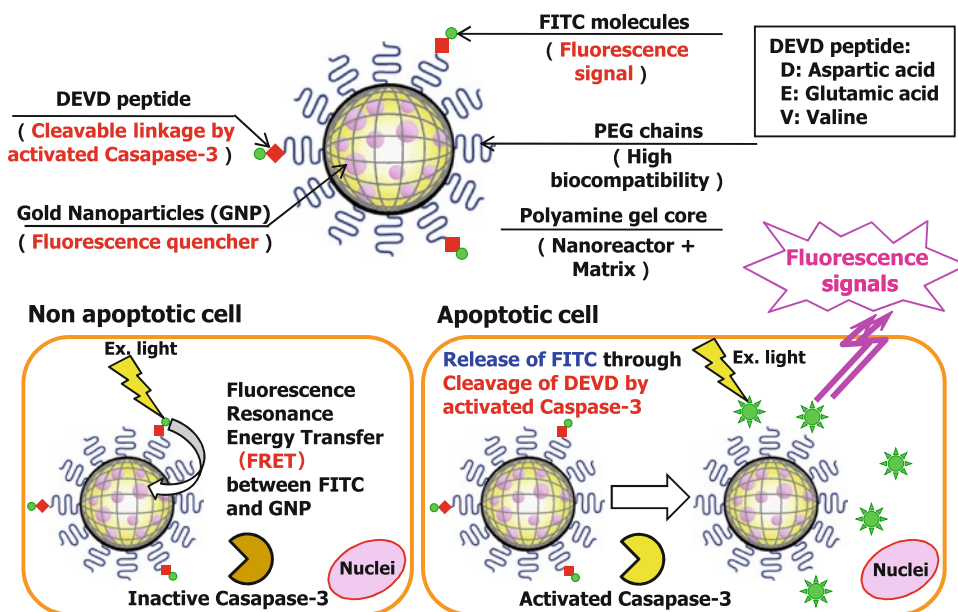
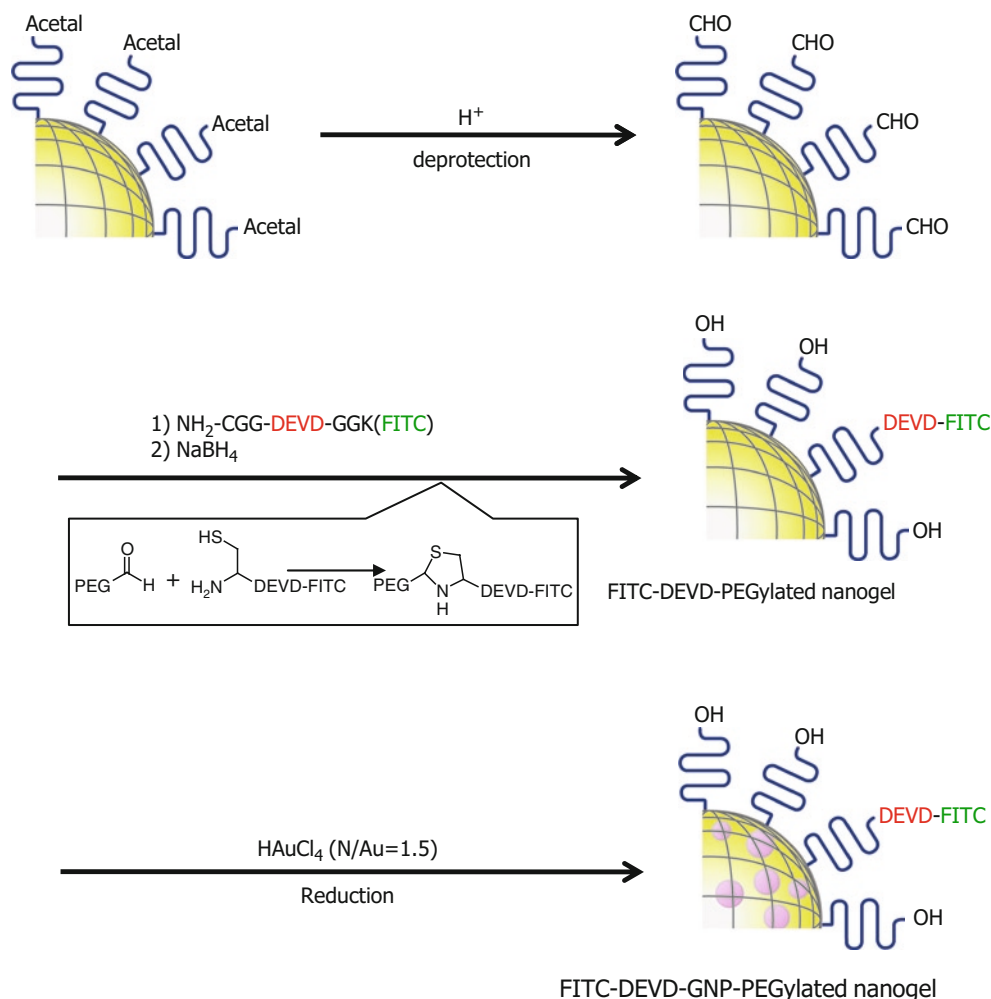


Fig. 15. Schematic illustration of the smart fluorescence-quenching apoptosis nanoprobe based on the PEGylated nanogel containing GNPs and FITC-labeled DEVD peptide at the tethered PEG chain end.

to activated caspase-3 after preferential accumulation in the solid tumor by the EPR effect [8]. Recently, a biocompatible, caspase-3-responsive, and fluorescence-quenching smart apoptosis nanoprobe, based on PEGylated nanogel containing GNPs as the fluorescence quencher in the PEAMA gels core and fluorescein isothiocyanate (FITC)-labeled DEVD peptide at the tethered PEG chain end (Fig. 15), was reported [20]. The fluorescence signal is quenched in the absence of activated caspase-3 in normal cells, due to the fluorescence resonance energy transfer (FRET) process [52, 53] between GNPs and FITC molecules, whereas recovery of the pronounced fluorescence signal arises from release of FITC molecules by the activated caspase-3 cleavage of the DEVD peptide, allowing high fluorescence imaging resolution.

A synthetic route to caspase-3-responsive PEGylated nanogel containing GNPs and FITC-labeled DEVD peptide is shown in Scheme 2. Low molecular weight of PEG (M_n 2,360) was used in this study, because FRET efficiency depends on the distance between the acceptor and donor molecules. Since the PEG chains immobilized on nanoparticles (micelles and liposomes) adopt a conformation of a slightly stretched random coil [54, 55], the end-to-end distance of PEG [Mw 2,360 g/mol and a degree of polymerization of 54] based on random coil models [56] was calculated to be ~ 2.3 nm, the distance between FITC molecules located at the PEG chain end and the core of nanogel is sufficient to effect the FRET [57]. Conversion of the acetal group to an aldehyde was carried out by acidic treatment of the PEGylated nanogel. The introduction of the FITC-labeled DEVD peptide to the aldehyde group was performed using 0.5 equivalents of H-Cys-Gly-Gly-DEVED-Gly-Gly-Lys(FITC) by the formation of a thiazolidine ring between the aldehyde group and N-terminal Cys moiety [58]; this was followed by the addition of NaBH_4 to reduce the unreacted aldehyde groups to hydroxyl groups. The degree of functionality of the FITC-labeled DEVD peptide (FITC-DEVD-PEGylated nanogel) was determined to be 53% based on the standard curve corresponding to the fluorescence intensity of the FITC. The synthesis of the FITC-DEVD-PEGylated nanogel containing GNPs (FITC-DEVD-GNP-PEGylated nanogel) was carried out at N/Au ratio of 1.5 (molar ratio of amino groups in the nanogel to HAuCl_4 of 1.5) by the



Scheme 2. A synthetic route to the caspase-3-responsive PEGylated nanogel containing GNPs and FITC-labeled DEVD peptide.

self-reduction of $HAuCl_4$ (III) with FITC-DEVD-PEGylated nanogel at pH 6.0 without any additional reducing agents [59]. The resulting FITC-DEVD-GNP-PEGylated nanogel was well-dispersed under physiological conditions in PBS at $37^\circ C$, although a slight increase in the size (78.8 nm) with unimodal size distribution ($\mu_2/\Gamma^2=0.072$) was observed probably due to the formation of the GNPs in the PEAMA gels core. A transmission electron microscopy (TEM) image of the FITC-DEVD-GNP-PEGylated nanogel showed GNP clusters and the average number of GNPs in a single nanogel (cluster) and the average diameter of the GNPs were about 6.7 ± 3.2 particles/nanogel and 8.5 ± 2.2 nm, respectively (Fig. 16).

The fluorescence spectra of the FITC-DEVD-PEGylated nanogel and FITC-DEVD-GNP-PEGylated nanogel are shown in Fig. 17. The FITC-DEVD-PEGylated nanogel showed pronounced fluorescence at 525 nm which was attributed to FITC molecules, whereas almost no fluorescence was observed for the FITC-DEVD-GNP-PEGylated nanogel. The fluorescence spectrum of the FITC-DEVD-GNP-PEGylated nanogel, after the addition of sodium cyanide to etch the GNPs [60–62], was almost the same as that of the FITC-DEVD-PEGylated nanogel, which indicated that fluorescence-quenching of

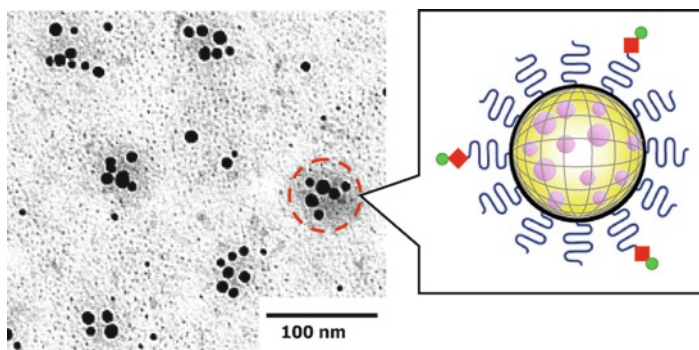


Fig. 16. TEM image of the FITC-DEVD-GNP-PEGylated nanogels.

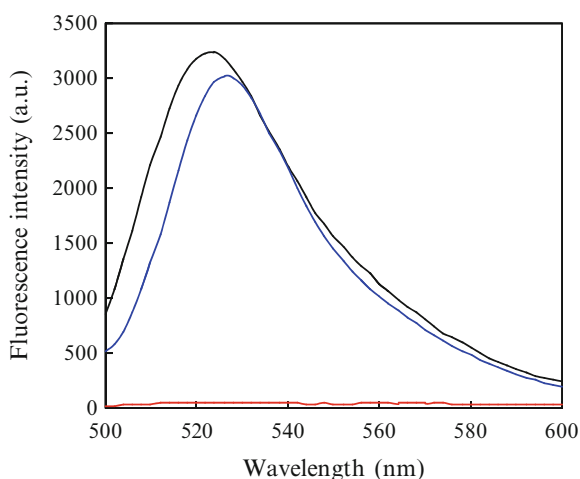


Fig. 17. Fluorescence spectra of the FITC-DEVD-PEGylated nanogel (*blue line*), FITC-DEVD-GNP-PEGylated nanogel (*red line*), and the FITC-DEVD-GNP-PEGylated nanogel after treatment of cyanide etching (*black line*).

the FITC-DEVD-GNP-PEGylated nanogel occurred due to the FRET between the GNPs and FITC molecules. The quenching efficiency of the FITC-DEVD-GNP-PEGylated nanogel was found to be 98% as determined from the fluorescence intensity between the FITC-DEVD-GNP-PEGylated nanogel and the FITC-DEVD-PEGylated nanogel treated with cyanide etching ratio.

The relative fluorescence intensity of the FITC-DEVD-GNP-PEGylated nanogel in the presence of activated caspase-3 as a function of time is shown in Fig. 18. Approximately a 4.8-fold increase in fluorescence intensity of the FITC-DEVD-GNP-PEGylated nanogel was immediately observed. The fluorescence intensity plateaus in 90 min, thus 23.5 ± 0.33 (%) of the fluorescence intensity (FL intensity of 368) was recovered by the activated caspase-3 cleavage of the DEVD peptide as determined from the fluorescence intensity (FL intensity of 1,565) of the FITC-DEVD-GNP-PEGylated nanogel after cyanide etching treatment. In contrast, the fluorescence intensity did not recover in the presence of activated caspase-9. Note that no change in fluorescence intensity of the FITC-DEVD-GNP-PEGylated nanogel was observed in the presence of both activated caspase-3 and caspase-3 inhibitor, indicating that the increase in fluorescence intensity of the FITC-DEVD-GNP-PEGylated nanogel is in fact a caspase-3-specific event.

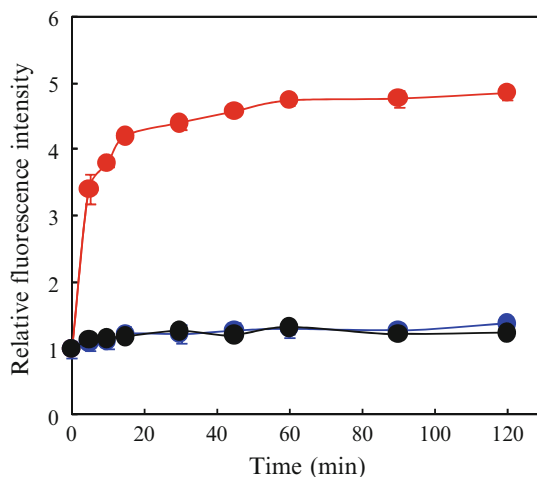


Fig. 18. Relative fluorescence intensity of the FITC–DEVD–GNP–PEGylated nanogel in the presence of caspase-3 (red line), caspase-3 with caspase-3 inhibitor (blue line), and caspase-9 (black line) as function of incubation time at 37°C. The plotted data are the average of three experiments \pm SD.

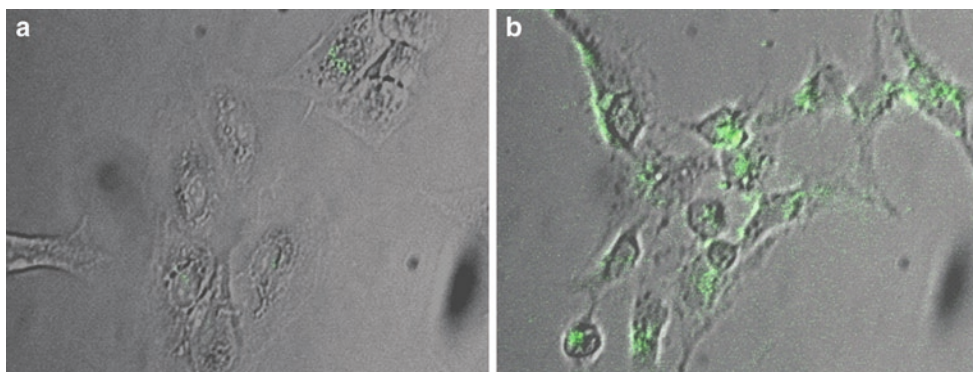


Fig. 19. Confocal fluorescence images of HuH-7 cells incubated with the FITC–DEVD–GNP–PEGylated nanogel in the (a) absence and (b) presence of staurosporine after 4 h incubation.

To determine whether the FITC–DEVD–GNP–PEGylated nanogel acts as an apoptosis nanoprobe for monitoring the cancer response, monolayer-cultured HuH-7 cells were visualized under a confocal fluorescence microscope after 4 h incubation in the presence and in the absence of staurosporine as an apoptosis inducer [63]. Before the treatment of the staurosporine for 4 h, HuH-7 cells were incubated with the FITC–DEVD–GNP–PEGylated nanogel (20 μ g/mL) for 24 h. As seen in Fig. 19, almost no fluorescence signal was observed for the HuH-7 cells incubated with the FITC–DEVD–GNP–PEGylated nanogel alone (Fig. 19a), yielding <5% of the fluorescence positive cells. In sharp contrast, pronounced fluorescence signals were observed for all apoptotic HuH-7 cells induced by staurosporine in the presence of the FITC–DEVD–GNP–PEGylated nanogel (Fig. 19b). Approximately 95% of fluorescence positive cells were observed, indicating the high specificity of the FITC–DEVD–GNP–PEGylated nanogel nanoprobe for apoptotic cells.

Monolayer-cultured tumor cells have been successfully used to determine antitumor activity of the drugs *in vitro* during short culture period. However, to date, the *in vivo* results

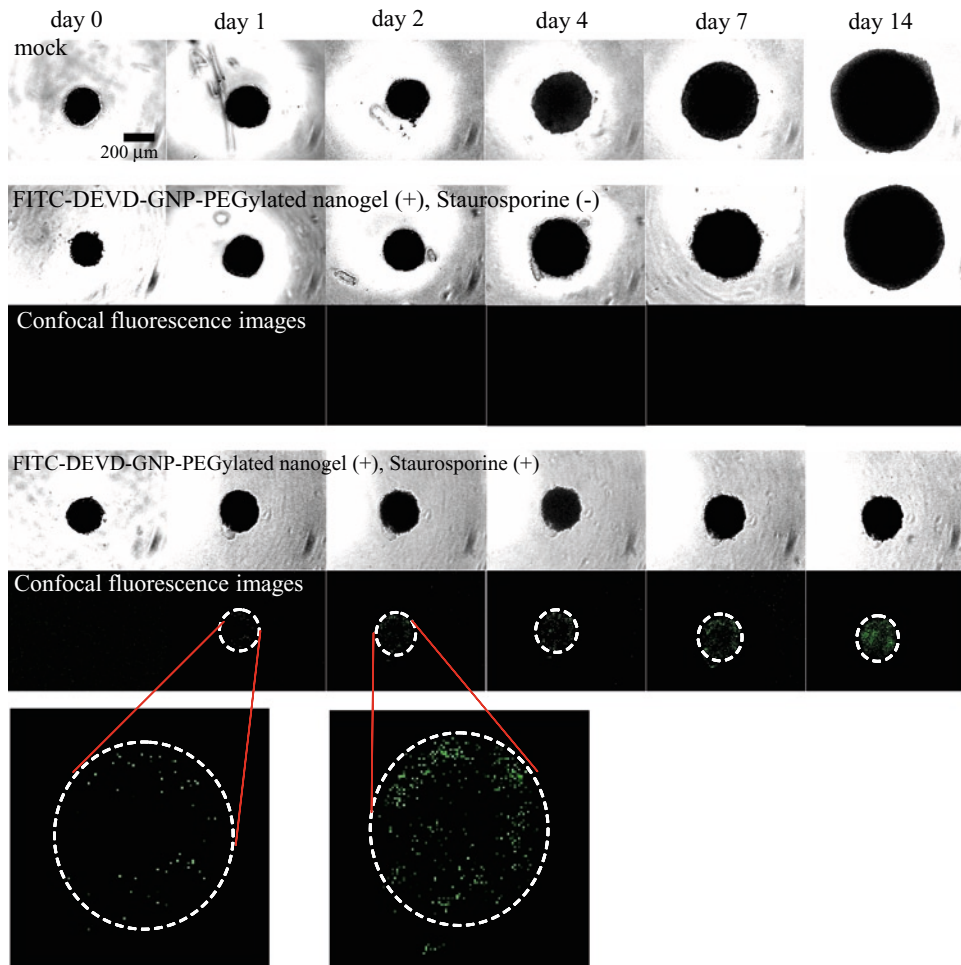


Fig. 20. Phase and confocal fluorescence images of the HuH-7 MCTSs incubated with PBS (mock), the FITC-DEVD-GNP-PEGylated nanogel alone, and the FITC-DEVD-GNP-PEGylated nanogel with staurosporine.

have not met the high expectations. One plausible reason for this discrepancy may be that the monolayer assay only reflects the acute efficacy for the first several days, possibly overlooking the delayed or sustained drug action appearing at later stages. In this regard, multicellular tumor spheroids (MCTSs) have attracted interest to evaluate drug-mediated antitumor activity during long-term *in vitro* tests [64–66]. Accordingly, MCTSs are used as the 3D *in vitro* tumor models for monitoring the cancer response to therapy. Thus, monitoring the cancer response (apoptosis) and staurosporine-induced growth inhibition of HuH-7 MCTSs were simultaneously assessed under prolonged culturing (up to 14 days). HuH-7 MCTSs (~200 μm) were used as the *in vitro* tumor model, since the maximum distance between the capillary blood vessels with intravascular solid tumors is believed to be 200 μm or less [67]. As seen in Fig. 20, the growth inhibition of the HuH-7 MCTSs was not observed for the FITC-DEVD-GNP-PEGylated nanogel alone or for the FITC-DEVD-GNP-PEGylated nanogel even in the presence of staurosporine on day 2. In addition, apoptotic cells (green fluorescence signal) were not observed for the FITC-DEVD-GNP-PEGylated nanogel alone. In contrast, apoptotic cells (green fluorescence signal) were observed as early as day 1, and the number of

apoptotic cells (fluorescence intensity) increased with prolonged incubation time. The growth inhibition of the HuH-7 MCTSs, treated with staurosporine, was observed after a delay of 3 days. Thus, the FITC–DEVD–GNP–PEGylated nanogel acts as a nanoprobe for monitoring apoptosis that is applicable to rapid assessment of cancer response to therapy compared with the simple direct observation of MCTS size.

Summary

Novel approaches to the synthesis, characterization, and biomedical applications of the smart stimuli-responsive PEGylated nanogels are ongoing. In particular, the pH-responsive PEGylated nanogels composed of a PEAMA-co-PTFEMA gels core and tethered PEG chains have remarkable on–off regulation of ^{19}F MR signals (T_2 values of ^{19}F) as well as S/N ratio in response to extracellular pH=6.5 of tumor environment, which potentially makes them excellent candidates as smart tumor-specific ^{19}F -MRI nanoprobes. Additionally, the DOX-loaded pH-responsive PEGylated nanogels exhibit intracellular release of DOX in response to endosome/lysosomal pH, thereby conferring a higher level of bioavailability than free DOX and far more effective antitumor activity than free DOX against naturally drug-resistant human hepatoma cells. The caspase-3-responsive and fluorescence-quenched smart apoptosis nanoprobe based on the PEGylated nanogel containing GNPs in the PEAMA gels core and FITC-labeled DEVD peptide at the tethered PEG chain end results are very exciting. The FITC–DEVD–GNP–PEGylated nanogel showed quenching/dequenching of the fluorescence signal synchronizing with the apoptosis in living cells, allowing real-time monitoring of early cancer response to staurosporine against monolayer-cultured HuH-7 cells as well as HuH-7 MCTSs. The apoptotic cells in HuH-7 MCTSs were detected as early as day 1 after treatment with staurosporine, whereas the growth inhibition (change in size) of the HuH-7 MCTSs was only observed on day 4. It is anticipated that the stimuli-responsive PEGylated nanogel has great promise to be used for cancer diagnosis and therapy in vivo as well as provide another approach to the creation of smart nanomedicines [68, 69].

References

1. Yallapu MM, Reddy MK, Labhasetwar V (2007) Nanogels: chemistry to drug delivery. In: Biomedical Applications Nanotechnology. Wiley, NY, pp 131–171
2. Morimoto N, Hasegawa U, Sugawara A, Yamane S, Akiyoshi K (2007) Polysaccharide nanogel engineering: Design of nano-structured hydrogel materials and application to biotechnology and medicine. In: Nanotechnology Carbohydrate Chemistry. Transworld Research Network, Trivandrum, India, pp 67–85
3. Vinogradov SV, Bronich TK, Kabanov AV (2002) Adv Drug Deliv Rev 54:135–147
4. Bronich TK, Bontha S, Shlyakhtenko LS, Bromberg L, Hatton TA, Kabanov AV (2006) J Drug Target 14:357–366
5. Bontha S, Kabanov AV, Bronich TK (2006) J Control Release 114:163–174
6. Vinogradov SV, Zeman AD, Batrakova EV, Kabanov AV (2005) J Control Release 107:143–157
7. Bronich TK, Keifer PA, Shlyakhtenko LS, Kabanov AV (2005) J Am Chem Soc 127:8236–8237
8. Matsumura Y, Maeda H (1986) Cancer Res 46:6387–6392
9. Oishi M, Nagasaki Y (2007) React Funct Polym 67:1311–1329
10. Oishi M, Hayashi H, Itaka K, Kataoka K, Nagasaki Y (2007) Colloid Polym Sci 285:1055–1060
11. Oishi M, Miyagawa N, Sakura T, Nagasaki Y (2007) React Funct Polym 67:662–668
12. Hayashi H, Iijima M, Kataoka K, Nagasaki Y (2004) Macromolecules 37:5389–5396
13. Gerweck LE, Seetharaman K (1996) Cancer Res 56:1194–1198
14. Wike-Hooley JL, Haveman J, Reinhold HS (1984) Radiother Oncol 2:343–366
15. Gruenberg J (2001) Nat Rev Mol Cell Biol 2:721–730
16. Clague MJ (1998) Biochem J 336:271–282
17. Mukherjee S, Ghosh RN, Maxfield FR (1997) Physiol Rev 77:759–803

18. Oishi M, Sumitani S, Nagasaki Y (2007) *Bioconjugate Chem* 18:1379–1382
19. Oishi M, Hayashi H, Iijima M, Nagasaki Y (2007) *J Mater Chem* 17:3720–3725
20. Oishi M, Tamura A, Nakamura T, Nagasaki Y (2009) *Adv Funct Mater* 19:827–834
21. Poehlein GW (1986) Emulsion polymerization. In: Mark HF, Bikales NM, Overberger CG, Menges G, Kroschwitz JJ (eds) *Encyclopedia of polymer science and engineering*, vol 6.1, 2nd edn. Wiley, New York, p 1986
22. Westby MJ (1988) *Colloid Polym Sci* 266:46–51
23. Hoshino F, Sasaki M, Kawaguchi H, Ohtsuka Y (1987) *Polym J* 19:383–389
24. Lee AS, Gast AP, Büttin V, Armes SP (1999) *Macromolecules* 32:4302–4310
25. Wetering VP, Moret EE, Schuurmans-Nieuwenbroek MME, Steenberg VMJ, Hennink WE (1999) *Bioconjug Chem* 10:589–597
26. Kobayashi H, Brechbiel MW (2005) *Adv Drug Deliv Rev* 57:2271–2286
27. Caravan P, Ellison JJ, McMurry TJ, Lauffer RB (1999) *Chem Rev* 99:2293–2352
28. Yu J-X, Kodibagkar VD, Cui W, Mason RP (2005) *Curr Med Chem* 12:819–848
29. Butun V, Billingham NC, Armes SPJ (1998) *Am Chem Soc* 120:11818–11819
30. Duncan R (2003) *Nat Rev Drug Discov* 2:347–360
31. Jain RK (2003) *Eur J Pharm Sci* 20:1–16
32. Maeda H (2001) *Adv Drug Delivery Rev* 46:149–168
33. Avicheckter D, Schechter B, Arnon R (1998) *React Funct Polym* 36:59–69
34. Bogdanov A Jr, Wright SC, Marecos EM, Bogdabova A, Martin C, Petherick P, Weissleder R (1997) *J Drug Target* 4:321–330
35. Lee CM, Tanaka T, Murai T, Kondo M, Kimura J, Su W, Kitagawa T, Ito T, Matsuda H, Miyasaka M (2002) *Cancer Res* 62:4282–4288
36. Gordon AN, Fleagle JT, Guthrie D, Parkin DE, Gore ME, Lacave A (2001) *J Clin Oncol* 19:3312–3322
37. Newman MS, Colbern GT, Working PK, Engbers C, Amntea MA (1999) *Cancer Chemother Pharmacol* 43:1–7
38. Nakanishi T, Fukushima S, Okano K, Suzuki M, Matsumura Y, Yokoyama M, Okano T, Sakurai Y, Kataoka K (2001) *J Control Release* 74:295–302
39. Yokoyama M, Okano T, Sakurai Y, Suwa S, Kataoka K (1996) *J Control Release* 39:351–356
40. Maeda H, Sawa T, Konno T (2001) *J Control Release* 74:47–61
41. Tsukioaka Y, Matsumura Y, Hamaguchi T, Koike H, Moriyasu F, Kakizone T (2002) *Jpn J Cancer Res* 93:1145–1153
42. Kwon G, Naito M, Yokoyama M, Okano T, Sakurai Y, Kataoka K (1997) *J Control Release* 48:195–201
43. Gillies ER, Frechet JM (2005) *Bioconjug Chem* 16:361–368
44. Bae Y, Fukushima S, Harada A, Kataoka K (2003) *Angew Chem Int Ed Engl* 42:4640–4643
45. Wirth T, Kuhnel F, Fleischmann-Mundt B, Woller N, Djojusbrotro M, Rudolph KL, Manns M, Zender L, Kubuka S (2005) *Cancer Res* 65:7393–7402
46. Huesker M, Folmer Y, Schneider M, Fulda C, Blum HE, Hafkemeyer P (2002) *Hepatology* 36:874–884
47. Omelyanenko V, Kopečková P, Kopeček J (1998) *J Control Release* 53:25–37
48. Schoenberger J, Bauer J, Moosbauer J, Eilles C, Grimm D (2008) *Curr Med Chem* 15:187–194
49. Thornberry NA, Lazebnik Y (1998) *Science* 281:1312–1316
50. Lazebnik YA, Kaufmann SH, Desnoyers S, Poirier GG, Earnshaw WC (1994) *Nature* 371:346–347
51. Wyllie AH (1980) *Nature* 284:555–556
52. Stefflova K, Chen J, Marotta D, Li H, Zheng G (2006) *J Med Chem* 49:3850–3856
53. Wu Y, Xing D, Luo S, Tang Y, Chen Q (2006) *Cancer Lett* 235:239–247
54. Harada A, Kataoka K (1998) *Macromolecules* 31:288–294
55. Kenworthy AK, Hristova K, Needham D, McIntosh TJ (1995) *Biophys J* 68:1921–1936
56. Tanford C, Nozaki Y, Rohde MF (1977) *J Phys Chem* 81:1555–1560
57. Gueroui Z, Libchaber A (2004) *Phys Rev Lett* 93:166108/1–166108/4
58. Zhang L, Torgerson TR, Liu X-Y, Timmons S, Colosia AD, Hawiger J, Tam JP (1998) *Proc Natl Acad Sci USA* 95:9184–9189
59. Oishi M, Hayashi H, Uno T, Ishii T, Iijima M, Nagasaki Y (2007) *Macromol Chem Phys* 208:1176–1182
60. Agasti SS, You C-C, Arumugam P, Rotello VM (2008) *J Mater Chem* 18:70–73
61. Isaacs SR, Cutler EC, Park JS, Lee TR, Shon Y-S (2005) *Langmuir* 21:5689–5692
62. Templeton AC, Hostetler MJ, Kraft CT, Murray RW (1998) *J Am Chem Soc* 120:1906–1911
63. Falcieri E, Matelli AM, Bareggi R, Cataldi A, Cocco L (1993) *Biochem Biophys Res Commun* 193:19–25
64. Santini MT, Rainaldi G, Indovina PL (1999) *Int J Radiat Biol* 75:787–799
65. Sutherland RM (1998) *Science* 240:177–184
66. Moscona A (1957) *Proc Natl Acad Sci USA* 43:184–194
67. Konerding MA, Fait E, Gaumann A (2001) *Br J Cancer* 84:1354–1362
68. Lian T, Ho RJY (2001) *J Pharm Sci* 90:667–680
69. Vasey PA, Kaye SB, Morrison R, Twelves C, Wilson P, Duncan R, Thoson AH, Murray LS, Hilditch TE, Murray T, Burtles S, Fraier D, Frigerio E, Cassidy J (1999) *Clin Cancer Res* 5:83–94

Stimuli-Sensitive Microhydrogels

Haruma Kawaguchi

Abstract Microhydrogels have become a very interesting and important material in hydrogels bioapplications. New techniques for the design, synthesis, characterization, function, and application of microhydrogels are providing exciting new possibilities in the micronized science. Hydrogels are a soft material with sizes and shapes that are subject to change depending on environmental conditions such as temperature, pH, coexisting materials, and light. Hydrogels that respond to these environmental stimuli and cause swelling changes in aqueous media are known as “stimuli-sensitive hydrogels.”

Introduction

Hydrogels are classified according to their size: bulk gels, macrogel, microgel, and nanogel. The microgels range from submicron to millimeter, whereas the size of nanogel is less than 100 nm. The size of materials is a crucial factor that determines their properties. The dependence of physical properties (x) on diameter (D) of spherical materials is presented in (1):

$$x = kD^n \quad (1)$$

The specific surface area of a spherical particle is inversely proportional to the diameter. The diffusion rate is also inversely proportional to the diameter. The time needed for the gels to transfer stimuli to its center was proportional to the square of the diameter of the gels (Table 1) [1]. Therefore, smaller gels provide much quicker and more efficient performance. If the particles are too small then they can cause problems; this makes microgels, in some cases, preferable to nanogels. Microgels have an additional merit, in that their size is in the same range as the wavelength of visible light. This unique feature enables the microgels to be applied for optically functionalized devices.

Stimuli-Sensitive Microgels

There are many kinds of thermosensitive hydrogels that include synthetic polymers, such as poly(acrylamide) derivatives, poly(methacrylamide) derivatives, poly(butyl vinyl ether), poly(ϵ -caprolactam), and derivatives of naturally occurring polymers, such as hydroxypropylcellulose and methylcellulose [2, 3].

Preparation of Microhydrogels

Polymerizations, such as inverse emulsion polymerization, precipitation polymerization, and dispersion polymerization, are the main methods for preparing polymer particles. Other routes include polymer molecule assembling in water, spray drying of polymer solutions,

H. Kawaguchi • Department of Chemistry, Kanagawa University, Yokohama, Kanagawa, Japan
e-mail: haruma@apple.keio.ac.jp

Table 1. Parameters determining the gels size

x	n
Volume	3
Specific surface area	-1
Period for stimuli to reach the center	2
Diffusion rate	-1
Sedimentation rate	2
Interparticle distance ^a	1

^aAt a constant volume fraction

evaporation or extraction of solvent from oil-in-water (O/W) emulsions in which polymer is added in the oil phase.

Microgel Preparation by Particle-Forming Polymerization

In an aqueous polymerization of *N*-isopropylacrylamide (NIPAM) at 70°C, the reaction system is homogeneous. Once polymerization is initiated, the polymer molecules are phase separated to give a condensed poly(*N*-isopropylacrylamide) (PNIPAM) phase of PNIPAM nanoaggregates [4]. The nanoaggregates grow with increasing conversion and finally become microhydrogels. Precipitation polymerization of acrylamide in aqueous alcohol forms monodispersed microgels [5, 6]. In this system, the number of nanoaggregates or nanogels is fixed at an early stage of polymerization; as a result, the size distribution of final microgels is quite narrow. The size of microgels is controlled by the composition of polymerization medium and the addition of surfactant to the aqueous polymerization of NIPAM in order to form smaller microgels. The addition of a hydrophilic comonomer, such as acrylic acid (AAc), makes smaller microgel particles.

Copolymerization of NIPAM and other monomers causes not only a change in microgel size, but also a change in thermosensitivity. For these microgels, depending on the crosslinking density of the shell, compression or shrink-wrapping of the core was observed [7]. The significance of the crosslinker used was shown in the study of *N*-vinylcaprolactam (VCL)-based microgels using two kinds of crosslinkers [8]. The compatibility between VCL and the crosslinker is the most important factor for well-structured temperature-sensitive microgels.

Microgel Preparation by Surface Modification of Core Particle

Core-shell microspheres, with the shell being composed of a hydrogel, are regarded as microgels. The core-shell particles are made by seeded polymerization and graft polymerization, although some core-shell particles are prepared by molecular assembly of amphiphilic block copolymers. When grafting reactions are carried out without using a crosslinker, “hairy-like” particles are obtained. Hairy PNIPAM particles are prepared using core particles with iniferters on the surface. The polymerization is carried out by UV irradiation at a temperature lower than the LCST of PNIPAM [9–11]. This controlled radical polymerization produces hairy-like PNIPAM particles with controlled chain lengths. When the dispersion is dried on a substrate, these PNIPAM particles form two-dimensional colloidal arrays. The inter particle distance of the colloidal array usually corresponds to twice the thickness of hairy layers.

Microgel Preparation by Assembling Polymer Molecules in Solution

Some polymer molecules dissolved in aqueous medium can be assembled by using stimuli. For example, PNIPAM microgels are obtained from an aqueous solution of PNIPAM by increasing the temperature which causes phase separation. The suitable temperature, for PNIPAM microgels to form from a solution, is well above the LCST of PNIPAM, and is usually, around 70°C [12]. Hydroxypropyl cellulose (HPC) is an amphiphilic cellulose derivative and its amphiphilicity depends on temperature with an LCST of ~41°C [13]. Thus, the HPC in aqueous solution can be converted to microaggregates by warming the solution above 41°C [14].

Amphiphilic block copolymers, for example, block copolymer of polyethyleneoxide (PEO) and PNIPAM, form micelles when the aqueous solution is warmed above the LCST of PNIPAM. On cooling, the micelles disappear and polymers dissolve to avoid this break down, the core (PNIPAM) or shell (PEO) must be crosslinked. Poly(glycerol methacrylate) (PGLM)-block-PNIPAM can actually form two types of micelles [15]; one is with a PNIPAM core and a PGLM micellar shell and the other is a PGLM core with a PNIPAM micellar shell. The first one is formed by warming the polymer as described earlier. Another technique is as follows: a methanol solution of the two polymer systems is made and then tetrahydrofuran (THF) is slowly added to the solution under stirring. This method is based on the principle that methanol is a common solvent for both of PGLM and PNIPAM blocks but THF is a nonsolvent of PGLM.

Polyelectrolytes in aqueous solution assemble as microaggregates by adding molecules with opposite charges; the electrostatic interactions between them facilitate particle formation. For example, carboxymethylcellulose (CMC) molecules dissolved in water assemble when a cationic surfactant, polycation or multivalent metal ion are added [16]. Similarly, CMC is converted to a microgel by assembling with chitosan.

Stimuli Responsiveness of Microhydrogels

Temperature Responsiveness of Microhydrogels

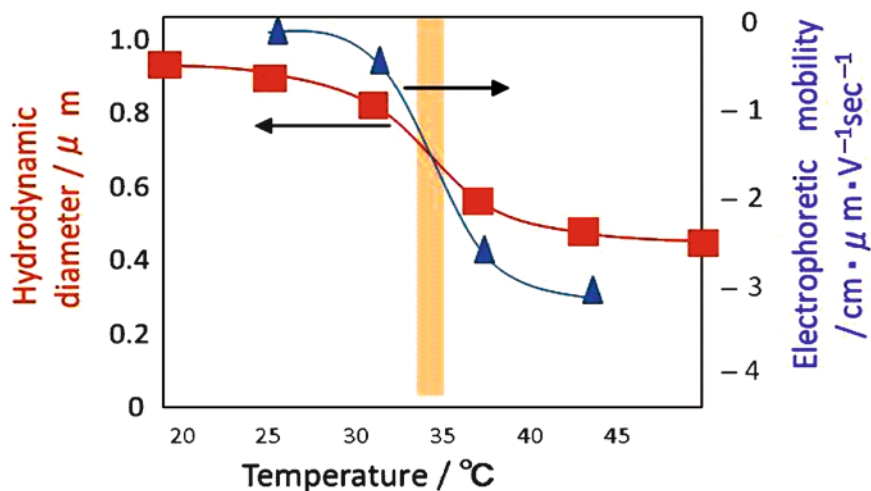
Acrylamide derivative polymers (LCSTs in Table 2, poly(vinyl methylether) (LCST: 36°C), poly(*N*-vinylcaprolactam) (LCST: 26°C), PEO-block-polypropyleneoxide-block-REO, Pluronics, and hydroxypropyl cellulose (LCST: 41°C) are well known thermo-sensitive polymers. The LCST can be changed by copolymerizing hydrophilic and hydrophobic comonomers that made the LCST of copolymers higher or lower, respectively. For example, microgels composed of poly(NIPAM-*co*-butyl acrylate) has a lower LCST and poly(NIPAM-*co*-AAc) has a higher LCST than 32°C. The combination of two acrylamide derivatives, *N*-acryloylpyrrolidine (LCST: 5°C) and *N*-acryloyl piperidine (LCST: 55°C), forms microgels with predictable LCST based on the molar fraction of two components [17].

Microgel Volume Phase Transition Temperature

Temperature responsiveness of microhydrogels is usually discussed by the microgel size change at their LCST at which the polymer molecule dehydrates and the gels collapses with a drastic decrease in volume. The temperature responsiveness of a microgel can also be volume phase transition temperature (VPTT) responsive instead of LCST [18]. The size of interest is not that of the dried microgel but that of the hydrodynamic form which is the effective size of the swollen hydrogels in an aqueous medium. The hydrodynamic size is commonly

Table 2. LCST of poly(acrylamide) derivatives

	$\begin{array}{c} \text{CH}_3 \\ \\ -\text{CH}_2-\text{C}- \\ \\ \text{C}=\text{O} \\ \end{array}$	$-\text{CH}_2-\text{CH}- \\ \\ \text{C}=\text{O} \\ \end{array}$
$\begin{array}{c} \text{CH}_2 \\ \\ -\text{NHCH} \\ \\ \text{CH}_2 \end{array}$	61	47
$\begin{array}{c} \text{CH}_3 \\ \\ -\text{NHCH} \\ \\ \text{CH}_3 \end{array}$	45	31
$-\text{NH}-\text{CH}_2-\text{CH}_2-\text{CH}_3$	27	23
$\begin{array}{c} \text{CH}_2-\text{CH}_2 \\ \\ -\text{N} \\ \\ \text{CH}_2-\text{CH}_2 \end{array}$		55
$\begin{array}{c} \text{CH}_2-\text{CH}_2 \\ \\ -\text{N} \\ \\ \text{CH}_2-\text{CH}_2 \\ \\ \text{CH}_2 \end{array}$		05

**Fig. 1.** Hydrodynamic size and electrophoretic mobility of poly(*N*-isopropylacrylamide) (PNIPAM) microgels as functions of temperature.

measured by dynamic light scattering (Fig. 1). Careful use of this data must be taken since the correlation function obtained by the dynamic light scattering measurements gives the diffusion constant of the particles, from which, the hydrodynamic diameter of particles is calculated; however, the swollen particles have an unclear interface. The real amount of water held in PNIPAM microgel is determined by DSC or other analyses.

Volume phase transitions cause changes in the electrophoretic mobility of the microgels because the charges, which remain buried in the gels at low temperatures, are concentrated at the surface layer of the shrunken gels at temperatures $>LCST$. However, the electrophoretic mobility does not serve for ζ potential determination because the ζ potential is not related to microgels that have no clear interface [19]. Measurements by force microscopy and incoherent elastic scattering reveal the elastic modulus of microgel. A difference of two orders in the elastic modulus has been seen between the temperatures above and below VPTT [20].

Temperature Dependent Hydrophilicity–Hydrophobicity of Microgel

The reversible swelling–deswelling of PNIPAM microgel reflects the reversible change in hydrophilicity–hydrophobicity of the gels. PNIPAM molecule dissolved in water is amphiphilic based on surface tension measurements. The surface tension of an aqueous solution of PNIPAM decreases with increasing temperature; this also occurs for dispersions of PNIPAM microgel. This property is utilized in the preparation of thermoreversible Pickering emulsions. PNIPAM microgels form micelle-like assemblies in organic solvent/water systems to give an O/W or W/O emulsion. Several aliphatic and aromatic solvents are mixed with aqueous dispersion of PNIPAM microgel. The mixture is stirred for 5 minutes at room temperature. Pickering emulsions form when the organic solvent has a low “work of adhesion” value whereas 1-undecanol which has a high “work of adhesion” does not form a Pickering emulsion. The Pickering emulsion is deformed when it is warmed above the VPTT of PNIPAM. The emulsion collapses at 40°C, and a stable emulsion is regenerated by agitation at 25°C [21].

PNIPAM-*co*-methacrylic acid (MAc) microgels, which are prepared under different pHs, are used as stimuli-responsive Pickering emulsion stabilizers [22]. The stability of the microgels depends on the pH during synthesis; the microgels with high charges appreciably stabilize the emulsion. PNIPAM microgel-based Pickering emulsion was utilized for the preparation of Janus microgels [23].

pH Responsiveness of Microhydrogels

Weak acid or base containing microgels are pH and ionic strength sensitive. They are prepared by combining a small amount of an ionizable component with a hydrophilic monomer, and if necessary, a crosslinker [24, 25]. For example, ethyl acrylate, MAc, and butanediol diacrylate are copolymerized in water to form microgels used to repair damaged load-bearing soft tissue [26]. When used for biomedical purposes, the sensitivity of the microgel to divalent ions, such as Ca^{2+} and Mg^{2+} , must be taken into account [27]. Addition of Ca^{2+} causes significant decreases in the critical coagulation concentration (CCC), the degree of swelling and the electrophoretic mobility due to the ionic crosslinking of neighboring COO^- groups by the Ca^{2+} . However, the extent of ionic crosslinking is limited because the covalent crosslinks suppress the large-scale conformational rearrangement of polymer chains and decrease the chances for ionic crosslinking. Thus, the change in properties of a microgel caused by Ca^{2+} is controlled by the degree of covalent crosslinking.

Tertiary amine-carrying pH responsive microgels are prepared by copolymerizing diethylamino- or diisopropylaminoethyl methacrylate (DEAEMA and DPAEMA, respectively) with poly(propyleneglycol) diacrylate in the presence of macromonomer stabilizer. The transition between the swollen and shrunken states of the particle occur in the arPKs of DEAEMA and DPAEMA [28].

Responsiveness of Microhydrogels to Other Stimuli

Other stimuli-sensitive microgels include UV-, light-, and biomolecule-sensitive microgels. Photosensitive microhydrogels are created by the insertion of azobenzene as a pendant group to the hydrophilic polymer chain or in the main chain.

Multistimuli-Sensitive Microhydrogels

In addition to NIPAM homopolymeric microgel, copolymerization of NIPAM with carboxylic acid-containing monomers, such as AAc, MAc, and allylacetic acid [29], or amine-containing monomers, such as vinyl pyridine [30], form multistimuli-sensitive microgels that are temperature, pH, and ionic strength-sensitive. The incorporation of NIPAM and AAc to copolymerize with acrylamido-2-deoxyglucose (AADG) at different ratios of AADG to AAc forms temperature, pH, and ionic strength-sensitive microgels with different VPTTs and greater biocompatibility [29].

PMAC-poly(2-dimethylamino)ethyl methacrylate (DMAEMA) microgels, prepared by inverse microemulsion polymerization and stabilized with grafted poly(ethylene glycol), show not only pH responsiveness but also temperature responsiveness due to the LCST of PDMAEMA [31]. Generally, only small amounts of comonomers are added relative to the amount of NIPAM. Simple copolymerization using larger amounts of comonomer causes shifts in the VPTT as well as broadening or loss of transition. Microgels, with two components in the block structure, form core-shell microgels under more suitable conditions [32]. An alternative method to maintain the individual stimuli-sensitivity of each component is to make a division between different stimuli-sensitive components. Multistimuli-sensitive microgels made of microgel-polyelectrolyte complexes that are composed of poly(NIPAM-co-MAc) and poly(diallyldimethyl ammonium chloride) are stable irrespective of the complex composition [33]. The size, zeta-potential and pH and temperature-sensitivity of the microgel-polyelectrolyte complexes are influenced by the adsorbed polyelectrolytes.

Preparation of Inorganic Nanoparticles/Polymer Composite Microgel

Inorganic nanoparticles have several interesting functions. For example, Au and Ag exhibit surface plasmon resonance that emit specific colors depending on the particle size, refractive index of the medium, and inter particle interactions. Magnetic nanoparticles made from iron oxide are used as MRI contrast enhancer and hyperthermia materials and titanium nanoparticles have photocatalytic properties. These versatile inorganic nanoparticles present novel functions when they are incorporated with polymeric particles. Several inorganic/polymer composite microgels have been prepared that have unique features [34–36].

Preparation of Inorganic Microgel Composites

The preparation methods for inorganic microgel composites are categorized into six patterns; these patterns are illustrated in Fig. 2 except for methods 2 and 4. The steps are as follows:

1. Particles formed by polymerization in the presence of inorganic nanoparticles
2. Simultaneous reactions of particle-forming polymerization with inorganic nanoparticle precursors

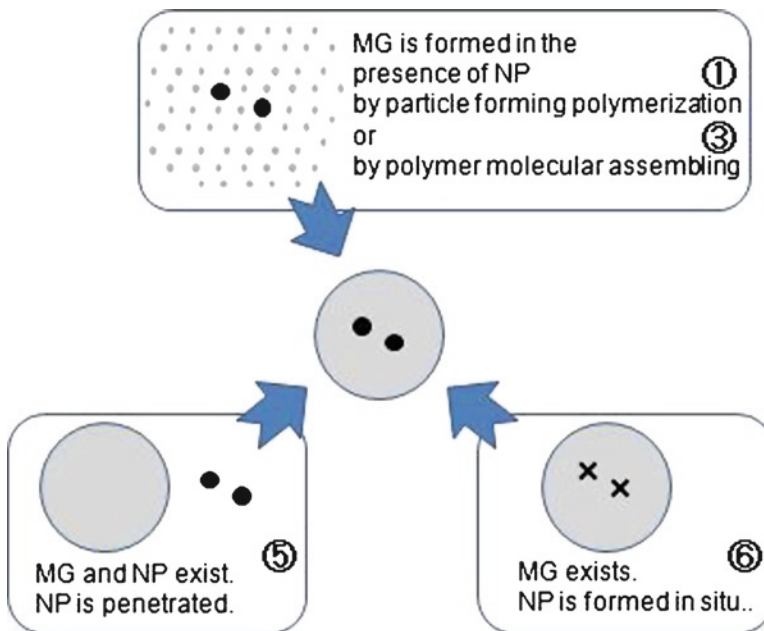


Fig. 2. Synthesis routes for nanoparticle (NP) containing composite microgel (MG).

3. Polymer molecular assembly involving inorganic nanoparticle as composites
4. Polymer molecule assembly involving inorganic nanoparticle precursors followed by in situ formation of nanoparticles
5. Introduction of inorganic nanoparticles onto/into polymeric microgels
6. Introduction of precursor of inorganic nanoparticles into polymeric microgel followed by in situ formation of inorganic nanoparticles

In method 1, an inverse mini-emulsion polymerization of a hydrophilic monomer in which inorganic nanoparticles are stably dispersed is used. The second method is not very practical because it is too difficult to carry two reactions at a comparable rate. Method 3 involves the formation of magnetite/CMC composite microgels; an affinity of magnetite for the COOH and OH groups causes the composite formation. A modified method of 3 entails successive deposition of polymer molecules onto magnetite particles. Negatively charged PNIPAM and positively charged PNIPAM are alternatively deposited layer-by-layer to prevent the deposited polymers from detaching from the magnetic particles [37].

The fourth method is not as common. It uses ferric and ferrous ions instead of magnetic nanoparticles. The ions have an affinity for $-\text{COOH}$ and $-\text{OH}$ groups of CMC. Therefore, combinations of ferric and ferrous ions and CMC form composite microgels by the conversion of ferric and ferrous ions to magnetite nanoparticles in the CMC matrix. In method 5, the network structure of the microgels allows inorganic nanoparticles to penetrate into the microgels that have an affinity with inorganic nanoparticles. The electro-attractive interaction is very strong between the inorganic nanoparticles, and the microgels enable composite microgel formation. Method 6 is the most promising in which the location of the inorganic nanoparticles inside of the microgel can be controlled.

Precipitation polymerization of NIPAM with a small amount of glycidyl methacrylate (GMA) forms PNIPAM microgels with the GMA evenly distributed. The GMA glycidyl groups react with the alkyl diamine to form ammonium sites in the microgel; when AuCl_4^- is added to the dispersion, it is electrostatically attracted to the amino groups in the core of the microgel. After reaching equilibrium, the Au ions are reduced with NaBH_4 in situ to Au, to provide microgels that contain evenly distributed Au^0 nanoparticles [38–40].

Polymer Composite Microgel Functions

Noble Metal Nanoparticles/PNIPAM Composite Microgel

The Au^0 nanoparticles, prepared above, can be grown by successive reduction of additional Au and Ag ions in the microgel. The size of the metal nanoparticles/PNIPAM composite microgel significantly affects the VPTT of PNIPAM. A change in the Au nanoparticles distribution in the microgel occurs that changes the spectrum of the surface plasmon resonance and consequently, and the color emitted [41]. To expand the application of Au^0 nanoparticle-containing PNIPAM microgel, more sophisticated microgels with layered structures were prepared [42]. Another efficient method to entrap Au nanoparticles in PNIPAM microgel involves a two-step protocol. In the first step, Au nanoparticles are coated with cetyltrimethyl ammonium bromide (CTAB) and a thin polystyrene shell; in the second step, the coated Au nanoparticles are emulsion polymerized. The resulting Au nanoparticle core/PNIPAM shell microgels exhibit changes in UV-visible light in response to the VPTT of PNIPAM with changes in temperature [26]. Thermosensitive PNIPAM hairy nanoparticles that have temperature-responsive catalytic activity can also be made [43].

Metal Oxide Nanoparticles/Thermosensitive Polymer Composite Microgels

Magnetite Nanoparticles/PNIPAM Composite Microgels

Composite microgels, composed of magnetic nanoparticles and PNIPAM, are used for heat-triggered release of drugs. The heat generated by the magnetic nanoparticles is transferred to thermosensitive matrix which leads to the collapse of the gels when the temperature of matrix exceeds the VPTT. The morphology ranges from a magnetic island/PNIPAM to a magnetic core/PNIPAM shell [44]. Control of location and the amount of magnetic nanoparticles in the thermosensitive microgel are very important [45]. A series of microgels composed of

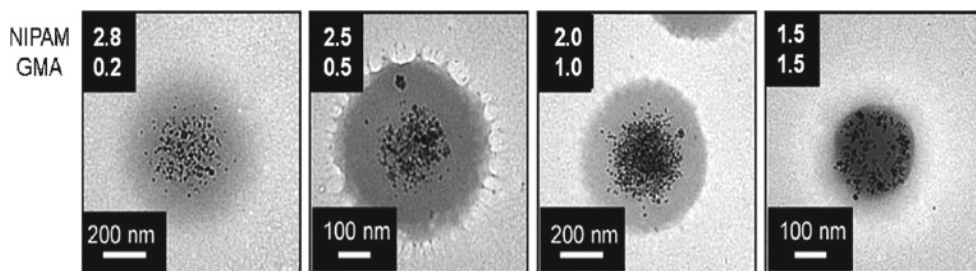


Fig. 3. Magnetite nanoparticles in poly(NIPAM-co-glycidyl methacrylate) microgel.

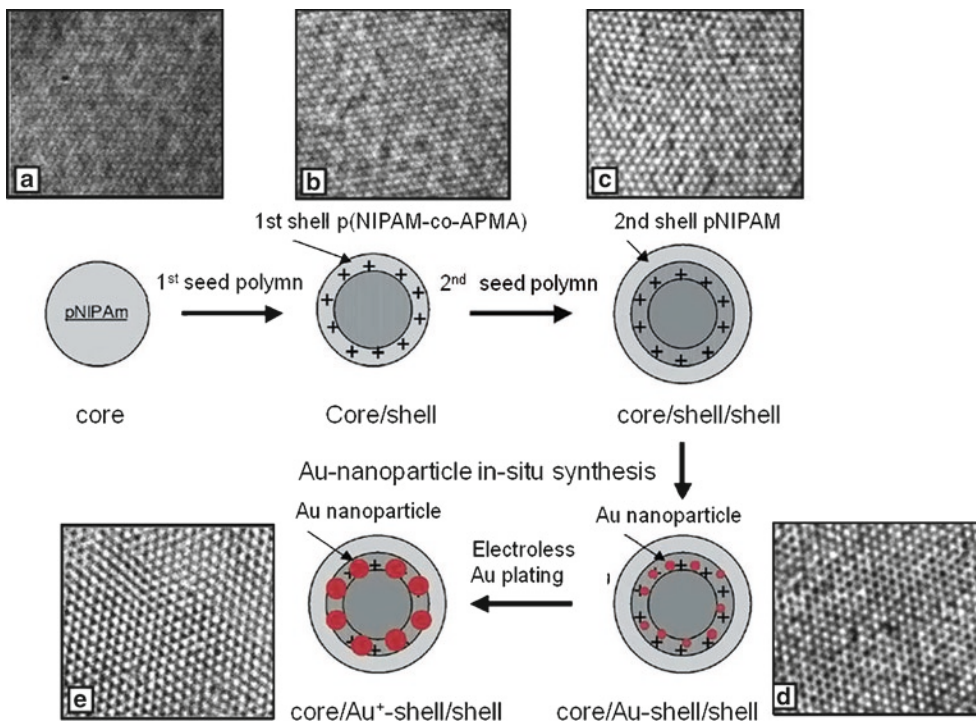


Fig. 4. Composite microgels with designed inner structures and their colloid crystal.

poly(NIPAM-*co*-GMA) with different monomer ratio are formed using radial gradient monomer compositions (Fig. 3). The core of microgel is rich in GMA and the shell is rich in NIPAM. This gradient is attributed to the difference in reactivity and solubility-in-water between GMA and NIPAM. The glycidyl groups of GMA react with 3-mercaptopropyl sulfonic acid sodium salt (MPSA) and then ferrous ions (Fe_2^+) are added which are attracted to the negative sulfonic groups in the core of microgel. After reaching equilibrium, the ferrous ions are reduced to magnetite (Fe_3O_4) to form microgels containing magnetite nanoparticles in the core. As shown in Fig. 4, more magnetite nanoparticles are in the microgels that contained more GMA. However, if the amount of GMA in the core is too high, they pack so densely that the diffusion of ferrous ions in the gels is prevented limiting the magnetite nanoparticles content.

Zinc Oxide Nanoparticles/Thermosensitive Composite Microgels

A precursor of ZnO, $\text{Zn}(\text{CH}_3\text{COO})_2 \cdot 2\text{H}_2\text{O}$, was introduced into poly(VCL-*co*-acetoacetoxyethyl methacrylate (AEM)), a thermosensitive microgel, and then hydrolyzed in situ. The composite microgel formed retained thermosensitivity similar to that of P(VCL-*co*-AEM) even with ZnO nanoparticles as high as 16 wt%. A dispersion of these composite microgels cast on a glass substrate forms a transparent film that is used for UV-shielding. These composite microgels are also used in optoelectronic and photonic fields. As optoelectronic microdevices, UV-detectors, and photocatalysts [46].

Titania Nanoparticles/Thermosensitive Composite Microgels

The incorporation of titanium dioxide into poly(NIPAM-*co*-AAc) microgel was carried out by reacting ammonia with the AAc carboxyl groups in the copolymer microgel [47, 48]. The microgels are added into an ethanolic solution of poly(vinylpyrrolidone) and then titanium tetraisopropoxide is added under stirring for 24 hours. The composite microgels exhibit high catalytic activity in the decomposition reaction of methylene blue under UV irradiation at room temperature, but lose their catalytic activity at high temperatures. It seems that the titania is shielded in the shrunken, opaque PNIPAM matrix at temperatures above the VPTT.

Interpenetrating PNIPAM-PAAc microgels (average diameters at swollen and shrunken states: 750 and 350 nm, respectively), prepared by precipitation polymerization of NIPAM in the presence of PAAc, are used to absorb titania nanoparticles (71 nm). The absorption is carried out at pH 6, near the isoelectric point of titania (6.2). The titania/PNIPAM/PAAc composite microgels thus obtained contain 10–75 wt% titania. The composite microgels exhibit rapid sedimentation which is useful for gravity separation of composite microgels from dispersions after photocatalytic application of microgels, while the sedimentation behavior is temperature controlled [49].

Photoluminescent Nanocrystals/Thermosensitive Composite Microgels

Fluorescent thermosensitive composite microgels are prepared by covering PNIPAM microgels with CdTs nanocrystals [44]. The nanocrystals are covalently immobilized on the microgel surface to form composite microgels that respond to the changes of environmental conditions reversibly and reproducibly. The nanocrystal photoluminescence of microgel is quenched under the VPTT of PNIPAM and restored above the VPTT.

CdSe quantum dots, stabilized with trioctylphosphine oxide, can be incorporated into PNIPAM microgels via ligand exchange, and those stabilized with oleic acid are incorporated into microgels with pendant COOH groups. This method is also used to prepare thermosensitive microgels composed of poly(AEM-*co*-*N*-vinylcaprolactam) [50]. Photoluminescent nanocrystal/thermosensitive polymer composite microgels were prepared by incorporating PbS quantum dots in the interior of PNIPAM microgel [51]. The composite microgels exhibit room temperature quantum efficiency and strong luminescence.

Miscellaneous Nanoparticles/Thermosensitive Composite Microgels

Poly(3,4-ethylenedioxythiophene) (PEDOT) nanorods were incorporated into the shell of PVCL core/poly(AEM) shell microgels [52]. The responses of these composite microgels to environmental temperature and to the repulsion/attraction due to reversible oxidation/reduction by addition of acid and base are very interesting. PEDOT nanorods in microgel are oxidized when the pH is decreased and the Cl⁻ ions are transformed from the aqueous phase into microgels interior, causing the microgels to shrink. Reduction of the PEDOT causes a reversion; consequently, shrinking/swelling can be controlled reversibly by oxidation/reduction. Microgels, which contain ruthenium complexes, catalyze the Belousov–Zhabotinsky self-oscillation reaction [53]. Clay can serve as a crosslinker in PNIPAM microgels; the amount of clay affects the size of microgels [37].

Assemblies and Colloid Crystals of Thermosensitive Microgels

PNIPAM-based microgels self-assemble to form colloid crystals. For example, a dispersion of layered PNIPAM composite microgels was condensed and then a heating–cooling cycle was applied to complete the crystallization [42]. PNIPAM colloid crystal was fixed by self-crosslinking using *N*-hydroxymethylacrylamide [54]. The thermosensitive properties of PNIPAM microgels embedded in the hydrogels remain unperturbed in the volume transition of microgels [55].

Summary

Stimuli-sensitive microgels, also called smart microgels, have significant potential as sensors, energy transferring devices, photonic devices, and bio-separators. Among the many stimuli-sensitive microgels available, PNIPAM microgels have been extensively studied and used for variety of bioapplications. The inorganic nanoparticles, included into PNIPAM microgels, and provide the potential for many new bioapplications without affecting the thermosensitive properties of PNIPAM.

References

1. Tanaka T, Fillmore DJ (1979) Kinetics of swelling of gels. *J Chem Phys* 70:1214–1218
2. Schield HG (1992) Poly(*N*-isopropylacrylamide): experiment, theory and application. *Prog Polym Sci* 17:163–249
3. Ito S (1987) Phase-transition of aqueous solution of poly(*N*-alkylacrylamide) derivatives. Effect of side chain structure. *Kobunshi Ronbunshu* 46(7):437–443
4. Pelton RH, Chibante P (1986) Preparation of aqueous latexes with *N*-isopropylacrylamide. *Coll Surf* 20:247–256
5. Kawaguchi H, Yamada Y, Kataoka S, Morita Y, Ohtsuka Y (1991) Hydrogel microspheres. 2. Precipitation copolymerization of acrylamide with comonomers to prepare monodisperse hydrogel microspheres. *Polym J* 23:955–962
6. Nakazawa Y, Kamijo Y, Fujimoto K, Kawaguchi H, Yuguchi Y, Urakawa H, Kajiwara K (1996) Preparation and structural characteristics of stimuli-responsive hydrogel microsphere. *Angew Makromol Chem* 240:187–196
7. Jones CD, Lyon LA (2003) *Macromolecules* 19:4544
8. Imaz A, Forcada J (2008) *N*-vinylcaprolactam-based microgels: effect of the concentration and type of cross-linker. *J Polym Sci A Polym Chem* 46(8):2766–2775
9. Tsuji S, Kawaguchi H (2004) Temperature-sensitive hairy particles prepared by living radical graft polymerization. *Langmuir* 20:2449–2455
10. Tsuji S, Kawaguchi H (2005) Self-assembly of poly(*N*-isopropylacrylamide)-carrying microspheres into two-dimensional colloidal arrays. *Langmuir* 21(6):2434–2437
11. Tsuji S, Kawaguchi H (2006) Effect of graft chain length and structure design on temperature-sensitive hairy particles. *Macromolecules* 39(13):4338–4344
12. Heskins M, Guillet JE, James E (1968) Solution properties of poly(*N*-isopropylacrylamide). *J Macromol Sci Chem* A2:1441–1455
13. Harsh DC, Gehrke SH (1991) *J Control Release* 17:175
14. Lu X, Hu Z, Gao J (2001) *Macromolecules* 34:2242
15. Sato T, Tsuji S, Kawaguchi H (2008) Preparation of functional nanoparticles by assembling block copolymers formed by living radical polymerization. *Ind Eng Chem Res* 47:6358–6361
16. Guillot S, Delsanti M, Désert S, Langevin D (2003) Surfactant-Induced Collapse of Polymer Chains and Monodisperse Growth of Aggregates near the Precipitation Boundary in Carboxymethylcellulose–DTAB Aqueous Solutions. *Langmuir* 19(2):230–237

17. Hoshino F, Fujimoto T, Kawaguchi H, Ohtsuka Y (1987) N-substituted acrylamide-styrene copolymer latexes II. Polymerization behavior and thermosensitive stability of latexes. *Polym J* 19(2):241–247
18. Wu C, Zhou S (1997) *Macromolecules* 30:574
19. Ohshima H, Makino K, Kato T, Fujimoto K, Kondo T (1993) Kawaguchi, Electrophoretic mobility of latex particles covered with temperature-sensitive hydrogel layers. *J Colloid Interface Sci* 159:512–514
20. Rubio RJ, Frick B, Seydel T, Stamm M, Fernandez BA, Lopez CE (2008) Polymer chain dynamics of core-shell thermosensitive microgels. *Macromolecules* 41(13):4739–4745
21. Tsuji S, Kawaguchi H (2008) Thermosensitive Pickering emulsion stabilized by poly(N-isopropylacrylamide)-carrying particles. *Langmuir* 24(7):3300–3305
22. Brugger B, Richtering W (2008) Emulsions stabilized by stimuli-sensitive poly(N-isopropylacrylamide)-co-methacrylic acid polymers: microgels versus low molecular weight polymers. *Langmuir* 24(15):7769–7777
23. Suzuki D, Tsuji S, Kawaguchi H (2008) Janus microgels prepared by surfactant-free Pickering emulsion-based modification and their self-assembly. *J Am Chem Soc* 129(26):8088–8089
24. Ni H, Kawaguchi H, Endo T (2007) Preparation of pH-sensitive hydrogel microspheres of poly(acrylamide-co-methacrylic acid) with sharp pH–volume transition. *Colloid Polym Sci* 285:819–826
25. Ni H, Kawaguchi H (2007) Preparation of amphoteric microgels of poly (acrylamide/methacrylic acid/dimethylamino ethylene methacrylate) with a novel pH-volume transition. *Macromolecules* 40:6370–6376
26. Freemont TJ, Saunders BR (2008) pH-Responsive microgel dispersions for repairing damaged load-bearing soft tissue. *Soft Matter* 4(5):919–924
27. Dalmont H, Pinprayoon O, Saunders BR (2008) Study of pH-responsive microgels containing methacrylic acid: effects of particle composition and added calcium. *Langmuir* 24:2834–2840
28. Amalvy JL, Wanless EJ, Li Y, Michailidou V, Armes SP (2004) Synthesis and characterization of novel pH responsive microgels based on tertiary amine methacrylates. *Langmuir* 20:8992–8999
29. Teng D, Hou J, Zhang X, Wang X, Wang Z, Li C (2008) Glucosamine-carrying temperature- and pH-sensitive microgels: preparation, characterization, and in vitro drug release studies. *J Colloid Interface Sci* 322(1):333–341
30. Bredley M, Vincent B (2008) Poly(vinylpyridine) core/poly(N-isopropylacrylamide) shell microgel particles: their characterization and the uptake and release of anionic surfactant. *Langmuir* 24(6):2421–2425
31. Ho BS, Tan BH, Tan JPK, Tam KC (2008) Inverse microemulsion polymerization of sterically stabilized polyampholyte microgels. *Langmuir* 24(15):7698–7703
32. Ni P (2008) Nanoparticles comprising pH/temperature-responsive amphiphilic block copolymers and their applications in biotechnology. In: Elaissari A (ed) *Colloidal nanoparticles in biotechnology*. Wiley, New York
33. Kleinen J, Richtering W (2008) Defined complexes of negatively charged multisensitive poly(N-isopropylacrylamide-co-methacrylic acid) microgels and poly(diallyldimethylammonium chloride). *Macromolecules* 41:1785–1790
34. Zhang J, Xu S, Kumacheva E (2004) Polymer microgels: reactors for semiconductor, metal, and magnetic nanoparticles. *J Am Chem Soc* 126(25):7908–7914
35. Liu S, Weaver JVM, Save M, Armes SP (2003) Synthesis of pH-responsive shell cross-linked micelles and their use as nanoreactors for the preparation of gold nanoparticles. *Langmuir* 18:8350
36. Nassif N, Gehrke N, Pinna N, Shirshova N, Tauer K, Antonietti M, Colfen H (2005) Synthesis of stable aragonite superstructures by a biomimetic crystallization pathway. *Angew Chem Int Ed Engl* 117:6158
37. Zhang Q, Tang Y, Zha L, Ma J, Liang B (2008) Effects of hectorite content on the temperature-sensitivity of PNIPAM microgels. *Eur Polym J* 44(5):1358–1367
38. Suzuki D, Kawaguchi H (2005) Modification of gold nanoparticle composite nanostructures using thermosensitive core-shell particles as a template. *Langmuir* 21(18):8175–8179
39. Suzuki D, Kawaguchi H (2005) Gold nanoparticle localization at the core surface by using thermosensitive core-shell particles as a template. *Langmuir* 21:12016–12024
40. Hantzschel N, Zhang F, Eckert F, Pich A, Winnik M (2007) Poly(N-vinylcaprolactam-co-glycidyl methacrylate) aqueous microgels labeled with fluorescent LaF₃:Eu nanoparticles. *Langmuir* 23:10793–10800
41. Suzuki D, Kawaguchi H (2006) Hybrid microgels with reversibly changeable multiple brilliant color. *Langmuir* 22:3818–3822
42. Suzuki D, McGrath J, Kawaguchi H, Lyon LA (2007) Colloidal crystals of thermosensitive, core/shell hybrid microgels. *J Phys Chem C* 111:5667–5672
43. Schrinner M, Proch S, Mei Y, Kempe R, Miyajima N, Ballauff M (2008) Stable bimetallic gold-platinum nanoparticles immobilized on spherical polyelectrolyte brushes: synthesis, characterization, and application for the oxidation of alcohols. *Adv Mater* 20(10):1928–1933

44. Wong JE, Gaharwar AK, Mueller-Schulte D, Bahadur D, Richtering W (2008) Dual-stimuli responsive PNIPAM microgel achieved via layer-by-layer assembly: magnetic and thermoresponsive. *J Colloid Interface Sci* 324:47–54
45. Suzuki D, Kawaguchi H (2006) Stimuli-sensitive core/shell template particles for immobilizing inorganic nanoparticles in the core. *Colloid Polym Sci* 284:1443–1451
46. Agrawal M, Pich A, Gupta S, Zafeiropoulos NE, Rubio-Retama J, Simon F, Stamm M (2008) Temperature sensitive hybrid microgels loaded with ZnO nanoparticles. *J Mater Chem* 18(22):2581–2586
47. Wang P, Chen D, Tang FQ (2006) Preparation of titania-coated polystyrene particles in mixed solvents by ammonia catalysis. *Langmuir* 22:4832–4835
48. Kawaguchi H, Suzuki D, Kaneshima D (2008) Synthesis and application of polymeric microspheres containing inorganic particles. *Trans Mater Res Soc Jpn* 33(2):205–208
49. Coutinho CA, Harrinath RK, Gupta VK (2008) Settling characteristics of composites of PNIPAM microgels and TiO₂ nanoparticles. *Colloids Surf A Physicochem Eng Asp* 318(1–3):111–121
50. Shen L, Pich A, Fava D, Wang M, Kumar S, Wu C, Scholes GD, Winnik MA (2008) Loading quantum dots into thermo-responsive microgels by reversible transfer from organic solvents to water. *J Mater Chem* 18(7):763–770
51. Zhao X, Gan J, Chuchi S, Liu G, Chen A (2007) Poly(N-isopropyl acrylamide) microgel doped with luminescent PbS quantum dots. *Chinese J React Polym* 16(1–2):55–60
52. Hain J, Eckert F, Pich A, Hans-Juergen A (2008) Multi-sensitive microgels filled with conducting poly(3, 4-ethylenedioxythiophene) nanorods. *Macromol Rapid Commun* 29(6):472–478
53. Suzuki D, Yoshida R (2008) Temporal control of self-oscillation for microgels by cross-linking network structure. *Macromolecules* 41(15):5830–5838
54. Zhou J, Wang G, Marquez M, Hu ZB (2008) The formation of crystalline hydrogel films by self-crosslinking microgels. *Soft Matter* 5:820–826
55. Musch J, Schneider S, Lindner P, Richtering W (2008) Unperturbed volume transition of thermosensitive poly(N-isopropylacrylamide) microgel particles embedded in a hydrogel matrix. *J Phys Chem B* 112(20):6309–6314

Part II

Hydrogels For Drug Delivery

In-Situ Gelling Stimuli-Sensitive PEG-Based Amphiphilic Copolymer Hydrogels

Doo Sung Lee and Chaoliang He

Abstract In-situ gelling stimuli-sensitive block copolymer hydrogels exhibit sol–gel phase-transitions in response to external stimuli, due to the formation of reversible polymer networks caused by physical interactions. In-situ gelling stimuli-sensitive block copolymer hydrogels show many advantages, such as simple drug formulation and administration procedures, no organic solvent, site-specificity, a sustained drug release behavior, less systemic toxicity, and ability to delivery both hydrophilic and hydrophobic drugs. Poly(ethylene glycol)s with relatively low molecular weight are hydrophilic, nontoxic, absent of antigenicity and immunogenicity, and can be directly excreted by the kidneys. PEG-based amphiphilic copolymers have attracted extensive interest for their unique self-assembly and biocompatibility. The PEG-based amphiphilic copolymers exhibit unique changes in micellar architecture and aggregation number in response to changes near physiological temperature; therefore, in-situ gelling systems made of the PEG-based amphiphilic copolymers have received worldwide investigation. This article stresses the recent development and biomedical evaluation of the in-situ gelling stimuli-sensitive PEG-based amphiphilic copolymers that are capable of responding to changes in temperature and/or pH.

Introduction

The hydrogels systems are three-dimension hydrophilic polymer networks that can absorb considerable water and exhibit considerable flexibility [1, 2]. Many polymer networks can undergo reversible volume phase transitions or sol–gel phase transitions in response to the external physical or chemical stimuli, such as temperature, pH, ionic strength, light, electromagnetic radiation, and biomolecules, are called stimuli-sensitive or intelligent hydrogels, which have received increasing attention for their great potential in industrial applications, such as drug delivery systems (DDS), tissue engineering, and separation. Under the influence of external stimuli, hydrogels based on covalently crosslinked networks can undergo drastic volume phase transitions, while some physical networks show reversible sol–gel phase transitions without marked volume changes. Reversible hydrogels formed by stimuli-induced sol–gel phase transitions are called in-situ forming hydrogels and exist as flowable aqueous solutions (or sol state) before administration but immediately turn into standing gels after administration. These are of considerable interest for their applications in drug delivery and tissue engineering [3, 4].

D.S. Lee and C. He • Department of Polymer Science and Engineering, Sungkyunkwan University, Suwon, Gyeonggi, 440-746 Republic of Korea
e-mail: dslee@skku.edu

Table 2. LCSTs of several typical thermosensitive polymers

Polymer	LCST (°C)	References
Poly(<i>N</i> -isopropylacrylamide) (PNIPAM)	32	[5]
Poly(<i>N,N</i> -diethylacrylamide) (DEAM)	25	[6]
Poly(<i>N</i> -ethylmethacrylamide) (PNEMAM)	58	[6]
Poly(methyl vinyl ether) (PMVE)	34	[7]
Poly(2-ethoxyethyl vinyl ether) (PEOVE)	20	[8]
Poly(<i>N</i> -vinylisobutyramide) (PNVIBAM)	39	[9]
Poly(<i>N</i> -vinylcaprolactam) (PNVCa)	30~50	[10]
Poly(organophosphazenes)	25.0~98.5	[11]
Poly(<i>N</i> -(2-hydroxypropyl) methacrylamide mono/di lactate) (PHPMAM-mono/di lactate)	13~65	[12]

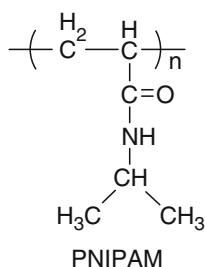
Thermo-sensitive hydrogels exhibit volume phase transitions or sol–gel phase-transitions at critical temperatures, i.e., lower critical solution temperatures (LCST) or upper critical solution temperatures (UCST). The LCST polymers exhibit swelling-to-shrinking (or sol-to-gels) transition with increasing temperature, whereas the UCST systems undergo the opposite transitions. Typical LCST polymers include poly(*N*-isopropylacrylamide) (PNIPAM) [5], poly(*N,N*-diethylacrylamide) (PDEAM) [6], poly(vinyl ether)s (PVE) [7, 8], poly(*N*-vinylalkylamide) [9], poly(*N*-vinylcaprolactam) (PVNCa) [10], polyphosphazene derivatives [11], and poly(*N*-(2-hydroxypropyl) methacrylamide mono/di lactate) (PHPMAM-mono/di lactate) [12, 13]. The LCSTs of several typical thermosensitive polymers are listed in Table 1.

In contrast to the permanent networks formed by chemical crosslinking, the in-situ forming hydrogels are transient (or reversible) physical networks and can be reversibly transformed into sol state by varying the environmental conditions [14]. Typical in-situ forming thermosensitive hydrogels based on natural polymers include methylcellulose [15] and chitosan/glycerophosphate blends [16]. Examples of in-situ forming hydrogels based on synthetic polymers are poly(*N*-isopropylacrylamide-*co*-acrylic acid) (P(NIPAM-*co*-AA)) [17], poly(*N*-isopropylacrylamide)-*block*-poly(ethylene glycol) (PNIPAM-*b*-PEG) [18], and poly(ethylene oxide)-*b*-poly(propylene oxide)-*b*-poly(ethylene oxide) (PEO-PPO-PEO) [19]. Poly(ethylene glycol) (PEG) with lower molecular weight (MW < 10,000) is known as a kind of polymer that is hydrophilic, nontoxic, absent of antigenicity and immunogenicity, and can be excreted by kidney [20, 21]. PEG-based amphiphilic copolymers exhibit unique changes in micellar architecture and aggregation number in response to a temperature change at physiological temperatures [22, 23]. The in-situ gelling systems based on the PEG-based amphiphilic copolymers have also attracted increasing attention.

This article is focused on the development and biomedical evaluation of the in-situ gelling stimuli-sensitive PEG-based amphiphilic copolymers and Pluronic-based amphiphilic copolymers.

Thermogelling PEG–PNIPAM Block Copolymers

Poly(*N*-isopropylacrylamide) (PNIPAM), shown in Scheme 1, is one of the most popular thermosensitive polymers. The linear PNIPAM chain undergoes a rapid coil-to-globule transition in aqueous solution at ~32°C, its LCST, while the crosslinked PNIPAM



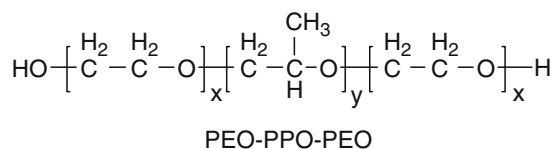
Scheme 1. Chemical structure of PNIPAM.

network shows an abrupt swelling–deswelling transition at LCST [5]. This unique hydration-to-dehydration transition is attributed to the isopropyl side groups, as the associated water separation in the gels (syneresis) due to the entropic increase when the temperature is increased above LCST [24]. The LCST of PNIPAM can be elevated or reduced by incorporating *N*-isopropylacrylamide (NIPAM) with a more hydrophilic monomer or a more hydrophobic monomer [25]. Homo- and co-polymers of PNIPAM have been synthesized by different methods, including conventional radical polymerization [5] and controlled radical polymerization, such as reversible addition fragmentation chain transfer (RAFT) [26], atom transfer radical polymerization (ATRP) [27], and Cerium (IV) redox-initiation polymerization [28]. The NIPAM monomer is cytotoxic, but PNIPAM is nontoxic and PNIPAM with limited molecular weight is excreted by glomerular filtration without long-term accumulation in vivo [29]. PNIPAM and its copolymers have been extensively developed because of their potential industrial applications such as in separation [30], conductivity control [31], controlled drug delivery [32], and tissue engineering [33].

Compared with the volume phase transitions of the chemically crosslinked PNIPAM homopolymer systems, the in-situ forming PNIPAM-based hydrogels exhibit simple sol–gel phase transitions. These hydrogels contain a certain hydrophilic component that can retain the water above the LCST. For example, monomethoxy PEG–PNIPAM diblock copolymers (MPEG–PNIPAM), prepared by quasi-living polymerization using cerium (IV) redox [28], exhibit sol-to-gel-to-syneresis transitions with increasing temperature and the gels window is markedly influenced by the composition of the copolymer [18, 34]. The gelation of the AB diblock copolymer is driven by micellar ordered-packing and entanglement. A series of AB, BAB, A(B)₄, and A(B)₈ linear and star-shaped block copolymers with poly(ethylene glycol) (PEG) as the A block and PNIPAM as the B block was synthesized by cerium (IV) redox initiated free radical polymerization [18]. A 20 wt% copolymer aqueous solutions exist as a sol state at a lower temperature (5°C), whereas gelation occurred rapidly when the temperature was increased to 37°C. In contrast to the micellar packing and entanglement mechanism for the diblock copolymers, the BAB, A(B)₄, and A(B)₈ type copolymers form a strong associative network due to the hydrophobic aggregation of the PNIPAM segments at temperatures above LCST. The PEG/PNIPAM block copolymer hydrogels show no significant syneresis (water separation in the gels) after 2 months at 37°C, as compared with a high degree of syneresis for the hydrogels based on the PNIPAM homopolymer or the systems composed of PNIPAM and hydrophobic blocks, such as the poly(methyl methacrylate)–PNIPAM diblock (PMMA–PNIPAM) [35] and polystyrene–PNIPAM–polystyrene triblock copolymers (PS–PNIPAM–PS) [36]. Similar block copolymers composed of PEG and PNIPAM are used for immobilization and culturing rabbit chondrocytes [37]. Higher PNIPAM contents and polymer concentration lead to higher cell viability after a 7-day culture, probably due to a more appropriate mechanical strength and higher porosity.

Pluronic-Based In-Situ Forming Hydrogels

Widely used in pharmaceutical systems, Pluronics (BASF) and Poloxamers (ICI) are PEO–PPO–PEO triblock copolymers (Scheme 2). The PEO block is predominantly hydrophilic from 0 to 100°C, whereas the PPO block undergoes a hydrophilic-to-hydrophobic transition as temperature is increased about 15°C [38]. With increasing temperature, some concentrated Pluronic aqueous solutions exhibit a sol-to-gels phase transition at the lower critical gelation temperature (LCGT) and a gels-to-sol transition at the upper phase transition temperature. As the temperature increases, a unimers-to-micelles transition first occurs in the Pluronic solution and the micelle number increases with further temperature increases (Fig. 1). When the micellar volume fraction is increased to a critical value (~0.53), the micelles are packed into a crystallization-like structure of hard-spheres and gelation occurs [38]. As the temperature increases further, the aggregation conformation of some Pluronic hydrogels changes from the spherical micelles closely packed in a cubic lattice into rod-like micelles packed in a hexagonal system; this results in a decrease in the intermicellar interactions and the upper gels-to-sol transition to occur at a higher temperature.



Scheme 2. Chemical structure of PEO–PPO–PEO.

The Pluronic hydrogels exhibit high viscosity, partial rigidity, and time persistence, due to the ordered micellar packing structure and micellar interactions. Some concentrated Pluronic aqueous solutions exist in the sol state at room temperature but form a gels at physiological temperatures. Consequently, Pluronics are used as injectable in-situ forming matrices for drug and cell deliveries. However, there are drawbacks to Pluronic hydrogels systems, such as weak mechanical strength, short residence time, high permeability, nonbiodegradability, and molecular weight limitations [3]. To overcome these drawbacks, several oligomers of Pluronic F127 were coupled using hexamethylene diisocyanate (HMDI) or phosgene as the coupling reagent [39]. These oligomers exhibited viscosities 15 times greater than F127 alone at 37°C.

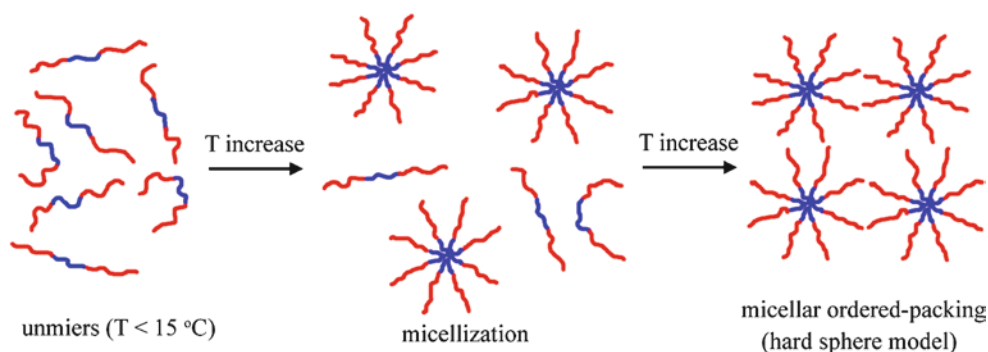


Fig. 1. Schematical illustration for the phase transition of PEO–PPO–PEO aqueous solution in response to temperature.

The in vitro release of an antirestenosis drug (RG-13577) from a 30 wt% p[F127]₄ hydrogels persisted over 40 days; in contrast, only 7 days from a 30 wt% F127 hydrogels. A series of biodegradable multiblock Pluronics with the molecular weights of 4,000–40,000 was prepared by coupling Pluronic P85 using terephthaloyl chloride [40]. The gels duration of the multiblock Pluronic is controllable from 8 h to 4 weeks by tailoring the molecular weight.

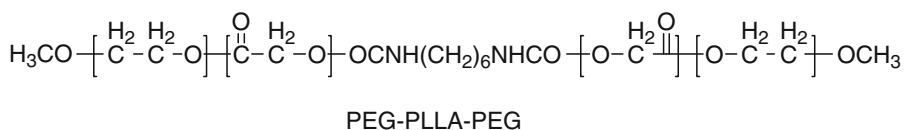
PEO/PPO alternating multiblock copolymers were synthesized by coupling PEO and PPO using carbonyl chloride or diacyl chloride [41]. The hydrogels based on the multiblock copolymers have markedly higher viscosities than Pluronic F127 hydrogels. In addition, the alternating ether-carbonate structure within the backbone renders the copolymers biodegradable. A family of pentablock copolymers composed of Pluronic F87 flanked by two short polyester blocks [poly(D,L-lactide) (PLA) or poly(ε-caprolactone) (PCL)] have been developed [42, 43]. The pentablock copolymers retained the thermoreversible sol–gel transition properties and have a lower critical micellization temperature (CMT) in comparison with F87. The in vitro release of hydrophilic procain hydrochloride (PrHy) and hydrophobic 9-(methylaminomethyl) anthracene (MAMA) was performed using PLA₆–F87–PLA₆ and PCL₄–F87–PCL₄ hydrogels, respectively. No initial burst was observed in either release curve, while the drug release from the hydrogels copolymer at 37°C was almost equal to or faster than that from the corresponding polymer solution at 25°C.

A Pluronic-based poly(ether-ester-urethane) multiblock copolymer was synthesized by coupling the oligo(ester)-Pluronic(F127)-oligo(ester) pentablock copolymers using HMDI [44]. The rheology and degradation behavior of the copolymer hydrogels are tunable by varying the polyester block length and the degree of the chain extension.

Thermogelling PEG/PLGA Amphiphilic Block Copolymers

Aliphatic polyesters, such as poly(lactic acid) (PLA), poly(ε-caprolactone) (PCL), and poly(glycolic acid) (PGA), are biodegradable and biocompatible polymers; therefore, they have potential biomedical applications as well as being environmental-friendly materials [45]. PEG-polyester copolymers have also been developed as unique polymers, such as amphiphilicity, self-assembly, permeability, biocompatibility, and biodegradability [46].

The first biodegradable thermosensitive hydrogels, based on the PEG-polyester block copolymer, were ABA-type PEG–poly(L-lactide)–PEG triblock copolymers (Scheme 3) [47]. These PEG–PLLA–PEG triblock copolymers are prepared in two steps: first, the MPEG–PLLA diblock copolymers are synthesized by ring-opening polymerization of L-lactide (LLA) using the monomethoxy PEG (MPEG, Mw=5,000) as the macroinitiator; then the PEG–PLLA–PEG triblock copolymers are obtained by coupling MPEG–PLLA using HMDI. The molecular weight (Mw) of the PLLA block varied from 2,000 to 5,000. The concentrated PEG–PLLA–PEG solutions exhibited a gels-to-sol transition as temperatures increased.

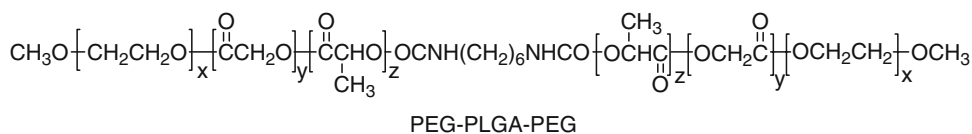


Scheme 3. Chemical structure of PEG–PLLA–PEG.

The *in vitro* release of fluorescein isothiocyanate (FITC) labeled dextran from the PEG–PLLA–PEG (5,000–2,040–5,000) hydrogels was investigated. Polymer aqueous solutions containing a drug were first prepared at 45°C, and then drug-loaded hydrogels were formed by lowering the temperature to 37°C. The release of dextran from the 35 wt% gels is a constant rate up to 12 days without an initial burst, in contrast to an initial burst in the release curve of the 23 wt% gels (Fig. 3). The influence of the hydrophilic/hydrophobic balance, block length, hydrophobicity, and stereoregularity of the hydrophobic block on the gels–sol transition properties of some PEG/polyester diblock and triblock copolymers has been reported [48, 49].

In general, a longer polyester block, shorter PEG block, higher hydrophobicity, or higher crystallizability of the polyester block lead to a lower critical gelation concentration (CGC) and a higher gels-to-sol transition temperature. The PEG–poly(D,L-lactide)–PEG (PEG–PLA–PEG) triblock copolymers with PEG block lengths of 2,000 and 5,000 were recently synthesized by coupling the corresponding MPEG–PLA diblock copolymers using adipoyl chloride [50]. A similar gels-to-sol transition was observed for the concentrated copolymer solutions. The H-bonding between PEG blocks was thought to be responsible for gelation at lower temperature. A series of star-shaped PLLA–PEG block copolymers was synthesized by coupling star PLLA with monocarboxy-MPEG using dicyclohexylcarbodiimide (DCC) [51, 52]. The concentrated block copolymer solutions showed a gels-to-sol transition with increasing temperature. The gelation and gels-to-sol transition were assumed to be attributed to micellar packing and the decrease in the micellar volume caused by the partial dehydration of the PEG block, respectively.

The PEG/PLA-based block copolymers, however, exhibited UCST behavior and did not show a sol-to-gels transition at lower temperatures; this is frequently observed in Pluronic systems. The use of UCST polymers may lead to an adverse effect to some drugs and proteins and bring inconvenience into practical applications. Additionally, the long PEG chains (Mw 5,000) in such block copolymers are likely to accumulate in the body after the degradation of the polyester block. More recently, new thermosensitive hydrogels made of the PEG–poly(D,L-lactide-*co*-glycolide)–PEG triblock copolymers (PEG–PLGA–PEG, Scheme 4) containing shorter PEG blocks (MW ≤ 750) were reported [53, 54]. The PEG–PLGA–PEG aqueous solutions showed a sol-to-gels transition as well as a gels-to-sol transition with rising temperature. Moreover, the gels window covered the physiological temperature (37°C), and the CGC and sol-to-gels transition temperature could be tuned by tailoring the block length and composition as well as by adding additives. In this case, the drugs could be mixed with the polymer solution at lower temperature and incorporated in the hydrogels after administration, such as injection. The sol-to-gels transition mechanism of PEG–PLGA–PEG was investigated by temperature-dependent ¹³C nuclear magnetic resonance (NMR) spectra and dynamic light scattering (DLS), which indicates a mechanism of micellar growth and close packing. It is noteworthy that the CGC (~16 wt%) of PEG–PLGA–PEG system does not fit the theoretic calculation result from the “hard sphere crystallization model.” A “soft sphere model” was assumed for the close packing of the PEG–PLGA–PEG micelles, indicating



Scheme 4. Chemical structure of PEG–PLGA–PEG.

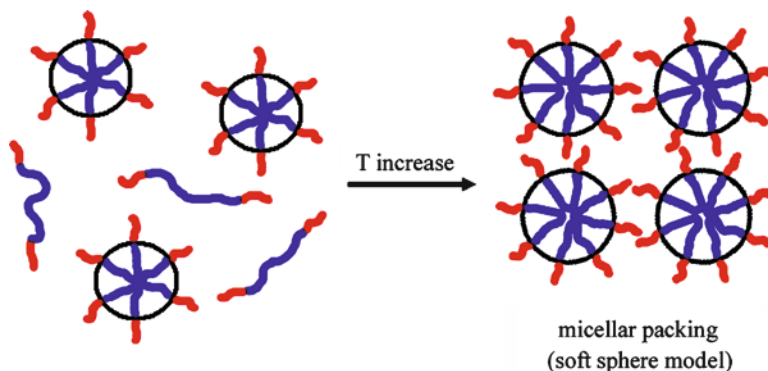
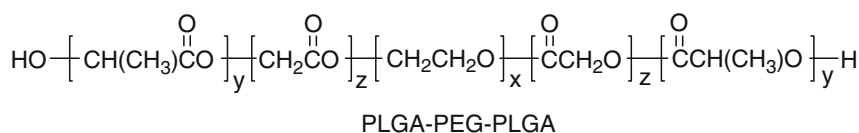


Fig. 2. Schematic illustration for the phase transition of PEG–PLGA–PEG aqueous solution in response to temperature.

marked micellar phase-mixing and overlapping for the later system (Fig. 2). Additionally, the much longer duration of the PEG–PLGA–PEG hydrogels in comparison with the Pluronic hydrogels may be attributed the fact that the dissolution of the PLGA hydrophobic cores is much more difficult than that of the PPO cores. The upper gels-to-sol transition was proved to be due to the breakage of micellar structure caused by partial dehydration of the PLGA and PEG block [54, 55]. In a separate study, the gelation behavior of the PEG–PLGA–PEG (750–3,500–750) triblock copolymer aqueous solutions was studied by using DLS, rheology, SANS, and differential scanning calorimetry (DSC) [56, 57]. A mechanism of macroscopic liquid–liquid phase separation was proposed to be responsible for the gelation. After the 33 wt% aqueous solution of PEG–PLGA–PEG (550–2,810–550) was subcutaneously injected into rats, a transparent hydrogels was formed in situ [58]. The gels exhibited good mechanical strength and the gels duration was over 1 month. The difference between the duration of the PEG–PLGA–PEG hydrogels and that of the Pluronic gels (1 day) was attributed to different erosion mechanisms. The latter disintegrated through surface erosion while the former through a degradation process. The PEG-rich components were lost preferentially during the degradation of the PEG–PLGA–PEG hydrogels. The in vitro drug release behavior of the PEG–PLGA–PEG hydrogels was evaluated by using ketoprofen and spironolactone as the hydrophilic and hydrophobic model drugs, respectively [59]. The release of ketoprofen showed a first-order release trace over 2 weeks, indicating a diffusion-controlled mechanism. In contrast, the release of spironolactone exhibited an S-shaped release profile over 2 months, suggesting a combined process composed of the initial diffusion-controlled process followed by the degradation-dominated process. The release rate was reduced with increasing the hydrophobic PLGA block length. The drug-contained PEG–PLGA–PEG aqueous solutions were directly instilled into the bladder of normal adult female Sprague–Dawley (SD) rats or cyclophosphamide-induced cystitis rats [60]. The in-situ formed hydrogels exhibited a sustained release profile, significant efficacy, and less systemic adverse effects. In addition, controlled gene delivery systems were also prepared by the PEG–PLGA–PEG hydrogels [61, 62]. The plasmid DNA (pDNA) was released in a zero-order profile for 12 days [61]. Most of the released pDNA were proven to maintain a supercoiled conformation at 12 days, even though the pH in the hydrogels markedly decreased from 7.4 to around 4 after incubation for 12 days caused by the degradation of the PLGA block. When the hydrogels loaded with luciferase pDNA were administered to the skin wounds of CD-1 mice, the expression of luciferase exhibited the maximum at 24 h and then decreased markedly. After administration to the

skin wounds of genetically diabetic mice, the hydrogels containing plasmid TGF- β 1 showed significantly higher levels of reepithelialization, cell proliferation, and collagen organization, as compared either with the commercial wound dressing, Humatrix[®], or with the plasmid TGF- β 1-loaded Humatrix[®] [62].

The thermosensitive hydrogels based on the BAB-type PLGA-PEG-PLGA triblock copolymers was subsequently developed (Scheme 5) [63, 64]. The synthesis of PLGA-PEG-PLGA was simpler than that of PEG-PLGA-PEG, because the coupling procedure using HMDI could be avoided in the former synthesis. PLGA-PEG-PLGA also exhibited a reversible sol-gel-sol transition with increasing temperature, and the phase diagram was influenced by the block length and composition as well as by additives [63, 65]. PLGA-PEG-PLGA showed marked lower CGC and lower sol-to-gels transition temperature in comparison with PEG-PLGA-PEG, suggesting different gelation mechanisms for them. At a lower temperature, some interconnected micelles composed of PLGA-PEG-PLGA are formed in the aqueous solution, but no stable network is formed, due to the less hydrophobicity of the PLGA blocks at lower temperatures. As the temperature is increased to LCGT, an interconnected micelle network is formed and gelation occurs (Fig. 3). The release behaviors of proteins and several conventional drugs from the PLGA-PEG-PLGA (1,500–1,000–1,500) hydrogels (commercially available as ReGel[®]) were studied [64]. The in vivo degradation of ReGel[®] after subcutaneous injection into rats was over 4 weeks. ReGel[®] showed significant solubilization and stabilization to the hydrophobic drugs, such as paclitaxel and cyclosporin A. The in vitro release of paclitaxel from the ReGel[®] exhibited a diffusion-controlled release profile in the initial 2 weeks, followed by a combined diffusion/degradation process for about 5 weeks. In contrast, the in vitro release of paclitaxel from the Pluronic F127 hydrogels was complete in around 1 day. The in vivo distribution of paclitaxel was monitored after an intratumor injection of ReGel[®] containing paclitaxel and [¹⁴C] paclitaxel. The C-14 levels in tumors were reduced slowly over 6 weeks. The elimination of C-14 was mainly through the feces and urine, with less than 0.1% being distributed to other organs. The ReGel[®]/paclitaxel showed higher antitumor efficacy and



Scheme 5. Chemical structure of PLGA-PEG-PLGA.

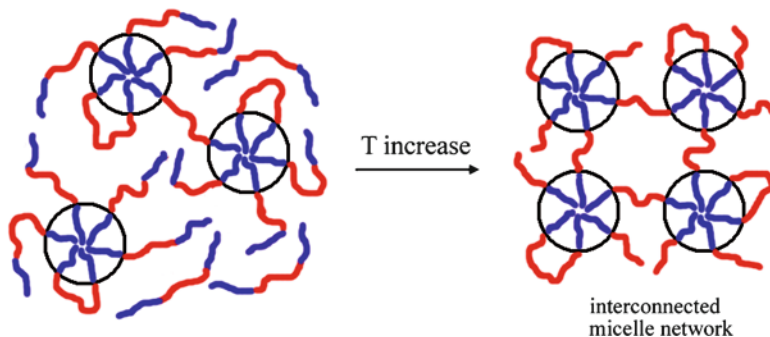


Fig. 3. Schematic illustration for the phase transition of PLGA-PEG-PLGA aqueous solution in response to temperature.

lower drug-related adverse effects, as compared with the maximum tolerated systemic dose of the commercial paclitaxel product (Taxol[®]). In addition, the sustained releases of some proteins, such as porcine growth hormone (pGH), glycosylated, insulin, and recombinant hepatitis B surface antigen (rHBsAg), were investigated and discussed. Separate studies on the release of insulin from ReGel[®] were reported [66, 67]. The *in vitro* release of insulin from ReGel[®] showed a zero-order release trace without initial burst [66]. The insulin with 0.2 wt% zinc obtained a higher release rate, and was almost released completely over 15 days. The *in vivo* insulin level was maintained over 15 days after a subcutaneous injection of ReGel[®]/0.2 wt% Zn-insulin into Sprague–Dawley (SD) rats (Fig. 5). The insulin released from ReGel[®] was confirmed to be bioactive after being injected into Zucker Diabetic Fatty (ZDF) rats [67]. The blood glucose concentration in the ZDF rats was reduced to normal level during the insulin release period. ReGel[®] also showed sustained release of the incretin hormone glucagons-like peptide-1 (GLP-1), which was a very useful drug for type 2 diabetes but exhibited extremely short plasma half-life due to rapid degradation [68]. The *in vitro* release of zinc-complexed GLP-1 from ReGel[®] exhibited almost a linear release profile over 2 weeks without initial burst. After one subcutaneous injection of zinc-complexed GLP-1/ReGel[®] into rats, the plasma GLP-1 level was maintained significantly higher than that of the control group for about 2 weeks, and the insulin level induced by GLP-1 stayed at a higher level over 2 weeks, leading to the obvious reduction of the blood glucose concentration during the same period.

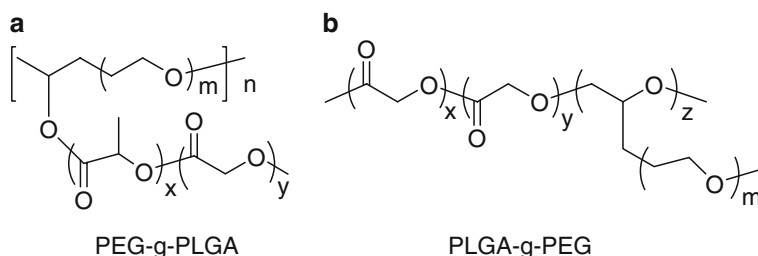
The effects of composition and sequential distribution on the phase-transition and drug release behavior of the PLGA/PEG block copolymers were investigated. A series of poly(D,L-3-methylglycolide)–PEG–poly(D,L-3-methylglycolide) triblock copolymers (PMG–PEG–PMG) was synthesized by using D,L-3-Methylglycolide (MG) as the cyclic monomer, leading to the well-defined alternating LA/GA sequence in the PMG blocks [69]. The sol–gel transition temperature of PMG–PEG–PMG was higher than that of ReGel[®], due to less hydrophobicity of the PMG block with higher GA content (50 mol%). The effect of composition of PLGA–PEG–PLGA on the drug release behavior was investigated [70]. The results indicated that the LA/GA ratio exhibited less effect on the release of a diffusion-controlled stage, but markedly affected the release of a degradation-dominative stage. The phase-transition behavior of the PEG/PLGA copolymers can be also tuned by modifying the polymer structure. A series of PLGA–PEG–PLGA end-capped with small alkyl groups (acetate or propionate) was prepared [71, 72]. The CGC and CGT of the alkyl-capped triblock copolymers were markedly lower than those of the unmodified triblock copolymers, and decreased with increasing the length of the terminal alkyl groups [72]. It was also found that the CGC of the end-modified triblock copolymers was significantly affected by the degree of end-modification [73]. A micellar network caused by the micellar hydrophobic aggregation was proposed to be responsible for the gels formation [72].

Thermogelling Star-Shaped and Graft PEG/PLGA Amphiphilic Copolymers

The topology structure is known to affect the polymer properties and self-assembly behaviors; therefore, developing PEG-polyester amphiphilic copolymers with different structures may be interesting. In addition, because the MW of the PEG block is limited due to its nonbiodegradability, there is also a limitation of molecular weight for the PEG–PLGA–PEG triblock copolymers [74]. Accordingly, PEG–PLGA amphiphilic copolymers with nonlinear architectures, including star-shaped and graft structures, have been developed. Three-arm and four-arm star-shaped PLGA–PEG block copolymers were prepared by coupling 3-arm and 4-arm

PLGA with carboxyl terminated MPEG ($M_n=550$) [75]. The concentrated PLGA–PEG star-shaped block copolymers aqueous solutions displayed sol–gel–sol transitions with increasing temperature. The CGCs of the star-shaped block copolymers were higher than those of the PEG–PLGA–PEG triblock copolymers, and the CGC and CMT decreased with increasing the PLGA block length. The in vitro and in vivo release of Doxorubicin (DOX) from the 4-arm star-shaped copolymer hydrogels was investigated [76]. The in vitro release of DOX showed sustained profiles. After the subcutaneous injections of the DOX-loaded polymer solutions into tumor-bearing mice, the growth of tumor was significantly suppressed. Additionally, the antitumor efficacy was also found to be affected by the PLGA block length.

PEG-*g*-PLGA graft copolymers with hydrophilic backbones were synthesized by the ring-opening polymerization of LA and GA using PEG with hydroxyl pendant groups [77]. The schematically chemical structure of PEG-*g*-PLGA is shown in Scheme 6a. The PEG-*g*-PLGA graft copolymer solutions exhibited sol–gel–sol transitions at concentrations above 16 wt%. The hydrogels remained a gels state for 1 week at physiological conditions. PLGA-*g*-PEG graft copolymers with hydrophobic backbones were also developed by the one-step ROP of LA, GA, and epoxy-terminated PEG (Scheme 6b) [74, 78]. After a subcutaneous injection of the PLGA-*g*-PEG aqueous solution into a rat, a round shaped gels was formed in situ [78]. In comparison with 1 week for the PEG-*g*-PLGA hydrogels, the PLGA-*g*-PEG hydrogels persisted more than 2 months in vivo. The sol–gel transition temperature could be adjusted within a range of 15–45°C by changing the number of PEG grafts and the composition of the copolymer [79], or by mixing two PLGA-*g*-PEG copolymers with different compositions [78]. Based on the IR, ^{13}C NMR, small-angle neutron scattering (SANS), and rheological studies, PEG dehydration is assumed to be the major driving force for the phase transition [78]. After one injection of the insulin-loaded PLGA-*g*-PEG solution into a diabetic SD rat, the blood glucose level was adjusted to maintain normal level for 16 days, caused by the sustained release of insulin from the hydrogels [80]. Interestingly, the normal blood glucose level could be controlled from 5 to 16 days by using the hydrogels based on the PEG-*g*-PLGA/PLGA-*g*-PEG blends. In addition, the biodegradable PLGA-*g*-PEG hydrogels containing chondrocyte cell showed a superior efficacy in cartilage defect repairing, as compared with the nonbiodegradable PNIPAM-*co*-PAA/hydroxyapatite collagen sponge.

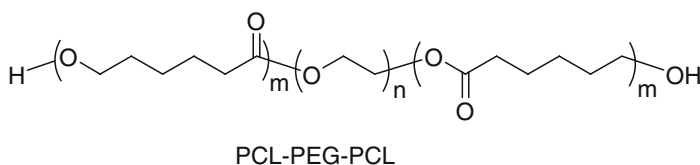


Scheme 6. Chemical structures of (a) PEG-*g*-PLGA and (b) PLGA-*g*-PEG.

Thermogelling PEG–PCL Amphiphilic Copolymers

Many amphilic copolymers composed of PEG and other biodegradable aliphatic polyesters also showed a thermoreversible sol–gel transition in the aqueous solutions. Different PEG-polyester diblock copolymers, including PEG–PCL, PEG–poly(δ -valerolactone) (PEG–PVL), PEG–PLLA, and PEG–PLGA, with well-defined structure were synthesized by living ring-

opening polymerization [81]. The concentrated aqueous solutions of the diblock copolymers (PEG $\geq 2,000$) showed a gels-to-sol transition with increasing temperature. The gels-to-sol transition was highly affected by the block length and the hydrophobic nature of the polyester block [81, 82]. When the 23 wt% PEG-PCL (2,000–2,300) aqueous solution was heated to 42°C and then injected into a mouse, it formed a gels immediately at normal body temperature [83]. The hydrogels maintained in vivo for 1 month, due to the slow degradation of the PCL block. In subsequent reports, PEG-polyester diblock copolymers with shorter PEG blocks ($M_w = 750$), including PEG-PCL, PEG-poly(ϵ -caprolactone-*co*-trimethylene carbonate) (PEG-P(ϵ -CL-*co*-TMC)), and PEG-poly(ϵ -CL-*co*-1,4-dioxan-2-one) (PEG-P(ϵ -CL-*co*-DO)), were prepared [84, 85]. It was claimed that the slow degradation of these copolymers did not lead to an acidic environment, which is often observed with the rapid degradation of PLLA and PLGA. In addition, these PEG-polyester diblock copolymers with shorter PEG length ($M_w = 750$) display a sol-gel-sol transition as temperatures increased; the gels window was highly dependent on the polyester block length. Contrary to the PEG/PLGA block copolymer systems, the lower sol-to-gels transition temperature of the PEG-PCL systems is markedly influenced by polymer concentration as compared with almost no concentration-dependence for the upper gels-to-sol transition temperature. As the PEG-PCL (750–2,440) solution loading rat bone marrow stromal cells (rBMSC) and dexamethasone was subcutaneously injected into SD rats, a gels formed in situ and maintained its integrity for over 4 weeks [86]. Histological analysis indicated that the in-situ formed scaffolds were biocompatible and accelerated the bone formation. The in vitro release of FITC-labeled bovine serum albumin (BSA-FITC) from the PEG-PCL (750–2,490) hydrogels exhibited a sustained profile over 20 days [87]. Even though an initial burst was observed, the release of BSA-FITC persisted over 30 days after the PEG-PCL (750–2,490) solutions containing BSA-FITC were subcutaneously injected into SD rats.



Scheme 7. Chemical structure of PCL-PEG-PCL.

Recently, a series of ABA- and BAB-type triblock copolymers consisting of PEG and PCL, i.e., PEG-PCL-PEG and PCL-PEG-PCL, was prepared (Scheme 7) [88, 89]. Both types of triblock copolymers display a clear sol-to-gels-to-turbid sol transition as the temperature increases from 10 to 60°C. Light scattering and ^{13}C NMR studies indicated that the sol-to-gels transition at lower temperature followed the micellar association mechanism; the upper gels-to-sol transition was due to the breakage of the micellar core-shell structure. Similar to the previous PEG-PCL diblock copolymer system, the polymer concentration only significantly influenced the lower sol-gel transition temperature of PCL-PEG-PCL system. Both types of triblock copolymers lyophilize into a powder form, and easily redissolve in water at lower temperatures. In contrast to PEG-PCL-PEG, the PCL-PEG-PCL has a wider gels domain and a higher gels modulus. However, the concentrated PCL-PEG-PCL aqueous solution (20 wt%) is not stable and turns into an opaque gels in 1 h at room temperature [90]. The Raman spectra, X-ray diffraction (XRD), DSC, and polarized optical microscope (POM) studies clearly indicate that the slow gelation at room temperature is attributed to the crystallization of the copolymer, which is quite different from the micellar aggregation mechanism

of the thermo-induced gelation at 37°C. The unstable PCL–PEG–PCL solution would be impractical for application. Therefore, the above PCL–PEG–PCL (1,000–1,000–1,000) was coupled, by terephthaloyl chloride, to fabricate PEG–PCL multiblock copolymers. The 20 wt% aqueous solution of the PEG/PCL multiblock copolymer has a sol–gel–sol transition as temperature increased and exists as a stable transparent solution at room temperature, which is convenient for drug delivery applications. Based on the ¹³C NMR and DLS studies, the gelation of the multiblock copolymer aqueous solution was thought to be driven by the increase in polymer–polymer attraction.

Thermogelling PEG-Based Amphiphilic Multiblock Copolymers

In addition to PEG–PCL multiblock block copolymers above, the thermo-dependent phase behavior is also observed in other PEG-based poly(ether ester) multiblock copolymer systems. A series of PEG/PLLA multiblock copolymers, synthesized by the coupling reaction between dicarboxylated PLLA and PEG [91], has sharp LCST transitions in aqueous solution. This copolymer matrix loaded with basic fibroblast growth factor has significant wound healing activity [91, 92]. A range of PEG/PLLA multiblock copolymers with lower PEG Mw were prepared by coupling PEG (Mw=600) and PLLA (Mw=1,100–1,500) using succinic anhydride [93]. The PEG/PLLA multiblock copolymer solutions exhibit a sol–gel–sol transition with increasing temperature and the maximum gels modulus was displayed at around body temperature. The transition temperature and gels window were affected by the PLLA block length and PEG/PLLA ratio. Compared with the PEG/poly(D,L-lactide) (PEG/PLA) multiblock copolymer, the PEG/PLLA multiblock copolymer exhibited a lower CGC, a lower sol-to-gels transition temperature, and a broader gels window [94]. The isotactic arrangement of the methyl groups within the PLLA blocks developed a strong aggregate of the polyester blocks. It is noteworthy that the phase-transition of the above PEG/PCL (or PEG/PLA) multiblock copolymers could be changed to a UCST manner (gels-to-sol) by increasing the PCL (or PEG) block length, probably due to the increase in crystallizing ability of the PCL block [95, 96] (or the increase of interactions between PEG blocks [97]). A soft thermosensitive hydrogels made of PEG–sebacate (PEG–SA) multiblock copolymers was prepared by simple condensation polymerization [98]. When the 25 wt% aqueous solution of the PEG–SA multiblock copolymer was heated from room temperature to 37°C, a very soft gels was formed with a gels modulus less than 5 Pa. However, the gels retained its integrity for over 3 weeks. The release of hydrophilic FITC-dextran from the poly(PEG–SA) hydrogels indicated a constant rate during 5–24 h without an initial burst. A series of biodegradable poly(ether ester urethane) multiblock copolymers consisting of poly[(R)-3-hydroxybutyrate] (PHB), PEG, and poly(propylene glycol) (PPG) was reported very recently [99]. The poly(ether ester urethane) aqueous solutions underwent a sol–gel–sol transition with increasing temperature from 4 to 80°C. Notably, the poly(ether ester urethane) solutions showed a very low CGC ranging from 2 to 5 wt% depending on the composition and block lengths. An associated micellar packing was assumed to be responsible for the gelation.

pH- and Thermo-Sensitive PEG–Polyester Amphiphilic Copolymer Hydrogels

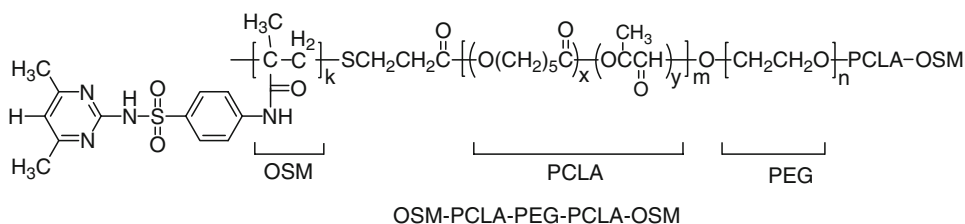
The in-situ gelling PEG/polyester amphiphilic copolymers have shown potential applications in the injectable drug and cell delivery systems. There are some limitations in the PEG–polyester systems. For example, when a thermosensitive polymer solution is

injected into the body, the increase in temperature by the body can cause a sol–gel transition within the needle and can plug the needle. However, the PEG–polyester amphiphilic copolymers, such as PLGA–PEG–PLGA, are nonionic systems, in which the drugs and proteins are loaded by hydrophobic association and/or simple physical encapsulation. The release of hydrophilic drugs or proteins from these systems is expected to be a diffusion process, and so difficult to obtain desirable profiles. Additionally, the reconstitution problem of the PEG–PLGA systems is a disadvantage. The PEG–PLGA copolymers need to be stored in solution, and the reversible gels-to-sol transition with decreasing temperature is rather slow. To overcome the above drawbacks, the pH-sensitive moieties are introduced into the PEG–polyester amphiphilic systems.

PEG-Based Amphiphilic Copolymers Modified by Anionic Weak Polyelectrolytes

The pH-sensitive polymers are classified as acidic weak polyelectrolytes and basic weak polyelectrolytes. Corresponding to the pH variation range in vivo, weak polyelectrolytes with the pK_a between 3 and 10 are suitable candidates for biomedical applications [100]. Representative acidic pH-sensitive polymers are based on the polymers containing pendant carboxylic groups, such as poly(acrylic acid) (PAA) [101] and poly(L-glutamic acid) (PLG) [102], and polymers containing sulfonamide groups [103]. Both PAA and PLG show continuous transitions rather than sharp transition in response to the pH change. The PAA and PLG systems were modified by hydrophobic groups, such as propyl [104] and benzyl groups [105], to obtain sharper transition behavior and smaller pH-responsive ranges. Compared with the PAA and PLG systems, the sulfamethazine oligomers exhibit very sharp pH-dependent transitions within a narrow pH range around pH 7.4 [103]; therefore, sulfamethazine oligomers were introduced into the PEG–polyester amphiphilic systems.

pH-sensitive sulfamethazine oligomers (OSM) were introduced to both ends of poly(ϵ -CL-*co*-LA)–PEG–poly(ϵ -CL-*co*-LA) (PCLA–PEG–PCLA) to create a pH- and temperature-sensitive pentablock copolymers (OSM–PCLA–PEG–PCLA–OSM, Scheme 8) [106, 107]. The thermo-induced sol–gel–sol transition of the parent PCLA–PEG–PCLA is not affected by the pH changes between 7.2 and 8.0 (Fig. 4a). In contrast, the concentrated (15 wt%) OSM–PCLA–PEG–PCLA–OSM aqueous solution exhibited a thermoreversible sol–gel–sol transition only at a pH below 8.0, and the gels window became broader from pH 7.8 to 7.2 (Fig. 4b). The gels window can also be tuned wider by increasing the PCLA/PEG ratio. The sol–gel transition of the pentablock copolymer solutions can be tailored by varying the PEG block length, PCLA/PEG ratio, the OSM molecular weight, and the polymer concentration. An interconnected-micelle association mechanism was proposed for the gelation of the pentablock copolymer solution, as schematically illustrated in Fig. 5. At lower temperature (15°C) or/and



Scheme 8. Chemical structure of OSM–PCLA–PEG–PCLA–OSM.

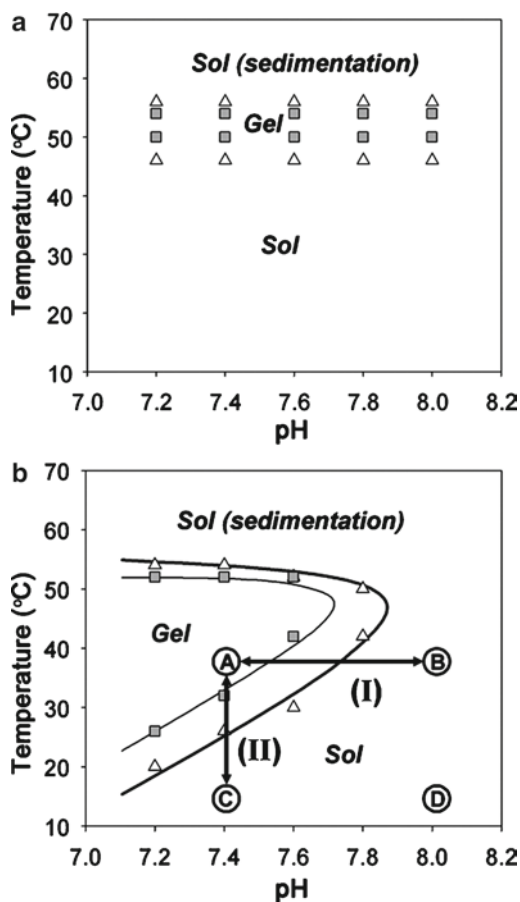


Fig. 4. Phase diagram of block copolymers in buffer solution. M_n of PEG=1,750; concentration, 15 wt%; PEG/PCLA weight ratio, 1/1.89 (■), 1/2.08 (Δ). (a) PCLA-PEG-PCLA solution (b) OSM-PCLA-PEG-PCLA-OSM solution. (A) pH 7.4, 37°C; (B) pH 8.0, 37°C; (C) pH 7.4, 15°C; (D) pH 8.0, 15°C. Reproduced with permission from [106]. Copyright 2005 American Chemical Society.

higher pH (pH 8.0), the block copolymer solution exists as a sol state, due to less hydrophobicity of the PCLA-OSM block. In contrast, at 37°C and pH 7.4, a macrolattice composed of interconnected micelles was formed by the strong hydrophobic associations between the PCLA-OSM blocks. The 15 wt% OSM-PCLA-PEG-PCLA-OSM aqueous solution at pH 8.0 can be easily injected into the buffer solution at 37°C even with a long guide catheter. The state of the polymer solution after injection is highly sensitive to a small change in pH. A stable and compact gels is formed immediately in the pH 7.4 buffer solution, whereas the polymer dispersed quickly in the pH 8.0 buffer solution. In addition, the pentablock copolymer hydrogels exhibited a rapid gels-to-sol transition after temperature is lowered. The pentablock copolymer hydrogels maintains its integrity in the pH 7.4 PBS buffer solution at 37°C for over 2 weeks and has a slower degradation rate in comparison with the hydrogels made of the parent PCLA-PEG-PCLA triblock copolymer. Notably, in contrast to the marked pH decrease from 7.4 to 2.2 in the PCLA-PEG-PCLA triblock copolymer hydrogels, the pH maintained at round 5.5 in the pentablock copolymer hydrogels after incubation at 37°C for 1 month [108]. This was believed to be attributed to the proton sponge effect of the OSM block.

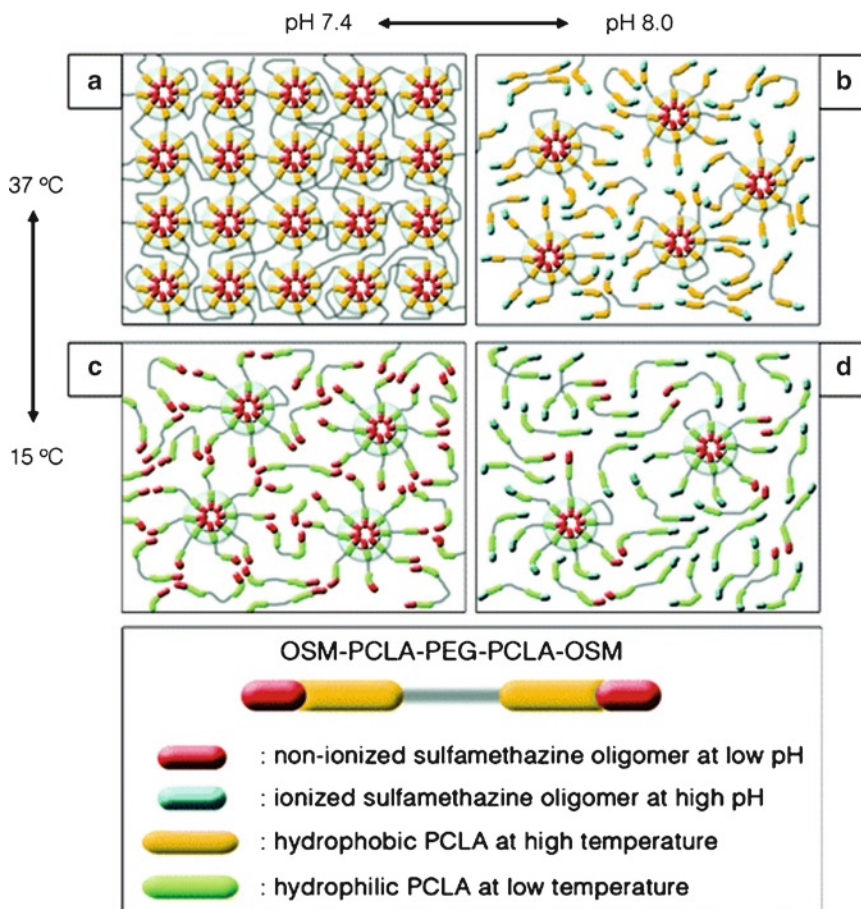


Fig. 5. Schematic diagram of the sol–gel mechanism of the pH and temperature sensitive block copolymer solution. (a) pH 7.4, 37°C; (b) pH 8.0, 37°C; (c) pH 7.4, 15°C; (d) pH 8.0, 15°C. Reproduced with permission from [106]. Copyright 2005 American Chemical Society.

A gels immediately forms *in vivo* after the OSM–PCLA–PEG–PCLA–OSM aqueous solution (20 wt% in PBS at pH 8.0) is subcutaneously injected into rats (Fig. 6) [108]. OSM–PCLA–PEG–PCLA–OSM has good *in vitro* biocompatibility. Although the pentablock copolymer hydrogels brought a typical acute inflammation within 2 weeks *in vivo*, chronic inflammation was not observed during the first 6 weeks. The *in vitro* release of paclitaxel (PTX) from the OSM–PCLA–PEG–PCLA–OSM hydrogels indicated a zero-order release profile over 20 days, which was independent of the initial loading amount [109]. The subcutaneously injected pentablock copolymer hydrogels containing PTX showed significant antitumor efficacy. OSM–PCLA–PEG–PCLA–OSM copolymers, as well-defined pentablock copolymers, were prepared by the polymerization of sulfamethazine methacrylate monomer using Br–PCLA–PEG–PCLA–Br as the ATRP macroinitiator. A series of OSM–poly(ϵ -CL-*co*-GA)–PEG–poly(ϵ -CL-*co*-GA)–OSM pentablock copolymers (OSM–PCGA–PEG–PCGA–OSM) was subsequently reported [110, 111]. The OSM–PCGA–PEG–PCGA–OSM aqueous solutions also exhibited a thermoreversible sol–gel–sol transition with the gels window depending

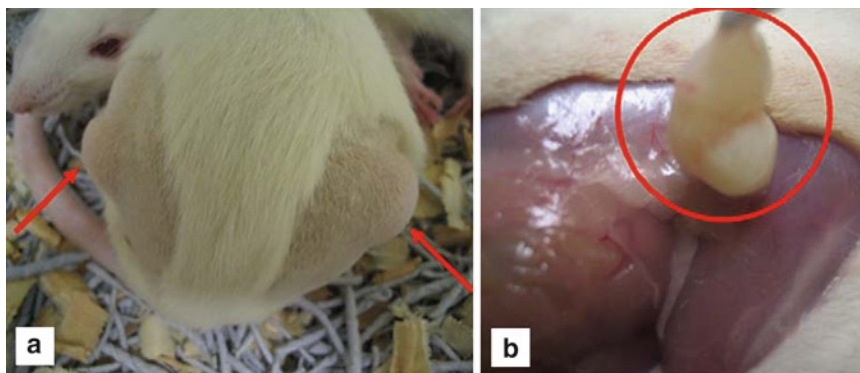


Fig. 6. Spontaneous forming hydrogels of a OSM-PCLA-PEG-PCLA-OSM block copolymer solution (20 wt% in PBS at pH 8.0). About 200 μ l of the block copolymer solution was subcutaneously injected into SD rats with a syringe needle (a), and the resulting hydrogels was isolated by tweezers after only 10 min (b). Reproduced with permission from [108].

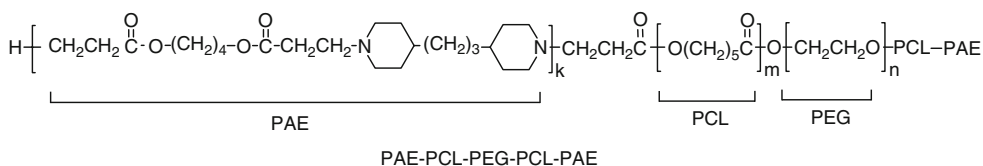
on pH. The sol-gel transition phase diagram can be controlled by changing the block length and PEG/PCGA ratio. The *in vitro* release of PTX from the OSM-PCGA-PEG-PCGA-OSM hydrogels also followed near zero-order kinetics without an initial burst. Compared with the OSM-PCLA-PEG-PCLA-OSM hydrogels, the OSM-PCGA-PEG-PCGA-OSM hydrogels have a faster release rate, due to the faster degradation of the PCGA block.

PEG-Based Amphiphilic Copolymers Modified by Cationic Weak Polyelectrolytes

In addition to the anionic weak polyelectrolytes, the cationic weak polyelectrolytes are of interest due to their pH-sensitivity and the ability to form electrostatic interaction with ionic DNA and proteins. Some therapeutic proteins, such as insulin and human growth hormone (hGH), are ampholytes and have net negative charges in aqueous solutions at physiological pH (7.4) because of their relatively low isoelectric points (\sim 5.3) [112]. The cationic segments within the hydrogels network are expected to form electrostatic interactions with the negatively charged proteins at pH 7.4, and may lead to more sustained and controllable release profiles.

Typical examples of basic polyelectrolytes include poly(tertiary amine methacrylate), such as poly(2-(dimethylamino)ethyl methacrylate) (PDMAEMA) and poly(2-(diethylamino)ethyl methacrylate) (PDEAEMA) [113], poly(2-vinylpyridine) (P2VP) [114] and poly(β -amino ester) (PAE) [115]. Some poly(tertiary amine methacrylate)s and P2VP exhibit sharp hydrophilic-hydrophobic transitions at around physiological pH; however, they are nonbiodegradable and, therefore, have limited applications as *in-situ* forming hydrogels. In contrast, a series of biodegradable cationic polyelectrolytes, poly(β -amino ester) (PAE), was developed recently for gene delivery [115]. PAE exhibits a sharp hydrophilic-hydrophobic transition in aqueous solution at pH around 6.5 [115]. It was established that PAE was noncytotoxic and could be degraded into nontoxic small molecular byproducts. In addition, the partially positively charged PAE forms electrostatic complexes with negatively charged pDNA at physiological pH (pH 7.2) [116]. A series of PEG-PCL-PAE triblock copolymers was synthesized

by Michael addition of piperazine, MPEG-PCL acrylate, and 1,6-hexanediol diacrylate [117]. When the pH was below 6.0, the 30 wt% triblock copolymer aqueous solution existed as a sol state within the temperature range of 0–60°C, whereas it showed a gels-to-sol transition upon heating at a pH above 6.0. The gels–sol phase-diagram could be tailored by varying the block length and composition. A PAE–PCL–PEG–PCL–PAE pentablock copolymer was subsequently prepared by the Michael addition of 4,4'-trimethylene dipiperidine, PCL–PEG–PCL diacrylate, and 1,4-butandiol diacrylate (Scheme 9) [118]. These pentablock copolymers have sol-to-gels-to-sol (sedimentation) transitions with increasing temperature (Fig. 7). In contrast to the OSM-based system, the gels window of PAE–PCL–PEG–PCL–PAE is observed in the pH region above the pKa of PAE. The cytotoxicity was ~100% cell viability even when the polymer concentration was increased to 100 µg/mL, indicating a good cellular compatibility. The degradation of the copolymer is a two-step process; a fast degradation of the PAE segments within about 10 days and a slower degradation of the PCL segments. The in vitro release of insulin exhibited sustained release profiles at constant rates. On loading insulin, the sol–gel phase diagram slightly shifts to lower temperature range. After a subcutaneous injection of the polymer solution containing insulin into SD rats, the elevated plasma insulin level maintained at constant level over 15 days without an initial burst for the PAE–PCL–PEG–PCL–PAE/insulin group. A marked initial bursts and shorter durations of the elevated insulin levels were observed for the PCL–PEG–PCL/insulin group and insulin solution group (Fig. 8). The sustained release behavior of the pentablock copolymer hydrogels is thought



Scheme 9. Chemical structure of PAE–PCL–PEG–PCL–PAE.

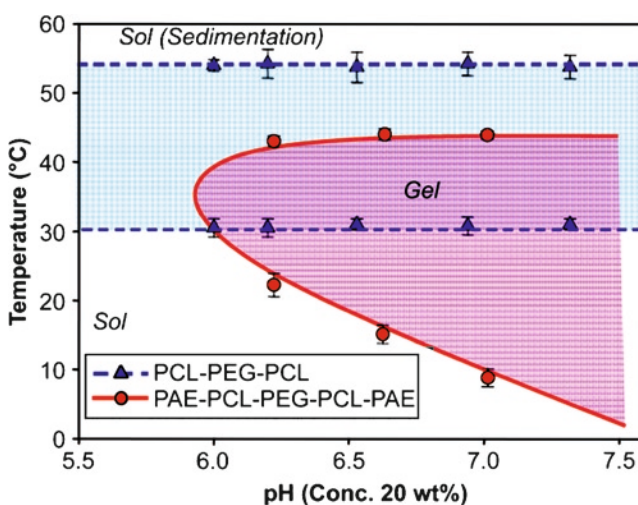


Fig. 7. Sol–gel phase diagram of triblock and pentablock copolymer solutions at 20 wt%. Reproduced with permission from [118].

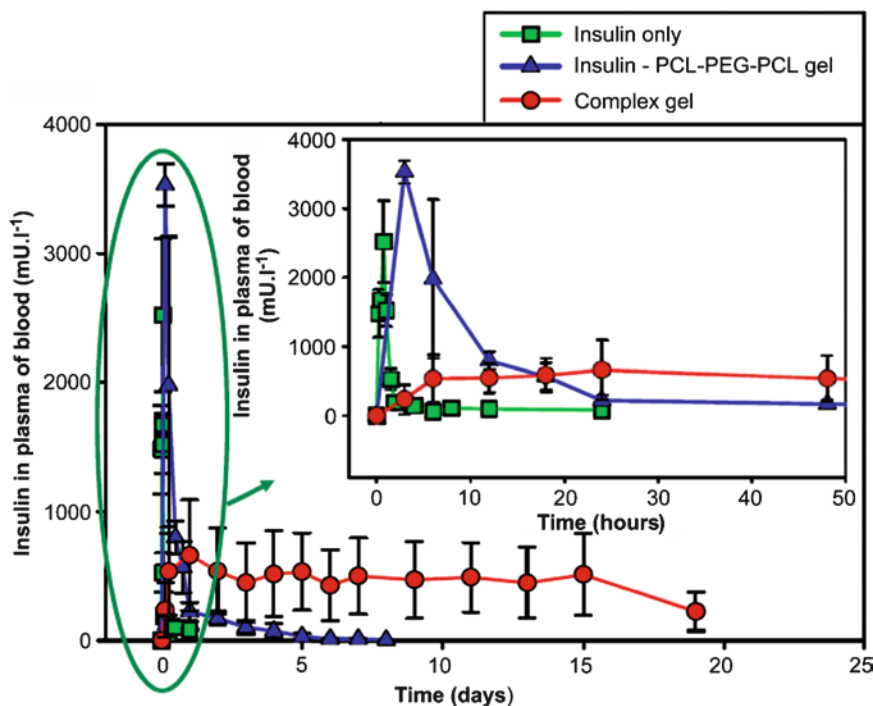
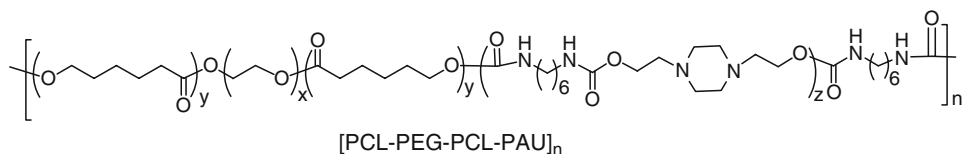


Fig. 8. Insulin release experiment in vivo. In insulin-only group, 200 mL insulin solution 0.25 mg mL⁻¹ (in PBS buffer (pH 7.4) is administered by subcutaneous injection (0.05 mg insulin for each rat)). In insulin-PCL-PEG-PVL gels group, 200 mL of solution (5 mg mL⁻¹ insulin in PCL-PEG-PCL solutions 25 wt%) at pH 7.0 and 10°C is subcutaneously injected (1 mg insulin for each rat). In complex gels group, 200 mL of the complexation insulin solution (5 mg mL⁻¹ in PAE-PCL-PEG-PCL-PAE solutions 25 wt%) at pH 7.0 and 10°C is subcutaneously injected (1 mg insulin for each rat). (Male SD rats, error bars represent the standard deviation ($n=5$)). Reproduced with permission from [118].

to be related to the electrostatic interactions between the partially positively charged PAE blocks and the negatively charged insulin at physiological pH. The release of insulin is mainly based on the breakage of the electrostatic complex caused by the degradation of the PAE segments, indicating that a degradation-controlled process is the major mechanism for the insulin release.

A series of the novel pH- and temperature-sensitive multiblock poly(ester amino urethane) (PCL-PEG-PCL-PAU)_n, was synthesized by reacting together hexamethylene diisocyanate (HDI), hydroxyl-terminated PCL-PEG-PCL, and bis-1,4-(hydroxyethyl)piperazine (HEP) with the OH/NCO molar ratio of 1:1 (Scheme 10) [119]. The tertiary amino groups of the poly(amino urethane) segments act as pH-responsive moieties, while the PCL-PEG-PCL



Scheme 10. Chemical structure of [PCL-PEG-PCL-PAU]_n.

blocks act as biodegradable and temperature-sensitive segments. At a relatively high pH (7.0 or above), the multiblock copolymer aqueous solution shows a sol-to-gels-to-aggregation transition with increasing temperature. In contrast, at a lower pH (<7.0), the polymer solution exists as a sol state within the experimental temperature range. The gelation was attributed to the formation of strong micellar interactions and aggregation. After a subcutaneous injection of a 20 wt% multiblock copolymer solution into mice, polymeric hydrogels are quickly formed in situ. The in vitro release of an anticancer drug, paclitaxel, persists over a month under physiological conditions.

Summary

Poly(ethylene glycol)s with relatively low molecular weight (<5,000) are widely used in biomedical applications because they are hydrophilic, nontoxic, absent of antigenicity and immunogenicity, and can be directly excreted by the kidneys. PEG-based amphiphilic copolymers are of interest for their unique self-assembly and biocompatibility. Additionally, the PEG-based amphiphilic copolymers exhibit unique changes in micellar architecture and aggregation number in response to changes near physiological temperature as this unique amphiphilic system may retain water molecules in the network during the sol–gel phase transition. Therefore, in-situ gelling systems made of the PEG-based amphiphilic copolymers are extensively used. Aqueous solutions of these block copolymers exhibit a sol–gel transition without syneresis in response to the changes in temperature or/and pH. These systems have many advantages, such as: simple drug formulation and administration procedure, no organic solvent, site-specificity, a sustained release behavior, less systemic toxicity, and ability to deliver both hydrophilic and hydrophobic drugs. The gelation of the block copolymer systems is due to the formation of the transient (or reversible) polymer network with absorbing a large amount of water caused by the stimuli-induced physical interactions, such as micellar aggregation and packing, hydrophobic association, phase-separation, and crystallization.

The main challenges for the application of in-situ forming hydrogels include a short gelation time, appropriate gelation temperature and/or pH, appropriate mechanical strength, biocompatibility, proper persistent time, convenient practical procedure, no significant syneresis, and desirable drug release behavior. These properties depend on copolymer composition, hydrophilic/hydrophobic balance, hydrophilic/hydrophobic block length, molecular weight, and polymer architecture. In addition, drug release from the block copolymer hydrogels is based on drug diffusion and gels erosion mechanisms; therefore, the biodegradability or bio-eliminability of these block copolymers is important for in vivo applications.

Amphiphilic copolymer hydrogels with multifunctionality and multisensitivity are attractive because of their unique advantages. In contrast to the thermosensitive systems, the pH- and temperature-sensitive amphiphilic copolymer hydrogels have some practical advantages, such as no premature gelation, electrostatic interaction with some biomolecules, and easy to store. The double-responsive system is easily injected into sites deep in the body. Some in-situ gelling systems, which contain cationic groups, may form electrostatic interactions with ionic proteins and DNA under physiological conditions, leading to sustained and constant release profiles as well as environments that benefit maintaining protein and DNA stability.

Acknowledgments

This work was supported by a “Korea Research Foundation Grant” (KRF-2006-005-J04602)

References

1. Qiu Y, Park K (2001) Environment-sensitive hydrogels for drug delivery. *Adv Drug Deliv Rev* 53:321–329
2. Hoffman AS (2002) Hydrogels for biomedical applications. *Adv Drug Deliv Rev* 43:3–12
3. Ruel-Gariepy E, Leroux JC (2004) In situ-forming hydrogels – review of temperature-sensitive systems. *Eur J Pharm Biopharm* 58:409–426
4. He CL, Kim SW, Lee DS (2008) In situ gelling stimuli-sensitive hydrogels for drug delivery. *J Control Release* 127:189–207
5. Schild HG (1992) Poly(*N*-isopropylacrylamide): experiment, theory and application. *Prog Polym Sci* 17:163–249
6. Taylor LD, Cerankowski LD (1975) Preparation of films exhibiting a balanced temperature dependence to permeation by aqueous solution – a study of low consolute behavior. *J Polym Sci Polym Chem Ed* 13:2551–2570
7. Horne RA, Almeida JP, Day AF et al (1971) Macromolecule hydration and the effect of solutions of polyvinyl methyl ether: a possible model for protein denaturation and temperature control in homeothermic animals. *J Colloid Interface Sci* 35:77–84
8. Aoshima S, Oda H, Kobayashi E (1992) Synthesis of thermally-induced phase separating polymer with well-defined polymer structure by living cationic polymerization. I. Synthesis of poly(vinyl ether)s with oxyethylene units in the pendant and its phase separation behavior in aqueous solution. *J Polym Sci A Polym Chem* 30:2407–2413
9. Suwa K, Wada Y, Kikunaga Y et al (1997) Synthesis and functionalities of poly(*N*-vinylalkylamide). IV. Synthesis and free radical polymerization of *N*-vinylisobutyramide and thermosensitive of the polymers. *J Polym Sci A Polym Chem* 35:1763–1768
10. Mikheeva LM, Grinberg NV, Mashkevich AY et al (1997) Microcalorimetric study of thermal cooperation transitions in poly(*N*-vinylcaprolactam) hydrogels. *Macromolecules* 30:2693–2699
11. Song SC, Lee SB, Jin JI et al (1999) A new class of biodegradable thermosensitive polymers. I. Synthesis and characterization of poly(organo phosphazenes) with methoxy-poly(ethylene glycol) and amino acid esters as side groups. *Macromolecules* 32:2188–2193
12. Soga O, van Nostrum CF, Hennik WE (2004) Poly(*N*-(2-hydroxypropyl) methacrylamide mono/di lactate): a new class of biodegradable polymers with tunable thermosensitivity. *Biomacromolecules* 5:818–821
13. Vermonden T, Besseling NAM, van Steenberghe MJ et al (2006) Rheological studies of thermosensitive triblock copolymer hydrogels. *Langmuir* 22:10180–10184
14. Gil ES, Hudson SM (2004) Stimuli-responsive polymers and their bioconjugates. *Prog Polym Sci* 29:1173–1222
15. Sarkar N (1979) Thermal gelation properties of methyl and hydroxypropyl methycellulose. *J Appl Polym Sci* 24:1073–1087
16. Chenite A, Chaput C, Wang D et al (2000) Novel injectable neutral solutions of chitosan form biodegradable gels in situ. *Biomaterials* 21:2155–2161
17. Han CK, Bae YH (1998) Inverse thermally-reversible gelation of aqueous *N*-isopropylacrylamide copolymer solution. *Polymer* 39:2809–2814
18. Lin HH, Cheng YL (2001) In-situ thermoreversible gelation of block and star copolymers of poly(ethylene glycol) and poly(*N*-isopropylacrylamide) of varying architectures. *Macromolecules* 34:3710–3715
19. Brown W, Schillen K, Almgren M et al (1991) Micelle and gel formation in a poly(ethylene oxide)/poly(propylene oxide)/poly(ethylene oxide) triblock block copolymer in water solution. Dynamic and static light scattering and oscillatory shear measurements. *J Phys Chem* 95:1850–1858
20. Herold CB, Keil K, Bruns DE (1989) *Biochem Pharmacol* 38:73
21. Shaffer CB, Critchfield FH (1947) *J Am Pharm Assoc* 36:152
22. Rassing J, Attwood D (1983) Ultrasonic velocity and light-scattering studies on the polyoxyethylene-polyoxypropylene copolymer F127 in aqueous solution. *Int J Pharm* 13:47–55
23. Attwood D, Collett JH, Tait CJ (1985) The micellar properties of the poly(oxyethylene)-poly(oxypropylene) copolymer Pluronic F127 in water and electrolyte solution. *Int J Pharm* 26:25–33

24. Dimitrov I, Trzebicka B, Muller AHE et al (2007) Thermosensitive water-soluble copolymers with doubly responsive reversibly interacting entities. *Prog Polym Sci* 32:1275–1343
25. Feil H, Bae YH, Feijen J et al (1993) Effect of copolymer hydrophilicity and ionization on the lower critical solution temperature of *N*-isopropylacrylamide copolymers. *Macromolecules* 26:2496–2500
26. Liu QF, Zhang P, Lu MG (2005) Synthesis and swelling behavior of comb-type grafted hydrogels by reversible addition-fragmentation chain transfer polymerization. *Inc J Polym Sci A Polym Chem* 43:2615–2624
27. Masci G, Giacomelli L, Crescenzi V (2004) Atom transfer radical polymerization of *N*-isopropylacrylamide. *Macromol Rapid Commun* 25:559–564
28. Topp MDC, Dijkstra PJ, Talsma H et al (1997) Thermosensitive micelle-forming block copolymers of poly(ethylene glycol) and poly(*N*-isopropylacrylamide). *Macromolecules* 30:8518–8520
29. Kohori F, Sakai K, Aoyagi T et al (1998) Preparation and characterization of thermally responsive block copolymer micelles comprising poly(*N*-isopropylacrylamide-*b*-D,L-lactide). *J Control Release* 55:87–98
30. Zhuang YF, Chen LW, Zhu ZQ et al (2000) Preparation and separation function of *N*-isopropylacrylamide copolymer hydrogels. *Polym Adv Technol* 11:192–197
31. Chen JH, Maekawa YM et al (2002) Thermoresponsive conductivity of poly(*N*-isopropylacrylamide)/potassium chloride gel electrolytes. *J Polym Sci B Polym Phys* 40:134–141
32. Spohr R, Reber N, Wolf A et al (1998) Thermal control of drug release by a responsive ion track membrane observed by ratio tracer flow dialysis. *J Control Release* 50:1–11
33. Stile RA, Burghardt WR, Healy KE (1999) Synthesis and characterization of injectable poly(*N*-isopropylacrylamide)-based hydrogels that support tissue formation in vitro. *Macromolecules* 32:7370–7379
34. Motokawa R, Morishita K, Koizumi S et al (2005) Thermosensitive diblock copolymer of poly(*N*-isopropylacrylamide) and poly(ethylene glycol) in water: Polymer preparation and solution behavior. *Macromolecules* 38:5748–5760
35. Tang T, Castelletto V, Parras P et al (2006) Thermo-responsive poly(methyl methacrylate)-block- poly(*N*-isopropylacrylamide) block copolymers synthesized by RAFT polymerization: Micellization and gelation. *Macromol Chem Phys* 207:1718–1726
36. Nykanen A, Nuopponen M, Laukkanen A et al (2007) Phase behavior and temperature-responsive molecular filters based on self-assembly of polystyrene-block-poly(*N*-isopropylacrylamide)-block-polystyrene. *Macromolecules* 40:5827–5834
37. Kwon IK, Matsuda T (2006) Photo-inverter-based thermoresponsive block copolymers composed of poly(ethylene glycol) and poly(*N*-isopropylacrylamide) and chondrocyte immobilization. *Biomaterials* 27:986–995
38. Mortensen K, Pedersen JS (1993) Structural study on the micelle formation of poly(ethylene oxide)-poly(propylene oxide)-poly(ethylene oxide) triblock copolymer in aqueous solution. *Macromolecules* 26:805–812
39. Cohn D, Sosnik A, Levy A (2003) Improved reverse thermo-responsive polymeric systems. *Biomaterials* 24:3707–3714
40. Ahn JS, Suh JM, Lee M et al (2005) Slow eroding biodegradable multiblock poloxamer copolymers. *Polym Int* 54:842–847
41. Sosnik A, Cohn D et al (2005) Reverse thermo-responsive poly(ethylene oxide) and poly(propylene oxide) multiblock copolymers. *Biomaterials* 26:349–357
42. Xiong XY, Tam KC, Gan LH (2005) Synthesis and thermal responsive properties of P(LA-*b*-EO-*b*-PO-EO-*b*-LA) block copolymers with short hydrophobic poly(lactic acid) (PLA) segments. *Polymer* 46:1841–1850
43. Xiong XY, Tam KC, Gan LH (2006) Synthesis and thermally responsive properties of novel pluronic F87/polycaprolactone (PCL) block copolymers with short PCL blocks. *J Appl Polym Sci* 100:4163–4172
44. Cohn D, Lando G, Sosnik A et al (2006) PEO-PPO-PEO-based poly(ether ester urethane)s as degradable reverse thermo-responsive multiblock copolymers. *Biomaterials* 27:1718–1727
45. Masahiko O (2002) *Prog Polym Sci* 27:87
46. Yasin M, Tighe BJ (1992) *Biomaterials* 13:9
47. Jeong B, Bae YH, Lee DS et al (1997) Biodegradable block copolymers as injectable drug-delivery systems. *Nature* 388:860–862
48. Jeong B, Lee DS, Shon J et al (1999) Thermoreversible gelation of poly(ethylene oxide) biodegradable polyester block copolymers. *J Polym Sci A Polym Chem* 37:751–760
49. Choi SW, Choi SY, Jeong B et al (1999) Thermoreversible gelation of poly(ethylene oxide) biodegradable polyester block copolymers. II. *J Polym Sci A Polym Chem* 37:2207–2218
50. Li F, Li S, Ghzaoui AE et al (2007) Synthesis and gelation properties of PEG-PLA-PEG triblock copolymers obtained by coupling monohydroxylated PEG-PLA with adipoyl chloride. *Langmuir* 23:2778–2783
51. Park SY, Han DK, Kim SC et al (2001) Synthesis and characterization of star-shaped PLLA-PEO block copolymers with temperature-sensitive sol-gel transition behavior. *Macromolecules* 34:8821–8824

52. Park SY, Han BR, Na KM et al (2003) Micellization and gelation of aqueous solutions of star-shaped PLLA-PEO block copolymers. *Macromolecules* 36:4115–4124
53. Jeong B, Bae YH, Kim SW (1999) Thermoreversible gelation of PEG-PLGA-PEG triblock copolymer aqueous solutions. *Macromolecules* 32:7064–7069
54. Jeong B, Choi YK, Bae YH et al (1999) New biodegradable polymers for injectable drug delivery systems. *J Control Release* 62:109–114
55. Jeong B, Bae YH, Kim SW (1999) Biodegradable thermosensitive micelles of PEG-PLGA-PEG triblock copolymers. *Colloids Surf B Biointerfaces* 16:185–193
56. Park MJ, Char K (2004) Gelation behavior of PEO–PLGA–PEO triblock copolymers induced by macroscopic phase separation. *Langmuir* 20:2456–2465
57. Kwon KW, Park MJ, Bae YH et al (2002) Gelation behavior of PEO–PLGA–PEO triblock copolymers in water. *Polymer* 43:3353–3358
58. Jeong B, Bae YH, Kim SW et al (2000) In situ gelation of PEG–PLGA–PEG triblock copolymer aqueous solutions and degradation thereof. *J Biomed Mater Res* 50:171–177
59. Jeong B, Bae YH, Kim SW (2000) Drug release from biodegradable injectable thermosensitive hydrogel of PEG–PLGA–PEG triblock copolymers. *J Control Release* 63:155–163
60. Tyagi P, Li Z, Chancellor M et al (2004) Sustained intravesical drug delivery using thermosensitive hydrogel. *Pharm Res* 21:832–837
61. Li Z, Ning W, Wang J et al (2003) Controlled gene delivery system based on thermosensitive biodegradable hydrogel. *Pharm Res* 20:884–888
62. Lee PY, Li Z, Huang L (2003) Thermosensitive hydrogel as a Tgf- β 1 gene delivery vehicle enhances diabetic wound healing. *Pharm Res* 20:1995–2000
63. Lee DS, Shim MS, Kim SW et al (2001) Novel thermoreversible gelation of biodegradable PLGA-bolck-PEO-block-PLGA triblock copolymers in aqueous solution. *Macromol Rapid Commun* 22:587–592
64. Zentner GM, Rathi R, Shih C et al (2001) Biodegradable block copolymers for delivery of proteins and water-insoluble drugs. *J Control Release* 72:203–215
65. Shim MS, Lee HT, Shim WS et al (2002) Poly(D,L-lactic acid-co-glycolic acid)-b-poly(ethylene glycol)-b-poly(D,L-lactic acid-co-glycolic acid) triblock copolymer and thermoreversible phase transition in water. *J Biomed Mater Res* 61:188–196
66. Kim YJ, Choi S, Koh JJ et al (2001) Controlled release of insulin from injectable biodegradable triblock copolymer. *Pharm Res* 18:548–550
67. Choi S, Kim SW (2003) Controlled release of insulin from injectable biodegradable triblock copolymer depot in ZDF rats. *Pharm Res* 20:2008–2010
68. Choi S, Baudys M, Kim SW (2004) Control of blood glucose by novel GLP-1 delivery using biodegradable triblock copolymer of PLGA–PEG–PLGA in type-2 diabetic rats. *Pharm Res* 21:827–831
69. Zhong Z, Dijkstra PJ, Feijen J et al (2002) Synthesis and aqueous phase behavior of thermoresponsive biodegradable poly(D,L-3-methylglycolide)-block-poly(ethylene glycol)-block-poly(D,L-3-methyl-glycolide) triblock copolymers. *Macromol Chem Phys* 203:1797–1803
70. Qiao M, Chen D, Ma X et al (2005) Injectable biodegradable temperature-responsive PLGA–PEG–PLGA copolymers: synthesis and effect of copolymer composition on the drug release from the copolymer-based hydrogels. *Int J Pharm* 294:103–112
71. Yu L, Zhang H, Ding J (2006) A subtle end-group effect on macroscopic physical gelation of triblock copolymer aqueous solutions. *Angew Chem Int Ed* 45:2232–2235
72. Yu L, Chang G, Zhang H et al (2007) Temperature-induced spontaneous sol–gel transition of poly(D,L-lactic acid-co-glycolic acid)-b-poly(ethylene glycol)-b-poly(D,L-lactic acid-co-glycolic acid) triblock copolymers and their end-capped derivatives in water. *J Polym Sci A Polym Chem* 45:1122–1133
73. Jo S, Kim J, Kim SW (2006) Reverse thermal gelation of aliphatically modified biodegradable triblock copolymers. *Macromol Biosci* 6:923–928
74. Jeong B, Wang LQ, Gutowska A (2001) Biodegradable thermoreversible gelling PLGA-g-PEG copolymers. *Chem Commun* 16:1516–1517
75. Lee SJ, Han BR, Park SY et al (2006) Sol–gel transition behavior of biodegradable three-arm and four-arm star-shaped PLGA–PEG block copolymer aqueous solution. *J Polym Sci A Polym Chem* 44:888–899
76. Lee SJ, Bae Y, Kataoka K et al (2008) In vitro release and in vivo anti-tumor efficacy of doxorubicin from biodegradable temperature-sensitive star-shaped PLGA–PEG block copolymer hydrogel. *Polym J* 40:171–176
77. Jeong B, Kibbey MR, Birnbaum JC et al (2000) Thermogelling biodegradable polymers with hydrophilic backbones: PEG-g-PLGA. *Macromolecules* 33:8317–8322
78. Chung YM, Simmons KL, Gutowska A et al (2002) Sol–gel transition temperature of PLGA-g-PEG aqueous solutions. *Biomacromolecules* 3:511–516

79. Jeong B, Windisch CF, Park MJ et al (2003) Phase transition of the PLGA-g-PEG copolymer aqueous solutions. *J Phys Chem B* 107:10032–10039
80. Jeong B, Lee KM, Gutowska A et al (2002) Thermogelling biodegradable copolymer aqueous solutions for injectable protein delivery and tissue engineering. *Biomacromolecules* 3:865–868
81. Kim MS, Seo KS, Khang G et al (2004) Preparation of methoxy poly(ethylene glycol)/polyester diblock copolymers and examination of the gel-to-sol transition. *J Polym Sci A Polym Chem* 42:5784–5793
82. Yang J, Jia L, Hao Q et al (2005) A novel approach to biodegradable block copolymers of ϵ -caprolactone and δ -valerolactone catalyzed by new aluminum metal complexes II. Micellization and solution to gel transition. *Macromol Biosci* 5:896–903
83. Kim MS, Seo KS, Khang G et al (2004) Preparation of poly(ethylene glycol)-block-poly(caprolactone) copolymers and their applications as the thermo-sensitive materials. *J Biomed Mater Res* 70A:154–158
84. Kim MS, Hyun H, Khang G et al (2006) Preparation of thermosensitive diblock copolymers consisting of MPEG and polyesters. *Macromolecules* 39:3099–3102
85. Kim MS, Hyun H, Seo KS et al (2006) Preparation and characterization of MPEG–PCL diblock copolymers with thermo-responsive sol–gel–sol phase transition. *J Polym Sci A Polym Chem* 44:5413–5423
86. Kim MS, Kim SK, Kim SH et al (2006) In vivo osteogenic differentiation of rat bone marrow stromal cells in thermosensitive MPEG–PCL diblock copolymer gels. *Tissue Eng* 12:2863–2873
87. Hyun H, Kim YH, Song IB et al (2007) In vitro and in vivo release of albumin using a biodegradable MPEG–PCL diblock copolymer as an in situ gel-forming carrier. *Biomacromolecules* 8:1093–1100
88. Hwang MJ, Suh JM, Bae YH et al (2005) Caprolactonic poloxamer analog: PEG–PCL–PEG. *Biomacromolecules* 6:885–890
89. Bae SJ, Suh JM, Sohn YS et al (2005) Thermogelling poly(caprolactone-b-ethylene glycol-b-caprolactone) aqueous solutions. *Macromolecules* 38:5260–5265
90. Bae SJ, Joo MK, Jeong Y et al (2006) Gelation behavior of poly(ethylene glycol) and polycaprolactone triblock and multiblock copolymer aqueous solutions. *Macromolecules* 39:4873–4879
91. Huh KM, Bae YH (1999) Synthesis and characterization of poly(ethylene glycol)/poly(L-lactic acid) alternating multiblock copolymers. *Polymer* 40:6147–6155
92. Bae YH, Huh KM, Kim Y, Park KH (2000) Biodegradable amphiphilic multiblock copolymers and their implications for biomedical applications. *J Control Release* 64:3–13
93. Lee J, Bae YH, Sohn YS, Jeong B (2006) Thermogelling aqueous solutions of alternating multiblock copolymers of poly(L-lactic acid) and poly(ethylene glycol). *Biomacromolecules* 7:1729–1734
94. Joo MK, Sohn YS, Jeong B (2007) Stereoisomeric effect on reverse thermal gelation of poly(ethylene glycol)/poly(lactide) multiblock copolymers. *Macromolecules* 40:5111–5115
95. Lee JW, Hua FJ, Lee DS (2001) Thermoreversible gelation of biodegradable poly(ϵ -caprolactone) and poly(ethylene glycol) multiblock copolymers in aqueous solutions. *J Control Release* 73:315–327
96. Lee SC, Kang SW, Kim C, Kwon IC, Jeong SY (2000) Synthesis and characterization of amphiphilic poly(2-ethyl-2-oxazoline)/poly(ϵ -caprolactone) alternating multiblock copolymers. *Polymer* 41:7091–7097
97. Li F, Li S, Vert M (2005) Synthesis and rheological properties of polylactide/poly(ethylene glycol) multiblock copolymers. *Macromol Biosci* 5:1125–1131
98. Lee J, Joo MK, Oh H, Sohn YS, Jeong B (2006) Injectable gel: poly(ethylene glycol)-sebacic acid polyester. *Polymer* 47:3760–3766
99. Loh XJ, Goh SH, Li J (2007) New biodegradable thermogelling copolymers having very low gelation concentrations. *Biomacromolecules* 8:585–593
100. Schmaljohann D (2006) Thermo- and pH-responsive polymers in drug delivery. *Adv Drug Deliv Rev* 58:1655–1670
101. Philippova OE, Houdet D, Audebert R et al (1997) pH-responsive gels of hydrophobically modified poly(acrylic acid). *Macromolecules* 30:8278–8285
102. Yang Z, Zhang Y, Markland P et al (2002) Poly(glutamic acid)/poly(ethylene glycol) hydrogels prepared by photoinduced polymerization: synthesis, characterization, and preliminary release studies of protein drugs. *J Biomed Mater Res* 62:14–21
103. Park SY, Bae YH (1999) Novel pH-sensitive polymers containing sulfonamide groups. *Macromol Rapid Commun* 20:269–273
104. Yin XC, Hoffman AS, Stayton PS (2006) *Biomacromolecules* 7:1381
105. He CL, Zhao CW, Chen XS et al (2008) Novel pH- and temperature-sensitive block copolymers with tunable pH-responsive range. *Macromol Rapid Commun* 29:490–497
106. Shim WS, Yoo JS, Bae YH et al (2005) Novel injectable pH and temperature sensitive block copolymer hydrogels. *Biomacromolecules* 6:2930–2934

107. Shim WS, Kim SW, Lee DS (2006) Sulfonamide-based pH- and temperature-sensitive biodegradable block copolymer hydrogels. *Biomacromolecules* 7:1935–1941
108. Shim WS, Kim JH, Park H et al (2006) Biodegradability and biocompatibility of a pH- and thermo-sensitive hydrogel formed from a sulfonamide-modified poly(ϵ -caprolactone-co-lactide)-poly(ethylene glycol)-poly(ϵ -caprolactone-co-lactide) block copolymer. *Biomaterials* 27:5178–5185
109. Shim WS, Kim JH, Kim K et al (2007) pH- and temperature-sensitive, injectable, biodegradable block copolymer hydrogels as carriers for paclitaxel. *Int J Pharm* 331:11–18
110. Dayananda K, Pi BS, Kim BS et al (2007) Synthesis and characterization of pH/temperature-sensitive block copolymers via atom transfer radical polymerization. *Polymer* 48:758–762
111. Huynh DP, Shim WS, Kim JH et al (2006) pH/temperature sensitive poly(ethylene glycol)-based biodegradable polyester block copolymer hydrogels. *Polymer* 47:7918–7926
112. Wintersteiner O, Abramson HA (1933) The isoelectric point of insulin: electrical properties of adsorbed and crystalline insulin. *J Biol Chem* 99:741–753
113. Butun V, Armes SP, Billingham NC (2001) Synthesis and aqueous solution properties of near-monodisperse tertiary amine methacrylate homopolymers and diblock copolymers. *Polymer* 42:5993–6008
114. Gohy J, Lohmeijer BGG, Varshney SK et al (2002) Stimuli-responsive aqueous micelles from an ABC metallo-supramolecular triblock copolymer. *Macromolecules* 35:9748–9755
115. Lynn DM, Amiji MM, Langer R (2001) pH-responsive polymer microsphere: rapid release of encapsulated material within the range of intracellular pH. *Angew Chem Int Ed* 40:1707–1710
116. Lynn DM, Langer R (2000) Degradable poly(β -amino ester): synthesis, characterization, and self-assembly with plasmid DNA. *J Am Chem Soc* 122:10761–10768
117. Yoo JS, Kim MS, Lee DS et al (2006) Novel pH and temperature-sensitive block copolymer: poly(ethylene glycol)-*b*-poly(ϵ -caprolactone)-*b*-poly(β -amino ester). *Macromol Res* 14:117–120
118. Huynh DP, Nguyen MK, Pi BS et al (2008) Functionalized injectable hydrogel for controlled insulin delivery. *Biomaterials* 29:2527–2534
119. Dayananda K, He CL, Lee DS (2008) In situ gelling aqueous solutions of pH- and temperature-sensitive poly(ester amino urethane)s. *Polymer* 49:4620–4625

Biodegradable Hydrogels for Controlled Drug Release

Luis García, María Rosa Aguilar, and Julio San Román

Abstract Biodegradable hydrogels for controlled drug release are based on functionalized polymer systems and are of great importance in polymer therapeutics. The most relevant aspects of biodegradable polymeric hydrogels for the release of specific drugs and bio-active compounds are the nature of biodegradable polymer, the gelation process by physical or chemical crosslinking, and the properties of the bioactive compound. The design of bio-degradable hydrogels for drug delivery is an important aspect in the administration of therapeutics, such as the formulation and application of injectable hydrogels, are discussed on the basis of components and bioactive counterparts.

Introduction

Natural and synthetic polymeric materials offer many possibilities for the design and application of controlled drug delivery systems (DDS). The polymers provide bioresorbable supports for a number of bioactive compounds from small molecules with specific pharmacological activity to biomacromolecules, such as enzymes, hormones and growth factors. These prospects are based on the dynamic molecular characteristics of high molecular weight polymer chains and the supramolecular nature of the association of macromolecular chains with specific bioactive agents. The dynamics and movement of chain segments and monomeric sequences are two important characteristics to build bioactive systems into a biomimetic platform that provides alternatives to the classical application of bioactive compounds and specific drugs.

Basically, two approaches for polymeric chains to participate in dynamic and reversible processes of making bonds between macromolecules and of the monomeric functional components with the bioactive compounds. These interactions are established through physically dynamic noncovalent bonds by ionic and polar functional groups, that give rise to well known supramolecular structures, or by chemically dynamic situations through reversible covalent bonds that are important in the design and application of “targeting” systems and the development of “polymer drugs” which have open a very active discipline known as “polymer therapeutics” [1]. One of the most important characteristics of the systems based on physical supramolecular structures, or dynamic and reversible chemical blocks, is that all the systems have to offer the possibility to avoid the accumulation of the macromolecular support in the body, by the application of polymers that, after a controlled time interval, would bio-degrade or solubilize in physiological conditions to facilitate the clearance of nonbioactive residues in the body. To achieve this challenge, the application of biodegradable polymeric systems, it is necessary that biogradtion gives nontoxic low molecular weight

L. García, M. Rosa Aguilar, and J. San Román • Institute of Polymer Science and Technology, CSIC and CIBER-BBN, Juan de la Cierva 3 28006 Madrid, Spain
e-mail: jsroman@ictp.csic.es

products, or soluble polymer chains of the adequate molecular size, to be cleared by the normal metabolic route from the body. In this sense, the application of biodegradable or resorbable polymeric hydrogels becomes one of the most important concepts to be considered for the design and application of controlled release systems and polymer drugs.

From a physical point of view, the association of polymer–polymer, polymer–drug, or polymer–bioactive components can be established by means of: electrostatic interactions, hydrogen bonding, donor–acceptor, van der Waals forces, or even metal–ion coordination. There are clear examples of supramolecular systems in the living tissues constituted by this mechanism and even it is the basis for metabolic functions, cell growth and proliferation, or the pharmacological action of a great number of drugs. The chemical approach gives excellent opportunities for the design and development of bioactive polymer systems and polymer drugs, with a lot of possibilities for the modulation and control of the targeting of these very interesting bioactive systems. Reversible chemical reactions of functional groups present in monomeric components, building blocks in polymer chains, linear polymerization with control of the molecular weight and molecular weight distribution, and crosslinking, are some of the possibilities of this very wide and attractive approach for the development of bioactive macromolecules of very high interest in “polymer therapeutics.” The reversible chemical reactions are very frequent in nature and a single example is the reversible crosslinking of proteins based on disulfure links from aminoacid components of the macromolecular chains.

Bioactive degradable hydrogels based on natural macromolecules (polysaccharides, polypeptides, proteins), or designed with synthetic or biohybrid polymer systems, offer a wide range of possibilities and actuations in a biomimetic way, with the advantage of the precise selection of components not only from a chemical and structural point of view, but also from morphological considerations, the modulation of the resorption kinetics and mechanism, with the corresponding control of the targeting to the active local point and the release of the pharmacologically or bioactive main component.

Nature has developed evolutionary processes with elegant strategies for the specific application of bioactive agents, most of them are based on very well known macromolecules and supramolecular assemblies. Clear examples of that are; proteins like insulin, polysaccharides as hyaluronic acid or glucosaminoglicans such as chondroitin sulfate. Therefore, nature can be considered as the best model for the development of new and advanced targeting and DDS to be applied in the frame of new strategies in nanomedicine and therapeutic actions with high efficacy, local action, and reduced toxicity.

The current strategies for the development of systems for targeting and controlled release of specific drugs and bioactive molecules (growth factors, hormones, antioxidants, and cell activators for regenerative medicine) are based on the design and development of biodegradable hydrogels.

The Nature of Biodegradable Hydrogels

Hydrogels are three-dimensional, crosslinked physical or chemical networks of water-soluble polymers, that encompass a wide range of chemical compositions and bulk physical properties. Hydrogels can be classified according to the interactions between components into physical or chemical gels. Polymers with very different chemical structures as multivalent polymers, branched polymers, graft polymers, dendrimers, dendronized polymers, block copolymers, and stars [1] have been used for the preparation of biodegradable hydrogels for DDS (Fig. 1).

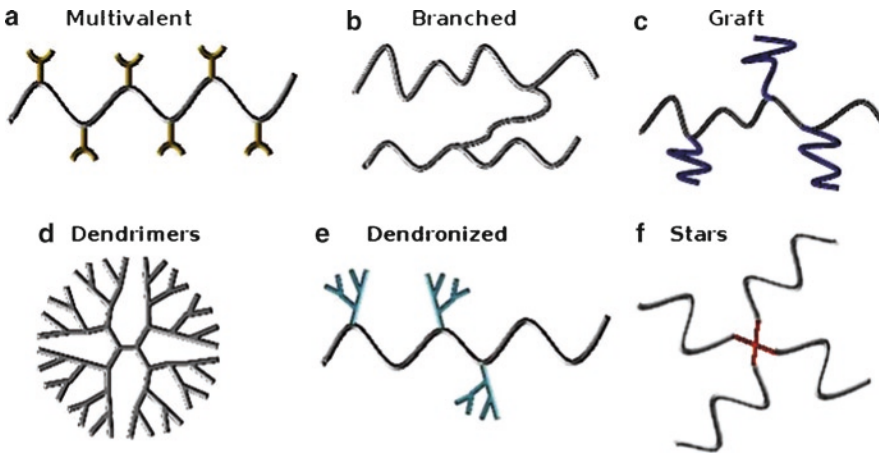


Fig. 1. Polymer structures used in the synthesis of hydrogels for drug delivery.

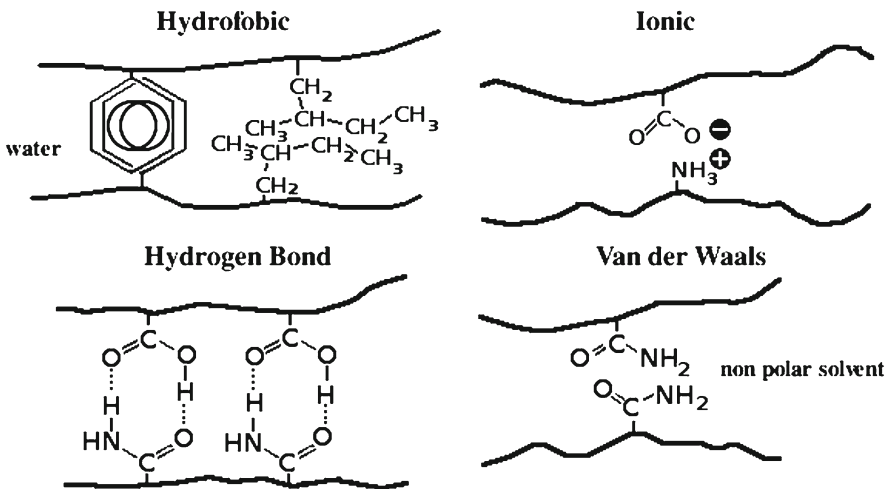


Fig. 2. Interactions of specific functional groups in the formation of physical gels.

Hydrogels can be prepared with natural or synthetic polymers. In general, natural macromolecules present inherent biocompatibility, biodegradability, and biological moieties that support cellular activities. However, they usually do not provide sufficient mechanical properties and may contain pathogens or evoke immune/inflammatory responses. On the other hand, synthetic hydrogels present well-defined structures that can be manipulated to obtain biodegradability and a specific functionality.

Physical Hydrogels

Hydrogels are “physical” gels when the networks are held together by the growth of physically connected aggregates (Fig. 2). Depending on the nature of each gelling system, the junctions may be molecular entanglements, ordered crystalline regions, phase-separated

microdomains, and/or secondary forces including ionic, H-bonding, or hydrophobic forces. Physical hydrogels are not homogeneous, since clusters of molecular entanglements, or hydrophobically or ionically associated domains, can create inhomogeneities. The common disadvantage of physical crosslinking is that the gels formed are unstable and may disintegrate rapidly and unpredictably.

Hydrophobic Interactions Hydrogels

Polymers with hydrophobic domains can crosslink in aqueous environments via reverse thermal gelation (sol–gel transition). The gelation occurs when a gelator (the hydrophobic segment) is coupled to the hydrophilic polymer segment of an amphiphilic polymer. These polymers are water soluble at low temperatures. As the temperature is increased the hydrophobic domains aggregate to minimize the hydrophobic surface area, reducing the amount of structured water surrounding the hydrophobic domains and maximizing the solvent entropy (Fig. 3). The temperature at which gelation occurs depends on the concentration of the polymer, the length of the hydrophobic block, and the chemical structure of the polymer. There is great versatility in composition, structure, and molecular weight of the synthetic polymers. Poly(ethylene glycol) (PEG) is one of the simplest and most used in the preparation of physical hydrogels.

A series of interesting biodegradable and biocompatible ABA-type triblock copolymers (PEG–PLLA–PEG) as thermo-sensitive hydrogels was developed [2]. Their sol–gel transitions were easily manipulated by changing the biodegradable block length; by increasing the PLLA block length, the aggregation tendency was increased to provide a lower critical gelation concentration (CGC) with steeper sol–gel transition curves. The system was designed for delivery of high Mw or low Mw hydrophobic protein drugs which have a low diffusion coefficient. These PEG–PLLA–PEG systems and their degradation products are known to be biocompatible and pharmacologically inactive, so there is no need for removal of an implanted delivery system.

Other ABA copolymers have been synthesized using shorter PEG ($M_w < 750$) and PLGA blocks [3]. This system showed gelation transitions near physiological temperature. These are tunable by tailoring the block length and compositions. The “in vitro” drug release

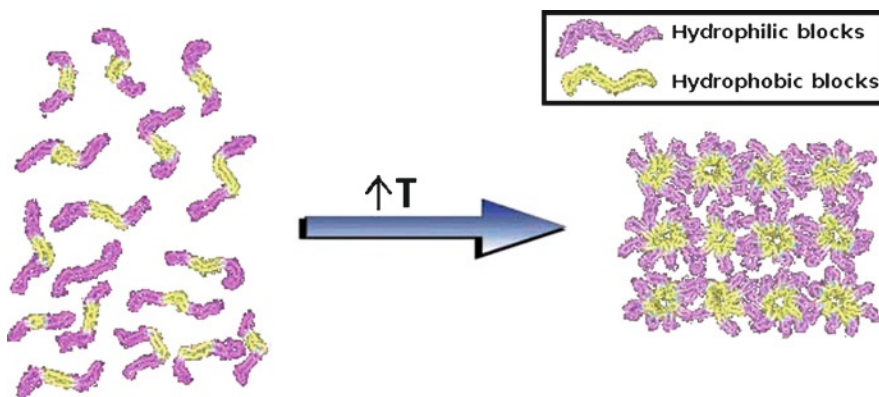


Fig. 3. Sol–gel transition of A-B-A block copolymers.

behavior of PEG–PLGA–PEG hydrogels was evaluated by using ketoprofen and spiro lactone as ionizable and nonionizable model drugs, respectively [4]. The release of ketoprofen was first-order release over 2 weeks, indicating a diffusion controlled mechanism. In contrast, the release of spiro lactone exhibited an S-shaped release profile over 2 months, suggesting a diffusion-controlled process followed by a degradation-dominated process.

PLGA–PEG–PLGA BAB-type triblock copolymers were synthesized using hexamethylene diisocyanate. Compared with PEG–PLGA–PEG, these copolymers have a lower sol–gel transition temperature that is influenced by the block length and composition [5]. ReGel[®] is a commercial biodegradable PLGA–PEG–PLGA (1,500–1,000–1,500) hydrogels. ReGel[®] drug release and degradation is a diffusion-controlled during the initial 2 weeks followed by a combined diffusion/degradation controlled process within a 4-week degradation time [6]. PLGA undergoes rapid degradation in the block copolymer releasing acidic products leading to an environment in the hydrogels, which is deleterious to bioactive proteins and to cells. Poly(η -caprolactone) was considered an alternative to hydrophobic blocks that release fewer acidic products during the degradation, but suffers from extremely slow degradation rates. New thermosensitive biodegradable triblock copolymers, based on PEG–[poly(β -caprolactone-*co*-glycolide)]–PEG, (PEG–[PCL-*co*-GA]–PEG), were prepared and characterized. The glycolide was incorporated into the hydrophobic block to avoid PCL crystallization and enhance biodegradation [7].

Pluronic[®] (BASF) and Poloxamer[®] (ICI) are block copolymers based on PEO–PPO sequences and are widely used in pharmaceutical systems. These systems have sol–gel transitions below or close to the physiological temperature as high as 50°C by tailoring the hydrophobic–hydrophilic balance which changes the three-dimensional packing of the micelles formed. Thermal transitions depend on polymer composition and solution concentration; therefore, these polymers are attractive for controlled release injectable formulations [8]. However, their applications in DDS are limited by their lack of biodegradability. Subsequently, a family of degradable pentablock copolymers, composed of Pluronic F87 flanked by two short biodegradable polyester blocks (PLA or PCL) [9, 10] that provided controlled release without an initial burst release, were prepared by these authors.

A high strength degradable hydrogels, based on an enantiomeric mixture of starburst triblock copolymers consisting of an 8-arm PEG and poly(L-lactide) (PLLA) or poly(D-lactide) (PDLA), was synthesized [11]. This hydrogels was stable after cooling below the transition temperature due to the formation of stable stereo complexes. The combination of rapid temperature-triggered irreversible hydrogels formation, high-mechanical strength, and degradation behavior renders this polymer suitable for injectable biomedical applications.

Synthetic block copolypeptides incorporating hydrophobic and hydrophilic segments, which are thermosensitive and present similar behavior to Pluronics[®], were developed [12, 13]. However, the sol–gel transition took place at lower concentrations since part of the molecule adopts an α -helix conformation that facilitates gelation. Bellomo et al. [14] prepared synthetic vesicles based on amphiphilic copolypeptides with a high degree of architectural control. The hydrophilic block, made of L-lysine was grafted with water soluble ethylene glycol to make the hydrophobic lysine block consistent with L-leucine. Each block presented a different secondary structure: poly(L-lysine), ionized polyelectrolyte, presented a stretched linear configuration and poly(L-leucine) an α -helix secondary structure, which produced a dramatic effect in the overall structure.

Reversible physical networks based on PAA and poly(2-vinylpyridine) triblock copolymers (PAA–P2VP–PAA) that have an isoelectric point at \sim 5.5 and form a gels at pH \sim 3.4 were prepared by Sfica and Tsitsilians [15]. When the pH was increased near the

isoelectric point the polyampholyte. Precipitated, and as the pH was further increased, the polymer redissolved due to the formation of micelles with P2VP as core and charged PAA chains as the shell.

Supramolecular structures based on amphiphilic block copolymers and cyclodextrins (CD) also formed interesting controlled DDS [16]. Supramolecular hydrogels based on the self-assembly of the inclusion complexes between CDs with biodegradable block copolymers were injectable DDS for macromolecular drugs. The CD-containing cationic polymers were described as “gene carriers” with reduced toxicity compared non-CD-containing polymer counterparts [16].

Dendritic structures provided an ideal platform for drug delivery. The advantages of these structures were the highly branched nanoscale architecture and the many surface reactive groups; these provided drug targeting and high drug payloads. The cytotoxicity and cell permeability of dendrimers was found to increase with increasing generation and concentration [17]. Many of their adverse effects were reduced by conjugation of poly(ethylene glycol) (PEG) to their surface. Conjugated PEG dendrimers reduced cytotoxicity and immunogenicity and also provided dendrimers with excellent solubility, favorable pharmacokinetic, and tissue biodistribution [18]. For example, the carbonyl group of ibuprofen formed electrostatic complexes with the PAMAM dendrimer amine groups. The complexed drug entered A549 cells more rapidly than pure drug, indicating that dendrimers may effectively carry complexed drugs inside cells [19].

Ionic Interaction Hydrogels

A physical “ionotropic” hydrogels is formed when a polyelectrolyte is combined with a multivalent ion of opposite charge. When polyelectrolytes of opposite charges are mixed, they may form a gels or precipitate depending on: the concentrations, the ionic strength, and pH of the solution. The products of ion-crosslinked systems are known as complex coacervates, polyion complexes, or polyelectrolyte complexes. Complex coacervates and polyion complex hydrogels are attractive as tissue engineering matrices as these physical gels can form biospecific recognitions. All these interactions are reversible and can be easily disrupted by simple changes in physical conditions, such as pH or ionic strength.

A 5-aminosalicylic acid colon-specific delivery system is based on chitosan-Ca²⁺-alginate by spray drying and followed by ionotropic gelation/polyelectrolyte complexation [20]. The highly cooperative ionic bonds between the positively charged chitosan and negatively charged alginate, the main driven force binding of the intermolecular and intramolecular hydrogen bonds and hydrophobic forces between the drug and the polymers, increased the mechanical strength of the gels network and decreased its porosity/permeability. “In vivo,” these microspheres have been localized in the colon of Wistar male rats that were previously induced with colitis.

Biodegradable nanoparticles that solidify “in situ” upon injection into isotonic phosphate buffered saline (PBS) with no additional initiators were developed [21]. These nanoparticles are prepared from different amine-modified polyesters: diethylaminopropylamine-poly(vinylalcohol)-g-poly(lactide-co-glycolide) (DEAPA (68)-PVA-g-PLGA(1:20)), diethylaminoethyl-amine-PVA-g-PLGA (DEAEA(33)-PVA-g-PLGA(1:20)), and dimethylaminopropyl-amine-PVAL-g-PLGA (DMAPEA(33)-PVA-g-PLGA(1:20)). The “in situ” depots are formed by ion-mediated aggregation. The “in vitro” insulin release from these systems gave good results [21].

Microspheres can also be formed crosslinking hydrogels by ionic interactions. An example is the preparation of microspheres by polymerization of acrylic acid in the presence of chitosan [22]. This kind of systems have been used as meclofenamic acid delivery systems. The release of this drug was controlled by the solubility of the drug and not by the swelling of the polymeric matrix at different pH. A constant release was observed during 2–4 weeks. The particles were biocompatible and bioresorbable by living tissues based on “in vivo” tests [23].

Hydrogen Bonded Hydrogels

Hydrogen bonded hydrogels as injectable hydrogels are formulated by mixing two or more natural polymers that exhibit rheological synergism. These blends are more gels-like than those of the individual polymers due to the extensive hydrogen bonding interactions. However, the hydrogen bonds are relatively weak and easily disrupted by shear forces within the needle. Hydrogen bonded natural polymers, such as gelatine-agar [24] and hyaluronic acid-methylcellulose [25], exhibit excellent biocompatibility; however, they are often diluted and dispersed in few hours due to an influx of water from surrounding tissues; consequently, their use is restricted to relatively short-acting drug release requirements.

New bioactive dressings based on chitosan-lactate (ChL) and PVA loaded with nitrofurazone for wound healing have been developed with good results both “in vitro” and “in vivo” [23]. Hydrogels were formed by the phase inversion technique after blending solutions of both polymers. ChL blended with PVA improved hemocompatibility and mechanical properties of the synthetic PVA, maintaining the bioresorbable character of this kind of hydrogels [23].

Chemically Bonded Hydrogels

The most common hydrogels are those obtained by chemical crosslinking of hydrophilic molecules to form a network. Covalent-linkages allow the material to swell without loss of structural integrity. Chemical hydrogels usually contain regions of high crosslink density with low water swelling, called “clusters,” dispersed within regions of low crosslink density with high swelling. This pattern could be due to hydrophobic aggregation of crosslinking agents, leading to high crosslink density clusters [26]. In some cases, temperature and solids concentration phase separation can occur during gelation to form water-filled “voids” and/or “macropores.”

Small-molecule crosslinkers can be used to produce “in situ” crosslinked hydrogels. For example, human serum albumin was crosslinked with the activated ester of tartaric acid to create a tissue adhesive hydrogels for primaquine[®] delivery and encapsulation of hepatocytes [27]. Several types of linkages with polymers with reactive functional groups can be used, depending on the rate of crosslinking and biodegradability needed. For example, a mixture of thiol-modified heparin and thiol-modified hyaluronic acid gels with PEG diacrylate forms a hydrogels that prolongs the release of bFGF in vivo [28].

N-isopropylacrylamide (NIPAM)-based hydrogels are extensively used as chemical gels [29, 30]. Thermosensitive NIPAM-based hydrogels were prepared using the biodegradable pseudo-peptide crosslinker DMTLT (a tri-molecular adduct of tyrosine, lysine, tyrosine) [31]. The volume phase transition temperature and the morphology of the gels were modulated by the amount of DMTLT. In aqueous media, these hydrogels exhibited a well-defined pulsate behavior in swelling and the release of benzoic acid and dextran as models of ionizable molecules and nonionizable macromolecules, respectively.

Summary

Biomimetic hydrophilic and amphiphilic hydrogels, based on combinations of biodegradable and/or resorbable biocompatible polymeric systems, provide excellent opportunities for controlled release and targeting of specific drugs and bioactive compounds. The problems with healing wounds of compromised patients are now well addressed, with good response, by the application of new polymeric hydrogels with bio-adhesive properties and controlled delivery mechanisms, thanks to the combination of effects associated to intermolecular interactions of polymers and polymer–drugs or polymer–bioactive compounds interactions. Smart polymers that are sensitive to the physiological conditions in a specific application (dermal, eyes, connective tissue) are of interest with the new and advanced hydrogels formulations being developed for clinical applications.

Hydrogels in bioactive scaffolds for “in situ” tissue regeneration are being developed by companies around the world with opportunities to advance the regeneration of tissues and organs. Applications in regenerative processes for soft tissues and cartilage or meniscus are good examples of the potential and relevant position of this kind of polymeric system in the advanced concepts of regenerative medicine.

References

1. Duncan R (2003) The dawning era of polymer therapeutics. *Nat Rev* 2:347–360
2. Jeong B, Bae Y, Lee D et al (1997) Biodegradable block copolymers as injectable drug-delivery systems. *Nature* 388:860–862
3. Jeong B, Bae Y, Kim S (1999) Thermoreversible gelation of PEG–PLGA–PEG triblock copolymer aqueous solutions. *Macromolecules* 32:7064–7069
4. Jeong B, Bae Y, Kim S (2000) Drug release from biodegradable injectable thermosensitive hydrogel of PEG–PLGA–PEG triblock copolymers. *J Control Release* 63:155–163
5. Lee D, Shim M, Kim S et al (2001) Novel thermoreversible gelation of biodegradable PLGA–PEO–PLGA triblock copolymers in aqueous solution. *Macromol Rapid Commun* 22:587–592
6. Zentner G, Rathi R, Shih C et al (2001) Biodegradable block copolymers for delivery of proteins and water-insoluble drugs. *J Control Release* 72:203–215
7. Jiang Z, Hao J, You Y et al (2008) Biodegradable and thermoreversible hydrogels of poly(ethylene glycol)-poly(ϵ -caprolactone-co-glycolide)-poly(ethylene glycol) aqueous solutions. *J Biomed Mater Res A* 87:45–51
8. Bromberg L, Ron E (1998) Temperature-responsive gels and thermogelling polymer matrices for protein and peptide delivery. *Adv Drug Deliv Rev* 31:197–221
9. Xiong X, Tam K, Gan L (2005) Synthesis and thermal responsive properties of P(LA-b-EO-b-PO-b-EO-b-LA) block copolymers with short hydrophobic PLA segments. *Polymer* 46:1841–1850
10. Xiong X, Tam K, Gan L (2006) Synthesis and thermal responsive properties of novel pluronic F87/PCL block copolymers with short PCL blocks. *J Appl Polym Sci* 100:4163–4172
11. Nagahama K, Fujiura K, Enami S et al (2008) Irreversible temperature-responsive formation of high-strength hydrogel from an enantiomeric mixture of starburst triblock copolymers consisting of 8-arm PEG and PLLA or PDLA. *J Polym Sci A Polym Chem* 46:6317–6332
12. Breedveld V, Nowak A, Sato J et al (2004) Rheology of block copolypeptide solutions: hydrogel with tunable properties. *Macromolecules* 37:3943–3953
13. Nowak A, Breedveld V, Pakstis L et al (2002) Rapidly recovering hydrogel scaffolds from self-assembling diblock copolypeptide amphiphiles. *Nature* 417:424–428
14. Bellomo EG, Wirsta MD, Pakstis L et al (2004) Stimuli-responsive polypeptide vesicles by conformation-specific assembly. *Nat Mater* 3:244–248
15. Sfika V, Tsitsilians C (2003) Association phenomena of poly(acrylic acid)-b-poly(2-vinylpyridine)-b-poly(acrylic acid) triblock polyampholyte in aqueous solutions: from transient network to compact micelles. *Macromolecules* 36:4983–4988

16. Li J, Loh X (2008) Cyclodextrin-based supramolecular architectures: syntheses, structures, and applications for drug and gene delivery. *Adv Drug Deliv Rev* 60:1000–1017
17. Crampton H, Simanek E (2007) Dendrimers as drug delivery vehicles: non-covalent interactions of bioactive compounds with dendrimers. *Polym Int* 56:489–496
18. Yang H, Lopina S, DiPersio L (2008) Stealth dendrimers for drug delivery: correlation between pegylation, citocompatibility and drug payload. *J Mater Sci Mater Med* 19:1991–1997
19. Kolhe P, Misra E, Kannan R et al (2003) Drug complexation, “in vitro” release and cellular entry of dendrimers and hyperbranched polymers. *Int J Pharm* 259:143–160
20. Mladenovska K, Raicki R, Janevik E et al (2007) Colon-specific delivery of 5-aminosalicylic acid from chitosan-Ca-alginate microparticles. *Int J Pharm* 342:124–136
21. Packhaeuser C, Kissel T (2007) On the design of “in situ forming” biodegradable parenteral depot systems based on insulin loaded dialkylaminoalkyl-amine-poly(vinyl alcohol)-g-poly(lactide-co-glycolide) nanoparticles. *J Control Release* 123:131–140
22. Peniche C, Argüelles-Monal W, Davidenko N et al (2003) Self-curing membranes of chitosan/PAA IPNs obtained by radical polymerization: preparation, characterization and interpolymer complexation. *Biomaterials* 20:1869–1875
23. Peniche C, Fernández M, Gallardo A et al (2003) Drug delivery systems based on porous chitosan/polyacrylic acid microspheres. *Macromol Biosci* 3:540–545
24. Liu J, Lin S, Li L et al (2005) Release of theophylline from polymer blend hydrogels. *Int J Pharm* 298:117–125
25. Gupta D, Tator C, Shoichet M (2006) Fast-gelling injectable blend of hyaluronan and methylcellulose for intrathecal, localized delivery to the injured spinal cord. *Biomaterials* 27:2370–2379
26. Drumheller P, Hubbell J (1995) Densely crosslinked polymer networks of PEG in trimethylolpropane triacrylate for cell adhesion-resistant surfaces. *J Biomed Mater Res* 29:201–215
27. Kakinoki S, Taguchi T, Saito H et al (2007) Injectable “in situ” forming drug delivery system for cancer chemotherapy using a novel tissue adhesive: characterization and “in vitro” evaluation. *Eur J Pharm Biopharm* 66:383–390
28. Cai S, Liu Y, Shu X et al (2005) Injectable glycosaminoglycan hydrogels for controlled release of human basic fibroblast growth factor. *Biomaterials* 26:6054–6067
29. Lugo-Medina E, Licea-Claverie A, Cornejo-Bravo J et al (2007) Effect of method of preparation on properties of temperature and pH-sensitive gels: chemical crosslinking versus irradiation with ϵ -beam. *React Funct Polym* 67:67–80
30. Schoenmakers R, Van de Wetering P, Elbert D et al (2004) The effect of the linker on the hydrolysis rate of drug-linked ester bonds. *J Control Release* 95:291–300
31. Pérez P, Gallardo A, Corrigan O et al (2008) Thermosensitivity of *N*-isopropylacrylamide hydrogels crosslinked with degradable crosslinker. *J Biomater Sci Polym Ed* 19:769–783

Thermo-Responsive Biodegradable Hydrogels from Stereocomplexed Poly(lactide)s

Tomoko Fujiwara, Tetsuji Yamaoka, and Yoshiharu Kimura

Abstract Hydrogels that form by responding to temperature changes are used for injectable biomaterials with many potential applications. Numerous techniques have been used to prepare biodegradable polymers for bioapplications. Specifically, biocompatible hydrogels that can be safely injected without surgery and sustained/disintegrated in a controlled manner are of interest. Poly(lactide), PLA, is the most studied and utilized biodegradable polymer, and its block copolymers provide a great variety of structures and properties. Utilizing stereocomplexation technology of enantiomeric PLAs on thermo-sensitive hydrogels of PLA-PEG block copolymers is an important aspect of bioapplications of hydrogels.

Introduction

Stimuli-sensitive hydrogels have the ability to respond to changes in the environment. Temperature is one of typical stimuli and can produce physically crosslinked gels. The physical gels are established by various interactions, such as van der Waals, hydrogen bonding, hydrophobic interaction, and molecular entanglement. Poly(*N*-isopropylacrylamide) (PNIPAM), which is the most widely known thermo-responsive physical gels, has a low critical solution temperature (LCST) around 32°C and forms a gels above the LCST as a result of dehydration of the hydrophobic isopropyl groups and hydrogen bonding to the carbonyl groups [1–4]. Triblock copolymers of poly(ethylene oxide) and poly(propylene oxide) (PEO-PPO-PEO), are nonionic surfactants known as Pluronic® and Poloxamer®, also exhibit sol-gel phase transition in water. The gelation mechanism [5–9] involves the formation and packing of micelles to induce sol-to-gels transition near LCST; the PEO corona blocks shrink to lead gel-to-sol transition at the higher temperature. In other cases, such as gelatin and agarose, helix formation is responsible for the gels formation in a cooled aqueous medium [10], while the hydration of poly(oxyethylene) grafted onto a substrate forms a gels [11].

Polymer gels, applied as biomedical materials, have achieved remarkable advances in medical science and biotechnology [12]. These applications include cell culture, tissue engineering, drug delivery system (DDS), and medical sensing. The biocompatibility, biodegradability, and safety of the gels are extremely important as well as the physicochemical properties for these applications. Hydrogels biodegradability, in particular, is essential for in vivo use; accordingly,

T. Fujiwara • Department of Chemistry, University of Memphis, Memphis, TN 38152, USA
e-mail: tfujiwara@memphis.edu

T. Yamaoka • Advanced Medical Engineering Center, National Cardiovascular Center Research Institute, Osaka 565–8565, Japan

Y. Kimura • Department of Biobased Materials Science, Kyoto Institute of Technology, Kyoto 606-8585, Japan

they are prepared from degradable polymers with good biocompatibility. Polylactides (PLA) are among the commonly used biodegradable polymers that are of special interest not only as eco-plastic materials [13] but also as biomedical materials as well [14]. Since lactic acid, the monomer for PLA, can be derived from renewable natural resources such as cornstarch, it is regarded as one of the sustainable materials.

There is a great need for the polymer systems that can respond to temperature changes and biodegrade safely in the body. Biodegradable hydrogels based on block copolymer systems consisting of PLAs and poly(ethylene glycol) (PEG), as well as thermo-responsive gels, that utilize stereocomplexation of enantiomeric PLAs are very important.

Micelles and Hydrogels with Various Block, Graft, and Armed PLA Copolymers

One of the approaches to these hydrogels is to synthesize copolymers that consist of block components; for example, PLA hydrophobic “hard” A-blocks and PEG hydrophilic “soft” B-blocks. Typical chemical structures of ABA, BAB, and AB block copolymers are shown in Fig. 1. Since both PLA and PEG are biocompatible and bioresorbable, the PLA–PEG block copolymers have many biomedical applications, such as temporary devices for clinical and pharmaceutical purposes.

The diblock copolymer, poly(DL-lactide)-*block*-poly(ethylene glycol) (PDLLA–PEG), was first used as a drug carrier in the early 1980s [15, 16]. The ABA triblock copolymer, PLA–PEG–PLA, was prepared in the late 1980s [17–24] and the properties were studied [25, 26], such as degradability [27–31] and drug release [32, 33]. In the ABA system, PEG acts as an intermolecular plasticizer for processing implant pastes, films, and scaffolds. This system has been used for biomedical application since early 1980s [23, 34–38]. Later, Vert et al. reported the utilization of hydrogels for protein release [39]. Microspheres prepared from the ABA block copolymers by emulsion technique [40–42] are used to encapsulate hydrophilic macromolecular drugs. Nanoparticles with much smaller diameters (10–1,000 nm) are used for the drug targeting [43] and as practical biodegradable materials [32, 44–46].

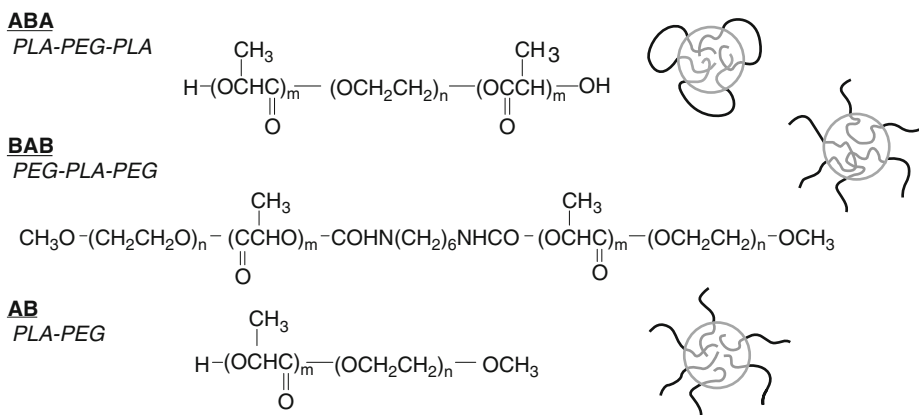


Fig. 1. Typical polymer structures and schematics of the micelles in aqueous medium.

Injectable microparticles for DDS were prepared from a BAB type triblock copolymer, PEG–PLLA–PEG [47, 48]. The aqueous micellar solution containing BAB copolymers exhibited a sol-to-gels phase transition with decreasing temperature from higher temperatures to the body temperature. The transition temperature is variable depending on the block lengths and polymer concentration. The mechanism of this hydrogels is a simple swelling and hydration of the PEG layers. Other BAB and ABA type thermo-sensitive hydrogels were made by incorporating poly(L-lactide-co-glycolide) (PLGA) as the A-block and PEG as the B-block; copolymer has a complicated phase diagram with both sol-to-gels and gels-to-sol transitions with increasing temperature, similar to PEO–PPO–PEO. From static (SLS) and dynamic light scattering (DLS) studies it appears that an increase in the aggregation number of the micelles causes the gelation [49, 50]. The in vitro drug release behavior of the PEG–PLGA–PEG hydrogels was evaluated by using both hydrophilic and hydrophobic model drugs [51, 52]. ABA or BAB block copolymer gels based on PLGA and PEG have also been studied [53–59]. AB diblock copolymers have been used for many years to prepare micelles to encapsulate drugs and DNA [41, 60–62]. These AB diblock copolymers form hydrogels by temperature change similar to PEG–PLLA–PEG or other simple BAB triblock copolymers [63].

The rheological properties of hydrogels are strongly influenced by polymer structures, i.e., the block length and type [64] and the crystallinity [65]. The latter was systematically studied by mixing ABA type and AB type copolymers and mixing crystalline PLLA–PEG and amorphous PDLLA–PEG copolymer systems. The effect of the synthesis method on rheological properties is important [66] as well as polymer structural effects [67].

There are several techniques for photo-crosslinking hydrogels of PLA–PEG block copolymer systems. For example, methacrylate capped triblock copolymer MA–PLLA–PEG–PLLA–MA and its' degradation properties were studied [68, 69] and the degradability of this high modulus gels can be controlled by tailoring the composition. Tissue-adhesive hydrogels were prepared using crosslinkable polymeric micelles of aldehyde-terminated PEG-*block*-PLA with a Schiff base polymer [70]. When the polymeric micelle solution and a polyallylamine solution are mixed, hydrogels are formed either in vivo or in vitro almost instantaneously.

Stereocomplexation of Enantiomeric PLAs, and the Hydrogels Applications

PLAs consisting of enantiomeric L- and D-lactic acids are generally differentiated as PLLA and PDLA, respectively. PLLA is now produced by ring-opening polymerization of L-lactide that is made from L-lactic acid manufactured by large-scale fermentation. A polymer blend of PLLA and PDLA forms a stereocomplex with a melting temperature (T_m) of 230°C which is approximately 50°C higher than that of single crystal of PLLA or PDLA, due to the differences in crystal formation (Fig. 2) [71–76]. Therefore, the improved properties are expected with the stereocomplex of PLLA and PDLA. Based on these backgrounds many attempts have been made to obtain polymer gels from PLA derivatives.

The use of stereocomplexation of PLLA and PDLA was first applied to form hydrogels in 2000 to form a system based on polymer of hydroxyethylmethacrylate P(HEMA) with grafts of lactide (LA) oligomers [78]. In 2001, a dextran-graft-oligo(LA) system was prepared [79–81]. Both systems involve P(HEMA) stereocomplexation of the lactide oligomers in the hydrogels. The hydrogels made with grafted oligo(LLA) and oligo(DLA) degraded more slowly than the gels made from the single p(HEMA)-graft-oligo(LA). The gelation mechanism of the stereocomplex interaction of oligo-LAs act as crosslinkers between main polymers as illustrated in Fig. 3.

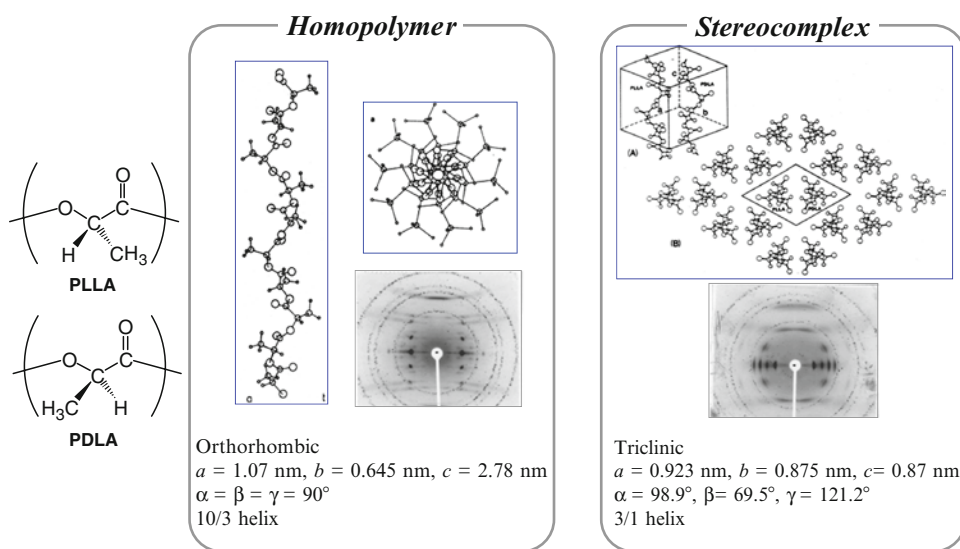


Fig. 2. Stereochemistry of PLLA and PDLA, and crystal forms of the homopolymer and stereocomplex. Reproduced from [77] with permission from ACS.

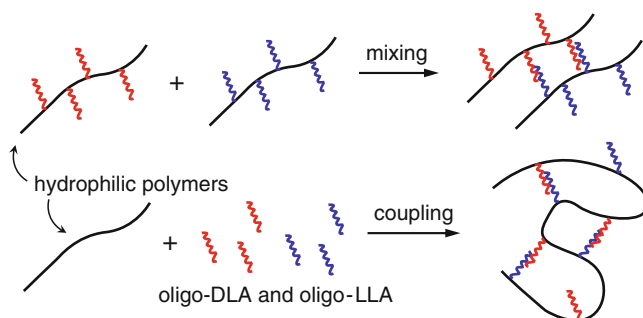


Fig. 3. Typical mechanisms of hydrogels formation using enantiomeric LA oligomers.

Fujiwara and Kimura, on the other hand, first reported the temperature-dependent, injectable hydrogels by stereocomplex formation of the enantiomeric micelle mixture of PLA-PEG-PLA triblock copolymers in 2001 [82]. Wide Angle X-ray Scattering (WAXS) and rheological analyses was used to monitor the increase of stereocomplex crystals and gelation process. The mechanism of this system was new and unique (vide infra) along with studies on BAB and AB block copolymers [83]. Similar hydrogels formations from enantiomeric PLA-PEG di- and triblock copolymers were studied using Raman spectroscopy in addition to WAXS and rheology measurements to confirm the stereocomplex crystals [84].

Another in-situ hydrogels system by stereocomplexation was developed from PEG-(PLLA)(8) and PEG-(PDLA)(8) star block copolymers [85]. Relatively short chain PLA

(9–17 lactate units per PLA block) was prepared by ring-opening polymerization of L- or D-lactide onto 8-arms PEG (Mw 22,000 and 44,000) as an initiator. Hydrogels were formed by mixing of solutions of L-star and D-star copolymers. With increasing PLA block length, water solubility and critical gels concentration (CGC) decreased. The protein delivery using these injectable hydrogels was evaluated in vitro and in vivo [86]. The relatively small protein lysozyme followed first order kinetics, wherein a high cumulative release of approximately 90% was obtained in 10 days. The larger protein IgG was released in vitro with nearly zero order kinetics for 16 days. The release of the therapeutic protein rhIL-2 followed almost zero order kinetics for 7 days, wherein up to 45% was released. To prepare robust hydrogels of stereocomplexed PLA copolymers, co-crosslinking systems by photo reactive groups are used by adding methacrylate groups on to star-block PLA-PEG chain ends [87]. Stereocomplexation from the enantiomeric PLA still occurred. After UV-polymerization, the hydrogels showed significantly higher storage modulus and prolonged degradation times. Biodegradability of these stereocomplexed-photopolymerized hydrogels varied depends on the design and procedures.

A thermo-sensitive and biodegradable stereocomplexed hydrogels composed of multiblock Pluronic copolymers were developed by linking oligo-LLA and oligo-DLA [88]. A scheme of the gelation mechanism is shown in Fig. 4. The stereocomplexed multiblock hydrogels showed enhanced gels stability and mechanical strength, linear mass erosion profiles, and near zero-order hGH release patterns.

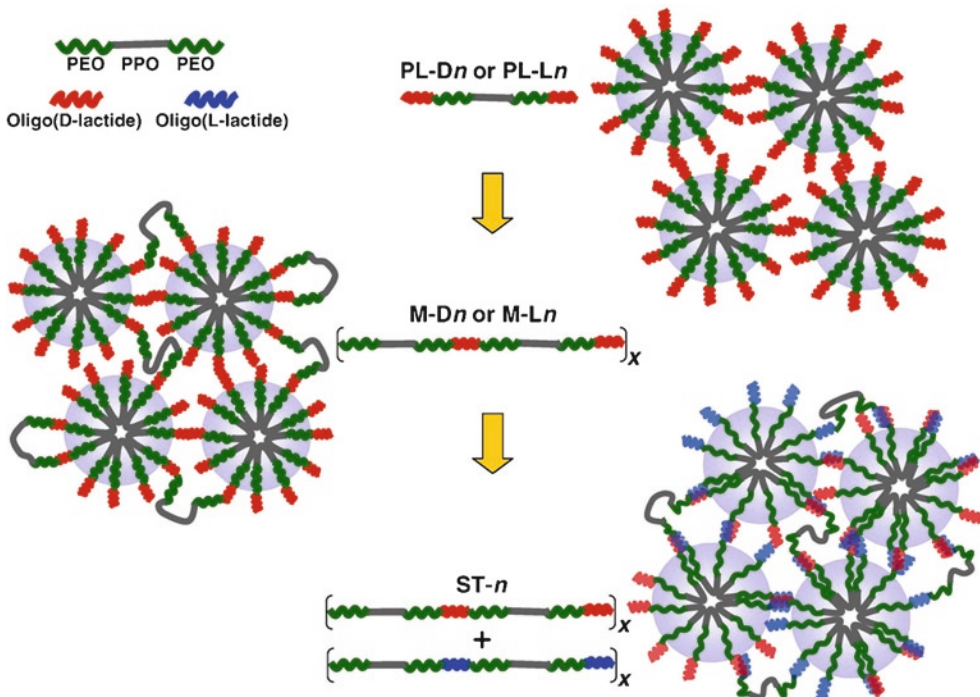


Fig. 4. Schematic illustration for molecular structure of hydrogels formed by PN-multi-oligo(LLA) and PN-multi-oligo(DLA) developed by Park et al. With permission from [88]. Copyright Elsevier.

Hydrogels Study on Enantiomeric PLA–PEG Linear Block Copolymers

Hereafter, the systematic studies on ABA, BAB, and AB type enantiomeric PLA–PEG block copolymers by the authors are described.

Motivation for the Study of Stereocomplexed Micellar Hydrogels

In late 1990s, the authors discovered interesting band morphology formed from the micellar nanoparticles of PLLA–PEG diblock and PLLA–PEG–PLLA triblock copolymers that were placed on a flat substrate surface [89–91]. The nanoparticles on the mica surface were self-organized into different structures by mild thermal treatment. It has been verified that the band morphology is directed by crystallization of the PLLA segments and that the PLLA chains take a doubly twisted structure in it with the ordinary 10/3 helical conformation preserved. Prior to this PLLA band formation, PEG blocks phase-separate and plays an important role. The two-dimensional network formed by the PLLA–PEG–PLLA bands on the surface well simulates the structure of the three-dimensional network systems observed in melt, concentrated solution, and hydrogels. These studies directed us to thermo-responsive hydrogels formation from PLA–PEG block copolymers.

The atomic force microscopic (AFM) images of the bicontinuous network structure (for high concentration sample) and nanofibers (for low concentration sample) formed from a mixture of PLLA–PEG (5,000–5,000) and PDLA–PEG (5,000–5,000) micellar solutions are shown in Fig. 5. Aqueous solutions (0.2 and 0.01 wt%) of both enantiomeric micelles were mixed at room temperature, cast on the mica surface, and then heated at 60°C for 1 h. For the high concentration samples of the enantiomeric mixture, gel-type network formation was clearly seen, which was totally different from the structure of a single polymer system of PLLA–PEG high concentration micelles [90]. As previously observed from single PLLA–PEG of low concentration samples, the mixed system also formed similar crystal nanofibers (Fig. 5). An interesting phenomenon observed only in this enantiomeric mixture is that the nanofibers are aligned in pairs. Analysis by TEM diffraction indicated that the two bands in pair consist of the single PLLA and PDLA crystals. These facts suggest that the PEG blocks connected with PLLA and PDLA interact so strongly prior to the band formation and guide the separate crystallization of the PLLA and PDLA blocks with opposite helical sense. Under different conditions, the enantiomeric micelle mixture was found to reorganize in different ways by thermal treatment, which inspired us to the temperature responsive network formation by PLA stereocomplexation.

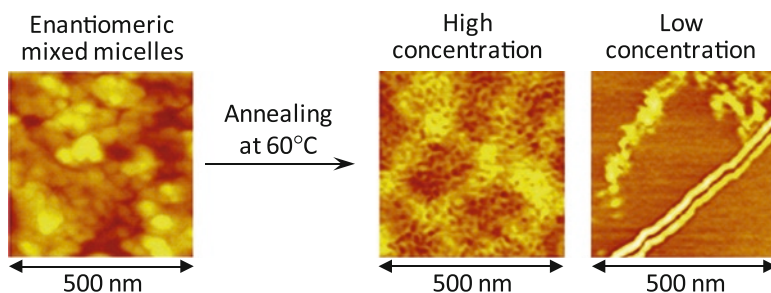


Fig. 5. AFM height images of thermal reorganization of micelles casted from the enantiomeric mixture of PLLA–PEG (5,000–5,000) and PDLA–PEG (5,000–5,000) micellar solutions.

Table 1. Typical block copolymers and the molecular weight

Type	Copolymers	PLA block (Mn)	PEG block (Mn)	Total (Mn)	PLA/PEG (wt/wt)
ABA	PLLA-PEG-PLLA	1,300	4,600	7,200	0.56
	PDLA-PEG-PDLA	1,100	4,600	6,800	0.48
BAB	PEG-PLLA-PEG	2,000	2,000	6,000	0.50
	PEG-PDLA-PEG	2,000	2,000	6,000	0.50
AB	PLLA-PEG	1,100	2,000	3,100	0.55
	PDLA-PEG	900	2,000	2,900	0.45

Copolymer Synthesis and Gels Formation

A number of PLA-PEG block copolymers with various molecular weights (Mn) and block ratios have been synthesized. Summarized in Table 1 are copolymers of ABA, BAB, and AB types that induce thermo-sensitive gelation when L- and D-copolymers are mixed. Interestingly, the PLA/PEG ratio of all the different types is near 0.5. The ordinary ring-opening polymerization of L- or D-lactide, initiated with PEG and MePEG, generated the ABA and AB block copolymers, respectively, in high yields [82, 83]. The BAB triblock copolymers were obtained by the coupling the AB diblock copolymers with hexamethylene diisocyanate (HMDI) (Fig. 1) [47]. These copolymers readily formed the core-shell type amphiphilic micelles in water as illustrated in Fig. 1. The average hydrodynamic diameters of the micelles measured by DLS were in the range of 20–30 nm for 1 wt% solutions of all these copolymers. To obtain sol-to-gels or gels-to-sol transition, micellar solutions were prepared at various concentrations, and both solutions of L- and D-copolymers were mixed together at low temperature (typically at 4°C). Then the temperature was increased up to 75°C to observe the sol-gel behavior. All solutions were prepared in water.

The molecular weights of ABA, BAB, and AB copolymers listed in Table 1 showed the best performance as a thermo-sensitive hydrogels. A variety of length and composition of copolymers for each block type was prepared and it was found that the PLA/PEG composition ratio and the thickness of appearance of PEG shell layer (since the PEG of ABA micelle makes a loop) were similar for the three types of micelles rather than the molecular weights of PLA blocks [83].

Hydrogels from Micellar Solutions of ABA Triblock Copolymers

Spontaneous gels formation occurs when a micellar solution of the enantiomeric ABA triblock copolymers, PLLA-PEG-PLLA and PDLA-PEG-PDLA, are mixed. This system is characterized by an interesting temperature-dependent sol-to-gels transition that is induced around 37°C by the stereocomplexation of the PLLA and PDLA block segments [82]. As seen in Fig. 6, only enantiomeric mixture of micellar solutions formed hydrogels. The gels formation was successfully monitored by the rheological change of a micellar solution, and the stereocomplex formation was confirmed by wide-angle X-ray scattering (WAXS).

The sol-gel transition diagram of the mixed micellar solutions of PLLA-PEG-PLLA and PDLA-PEG-PDLA with respect to temperature and polymer concentration is shown in Fig. 7.

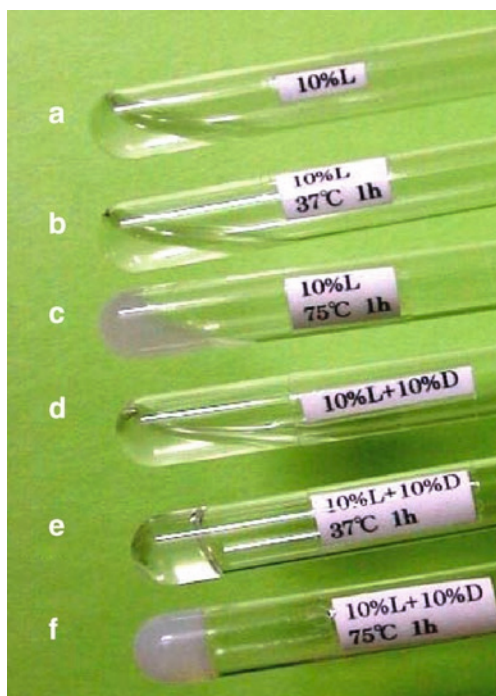


Fig. 6. The appearances of 10 wt% of ABA micellar solutions; PLLA–PEG–PLLA at room temperature (a), 37°C (b), 75°C (c), and enantiomeric mixture of L- and D-triblock copolymers at room temperature (d), 37°C (e), 75°C (f). Reproduced from [82]. Copyright 2001 Wiley-VCH.

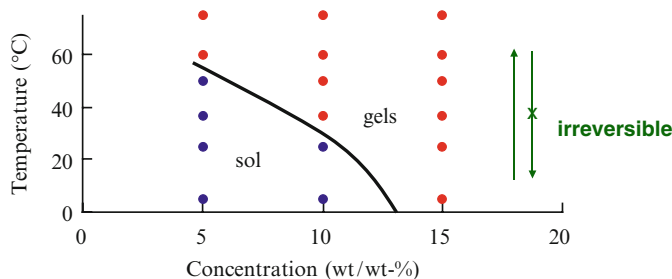


Fig. 7. The phase diagram of mixed micellar solutions of PLLA–PEG–PLLA and PDLA–PEG–PDLA.

The single PLLA–PEG–PLLA micellar solution had only the solution state at all temperatures and concentrations plotted in Fig. 7 and all later phase diagrams. With the 10 wt% enantiomeric mixture, the sol-to-gels transition was between room temperature (25°C) and the body temperature (37°C) as shown in Fig. 6d, e. While the single micellar solution of PLLA–PEG–PLLA (control) turned white fluid after heating to 75°C (c) by the crystallization of homocrystals, the mixture became a white gels at 75°C (f).

The responsibility for the stereocomplex formation of the enantiomeric polylactide blocks on the gelation was confirmed by synchrotron Wide Angle X-ray Scattering (WAXS) measurements.

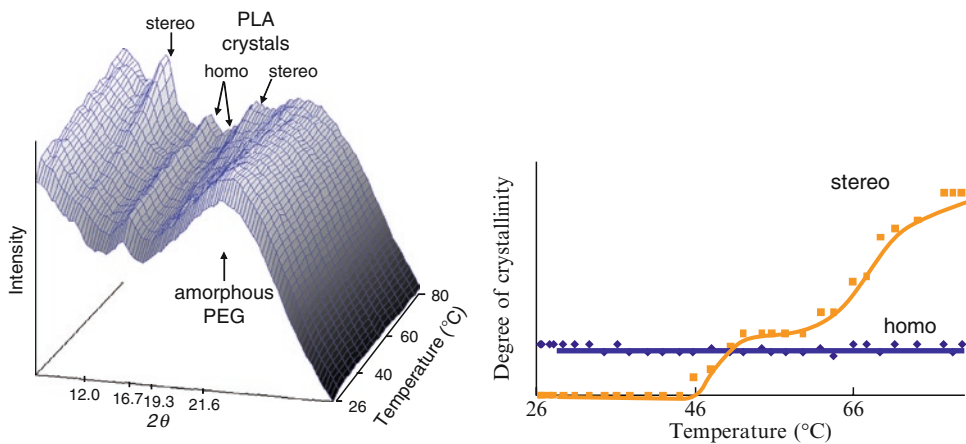


Fig. 8. The temperature-dependent WAXS measurement of the 10% enantiomeric mixture at a heating rate $2^{\circ}\text{C}/\text{min}$. Two-dimensional WAXS data were collected every 30 s with a synchrotron X-ray at the BL-15A beamline (PF, Tsukuba, Japan).

The temperature-dependent WAXS profiles for the mixed solution are shown in Fig. 8. The measurement was started immediately after the 10 wt% micellar solutions of PLLA-PEG-PLLA and PDLA-PEG-PDLA were mixed at room temperature, and the data was collected every half minute by in situ heating at a rate of $2^{\circ}\text{C}/\text{min}$. Small diffraction peaks are confirmed at $2\theta = 16.8^{\circ}$ and 19.4° in the starting mixture, which means that the small amount of hexagonal crystals of PLLA and PDLA exists in the core of the micelles at room temperature. These diffractions are attributed to the (200) or (110) plane and the (203) or (113) plane of the hexagonal crystal lattice comprising the PLLA or PDLA 10/3-helices [92]. With increasing temperature, the WAXS data exhibits two different reflections, at $2\theta = 12.1$ and 21.7° , in addition to the small reflections of the hexagonal crystals. These new peaks can be reasonably ascribed to the crystals of the stereocomplex of PLLA and PDLA [82, 83]. Around 37°C , these reflections are still weak, indicating that both the PLLA and PDLA chains may be mixed into a complexation state prior to the crystallization. At 75°C , the significant crystal growth of the stereocomplex is clearly seen.

In the single PLLA-PEG-PLLA micellar solution (control experiment), the hexagonal crystal growth was also observed with increasing temperature despite its continuous sol nature. The total degree of crystallinity estimated from the WAXS was almost identical with that observed in the mixed solution at each temperature. Since the single and mixed solutions have same degree of crystallinity but have different major crystal forms which are hexagonal and stereocomplex, respectively, it is suggested that the gels formation in the mixed solution is closely related with the stereocomplexation of the enantiomeric PLA blocks.

In the micellar solutions of the enantiomeric ABA triblock copolymers, the hydrophobic PLLA or PDLA segments aggregate to form a core region, around which, the hydrophilic PEG segments settle to form a shell when the micelles are prepared separately. Consequently, the PLLA and PDLA segments can be isolated from each other when the micellar solutions of the enantiomeric block copolymers are mixed. Illustrated in Fig. 9 is a schematic of an ABA system gelation. When heated, the aggregation of the PLLA and PDLA segments in the core/shell interface is weakened to allow the segments to mix outside of the core. The shorter block length of PLLA and

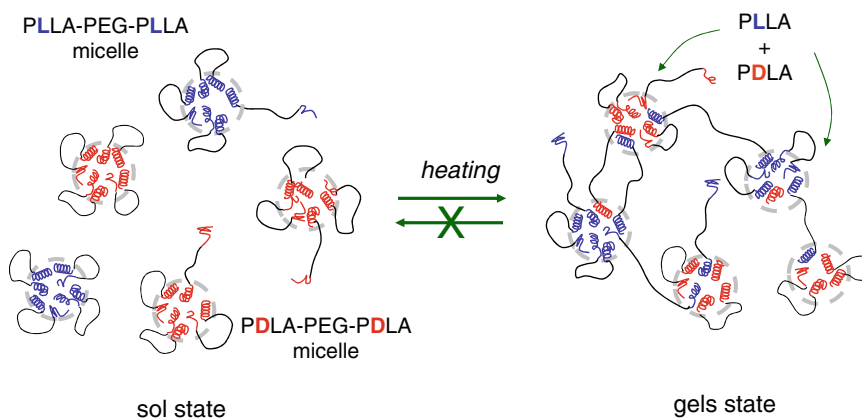


Fig. 9. Proposed gelation mechanism of enantiomeric mixture of ABA triblock copolymers.

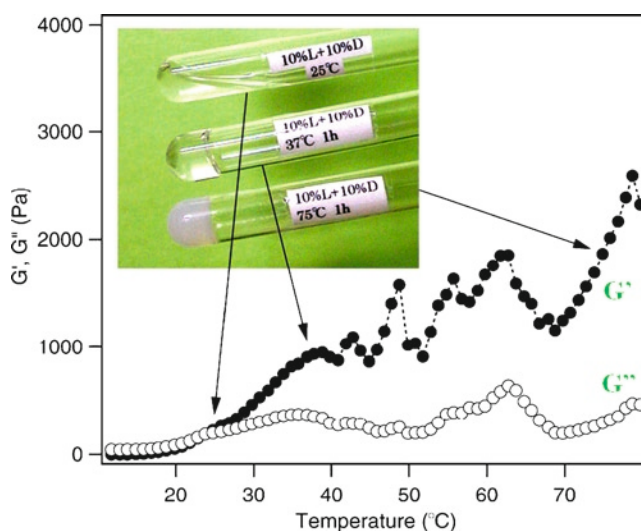


Fig. 10. Rheological changes of the mixed dispersion of ABA copolymers in regard to temperature increase; slit-shear mode with frequency 128 Hz.

PDLA is favorable for this chain scrambling and mixing. Consequently, the stereocomplexation starts as indicated by the WAXS data (Fig. 8), and the micelles are wholly crosslinked with each other at 37°C to form a gels. With increasing temperature, the crosslinking state is changed by reorganization of the hydrophobic cores and increased crystallization of the stereocomplex.

This process was also supported by fluctuations in the storage modulus (G') in the rheology measurement [83]. Plotted in Fig. 10 are the temperature-dependent rheological changes with the gelation of the mixed dispersion of ABA-type block copolymers. A dramatic increase in storage modulus (G') was observed from 20 to 37°C. The crossing of the G' and loss modulus (G'') curves is detectable around 23°C. This change corresponds to the crosslinking reaction that leads to gels formation. Above 37°C, G' fluctuates around 10^3 Pa, which

is an ordinary G' level for physically crosslinked gels. It starts to elevate again above 70°C , corresponding to the turbidity of the gels. Since this turbid gels regains its transparency to some degree when cooled, this turbidity change is mainly attributed to the clouding phenomenon resulting from the desolubilization of nonionic surfactants (such as PEG). This data supports the gels formation of the mixed dispersion at around 37°C . Because the stereocomplex formation depresses the mobility of the PLA chains and stabilizes the PEG crosslinkers, gels formation is only possible for the enantiomeric mixture. This sol–gel transition is irreversible though the crosslinking is performed by an ordinary physical mechanism.

Hydrogels from BAB Triblock Copolymers

The second gels system consists of the enantiomeric BAB type triblock copolymers, PEG–PLLA–PEG and PEG–PDLA–PEG. The sol–gel transition of this system should be induced by the stereo interaction of L- and D-copolymers, being much different from that of the single BAB (PEG–PLLA–PEG) system that has previously been described to undergo gelation by the ordinary hydrophobic/hydrophilic interaction [47].

The aqueous micellar solution of single enantiomer, PEG–PLLA–PEG (2,000–2,000–2,000) or PEG–PDLA–PEG (2,000–2,000–2,000), remains a “sol” phase at all temperatures in the concentration range of 10–40 wt%. Shown in Fig. 11 is a sol–gel transition diagram plotted for 1:1 (v/v) mixed micellar solutions of PEG–PLLA–PEG and PEG–PDLA–PEG with respect to temperature and polymer concentration. It is found that the gels state cannot be formed at concentrations lower than 30 wt% and that the gels state is preferentially kept below 75°C at concentrations higher than 40 wt%. The gels-to-sol transition temperature increases up to 75°C at higher concentrations. It should be noted here that in the present BAB system the gels and sol are formed, respectively, at low and high temperatures in a reversible manner. This is opposite to the above ABA system where gelation is induced with increasing temperature in an irreversible manner.

Shown in Fig. 12a are the typical changes in the mixed solution at 35 wt% concentration before and after the heat treatment from 37°C (c) to 75°C (d). This gels is formed immediately after the L- and D-solutions are mixed at room temperature. It is observed that the mixed solution is in gels and sol states at 37 and 75°C , respectively, while the single solution remained fluid irrespective of the temperature (a, b). Since gels-to-sol transformation of the mixed solutions is reversible with the temperature change, sample (d) returns to gels after cooling to room temperature.

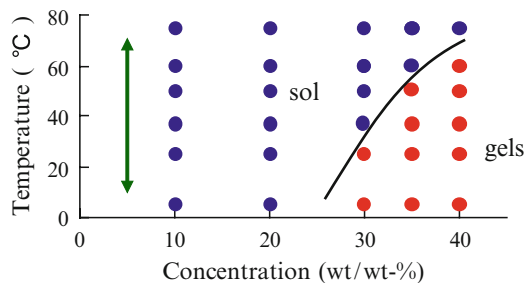


Fig. 11. The phase diagram of mixed micellar solutions of PEG–PLLA–PEG and PEG–PDLA–PEG. Reproduced from [83]. Copyright 2004 Wiley-VCH.

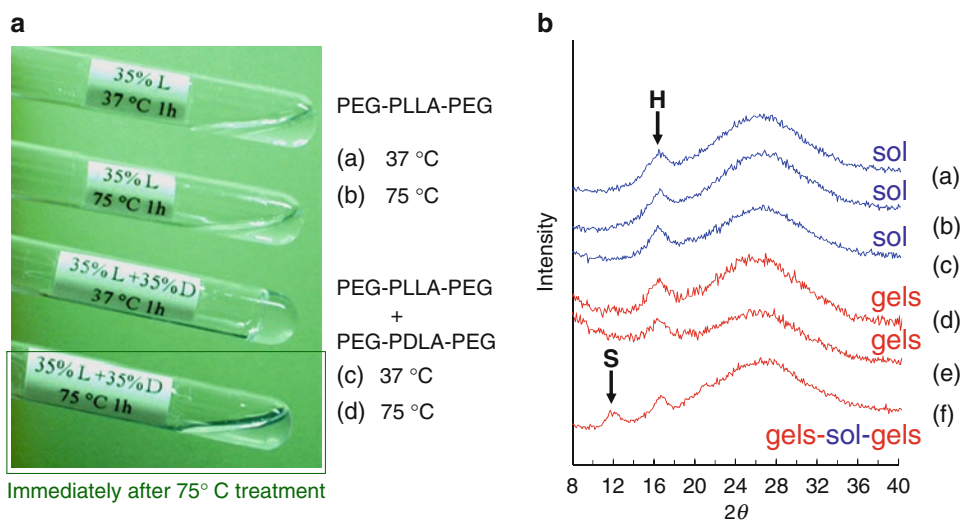


Fig. 12. The appearance of 35 wt% of BAB micellar solutions (a); PEG-PLLA-PEG at 37°C (a), 75°C (b), and enantio-mixture at 37°C (c), 75°C (d). The WAXS profiles of BAB micellar solutions (b); PEG-PLLA-PEG at room temperature (a), after 37°C (b), after 75°C (c), and enantio-mixture at room temperature (d), after 37°C (e), and after 75°C (f). Reproduced from [83]. Copyright 2004 Wiley-VCH.

The WAXS profiles of the single and mixed solutions at different temperatures are shown in Fig. 12b. The mixed solution gave very small reflections at $2\theta = 12.1$ and 21.7° in addition to the reflections of the hexagonal crystals ($2\theta = 16.8^\circ$) of PLLA or PDLA only when heated at 75°C. This indicates that the stereocomplexation of the PLLA and PDLA blocks is induced even in the mixed solution heated at high temperatures where the sol state is achieved. When this BAB sol is cooled, the gelation is restored without significant change in the WAXS profile. Furthermore, the degree of crystallinity which was estimated by peak separation of each crystal and amorphous peaks does not increase by the heat treatment, being obviously different from the ABA gels system. It is, therefore, concluded that the stereocomplexation is not directly related with the gels formation mechanism for the BAB system.

Hydrogels from AB Diblock Copolymers

Mixed micellar solutions of enantiomeric ABA and BAB block copolymers exhibit very different gelation behavior and crystal structure. As a third system, the micellar solutions of AB block copolymers, PLLA-PEG and PDLA-PEG, were examined for the hydrogels formation. The AB system is similar to ABA in that the A-blocks associate in the core of the micelles as illustrated in Fig. 10, while being similar to BAB because the mobility of the corona B-blocks is comparable to each other.

A typical sol-gel phase diagram, plotted for the mixed solutions of the enantiomeric AB diblock copolymers, is illustrated in Fig. 13. It resembles the BAB system diagram shown in Fig. 11, where the gels-to-sol transition occurs with increasing temperature. The typical phase changes of a mixed solution of the PLLA-PEG and PDLA-PEG (total 30 wt%) are shown in Fig. 14a at 37°C (c) and 75°C (d) as compared with those of the corresponding single

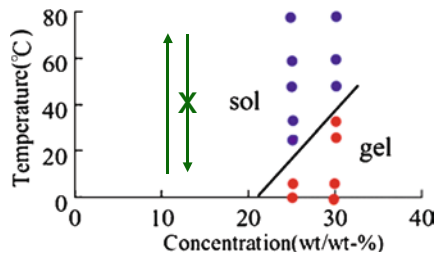


Fig. 13. The phase diagram of mixed micelle solution of PLLA-PEG and PDLA-PEG.

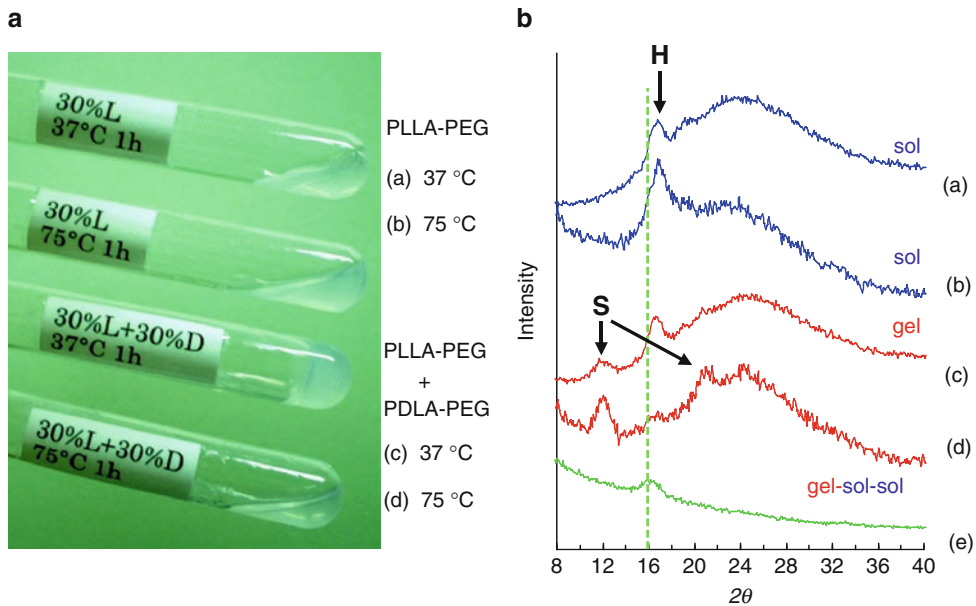


Fig. 14. The appearance of 30 wt% of AB micellar solutions (a); PLLA-PEG at 37°C (a), 75°C (b), and enantio-mixture at 37°C (c), 75°C (d). The WAXS profiles of AB micellar solutions (b); PLLA-PEG after 37°C (a), after 75°C (b), and enantio-mixture after 37°C (c), and after 75°C (d), PET film (e). Reproduced from [83]. Copyright 2004 Wiley-VCH.

micellar solution of PLLA-PEG (30 wt%) (a, b). Although the latter solution does not form a gels at any temperature, the mixed solution forms a gels on mixing at room temperature. The difference from the BAB system is that the sol formed at 75°C never returns to a gels again when cooled. This irreversible nature suggests that the interaction of the micelles formed in the hydrogels at lower temperature may be changed after turning to sol state by heating. Note that the normally synthesized AB diblock copolymer should involve a small amount of ABA triblock copolymer because MePEG is contaminated with dihydroxyterminated PEG [93, 94]. This impurity can be eliminated by high osmotic pressure chromatography; the same hydrogels formation for the pure enantiomeric AB system is also confirmed.

The WAXS profiles of the AB systems are shown in Fig. 14b, which are significantly different from those of the BAB system. The single micellar solution of PLLA-PEG shows

an increase in the crystallinity (a, b) with increasing temperature, while that of PEG–PLLA–PEG does not have this behavior. In the mixed AB solution, the gels state formed at the lower temperature involves the hexagonal crystals, as shown by the reflection at $2\theta=16.8^\circ$ (c); the sol state attained by heating at 75°C produces the stereocomplex crystals ($2\theta=12.1$ and 21.7°) with most of the hexagonal crystals being lost (d). This feature is similar to that of the ABA system rather than the BAB system.

Gelation mechanism of the mixtures of enantiomeric BAB and AB block polymers may be much different from that of ABA system since the PEG blocks cannot act as direct cross-linkers between the micelles. The sol–gel transition diagrams and WAXS data suggest that the stereocomplexation between the PLLA and PDLA blocks is not directly correlated with the gelation of the mixed solution. Since, in the BAB triblock copolymers the hydrophobic PLLA and PDLA are confined in the core of the micelles and surrounded by the hydrophilic PEG shell, a sort of macromolecular reorganization is needed to grow the PLLA stereocomplexes and PDLA blocks in the micelles. Even when heated at high temperatures, the block chains are not easily exchanged among the micelles in the BAB system since PLLA and PDLA blocks are in the middle of copolymers (Fig. 15a), so that the degree of stereocomplexation is limited. Even if the stereocomplex crystals could be formed, they are confined to the micelle core and cannot achieve an interaction between the particles strong enough as to induce gelation.

The WAXS data (Fig. 12b) revealed that both PLLA and PDLA blocks of the AB block copolymers form the hexagonal crystals in the micellar cores at room temperature. The IR spectra of the micellar solutions both in gels and sol states also have absorption bands at 921 and $1,210\text{ cm}^{-1}$, supporting the presence of the $10/3$ helical structure of the

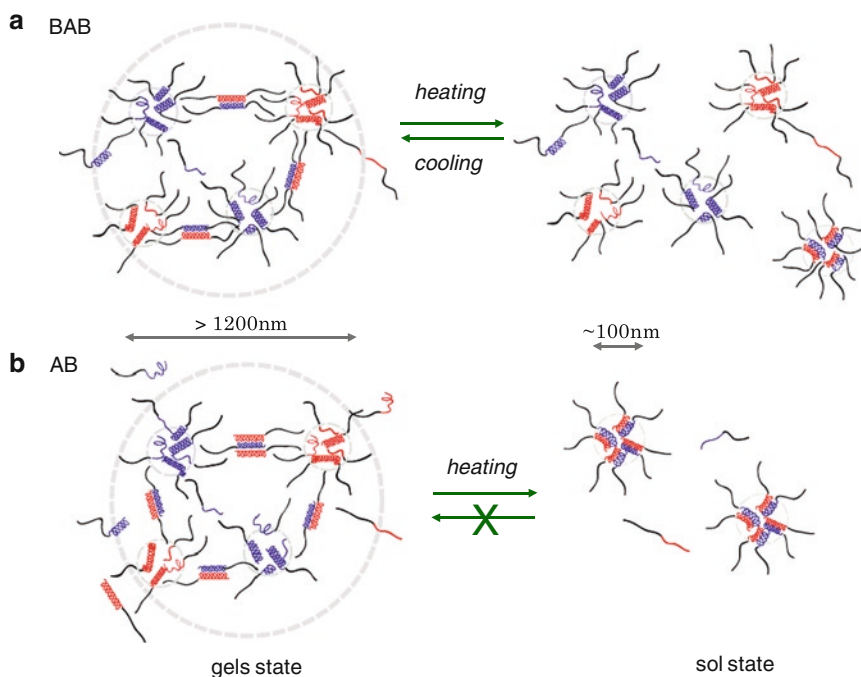


Fig. 15. Proposed gelation mechanisms of enantiomeric mixture of BAB triblock (a) and AB diblock (b) copolymers.

PLLA and PDLA blocks [95]. One possible explanation of this gel-to-sol behavior is that PEG blocks between micelles act as crosslinkers at low temperature even though they are free to move. This helix formation of PLLA and PDLA blocks is possibly transmitted to the PEG chains through the block-linking bonds, because the PEG chain can readily take on a similar helical conformation. In fact, ordinary monoclinic crystals of PEG are known to consist of 7/2-helical chains.

Since the helical senses of PLLA and PDLA are opposite to each other, the induced helices of the PEG chains should be right- and left-handed depending on the connecting PLA chains. Maybe, the helical chains of PEG, with opposite senses, aggregate through the chain interdigitation mechanism and change the hydrophilic/hydrophobic balance that leads to the interchain cohesion of the PEG blocks even in an aqueous environment. With the helical conformation, the hydrophilic ether linkages are surrounded by the hydrophobic alkylene chains to make the whole chain hydrophobic. With a single BAB copolymer, the helices have an identical sense, and the chain interdigitation to cause gelation is impossible. The interaction of the PEG chains in opposite helical senses was supported by the gelation behavior of the mixed micellar solution of the enantiomeric AB diblock copolymers (Fig. 15b). In this case, the exchange of the core PLA blocks between micelles is much faster than that of the BAB system; in fact, the stereocomplex crystals grow with increasing temperatures of the mixture. At 75°C, most of the PLA crystals were replaced by the stereocomplex crystals. Therefore, most of the micelles comprise both PLLA and PDLA blocks in their core due to the exchange of PLA blocks at high temperature and intermicelle interaction through the PEG is weakened even after cooling. The PEG interaction changed to intramicellar instead of intermicellar. This is why in the AB system the gels is irreversible.

Another effect on these BAB and AB-type hydrogels formation is that micelles are aggregating into microgel size as depicted in Fig. 15; a negligible amount of stereocomplex crystals of PLLA and PDLA blocks is still responsible for the gels formation. Dynamic light scattering revealed a bimodal size distribution of the AB-type gels of 120 and 1,200 nm (Fig. 16). Upon heating, the microparticles at 1,200 nm disappear. The difference in reversibility for the BAB and AB gels is due to the rate of micelle reformation. If the core of all micelles becomes stereocomplexed PLA as seen in WAXS data of AB micelles (Fig. 14b(d)), no more intermicelle interaction occurs.

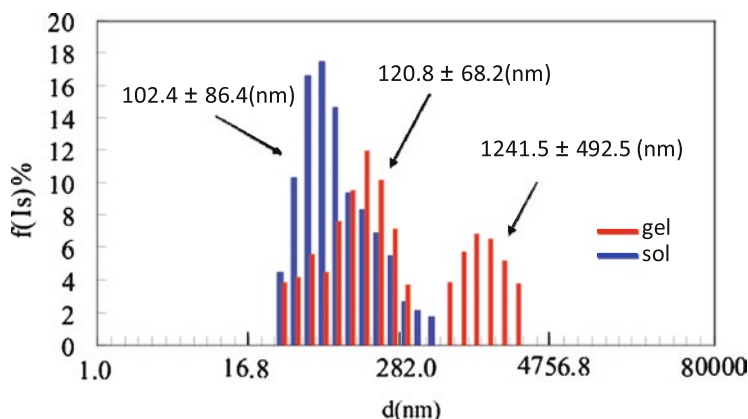


Fig. 16. Particle sizes of the micelles (30 wt%) in the mixed gels and sol (after heating) states of a mixture of PLLA-PEG (1,100–2,000) and PDLA-PEG (900–2,000) determined by DLS.

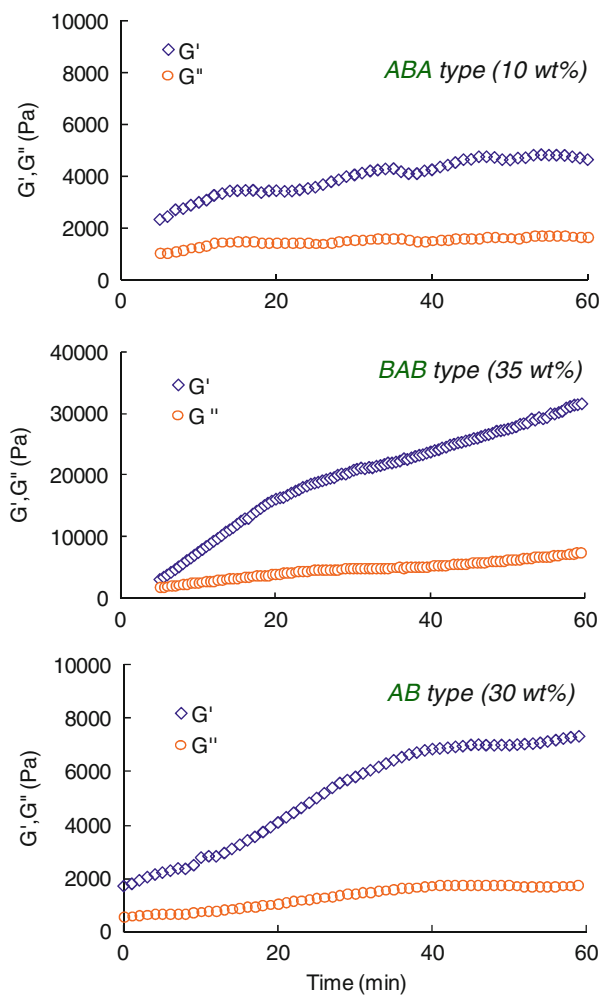


Fig. 17. Rheological change of the hydrogels of enantiomeric micelle mixtures at 37°C, 128 Hz.

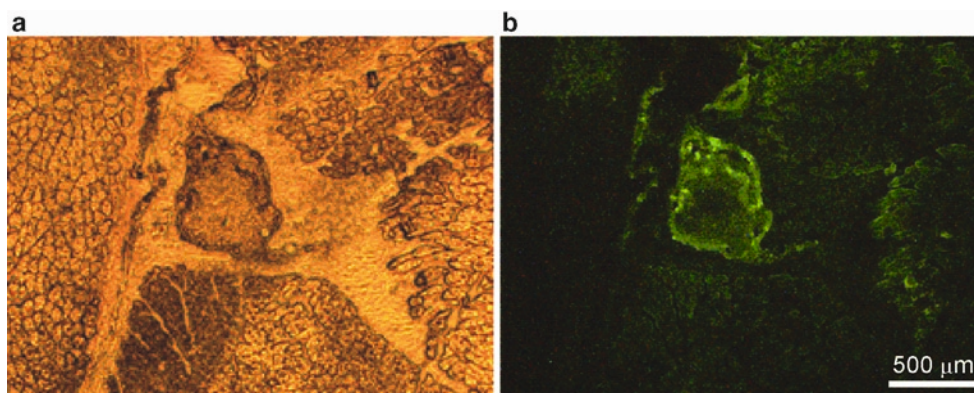


Fig. 18. The sectioned tissue from the femoral region of mouse; (a) optical and (b) fluorescent microscopes.

Hydrogels Properties and Applications

The time-dependent rheological changes in the mixed micellar solutions of ABA, BAB, and AB copolymers at 37°C are shown in Fig. 17. The mechanical properties of the BAB system are dramatically greater than those of the ABA system [82, 83]. For the BAB system, the storage modulus (G') gradually rises to 31 kPa after 60 min with gelation. The physical crosslinking through the PEG interaction provides the mechanical properties of the gels. The G' value of AB-type hydrogels from PLLA-PEG (1,100–2,000) and PDLA-PEG (900–2,000) reaches 7 kPa, which is lower than the BAB triblock system.

The mechanical properties of ABA thermo-responsive gels, copolymers with different molecular weight and different block ratios examined for improvements [84]. It is still a challenge to find better systems with sol-to-gels transitions between room temperature and body temperature as well as with superior mechanical properties, that do not cause other crosslinking mechanisms to occur, such as photoreactions with other low LCST polymers.

The biodegradable thermo-sensitive hydrogels formed by the enantiomeric PLA-PEG block copolymers can potentially be used as an injectable biomedical matrix. The injection of ABA mixed micellar solutions results successful gels formation in the body of mice, and the hydrogels is absorbed within 3 days after implantation. A suspension of mouse embryonic fibroblast (MEF) cells, with 9% PLLA-PEG-PLLA and 9% PDLA-PEG-PDLA micelles, was injected into the femoral region of an inbred mouse. After 3 days, the femoral regions were removed and examined; the microscopic images of a section of the femoral region are shown in Fig. 18. The tissues contain some domains that are different from the muscular tissue seen in the optical image. The observed fluorescent cells indicate that the injected cells survived among the muscular cells. In contrast, no living cells were observed when the cells were injected as a PBS solution without enantiomeric micelles.

Summary

The combination of “thermo-responsive” and “biodegradable” properties is the grail that is being sought by scientists for biomedical use. Consequently, the hydrogels formation via block copolymer micelles consisting of enantiomeric PLA and PEG has an important role in many hydrogels bioapplications. The mixture of ABA-type block copolymers, PLLA-PEG-PLLA and PDLA-PEG-PDLA, with specific molecular weight and block ratio exhibits attractive sol-to-gels transition between room and body temperature, can be used as an injectable biodegradable scaffold. The reversible gels-sol transitions occur in the mixed micellar solution of the enantiomeric BAB triblock copolymers, PEG-PLLA-PEG and PEG-PDLA-PEG, depending on the polymer concentration and temperature. An understanding of the gelation mechanisms for ABA, BAB, and AB systems involving stereocomplex crystals is critical to achieve their potential for bioapplications. There are many hydrogels formation theories and understanding gelation mechanisms will provide new perspectives for biomaterial applications.

References

1. Ringsdorf H, Venzmer J, Winnik FM (1991) Fluorescence studies of hydrophobically modified poly(*N*-isopropylacrylamides). *Macromolecules* 24:1678–1686

2. Takei YG, Aoki T, Sanui K et al (1994) Dynamic contact-angle measurement of temperature-responsive surface-properties for poly(*N*-isopropylacrylamide) grafted surfaces. *Macromolecules* 27:6163–6166
3. Zareie HM, Bulmus EV, Gunning AP et al (2000) Investigation of a stimuli-responsive copolymer by atomic force microscopy. *Polymer* 41:6723–6727
4. Maeda Y, Higuchi T, Ikeda I (2000) Change in hydration state during the coil-globule transition of aqueous solutions of poly(*N*-isopropylacrylamide) as evidenced by FTIR spectroscopy. *Langmuir* 16:7503–7509
5. Vadnere M, Amidon G, Lindenbaum S et al (1984) Thermodynamic studies on the gel sol transition of some pluronic polyols. *Int J Pharm* 22:207–218
6. Wanka G, Hoffmann H, Ulbricht W (1990) The aggregation behavior of poly-(oxyethylene)–poly-(oxypropylene)–poly-(oxyethylene)-block-copolymers in aqueous-solution. *Colloid Polym Sci* 268:101–117
7. Jorgensen EB, Hvidt S, Brown W et al (1997) Effects of salts on the micellization and gelation of a triblock copolymer studied by rheology and light scattering. *Macromolecules* 30:2355–2364
8. Deng Y, Yu GE, Price C et al (1992) Thermodynamics of micellization and gelation of oxyethylene oxypropylene diblock copolymers in aqueous-solution studied by light-scattering and differential scanning calorimetry. *J Chem Soc Faraday Trans* 88:1441–1446
9. Alexandridis P, Holzwarth JF, Hatton TA (1994) Micellization of poly(ethylene oxide)–poly(propylene oxide)–poly(ethylene oxide) triblock copolymers in aqueous-solutions – thermodynamics of copolymer association. *Macromolecules* 27:2414–2425
10. Rees DA (1969) Conformational analysis of polysaccharides. Part II. Alternating copolymers of agar–carrageenan–chondroitin type by model building in computer with calculation of helical parameters. *J Chem Soc B* 217–226
11. Hubbell JA, West JL, Chowdhury SM (eds) (1996) *Advanced biomaterials in biomedical engineering and drug delivery systems*. Springer, Tokyo
12. Nagata Y, Kajiwara K (1997) *Gel handbook*. NTS, Tokyo
13. Steinbuechel A (2001) *Biopolymers*. Wiley-VCH, Weinheim
14. Tsuruta T, Hayashi T, Ishihara K et al (1993) *Biomedical applications of polymeric materials*. CRC Press, Boca Raton
15. Zhu KJ, Song BH, Yang SL (1989) Super microcapsules (Smc). 1. Preparation and characterization of star polyethylene oxide (Peg)–polylactide (Pla) copolymers. *J Polym Sci A Polym Chem* 27:2151–2159
16. Zhu KJ, Lin XZ, Yang SL (1990) Preparation, characterization, and properties of polylactide (Pla) poly(ethylene glycol) (Peg) copolymers – a potential-drug carrier. *J Appl Polym Sci* 39:1–9
17. Kricheldorf HR, Boettcher C (1993) Polylactones. 27. Anionic-polymerization of L-lactide – variation of end-groups and synthesis of block-copolymers with poly(ethylene oxide). *Macromol Symp* 73:47–64
18. Kricheldorf HR, Kreiseraunders I, Boettcher C (1995) Polylactones. 31. Sn(II)octoate-initiated polymerization of L-lactide – a mechanistic study. *Polymer* 36:1253–1259
19. Kricheldorf HR, Meierhaack J (1993) Polylactones. 22. ABA triblock copolymers of L-lactide and poly(ethylene glycol). *Macromol Chem Phys* 194:715–725
20. Cerrai P, Tricoli M (1993) Block-copolymers from L-lactide and poly(ethylene glycol) through a noncatalyzed route. *Macromol Rapid Commun* 14:529–538
21. Jedlinski Z, Kurcok P, Walach W et al (1993) Polymerization of lactones. 17. Synthesis of ethylene glycol-L-lactide block-copolymers. *Macromol Chem Phys* 194:1681–1689
22. Xie WH, Chen DP, Fan XH et al (1999) Lithium chloride as catalyst for the ring-opening polymerization of lactide in the presence of hydroxyl-containing compounds. *J Polym Sci A Polym Chem* 37:3486–3491
23. Li SM, Rashkov I, Espartero JL et al (1996) Synthesis, characterization, and hydrolytic degradation of PLA/PEO/PLA triblock copolymers with long poly(L-lactic acid) blocks. *Macromolecules* 29:57–62
24. Goraltchouk A, Freier T, Shoichet MS (2005) Synthesis of degradable poly(L-lactide-co-ethylene glycol) porous tubes by liquid–liquid centrifugal casting for use as nerve guidance channels. *Biomaterials* 26:7555–7563
25. Younes H, Cohn D (1987) Morphological-study of biodegradable PEO/PLA block copolymers. *J Biomed Mater Res* 21:1301–1316
26. Kubies D, Rypacek F, Kovarova J et al (2000) Microdomain structure in polylactide-block-poly(ethylene oxide) copolymer films. *Biomaterials* 21:529–536
27. Li YX, Volland C, Kissel T (1994) In-vitro degradation and bovine serum-albumin release of the ABA triblock copolymers consisting of poly(L(+))lactic acid, or poly(L(+))lactic acid-co-glycolic acid A-blocks attached to central polyoxyethylene B-blocks. *J Controlled Release* 32:121–128
28. Rashkov I, Manolova N, Li SM et al (1996) Synthesis, characterization, and hydrolytic degradation of PLA/PEO/PLA triblock copolymers with short poly(L-lactic acid) chains. *Macromolecules* 29:50–56
29. Shah SS, Zhu KJ, Pitt CG (1994) Poly-DL-lactic acid–polyethylene-glycol block-copolymers – the influence of polyethylene-glycol on the degradation of poly-DL-lactic acid. *J Biomater Sci Polym Ed* 5:421–431

30. Li SM, Garreau H, Vert M (1990) Structure property relationships in the case of the degradation of massive aliphatic poly-(alpha-hydroxy acids) in aqueous-media. 1. Poly(DL-lactic acid). *J Mater Sci Mater Med* 1:123–130
31. Hu DSG, Liu HJ (1993) Effect of soft segment on degradation kinetics in polyethylene glycol/poly(L-lactide) block-copolymers. *Polymer Bull* 30:669–676
32. Mason MN, Metters AT, Bowman CN et al (2001) Predicting controlled-release behavior of degradable PLA-b-PEG-b-PLA hydrogels. *Macromolecules* 34:4630–4635
33. Shah NM, Pool MD, Metters AT (2006) Influence of network structure on the degradation of photo-cross-linked PLA-b-PEG-b-PLA hydrogels. *Biomacromolecules* 7:3171–3177
34. Graham NB, McNeill ME (1984) Hydrogels for controlled drug delivery. *Biomaterials* 5:27–36
35. Metters AT, Anseth KS, Bowman CN (2000) Fundamental studies of a novel, biodegradable PEG-b-PLA hydrogel. *Polymer* 41:3993–4004
36. Metters AT, Bowman CN, Anseth KS (2000) A statistical kinetic model for the bulk degradation of PLA-b-PEG-b-PLA hydrogel networks. *J Phys Chem B* 104:7043–7049
37. Metters AT, Bowman CN, Anseth KS (2001) Verification of scaling laws for degrading PLA-b-PEG-b-PLA hydrogels. *AIChE J* 47:1432–1437
38. Metters AT, Anseth KS, Bowman CN (2001) A statistical kinetic model for the bulk degradation of PLA-b-PEG-b-PLA hydrogel networks: incorporating network non-idealities. *J Phys Chem B* 105:8069–8076
39. Molina I, Li SM, Martinez MB et al (2001) Protein release from physically crosslinked hydrogels of the PLA/PEO/PLA triblock copolymer-type. *Biomaterials* 22:363–369
40. Deng XM, Li XH, Yuan ML et al (1999) Optimization of preparative conditions for poly-DL-lactide–polyethylene glycol microspheres with entrapped *Vibrio cholera* antigens. *J Controlled Release* 58:123–131
41. Perez C, Sanchez A, Putnam D et al (2001) Poly(lactic acid)–poly(ethylene glycol) nanoparticles as new carriers for the delivery of plasmid DNA. *J Controlled Release* 75:211–224
42. Beck LR, Cowsar DR, Lewis DH et al (1979) New long-acting injectable microcapsule contraceptive system. *Am J Obstet Gynecol* 135:419–426
43. Gref R, Domb A, Quellec P et al (1995) The controlled intravenous delivery of drugs using PEG-coated sterically stabilized nanospheres. *Adv Drug Delivery Rev* 16:215–233
44. Sakurai K, Nakada Y, Nakamura T et al (1999) Preparation and characterization of polylactide–poly(ethylene glycol)–polylactide triblock polymers and a preliminary in vivo examination of the blood circulation time for the nanoparticles made therefrom. *J Macromol Sci Pure Appl Chem* 36:1863–1877
45. Matsumoto J, Nakada Y, Sakurai K et al (1999) Preparation of nanoparticles consisted of poly(L-lactide)–poly(ethylene glycol)–poly(L-lactide) and their evaluation in vitro. *Int J Pharm* 185:93–101
46. De Jaeghere F, Allemann E, Feijen J et al (2000) Cellular uptake of PEO surface-modified nanoparticles: evaluation of nanoparticles made of PLA:PEO diblock and triblock copolymers. *J Drug Targeting* 8:143–153
47. Jeong B, Bae YH, Lee DS et al (1997) Biodegradable block copolymers as injectable drug-delivery systems. *Nature* 388:860–862
48. Jeong B, Kim SW, Bae YH (2002) Thermosensitive sol–gel reversible hydrogels. *Adv Drug Delivery Rev* 54:37–51
49. Jeong B, Bae YH, Kim SW (1999) Thermoreversible gelation of PEG–PLGA–PEG triblock copolymer aqueous solutions. *Macromolecules* 32:7064–7069
50. Jeong JH, Kim SW, Park TG (2004) Biodegradable triblock copolymer of PLGA–PEG–PLGA enhances gene transfection efficiency. *Pharm Res* 21:50–54
51. Jeong B, Bae YH, Kim SW (2000) Drug release from biodegradable injectable thermosensitive hydrogel of PEG–PLGA–PEG triblock copolymers. *J Controlled Release* 63:155–163
52. Kim YJ, Kim SW (2003) Controlled drug delivery from injectable biodegradable triblock copolymer. In 'Polymer Gels: Fundamentals and Applications', Bohidar HB, Dubin P, Osada Y Eds, ACS, 833:300–311
53. Li ZH, Ning W, Wang JM et al (2003) Controlled gene delivery system based on thermosensitive biodegradable hydrogel. *Pharm Res* 20:884–888
54. Lee PY, Li ZH, Huang L (2003) Thermosensitive hydrogel as a Tgf-beta 1 gene delivery vehicle enhances diabetic wound healing. *Pharm Res* 20:1995–2000
55. Lee PY, Cobain E, Huard J et al (2007) Thermosensitive hydrogel PEG–PLGA–PEG enhances engraftment of muscle-derived stem cells and promotes healing in diabetic wound. *Mol Ther* 15:1189–1194
56. Yu L, Chang GT, Zhang H et al (2008) Injectable block copolymer hydrogels for sustained release of a PEGylated drug. *Int J Pharm* 348:95–106
57. Qiao MX, Chen DW, Hao TN et al (2008) Injectable thermosensitive PLGA–PEG–PLGA triblock copolymers-based hydrogels as carriers for interleukin-2. *Pharmazie* 63:27–30
58. Qiao MX, Chen DW, Ma XC et al (2006) Sustained release of bee venom peptide from biodegradable thermosensitive PLGA–PEG–PLGA triblock copolymer-based hydrogel in vitro. *Pharmazie* 61:199–202

59. Pratoomsoot C, Tanioka H, Hori K et al (2008) A thermoreversible hydrogel as a biosynthetic bandage for corneal wound repair. *Biomaterials* 29:272–281
60. Gref R, Minamitake Y, Peracchia MT et al (1994) Biodegradable long-circulating polymeric nanospheres. *Science* 263:1600–1603
61. Miyamoto S, Takaoka K, Okada T et al (1993) Polylactic acid polyethyleneglycol block-copolymer – a new biodegradable synthetic carrier for bone morphogenetic protein. *Clin Orthop*:333–343
62. Iijima M, Nagasaki Y, Okada T et al (1999) Core-polymerized reactive micelles from heterotelechelic amphiphilic block copolymers. *Macromolecules* 32:1140–1146
63. Choi SW, Choi SY, Jeong B et al (1999) Thermoreversible gelation of poly(ethylene oxide) biodegradable polyester block copolymers. Part II. *J Polym Sci A Polym Chem* 37:2207–2218
64. Aamer KA, Sardinha H, Bhatia SR et al (2004) Rheological studies of PLLA–PEO–PLLA triblock copolymer hydrogels. *Biomaterials* 25:1087–1093
65. Sanabria-DeLong N, Agrawal SK, Bhatia SR et al (2006) Controlling hydrogel properties by crystallization of hydrophobic domains. *Macromolecules* 39:1308–1310
66. Sanabria-DeLong N, Agrawal SK, Bhatia SR et al (2007) Impact of synthetic technique on PLA–PEO–PLA physical hydrogel properties. *Macromolecules* 40:7864–7873
67. Agrawal SK, Sanabria-DeLong N, Tew GN et al (2008) Structural characterization of PLA–PEO–PLA solutions and hydrogels: crystalline vs. amorphous PLA domains. *Macromolecules* 41:1774–1784
68. Bryant SJ, Bender RJ, Durand KL et al (2004) Encapsulating chondrocytes in degrading PEG hydrogels with high modulus: engineering gel structural changes to facilitate cartilaginous tissue production. *Biotechnol Bioeng* 86:747–755
69. Rice MA, Anseth KS (2004) Encapsulating chondrocytes in copolymer gels: bimodal degradation kinetics influence cell phenotype and extracellular matrix development. *J Biomed Mater Res A* 70A:560–568
70. Murakami Y, Yokoyama M, Okano T et al (2007) A novel synthetic tissue-adhesive hydrogel using a crosslinkable polymeric micelle. *J Biomed Mater Res A* 80A:421–427
71. Ikada Y, Jamshidi K, Tsuji H et al (1987) Stereocomplex formation between enantiomeric poly(lactides). *Macromolecules* 20:904–906
72. Okihara T, Tsuji M, Kawaguchi A et al (1991) Crystal-structure of stereocomplex of poly(L-lactide) and poly(D-lactide). *J Macromol Sci Phys B30*:119–140
73. Tsuji H, Horii F, Hyon SH et al (1991) Stereocomplex formation between enantiomeric poly(lactic acid)s. 2. Stereocomplex formation in concentrated-solutions. *Macromolecules* 24:2719–2724
74. Tsuji H (2000) In vitro hydrolysis of blends from enantiomeric poly(lactide)s. Part 1. Well-stereo-complexed blend and non-blended films. *Polymer* 41:3621–3630
75. Brochu S, Prudhomme RE, Barakat I et al (1995) Stereocomplexation and morphology of poly(lactides). *Macromolecules* 28:5230–5239
76. Brizzolara D, Cantow HJ, Diederichs K et al (1996) Mechanism of the stereocomplex formation between enantiomeric poly(lactide)s. *Macromolecules* 29:191–197
77. Hoogsteen W, Postema AR, Pennings AJ et al (1990) Crystal-structure, conformation, and morphology of solution-spun poly(L-lactide) fibers. *Macromolecules* 23:634–642
78. Lim DW, Choi SH, Park TG (2000) A new class of biodegradable hydrogels stereocomplexed by enantiomeric oligo(lactide) side chains of poly(HEMA-g-OLA)s. *Macromol Rapid Commun* 21:464–471
79. de Jong SJ, De Smedt SC, Wahls MWC et al (2000) Novel self-assembled hydrogels by stereocomplex formation in aqueous solution of enantiomeric lactic acid oligomers grafted to dextran. *Macromolecules* 33:3680–3686
80. de Jong SJ, De Smedt SC, Demeester J et al (2001) Biodegradable hydrogels based on stereocomplex formation between lactic acid oligomers grafted to dextran. *J Controlled Release* 72:47–56
81. de Jong SJ, van Eerdenbrugh B, van Nostrum CF et al (2001) Physically crosslinked dextran hydrogels by stereocomplex formation of lactic acid oligomers: degradation and protein release behavior. *J Controlled Release* 71:261–275
82. Fujiwara T, Mukose T, Yamaoka T et al (2001) Novel thermo-responsive formation of a hydrogel by stereo-complexation between PLLA–PEG–PLLA and PDLA–PEG–PDLA block copolymers. *Macromol Biosci* 1:204–208
83. Mukose T, Fujiwara T, Nakano J et al (2004) Hydrogel formation between enantiomeric B-A-B-type block copolymers of polylactides (PLLA or PDLA: A) and polyoxyethylene (PEG: B); PEG–PLLA–PEG and PEG–PDLA–PEG. *Macromol Biosci* 4:361–367
84. Li SM, Vert M (2003) Synthesis, characterization, and stereocomplex-induced gelation of block copolymers prepared by ring-opening polymerization of L(D)-lactide in the presence of poly(ethylene glycol). *Macromolecules* 36:8008–8014
85. Hiemstra C, Zhong ZY, Li LB et al (2006) In-situ formation of biodegradable hydrogels by stereocomplexation of PEG-(PLLA)(8) and PEG-(PDLA)(8) star block copolymers. *Biomacromolecules* 7:2790–2795

86. Hiemstra C, Zhong Z, Van Tomme SR et al (2007) In vitro and in vivo protein delivery from in situ forming poly(ethylene glycol)–poly(lactide) hydrogels. *J Controlled Release* 119:320–327
87. Hiemstra C, Zhou W, Zhong ZY et al (2007) Rapidly in situ forming biodegradable robust hydrogels by combining stereocomplexation and photopolymerization. *J Am Chem Soc* 129:9918–9926
88. Chung HJ, Lee YH, Park TG (2008) Thermo-sensitive and biodegradable hydrogels based on stereocomplexed Pluronic multi-block copolymers for controlled protein delivery. *J Controlled Release* 127:22–30
89. Fujiwara T, Miyamoto M, Kimura Y (2000) Crystallization-induced morphological changes of a poly(L-lactide)/poly(oxyethylene) diblock copolymer from sphere to band via disk: a novel macromolecular self-organization process from core-shell nanoparticles on surface. *Macromolecules* 33:2782–2785
90. Fujiwara T, Miyamoto M, Kimura Y et al (2001) Self-organization of diblock and triblock copolymers of poly(L-lactide) and poly(oxyethylene) into nanostructured bands and their network system. Proposition of a doubly twisted chain conformation of poly(L-lactide). *Macromolecules* 34:4043–4050
91. Fujiwara T, Kimura Y (2002) Macromolecular organization of poly(L-lactide)-block-polyoxyethylene into bio-inspired nano-architectures. *Macromol Biosci* 2:11–23
92. Fujiwara T, Miyamoto M, Kimura Y et al (2001) Intriguing morphology transformation due to the macromolecular rearrangement of poly(L-lactide)-block-poly(oxyethylene): from core-shell nanoparticles to band structures via fragments of unimolecular size. *Polymer* 42:1515–1523
93. Lee D, Teraoka I (2002) Termini and main-chain composition of monomethoxy-terminated poly(ethylene glycol) studied by two-dimensional column chromatography. *Polymer* 43:2691–2697
94. Lee D, Teraoka I (2003) Removal of dihydroxy-terminated components from monomethoxy-terminated poly(ethylene glycol). *Biomaterials* 24:329–336
95. Kister G, Cassanas G, Vert M (1998) Effects of morphology, conformation and configuration on the IR and Raman spectra of various poly(lactic acid)s. *Polymer* 39:267–273

Hydrogels-Based Drug Delivery System with Molecular Imaging

Keun Sang Oh and Soon Hong Yuk

Abstract Drug delivery systems with molecular imaging capability are usually nanoscopic therapeutic systems that incorporate therapeutic agents and diagnostic imaging probes. Polymers (which form hydrogels) and molecular imaging probes used currently were reviewed firstly. Polymer-coated molecular imaging probes were also reviewed to introduce the basic component in the preparation of drug delivery systems with molecular imaging capability. Finally, the recent studies on the drug delivery systems with molecular imaging capability were summarized and their prospect was addressed.

Introduction

Hydrogels, a three dimensional polymer network, may absorb a large quantity of contact liquid. Because of this swelling phenomenon, hydrogels gives a new insight into a model system for the study of a viscoelastic body that is a major topic in polymer physics. In addition to its importance in science, it has many direct applications in the biomedical area, especially in the area of drug and cell delivery.

The concept of drug delivery system in the pharmaceutical area has been investigated using hydrogels as a candidate material. The three dimensional network of hydrogels demonstrated the sustained release of loaded drug [1–3]. Because of presence of a large quantity of water, the swelling transition in response to various stimuli (pH, temperature, light, ionic concentration, metabolites...) is being intensively investigated with respect to the concept of stimulus-sensitive drug delivery [3–7]. In addition, hydrogels have the potential to execute cell delivery, such as pancreatic islet transplantation for diabetes. Transplanted islets are subject to immunologically mediated destruction by both autoimmunity and transplant rejection. Hydrogels can be used as a semipermeable, biocompatible membrane to protect the islets from host immune responses [8–10].

Current interest is focused on the development of nanomedicine platforms in drug delivery and molecular imaging applications. This led to the emergence of nanoscopic therapeutic systems that incorporate therapeutic agents and diagnostic imaging probes (Fig. 1). Studies have shown that this multifunctional nanomedicine improves the therapeutic outcome of drug therapy. To efficiently obtain information on nanomedicine (the drug delivery systems with molecular imaging capability), the nanomedicine should have the reservoir to contain drugs and molecular imaging probes.

K.S. Oh and S.H. Yuk • Department of Advanced Materials, Hannam University, 461-6 Jeonmin Dong, Yusung Gu, Daejeon 305-811, Korea
e-mail: shyuk@hnu.kr

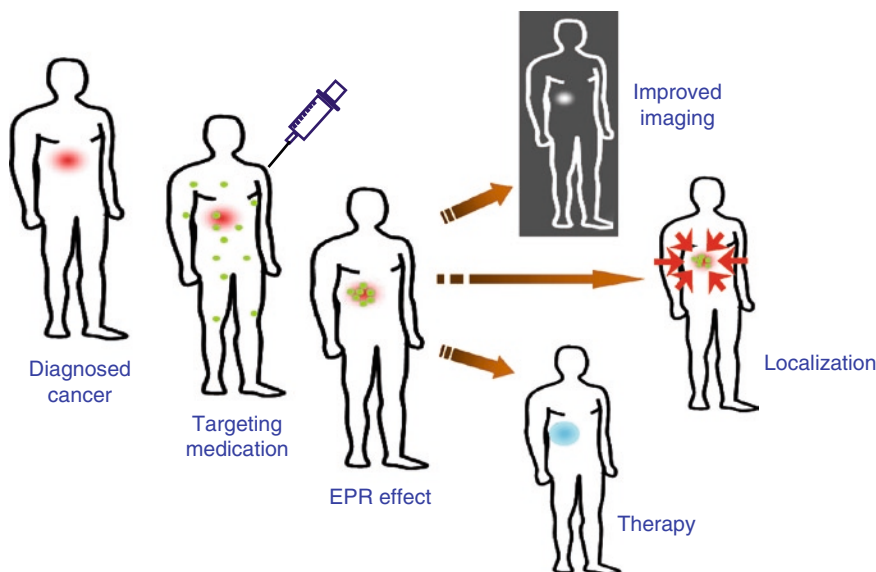


Fig. 1. Therapeutic agents and diagnostic imaging capabilities.

Hydrogels Polymers for Imaging Probes

Poly(vinyl pyrrolidone): Poly(vinyl pyrrolidone) (PVP) is a biocompatible, water-soluble, and nontoxic polymer. Using the hydrogen bonding between the carbonyl groups of PVP and the carboxyl groups of poly(acrylic acid) (PAA) [11] or chitosan [12], various forms of physical gels have been prepared and characterized. PVP gels are utilized as drug delivery systems with the forms of microspheres, nanoparticles, liposomes, and polymer conjugates [13–16].

Self-assembly in aqueous solutions of PVP-block-poly(D,L-lactide) [15], PVP-block-poly(D,L-lactide)-block-PVP, PVP-block-poly(ϵ -caprolactone)-block-PVP [17], and PVP-block-poly(ϵ -caprolactone) [18] is a very important property. As a consequence, PVP can be used to form polymeric micelles to deliver the medical drugs or molecular imaging probes.

Poly(vinyl alcohol): Poly(vinyl alcohol) (PVA) is a linear hydrophilic polymer that is nontoxic and biocompatible. Because of intra/intermolecular interactions via hydrogen bonding, PVA forms hydrogels (physical gels). The freeze-thawing method is often used to enhance the mechanical properties [19, 20]. PVA hydrogels are also prepared by chemical crosslinking using irradiation or crosslinkers, such as glutaraldehyde or sodium borate and boric acid [21, 22].

The use of PVA as the base component for hydrogels formation is particularly advantageous, due to the abundance of hydroxyl pendant groups on the PVA chains that can be further substituted with various functional groups. Several research groups have investigated the addition of methacrylate and acrylate pendant groups [23–25], sulfosalicylic acid [26], chitosan [27], hydroxyapatite [28], and alginate [29, 30].

Dextran Hydrogels: Dextran is a polysaccharide consisting of glucose molecules coupled into long branched chains, mainly through 1,6- and some through 1,3-glucosidic linkages. Dextran is colloidal, hydrophilic, and water-soluble substances that have excellent biocompatibility and hence, they do not affect cell viability. It is susceptible to enzymatic digestion in the body [31]. Dextran has abundant pendant hydroxyl functional groups making it amenable

to chemical modification [32–34]. Hydrophobically modified dextrans are used as stabilizers to produce stable hydrophilic poly(styrene) or poly(lactic acid) nanoparticles by the oil in water (o/w) emulsion and evaporation technique [35–37].

An interconnected macroporous glycidyl methacrylated dextran (Dex-GMA)/gelatin hydrogels scaffold containing microspheres loaded with bone morphogenetic proteins (BMP) has been developed [38]. Microspheres are formed when gelatin was mixed with glycidyl methacrylate dextrans (Dex-GMA); the characteristics of the dextran-co-gelatin hydrogels microspheres can be controlled by the crosslinking density and added substituents to Dex-GMA. Controlled release of bone morphogenetic proteins was observed from 18 to more than 28 days by changing the hydrogels/microsphere ratio.

As a drug delivery system, doxorubicin conjugated dextran nanoparticles have been prepared to improve its therapeutic efficacy in the treatment of solid tumors [39]. In vivo efficacy test of nanoparticles showed faster regression in tumor volume and increased survival time comparing with drug conjugate and free drug.

Chitosan Hydrogels: Chitosan (poly-b(1,4)-D-glucosamine) is a cationic polysaccharide which is obtained by alkaline deacetylation of chitin, the main exoskeletal component in crustaceans. Its molecular weight ranges from 3,000 to 10,000, with a degree of deacetylation from 30 to 95%, depending on the source and preparation method. The amine groups of chitosan are protonated in the acidic conditions (pH < 4). The quality and properties of chitosan products, such as purity, viscosity, deacetylation, and molecular weight, may vary widely because of many factors in the manufacturing process can influence the characteristics of the final product. Chitosan has biodegradability, nontoxicity, biocompatibility, and antifungal activity; chitosan and its derivatives have been studied as biomaterials which are used for drug delivery systems [40] and scaffolds for tissue engineering [41, 42].

Chitosan beads are prepared by simultaneous crosslinking with glutaraldehyde and precipitation in aqueous NaOH [40]. Metronidazole, an antiinfection agent, loaded chitosan beads give faster release at acidic conditions; this pH-sensitive release behavior can be utilized to design targeted delivery system for anticancer drugs.

The differentiation of mesenchymal stem cells (MSCs) and the mass formation of cartilage are possible using an injectable hydrogels composed of copolymer of thermosensitive poly(*N*-isopropylacrylamide) and water-soluble chitosan. Cartilage formation in the submucosal layer of the bladder of rabbits and the in situ hydrogels system composed of dextran copolymer as a scaffold are being pursued [41].

The reactive amino groups in the backbone of chitosan make it possible to chemically conjugate various biological molecules such as different ligands and antibodies, which may improve targeting efficiency of the drug to the site of action [43, 44]. Chitosan-based polymeric vesicles and niosomes bearing glucose or transferrin ligands for drug targeting have been prepared [43]. Transferrin (TF) coupled to the surface of the polymeric vesicles appears to be accessible to the TF receptor in the A431 cell line. The TF receptors are over expressed on the surface of many proliferating cells and the active targeting of polymeric vesicles for drug/gene delivery can be accomplished.

One of the most useful properties of chitosan is ionic chelation. The strong positive charge of chitosan enables it to bind to negatively charged substrates, such as cholesterol, fats, metal ions, and proteins [45–48]. As a nutritional supplement, chitosan has been reported to reduce lipid absorption in the intestine by binding fatty acids and bile acids and by increasing their excretion [45, 46]. Therefore, oral administration of chitosan inhibits the development of atherosclerosis in individuals with hypercholesterolemia by lowering the serum cholesterol levels.

Alginate: Alginate is a naturally derived anionic polysaccharide, obtained mainly from marine algae; it is widely utilized as a food additive and in drug formulations. Alginate consists of two sugar moieties, 1, 4-linked D-mannuronic acid (M) and L-gluronic acid (G), either block or random sequences [49–53]. Alginate forms complexes with divalent ions, such as Ca^{2+} , Ba^{2+} , and so on [52, 53].

Alginate hydrogels have pH-sensitive swelling transitions that are used in the design of drug delivery systems [54, 55]. Drug release from alginate gels is known to be blocked or sustained at low pH by forming a surface gels cover by deswelling, while drug release is accelerated at neutral pH by the swelling increase [56–59]. Alginate can potentially be used for cell delivery, such as microencapsulation of artificial pancreas [60]. The isolated islets of Langerhans suspended in the alginate aqueous solution are effectively encapsulated in the alginate gels when the solution is treated with divalent cations. For further stabilization of islet-encapsulated alginate gels, the polymer complex (an ionic complex) is usually formed at the surface of alginate gels with polycations, such as poly(L-lysine) [61, 62].

Pluronics: Pluronic is a triblock copolymer of poly(ethylene oxide)–poly(propylene oxide)–poly(ethylene oxide) (PEO–PPO–PEO, Poloxamers, Pluronics). Because of its nontoxicity and ability to form a gels, it is widely used in the pharmaceutical area [63–65]. For example, at 20% (w/v), aqueous solutions of poloxamer 407 form hydrogels at body temperature [66].

Poloxamer 188 ($\text{PEO}_{80}\text{--PPO}_{27}\text{--PEO}_{80}$, molecular weight: 7,680–9,510) is used in intravenous injections and oral formulations and Poloxamer 407 ($\text{PEO}_{101}\text{--PPO}_{56}\text{--PEO}_{101}$, molecular weight 9,840–14,600) is used in ophthalmic solutions. The sol–gel phase diagrams of poloxamer 188 and poloxamer 407, as a function of concentrations, are shown in Fig. 2.

In addition to the enhancement of the bioavailability of low-solubility drugs in oral solid dosage forms, Pluronics are used as an emulsifier, solubilizer, dispersant, and wetting agent in the preparation of solid dispersions [67, 68]. When these polymers are bound to the surface of nanospheres by the hydrophobic interaction of the PPO chains, the hydrophilic PEO chains stretch into the surrounding medium creating a steric barrier [69, 70]. This barrier

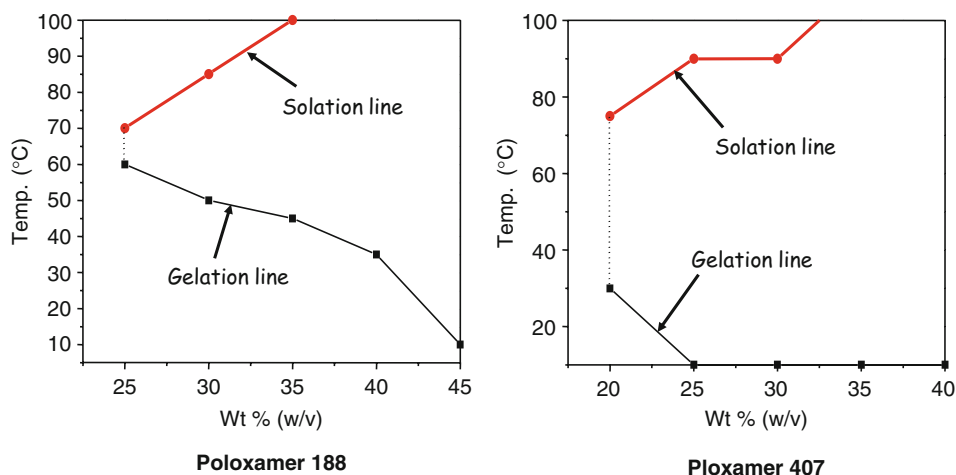


Fig. 2. Sol–gel phase diagram with different concentration of poloxamer 188 and poloxamer 407.

prevents or restricts the adsorption of plasma proteins onto the particle surface decreasing recognition by liver and spleen macrophages [71, 72].

The adsorption of these surfactants is the most widely used procedure to modify the surface characteristics of the primitive carriers; the incorporation of these copolymers into the particles during the manufacturing process has become a significant alternative strategy.

Poly(Ethylene Glycol) (PEG) and Its Copolymers

Poly(ethylene glycol) (PEG) is a neutral, water-soluble, and nontoxic synthetic polymer approved by the FDA for internal use and inclusion in a variety of foods, cosmetics, and drug delivery systems. For prolong blood circulation time, PEG is used to modify nanoparticles to avoid uptake by the reticuloendothelial system (RES). This is important in the design of effective therapeutic systems for injectable delivery and for the controlled drug delivery [73–75].

Modifying the polymer composition, particularly, the middle block composition, the block length, and the block ratio, produced a new generation of PEG–(poly(L-lactic acid-co-glycolide acid))–PEG (PEG–PLGA–PEG) triblock copolymers. The sol–gel transition temperature can be controlled by changing the repeating units of PEG–PLGA–PEG triblock copolymers, such as the PLGA length. As the hydrophobic block (PLGA) length is increased, a stronger shear stress is required to make the gels system. Increasing the PEG length of a PEG–PLGA–PEG triblock copolymer shifts the thermo-phase diagrams to higher temperatures [76, 77].

In situ gels formation in vivo was first made by subcutaneous injection of PEG–PLGA–PEG triblock copolymer aqueous solutions into rats [78]. Based on this phenomenon, paclitaxel-loaded biodegradable polymeric micellar system using low molecular weight and biodegradable amphiphilic diblock copolymer and monomethoxy PEO₂₀₀₀-Poly(D,L-Lactide)₁₇₅₀ micelles (Genexol®-PM) were published by Kim et al. [79, 80]. In Phase I human trials, micellar encapsulation of paclitaxel allowed safer administration of high doses of paclitaxel.

Poly(*N*-isopropylacrylamide) (PNIPAm)

Poly(*N*-isopropylacrylamide) (PNIPAm) is one of the most widely used thermosensitive polymers. PNIPAm has a hydrophilic amide group and a hydrophobic isopropyl group. The linear PNIPAm chain undergoes a rapid dehydration of the hydrophobic isopropyl groups in aqueous solution at its lower critical solution temperature (LCST) of around 32–34°C in water due to its coil-to-globule transition [81–85]. The potential of PNIPAm for drug delivery system [86–89] and cell engineering [90–92] has been well documented. For example, hybrid block and graft copolymers of PNIPAm containing phosphocholine [93, 94], poly(D,L-lactide) [95], and alginate [96, 97] have been successfully synthesized and well characterized as bio-material candidates.

The copolymers that include the LCST block and a hydrophilic block, such as PEG–PNIPAm copolymers, form micelles above the LCST of PNIPAm, with PNIPAm block forming a micelle core [98]. Block copolymers consisting of the LCST block and a hydrophobic block, such as poly(*N*-isopropylacrylamide)-poly(methyl methacrylate) (PNIPAm–PMMA), form micelles below the LCST, with PMMA block forming a core and PNIPAm block forming a shell [99].

Table 1. Noninvasive imaging in medical application

Technique	Detection	Contrast agent
Computered Tomography (CT)	X-rays	Iodine (Ultravist [®]), Barium, Barium sulfate Gastrografin
Magnetic Resonance Imaging (MRI)	Magnetic field	Paramagnetic agents: Gd-DTPA(Magnevist [®]), Gd-DTPA-BMA (Omniscan [®]) Superparamagnetic agents: iron oxide nanoparticles (Resovist [®] , Feridex [®])
Positron Emission Tomography (PET)	Gamma rays	F18-FDG(2-Deoxy-2-fluoro-D-glucose)
Ultra-sonography	Ultrasonic waves	Microbubbles(Albunex [®] , Levovist [®])

Molecular Probes for Imaging

With the advances in imaging technology, the importance of molecular imaging probes has increased for precise diagnosis. The visualization of the cellular function and the follow-up of the molecular process in living organisms without surgical operation are facily carried out. Some of the techniques used for noninvasive imaging in diagnosis medicine are listed in Table 1.

Gold Nanoparticles

One of the most interesting aspects of gold nanoparticles is that their optical properties are varyingly dependant on the particle size and shape. Bulk gold looks yellow in reflected light, but this characteristic changes to orange, through several tones of purple and red, as particle size is reduced to ~20 nm. These effects are the result of changes in the so-called surface plasmon resonance (SPR) [100].

Gold nanoparticles are usually prepared by reduction in a boiling sodium citrate solution [101]. The formation of gold nanoparticles appears as a deep wine red color and the UV absorption in the aqueous media at around 520 nm. Functionalization of gold nanoparticles (gold surfaces) with molecules containing thiol (-SH), which has a high affinity for gold atoms is commonly used. A number of biosensors are designed based on this phenomenon.

The gold nanoparticles are biocompatible and nontoxic in vivo [102, 103]. However, plasma proteins and salts in the blood nonspecifically adsorb onto the surface of gold nanoparticles, this often causes aggregation; therefore, the direct use of gold nanoparticles in vivo can lead to clearance from the bloodstream due to uptake by the reticular endothelial system (RES) (Kupffer cells of the liver) [104–107]. Therefore, gold nanoparticles used in vivo are usually surface modified with PEG [104].

Magnetic Nanoparticles

Magnetic nanoparticles are manipulated under the influence of a magnetic field and are commonly composed of magnetic elements such as iron oxide (superparamagnetic iron oxide (SPIO) and ultrasuperparamagnetic iron oxide (USPIO)) and gadolinium compounds. Because of difficulties in recognizing tumors from normal tissues by magnetic resonance

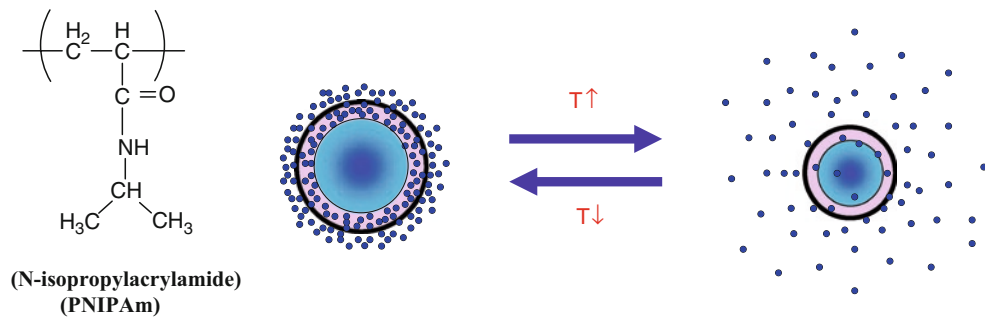


Fig. 3. Schematic description for molecular structure of poly(*N*-isopropylacrylamide) (PNIPAm) and drug release mechanism in response to temperature (*T*) changes.

imaging (MRI), patients are often injected with a contrast agent, such as iron oxide nanoparticles or gadolinium chelates.

Nanoparticles are prepared by either coprecipitation [108–110], high-temperature decomposition [111–113], or microemulsion [114, 115]. Coprecipitation is a facile and convenient way to synthesize iron oxides (Fe_3O_4 or $\gamma\text{-Fe}_2\text{O}_3$) from aqueous Fe^{2+} and Fe^{3+} salt solutions by the addition of base at room temperature or at raised temperatures. The stability is maintained by electrostatic and repulsive interaction between counter-ions. The size, shape, and composition of the magnetic nanoparticles mainly depend on the type of salts used, the $\text{Fe}^{2+}/\text{Fe}^{3+}$ molar ratio, reaction temperature, the pH, and ionic strength of the media [116–118].

The high-temperature decomposition ($>200^\circ\text{C}$) of an organic iron precursor in the presence of hydrophobic ligands, such as oleic acid, is typically used; the hydrophobic ligands form a dense coating around the nanoparticles, thereby avoiding their aggregation.

Microemulsions are used to obtain relatively small particles (high surface area) with well controlled properties; water-in-oil microemulsions are usually used to produce iron oxide nanoparticles. The type and concentration of surfactant [119, 120], type of oil [121] and alcohol [122–124], droplet core size [125], and the speed of microemulsion mixing [126] all play an important role in the formation of iron oxide nanoparticles by microemulsion techniques.

Iron oxide nanoparticles have been approved for clinical use, especially for MRI, for example, Endorem[®] (diameter 80–150 nm, Advanced Magnetix) and Resovist[®] (diameter 60 nm, Schering) for liver/spleen imaging [127–129].

Gadolinium is also an FDA approved contrast agent for MRI. Gadolinium, or gadodiamide, provides greater contrast between normal tissue and abnormal tissue in the brain and body. Because of their paramagnetic properties, solutions of organic gadolinium complexes and gadolinium compounds are used as intravenous radiocontrast agents to enhance images in medical MRI. After it is injected into a vein, gadolinium accumulates in the abnormal tissue with bright (enhanced) images on the MRI. With the administration of MRI contrast agents, the relaxation times T_1 and/or T_2 of a proton in the vicinity of an agent change, thus generating image contrast (bright/dark) (Fig. 4) [130].

Fluorescence Dyes

Optical fluorescence depends on the inherent property of fluorophores, such as fluorescein isothiocyanate (FITC) and FITC derivatives, cysteine, cyanine dye (cydye), and Indocyanine green dye (ICG) are used for fluorescence imaging (Fig. 5) [130].

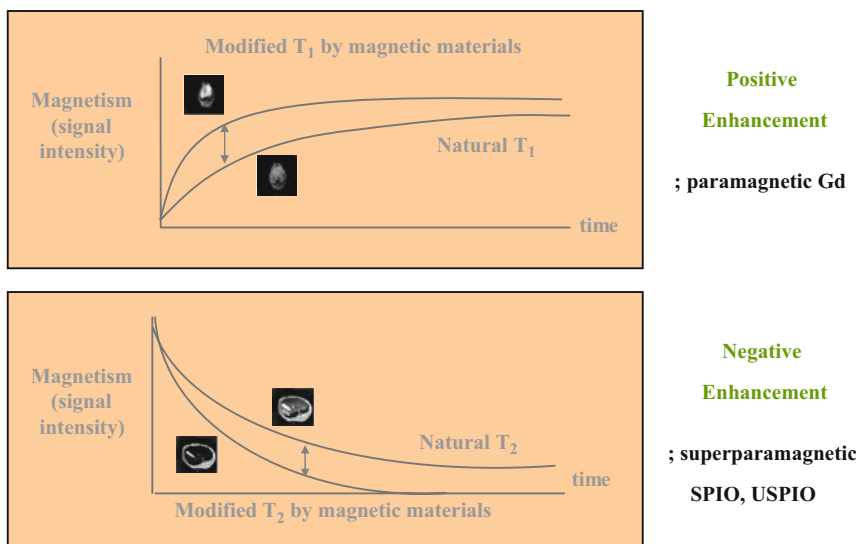


Fig. 4. T1 and T2 relaxation processes [130].

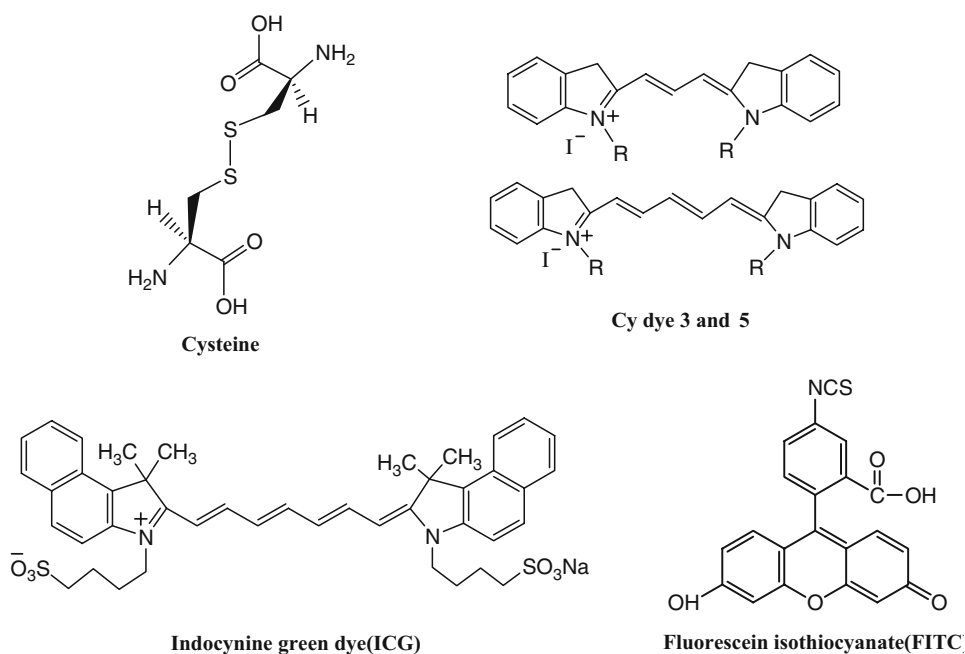


Fig. 5. Various used fluorophores in biological imaging.

Fluorescein isothiocyanate (FITC) is used in several biological applications, such as fluorescent-labeled antibodies and molecules that are taken up by cells or organelles. Usually, the energy from an external source is absorbed by the fluorophores injected or accumulated at the tumor site.

Microbubbles

Ultrasound contrast agents, which consist of a hydrophobic gas (microbubbles) and a stabilizing shell, have enabled clinical contrast echocardiography due to their enhanced stability in circulation. Moderate intensity ultrasound assisted by encapsulated microbubbles has been used in *in vitro* and *in vivo* targeting drug delivery via a process called “sonoporation.” Ultrasound imaging is used to molecularly target microbubbles to the liver [131], breast [132], and prostate tumors [133].

These advances have created interest in ultrasound as a molecular imaging modality. Ultrasonic imaging of molecular targets associated with angiogenesis [134–137], thrombosis [138], and inflammation is being used [139, 140].

There are two types of bubbles that are related to sonoporation process: free bubbles and encapsulated microbubbles. Free bubbles are usually cavities filled with air, other gases, or gas vapor from surrounding liquid. However, due to their instability, free bubbles are usually encapsulated in biocompatible polymers as microbubbles for the ultrasonic imaging of angiogenesis [136, 141–146].

Quantum Dots

In general, the quantum dots are prepared in the organic solvent at high temperatures between 180 and 310°C, depending on the ligands and solvents employed in the preparation.

Quantum dots are nanoscale semiconductor crystals composed of Group II B (Transition metal)-Group VI A compounds (CdTe, CdS, CdHg, ZnS) or Group III A-Group V A elemental groups (InAs, InP, GaAs). A noble class of inorganic fluorophores is gaining widespread recognition as a result of their exceptional photophysical properties. Both the optical absorption and emission of quantum dots shift to the blue (higher energies) as the size of the dots gets smaller (Fig. 6) [147, 148].

Quantum dots have broad excitation spectrum; therefore, different-colored quantum dots can be activated by using a single source laser at the same time, making them extremely attractive in multiplexing studies [149–151]. For biological imaging applications, quantum dot materials are chosen based on size, optical properties, and toxicity. The emission wavelength should be in a region of the spectrum where blood and tissue absorb minimally but detectors are still efficient, approximately in the near-infrared (700–900 nm).

In spite of these attractive features the use of quantum dots in the biomedical application has been limited due to their hydrophobic character; now hydrophilic surface ligands, such as mercaptoacetic acid [152, 153] and polyethylene glycol (PEG), are used to increase their stability in aqueous media and to reduce the nonspecific adsorption. However, quantum dots capped with these small molecules are easily degraded by hydrolysis or oxidation of the capping ligands [153]. Heavy metal ions, such as Cd²⁺, that can escape from the quantum dot matrix are cytotoxic and cause biocompatibility concerns [154, 155].

Molecular Probe/Polymer Composite Systems

Metal nanoparticles used in the biological imaging applications, such as gold and iron oxide, are easily cleared from the body because of biofouling of metal nanoparticles in the body.

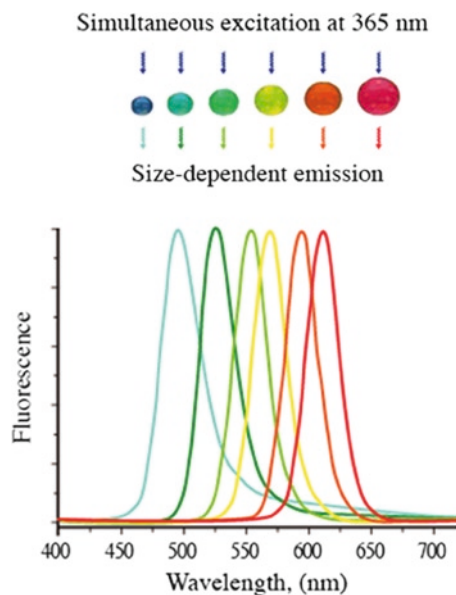


Fig. 6. Fluorescence spectra depending on the size of quantum dots [147, 148] (Blue fluorescence can be emitted from small particles of approximately 2 nm in diameter, green from ~3 nm particles, yellow from ~4 nm particles, and red from large particles of ~5 nm. The wavelength of the excitation light is 365 nm).

To overcome this limitation, the polymers used in the fabrication of hydrogels are utilized to stabilize the metal nanoparticles as molecular probe/polymer composite systems.

Contrast agents for Computer Tomography (CT) are based on iodinated small molecules because, among nonmetal atoms, iodine has a high X-ray absorption coefficient. However, iodinated compounds have very short imaging times due to rapid clearance by the kidney. Therefore, gold nanoparticles are used as they have a higher atomic number and X-ray absorption coefficient than iodine [156, 157]. However, gold nanoparticles also showed the rapid clearance by biofouling [158]. Gold nanoparticles can be combined with polymers containing thiol (-SH), which has a high affinity for gold atoms. Numerous modifications have been made based on this chemical nature of gold nanoparticles and this has led to several kinds of biosensors.

Poly(ethylene glycol)-SH (PEG-SH) can be design with CT contrast agents; the formation of PEG-coated gold nanoparticles enhances antibiofouling capability [159]. The X-ray absorption coefficient in vitro indicates that the attenuation of PEG-coated gold nanoparticles is 5.7 times higher than the iodine-based CT-contrast agent Ultravist in in-vivo animal test using rat.

The anionic character of gold nanoparticles stabilized with citrate attracts macromolecules with cationic character (positively charged polymers), such as chitosan and poly(ethyleneimine) (PEI). Through this electrostatic interaction gold nanoparticles/polymer composite systems are formed.

Multilayer film composites of gold nanoparticles and chitosan are constructed using layer by layer assembly [160]. The formation of the multilayer film was verified by UV-Vis Spectrometry, Atomic Force Microscopy, and Electrochemical Impedance Spectroscopy, and applied to nanodevices.

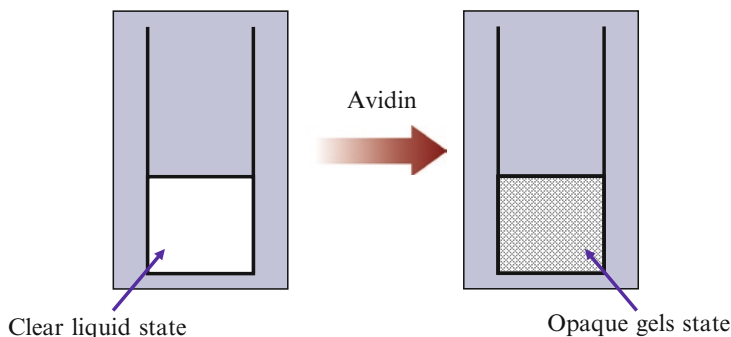


Fig. 7. Gold nanoparticles stabilized by biotinylated PNIPAM before and after the addition of avidin [161].

Gold nanoparticles protected/stabilized by biotinylated PNIPAM were prepared via a thiol anchoring end-group. The introduction of a biotin at the free chain-end of the stabilizer is to induce the supramolecular assembly containing gold nanoparticles via complexation with avidin in water [161].

As shown in Fig. 7, the gold nanoparticles stabilized by biotinylated PNIPAM demonstrated the nanostructure organization at the supramolecular level by biotin/avidin complexation in response to the biochemical species in the aqueous media, which can be utilized in the design of biosensors.

Iron Oxide Nanoparticle/Polymer Composite Systems

Iron oxide nanoparticles have been evaluated as an MRI contrast agent for the liver and the spleen. However, the applications are still subject to many limitations such as size monodispersity, magnetization, stability, nontoxicity, biocompatibility, injectability, and the short blood half-life of magnetic nanoparticles for in vivo applications. To overcome these limitations, a variety of biocompatible polymeric materials, such as PVP [162], Pluronic [163], dextran [164], chitosan [165], poly(D,L-lactid-co-glycolide) [166], and ϵ -caprolactone [167], have been employed as coating materials for MRI contrast agents.

Magnetic nanoparticles composites are prepared with Fe_3O_4 as core and chitosan as polymeric shell [168]. Chitosan and Fe_3O_4 aqueous suspensions are mixed in appropriate proportions using reverse-phase suspension crosslinking. The saturated magnetization of composite nanoparticles shows the characteristics of superparamagnets. The decrease in the saturated magnetization is related to the increased amounts of polymer incorporated in the polymer-coated magnetite suspension.

Similarly, sonochemistry can be employed to prepare iron oxide-loaded chitosan nanoparticles [165]. The magnetic Fe_3O_4 nanoparticles have been prepared by coprecipitation. Ferric chloride hexahydrate ($\text{FeCl}_3 \cdot 6\text{H}_2\text{O}$) and ferrous chloride tetrahydrate ($\text{FeCl}_2 \cdot 4\text{H}_2\text{O}$) are mixed with ammonium hydroxide (NH_4OH) under irradiated ultrasonic waves. The ferrofluid, made of iron oxide nanoparticles and chitosan, is sprayed on the surface of the alkali solution (NaOH /ethanol/water, 4/30/66, w/v/v) to form iron oxide-loaded chitosan nanoparticles.

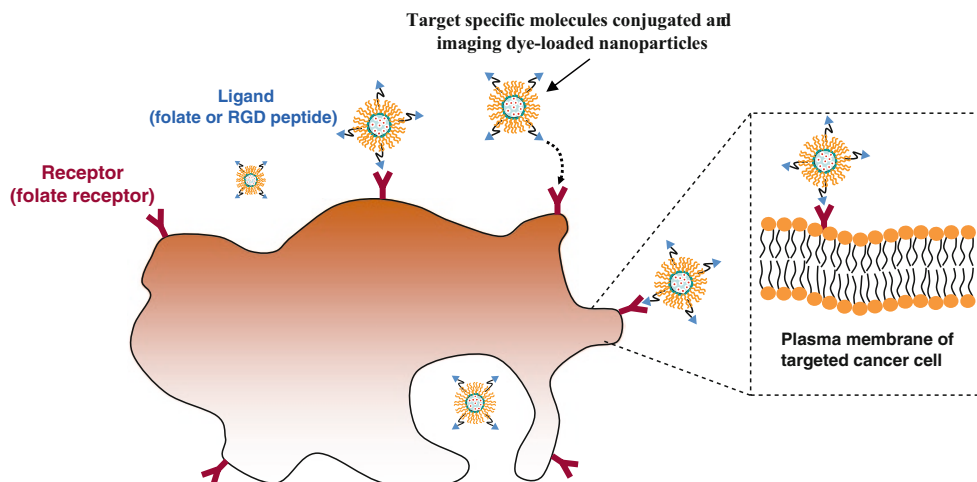


Fig. 8. Scheme of active cellular targeting [170].

These nanoparticles were injected into the left kidney of a rabbit and T2-weighted MR images of the kidney were obtained. The iron oxide-loaded chitosan nanoparticles enhanced contrast of the T2-weighted MR images.

Recently, active localizing imaging probes (gold nanoparticles and metal nanoparticles) in tumor tissue were accomplished by conjugating target specific molecules, such as folic acid [169], RGD peptide [170], or integrins [171] (Fig. 8).

The surface modification of iron oxide nanoparticles with folic acid was carried out to improve receptor binding and the efficiency of cellular internalization of nanoparticles [169]. To evaluate the targeting specificity of the nanoparticle-PEG-folic acid (NP-PEG-FA) conjugate to tumor cells, the uptake of the nanoconjugate by HeLa cells was compared with that by human osteosarcoma MG-63 cells (folate receptor negative cell line). Human osteosarcoma MG-63 cells express very low levels of the α and β forms of the folate receptor. The level of nanoparticle conjugate uptake by HeLa cells ranged from twice to as much as ten times that by MG-63 cells. Concomitant with this nanoparticle uptake, the T2-weighted MR phantom image showed a significant increase in the negative contrast enhancement of the HeLa cells compared with that of the MG-63 cells.

Quantum Dot/Polymer Composite Systems

Fluorescent semiconductor nanocrystals or quantum dots provide a new class of biomarkers that could overcome the limitations of organic dyes as *in vitro* and *in vivo* imaging probes. Despite of their advantages as a molecular probe, the semiconductor core of quantum dots has raised concerns regarding heavy metal cytotoxicity. In fact, quantum dots are cytotoxic due to cadmium oxidation and the leaching of heavy metal ions [171–173]. As quantum dots applications broaden in biotechnology research, it is important to consider these potential hazards and develop novel approaches to avoid toxicity, such as encapsulation or polymer coating, to form a protective insulating material or wide band gap semiconductor structurally matched with the core material.

The formation of quantum dot/polymer nanocomposites involves strong noncovalent interactions, such as hydrogen bonding, ionic attraction [174–176], and physically entrapping quantum dots into particles formed by emulsion polymerization [177] or sol–gel synthesis [178].

Quantum dot-encapsulated nanoparticles are noncytotoxic during long-term incubation with viable cells in the absence of light exposure, which makes them appropriate for cell monitoring and drug delivery [179, 180]. The quantum dots were conjugated with various molecules and proteins, such as myosin VI, transferrin, and kinesin; when these bioconjugated quantum dots were present, receptor-mediated endocytosis occurred and the luminescent quantum dots enabled the investigation of cellular uptake pathways and detection within cells due to the bright fluorescence of the colloids. Since the quantum dots have broad excitation properties for all colors, multiple colors can be efficiently excited simultaneously with one light source, such as blue-violet filtered light or a 405 nm or 488 nm laser [181, 182].

Microbubble/Polymer Composite Systems

Ultrasound contrast agents are widely used to image perfusion and have potential for drug and gene delivery, where therapeutic release is initiated by local sonication [183–192]. Microbubble-loaded and lipid-based contrast agents have a self-assembled shell that provides a flexible, protective membrane around a perfluorocarbon gas core. In the diagnosis, these agents have been successfully used in the measurement of blood volume and flow in cardiology and radiology [192, 193].

Lipid-based microbubbles are usually stabilized with ligand and/or polymer molecules before bubble production, and the stabilized lipids are self-assembled into a shell with exposure to the aqueous medium. The approach for these lipid-stabilized contrast agents (diameters ~1–10) utilizes the lipid with PEG or PEG/ligand to specifically bind to a preferred target site [194].

Drug Delivery System with Molecular Imaging Capability

The development of noninvasive imaging technology (MRI, CT, PET, and Ultrasound) that integrates drug delivery systems with medical imaging is an important technology. A drug loaded with an imaging probe will enable real-time, targeted monitoring of drug delivery with medical imaging devices and to quantify drug uptake at the site as well as monitor the response to the therapy.

Yuk recently used composite gold nanoparticles, for the delivery of an anticancer drug; the ionic interaction between the gold nanoparticles and chitosan to form the composite nanoparticles loaded with paclitaxel [195]. Considering the optical property of gold nanoparticles, the gold nanoparticles/chitosan composite was utilized as a drug delivery system with molecular imaging capability (Fig. 9) [195].

The oleic acid (OA)-Pluronic (F-127)-coated iron oxide nanoparticles were formed with high doses of water insoluble doxorubicin [163]. Because of drug partitions into the OA shell, the surrounding iron oxide nanoparticles and the Pluronic anchor at the water–OA interface which significantly increased the solubility (dispersity) of the doxorubicin. Neither the formulation components nor the drug loading affected the magnetic properties of the core iron oxide nanoparticles and sustained release of doxorubin was observed 2 weeks under *in vitro* conditions. The nanoparticles in this study showed an enhanced intracellular drug retention, comparing with free drug in the aqueous solution, and a dose-dependent antiproliferative effect in breast and prostate cancer cell lines.

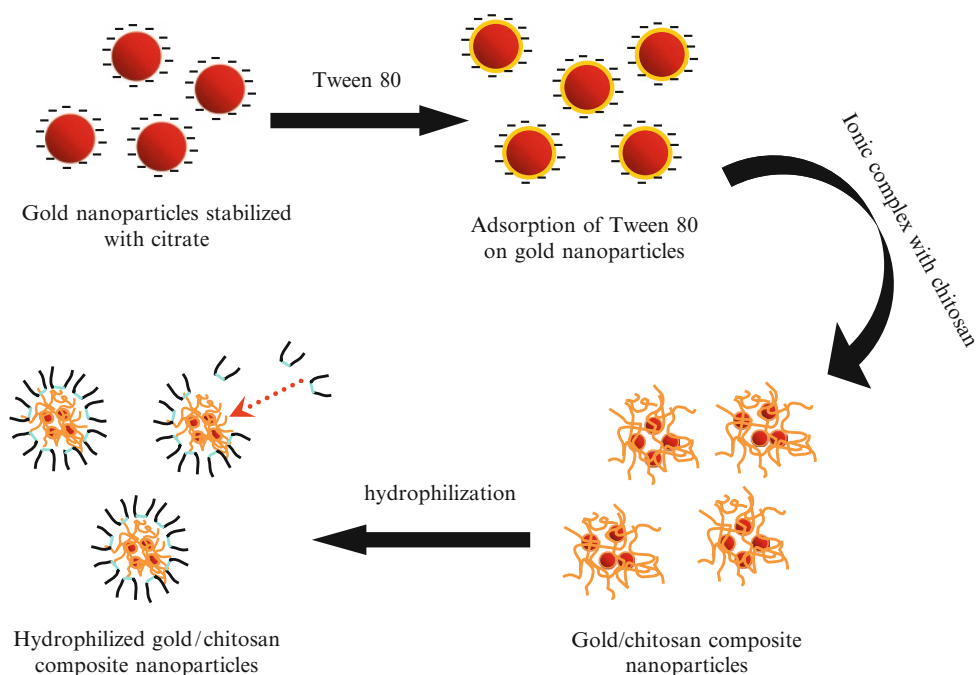


Fig. 9. Schematic description of gold/chitosan composite nanoparticles [195].

Doxorubicin-loaded superparamagnetic iron oxide (SPIO) nanoparticles were made using polymeric micelles with cRGD attached onto the surface of polymeric micelles for efficient targeting to tumors [196]. Amphiphilic block copolymers of maleimide-terminated poly(ethylene glycol)-block-poly(D,L-lactide) [MAL-PEG-PLA, $M_n=7,200$, $M_n(\text{PEG})=3,200$] and methoxy-terminated poly-(ethylene glycol)-block-poly(D,L-lactide) copolymer [MPEG-PLA, $M_n=6,400$, $M_n(\text{PEG})=2,000$] were used to form micelles with cRGD attached to the surface through a thiol-maleimide linkage. The cRGD on the surface of polymeric micelle targeted the delivery of doxorubicin to $\alpha_v\beta_3$ -expressing tumor cells. The *in vitro* MRI and cytotoxicity of the $\alpha_v\beta_3$ -specific cytotoxic response of these multifunctional polymeric micelles were observed by ultrasensitive MRI.

To combine contrast-enhanced ultrasound tumor imaging with targeted drug delivery is a challenging task [197–199]. Rapoport et al. developed novel ultrasound-sensitive multifunctional nanoparticles composed of nanoscale polymeric micelles that function as drug carriers and nano- or microscale echogenic bubbles that combine the properties of drug carriers, enhancers of ultrasound-mediated drug delivery with long-lasting ultrasound contrast agents [200, 201]. In their study, perfluoropentane (PFP) nanoemulsions dispersed in a solution of polymeric micelles were produced by introducing an aliquot of a sterilized PFP into a micellar solution of a copolymer which was subsequently subject to sonication to produce cavitation. Biodegradable diblock copolymers poly(ethylene oxide)-block-poly(lactide) and poly(ethylene oxide)-block-poly(caprolactone) were used to form polymeric micelles with doxorubicin as the drug model. The copolymer-stabilized PFP nanoemulsion systems undergo nanodroplet/nanobubble conversion *in vivo*, accumulate locally in the tumor tissue and coalesce into larger,

highly echogenic microbubbles, which provide long-lasting ultrasound contrast in the tumor while maintaining effective levels of doxorubicin at the tumor site.

The visualization and monitoring of transplanted islets using iron oxide nanoparticles covered with a modified dextran was carried out by incubating the Islets with magnetic nanoparticles consisting of a superparamagnetic iron core covered with a modified dextran coating [202]. The MRI showed a marked decrease in signal intensity on T2-weighted images at the implantation site in the left kidney as compared with the right kidney (implanted unlabeled islets). Thus, *in vivo* detection of transplanted human pancreatic islets using magnetic resonance imaging (MRI) that allowed noninvasive monitoring of islet grafts in diabetic mice in real time is now possible [202].

Summary

The unique feature of hydrogel-based drug delivery systems with molecular imaging capability involves loading a therapeutic agent into polymer network (hydrogels) surrounding molecular imaging probes. Although understanding and demonstrating the combination of hydrogels containing therapeutic agents with molecular imaging probes has been performed successfully, there remains the challenge for efficient application of this technology to diagnosis and therapy. The realization of hydrogels/molecular imaging probe composite systems on the nanoscale and the optimized drug release in response to the diagnosis is an important step. In the near future, this integrated smart system will open many potential opportunities for the effective therapeutic delivery and monitoring as well as molecular imaging probes for noninvasive procedures in early detection of disease.

References

1. Liu YY, Fan XD (2005) Synthesis, properties and controlled release behaviors of hydrogel networks using cyclodextrin as pendant groups. *Biomaterials* 26:6367–6374
2. John C, Lev EB, Edmond M (2003) Diffusion and release of solutes in pluronic-g-poly(acrylic acid) hydrogels. *Langmuir* 19:9162–9172
3. Alvarez-Lorenzo C, Concheiro A, Dubovik AS (2005) Temperature-sensitive chitosan-poly(*N*-isopropylacrylamide) interpenetrated networks with enhanced loading capacity and controlled release properties. *J Control Release* 102:629–641
4. Wang SC, Chen BH, Wang LF et al (2007) Release characteristics of lidocaine from local implant of polyanionic and polycationic hydrogels. *J Control Release* 118:333–339
5. Dayananda K, He C, Park DK et al (2008) pH- and temperature-sensitive multiblock copolymer hydrogels composed of poly(ethylene glycol) and poly(amino urethane). *Polymer* 49(23):4968–4973
6. Bhattarai N, Ramay HR, Gunn J et al (2005) PEG-grafted chitosan as an injectable thermosensitive hydrogel for sustained protein release. *J Control Release* 103:609–624
7. Zhang R, Tang M, Bowyer A et al (2005) A novel pH and ionic strength-sensitive carboxymethyl dextran hydrogel. *Biomaterials* 26:4677–4683
8. Mikos AG, Papadaki MG, Kouvrokoglou S (1994) Mini-review: islet transplantation to create a bioartificial pancreas. *Biotechnol Bioeng* 43:673–677
9. Laney MW, Kirsten NH, Kathryn H et al (2007) The effects of cell–matrix interactions on encapsulated b-cell function within hydrogels functionalized with matrix-derived adhesive peptides. *Biomaterials* 28:3004–3011
10. Hou QP, Bae YH (1999) Biohybrid artificial pancreas based on macrocapsule device. *Adv Drug Deliv Rev* 35:271–287

11. Chun MK, Cho CS, Choi HK (2002) Mucoadhesive drug carrier based on interpolymer complex of poly(vinyl pyrrolidone) and poly(acrylic acid) prepared by template polymerization. *J Control Release* 81:327–334
12. Siegel RA, Falamarzian M, Firestone BA et al (1988) pH controlled release from hydrophobic/polyelectrolyte copolymer hydrogel. *J Control Release* 8:179–182
13. Moneghini M, Voinovich D, Princivale F et al (2000) Formulation and evaluation of vinylpyrrolidone/vinylacetate copolymer microspheres with carbamazepine. *Pharm Dev Technol* 5:347–353
14. Torchilin VP, Shtilman MI, Trubetsky VS et al (1994) Amphiphilic vinyl polymers effectively prolong liposome circulation time in vivo. *Biochim Biophys Acta* 1195:181–184
15. Kamada H, Tsutsumi Y, Yamamoto Y et al (2000) Antitumor activity of tumor necrosis factor- α conjugated with polyvinylpyrrolidone on solid tumors in mice. *Cancer Res* 60:6416–6420
16. D'souza AJM, Schowen RL, Topp EM (2003) Polyvinylpyrrolidone-drug conjugate: synthesis and release mechanism. *J Control Release* 94:91–100
17. Luo L, Ranger M, Lessard DG et al (2004) Novel amphiphilic diblock copolymer of low molecular weight poly(*N*-vinylpyrrolidone)-block-poly(D,L-lactide): synthesis, characterization, and micellization. *Macromolecules* 37:4008–4013
18. Lele BS, Leroux JC (2002) Synthesis and micellar characterization of novel amphiphilic A-B-A triblock copolymers of *N*-(2-Hydroxypropyl) methacrylamide or *N*-Vinyl-2-pyrrolidone with poly(ϵ -caprolactone). *Macromolecules* 35:6714–6723
19. Yokoyama F, Masada I, Shimamura K et al (1986) Morphology and structure of highly elastic poly-(vinyl alcohol) hydrogel prepared by repeated freezing-and-melting. *Colloid Polym Sci* 264:559–561
20. Hassan CM, Stewart JE, Peppas NA (2000) Diffusional characteristics of freeze/thawed poly(vinyl alcohol) hydrogels: applications to protein controlled release from multilaminate devices. *Eur J Pharm Biopharm* 49:161–165
21. Mansur HS, Sadahira CM, Souza AN et al (2008) FT-IR spectroscopy characterization of poly (vinyl alcohol) hydrogel with different hydrolysis degree and chemically crosslinked with glutaraldehyde. *Mater Sci Eng C* 28(4):539–548
22. Lin HL, Liu YF, Yu TL et al (2005) Light scattering and viscoelasticity study of poly(vinyl alcohol)-borax aqueous solutions and gels. *Polymer* 46:5541–5549
23. Mühlebach A, Müller B, Pharisa C et al (1997) New water-soluble photo crosslinkable polymers based on modified poly(vinyl alcohol). *J Polym Sci A Polym Chem* 35(16):3603–3611
24. Peppas NA, Wright SL (1996) Solute diffusion in poly(vinyl alcohol)/poly(acrylic acid) interpenetrating networks. *Macromolecules* 29:8798–8804
25. Peppas NA, Wright SL (1998) Drug diffusion and binding in ionisable interpenetrating networks from poly(vinyl alcohol) and poly(acrylic acid). *Eur J Pharm Biopharm* 4:15–29
26. Juntanon K, Niamlang S, Rujiravanit R et al (2008) Electrically controlled release of sulfosalicylic acid from crosslinked poly(vinyl alcohol) hydrogel. *Int J Pharm* 356:1–11
27. Yu FT, Yu MD, Xian WH et al (2007) Rheological characterisation of a novel thermosensitive chitosan/poly(vinyl alcohol) blend hydrogel. *Carbohydr Polym* 67:491–499
28. Wu G, Suc B, Zhang W et al (2008) In vitro behaviors of hydroxyapatite reinforced poly(vinyl alcohol) hydrogel composite. *Mater Chem Phys* 107:364–369
29. Kim JO, Park JK, Kim JH et al (2004) Development of poly(vinyl alcohol)-sodium alginate gel-matrix-based wound dressing system containing nitrofurazone. *Polymer* 45:7129–7136
30. Nishioa Y, Yamada A, Ezaki K et al (2004) Preparation and magnetometric characterization of iron oxide-containing alginate/poly(vinyl alcohol) networks. *Polymer* 45:7129–7136
31. Franssen O, van oojien RD, de Boer D et al (1999) Enzymatic degradation of cross-linked dextrans. *Macromolecules* 32:2896–2902
32. Stenekes RJH, Loebis AE, Fernandes CM et al (2001) Degradable dextran microspheres for the controlled release of liposomes. *Int J Pharm* 214:17–20
33. van Dijk-Wolthuis WNE, Franssen O, Talsma H et al (1995) Synthesis, characterization and polymerization of glycidyl methacrylate derivatized dextran. *Macromolecules* 28:6317–6322
34. Massia SP, Stark J (2001) Immobilized RGD peptides on surface-grafted dextran promote biospecific cell attachment. *J Biomed Mater Res* 56(3):390–399
35. Rouzes C, Leonard M, Durand A et al (2003) Influence of polymeric surfactants on the properties of drug-loaded PLA nanospheres. *Colloids Surf B* 32:125–135
36. De Sousa DA, Leonard M, Dellacherie E (2001) Surface properties of polystyrene nanoparticles coated with dextrans and dextran-PEO Copolymers. Effect of polymer architecture on protein adsorption. *Langmuir* 17:4386–4391

37. De Sousa DA, Leonard M, Dellacherie E (2000) Surface modification of polystyrene nanoparticles using dextrans and dextran-POE copolymers: polymer adsorption and colloidal characterization. *J Biomater Sci Polym Ed* 11:1395–1410
38. Chen FM, Zhao YM, Sun HH et al (2007) Novel glycidyl methacrylated dextran (Dex-GMA)/gelatin hydrogel scaffolds containing microspheres loaded with bone morphogenetic proteins: Formulation and characteristics. *J Control Release* 118:65–77
39. Mitra S, Gaur U, Ghosh PC et al (2001) Tumour targeted delivery of encapsulated dextran–doxorubicin conjugate using chitosan nanoparticles as carrier. *J Control Release* 74:317–323
40. Barreiro-Iglesias R, Coronilla R, Concheiro A et al (2005) Preparation of chitosan beads by simultaneous cross-linking/insolubilisation in basic pH rheological optimisation and drug loading/release behaviour. *Eur J Pharm Sci* 24:77–84
41. Cho JH, Kim SH, Park KD et al (2004) Chondrogenic differentiation of human mesenchymal stem cells using a thermosensitive poly(*N*-isopropylacrylamide) and water-soluble chitosan copolymer. *Biomaterials* 25:5743–5751
42. Chung HJ, Go DH, Ba JW et al (2005) Synthesis and characterization of Pluronic grafted chitosan copolymer as a novel injectable biomaterial. *Curr Appl Phys* 5:485–488
43. Dufes C, Schätzlein AG, Tetley L et al (2000) Niosomes and polymeric chitosan based vesicles bearing transferring and glucose ligands for drug targeting. *Pharm Res* 17:1250–1258
44. Hejazi R, Amiji M (2003) Chitosan-based gastrointestinal delivery systems. *J Control Release* 89:151–165
45. Ormrod DJ, Holmes CC, Miller TE (1998) Dietary chitosan inhibits hypercholesterolaemia and atherogenesis in the apolipoprotein E-deficient mouse model of atherosclerosis. *Atherosclerosis* 138:329–334
46. Gallaher CM, Munion J, Hesslink R Jr et al (2000) Cholesterol reduction by glucomannan and chitosan is mediated by changes in cholesterol absorption and bile acid and fat excretion in rats. *J Nutr* 130:2753–2759
47. Chen AH, Liu SC, Chen CY et al (2008) Comparative adsorption of Cu(II), Zn(II), and Pb(II) ions in aqueous solution on the crosslinked chitosan with epichlorohydrin. *J Hazard Mater* 154(1–3):184–191
48. Chen F, Zhang ZR, Yuan F et al (2008) In vitro and in vivo study of *N*-trimethyl chitosan nanoparticles for oral protein delivery. *Int J Pharm* 349:226–233
49. Grant GT, Morris ER, Rees DA et al (1973) Biological interactions between polysaccharides and divalent cations: the egg-box model. *FEBS Lett* 32(1):195–198
50. Morris ER (1974) Molecular interactions in polysaccharide gelation. *Br Polym J* 18:14–21
51. Smidsrod O (1974) Molecular basis for some physical properties of alginates in gel state. *Faraday Discuss Chem Soc* 57:263–274
52. Ouwerx C, Velings N, Mestdagh MM et al (1998) Physico-chemical properties and rheology of alginate gel beads formed with various divalent cations. *Polym Gels Netw* 6:393–408
53. Montero P, Pérez-Mateos M (2002) Effects of Na⁺, K⁺ and Ca²⁺ on gels formed from fish mince containing a carrageenan or alginate. *Food Hydrocol* 16:375–385
54. Murata Y, Hirai D, Kofuji KE (2004) Properties of an alginate gel bead containing a chitosan-drug salt. *Biol Pharm Bull* 27:440–442
55. Murata Y, Jinno D, Kofuji K et al (2004) Properties of calcium-induced gel beads prepared with alginate and hydrolysates. *Chem Pharm Bull* 52:605–607
56. Liu X, Xu W, Liu Q et al (2004) Swelling behaviour of alginate–chitosan microcapsules prepared by external gelation or internal gelation technology. *Carbohydr Polym* 56:459–464
57. Lin YH, Liang HF, Chung CK et al (2005) Physical crosslinked alginate/*N*, *O*-carboxymethyl chitosan hydrogels with calcium for oral delivery of protein drugs. *Biomaterials* 26:2105–2113
58. Holte Ø, Onsøyen E, Myrvold R et al (2003) Sustained release of water-soluble drug from directly compressed alginate tablets. *Eur J Pharm Sci* 20:403–407
59. Bajpai SK, Shubhra S (2004) Investigation of swelling/degradation behaviour of alginate beads crosslinked with Ca²⁺ and Ba²⁺ ions. *React Funct Polym* 59:129–140
60. Denis D, van Mathieu S, Rose MG et al (2006) The influence of implantation site on the biocompatibility and survival of alginate encapsulated pig islets in rats. *Biomaterials* 27:3201–3208
61. Choi YH, Lee JH, Yuk SH (2006) Core/shell macrobeads for the protection of islets from immune system rejection. *J Bioact Compat Polym* 21:71–81
62. Koch S, Schwinger C, Kressler J et al (2003) Alginate encapsulation of genetically engineered mammalian cells: comparison of production devices, methods and microcapsule characteristics. *J Microencapsul* 20:303–316
63. Xiong XY, Tam KC, Gan LH (2006) Polymeric nanostructures for drug delivery applications based on pluronic copolymer systems. *J Nanosci Nanotechnol* 6(9–10):2638–2650

64. Alexandridis P, Hatton TA (1995) Poly (ethylene oxide)–poly (propylene oxide)–poly (ethylene oxide) block copolymer surfactants in aqueous solutions and at interfaces: thermodynamics, structure, dynamics, and modeling. *Colloids Surf A Physicochem Eng Asp* 96:1–46
65. Ruel-Gariepy E, Leroux JC (2004) In situ-forming hydrogels-review of temperature-sensitive systems. *Eur J Pharm Biopharm* 58:409–426
66. Dumortier G, Grossiord JL, Agnely F et al (2006) A review of Poloxamer 407 pharmaceutical and pharmacological characteristics. *Pharm Res* 23:2709–2728
67. Newa M, Bhandari KH, Li DX (2007) Preparation, characterization and in vivo evaluation of ibuprofen binary solid dispersions with poloxamer 188. *Int J Pharm* 343(1–2):228–237
68. Yong CS, Oh YK, Kim YI et al (2005) Physicochemical characterization and in vivo evaluation of poloxamer-based solid suppository containing diclofenac sodium in rats. *Int J Pharm* 301(1–2):54–61
69. Kayes JB, Rawlins DA (1979) Adsorption characteristics of certain polyoxyethylene polyoxypropylene block co-polymers on polystyrene latex. *Colloid Polym Sci* 257:622–629
70. Li JT, Caldwell KD, Rapoport N (1994) Surface properties of pluronic-coated polymeric colloids. *Langmuir* 10:4475–4482
71. Illum L, Jacobsen LO, Muller RH et al (1987) Surface characteristics and the interaction of colloidal particles with mouse peritoneal macrophages. *Biomaterials* 8:113–117
72. Tan JS, Butterfield DE, Voycheck CL et al (1993) Surface modification of nanoparticles by PEO/PPO block copolymers to minimize interactions with blood components and prolong blood circulation in rats. *Biomaterials* 14:823–833
73. Stolnik S, Dunn SE, Garnett MC et al (1994) Surface modification of poly(lactide-co-glycolide) nanoparticles by biodegradable poly(lactide)-poly(ethylene glycol) copolymer. *Pharm Res* 11:1800–1808
74. Bazile D, Prud'homme C, Bassoulet MT et al (1995) Stealth Me.PEG-PLA nanoparticles avoid uptake by the mononuclear phagocyte system. *J Pharm Sci* 84:493–498
75. Jeong B, Bae YH, Kim SW (2000) Drug release from biodegradable injectable thermosensitive hydrogel of PEG–PLGA–PEG triblock copolymer. *J Control Release* 63:155–163
76. Jeong B, Bae YH, Kim SW (1999) Thermoreversible gelation of PEG–PLGA–PEG triblock copolymer aqueous solutions. *Macromolecules* 32:7064–7069
77. Lee DS, Shim MS, Kim SW et al (2001) Novel thermoreversible gelation of biodegradable PLGA-block-PEO-block-PLGA triblock copolymers in aqueous solution. *Macromol Rapid Commun* 22:587–592
78. Jeong B, Bae YH, Kim SW (2000) In situ gelation of PEG–PLGA–PEG triblock copolymer aqueous solutions and degradation thereof. *J Biomed Mater Res* 50:171–177
79. Kim SC, Kim DW, Shim YH et al (2001) In vivo evaluation of polymeric micellar paclitaxel formulation: toxicity and efficacy. *J Control Release* 72:191–202
80. Kim T, Kim D, Chung J (2004) Phase I and pharmacokinetic study of genexol-PM, a cremophor-free, polymeric micelleformulated paclitaxel, in patients with advanced malignancies. *Clin Cancer Res* 10:3708–3716
81. Heskings M, Guillet JJ (1968) Solution properties of poly(*N*-isopropylacrylamide). *J Macromol Sci Part A Pure Appl Chem* 2(8):1441–1455
82. Xu J, Ye J, Liu S (2007) Synthesis of well-defined cyclic poly(*N*-isopropylacrylamide) via click chemistry and its unique thermal phase transition behavior. *Macromolecules* 40(25):9103–9110
83. Feil H, Bae YH, Feijen J et al (1993) Effect of comonomer hydrophilicity and ionization on the lower critical solution temperature of *N*-isopropylacrylamide copolymers. *Macromolecules* 26(10):2496–2500
84. Zhang J, Pelton R, Deng Y (1995) Temperature-dependent contact angles of water on poly(*N*-isopropylacrylamide) gels. *Langmuir* 11(6):2301–2302
85. Maeda T, Kanda T, Yonekura Y et al (2006) Hydroxylated poly(*N*-isopropylacrylamide) as functional thermoresponsive materials. *Biomacromolecules* 7(2):545–549
86. Canavan HE, Cheng X, Graham DJ et al (2005) Surface characterization of the extracellular matrix remaining after cell detachment from a thermoresponsive polymer. *Langmuir* 21:1949–1955
87. Yoshida R, Uchida K, Kaneko Y et al (1995) Comb-type grafted hydrogels with rapid de-swelling response to temperature changes. *Nature* 374:240–242
88. Tuncel A, Ozdemir A (2000) Thermally reversible VPBA–NIPAM copolymer gels for nucleotide adsorption. *J Biomater Sci Polym Ed* 11:817–831
89. Lin HH, Cheng YL (2001) In-situ thermoreversible gelation of block and star copolymers of Poly(ethylene glycol) and Poly(*N*-isopropylacrylamide) of varying architectures. *Macromolecules* 34:3710–3715
90. Kwon OH, Kikuchi A, Yamato M et al (2000) Rapid cell sheet detachment from Poly(*N*-isopropylacrylamide)-grafted porous cell culture membranes. *J Biomed Mater Res* 50:82–89
91. Yamato M, Kwon OH, Hirose M et al (2000) Novel patterned cell coculture utilizing thermally responsive grafted polymer surfaces. *J Biomed Mater Res* 55:137–140

92. Shimizu T, Yamato M, Kikuchi A et al (2001) Two-dimensional manipulation of cardiac myocyte sheets utilizing temperature-responsive culture dishes augments the pulsatile amplitude. *Tissue Eng* 7:141–151
93. Li C, Buurma NJ, Haq I et al (2005) Synthesis and characterization of biocompatible, thermoresponsive ABC and ABA triblock copolymer gelators. *Langmuir* 21(24):11026–11033
94. Hay DNT, Rickert PG, Seifert S et al (2004) Thermoresponsive nanostructures by self-assembly of a poly(*N*-isopropylacrylamide)-lipid conjugate. *J Am Chem Soc* 126(8):2290–2291
95. Jeong B, Choi YK, Bae YH et al (1999) New biodegradable polymers for injectable drug delivery systems. *J Control Release* 62:109–114
96. Lee SB, Park EK, Lim YM et al (2006) Preparation of alginate/poly(*N*-isopropylacrylamide) semi-interpenetrating and fully interpenetrating polymer network hydrogels with γ -ray irradiation and their swelling behaviors. *J Appl Pol Sci* 100:4439–4446
97. Kim MH, Kim JC, Lee HY et al (2005) Release property of temperature-sensitive alginate beads containing poly(*N*-isopropylacrylamide). *Colloids Surf B Biointerfaces* 46:57–61
98. Neradovic D, Soga O, van Nostrum CF et al (2004) The effect of the processing and formulation parameters on the size of nanoparticles based on block copolymers of poly(ethylene glycol) and poly(*N*-isopropylacrylamide) with and without hydrolytically sensitive groups. *Biomaterials* 25:2409–2418
99. Wei H, Zhang XZ, Zhou Y et al (2006) Self-assembled thermoresponsive micelles of poly(*N*-isopropylacrylamide-*b*-methyl methacrylate). *Biomaterials* 27:2028–2034
100. Kreibitz U, Vollmer M (1996) Optical properties of metal clusters. Springer verlag, Berlin
101. Turkevich J, Stevenson PC, Hillier J (1951) A study of the nucleation and growth processes in the synthesis of colloidal gold. *Discuss Faraday Soc* 11:55
102. Shukla R, Bansal V, Chaudhary M et al (2005) Biocompatibility of gold nanoparticles and their endocytotic fate inside the cellular compartment: a microscopic overview. *Langmuir* 21:10644–10654
103. Connor EE, Mwamuka J, Gole A et al (2005) Gold nanoparticles are taken up by human cells but do not cause acute cytotoxicity. *Small* 1:325–327
104. Kim DK, Park SJ, Lee JH et al (2007) Antibiofouling polymer-coated gold nanoparticles as a contrast agent for in vivo X-ray computed tomography imaging. *J Am Chem Soc* 129:7661–7665
105. Raynal I, Prigent P, Peyramaure S et al (2004) Macrophage endocytosis of superparamagnetic iron oxide nanoparticles mechanisms and comparison of ferumoxides and ferumoxtran-10. *Invest Radiol* 39:56–63
106. Rogers WJ, Basu P (2005) Factors regulating macrophage endocytosis of nanoparticles: implications for targeted magnetic resonance plaque imaging. *Atherosclerosis* 178:67–73
107. Woodle MC, Engbers CM, Zalipsky S (1994) New amphipatic polymer-lipid conjugates forming long-circulating reticuloendothelial system-evading liposomes. *Bioconj Chem* 5:493–496
108. Fong YC, Chia HS, Yu SY (2005) Characterization of aqueous dispersions of Fe₃O₄ nanoparticles and their biomedical applications. *Biomaterials* 26:729–738
109. Knag YS, Risbud S, Rabolt JF et al (1996) Synthesis and characterizations of nanometer-size Fe₃O₄ and Fe₂O₃ particles. *Chem Mater* 8:2209–2211
110. Mann S, Hannington JP (1988) Formation of iron oxides in unilamellar vesicles. *J Colloid Interface Sci* 122:326–335
111. Domingo C, Rodriguez Clemente R, Blesa MA (1993) Kinetics of oxidative precipitation of iron oxide particles. *Colloids Surf A* 79:177–189
112. Euliss LE, Grancharov SG, O'Brien S et al (2003) Cooperative assembly of magnetic nanoparticles and block copolypeptides in aqueous media. *Nano Lett* 3:1489–1493
113. Park J, An K, Hwang Y et al (2004) Ultra-large-scale syntheses of monodisperse nanocrystals. *Nat Mater* 3:891–895
114. Swadeshmukul S, Rovelyn T, Nikoleta T et al (2001) Synthesis and characterization of silica-coated iron oxide nanoparticles in microemulsion: the effect of nonionic surfactants. *Langmuir* 17:2900–2906
115. Li L, Choo ESG, Yi JB et al (2008) Superparamagnetic silica composite nanospheres (SSCNs) with ultrahigh loading of iron oxide nanoparticles via an oil-in-DEG microemulsion route. *Chem Mater* 20:6292–6294
116. Jolivet JP, Belleville P, Tronc E et al (1992) Influence of Fe(II) on the formation of the spinel iron oxide in alkaline medium. *Clays Clay Miner* 40:531–539
117. Cuyper MD, Joniau M (1988) Magnetoliposomes. *Eur Biophys J* 15:311–319
118. Massart R (1981) Preparation of aqueous magnetic liquids in alkaline and acidic media. *IEEE Trans Magn* 17:1247–1248
119. Shah PS, Holmes JD, Johnston KP et al (2002) Size-selective dispersion of dodecanethiol-coated nanocrystals in liquid and supercritical ethane by density tuning. *J Phys Chem B* 106:2545–2551
120. Kitchens C, McLeod MC, Roberts B (2003) Solvent effects on the growth and steric stabilization of copper metallic nanoparticles in AOT reverse micelle systems. *J Phys Chem B* 107:11331–11338

121. Summers M, Eastoe J, Davis S (2002) Formation of BaSO₄ nanoparticles in microemulsions with polymerized surfactant shells. *Langmuir* 18:5023–5026
122. Marchand KE, Tarret M, Lechaire JP et al (2003) Investigation of AOT-based microemulsions for the controlled synthesis of MoS_x nanoparticles: an electron microscopy study. *Colloids Surf A Physicochem Eng Asp* 214:239–248
123. Husein M, Rodil E, Vera J (2003) Formation of silver chloride nanoparticles in microemulsions by direct precipitation with the surfactant counterion. *Langmuir* 19:8467–8474
124. Charinpanitkul T, Chanagul A, Dutta J et al (2005) Effects of cosurfactant on ZnS nanoparticle synthesis in microemulsion. *Sci Technol Adv Mater* 6:266–271
125. Pileni MP (2003) The role of soft colloidal templates in controlling the size and shape of inorganic nanocrystals. *Nat Mater* 2:145–150
126. Singh R, Kumar S (2006) Effect of mixing on nanoparticle formation in micellar route. *Chem Eng Sci* 61:192–204
127. Wang YX, Hussain SM, Krestin GP (2001) Superparamagnetic iron oxide contrast agents: physicochemical characteristics and applications in MR imaging. *Eur Radiol* 11:2319–2331
128. Stark DD, Weissleder R, Elizondo G et al (1988) Superparamagnetic iron oxide: clinical application as a contrast agent for MR imaging of the liver. *Radiology* 168:297–301
129. Hamm B, Staks T, Taupitz M et al (1994) Contrast-enhanced MR imaging of liver and spleen: first experience in humans with a new superparamagnetic iron oxide. *J Magn Reson Imag* 4:659–668
130. Weissleder R, Bogdanov A, Neuwelt EA (1995) Long-circulating iron oxides for MR imaging. *Adv Drug Deliv Rev* 16:321–334
131. Wilson SR, Burnes PN, Muradali D et al (2000) Harmonic hepatic US with microbubble contrast agent: initial experience showing improved characterization of hemangioma, hepatocellular carcinoma, and metastasis. *Radiology* 215:153–161
132. Kedar RP, Cosgrove D, McCready VR et al (1996) Microbubble contrast agent for color Doppler US: effect on breast masses. Work in progress. *Radiology* 198:679–686
133. Halpern EJ, Rosenberg M, Gomella LG (2001) Prostate cancer: contrast-enhanced US for detection. *Radiology* 219:219–225
134. Ellegala DB, Leong-Poi H, Carpenter JE et al (2003) Imaging tumor angiogenesis with contrast ultrasound and microbubbles targeted to alpha(v)beta3. *Circulation* 108:336–341
135. Leong-Poi H, Christiansen J, Klibanov AL et al (2003) Noninvasive assessment of angiogenesis by ultrasound and microbubbles targeted to alpha(v)-integrins. *Circulation* 107:455–460
136. Weller GER, Wong MKK, Modzelewski RA et al (2005) Ultrasonic imaging of tumor angiogenesis using contrast microbubbles targeted via the tumor-binding peptide arginine–arginine–leucine. *Cancer Res* 65:533–539
137. Stieger SM, Dayton PA, Borden MA et al (2007) Imaging of angiogenesis using cadence contrast pulse sequencing and targeted contrast agents. *Contrast Media Mol Imaging* 3(1):9–18
138. Unger E, Metzger P, Krupinski E et al (2000) The use of a thrombus-specific ultrasound contrast agent to detect thrombus in arteriovenous fistulae. *Invest Radiol* 35:86–89
139. Lindner JR, Song J, Christiansen J et al (2001) Ultrasound assessment of inflammation and renal tissue injury with microbubbles targeted to P-selectin. *Circulation* 104:2107–2112
140. Linker RA, Reinhardt M, Bendszus M et al (2005) In vivo molecular imaging of adhesion molecules in experimental autoimmune encephalomyelitis (EAE). *J Autoimmun* 25:199–205
141. Takalkar AM, Klibanov AL, Rychak JJ et al (2004) Binding and detachment dynamics of microbubbles targeted to P-selectin under controlled shear flow. *J Control Release* 96:473–482
142. Rychak JJ, Li B, Acton ST et al (2006) Selectin ligands promote ultrasound contrast agent adhesion under shear flow. *Mol Pharmacol* 3:516–524
143. Lankford M, Behm CZ, Yeh J et al (2006) Effect of microbubble ligation to cells on ultrasound signal enhancement: implications for targeted imaging. *Invest Radiol* 41(10):721–728
144. Rychak JJ, Lindner JR, Ley K et al (2006) Deformable gas-filled microbubbles targeted to P-selectin. *J Control Release* 114(3):288–299
145. Klibanov AL (2005) Ligand-carrying gas-filled microbubbles: ultrasound contrast agents for targeted molecular imaging. *Bioconjug Chem* 16:9–17
146. Rychak JJ, Klibanov AL, Ley KF et al (2007) Enhanced targeting of ultrasound contrast agents using acoustic radiation force. *Ultrasound Med Biol* 33(7):1132–1139
147. Bakalova R, Zhelev Z, Ohba H et al (2005) Quantum dot-based western blot technology for ultrasensitive detection of tracer proteins. *J Am Chem Soc* 127(26):9328–9329
148. Zhelev Z, Bakalova R, Ohba H (2006) Uncoated, broad fluorescent, and size-homogeneous CdSe quantum dots for bioanalyses. *Anal Chem* 78(1):321–330

149. Mingyong H, Xiaohu G, Jack ZS (2001) Quantum-dot-tagged microbeads for multiplexed optical coding of biomolecules. *Nat Biotechnol* 19:631–635
150. Bruchez M Jr, Moronne M, Gin P (1998) Semiconductor nanocrystals as fluorescent biological labels. *Science* 281:2013–2016
151. Han M, Gao X, Su JZ (2001) Quantum-dot-tagged microbeads for multiplexed optical coding of biomolecules. *Nat Biotechnol* 19:631–635
152. Chan WC, Nie S (1998) Quantum dot bioconjugates for ultrasensitive nonisotopic detection. *Science* 281:2016–2018
153. Chen Y, Rosenzweig Z (2002) Luminescent CdSe quantum dot doped stabilized micelles. *Nano Lett* 2(11):1299–1302
154. Kirchner C, Liedl T, Kudera S et al (2005) Cytotoxicity of colloidal CdSe and CdSe/ZnS nanoparticles. *Nano Lett* 5:331–338
155. O'Brien P, Cummins SS, Darcy D et al (2003) Quantum dot-labelled polymer beads by suspension polymerization. *Chem Commun* 3:2532–2533
156. Rabin O, Manuel Perez J, Grimm J (2006) An X-ray computed tomography imaging agent based on long-circulating bismuth sulphide nanoparticles. *Nat Mater* 5(2):118–122
157. Hainfeld JF, Slatkin DN, Focella TM (2006) Gold nanoparticles: a new X-ray contrast agent. *Br J Radiol* 79(939):248–253
158. Lee HR, Lee EH, Kim DK et al (2006) Antibiofouling polymer-coated superparamagnetic iron oxide nanoparticles as potential magnetic resonance contrast agents for in vivo cancer imaging. *J Am Chem Soc* 128:7383–7389
159. Kim DK, Park SJ, Lee JH et al (2007) Antibiofouling polymer-coated gold nanoparticles as a contrast agent for in vivo X-ray computed tomography imaging. *J Am Chem Soc* 129:7661–7665
160. Huang H, Yang X (2003) Chitosan mediated assembly of gold nanoparticles multilayer. *Colloids Surf A Physicochem Eng Asp* 226(1–3):77–86
161. Aqil A, Qiu H, Greisch JF et al (2008) Coating of gold nanoparticles by thermosensitive poly(*N*-isopropylacrylamide) end-capped by biotin. *Polymer* 49:1145–1153
162. Lee HY, Lee SH, Xu C et al (2008) Synthesis and characterization of PVP-coated large core iron oxide nanoparticles as an MRI contrast agent. *Nanotechnology* 19:165101–165107
163. Jain TK, Morales MA, Sahoo SK et al (2005) Iron oxide nanoparticles for sustained delivery of anticancer agents. *Mol Pharm* 2(3):194–205
164. Dutza S, Andrä W, Hergta R et al (2007) Influence of dextran coating on the magnetic behaviour of iron oxide nanoparticles. *J Magn Magn Mater* 311:51–54
165. Kim EH, Ahn YK, Lee HS (2007) Biomedical applications of superparamagnetic iron oxide nanoparticles encapsulated within chitosan. *J Alloys Compd* 434–435:633–636
166. Patel D, Moon JY, Chang YM et al (2008) Poly(D,L-lactide-co-glycolide) coated superparamagnetic iron oxide nanoparticles: synthesis, characterization and in vivo study as MRI contrast agent. *Colloids Surf A Physicochem Eng Asp* 313–314:91–94
167. Yang X, Chen Y, Yuan R et al (2008) Folate-encoded and Fe₃O₄-loaded polymeric micelles for dual targeting of cancer cells. *Polymer* 49:3477–3485
168. Li GY, Jiang YR, Huang KL et al (2008) Preparation and properties of magnetic Fe₃O₄-chitosan nanoparticles. *J Alloys Compd* 466(1–2):451–456
169. Conroy S, Raymond S, Miqin Z (2006) Folic acid-PEG conjugated superparamagnetic nanoparticles for targeted cellular uptake and detection by MRI. *J Biomed Mater Res* 78A:550–570
170. Peer D, Karp JM, Hong SP et al (2007) Nanocarriers as an emerging platform for cancer therapy. *Nat Nanotechnol* 2:751–760
171. Norased N, Erik B, Jimin R (2006) Multifunctional polymeric micelles as cancer-targeted, MRI-ultrasensitive drug delivery systems. *Nano Lett* 6(11):2427–2430
172. von zur Muhlena C, von Elverfeldt D, Bassler N et al (2007) Superparamagnetic iron oxide binding and uptake as imaged by magnetic resonance is mediated by the integrin receptor Mac-1 (CD11b/CD18): implications on imaging of atherosclerotic plaques. *Atherosclerosis* 193:102–111
173. Derfus AM, Chan WCW, Bhatia SN (2004) Probing the cytotoxicity of semiconductor quantum dots. *Nano Lett* 4:11–18
174. Hardman RA (2006) Toxicological review of quantum dots: toxicity depends on physicochemical and environmental factors. *Environ Health Perspect* 114:165–172
175. Guo G, Liu W, Liang J et al (2006) Preparation and characterization of novel CdSe quantum dots modified with poly(D,L-lactide) nanoparticles. *Mater Lett* 60:2565–2568
176. Zhang H, Wang C, Li M et al (2005) Fluorescent nanocrystal–polymer composites from aqueous nanocrystals: methods without ligand exchange. *Chem Mater* 17:4783–4788

177. Zhang H, Wang C, Li M et al (2005) Fluorescent nanocrystal-polymer complexes with flexible processability. *Adv Mater* 17:853-857
178. Gong Y, Gao M, Wang D et al (2005) Incorporating fluorescent CdTe nanocrystals into a hydrogel via hydrogen bonding: toward fluorescent microspheres with temperature-responsive properties. *Chem Mater* 17:2648-2653
179. Yang X, Zhang Y (2004) Encapsulation of quantum nanodots in polystyrene and silica micro-/nanoparticles. *Langmuir* 20:6071-6073
180. Mokari T, Sertchook H, Aharoni A et al (2005) Nano@micro: general method for entrapment of nanocrystals in sol-gel-derived composite hydrophobic silica spheres. *Chem Mater* 17:258-263
181. Watanabe TM, Higuchi H (2007) Stepwise movements in vesicle transport of HER2 by motor proteins in living cells. *Biophys J* 92:4109-4120
182. Bruchez MP (2005) Turning all the lights on: quantum dots in cellular assays. *Curr Opin Chem Biol* 9(5):533-537
183. Tartis MS, McCallan J, Lum AF et al (2006) Therapeutic effects of paclitaxel-containing ultrasound contrast agents. *Ultrasound Med Biol* 32(11):1771-1780
184. Chen SY, Ding JH, Bekeredjian R et al (2006) Efficient gene delivery to pancreatic islets with ultrasonic microbubble destruction technology. *Proc Natl Acad Sci U S A* 103(22):8469-8474
185. Kimmel E (2006) Cavitation bioeffects. *Crit Rev Biomed Eng* 34(2):105-161
186. Kipshidze NN, Porter TR, Dangas G et al (2005) Novel site-specific systemic delivery of Rapamycin with perfluorobutane gas microbubble carrier reduced neointimal formation in a porcine coronary restenosis model. *Catheter Cardiovasc Interv* 64(3):389-394
187. Korpanty G, Chen S, Shohet RV et al (2005) Targeting of VEGF-mediated angiogenesis to rat myocardium using ultrasonic destruction of microbubbles. *Gene Ther* 12(17):1305-1312
188. Unger EC, Hersh E, Vannan M et al (2001) Local drug and gene delivery through microbubbles. *Prog Cardiovasc Dis* 44(1):45-54
189. Kheirloomoom A, Dayton PA, Lum AFH et al (2007) Acoustically-active microbubbles conjugated to liposomes: characterization of a proposed drug delivery vehicle. *J Control Release* 118(3):275-284
190. Lee LY, Wang CH, Smith KA (2008) Supercritical antisolvent production of biodegradable micro- and nanoparticles for controlled delivery of paclitaxel. *J Control Release* 125:96-106
191. Suzaki R, Takizawa T, Negishi Y et al (2008) Tumor specific ultrasound enhanced gene transfer in vivo with novel liposomal bubbles. *J Control Release* 125:137-144
192. Leong-Poi H, Song J, Rim SJ et al (2002) Influence of microbubble shell properties on ultrasound signal: implications for low-power perfusion imaging. *J Am Soc Echocardiogr* 15(10):1269-1276
193. Brannigan M, Burns PN, Wilson SR (2004) Blood flow patterns in focal liver lesions at microbubble-enhanced US. *Radiographics* 24(4):921-935
194. Toublan FJJ, Boppart SA, Suslick KS (2006) Tumor targeting by surface-modified protein microspheres. *J Am Chem Soc* 128:3472-3473
195. Oh KS, Kim RS, Yuk SH et al (2008) Gold/chitosan/pluronic composite nanoparticles for drug delivery. *J Appl Polym Sci* 108:3239-3244
196. Nasongkla N, Bey E, Ren J et al (2006) Multifunctional polymeric micelles as cancer-targeted, MRI-ultrasensitive drug delivery systems. *Nano Lett* 6(11):2427-2430
197. Ungar EC, Porter T, Culp W et al (2004) Therapeutic applications of lipid-coated microbubbles. *Adv Drug Deliv Rev* 56:1291-1314
198. Lum AFH, Borden MA, Dayton PA et al (2006) Ultrasound radiation force enables targeted deposition of model drug carriers loaded on microbubbles. *J Control Release* 111:128-134
199. Shortencarrier MJ, Dayton PA, Bloch SH et al (2004) A method for radiation-force localized drug delivery using gas-filled lipospheres. *IEEE Trans Ultrason Ferroelectr Freq Control* 51(7):822-831
200. Rapoport N, Gao Z, Kennedy A (2007) Multifunctional nanoparticles for combining ultrasonic tumor imaging and targeted chemotherapy. *J Natl Cancer Inst* 99(14):1095-1106
201. Gao Z, Fain H, Rapoport N (2005) Controlled and targeted tumor chemotherapy by micellar-encapsulated drug and ultrasound. *J Control Release* 102:203-221
202. Brad PB, Aravind A, Parag V et al (2007) Magnetic resonance-guided, real-time targeted delivery and imaging of magnetocapsules immunoprotecting pancreatic islet cells. *Nat Med*. doi:10.1038/nm1581

Part III

Hydrogels for Tissue Engineering

Hydrogels for Tissue Engineering Applications

Rong Jin and Pieter J. Dijkstra

Abstract Hydrogels have been widely applied in biomedical applications, such as drug delivery and tissue engineering, due to their many favorable characteristics. Their high water content renders them compatible with living tissues and proteins and their rubbery nature minimizes damage to the surrounding tissue. Their mechanical properties parallel those of soft tissues, making them particularly appealing for engineering of these tissues. Hydrogels used in tissue engineering are preferably biodegradable, thus further surgery, after the hydrogels has performed its function, is not required. Also, biodegradable hydrogels allow for the replacement of the hydrogels over time by the extracellular matrix produced when cells are incorporated. The biofunctionality of hydrogels is essential to guide cellular behavior such as proliferation, differentiation, and matrix production. An on-demand biofunction can be obtained by the incorporation of growth factors into hydrogels to enhance cellular proliferation in the tissue-engineered matrices.

Introduction

Tissue engineering (TE) represents a promising method to regenerate damaged tissue or to replace organs that fail to function in the body [1]. The concept of tissue engineering was proposed by Langer et al. in the early 1990s as “the application of the principles and methods of engineering and the life sciences toward the fundamental understanding of structure–function relationships in normal and pathological mammalian tissues and the development of biological substitutes that restore, maintain or improve tissue function” [1]. This strategy of tissue engineering generally involves the incorporation of the appropriate cells into a tissue-engineered scaffold, which serves as a temporary extracellular matrix (ECM) until cells produce the matrix along time and finally neo-tissue replaces the scaffold. The scaffold plays an important role in regulating cell migration, proliferation, and ECM production [2, 3]. The scaffolds should provide physical and biological properties such as sufficient mechanical strength, preventing cells from floating out of the defect, facilitating cell proliferation, cell signaling, and stimulating matrix production by cells. Therefore, the macromolecular engineering of scaffolds is an essential requisite for successful tissue engineering.

The scaffolds commonly involved in tissue engineering are either solid-type substances like foams, meshes, and sponges, or gels-like materials. The use of hydrogels can be traced back to 1960 when Wichterle and Lim first reported crosslinked hydroxyethyl methacrylate (HEMA) hydrogels for biological use [4]. Many hydrogels have desired biotraits, such as high and tissue-like water content as well as excellent permeability for influx of nutrients and excretion of metabolites. Hydrogels, unlike solid-type scaffolds, such as fibrous meshes and porous sponges, encapsulate and retain cells in a 3-D environment surrounded by gels

R. Jin and P.J. Dijkstra • Polymer Chemistry and Biomaterials, Faculty of Science and Technology, University of Twente, Enschede, The Netherlands
e-mail: P.J.Dijkstra@utwente.nl

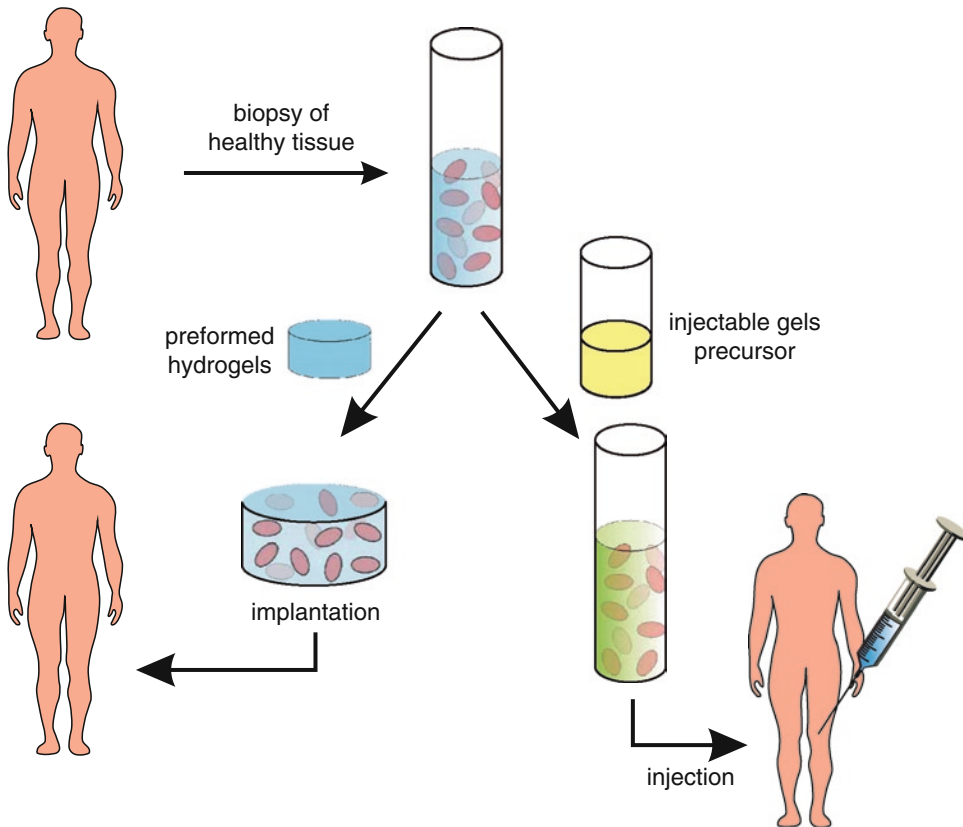


Fig. 1. TE strategies using preformed and injectable hydrogels in combination with cells.

matrix rather than promote attachment, preventing potential phenotype dedifferentiation [5]. These features make hydrogels especially suitable as engineered scaffolds. Hydrogels can be either preformed and inserted, or injected. The preformed hydrogels are processed in vitro prior to cell seeding and in vivo implantation. The injectable hydrogels can be implanted into the body as a liquid that gels in situ. Importantly, cells and growth factors can be incorporated and suspended in the gels precursors prior to gelation [6], enabling homogenous cell seeding and easy implantation (Fig. 1).

The criteria for design of hydrogels in tissue engineering and the strategies used for developing hydrogels materials for this purpose are extremely critical.

Hydrogels Designs for Tissue Engineering

There are several important requisites that have to be met in the design of hydrogels as scaffolds for tissue engineering. These requisites include biocompatibility, biodegradability, mechanical strength, and multiple biofunctionality. Hydrogels must be biocompatible so as to not induce an immune response and severe inflammation nor have any influence (e.g., temperature, pH value) on the surrounding tissue and cells within the gels, maintain tissue bioactivity and cell survival. Hence, toxic crosslinkers, initiators, or organic solvents used

should be completely leached out from a preformed hydrogels. For an injectable process, the precursors and the hydrogels must be completely biocompatible. Since the gels are generally formed under physiological conditions at a temperature of 37°C and a pH of about 7.4, organic solvents and harsh gelation conditions like strong bases or acids must be avoided. Moreover, during the regeneration process of neo-tissue, the degradation products leaching from or generated by the hydrogels should not accumulate in the body but be readily metabolized or excreted from the body.

Biodegradability of hydrogels is essential for tissue engineering (TE) scaffolds. Biodegradable hydrogels usually function as a temporary extracellular matrix (ECM) until replaced by neo-tissue. The degradation properties of hydrogels play an important role in controlling cell migration [7, 8] and influencing ECM production and distribution [9–14]. Degradable hydrogels are derived from biodegradable polymers or water soluble hydrogels, which are based on hyaluronic acid (HA) [15], collagen [16], chitosan [17], and poly(lactic acid) (PLA) [10, 11]. Degradation of hydrogels will generally lead to a loss in mechanical strength and final disintegration. Hence, the degradation rate of the gels needs to be carefully adjusted to match the rate of neo-tissue formation. This rate can be controlled by the molecular weight of the polymers used, in combination with hydrolytically unstable groups and crosslinking density.

In the design of hydrogels as tissue-engineered scaffolds, adequate mechanical support is a critical requirement. Mechanical moduli of tissues range from 10 kPa–350 MPa for soft tissues and 10 MPa–30 GPa for hard tissues [2, 18]. Depending on the intended application, the scaffold should provide sufficient mechanical support in order to protect the seeded cells and the developing neo-tissue as well as to withstand the physiologic load. The mechanical properties of a scaffold are highly potent regulators of cell migration and their phenotype [19]. Mesenchymal stem cells differentiated into various cell types depending on the elasticity of the polyacrylamide gels substrates on which they were cultured [20]. Mechanical moduli of hydrogels are generally increasing with increasing crosslinking density. However, increase in mechanical moduli can result in decreased cell metabolic activity, giving an inferior biocompatibility [21].

The biofunctionality of hydrogels is essential to guide cellular behavior such as proliferation, differentiation, and matrix production. It has been shown that an on-demand biofunction can be obtained by incorporation of growth factors into hydrogels to enhance cellular proliferation [22]. Growth factors commonly used in tissue engineering include bone morphogenetic protein (BMP), transforming growth factor (TGF), insulin-like growth factor (IGF), vascular endothelial growth factor (VEGF), and basic fibroblast growth factor (bFGF) (Table 1).

Researchers are also seeking to make hydrogels without growth factors that structurally and functionally resemble the natural ECM. A straightforward method is the use of natural ECM components such as collagen, hyaluronic acid, and fibrin to create hybrid hydrogels that are biocompatible and can provide appropriate signals to regulate cell behavior [23]. Hydrogels, modified with bioactive molecules, can also elicit specific cellular functions and direct cell–cell and cell–materials interactions. For example, hydrogels can promote cell adhesion and migration when they incorporate long chain ECM proteins such as fibronectin (FN) [24] and laminin (LN) [25]. Recently, short peptide sequences have been covalently conjugated to hydrogels, including Arg-Gly-Asp (RGD), Ile-Lys-Val-Ala-Val (IKVAV), and Tyr-Ile-Gly-Ser-Arg (YIGSR) since they are identified as dominant segments to perform bioactive functions in receptor binding and host cell attachment.

Table 1. Commonly used growth factors in hydrogels for tissue engineering [178]

Growth factor	Function	Hydrogels scaffold	Tissue regenerated	Ref.
BMP	Differentiation and migration of bone forming cells; Stimulating the synthesis and inhibiting degradation of proteoglycans	Acrylated HA/ PEG-thiol	Bone	[6]
		Alginate	Cartilage	[179]
TGF- β	Regulation of cell proliferation, differentiation; Stimulating production of proteoglycans and other matrix components	PLA-PEG-PLA	Bone	[180]
		OPF	Cartilage	[118]
IGF	Enhancing the differentiated function of osteoblast; promotion of cartilage and bone formation	PEODM	Cartilage	[181]
VEGF	Migration, proliferation, and survival of endothelial cells; initiation of angiogenesis	HA-thiol/PEGDA	Angiogenesis	[42]
bFGF	Potent modulators of cell proliferation, motility, differentiation, and survival; initiation of angiogenesis osteogenesis and chondrogenesis	Pluronic/heparin	Angiogenesis	[103]
		Matrigel	Adipogenesis	[182]
		Gelatin	Bone	[183]
		P(NIPAAm-co-AAc)	Cartilage	[184]

Crosslinking Methods to Form Hydrogels

Hydrogels can be classified into chemical and physical gels according to their crosslinks present. Various crosslinking approaches to prepare hydrogels are used in order to achieve specific properties, such as gelation time, mechanical modulus, and biocompatibility of the ensuing hydrogels that are important for tissue engineering applications.

Chemical Crosslinking by Radical Polymerization

Free radical polymerization is frequently used to prepare hydrogels for bioapplications [26, 27]. Vinyl-bearing macromers polymerize to form hydrogels using redox or thermal initiators or photopolymerization using UV light. Commonly used synthetic polymers are poly(vinyl alcohol) (PVA) and poly(ethylene glycol) (PEG) [9–11, 28, 29] and natural polymers are hyaluronic acid [30], chitosan [31], and dextran [32]; others are illustrated in Fig. 2. The advantage of photo-initiation is fast crosslinking rates and the disadvantage is that cells exposed to UV at high intensity or for long times may have an adverse effect on cellular metabolic activity [33]. In addition, the heat release during the crosslinking process may cause cellular necrosis [34]. Therefore, the intensity of the UV light is limited to approximately 5–10 mW/cm² in order to prevent cell damage [35]. In vivo Polymerization by UV is hampered due to limited tissue penetration and absorption of the UV-light by the skin (>99%) [35]. Alternatively, thermal- or redox-initiated polymerization can be applied. Several groups reported on hydrogels for tissue engineering using the redox-initiator N,N,N',N'-tetramethyl ethylenediamine (TEMED) and ammonium peroxydisulfate (APS) [17, 36]. Increasing the concentration of the initiator resulted in a reduced gelation time and

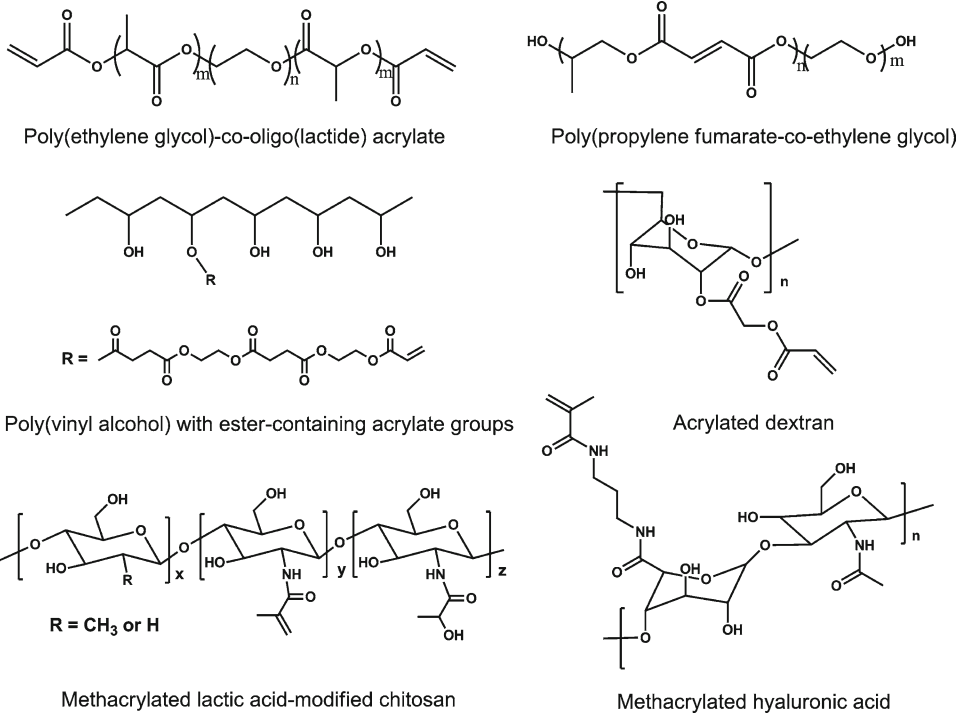


Fig. 2. Chemical structures of macromers used for the preparation of hydrogels by radical polymerization.

enhanced mechanical properties. However, a concomitant high cytotoxicity with low cell viability (<30%) at high concentrations of initiator (10 mM) was observed after a short cell culturing time of 4 days [17]. Therefore, a suitable method of free radical polymerization is necessary to arrive at appropriate hydrogels for tissue engineering.

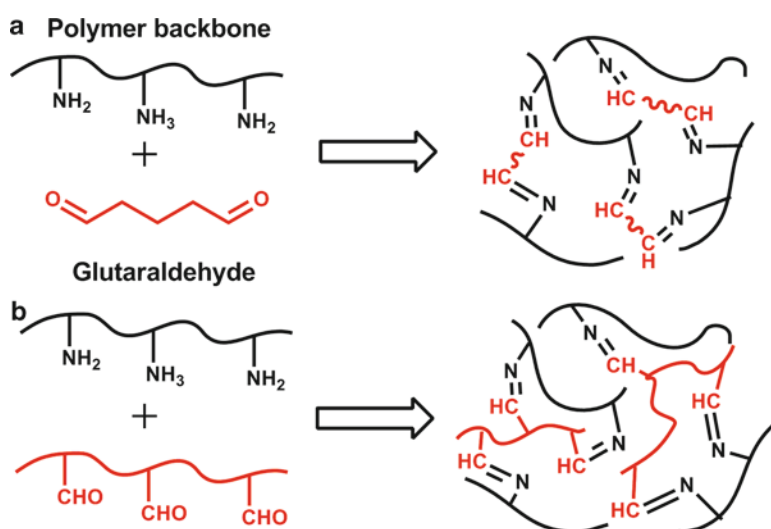
Crosslinking Functional Groups

Hydrogels can be prepared via reactions between functional groups present in the water-soluble monomers or macromonomers. Typical reactions are Schiff-base formation, Michael-type additions, peptide ligation as well as “click” chemistry (Table 2).

Schiff-base formation between an aldehyde and an amino group is often used to prepare crosslinked hydrogels [37, 38]. Glutaraldehyde as a crosslinker in this respect was frequently used (Fig. 3a). However, glutaraldehyde is toxic even at low concentrations and may leach out into the body during matrix degradation, inhibiting cell growth [39]. Thus, hydrogels prepared via glutaraldehyde crosslinking have to be extensively extracted to remove unreacted reagent. To avoid the toxicity associated with the use of glutaraldehyde, aldehyde-containing compounds are coupled to a nontoxic polymer such as hyaluronic acid [40] (Fig. 3b). Besides, reactive aldehyde groups can also be generated by oxidation of a polysaccharide, such as dextran [37], hyaluronic acid [38], and alginate [41]. Since Schiff bases are prone to degradation via hydrolysis of the imine bond at low pH, the addition of basic components like borax can facilitate Schiff-base formation to yield relatively stable hydrogels with fast gelation times [41].

Table 2. Summary of crosslinking methods via reactions between functional groups

Chemical reactions	Typical functional groups	Advantages	Limitations
Schiff-base formation	Amine/hydrazide & aldehyde	Easy incorporation and crosslinking of amine-bearing peptides and proteins	Aldehyde may induce side reactions in the body. Schiff-base linkages are usually unstable at low pH.
Michael-type addition	Acrylate/vinyl sulfone & thiol/amine	Mild reaction conditions, tunable properties, suitable for cell encapsulation	Unreacted thiol groups may influence cell viability
Peptide ligation	N-terminal cysteine & aldehyde	High substrate specificity, efficient crosslinking, mild reaction conditions	Complicated synthesis procedures of peptides due to protection and deprotection steps
Click chemistry	Azide & alkyne	An efficient, high-yielding reaction	Involvement of catalytic amounts of potentially toxic Cu

**Fig. 3.** Aldehyde/amine-containing polymers to prepare hydrogels via Schiff bases formation.

The Michael addition reaction between a nucleophile (an amine or a thiol group) and an electrophile (vinyl/acrylate/maleimide group) is another approach for preparation of hydrogels, especially for injectable hydrogels for tissue engineering (Fig. 4). Hydrogels are formed simply by mixing two polymers bearing nucleophilic and electrophilic groups. Many polymers, such as hyaluronic acid [42–44], dextran [45, 46], PVA [47], and PEG [44, 48, 49], have been conjugated with these groups to prepare hydrogels via Michael reactions. Using this reaction, thiol-bearing functional peptides (e.g., containing cysteine) were incorporated to yield biofunctional hydrogels, enhancing cell adhesion or matrix production [14, 49, 50]. Generally, the hydrogels that are prepared via Michael type addition have moderate gelation

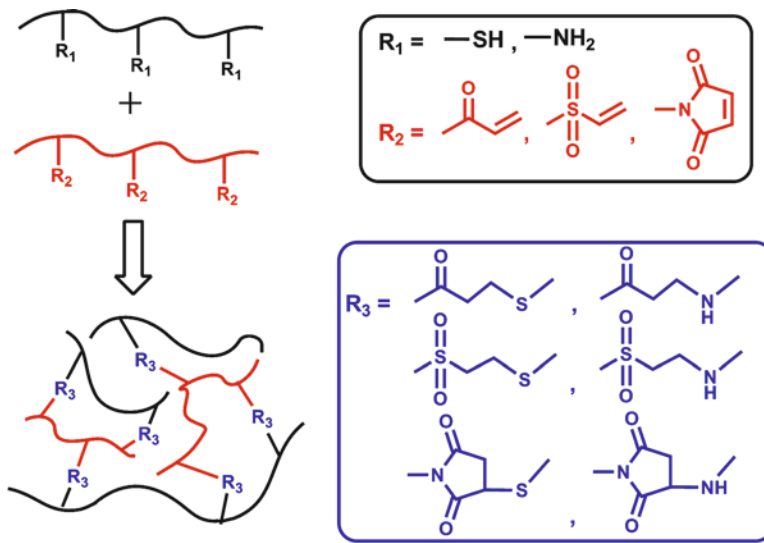


Fig. 4. Strategy of injectable hydrogels preparation via Michael-type additions

times (<0.5 to ~60 min) and moderate mechanical strength, and their properties can be adjusted by tuning the reactivity of the functional groups and crosslinking density [44–47]. Since Michael addition reactions take place under mild conditions, the reactions do not seriously influence cell viability during hydrogels formation. Usually, incorporated cells in hydrogels remain viable and survived from days to months [6, 50]. However, some caution has to be taken in the use of an excess of thiol functional groups as thiols may cause cell death [51].

Chemical peptide ligation, for the synthesis of proteins and enzymes is based on the chemoselective reaction of two unprotected peptide segments [52]. Peptide ligation for the preparation of hydrogels is based on the aldehyde groups of PEG derivatives and NH_2 -terminal cysteine moieties of peptide dendrons to form thiazolidine rings (Fig. 5a) [53]. The reactions were carried out under mild conditions and gelation took place within a few minutes. However, these hydrogels were intact for short periods of time (about 1 week) due to the reversible thiazolidine ring formation. Relatively stable hydrogels were prepared using PEG with end-capped ester-aldehyde groups instead of aldehyde groups via pseudoproline ring formation (Fig. 5b) [54]. The hydrogels retained their shape and size with less than 10% weight loss for more than 6 months.

“Click chemistry,” a highly efficient, quantitative reaction, can be carried out at physiological temperatures and pH by the copper-catalyzed 1,3-dipolar cycloaddition of azide and alkyne moieties (Fig. 6) [55]. Click chemistry has been used to synthesize polymer networks from functionalized synthetic polymers, such as PVA [56], PEG [57], poly(*N*-isopropylacrylamide-*co*-hydroxyethyl methacrylate) (P(NIPAAm-*co*-HEMA)) [58] as well as natural polymers like hyaluronic acid [59]. Lower degree of substitution with active pendant groups on polymers induces faster gelation [56]. Although copper-catalyzed click chemistry can be performed inside living cells [60], copper is known to be toxic to most bacterial and mammalian cells [61]. The removal of copper catalyst from hydrogels is difficult. Copper-free click reactions as an alternative to the conventional copper-catalyzed click chemistry offers a new route to prepare hydrogels for tissue engineering [61].

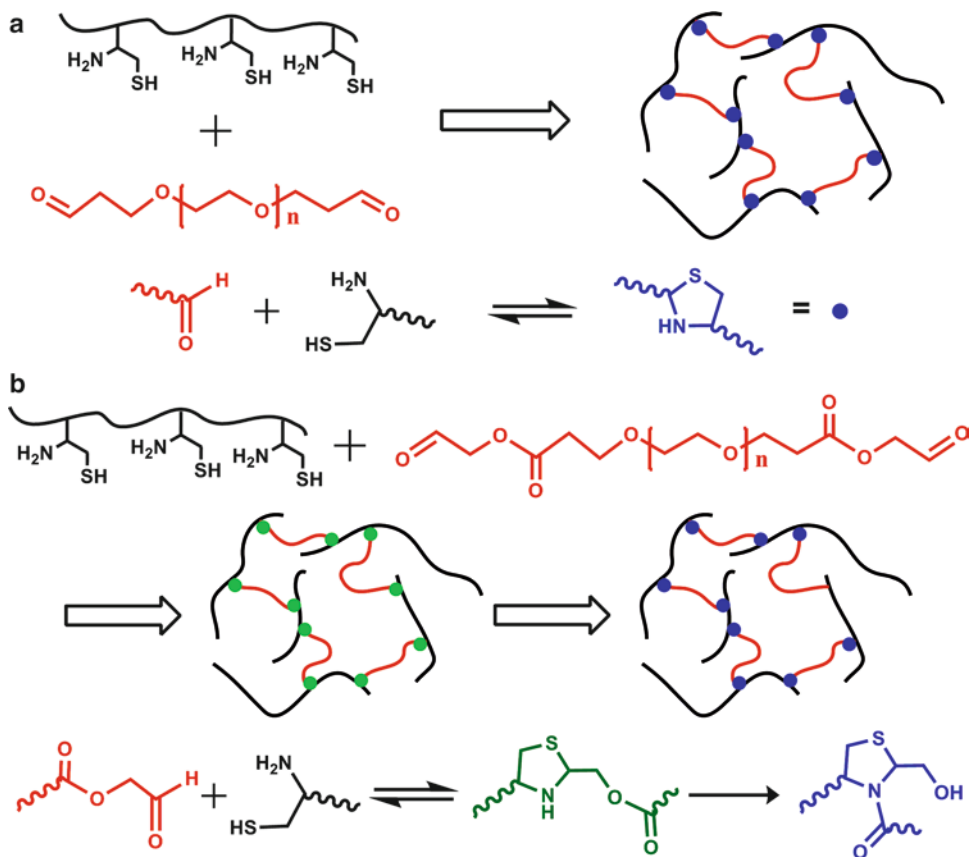


Fig. 5. Preparation of hydrogels via peptide ligation.

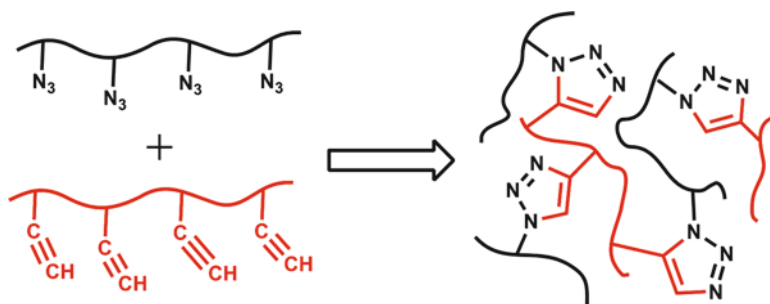


Fig. 6. Preparation of hydrogels via click chemistry.

Crosslinking by Enzymatic Reactions

Enzymes often exhibit a high degree of substrate specificity, potentially avoiding side reactions during crosslinking. With this advantage, it is possible to control and predict the gelation kinetics and increase the overall crosslinking rate by the enzyme concentration. Transglutaminase (TG) is a typical enzyme that is capable of catalyzing crosslinking reactions;

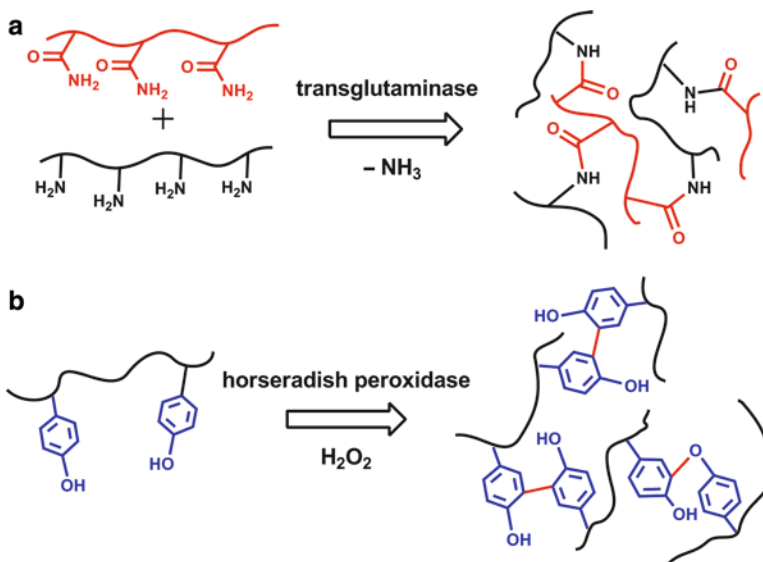


Fig. 7. Enzymatic crosslinking of (a) PEG or polypeptide conjugates or (b) polysaccharide conjugates.

it is a calcium-dependent enzyme that crosslinks proteins in vivo [62]. TG-catalyzed covalent crosslinking occurs via the formation of an amide linkage between the carboxamide and primary amines on polymers or polypeptides (Fig. 7a) [63]. TG hydrogels formation has been successfully used in a variety of systems, including PEG-peptide and polypeptide hydrogels [62, 64–68]. The gelation times can be shortened to a few minutes by rational designs of the peptide sequences that increase substrate specificity [67]. In addition, these hydrogels have good adhesive properties and are used as surgical tissue adhesives [68].

Horseradish peroxidase (HRP) (Fig. 7b) is a single-chain β -type hemoprotein that catalyzes the coupling of phenols or aniline derivatives in the presence of hydrogen peroxide [69]. Phenol conjugated poly(aspartic acid)s have been crosslinked with HRP and H₂O₂ to give hydrogels [70]. Similar approaches have been adopted to design hydrogels based on hyaluronic acid [6, 71], dextran [72], cellulose [73], and alginate [74]. These systems provide fast gelation (within 1 min), good mechanical, and degradation properties in hydrogels that can be tailored by varying the HRP/H₂O₂/substrate ratio.

Crosslinking by Stereocomplexation

Enantiomeric mixtures of polylactides (D- and L-PLA) that co-crystallize into a stereocomplex [75], are used in the design of hydrogels. Hydrogels formation occurs by mixing two water-soluble polymers containing PLLA and PDLA blocks. Stereocomplexed hydrogels have been made using dextran grafted with monodisperse L-lactic acid and D-lactic acid oligomers, respectively. At least eleven lactic acid units in the grafts appeared to be necessary for hydrogels formation [76, 77]. In similar approaches, hydrogels were based on poly(HEMA-g-OLA) [78] and stereocomplexation using PEG-PLLA and PEG-PDLA block copolymers [79, 80]. Hydrogels based on multi-arm block PEG-PLA copolymers have shorter gelation times and greater moduli than the triblock PEG-PLA copolymers (Fig. 8) [79].

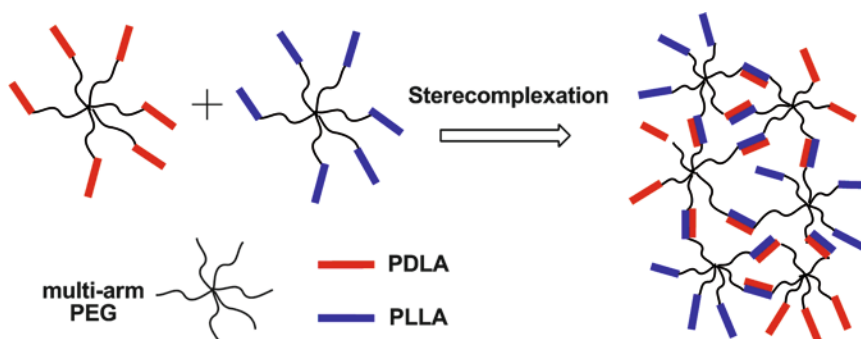


Fig. 8. Stereocomplexed hydrogels based on PEG and PLA star block copolymers.

Hydrogels by Thermo-Gelation

Thermo-sensitive gelation is triggered by hydrophobic interactions upon a change in temperature [39, 81]. Thermosensitive hydrogels based on poly(ethylene oxide)-poly(propylene oxide)-poly(ethylene oxide) (PEO-PPO-PEO, known as Pluronics) and poly(N-isopropylacrylamide) (PNIPAAm) are most commonly used. However, nondegradability and potential cytotoxicity of these gels limit their applications in tissue engineering. For example, significant decreases in cell viability of HepG2 cells occur in a 10% (w/w) Pluronic F127 solution. Cells encapsulation in hydrogels with F127 concentrations ranging from 15 to 20% (w/w) result in complete cell death within 5 days [82]. Alternatively, biodegradable thermo-sensitive hydrogels, such as block or graft copolymers containing hydrophilic PEO moieties and hydrophobic PLA moieties have lower cytotoxicity [83, 84]. Thermosensitive biodegradable gels can also be prepared from naturally occurring polymers, such as gelatin and agarose. Other natural water-soluble polymers, like polysaccharides, can be modified with a hydrophobic moiety to prepare physical hydrogels. A variety of temperature-sensitive hydrogels systems have been reported in other chapters [81, 85–87].

Crosslinking by Self Assembly

Supramolecular self-assembly is a powerful concept used in the design of biohydrogels. The coiled-coil, one of the basic folding patterns of native proteins, is utilized to design physically crosslinked hydrogels. Gelation is triggered when coils form during protein folding with two or more helices wind together to form a superhelix [88]. A series of self-assembly hydrogels containing coiled-coil protein motifs were made by either noncovalent or covalent grafts to a synthetic N-(2-hydroxypropyl)methacrylamide (HPMAm) copolymer backbone to form hybrid hydrogels (Fig. 9) [89–92]. The gelation process is influenced by the length and the number of coiled-coil grafts per chain. At least 4 heptads are needed to achieve hydrogels formation with gelation times ranging from a few minutes to several days [90]. Moreover, by changing the structural specificity of coiled-coils, gelation in PBS at concentrations as low as 0.1 wt% is possible [89]. In similar approaches, hydrogels were prepared from block polypeptides [93–96]. The gelation process of hydrogels from polypeptide amphiphiles depended not only on the overall amphiphilic nature of the polypeptides, but also on the chain conformation (α -helix, β -strand, or random coil) [95]. The thermal stability and self-assembling properties of these hydrogels are related to hydrophobic and electrostatic

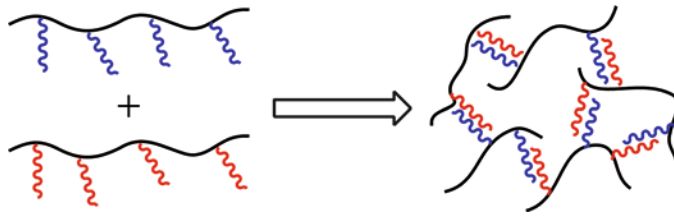


Fig. 9. Hydrogels formation through coiled-coil association.

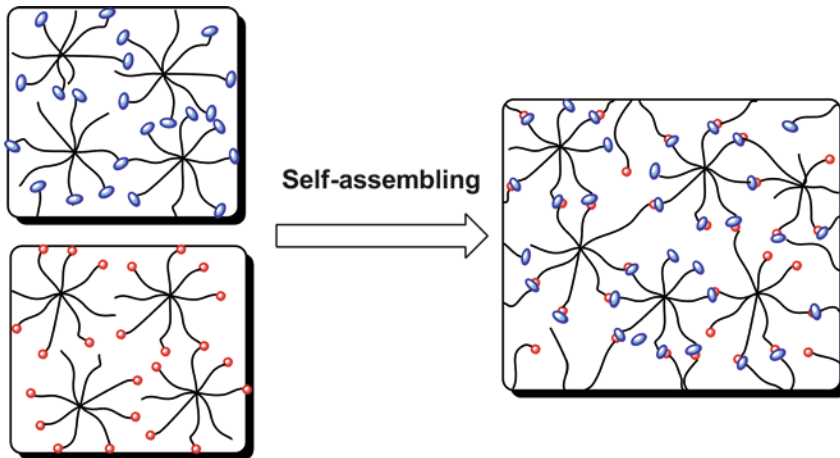


Fig. 10. Hydrogels concept based on inclusion complexes between cholesterol and α -CD moieties coupled to star-shaped 8-arm PEG (P).

interactions, which can be controlled by manipulating the amino acid sequences and block length of the coiled-coil domains [93, 94].

Crosslinking by Inclusion Complexation

Inclusion complexes between cyclodextrin (CD) and guest molecules represent a type of physical crosslinking that can be exploited for network formation. Cyclodextrins are cyclic oligosaccharides linked by α -1,4-glucosidic linkages. The three subtypes, α -, β -, and γ -CDs consisting of 6, 7, and 8 glucopyranose units, respectively, have a relatively hydrophobic interior cavity and a relatively hydrophilic outer surface [97]. These characteristic gives CDs the unique ability to form complexes in which lipophilic guest molecules are surrounded by the hydrophobic environment of the cavity. PEG hydrogels based on inclusion complexes between β -CD and cholesterol have been linked to the end groups of PEG [98]. The stability of these gels is influenced by temperature as they have significantly lower storage moduli at 37°C than at 4°C. Hydrogels have been formed by inclusion complexes between adamantyl-containing copolymers and CD dimers [99]. In addition to complexation with guest molecules, complex formation also takes place between CD and polymers, such as poly(ϵ -caprolactone) (PCL) and PEG [100]; for example, α -CDs form rapid gelation hydrogels with PLA-PEG-PLA and PEO-poly([R]-3-hydroxybutyrate)-PEO (PEO-PHB-PEO) (Fig. 10) [101, 102].

Combining Physical and Chemical Crosslinking

Due to the reversible interactions, physically in-situ formed hydrogels generally have lower mechanical properties than chemical hydrogels. The mechanical properties can be improved by increasing the crosslinking density and molecular weight of polymers, however, the viscosity of hydrogels precursors increases the difficulty in handling. For chemically in-situ formed hydrogels, the mechanical properties are much higher, but their preparation usually involves biologically unfavorable compounds that can lead to bio-incompatible materials. A combination of physical and chemical crosslinking offers the possibility of obtaining materials with improved physical and mechanical properties without compromising biocompatibility, for example, in the design of in situ hydrogels by combining stereocomplexation and photopolymerization an 8-arm PEG–PLLA and an 8-arm PEG–PDLLA, partly functionalized with methacrylate groups (40%), stereocomplexed hydrogels were formed upon mixing (Fig. 11) [35]. These hydrogels can be postcrosslinked by UV-irradiation. These double-crosslinked hydrogels showed increased mechanical moduli and prolonged degradation times compared to the hydrogels that were formed only by stereocomplexation. The photopolymerization takes place at much lower initiator concentrations (0.003 wt%) than conventional photocrosslinking systems (0.05 wt%), which greatly reduces the possibility of heating effects that can damage cells. Similar approaches are combinations of thermo-gelation, inclusive complexation, stereocomplexation, ligand-receptor interaction, Michael addition reactions, and photopolymerization [51, 101–111]. The advantages of combining two crosslinking mechanisms in one hydrogels system include fast gelation, controlled hydrogels properties, and improved biocompatibility with cells and proteins.

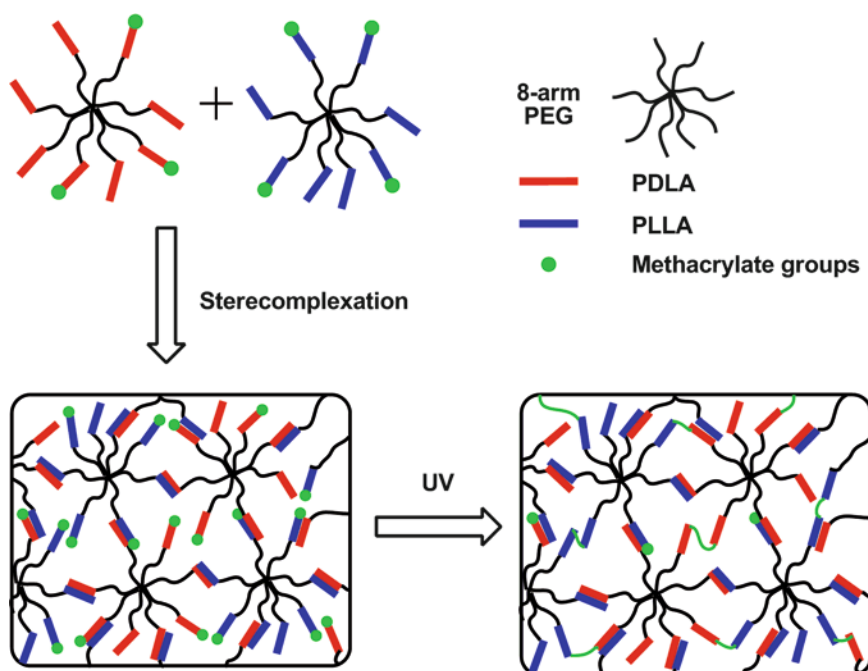


Fig. 11. Schematic representation of the preparation of hydrogels based on methacrylated PEG–PDLA and PEG–PLLA by stereocomplexation and post-UV irradiation.

Naturally Derived Hydrogels

Naturally derived polymers are widely used in the design of hydrogels for tissue engineering. Generally, these polymers are protein-based, such as collagen, gelatin and fibrin, or polysaccharide-based such as hyaluronic acid, alginate, chitosan, and dextran. Since naturally derived polymers are the components of the natural extracellular matrix, hydrogels prepared from these polymers may possess biofunctional features like modulating cell behavior and matrix production. Moreover, many naturally derived hydrogels are biocompatible, have a low cytotoxicity, and are enzymatically biodegraded in the human body [112].

Protein-Based Polymers

Collagen is the most abundant protein in connective tissues, such as cartilage, bone, skin, and tendon. It consists of specific peptide sequences that foster cell adhesion and cell-mediated degradation. Therefore, collagen-based hydrogels are regarded as the most suitable for scaffolds to repair damaged tissues and organs. Soluble collagen form physically-crosslinked hydrogels via thermo-gelation; however, rapid biodegradation and low mechanical strength of the hydrogels restrict their use in most tissue engineering applications [113]. Chemical crosslinking of soluble collagen can be used to produce hydrogels with a controlled degradation rate and improved mechanical properties. A typical collagen crosslinking method involves glutaraldehyde, but the potential toxicity of this crosslinker may compromise the *in vivo* biocompatibility of hydrogels [114], as an alternative, carbodiimides are used [115]. Chemical crosslinking methods that are used for collagen hydrogels can also be applied to form gelatin hydrogels for tissue engineering [23, 116, 117]. Gelatin microparticles, embedded in hydrogels networks for encapsulation and release of growth factors or plasmid DNA, enhance cellular and tissue regeneration [63, 118, 119].

The enzymatic polymerization of fibrinogen in the presence of thrombin is used to form fibrin gels [120]. Due to their biocompatibility and biodegradability, fibrin-based hydrogels are used in tissue engineering cartilage, bone, and adipose tissues [121]. Furthermore, fibrin is known to contain cell-binding sites and, therefore, is used as a substrate for cell adhesion and guiding cell migration. However, rapid degradation of fibrin before proper formation of neo-tissues represents a problem [122]. A number of strategies have been investigated to prolong the degradation time, such as addition of protease inhibitors to inhibit cell-excreted enzymes responsible for the degradation of fibrin [123] and chemical modifications, such as photocrosslinking PEGylated fibrin to increase the crosslinking density so as to hinder enzyme transport [124].

Peptide-based hydrogels are structurally and biofunctionally tunable at the genetic level to match the requirements in specific tissue regeneration applications. Genetically engineered peptides, such as elastin-like polypeptides (ELPs) that consists of the oligomeric repeats of the pentapeptide sequence Val-Pro-Gly-X-Gly (where X is any amino acid except proline) undergoes a sharp phase transition at 35°C to form coacervate hydrogels [125]. These coacervate hydrogels support chondrogenesis of chondrocytes [125] and human adipose derived adult stem cells *in vitro* [126]. ELP hydrogels prepared via enzymatic crosslinking by TG enzyme are used for cartilage repair [66], however, these ELP-based hydrogels generally have a low mechanical strength (moduli 80–280 Pa). Alternatively, lysine-containing ELP-based hydrogels that have a twofold to threefold higher modulus than noncrosslinked ELPs [127], were successfully implanted in a goat osteochondral defect model [128].

Similarly, hydrogels from silk-elastin like-polypeptides (SELPs), composed of amino acid sequence motifs from silk (Gly-Ala-Gly-Ala-Gly-Ser) and elastin (Gly-Val-Gly-Val-Pro), show in vitro chondrocytic differentiation and cartilage matrix accumulation of human mesenchymal stem cells [129].

Polysaccharides

Hyaluronic acid (HA) is a well-known polysaccharide that is composed of the repeating disaccharide units D-glucuronic acid and N-acetyl-D-glucosamine. It is one of the glycosaminoglycan (GAG) components in natural extracellular matrices (ECM) and plays an important role in many biological processes, such as lubrication, matrix assembly, cell proliferation, and differentiation [130, 131]. HA is nonimmunogenic and biodegradable, making it attractive in tissue engineering. In the ECM of most mature tissues, HA is present as a high molecular weight material (1–10MDa), therefore, an aqueous HA solution is highly viscous and difficult to handle. Low-molecular weight hyaluronic acid can be prepared by degradation either by acid or base treatment and is preferred for preparing hydrogels [132]. HA has abundant hydroxyl and carboxylic groups, which can be modified to give amine, hydrazide, thiol, acrylate, and phenol functionality [40, 43, 71, 133]. The mechanical and degradation properties of HA-based hydrogels are adjusted by the molecular weight, the degree of functionalization, and the polymer concentration [15, 134].

Chitosan is a partially deacetylated derivative of chitin, comprised of glucosamine and N-acetylglucosamine residues. Chitosan has a chemical structure similar to GAGs in the ECM of cartilage and may have related biofunctions favoring cartilage regeneration. Chitosan is known to be enzymatically degraded in vivo by lysozyme, which is found in cartilage [135–139]. Chitosan-based hydrogels are developed from acidified chitosan solutions, followed by neutralization with basic glycerophosphate [140, 141]. Chemical modifications of chitosan with different hydrophilic moieties are used to produce water-soluble chitosan derivatives [31, 142, 143]. Water-soluble chitosan derivatives can be used to prepare hydrogels either by physical or chemical crosslinking. Studies have demonstrated that chitosan-based hydrogels supported and enhanced chondrogenesis and osteogenesis both in vitro [144, 145] and in vivo [146].

Alginate, a naturally-occurring anionic polysaccharide composed of 1,4-linked β -D-mannuronate (M) and 1,4-linked α -L-guluronate (G) residues, is well-known for its gelling features with reversible crosslinking via ionic interactions between carboxylic groups and bivalent cations like Ca^{2+} [147]. The mild gelation conditions allow easy mixing of cells and active biomolecules in alginate hydrogels and make them attractive as cell and protein delivery carriers in tissue engineering. However, changes in the environment, such as pH and salt concentrations can release calcium ions and disruption of the gels. An alginate gels strength decreases ~40% within the first 9 days in vitro [148]. Covalent crosslinking of alginates by oxidative coupling [74] and Schiff-base formation [41] are being explored.

Dextran, a glucose homopolysaccharide consisting of an α -(1→6)-linked glucan with branches attached to the O-3 of the backbone chain units, is commercially available in a wide range of molecular weights. It is soluble in water forming low viscosity solutions, even at high concentrations (>20 wt%). Dextran can be chemically modified to introduce aldehyde groups [37] and other functional groups, such as (meth)acrylates [32, 149], thiols [46], phenols [72], maleimide [150], and vinyl sulfones [45]. Dextran-based hydrogels are used for sustained protein and drug delivery [151, 152] and, by incorporating specific cell-adhesive peptides, in tissue engineered scaffolds [153].

Synthetic Hydrogels

A wide variety of synthetic polymers are used in the design of hydrogels for tissue engineering. Synthetic hydrogels can be reliably produced in large quantities and are amenable to many structural variations. Moreover, the properties of synthetic hydrogels can be controlled by their composition, crosslinking density, and degradable linkages.

Hydrogels Based on PEG–PLA and PEG–PGA Copolymers

Poly(lactic acid) (PLA) and poly(glycolic acid) (PGA) are biocompatible and aliphatic biodegradable polyesters; however, they are hydrophobic and not soluble in water. PEG is a biocompatible water-soluble material. Using PEG as a starting material, water-soluble PEG–PLA, PEG–PGA, or PEG–PLGA block copolymers can be synthesized by ring-opening polymerization. By controlling the ratio of hydrophilic and hydrophobic moieties, these block copolymers can form physically-crosslinked hydrogels that exhibit thermosensitivity in water [86]. The block copolymers can also be endcapped with functional groups like acrylates enabling post chemical crosslinking as well [10, 101]. Hydrogels prepared from polyester-based polymers are degradable both *in vitro* and *in vivo* by hydrolytic cleavage of the ester linkages along the polymer backbones. Hydrolysis leads to degradation products, such as lactic acid and glycolic acid; as natural metabolites, these products are regarded as nontoxic.

Fumaric Acid-Based Hydrogels

Fumaric acid-based macromers including poly(propylene fumarate-co-ethylene glycol) (P(PF-co-EG)) and oligo(poly(ethylene glycol) fumarate) (OPF) are used as biocompatible biodegradable hydrogels. Degradation released fumaric acid is a well known product that is naturally formed in the Krebs cycle and is found in mammalian cell metabolism [154]. The presence of vinyl groups along the polymer backbone makes it an ideal substrate for crosslinking.

Hydrogels based on P(PF-co-EG) or OPF macromers are formed *in situ* in the presence of an initiator by photo- or redox-initiated crosslinking either between macromers or using crosslinking agents, such as N-vinyl-2-pyrrolidinone (NVP) and PEG diacrylate [155–157]. These hydrogels generally form mechanically strong networks that are biodegradable both *in vitro* and *in vivo* [155, 158–161]. Mechanical and swelling properties as well as degradation rates of the hydrogels are adjustable by changing the hydrophilicity and crosslinking density; these are controlled by changes in the molecular weight and molar ratio of the PEG, and the amount of macromers and crosslinkers, respectively [155, 162, 163]. The biocompatibility of these hydrogels is well-documented with respect to various cell types, such as chondrocytes [155], endothelial cells [154, 157] and marrow stromal cells [161, 164]. In cartilage and bone tissue engineering, these materials are used as carriers for marrow stromal cells or chondrocytes and have been shown to promote cellular differentiation and matrix production *in vitro* [155].

Hybrid Hydrogels

Successful tissue engineering requires biomimetic scaffolds that can be structurally and physically controlled, as well as to modulate specific cellular behavior. Synthetic polymers allow structural and compositional variations in the design of hydrogels, but mostly lack the

necessary biofunctionality. Hydrogels prepared from natural polymers encounter problems in batch-to-batch differences. Proteins and peptides are easily denatured by proteases or elicit immune responses in the body. These opportunities and limitations have been a motivation to develop hybrid hydrogels with tightly defined physical, chemical, and biological properties by the combination of synthetic polymers with natural polymers or peptide/protein sequences.

Illustrated in Fig. 12 are commonly used approaches to prepare hybrid hydrogels, and examples of hybrid hydrogels for tissue engineering are listed in Table 3. One approach is to crosslink proteins (collagen, albumin, and fibrinogen) conjugated with acrylated PEG and then photo-polymerized [165]. Enzymatic biodegradation and structural properties of these

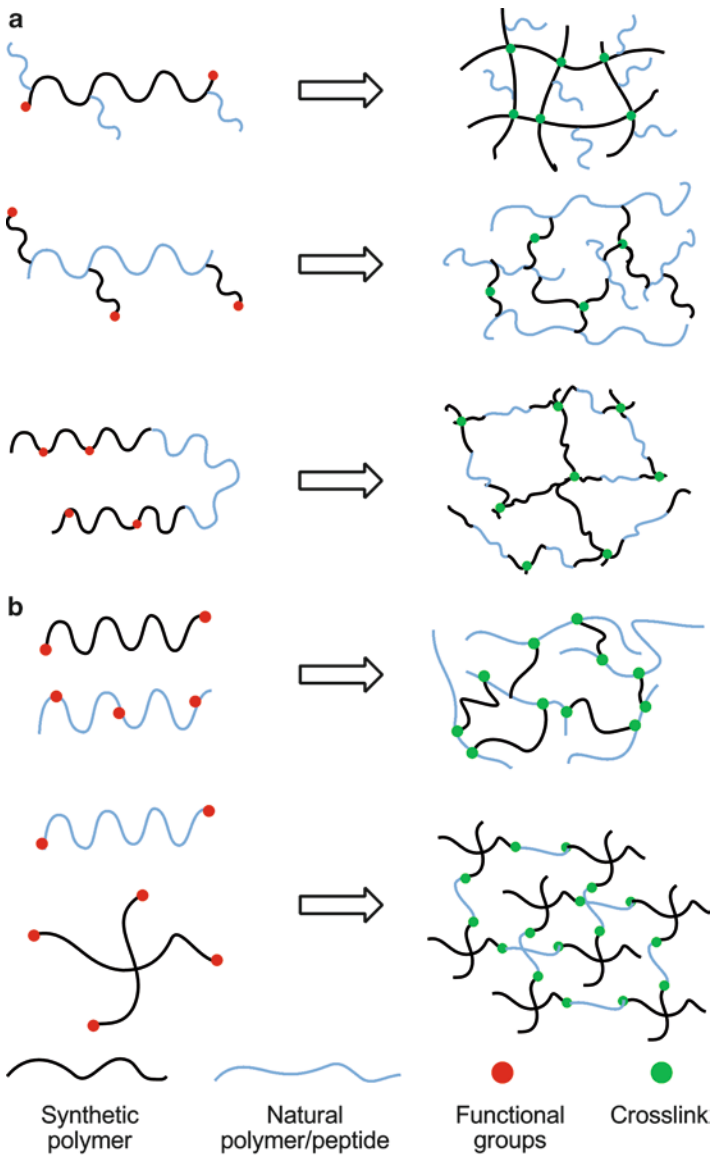


Fig. 12. Commonly used approaches in the preparation of hybrid hydrogels.

Table 3. Typical examples of hybrid hydrogels and their functionalities

Synthetic polymer	Biomimetic moiety	Bioconjugation method	Functionality	Ref.
PEG	Lysine and Glutamine substrate peptides	End group coupling	Enzymatic crosslinking, fast gelation	[185]
PEG	Heparin and VEGF	End group coupling	Growth factor-mediated crosslinking and gels erosion	[186]
PEG	MMP-sensitive peptide, engineered VEGF ₁₂₁ , RGD containing peptide	Crosslinking via Michael addition	Proteolytic degradability, cell adhesion, enhanced cell expression	[8, 14, 187]
PEG	Collagen, fibrinogen and albumin	Grafting	Cell adhesion, proteolytic degradability	[124, 188, 189]
PEG	collagen-mimic peptide	End group coupling	Retention of ECM production inside hydrogels via collagen binding	[165]
PVA or PEG	Chondroitin sulfate	Crosslinking via photopolymerization	Balance between modulus and swelling of hydrogels, enhanced matrix production	[28, 190]
Pluronic F127	Hyaluronic acid, RGD	Grafting and end group coupling	Improved cellular adhesion and proliferation, increased matrix production	[191]

hydrogels are easily controlled. The modified protein can maintain their cell-adhesive properties and support proteolytic degradability based on the specific characteristics of the protein backbone. Another approach is to crosslink mixtures of natural polymers and synthetic polymers; for example, proteolytically degradable hydrogels based on synthetic polymers and protease-sensitive peptide sequences [8, 14, 49, 150, 166, 167]. These peptide sequences are susceptible to local degradation upon excretion of cell-surface proteases, and the degradation rate of the hydrogels can be tailored by enzyme specificity to the peptide sequences [150]. The advantage of hybrid hydrogels is that multiple functionalities can be included in one gels system such as crosslinking ability, tunable physical properties, bioadhesive and proteolytic degradation properties, and enhanced extracellular matrix production.

Tissue Engineering Applications

Bone Graft Substitutes

Bone is a highly vascularized tissue that provides a rigid structure for muscle attachment in most higher vertebrates. Although bone tissue has a high capacity of self-healing, the repair and restoration of large segmental skeletal bone defects still remain a challenge. Hydrogels, embedded with progenitor or mature cells, may serve as bone graft substitutes for bone regeneration.

A variety of biofunctional sequences and/or growth factors can be introduced into hydrogels. Adhesive peptides, such as RGD sequences are incorporated into hydrogels to facilitate cell adhesion and spreading. Enhanced cell attachment and mineralized matrix deposition of osteoblasts embedded in RGD-modified PEG diacrylate (PEGDA) hydrogels were compared to RGD-free hydrogels [168], and that these hydrogels can promote the osteogenesis of bone marrow stromal cells in a dose-dependent manner [169]. The growth factor BMP-2 plays an important role in the expression of osteogenic markers, such as alkaline phosphatase (ALP) and osteocalcin [170]. However, direct incorporation of BMP-2 in hydrogels generally results in a burst release of about 18% during the first day [171]. Controlled release of the growth factor was achieved by using BMP-2 loaded nanoparticles (e.g., heparin functionalized PLGA) or microspheres (e.g., gelatin) [172]. In vivo experiments in rats showed that the maturity and the matrix mineralization of the regenerated bone are significantly improved in a fibrin hydrogels encapsulated with BMP-2 loaded PLGA nanoparticles [171]. The main limitation of hydrogels for bone tissue engineering is their inferior mechanical strength, which is at least 3–4 orders in magnitude lower than the native bone tissue. To address this limitation, novel matrix architectures were designed that combine a hydrogels with a 3-D bioresorbable synthetic framework, which is capable of maintaining structural integrity of tissue-engineered bone grafts in load-bearing applications [173]. For example, tricalcium phosphate (TCP) was combined with alginate gels for bone regeneration, and the addition of TCP helped to reduce swelling and gelation time and increase the stiffness [174].

Cartilage Regeneration

Cartilage is a flexible connective tissue in which chondrocytes are sparsely distributed in an extracellular matrix rich in proteoglycans (PGs) and collagen fibers. Cartilage has limited capacity for self-repair due to the avascular nature of cartilage and the low mitotic activity of chondrocytes. Chondrocytes readily undergo a dedifferentiation process during monolayer culturing and lose their phenotype. When cultured in hydrogels, chondrocytes were found to maintain their round morphology and be able to (re)differentiate [175]. Therefore, hydrogels are potential materials that can function as scaffolds for chondrocyte culturing and cartilage regeneration.

Several factors may influence cartilage regeneration and its ability to recover or maintain the chondrocyte phenotype. Recent studies showed that degradable hydrogels induced a more homogenous distribution of GAG than nondegradable hydrogels [9]. However, in fast degrading hydrogels, void spaces are generally present before new matrix formation [10, 11]. Therefore, the degradation rate of hydrogels are tailored by a combination of fast degrading linkages with slower degrading crosslinks [9–13]. Poor integration of neocartilage with native cartilage tissue is a major obstacle to cartilage regeneration. One main strategy is to take advantage of the presence of collagen type II in native cartilage that can chemically react with functional groups of the gels precursor molecules. For example, tissue-initiated polymerization was carried out between acrylate groups in polymerizable PEGDA macromers and tyrosine groups in collagen when exposed to light and an oxidative reagent like H_2O_2 , resulting in improved tissue adhesion and integration [176] (Fig. 13). In another approach, adhesion and integration with native cartilage were achieved using aldehyde functionalized methacrylated chondroitin sulfate (CSMA), which was covalently attached to collagen via Schiff-base formation [177]. The CSMA layer was further polymerized by photo-crosslinking of PEGDA to give a gels/cartilage integrated scaffold.

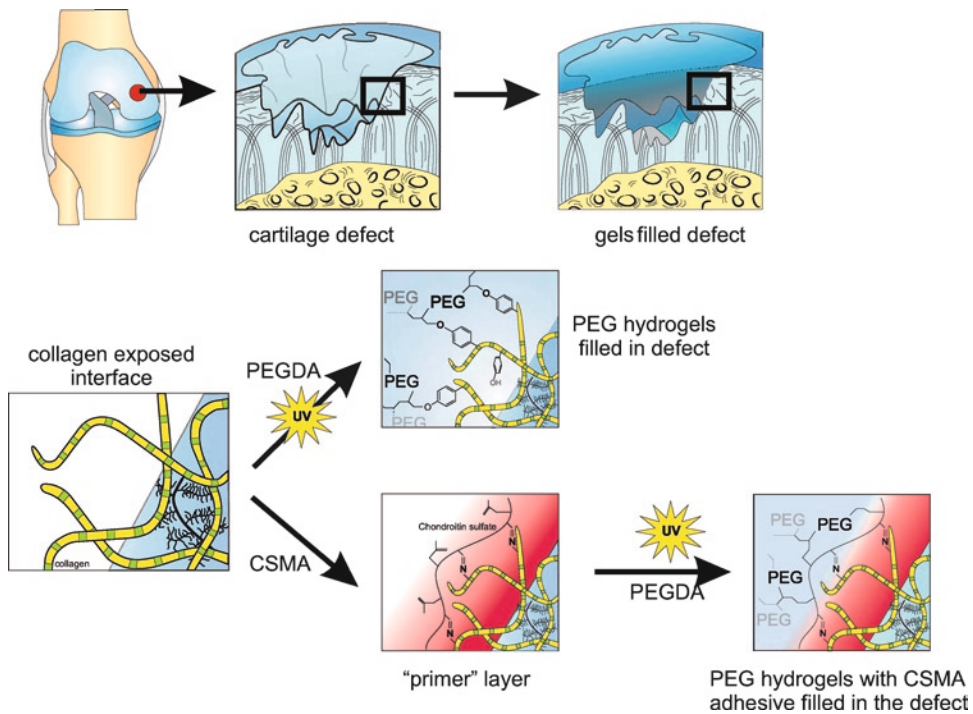


Fig. 13. Strategy of hydrogels-cartilage integration by tissue-initiated photopolymerization.

Summary

Chemical synthesis and protein engineering provide significant opportunities for the design of hydrogels with multifunctional properties on demand for tissue engineering applications. The fast progress in molecular biology inspires researchers to design smart and biofunctional hydrogels. Polymer composition and structures, hydrogels forming methods, degradation properties, mechanical strength, and biocompatibility are of significant importance. Artificial extracellular matrices combining hydrogels scaffolds, cells and growth factors hold great promise for tissue regeneration both *in vitro* and *in vivo*, and pave the way for treatment of diseases and replacement of organs. Preclinical studies show encouraging outcomes using these artificial matrices.

References

1. Langer R, Vacanti JP (1993) *Science* 260:920–926
2. Yang S, Leong K-F, Du Z et al (2001) *Tissue Eng* 7:679–689
3. Drury JL, Mooney DJ (2003) *Biomaterials* 24:4337–4351
4. Wichterle O, Lim D (1960) *Nature* 185:117–118
5. Kuo CK, Li W-J, Mauck RL et al (2006) *Curr Opin Rheumatol* 18:64–73
6. Kim J, Kim IS, Cho TH et al (2007) *Biomaterials* 28:1830–1837
7. Kamath KR, Park K (1993) *Adv Drug Deliv Rev* 11:59–84
8. Raebler GP, Lutolf MP, Hubbell JA (2005) *Biophys J* 89:1374–1388

9. Bryant SJ, Anseth KS (2002) *J Biomed Mater Res* 59:63–72
10. Bryant SJ, Anseth KS (2003) *J Biomed Mater Res A* 64A:70–79
11. Martens PJ, Bryant SJ, Anseth KS (2003) *Biomacromolecules* 4:283–292
12. Bryant SJ, Durand KL, Anseth KS (2003) *J Biomed Mater Res A* 67A:1430–1436
13. Bryant SJ, Bender RJ, Durand KL et al (2004) *Biotechnol Bioeng* 86:747–755
14. Lutolf MP, Lauer-Fields JL, Schmoekel HG et al (2003) *Proc Natl Acad Sci U S A* 100:5413–5418
15. Burdick JA, Chung C, Jia X et al (2005) *Biomacromolecules* 6:386–391
16. Ibusuki S, Halbesma GJ, Randolph MA et al (2007) *Tissue Eng* 13:1995–2001
17. Hong Y, Song H, Gong Y et al (2007) *Acta Biomater* 3:23–31
18. Lu L, Zhu X, Valenzuela RG et al (2001) *Clin Orthop Relat Res* 391S:S251–S270
19. Breuls RGM, Jiya TU, Smit TH (2008) *Open Orthop J* 2:103–109
20. Engler AJ, Sen S, Sweeney HL et al (2006) *Cell* 126:677–689
21. Chung C, Burdick JA (2008) *Adv Drug Deliv Rev* 60:243–262
22. Narine K, Wever OD, Valckenborgh DV et al (2006) *Tissue Eng* 12:2707–2716
23. Malafaya PB, Silva GA, Reis RL (2007) *Adv Drug Deliv Rev* 59:207–233
24. Nuttelman CR, Mortisen DJ, Henry SM et al (2001) *J Biomed Mater Res* 57:217–223
25. Stabenfeldt SE, Garcia AJ, LaPlaca MC (2006) *J Biomed Mater Res A* 77A:718–725
26. Ifkovits JL, Burdick JA (2007) *Tissue Eng* 13:2369–2385
27. Nguyen KT, West JL (2002) *Biomaterials* 23:4307–4314
28. Bryant SJ, Davis-Arehart KA, Luo N et al (2004) *Macromolecules* 37:6726–6733
29. Mawad D, Martens PJ, Odell RA et al (2007) *Biomaterials* 28:947–955
30. Park YD, Tirelli N, Hubbell JA (2003) *Biomaterials* 24:893–900
31. Hong Y, Mao Z, Wang H et al (2006) *J Biomed Mater Res A* 79A:913–922
32. Kim SH, Won CY, Chu CC (1999) *Carbohydr Polym* 40:183–190
33. Bryant SJ, Nuttelman CR, Anseth KS (2000) *J Biomater Sci Polym Ed* 11:439–457
34. Lukaszczyk J, Smiga M, Jaszcz K et al (2005) *Macromol Biosci* 5:64–69
35. Hiemstra C, Zhou W, Zhong Z et al (2007) *J Am Chem Soc* 129:9918–9926
36. Zhu W, Ding J (2006) *J Appl Polym Sci Symp* 99:2375–2383
37. Maia J, Ferreira L, Carvalho R et al (2005) *Polymer* 46:9604–9614
38. Lee KY, Alsberg E, Mooney DJ (2001) *J Biomed Mater Res* 56:228–233
39. Hennink WE, van Nostrum CF (2002) *Adv Drug Deliv Rev* 54:13–36
40. Bulpitt P, Aeschlimann D (1999) *J Biomed Mater Res* 47:152–169
41. Balakrishnan B, Jayakrishnan A (2005) *Biomaterials* 26:3941–3951
42. Riley CM, Fuegy PW, Firpo MA et al (2006) *Biomaterials* 27:5935–5943
43. Zheng Shu X, Liu Y, Palumbo FS et al (2004) *Biomaterials* 25:1339–1348
44. Vanderhooff JL, Mann BK, Prestwich GD (2007) *Biomacromolecules* 8:2883–2889
45. Hiemstra C, vanderAa LJ, Zhong Z et al (2007) *Macromolecules* 40:1165–1173
46. Hiemstra C, vanderAa LJ, Zhong Z et al (2007) *Biomacromolecules* 8:1548–1556
47. Tortora M, Cavalieri F, Chiessi E et al (2007) *Biomacromolecules* 8:209–214
48. Metters A, Hubbell J (2005) *Biomacromolecules* 6:290–301
49. Lutolf MP, Raeber GP, Zisch AH et al (2003) *Adv Mater* 15:888–892
50. Park Y, Lutolf MP, Hubbell JA et al (2004) *Tissue Eng* 10:515–522
51. Salinas CN, Cole BB, Kasko AM et al (2007) *Tissue Eng* 13:1025–1034
52. Cotton GJ, Muir TW (1999) *Chem & Biol* 6:R247–R256
53. Wathier M, Jung PJ, Carnahan MA et al (2004) *J Am Chem Soc* 126:12744–12745
54. Wathier M, Johnson CS, Kim T et al (2006) *Bioconjug Chem* 17:873–876
55. Rostovtsev VV, Green LG, Fokin VV et al (2002) *Angew Chem Int Edit* 41:2596–2599
56. Ossipov DA, Hilborn J (2006) *Macromolecules* 39:1709–1718
57. Malkoch M, Vestberg R, Gupta N et al (2006) *Chem Commun* 2006:2774–6
58. Xu X-D, Chen C-S, Wang Z-C et al (2008) *J Polym Sci A Polym Chem* 46:5263–5277
59. Crescenzi V, Cornelio L, DiMeo C et al (2007) *Biomacromolecules* 8:1844–1850
60. Speers AE, Cravatt BF (2004) *Chem & Biol* 11:535–546
61. Johnson JA, Baskin JM, Bertozzi CR et al (2008) *Chem Commun* 2008:3064–3066
62. Sanborn TJ, Messersmith PB, Barron AE (2002) *Biomaterials* 23:2703–2710
63. Park H, Temenoff JS, Holland TA et al (2005) *Biomaterials* 26:7095–7103
64. Sperinde JJ, Griffith LG (1997) *Macromolecules* 30:5255–5264
65. Sperinde JJ, Griffith LG (2000) *Macromolecules* 33:5476–5480
66. McHale MK, Setton LA, Chilkoti A (2005) *Tissue Eng* 11:1768–1779

67. Au A, Ha J, Polotsky A et al (2003) *J Biomed Mater Res A* 67A:1310–1319
68. Raeber GP, Lutolf MP, Hubbell JA (2005) *Biophys J* 89:1374–1388
69. Kobayashi S, Uyama H, Kimura S (2001) *Chem Rev* 101:3793–3818
70. Sofia SJ, Singh A, Kaplan DL (2002) *J Macromol Sci phys A* 39:1151–1181
71. Kurisawa M, Chung JE, Yang YY et al (2005) *Chem Commun* 2005:4312–4314
72. Jin R, Hiemstra C, Zhong Z et al (2007) *Biomaterials* 28:2791–2800
73. Ogushi Y, Sakai S, Kawakami K (2007) *J Biosci Bioeng* 104:30–33
74. Sakai S, Kawakami K (2007) *Acta Biomater* 3:495–501
75. Hideto T (2005) *Macromol Biosci* 5:569–597
76. de Jong SJ, De Smedt SC, Wahls MWC et al (2000) *Macromolecules* 33:3680–3686
77. De Jong SJ, van Eerdenbrugh B, van Nostrum CF et al (2001) *J Contr Release* 71:261–275
78. Lim DW, Choi SH, Park TG (2000) *Macromol Rapid Comm* 21:464–471
79. Hiemstra C, Zhong Z, Li L et al (2006) *Biomacromolecules* 7:2790–2795
80. Hiemstra C, Zhong Z, Dijkstra PJ et al (2005) *Macromol Symp* 224:119–132
81. Ruel-Gariepy E, Leroux J-C (2004) *Eur J Pharm Biopharm* 58:409–426
82. Khattak SF, Bhatia SR, Roberts SC (2005) *Tissue Eng* 11:974–983
83. Jeong B, Bae YH, Lee DS et al (1997) *Nature* 388:860–862
84. Jeong B, Lee KM, Gutowska A et al (2002) *Biomacromolecules* 3:865–868
85. Jeong B, Kim SW, Bae YH (2002) *Adv Drug Deliv Rev* 54:37–51
86. Klouda L, Mikos AG (2008) *Eur J Pharm Biopharm* 68:34–45
87. He C, Kim SW, Lee DS (2008) *J Contr Release* 127:189–207
88. Yu YB (2002) *Adv Drug Deliv Rev* 54:1113–1129
89. Yang J, Xu C, Wang C et al (2006) *Biomacromolecules* 7:1187–1195
90. Yang J, Xu C, Kopeckova P et al (2006) *Macromol Biosci* 6:201–209
91. Wang C, Stewart RJ, Kopecek J (1999) *Nature* 397:417–420
92. Wang C, Kopecek J, Stewart RJ (2001) *Biomacromolecules* 2:912–920
93. Xu C, Kopecek J (2008) *Pharm Res* 25:674–682
94. Xu C, Breedveld V, Kopecek J (2005) *Biomacromolecules* 6:1739–1749
95. Nowak AP, Breedveld V, Pakstis L et al (2002) *Nature* 417:424–428
96. Pakstis LM, Ozbas B, Hales KD et al (2004) *Biomacromolecules* 5:312–318
97. Uekama K, Hirayama F, Irie T (1998) *Chem Rev* 98:2045–2076
98. vandeManakker F, vanderPot M, Vermonden T et al (2008) *Macromolecules* 41:1766–1773
99. Kretschmann O, Choi SW, Miyauchi M et al (2006) *Angew Chem Int Edit* 45:4361–4365
100. Loethen S, Kim J-M, Thompson DH (2007) *Polymer Rev* 47:383–418
101. Wei H, He J, Sun L-g et al (2005) *Eur Polymer J* 41:948–957
102. Li J, Li X, Ni X et al (2006) *Biomaterials* 27:4132–4140
103. Yoon JJ, Chung HJ, Park TG (2007) *J Biomed Mater Res A* 83A:597–605
104. Cellesi F, Tirelli N, Hubbell JA (2004) *Biomaterials* 25:5115–5124
105. Kim MR, Park TG (2002) *J Contr Release* 80:69–77
106. Niu G, Zhang H, Song L et al (2008) *Biomacromolecules* 9:2621–2628
107. Robb SA, Lee BH, McLemore R et al (2007) *Biomacromolecules* 8:2294–2300
108. Lee JB, Yoon JJ, Lee DS et al (2004) *J Biomater Sci Polymer Ed* 15:1571–1583
109. Vermonden T, Fedorovich NE, van Geemen D et al (2008) *Biomacromolecules* 9:919–926
110. Chung HJ, Lee Y, Park TG (2008) *J Contr Release* 127:22–30
111. Seal BL, Panitch A (2006) *Acta Biomater* 2:241–251
112. Hayashi T (1994) *Prog Polymer Sci* 19:663–702
113. Ma L, Gao C, Mao Z et al (2003) *Biomaterials* 24:4833–4841
114. Gough JE, Scotchford CA, Downes S (2002) *J Biomed Mater Res* 61:121–130
115. Wissink MJB, Beernink R, Pieper JS et al (2001) *Biomaterials* 22:151–163
116. Kuijpers AJ, Engbers GHM, Krijgsveld J et al (2000) *J Biomater Sci Polym Ed* 11:225–243
117. Hoshikawa A, Nakayama Y, Matsuda T et al (2006) *Tissue Eng* 12:2333–2341
118. Park H, Temenoff JS, Tabata Y et al (2007) *Biomaterials* 28:3217–3227
119. Young S, Wong M, Tabata Y et al (2005) *J Contr Release* 109:256–274
120. Lee KY, Mooney DJ (2001) *Chem Rev* 101:1869–1880
121. Ahmed TAE, Dare EV, Hincke M (2008) *Tissue Eng B: Rev* 14:199–215
122. Fussenegger M, Meinhart J, Hobling W et al (2003) *Ann Plast Surg* 51:493–498
123. Ahmed TAE, Griffith M, Hincke M (2007) *Tissue Eng* 13:1469–1477
124. Dikovskiy D, Bianco-Peled H, Seliktar D (2006) *Biomaterials* 27:1496–1506

125. Betre H, Setton LA, Meyer DE et al (2002) *Biomacromolecules* 3:910–916
126. Betre H, Ong SR, Guilak F et al (2006) *Biomaterials* 27:91–99
127. Lim DW, Nettles DL, Setton LA et al (2007) *Biomacromolecules* 8:1463–1470
128. Nettles DL, Kitaoka K, Hanson NA et al (2008) *Tissue Eng A* 14:1133–1140
129. Haider M, Cappello J, Ghandehari H et al (2008) *Pharm Res* 25:692–699
130. Laurent TC, Fraser JR (1992) *FASEB J* 6:2397–2404
131. Kawasaki K, Ochi M, Uchio Y et al (1999) *J Cell Physiol* 179:142–148
132. Tokita Y, Okamoto A (1995) *Polymer Degrad Stabil* 48:269–273
133. Nettles DL, Vail TP, Morgan MT et al (2004) *Ann Biomed Eng* 32:391–397
134. Chung C, Mesa J, Randolph MA et al (2006) *J Biomed Mater Res A* 77A:518–525
135. Onishi H, Machida Y (1999) *Biomaterials* 20:175–182
136. Moss JM, Van Damme M-PI, Murphy WH et al (1997) *Arch Biochem Biophys* 339:172–182
137. Francis Suh JK, Matthew HWT (2000) *Biomaterials* 21:2589–2598
138. Di Martino A, Sittinger M, Risbud MV (2005) *Biomaterials* 26:5983–5990
139. Kim I-Y, Seo S-J, Moon H-S et al (2008) *Biotechnol Adv* 26:1–21
140. Wu J, Su Z-G, Ma G-H (2006) *Int J Pharm* 315:1–11
141. Chenite A, Chaput C, Wang D et al (2000) *Biomaterials* 21:2155–2161
142. Bhattarai N, Ramay HR, Gunn J et al (2005) *J Contr Release* 103:609–624
143. Ono K, Saito Y, Yura H et al (2000) *J Biomed Mater Res* 49:289–295
144. Marsich E, Borgogna M, Donati I et al (2008) *J Biomed Mater Res A* 84A:364–376
145. Sechrist VF, Miao YJ, Niyibizi C et al (2000) *J Biomed Mater Res* 49:534–541
146. Hoemann CD, Sun J, Légaré A et al (2005) *Osteoarthritis Cartilage* 13:318–329
147. Kuo CK, Ma PX (2001) *Biomaterials* 22:511–521
148. Shoichet MS, Li RH, White ML et al (1996) *Biotechnol Bioeng* 50:374–381
149. Levesque SG, Lim RM, Shoichet MS (2005) *Biomaterials* 26:7436–7446
150. Levesque SG, Shoichet MS (2007) *Bioconjug Chem* 18:874–885
151. Van Tomme SR, Hennink WE (2007) *Expert Rev Med Dev* 4:147–164
152. Coviello T, Matricardi P, Marianecchi C et al (2007) *J Contr Release* 119:5–24
153. Levesque SG, Shoichet MS (2006) *Biomaterials* 27:5277–5285
154. Suggs LJ, Shive MS, Garcia CA et al (1999) *J Biomed Mater Res* 46:22–32
155. Dadsetan M, Sztatowski JP, Yaszemski MJ et al (2007) *Biomacromolecules* 8:1702–1709
156. Suggs LJ, Payne RG, Yaszemski MJ et al (1997) *Macromolecules* 30:4318–4323
157. Shung AK, Behravesh E, Jo S et al (2003) *Tissue Eng* 9:243–254
158. Behravesh E, Jo S, Zygourakis K et al (2002) *Biomacromolecules* 3:374–381
159. Shin H, Quinten Ruh P, Mikos AG et al (2003) *Biomaterials* 24:3201–3211
160. Suggs LJ, Krishnan RS, Garcia CA et al (1998) *J Biomed Mater Res* 42:312–320
161. Temenoff JS, Park H, Jabbari E et al (2004) *Biomacromolecules* 5:5–10
162. Temenoff JS, Athanasiou KA, Lebaron RG et al (2002) *J Biomed Mater Res* 59:429–437
163. Tanahashi K, Mikos AG (2003) *J Biomed Mater Res A* 67A:1148–1154
164. Temenoff JS, Park H, Jabbari E et al (2004) *J Biomed Mater Res A* 70A:235–244
165. Lee HJ, Lee J-S, Chansakul T et al (2006) *Biomaterials* 27:5268–5276
166. He X, Jabbari E (2007) *Biomacromolecules* 8:780–792
167. Chau Y, Luo Y, Cheung ACY et al (2008) *Biomaterials* 29:1713–1719
168. Burdick JA, Anseth KS (2002) *Biomaterials* 23:4315–4323
169. Yang F, Williams CG, Wang D-a et al (2005) *Biomaterials* 26:5991–5998
170. Gallea S, Lallemand F, Atfi A et al (2001) *Bone* 28:491–498
171. Chung Y-I, Ahn K-M, Jeon S-H et al (2007) *J Contr Release* 121:91–99
172. Tessmar JK, Gopferich AM (2007) *Adv Drug Deliv Rev* 59:274–291
173. Endres M, Huttmacher DW, Salgado AJ et al (2003) *Tissue Eng* 9:689–702
174. Luginbuehl V, Wenk E, Koch A et al (2005) *Pharm Res* 22:940–950
175. Benya PD, Shaffer JD (1982) *Cell* 30:215–224
176. Wang DA, Williams CG, Yang F et al (2004) *Adv Funct Mater* 14:1152–1159
177. Wang D-A, Varghese S, Sharma B et al (2007) *Nat Mater* 6:385–392
178. Shin H, Jo S, Mikos AG (2003) *Biomaterials* 24:4353–4364
179. Park Y, Sugimoto M, Watrin A et al (2005) *Osteoarthritis Cartilage* 13:527–536
180. Burdick JA, Mason MN, Hinman AD et al (2002) *J Contr Release* 83:53–63
181. Elisseeff J, McIntosh W, Fu K et al (2001) *J Orthop Res* 19:1098–1104
182. Tabata Y, Miyao M, Inamoto T et al (2000) *Tissue Eng* 6:279–289

183. Hisatome T, Yasunaga Y, Yanada S et al (2005) *Biomaterials* 26:4550–4556
184. Park KH, Na K (2008) *J Biosci Bioeng* 106:74–79
185. Hu BH, Messersmith PB (2003) *J Am Chem Soc* 125:14298–14299
186. Yamaguchi N, Zhang L, Chae BS et al (2007) *J Am Chem Soc* 129:3040–3041
187. Seliktar D, Zisch AH, Lutolf MP et al (2004) *J Biomed Mater Res A* 68A:704–716
188. Gonen-Wadmany M, Oss-Ronen L, Seliktar D (2007) *Biomaterials* 28:3876–3886
189. Almany L, Seliktar D (2005) *Biomaterials* 26:2467–2477
190. Bryant SJ, Arthur JA, Anseth KS (2005) *Acta Biomater* 1:243–252
191. Lee H, Park TG (2009) *J Biomed Mater Res A* 88A:797–806

Composite Hydrogels for Scaffold Design, Tissue Engineering, and Prostheses

V. Guarino, A. Gloria, R. De Santis, and L. Ambrosio

Abstract Hydrogels have been successfully used in several biomedical applications, such as controlled drug release and micro-patterning. More recently, the ability to engineer composite hydrogels has generated new opportunities in addressing challenges in tissue engineering as well as in tissue function restoration via prostheses. Indeed, the knowledge of biocompatible materials and preparation technologies may be efficaciously used in synthesizing biocompatible hydrogels to develop state-of-the-art hydrogel-based devices for tissue regeneration and reconstruction. Important details with respect to the design of the materials adopted and with respect to specific tissues, such as tendons and ligaments, intervertebral discs, bone, menisci, and cartilage will be discussed.

Introduction

Biomaterials play a crucial role in modern strategies of the tissue replacement and restoration because they provide the reproduction of a designable biophysical and biochemical milieu able to direct cellular behaviour and functions [1]. The concept of regenerative and restorative design to engineer temporary or permanent devices, respectively, is a challenging task. Structural and biochemical peculiarities represent the basis upon which proper *in vivo* functions rely. The efficacy of the design strategy depends on mimicking natural tissue and supporting the engineered tissue. Tissue repair has been historically considered in two forms: tissue grafting and engineered organs. These two different approaches are based on the use of partially or completely synthetic biomaterials and alternatively biodegradable synthetic materials by designing novel bioactive materials capable (a) to interact with the host tissues, (b) to assist and to improve the healing process, and (c) to replace the functional tissue through the mimicry of morphological characteristics of the natural systems.

Hydrophilic composite structures may be efficaciously designed to mimic the transport and mechanical properties of natural soft tissue such as tendons, ligaments, and intervertebral discs. Indeed, non-degradable or partially degradable materials may reproduce the mechanical and viscoelastic behaviour of soft tissues due to the hydrogels matrix reinforced with bundles of non-degradable fibres. As for the approach related to tissue reconstruction, there is a need to develop third-generation prostheses based on multifunctional materials. In particular, focussing on the basic principle of “*learning from nature*”, the design of smart and multifunctional materials has to mimic the behaviour of natural soft tissues, which are characterized by a complex mechanical loading process, also taking part on specific biomechanical and physiological roles with respect to the surrounding tissues.

V. Guarino, A. Gloria, R. De Santis, and L. Ambrosio • Institute of Composite and Biomedical Materials, National Research Council, P.le Tecchio, 80, Naples 80125, Italy
e-mail: ambrosio@unina.it

The concept of designing bio-mimetic materials that actively direct the behaviour of cells to facilitate the regeneration of tissues and organs is being progressively explored in order to develop totally degradable biomaterials-based scaffolds. Indeed, the scaffold has to be designed as purely a structural support providing passive cues to the cells or with biological cues incorporated into the scaffold to guide cell and tissue growth [2]. In this context, tailor-made bio-composites may guide the tissue growth by bio-molecular interaction with cells or adjacent tissues to control their basic functions, also directing the spatially and temporally complex multi-cellular processes of tissue formation and regeneration, or restoring damaged or dysfunctional tissues.

Hydrogels based on both natural and synthetic polymers continued to be of interest in the field of “*tissue engineering*” for repairing and regenerating a wide variety of tissues and organs [3]. They can reproduce elastic, three-dimensional porous networks able to swell up to 90% in water solution and to adequately transfer stresses, making them an attractive material for biomedical and tissue engineering applications, such as bone and ligament replacement. Typically, hydrogels have lubricating properties, low coefficients of friction and tailorable mechanical strength, thus, resulting in very interesting cartilage and meniscus regeneration.

The addition of synthetic peptides in the design of hydrogels carriers with a wealth of bioactive signals programmed directly into the hydrogels matrix is another important step. It has been verified that incorporation of cell adhesion moieties and biochemical cues promote tissue deposition as well as specific enzyme-sensitive sequences as well as induce cell-mediated degradation [4]. In an effort to recapitulate the native microenvironment that surrounds cells, synthetic extracellular matrix (ECM) hydrogels may be designed by incorporating both proteins and glycosaminoglycans into a single hydrogels matrix. In this configuration, these synthetic ECM analogues could be degraded through hydrolysis of the ester bond associated with the acrylate with a glycosaminoglycan semi-dependent degradation level [5]. The traditional methods of hydrogels synthesis may impede to finely control the material structures because of side reactions related to the presence of un-reacted pendant groups and physical bonds (*entanglements*). Furthermore, gels compositions may rapidly degrade in the presence of enzymatic molecules (i.e. hyaluronidase, collagenase) which drastically undermine the mechanical performance after the implantation as well as presenting a slow or delayed response times to external stimuli [6, 32].

To overcome the drawbacks of traditional synthesized hydrogels, such as loss in mechanical properties with time [7], recent strategies have focussed on composite hydrogels, which afford greater control by combining different degradable or non-degradable polymers with tailored chemistry to create bioactive systems with customized functional properties.

Basic Concepts and Properties

Hydrogels are hydrophilic polymer networks that absorb from 10 to 20% up to thousands of times their dry weight in water. They may be chemically stable or they may degrade and eventually disintegrate and dissolve as the amount of water overcomes the absorption limit. They may be “*reversible*,” or “*physical*” gels when the networks are physically held together by molecular entanglements, and/or by secondary forces, such as ionic, H-bonding, and hydrophobic forces [8]. For example, the gels obtained by the hydrolysis of polyacrylonitrile (PAN) to amide and acid groups from the nitrile groups can be stabilized by hydrophobic interactions due to the presence of nitrile groups with appropriate concentration and combination.

The polymeric networks composed of chains joined through covalent bonds or crosslinks are defined “*permanent*” or “*chemical*” gels. For example, the hydrogels synthesized by Wichterle, [9] based on copolymerization of 2-hydroxyethyl methacrylate (HEMA) with ethylene glycol dimethacrylate (EGDMA) take part in this group. Water absorption capability of the crosslinked hydrogels depends mainly on the crosslink density estimated by the molecular weight between adjacent joined points [10].

In general, most hydrogels have good biocompatibility. They can homogeneously incorporate and suspend cells as well as growth factors and other bioactive compounds while allowing rapid diffusion of hydrophilic nutrients and metabolites to the incorporated cells. They can be processed under mild conditions or even be formed in situ. Hydrogels generally contain low amounts of dry mass, causing little irritation and a low quantity of degradation products. Hydrogels based on ECM polymers provide adhesive surfaces [11]. Although, hydrogels are considered to have great potential for biomedical applications, as they present several attractive physical properties such as, high water content and softness similar to living tissues, often in the swollen state, the mechanical properties are inadequate. This greatly limits the possibilities for the application as materials in artificial implants [12]. However, the incorporation of a hydrophobic component, such as poly(*caprolactone*) (PCL), into poly(2-hydroxyethyl-methacrylate) (PHEMA) hydrogels enhances mechanical properties.

Ambrosio et al. designed different PHEMA/PCL semi-interpenetrating polymer networks (semi-IPNs) hydrogels and their relative composite systems reinforced with polymeric fibres. These semi-IPNs were composed of 10, 20, and 30% by weight of PCL in PHEMA [12]. Compression tests were carried out on swollen PHEMA and PHEMA/PCL semi-IPNs in the form of cylindrical samples, according to the water content. The values of elastic modulus, maximum stress, and strain of PHEMA/PCL semi-IPNs are listed in Table 1 [12] which clearly shows that the presence of PCL crystalline micro-domains provides an increase in the elastic modulus and maximum stress of the modified hydrogels. In particular, the compression properties of the semi-IPNs improve as the concentration of PCL increases [12]. The possibility of improving the mechanical properties of these modified hydrogels by reinforcing the PHEMA/PCL semi-IPNs with 40–50% poly(ethylene terephthalate) (PET) fibres was investigated. These composite hydrogels were manufactured through filament winding technique varying the winding angle over a wide range of values. Compression tests performed on the swollen PHEMA/PCL semi-IPNs composite hydrogels reinforced with PET fibres have highlighted elastic modulus and maximum stress values higher than the PHEMA/PCL semi-IPNs alone [12].

Crosslinked PHEMA hydrogels were also investigated as interface material between bone and implant [13]. The aim was to use the force that PHEMA hydrogels generate on swelling in a constrained environment as a mechanism to fix an implant in an intramedullary cavity. The

Table 1. Compression properties of swollen PHEMA and PHEMA/PCL 90/10, PHEMA/PCL 80/20, PHEMA/PCL 70/30 semi-IPNs

PHEMA/PCL (w/w)	E (MPa)	σ_{\max} (MPa)	ϵ_{\max} (mm/mm)
100/0	1.02 ± 0.06	0.51 ± 0.02	0.51 ± 0.03
90/10	2.10 ± 0.16	1.45 ± 0.08	0.55 ± 0.02
80/20	6.21 ± 0.14	2.48 ± 0.06	0.44 ± 0.01
70/30	15.95 ± 1.07	7.27 ± 0.06	0.54 ± 0.02

Elastic modulus (E), maximum stress (σ_{\max}), and maximum strain (ϵ_{\max}) reported as mean value \pm standard deviation

in vitro mechanical tests were performed to evaluate the stress generated in the PHEMA when it was placed in water and not allowed to swell. The stainless steel pins were coated with PHEMA and then inserted in holes drilled through plaques of bovine cortical bone. The pin-hydrogels-bone systems were conditioned in distilled water at 37°C. Pull out loads up to 375°N were measured, indicating that the system could be successfully used in vivo [13].

Prostheses for tissue function replacement: Soft organic tissues are very complex both in terms of the constituents used and of the microstructure [14–16]. For example, tendons, ligaments, and intervertebral discs are dense connective tissues consisting of a protein phase of collagen and elastin, and a polysaccharide phase of proteoglycans. The mechanical properties of soft tissues are not homogeneous and their structural organisation plays an important role in terms of mechanical properties [14–16]. Specifically, the overall mechanical properties of these tissues are related to the relative amount of the two phases as well as the geometrical factors, the conformation, and orientation of the individual constituents [14–16]. Soft biological tissues, such as ligaments, tendons, and intervertebral discs are able to withstand high mechanical stresses due to the unique orientation of the collagen fibres embedded in a proteoglycan–water gels. Consequently, the design of prostheses has to take into account the high structural anisotropy degree in order to effectively mimic the complex functional response of these natural tissues. In particular, the non-linear mechanical behaviour and the viscoelastic properties of these natural tissues are uniquely related to their structure. Accordingly, the design of synthetic soft tissues for biomedical applications needs to involve fibre-reinforced composite hydrogels.

Composite Hydrogels for Tendons and Ligaments: The need to design artificial prostheses for the replacement of damaged ligaments is growing because of the increase in number of tendon and ligament injuries (anterior cruciate ligament) as well as enhanced and new medical techniques. In order to design appropriate artificial tendon or ligament prostheses that are able to stabilize a joint without inhibiting abnormal movement, it is necessary to mimic the anatomy and physiology of the natural structures to be replaced or augmented. More specifically, the complex structural architecture of the natural tissue characterized by the axial arrangement of collagen fibres contained in the ECM, confers peculiar mechanical response to the natural tissue. Thus, an accurate “ab initio” definition of the geometrical factors, such as the conformation and orientation of the single components, aids in the design of suitable prosthetic devices [17, 18].

Early attempts, using synthetic ligament prostheses, were unsuccessful, mainly due to material fatigue, creep, and the high degree of graft failure.

Current efforts are focussed on the use of tissue engineering technology to develop scaffolds that stimulate the formation of functional ligamentous tissue. Approaches based on hydrogels scaffolds [19] and scaffold-free constructs [20] do accumulate significant amounts of ligamentous ECM. However, mechanical performance of these materials is poor, bringing into question whether these approaches could be used clinically. For example, fibrous scaffolds are an attractive alternative, as an initial mechanical support to the joint which can be achieved by matching the mechanical properties of the scaffold to that of the native ligament [21, 22].

Comprising of large diameter knitted or braided polymeric fibres, these scaffolds are similar to the ligament prostheses developed in the 1970s with the exception of the use of biodegradable, as opposed to non-degradable synthetic polymers. However, by using this approach the knitted/braided design restricts cell seeding to the periphery of the scaffold

resulting in heterogeneous ECM accumulation within the construct [23]. Furthermore, the fibres are substantially larger than the size of ligament fibroblasts ($\sim 10 \mu\text{m}$) which is a problem as the cells are interacting with a planar surface as opposed to the aligned nanofibrous collagen network characteristic of ligament tissue [24]. The traditional synthetic devices, including the Gore-Tex[®] prosthesis, the Stryker–Dacron ligament, and the Kennedy ligament augmentation device (LAD), initially supply the mechanical function of the replaced ligaments, or protect the ligament that they augment. However, they fail over time because they cannot duplicate the necessary ligament behaviour [25, 26]. This is a direct consequence of the use of non-degradable materials which do not match the functional properties of biological tissue during “in vivo” evolution very well.

To mimic the morphology and mechanical properties of natural ligaments, composite systems based on degradable polymers are being explored. In particular, tensile tests have shown that the mechanical properties (i.e. modulus and strength) of natural connective tissues are higher than for hydrogels [16, 27]. Thus, the hydrogels need to be reinforced, creating a composite structure to match the mechanical properties of tendons and ligaments. Composite structures based on a hydrogels matrix reinforced with PET fibres were designed to reproduce the morphology, mechanical properties of natural ligaments, and to match the typical J-shaped stress–strain curve displayed by natural tendons and ligaments. Hence, hydrophilic composite structures, consisting of a soft hydrated hydrogels matrix (PHEMA) reinforced with a hydrophobic fibre phase [poly(ethylene terephthalate) (PET)] wound into a helix were made by filament winding technique.

These composite structures have tensile stress–strain curves that are similar to typical natural tendons and ligaments (Fig. 1a). An initial toe region (low modulus region), due to matrix response, is followed by a second higher modulus region, which due to the response of the fibres aligning along the loading direction. The first region of the stress–strain curve depends on the winding angle and the mechanical properties are mainly due to the matrix response. The mechanical behaviour of these composite hydrogels was investigated as a function of the winding angle. In composites with an identical fibre composition, higher winding angles resulted in a more extensive toe region; therefore, the difference in terms of stress/strain curves may only be due to the structural organization of the PET fibres derived from the different winding angles [27]. The increase of the modulus and strength with lower winding angles is due to the wider alignment of the fibres along the load direction. The tensile response of these fibre-reinforced devices can be tailored by varying the winding angle of the fibres, which determines the extent of the toe region and the mechanical response in the linear region. The behaviour of these soft composite prostheses can be controlled by a suitable design of the hydrophilic fibre-reinforced structures utilizing a filament winding technique. The control of the winding angle and the amount of fibres provides a wide range of mechanical properties [27].

Consequently, the static and dynamic-mechanical measurements on the proposed fibre-reinforced composite hydrogels indicate that the tensile stress/strain curves as well as the viscoelastic properties of natural ligaments and tendons can be emulated by selecting an appropriate matrix and an opportune geometrical design of the soft composite prostheses [27]. Composite hydrogels-based structures made of polyurethane matrix (HydroThane[™]) reinforced with PET fibres were also investigated [16] Although polyurethanes have good mechanical properties, their biocompatibility is compromised by their hydrophobicity; however, HydroThane[™] (Hydrophilic Thermoplastic Polyurethane by Cardio-Tech International) is a family of hydrophilic thermoplastic polyurethane elastomers with adequate mechanical

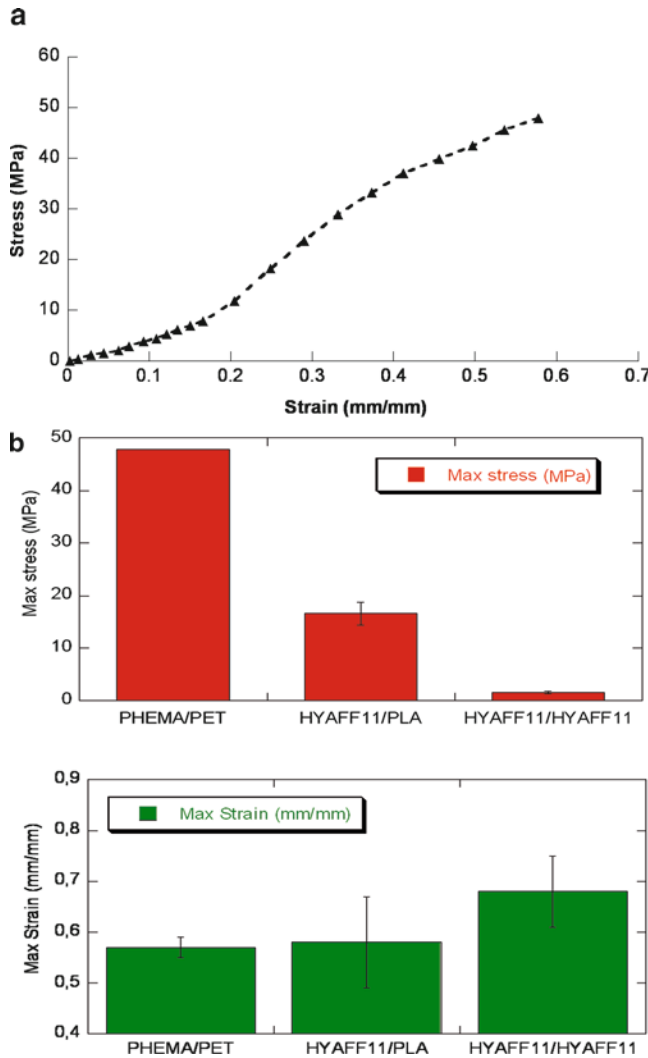


Fig. 1. ACL fibre-reinforced prostheses (a) Typical tensile stress–strain curve of PHEMA reinforced with PET fibres. (b) Comparison of mechanical parameters calculated for PHEMA/PET, HYAFF 11/PLA, and HYAFF 11/HYAFF 11 composite devices.

properties with an equilibrium water content that ranges between 5 and 25% by weight. These HydroThane™ matrices were reported to produce composites for ligament devices [16].

However, the need to assure an adequate transport of fluids through the implant should preclude the employment of synthetic material with hydrophobic behaviour. In fact, the presence of high amounts of water (~60%) associated with proteoglycans in the natural tissue, provides the lubrication and the structural spacing that are essential to enable the gliding function at the fibre/matrix interface [28].

This requirement embraces the philosophy of modern tissue engineering which is based on the use of porous scaffolds. Current tissue engineering for anterior cruciate ligament (ACL) regeneration allows the scaffolds to degrade while promoting tissue growth to enabling the

body to fully regenerate lost or damaged tissue without the risk of scaffold or neo-ligament rupture, or stress shielding of the new tissue.

Innovative designs to produce a new generation of composite scaffolds that can mimic the mechanics of natural ligament and provide quick and complete regeneration of new natural tissue are in the making. In this regard, the composite materials with a hydrogels-like phase is mandatory to provide an adequate supply of liquids to the neo-forming tissue. A scaffold for tissue engineering an ACL using composite materials for ligament devices is being pursued; the system is composed of a bioactive porous matrix, reinforced by a biodegradable fibre [29]. The matrix consists of a porous benzyl ester of hyaluronic acid reinforced with PLLA fibres. These fibres are wound to emulate the mechanical properties and function of collagen fibres. The possibility of using the benzyl ester of hyaluronic acid (HYAFF 11) as the fibrous component is also being explored. This system permits the attainment of the right balance between bioactivity, morphological features and mechanical performance for the ACL scaffold. Hyaluronan derivatives are bioactive and effectively reproduce the ECM domain. In particular, the benzyl ester of hyaluronic acid has good biocompatibility and the capability to promote cell adhesion and proliferation [8]. A porosity range from 100 to 500 μm is obtained through the solvent casting/salt leaching technique. A winding angle of 20° for PLLA fibres and HYAFF 11 was imposed through filament winding technique. The fibres are impregnated with the hyaluronan-derivative solution containing salt crystals (to be leached out later to form the pores) and then wound onto a mandrel. The mechanical properties are based on the stress/strain curve that displayed a tri-phasic diagram and the elastic modulus that depended upon the components and structural parameters of the scaffold (Fig. 1b). The *in vitro* degradation performed in lactate solution showed a large erosion of the mechanical properties after 84 days. Preliminary tests on adhesion and proliferation of 3 T3 mouse fibroblasts on the proposed scaffold showed higher adhesion on the more porosity scaffold (300–500 μm) for both the PLLA and HYAFF 11 fibres.

Polymeric substrates are able to match the starting mechanical properties, tailored degradation, and biocompatibility when used for “*in vivo*” ACL reconstruction. A current work on “*dual*” composite structures meets all basic scaffold requirements for ACL reconstruction [30]. The extreme parts allow osteogenesis with good integration of the substrate within the implant site. The middle part is composed of multiple growth factors loaded in layers with different properties that enable the host tissue to in-grow due to the timed degradation of each layer for total restoration of tissue functionality. The outer layer impedes the inflammatory phenomena due to the action of cytokines and macromolecules from the knee joints which maintain the free exchange of nutrient ions. The overall mechanical behaviour of the structure is assured by the fibre-reinforced cores that remain stable during degradation whereas controlled delivery of growth factors occurs at a later stage of the matrix degradation to promote the blood vessel supply for the complete tissue functionality.

Intervertebral disc: Similar to tendons and ligaments, intervertebral discs (IVDs) have non-linear, anisotropic, viscoelastic behaviour. Therefore, the stress/strain curve is non-linear with a marked toe or J-shaped region [15, 16, 31] However, the toe region, for the intervertebral disc loaded in compression, is due to the annulus fibres that gradually align themselves transversally to the load direction to withstand the tensile stress [32, 33]. The IVDs provide flexibility to the spine and enable the body to twist and bend into a wide range of postures. Each disc has a soft centre, called the “nucleus pulposus” surrounded by an outer wall, the “annulus fibrosus.” The annulus has a layered structure and each layer is reinforced by a regular pattern of collagen fibres [33]. Superiorly and inferiorly, there are two thin layers of vertebral cartilage endplates that are characterized by micropores for exchanging water and nutrients [33, 34].

The annulus consists mainly of collagen fibres embedded in a proteoglycan–water gels. The IVD is characterized by a gradation of collagen orientation from the annulus to the nucleus. From the edge of the disc inwards to the nucleus, the angle of collagen fibres in the concentric lamellae of the annulus decreases from 62 to 45°, with respect to the spinal axis [35]. The mechanical role of the nucleus is to resist and redistribute compression forces within the spine; while the major function of the annulus is to withstand tension.

The anisotropy of disc tissues and their specific biomechanical properties clearly suggest composite materials for IVD replacement. The design of homogeneous and isotropic devices at most reproduce the geometry of the natural structure; while composite material structural designs provide a wider set of options and possibilities for an implant [16, 36, 37]. The advantage of using composite designs to prepare soft replacement devices is that a wide selection range for the compliance and eventually the ability to control the chosen value is provided [31]. The selection of material characteristics, such as the aspect ratio, the fibres orientation, the matrix material, the fibres volume fraction, and the micromechanics are important. The lamination theory allows the design of a material with desired mechanical properties, such as elastic modulus and strength [12, 16, 27, 36, 37].

The need to match the mechanical behaviour of soft biological tissues with the anisotropy of an IVD has driven research towards designing soft fibre-reinforced composite materials.

The structural design of IVD prostheses suggests the use of continuous fibres embedded in a matrix, thus the filament winding technology was considered in order to create devices which mimic the complex natural structure. To design alternative IVD prostheses characterized by suitable transport, mechanical, and biological properties, research has focussed on the use of hydrogels [12, 16, 27, 36, 37]. The principle of mimicking the natural structure of IVD has led to engineering a novel fibre-reinforced hydrogels that is able to reproduce the structure and peculiar mechanical properties of a natural IVD [12, 16, 27, 36, 37].

PHEMA hydrogels are used in a wide variety of biomedical applications due to biocompatibility, high permeability, and high hydrophilicity properties [10, 13, 38, 39]. The drawbacks are related to poor mechanical properties of these materials in the hydrated state, which are not appropriate for applications where high mechanical strength is required [12, 27]. The mechanical properties of polymer hydrogels may be improved by incorporating a hydrophobic component, such as PCL, and polymeric fibres [12, 16, 27, 38]. PHEMA-based composite hydrogels reinforced networks with PET fibres have also been designed as potential IVD substitutes [12, 16, 27]. The mechanical behaviour of PHEMA/PCL semi-IPNs composite hydrogels reinforced with PET fibres has been investigated [12, 16, 27]. However, PCL rapidly degrades to create voids in the network and causing a decrease in the mechanical properties of the hydrogels-based devices. Accordingly, a biostable polymer, such as poly(methyl methacrylate) (PMMA), is being considered instead of PCL to improve the mechanical behaviour of the hydrophilic composite structures. This approach has led to the design and preparation of nucleus/annulus synthetic system for IVD prosthesis characterized by softer and more hydrophilic PHEMA-based semi-IPNs with harder and less hydrophilic outer fibrous part.

The compression J-shaped stress–strain curves obtained for these fibre-reinforced composite hydrogels (Fig. 2a) is typical of soft biological tissues, such as articular fibrocartilage and IVDs [37]. The typical values of the compression modulus for swollen PHEMA/PMMA 80/20 w/w semi-IPN fibre-reinforced hydrogels are shown in Fig. 2b [37]. The compression stress–strain behaviour of natural IVDs is reproducible by the hydrogels-based composite structure, while the dynamic-mechanical measurements indicate that the complex viscoelastic behaviour of the disc tissues can be emulated by selecting a suitable matrix and design of the composite structure [16, 27, 37]. Moreover, by varying the composition of the hydrogels-based matrix, the

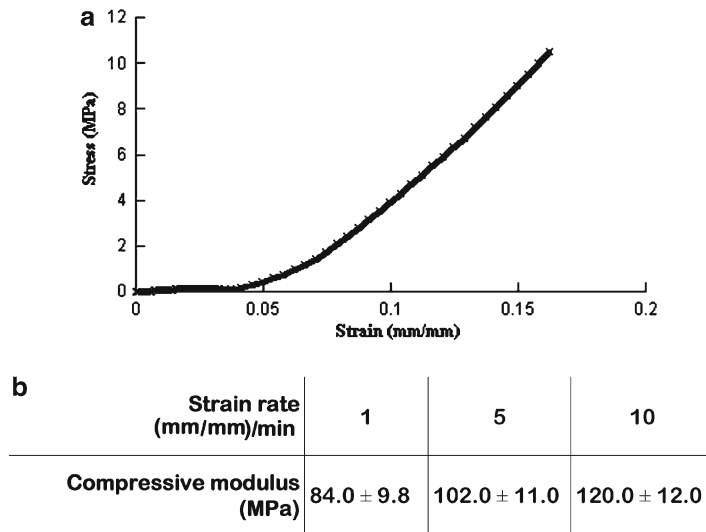


Fig. 2. Swollen PHEMA/PMMA 80/20 w/w semi-IPN composite hydrogels reinforced with PET fibres as nucleus/annulus system. (a) Typical stress–strain curve at a strain rate of 5 mm/min up to a load level of 15.8 kN without breaking; (b) compression modulus at different strain rates (1, 5, 10 (mm/mm)/min), expressed as mean value \pm standard deviation.

winding angle and the amount of the PET fibres, it is possible to modulate the hydrophilicity and the mechanical properties of the composite structure [16, 27, 37]. These results indicate that the use of fibre-reinforced composite hydrogels as nucleus/annulus system for IVD prostheses provides devices that are able to combine both the transport and mechanical properties.

Scaffolds for Tissue Regeneration

Although improvements have been made in skin and soft tissues regeneration, the regeneration of diseased tissue, such as bone, cartilage and menisci, are still far from appropriate solutions [40]. These limitations depend upon the properties of the scaffold which has to possess specific structural and functional cues capable of directing specific biological events for tissue formation [41]. The structure and architecture of scaffolds represent pivotal factors for scaffold-based tissue engineering to assure the right functionality of the tissue constructs for application in health care.

Porosity is essential to the performance of composite materials in scaffolds in order to provide a three-dimensional physical template able to support the new tissue formation. The main role of porosity on the biological behaviour of seeded cells in vitro culture is the capability to influence the correct response in the structures after in vivo implantation [42, 43]. The structural properties of a scaffold play an important role in all processes involved in tissue genesis including cell adhesion, migration, proliferation, growth, differentiation, and biosynthesis. The accurate control over the pore size and its distribution, pore shape, pore interconnectivity, and overall porosity of scaffolds is mandatory for tissue engineering. In general, the desirable porosities for tissue engineering scaffolds are around 80–90% of the structure with pore sizes ranging from 100 to 500 μm depending on the specific tissue to substitute (bone, cartilage, meniscus).

Consequently, there is a need to process polymers with different physicochemical characteristics into macroporous scaffolds with reproducible microstructure [29].

Current techniques include salt leaching [44, 45], fiber processing, gas foaming [46] phase separation [47], and solid freeform fabrication techniques [47, 48], which have been developed to generate highly porous polymer scaffolds from biodegradable polymers. These techniques are used to create a tailored environment able to offer the adequate surface area for cell attachment and thriving, while providing the free circulation of biological fluids for their maintenance [49]. To obtain a tissue-engineered construct for soft and hard tissues, repair and replacement requires several properties including biocompatibility, osteoconduction or induction, temporary mechanical support, controlled degradation, and adequate interstitial fluid flow [50]. In addition, the use of rate-controlled degradable materials is important to guarantee a greater penetration of extracellular substance to improve the nutrient/metabolites exchange and, to offer a better connection between neighbouring cells for the growth of forming tissue.

The hydrophilic nature of the natural ECM also plays a key role on the basic functions of the natural tissues. Synthetic hydrogels offer the ability to mimic various distinctive requirements of an ECM-like physicochemical environment to sustain cellular and tissue function. Hydrogels can also be implanted *in vivo* with minimal invasive techniques. The standard approach consists of seeding a three-dimensional (3D) biomaterial scaffold [46], incorporated with gene vectors, soluble factors, and chemical signals to help the new tissue development during implantation [51]. Furthermore, crosslinked hydrophilic polymers architecture may provide tissue-like viscoelastic, diffusive transport, and interstitial flow characteristics [2].

Naturally derived and synthetic scaffold materials have been used to exploit the regenerative capacities of host tissues or transplanted cells [52]. Current design and fabrication of organic scaffolds in skeletal tissue engineering (TE) involve a range of materials, such as, protein-based polymers (collagen, fibrin, gelatin, and synthetic polypeptides), natural carbohydrate-based polymers (agarose, alginate, hyaluronate, chitosan, dextran), fully synthetic polymers (polyactive, hyaluronan, and their copolymers with non-degradable polymers: Dacron, Teflon, polyesters, polyurethanes), and composite materials based on the coupling of hydrogels and inorganic compounds.

Although naturally derived biomaterials have proven effective in many basic and clinical applications, the need for custom-made matrices for tissue-specific cell biological investigation drives recapitulation of their key characteristics in synthetic materials. The use of synthetic material has been pursued because the immunogenic and purification issues relating to natural biomaterials are only partially overcome by recombinant protein technologies [1, 2] and the synthetic material properties can be finely controlled and tailored to perform required tissue responses. Although synthetic materials offer these advantages, and are more chemically programmable and reproducible, their deficiencies with respect to biological recognition limit their use as tissue regeneration scaffolds [52].

Currently, hydrogels are used as injectable *in situ* gelling networks and in cell-sheet engineering [53], wound healing and cellular patterning through spray deposition [54, 55]. Hydrogels combined with solid particles provide mechanically strong scaffolds largely used for load-bearing applications [56, 57]. To extend the biological performance of synthetic materials, a promising strategy consists of chemically encoding bio-molecular cues (morphogenic bone factors, growth factors, and gene factors) into synthetic platforms [11]. Composite hydrogels represent new frontiers for developing smart materials that are able to regulate and coordinate events in spatial and temporal modalities guided by biophysical and biochemical signals, as well as bio-molecular factors are naturally triggered by the extracellular microenvironment.

Composite hydrogels for bone replacement: Tissue regeneration through autogenous cell/tissue is a practice largely used in orthopaedic surgery and biomedical engineering to address the problems associated with donor site scarcity, immune rejection, and pathogen transfer. Synthetic platforms able to host osteoblasts, chondrocytes, and mesenchymal stem cells obtained from the patient's hard and soft tissues, and to slowly degrade and resorb as the tissue structures grow *in vitro* or *in vivo*, represent an invasiveness approach to reproduce the natural tissues. Efforts to design a variety of composite materials for tissue engineering scaffolds are based on biodegradable polymers with tailored degradation properties and specific biological cues. For example, manifold strategies of signalling usually involve the employment of ceramic particles like hydroxyapatite as bioactive factor or reinforcing agent within the polymeric matrix [58].

Currently, an approach based on the combination of hydrophobic and/or hydrophilic materials is emerging in scaffold design and preparation that represents a valid alternative to the traditional composite systems. To prevent the limitations of polyesters that include acute *in vivo* inflammatory phenomena [59], semi-synthetic materials like HYAFF formulations obtained by chemical modification of purified hyaluronan may be used in combination with them. The chemical modification of HYAFF consists of the partial or total esterification of the carboxyl groups of the hyaluronic acid that can be controlled by the selection of the chemical agents and the esterification extent with considerable effects on the composite biological properties either favouring or, conversely, inhibiting the adhesion of certain cell types [8]. HYAFF is being used for bone tissue engineering due to their positive tissue-forming abilities in the presence of chondrocytes and mesenchymal stem cells (MSCs) [60–63]. Furthermore, their use combined with aliphatic polyesters, such as PCL, polylactide (PLA), and poly(lactide-co-glycolide) (PLGA), may significantly reduce the inflammatory response during the degradation process [64, 65], because of a progressive increase in the hydrophilicity of the gels-like behaviour of material mimicking the native hyaluronan composing the ECM.

By changing the type of ester group introduced or the extent of the esterification, a broad variety of hyaluronan-based polymers (HYAFF 11, HYAFF 7) can be generated to produce membranes, fibres, sponges, microspheres, and other devices using different techniques (extrusion, lyophilization, and spray drying). For example, HYAFF 11 may be blended with PCL to develop porous scaffolds with tailored microstructure and degradation properties by phase inversion and salt leaching techniques (Fig. 3). The porous architecture is characterized by a well-interconnected and spatially well-distributed macroporosity ranging from 100 to 200 μm (Fig. 3a) obtained by leaching. The microporosity, ranging from 0.1 to 10 μm (Fig. 3b), generated by controlled extraction of solvents that do not active phase separation. The total porosity (92–93%) is consistent with theoretical value of sodium chloride porogen fraction (91%) as well as micro and macropore size distributions and surface areas (Fig. 3c, d). These have been calculated via imaging techniques by manipulating image parameters (brightness/contrast regulation, threshold definition). The shape and pore spatial distribution may be ascribable directly to the volumetric shrinkage of the HYAFF 11 which occurs during the preparation when the water content previously adsorbed during salt leaching step is lost. As a consequence, the volumetric shrinkage of the hydrogels determines a partial collapse of polymeric skeleton which explains the “microstructural disorder.” It may be possible to control the microstructural order by regulating the water adsorption properties which depend on the swelling ratios of the composites (Fig. 3e).

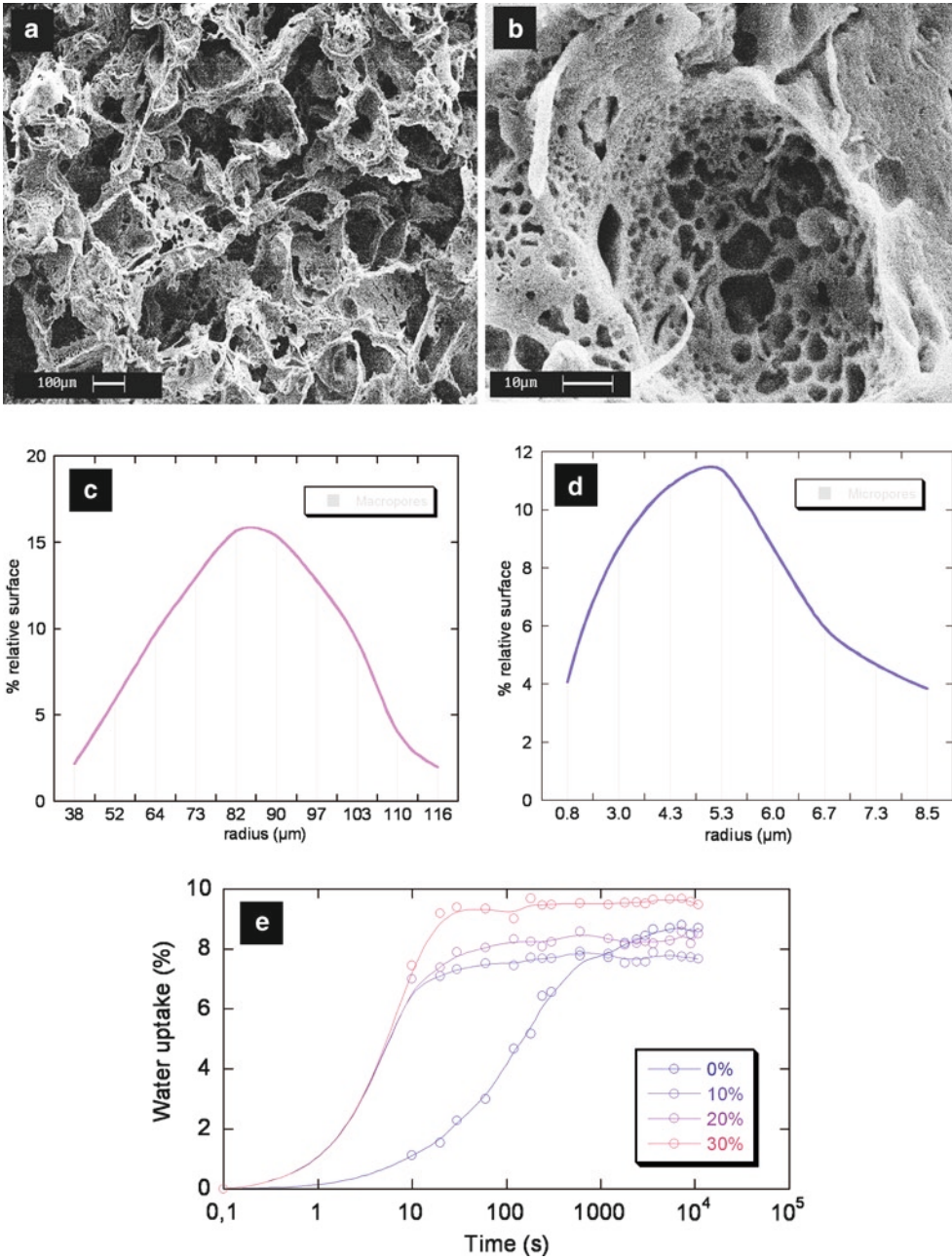


Fig. 3. HYAFF 11/PCL composite scaffolds for bone regeneration obtained by phase inversion and salt leaching technique. (a) Macropores and (b) micropores by SEM images at different magnifications for evidencing; (c) macropore and (d) micropore size distribution by imaging techniques; (e) swelling kinetic curves as a function of the HYAFF 11 content.

Composite hydrogels for menisci: The loss of meniscal tissue may lead to pain, degeneration of cartilage and osteoarthritis. Healing of ruptured meniscus is usually limited to the vascularized areas in the outer two-thirds of the meniscus. However, a large proportion of meniscal tears remains irreparable and partial, subtotal, or even total meniscectomy is often necessary. In cases of extensive destruction and complete loss of the meniscus, allograft transplantation and collagen meniscus implantation are two methods that are used in the clinical practice for meniscal substitution. In particular, collagen meniscus implants (CMI) is used for partial meniscus substitution in cases of extensive destruction with a meniscal rim left intact, while complete loss of the meniscus can only be treated by allograft transplantation [66, 67]. Meniscal allografts based on preservation techniques, such as fresh, fresh frozen, and cryopreserved, can foster healing and relieve pain. However, their long-term success, durability, safety, and chondroprotective effects are still uncertain.

Several materials have been tested as partial meniscus substitutes in animal models. While carbon fibres for meniscus repair in dogs did not result in meniscus-like tissue formation [68], small intestinal submucosa (SIS) was successfully used to repair posterior vascular meniscal defects, but not for total substitution [69]. A poly(vinyl alcohol) (PVA)-based meniscus in rabbits showed promising results in terms of chondroprotection, but problems related to the durability of the device, the fixation method and complete tissue regeneration remain unresolved. Two different types of porous polyester-urethane polymers as meniscus devices were used in dogs [70] with promising results in terms of tissue formation; however, one of the materials (4,4-diphenylmethanediisocyanate) is known to degrade to toxic products [66, 67]. Most porous polymer-based implants are not suitable as meniscus substitutes because of poor tissue in-growth related to the polymer degradation rate, and poor mechanical properties. However, tissue engineering is considered to be a possible solution for meniscal regeneration [71–73].

Animal studies indicate the possibility of using cells in a partial or total meniscal substitute [72, 73]. A collagenous sponge loaded with mesenchymal stem cells was used to heal a partial meniscus defect in rabbits; the presence of cells augmented the repair process but did not prevent degenerative osteoarthritis [71]. Positive histological results in CMI implants seeded with meniscal fibrochondrocytes were found compared to cell-free implants in sheep [72]. However, the tissue-engineered meniscus was biomechanically unstable [66, 67]. Several cell strategies have also been investigated *in vitro*, in order to find the most suitable source for cell augmentation of tissue-engineered meniscus. A new resorbable biomaterial, consisting of PCL and hyaluronic acid derivatives (HYAFF 11) was investigated [66, 67]. The material was designed for total meniscal substitution in an *in vivo* study in sheep [66]. Tissue integration between the joint capsule and the implant was observed with tissue formation, cellular infiltration, and vascularization. A second study investigated the feasibility of using this novel material for meniscus tissue engineering and to evaluate the tissue regeneration after the augmentation of the implant with autologous articular chondrocytes expanded *ex vivo* [66, 67]. With regard to the preparation of the HYAFF 11/PCL-based meniscus devices, they were manufactured through solvent casting, salt leaching, freeze-drying, and lamination techniques, using moulds that were designed according to original sheep menisci (Fig. 4). Using 3-D reconstructions of sheep menisci from microtomography and suitable software,

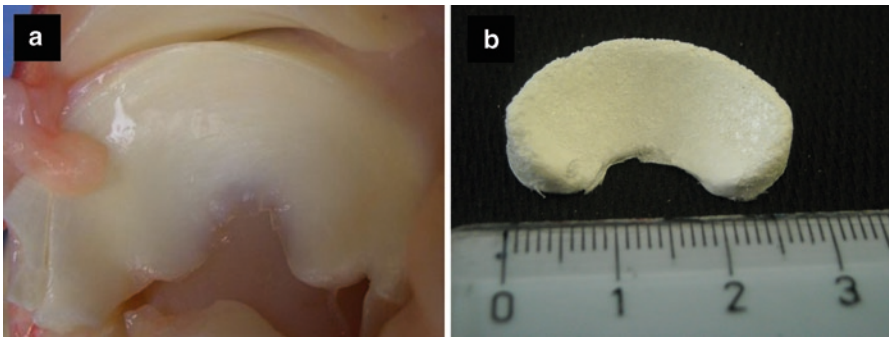


Fig. 4. Images of sheep meniscus (a) and HYAFF 11/PCL meniscus scaffold (b) obtained by integrating different techniques, such as computed tomography, computer numerical control (CNC) machining methods for mould realization, solvent casting, salt leaching, freeze-drying, and lamination.

3-D CAD drawings were designed in order to realize the appropriate moulds. Scanning electron micrographs and microtomographic reconstruction of the manufactured scaffolds indicate an average pore size of 200–250 μm with interconnectivity of the porous structure and a total porosity of 68% [67]. The HYAFF 11/PCL scaffold could be used for total meniscal substitution as it induces tissue in-growth, without rejection and no differences between the cell-free HYAFF 11/PCL-based scaffolds. The histological analysis showed cellular infiltration and vascularization throughout the implanted constructs. In addition, cartilaginous tissue formation was significantly more in the cell-seeded constructs [67]. Longer-term animal studies are necessary to evaluate the in situ conditions, particularly, cell augmentation in promoting fibro-cartilaginous tissue regeneration.

Composite hydrogels for cartilage: Tissue engineering of autologous cartilage is being investigated for repairing cartilage defects in reconstructive surgery. Chondrocytes are initially isolated from a tiny cartilage biopsy and then, expanded in conventional culture monolayers. Seeding into a porous scaffold network it is necessary to enable the organization of 3-dimensional (3-D) configurations [74].

Several suitable methods of culturing chondrocytes in gels substance such as agarose [75], hyaluronic acid gels [76], fibrin glue [77], collagen [78], and alginate [79] have been reported. However, these gels cultures do not provide suitable mechanical stability for creating cartilage structures with a specifically defined shape for transplantation. An additional problem is the de-differentiation of the chondrocytes into phenotypic fibroblast-like cells in substances like fibrin. Although gels substances such as agarose can induce cell re-differentiation, the use of agarose has not been approved for clinical treatment.

The integration of bio-molecular cues, such as growth or gene factors into synthetic platforms, enables to trigger a complex cascade of biological events involved in the tissue formation. For these reasons, a diffused strategy implies the development of polymeric matrices which may be easily synthesized with bioactive molecules.

Here, PEG can be successfully blended with hydrophobic materials like PCL to form a semi-hydrophilic scaffolds with high molecular transport capability and great potential for grafting bone morphogenic proteins and growth factors (Fig. 5a). The use of conventional techniques, like phase inversion and salt leaching, assures the formation of interconnected pore networks with desired pore sizes (Fig. 5b). The preliminary photo-polymerization by

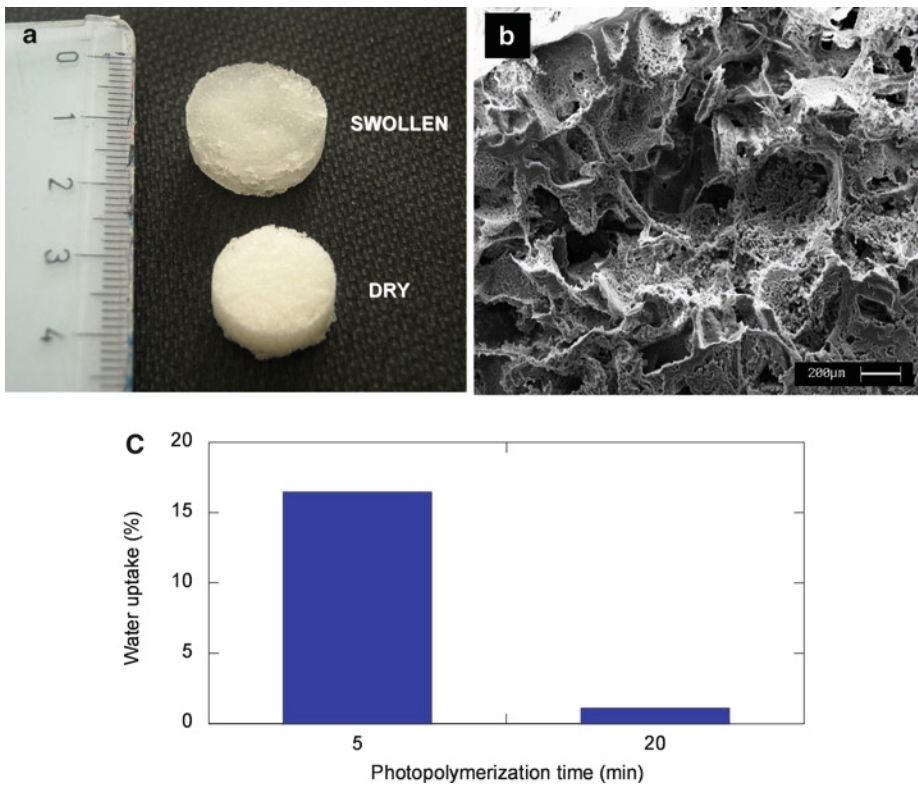


Fig. 5. PEG/PCL composite scaffold via photo-polymerization/phase inversion/salt leaching technique. (a) qualitative comparison of wet and dry samples; (b) SEM image of multi-porous structure; (c) swelling ratio as a function of the UV time exposure.

ultra-violet (UV) radiation of the composite prevents undesired removal of PEG during the ionic dissolution of the sodium chloride particles, improving the final mechanical response of the substrate.

In the case of avascular tissues, like articular cartilage, diffusion of nutrients and permeability of fluid through the ECM are essential for sustained cell viability [80–82]. The pore size, pore morphology, and interconnectivity are interrelated and influence the permeability of fluid through the scaffold as well as its mechanical properties [83].

Therefore, integration of hydrophilic biomaterials, such as PEG, may be able to provide properties similar to native cartilage with respect to fluid dynamics. Conversely, the mechanical integrity may be controlled by the crosslinking of the polymeric chain [84]. The hydrophilic properties of photopolymerized PEG-based scaffolds may be modulated by the variation of the reaction time (Fig. 5c). These hydrogels effectively encode morphological and functional properties, such as porosity and mechanical properties, through the synergic control of the chemical composition and processing parameters so as to mimic the behaviour of the mature cartilage. In particular, the modulated UV exposure time can control water uptake and transport properties of the substrate through the highly complex chemical composition and structural organization.

In this context, the adsorption properties of multi-porous hydrogels composites, coupled to the possibility to modulate the swelling capability acting on both chemical and physical parameters, such as PEG crosslinking, makes these materials suitable as low environmental impact substitutes in many industrial applications [85] as well as in regenerative medicine.

Summary

Currently, approaches based on the use of degradable materials have been largely applied to the reconstruction of many tissues and organs, including numerous soft and hard tissues like bone and bone/cartilage for osteochondral defects. Novel approaches in hydrogels and composite designs have been proposed for revitalizing the research on new functional biomaterials on the basic idea to jointly improve mechanical properties and morphological features. For instance, the introduction of crosslinking gels, semi-interpenetrating networks, and micro- or nano-composite hydrogels represent some valid solutions to improve the mechanical response of hydrogels under dynamic loading cycles. In addition, the adaptation of process technologies, traditionally used in scaffold design, to hydrogels science enables researchers to gain information related to transport properties of swollen materials, for the production of porous matrices with tailored pore morphology needful in tissue regeneration. In this context, hydrogels composites containing deliverable signals or functional proteins certainly have tremendous application potential. For example, the conjugation of peptide and/or protein segments to hydrogels chains may be used to introduce degradability [86], temperature-induced phase transition [87], and sensitivity to the presence of biologically active molecules [88] into the hydrogels network. Moreover, water-soluble synthetic polymers can be crosslinked with biological molecules, such as oligopeptides [89], oligodeoxyribonucleotides [90], stereospecific D,L-lactic acid oligomers [91], through antigen–antibody binding [92], or by intact native proteins to stimulate specific cell activities. The design of composite hydrogels may include the recent strategies of self-assembling that allow realizing hydrogel-forming copolymers, using recognition motifs found in nature. For example, DNA sequences have been frequently used as bio-recognition motifs in the design of new biomaterials [93]. The versatility of molecular motif, especially the possibility to manipulate its stability and specificity by modifying the primary structure, bodes well for the successful design of a new class of composite hydrogels with a great potential for the formation of precisely defined three-dimensional structures. However, several studies still need to be done with respect to analysing major factors involved in self-assembly of hybrid hydrogels. This would enhance the chance to implement structural and physicochemical criteria by using the self-assembly approach for the formation of highly reproducible, reversible three-dimensional hydrogels composites in the future.

References

1. Hubbell JA (1995) Biomaterials in tissue engineering. *Biotechnology* 13:565–576
2. Lutolf MP, Hubbell JA (2005) Synthetic biomaterials as instructive extracellular microenvironments for morphogenesis in tissue engineering. *Nat Biotechnol* 23(1):47–55
3. Woerly S (1997) Porous hydrogels for neural tissue engineering. *Porous Mater Tissue Eng* 250:53–68
4. Kisiday J, Jin M, Kurz B et al (2002) Self-assembling peptide hydrogel fosters chondrocyte extracellular matrix production and cell division: implications for cartilage tissue repair. *Proc Natl Acad Sci USA* 99:9996–10010

5. Shu XZ, Ahmad S, Liu YC et al (2006) Synthesis and evaluation of injectable, in situ crosslinkable synthetic extracellular matrices for tissue engineering. *J Biomed Mater Res A* 79A:902
6. Matthew HW, Salley SO, Peterson WD et al (1993) Complex coacervate microcapsules for mammalian cell culture and artificial organ development. *Biotechnol Prog* 9:510–519
7. Kopecek J, Yang J (2007) Hydrogels as smart materials. *Polym Int* 56:1078–1098
8. Campoccia D, Doherty P, Radice M et al (1998) Semisynthetic resorbable materials from hyaluronan esterification. *Biomaterials* 19:2101–2127
9. Wichterle O, Lim D (1960) Hydrophilic gels in biologic use. *Nature* 185:117
10. Hoffman AS (2002) Hydrogels for biomedical applications. *Adv Drug Deliv Rev* 43:3–12
11. Alblas FNE, De Wijn JR J et al (2007) Hydrogels as extracellular matrices for skeletal tissue engineering: state-of-the-art and novel application in organ printing. *Tissue Eng* 13(8):1905–1925
12. Ambrosio L, Netti PA, Iannace S et al (1996) Composite hydrogels for intervertebral disc prostheses. *J Mater Sci Mater Med* 7:251–254
13. Netti PA, Shelton JC, Revell PA et al (1993) Hydrogels as an interface between bone and an implant. *Biomaterials* 14(14):1098–1104
14. Fung YC (1993) *Biomechanics: mechanical properties of living tissues*. Springer, New York
15. Netti PA, D'Amore A, Ronca D et al (1996) Structure-mechanical properties relationship of natural tendons and ligaments. *J Mater Sci Mater Med* 7:525–530
16. De Santis R, Sarracino F, Mollica F, Netti PA, Ambrosio L, Nicolais L (2004) Continuous fibre reinforced polymers as connective tissue replacement. *Comp Sci Technol* 64:861–871
17. Iannace S, Sabatini G, Ambrosio L et al (1995) Mechanical behaviour of composite artificial tendons and ligaments. *Biomaterials* 16(9):675–680
18. Causa F, Sarracino F, De Santis R et al (2006) Basic structural parameters for the design of composite structures as ligament augmentation devices. *J Appl Biomater Biomech* 4:21–30
19. Noth U, Schupp K, Heymer A et al (2005) Anterior cruciate ligament constructs fabricated from human mesenchymal stem cells in a collagen type I hydrogel. *Cytherapy* 7(5):447–455
20. Calve S, Dennis R, Kosnik P et al (2004) Engineering of functional tendon. *Tissue Eng* 10(5/6):755–761
21. Gentleman E, Livesay G, Dee K et al (2006) Development of ligament-like structural organization and properties in cell-seeded collagen scaffolds in vitro. *Ann Biomed Eng* 34(5):726–736
22. Ouyang H, Goh J, Thambyah A et al (2003) Knitted poly-lactide-co-glycolide scaffold loaded with bone marrow stromal cells in repair and regeneration of rabbit achilles tendon. *Tissue Eng* 9(3):431–439
23. Cristino S, Grassi F, Toneguzzi S et al (2005) Analysis of mesenchymal stem cells grown on a three-dimensional HYAFF 11 based prototype ligament scaffold. *J Biomed Mater Res* 73A(3):275–283
24. Funakoshi T, Majima T, Iwasaki N et al (2005) Novel chitosan-based hyaluronan hybrid polymer fibres as a scaffold in ligament tissue engineering. *J Biomed Mater Res* 74A(3):338–346
25. McPherson GK, Mendenhall HV, Gibbons DF et al (1985) Experimental mechanical and histological evaluation of the Kennedy ligament augmentation device. *Clin Orthop* 196:186–195
26. Olson EJ, Kang JD, Fu FH et al (1988) The biochemical and histological effects of artificial ligament wear particles: in vitro and in vivo studies. *Am J Sports Med* 16:558–570
27. Ambrosio L, De Santis R, Nicolais L (1998) Composite hydrogels for implants. *Proc Inst Mech Eng* 212(Part H):93–99
28. Arnoczky SP, Matyas JR, Buckwalter JA et al (1963) Anatomy of the anterior cruciate ligament. In: Jackson DW (ed) *The anterior cruciate ligament*. Raven Press, New York, pp 5–23
29. Guarino V, Causa F, Ambrosio L (2007) Bioactive scaffolds for bone and ligament tissue. *Exp Rev Med Dev* 4(3):406–418
30. Ge Z, Yang F, Goh JCH et al (2006) Biomaterials and scaffolds for ligament tissue engineering. *J Biomed Mater Res* 77A:639–652
31. Gershon B, Cohn D, Marom G (1990) Utilization of composite laminate theory in the design of synthetic soft tissues for biomedical prostheses. *Biomaterials* 11:548–552
32. Cassidy JJ, Hiltner A, Baer A (1990) The response of the hierarchical structure of the intervertebral disc to uniaxial compression. *J Mater Sci Mat Med* 1:69–80
33. Hukins DWL (2005) Tissue engineering: a live disc. *Nat Mater* 4(12):881–882
34. Bao Q, McCullen GM, Higham PA et al (1996) The artificial disc: theory, design and materials. *Biomaterials* 17:1157–1167
35. Cassidy JJ, Hiltner A, Baer A (1989) Hierarchical structure of the intervertebral disc. *Connect Tissue Res* 23(1):75–88
36. Shikinami Y, Kotani Y, Cunningham BW et al (2004) A biomimetic artificial disc with improved mechanical properties compared to biological intervertebral discs. *Adv Funct Mater* 14:1039–1046

37. Gloria A, Causa F, De Santis R et al (2007) Dynamic-mechanical properties of a novel composite intervertebral disc prosthesis. *J Mater Sci Mater Med* 18:2159–2165
38. Peppas NA, Bures P, Leobandung W, Ichikawa H (2000) Hydrogels in pharmaceutical formulations. *Eur J Pharm Biopharm* 50:27–46
39. Davis PA, Huang SJ, Ambrosio L, Ronca D, Nicolais L (1991) A biodegradable composite artificial tendon. *J Mater Sci Mater Med* 3:359–364
40. Leach JB, Bivens KA, Patrick CW, Schmidt CE (2003) Photocrosslinked hyaluronic acid hydrogels: natural, biodegradable tissue engineering scaffolds. *Biotechnol Bioeng* 82:578–589
41. Khademhosseini A, Langer R (2007) Microengineered hydrogels for tissue engineering. *Biomaterials* 28:5087–5092
42. Ciapetti G, Ambrosio L, Marletta G et al (2006) Human bone marrow stromal cells: in vitro expansion and differentiation for bone engineering. *Biomaterials* 27:6150–6160
43. Savarino L, Baldini N, Greco M et al (2007) The performance of poly- ϵ -caprolactone scaffolds in a rabbit femur model with and without autologous stromal cells and BMP4. *Biomaterials* 28:3101–3109
44. Mikos AG, Sarakinos G, Leite SM et al (1993) Laminated three-dimensional biodegradable foams for use in tissue engineering. *Biomaterials* 14:323–330
45. Mikos AG, Thorsen AJ, Czerwonka LA et al (1994) Preparation and characterization of poly(L-lactic acid) foams. *Polymer* 35:1068–1077
46. Mooney DJ, Mikos AG (1999) Growing new organs. *Sci Am* 280:60–65
47. Nam YS, Park TG (1999) Biodegradable polymeric microcellular foams by modified thermally induced phase separation method. *Biomaterials* 20:1783–1790
48. Leong KF, Cheah CM, Chua CK (2003) Solid free-form fabrication of 3D scaffolds for engineering replacement tissues and organs. *Biomaterials* 24:2363–2378
49. Hollister SJ (2005) Porous scaffold design for tissue engineering. *Nat Mater* 4:518–524
50. Guarino V, Causa F, Salerno A et al (2008) Design and manufacture of microporous polymeric materials with hierarchical complex structure for biomedical application. *Mater Sci Technol* 24(9):1111–1117
51. Lum L, Elisseeff J (2003) Injectable hydrogels for cartilage tissue engineering. In: Ashammakhi N, Ferrettilov P (eds) *Topics in tissue engineering*, vol 1, pp1–25. www.tissue-engineering-oc.com [ebook]
52. Elisseeff J, Puleo C, Yang F et al (2005) Advances in skeletal tissue engineering with hydrogels. *Orthod Craniofac Res* 8:150–161
53. Griffith LG, Naughton G (2002) Tissue engineering – current challenges and expanding opportunities. *Science* 295:1009–1014
54. Causa F, Netti PA, Ambrosio L (2007) A multi-functional scaffold for tissue regeneration: the need to engineer a tissue analogue. *Biomaterials* 28:5093–5099
55. Kikuchi A, Okano T (2005) Nanostructured designs of biomedical materials: applications of cell sheet engineering to functional regenerative tissues and organs. *J Control Release* 101:69
56. Roberts A, Wyslouzil BE, Bonassar L (2005) Aerosol delivery of mammalian cells for tissue engineering. *Biotechnol Bioeng* 91:801
57. Nahmias Y, Arneja A, Tower TT et al (2005) Cell patterning on biological gels via cell spraying through a mask. *Tissue Eng* 11:701
58. Spitzer RS, Perka C, Lindenhayn K et al (2002) Matrix engineering for osteogenic differentiation of rabbit periosteal cells using alpha-tricalcium phosphate particles in a three-dimensional fibrin culture. *J Biomed Mater Res* 59:690
59. Xu XL, Lou J, Tang T et al (2005) Evaluation of different scaffolds for BMP-2 genetic orthopedic tissue engineering. *J Biomed Mater Res B Appl Biomater* 75:289
60. Guarino V, Causa F, Netti PA et al (2008) The role of hydroxyapatite as solid signal on performance of PCL porous scaffolds for bone tissue regeneration. *J Biomed Mater Res B Appl Biomater* 86B:548
61. Santavirta S, Konttinen YT, Saito T et al (1990) Immune response to polyglycolic acid implants. *J Bone Joint Surg Br* 72:597–600
62. Turner NJ, Kielty CM, Walker MG et al (2004) A novel hyaluronan-based biomaterial (HYAFF 11) as a scaffold for endothelial cells in tissue engineered vascular grafts. *Biomaterials* 25:5955–5964
63. Grigolo B, Roseti L, Fiorini M et al (2001) Transplantation of chondrocytes seeded on a hyaluronan derivative (HYAFF 11) into cartilage defects in rabbits. *Biomaterials* 22:2417–2424
64. Solchaga LA, Dennis JE, Goldberg VM et al (1999) Hyaluronic acid-based polymers as cell carriers for tissue-engineered repair of bone and cartilage. *J Orthop Res* 17:205–213
65. Solchaga LA, Gao J, Dennis JE et al (2002) Treatment of osteochondral defects with autologous bone marrow in a hyaluronan-based delivery vehicle. *Tissue Eng* 8:333–347

66. Seal BL, Otero TC, Panitch A (2001) Polymeric biomaterials for tissue and organ regeneration. *Mater Sci Eng R Rep* 34:147–230
67. Rezwani K, Chen QZ, Blaker JJ et al (2006) Biodegradable and bioactive porous polymer/inorganic composite scaffolds for bone tissue engineering. *Biomaterials* 27:3413–3431
68. Chiari C, Koller U, Dorotka R et al (2006) A tissue engineering approach to meniscus regeneration in a sheep model. *Osteoarthritis Cartilage* 14:1056–1065
69. Kon E, Chiari C, Marcacci M et al (2008) Tissue engineering for total meniscal substitution: animal study in sheep model. *Tissue Eng Part A* 14(6):1067–1080
70. Veth RP, Jansen HW, Leenslag JW et al (1986) Experimental meniscal lesions reconstructed with a carbon fibre-polyurethane-poly(L-lactide) graft. *Clin Orthop Relat Res* 202:286–293
71. Cook JL, Fox DB, Malaviya P et al (2005) Long-term outcome for large meniscal defects treated with small intestinal submucosa in a dog model. *Am J Sports Med* 34:32–42
72. Tienen TG, Heijkants RG, De Groot JH et al (2006) Meniscal replacement in dogs. Tissue regeneration in two different materials with similar properties. *J Biomed Mater Res B Appl Biomater* 76:389–396
73. Walsh CJ, Goodman D, Caplan AI et al (1999) Meniscus regeneration in a rabbit partial meniscectomy model. *Tissue Eng* 5:327–337
74. Martinek V, Uebliacker P, Braun K et al (2007) Second generation of meniscus transplantation: in-vivo study with tissue engineered meniscus replacement. *Arch Orthop Trauma Surg* 126:228–234
75. Weinand C, Peretti GM, Adams SBJ et al (2006) An allogenic cell-based implant for meniscal lesions. *Am J Sports Med* 34:1779–1789
76. Puelacher WC, Mooney D, Langer R et al (1994) Design of nasoseptal cartilage replacements synthesised from biodegradable polymers and chondrocytes. *Biomaterials* 15:774–778
77. Buschmann MD, Gluzband YA, Grodzinsky AJ et al (1991) Mechanical compression modulates matrix biosynthesis in chondrocyte/agarose gel culture. *J Cell Sci* 108:1497–1508
78. Butnariu-Ephrat M, Robinson D, Mendes DG et al (1996) Resurfacing of goat articular cartilage by chondrocytes derived from bone marrow. *Clin Orthop Relat Res* 330:234–243
79. Homming GN, Buma P, Koot HWJ et al (1993) Chondrocyte behaviour in fibrin glue in vitro. *Acta Orthop Scand* 64:441–445
80. Wakitani S, Kimura T, Hirooka A et al (1989) Repair of articular surfaces with allograft chondrocytes embedded in collagen gel. *J Bone Joint Surg* 71B:74–80
81. Grandolfo P, D'andrea P, Paoletti M et al (1993) Culture and differentiation of chondrocytes entrapped in alginate beads. *Calcif Tissue Int* 52:42–48
82. Lima EG, Mauck RL, Han SH et al (2004) Functional tissue engineering of chondral and osteochondral constructs. *Biorheology* 41(3–4):577–590
83. Shimko DA, Shimko VF, Sander EA et al (2005) Effect of porosity on the fluid flow characteristics and mechanical properties of tantalum scaffolds. *J Biomed Mater Res B Appl Biomater* 73(2):315–324
84. Mow V, Holmes M, Lai W (1984) Fluid transport and mechanical properties of articular cartilage: a review. *J Biomech* 17(5):377–394
85. Sander EA, Nauman EA (2003) Permeability of musculoskeletal tissues and scaffolding materials: experimental results and theoretical predictions. *Crit Rev Biomed Eng* 31(1–2):1–26
86. Hui PW, Leung PC, Sher A (1996) Fluid conductance of cancellous bone graft as a predictor for graft–host interface healing. *J Biomech* 29(1):123–132
87. Sannino A, Nicolais L (2005) Concurrent effect of microporosity and chemical structure on the equilibrium sorption properties of cellulose-based hydrogels. *Polymer* 46:4676–4685
88. Ulbrich K, Strohal J, Kopeček J (1982) Polymers containing enzymatically degradable bonds. 6. Hydrophilic gels cleavable by chymotrypsin. *Biomaterials* 3:150–154
89. Wang C, Kopeček J, Stewart RJ (2001) Hybrid hydrogels crosslinked by genetically engineered coiled-coil block proteins. *Biomacromolecules* 2:912–920
90. Nagahara S, Matsuda T (1996) Hydrogel formation via hybridization of oligonucleotides derivatized in water-soluble vinyl polymers. *Polymer Gels Networks* 4:111–127
91. De Jong SJ, De Smedt SC, Wahls MWC, Demeester J (2000) Kettenes-van den Bosch JJ, Hennink WE. Novel self-assembled hydrogels by stereocomplex formation in aqueous solution of enantiomeric lactic acid oligomers grafted to dextran. *Macromolecules* 33:3680–3686
92. Miyata T, Asami T, Urugami T (1999) A reversibly antigen-responsive hydrogels. *Nature* 399:766–769
93. Murakami Y, Maeda M (2005) DNA-responsive hydrogels that can shrink or swell. *Biomacromolecules* 6:2927–2929

Hydrogels for Cartilage Tissue Engineering

Pierre Weiss, Ahmed Fatimi, Jerome Guicheux, and Claire Vinatier

Abstract Tissue engineering is an emerging field of regenerative medicine that holds promise for the restoration of tissues and organs affected by chronic diseases, age-linked degeneration, congenital deformity, and trauma. Tissue engineering consists of building tissue and organs using cells grown on natural or artificial biomaterials outside the body. Recent efforts in bone and cartilage tissue regeneration have turned to tissue engineering, which have shown the proof of concept in clinical situations. Articular cartilage is composed of 70–80% of water retained in the form of a stable macromolecular gels. The extracellular matrix (ECM) and chondrocytes represent 20–30% of the articular cartilage. The lack of vascularization of the articular cartilage, however, prevents the development of an inflammatory response; this severely limits spontaneous repair. Currently, research is being directed to cell therapy associated with specific scaffold-like hydrogels. Articular cartilage, in particular, is considered to be a good candidate for tissue engineering, because it requires less metabolic involvement due to lower cellularity and avascular matrix. Cartilage organization and pathology have been highlighted here with respect to scaffold strategies using synthetic hydrogels as biomimetic extracellular matrices for tissue engineering.

Introduction

The loss of a tissue or an organ is one of the most serious problems in human health care. Tissue engineering is an emerging field of regenerative medicine that holds promise for the restoration of tissues and organs affected by chronic diseases, age-linked degeneration, congenital deformity, and trauma. Bone and cartilage tissue replacement has turned to recent efforts in tissue engineering, and proof of concept has been shown in clinical situations [1]. Currently tissue engineering consists of building tissue and organ using cells grown on natural or artificial biomaterials outside of the body. Many researchers throughout the world are interested in this unique matrix to manufacture supports for biotechnologies [2, 3]. The number of publications written to describe new hydrogels and their uses in the biomedical field is increasing dramatically from 300 to more than 2,000 publications in 7 years.

Numerous hydrogels are being used for bioapplications, [4] but none entirely satisfy the biorequisites. The polymers that are capable of forming hydrogels have a natural hydrogels origin, such as hyaluronic acid, alginate, chitosan, chondroitin sulfate, collagen, fibrin adhesive, and cellulose ether, or they are synthetic, such as poly(lactide-co-glycolide), poly(ethylene glycol), poly(vinyl alcohol), and poly(propylene fumarate). These reticulated three-dimensional (3D)

P. Weiss, A. Fatimi, J. Guicheux, and C. Vinatier • Inserm, UMR_S 791, Laboratoire d'ingénierie Ostéo-articulaire et dentaire, LIOAD, 1 place A. Ricordeau, Nantes, F-44042, France
e-mail: pweiss@sante.univ-nantes.fr

P. Weiss, A. Fatimi, J. Guicheux, and C. Vinatier • Université de Nantes, Laboratoire d'ingénierie Ostéo-articulaire et dentaire, LIOAD Faculté de chirurgie dentaire, IFR 26, 1 place A. Ricordeau, Nantes, F-44042, France

C. Vinatier • GRAFTYS SA, 415 rue Claude Ledoux, 13854 Aix en Provence, France

structures that enable the maintenance and proliferation of cells entrenched in a macromolecular structure while being made up of more than 90% water are rare. Hydrogels materials are used because they closely mimic tissue and can support the growth, multiplication, and differentiation of cells to produce regenerated organ transplants.

Hydrogels are water-swollen polymeric materials that are able to absorb and retain large volumes of water. The first hydrogels designed for use in the human body were introduced by the seminal 1960 paper in *Nature* by Wichterle and Lim. Traditional methods of biomaterial synthesis include cross linking copolymerization, cross linking of reactive polymer precursors, and crosslinking via polymer–polymer reaction. Hydrogels networks are widely used as 3D tissue engineering scaffolds to encapsulate cells by emulating the native extracellular matrix (ECM) due to their high water content and physical properties. In tissue engineering, it is crucial to control cell behavior to promote tissue regeneration. For example, degradable hydrogels have been investigated to generate space with time to provide room for cells to spread and migrate as the gels network degrades. The nature and the physical chemistry of hydrogels control the differentiation of stem cells and direct the strategy for tissue regeneration [5].

With regard to the applications of hydrogels in recent years, particular attention has been devoted to drug delivery, clinical application as well as to the use of hydrogels as scaffolds for tissue engineering and regenerative medicine. Among the materials used for regenerative applications, hydrogels are indeed very promising and are receiving increasing attention due to their ability to entrap large amount of water, good biocompatibility, and ability to mimic tissue environments.

Characterization of Hydrogels

Hydrogels are crosslinked hydrophilic polymers, which when placed in an aqueous media absorb large quantities of water and become highly swollen. The innate properties of a specific hydrogels are extremely important when selecting the material that is suitable for a given biomedical application. Hydrogels can be made from virtually any water-soluble polymer and encompasses a wide range of chemical compositions and bulk physical properties. However, hydrogels properties are highly dependent on environmental conditions as well. With this combination of factors, it is imperative that hydrogels properties are predetermined and that they are measured under specific conditions (pH, temperature) that are as close to the in situ conditions as possible.

One of the major challenges facing the use of hydrogels for tissue engineering is to replicate the mechanical and viscoelastic characteristics of the requisite tissues. In most cases, hydrogels-based tissues are significantly weaker mechanically than their native counterpart [6]. In general, hydrogels have poor mechanical properties, because they do not have the sophisticated complexity of native tissue.

Theory of Viscoelastic Behavior

Oscillatory measurements provide qualitative and/or quantitative information on the rheological properties of a hydrogels by determining the viscoelastic response of a sample as it is deformed under periodic stress or strain (Fig. 1a). The behavior is then defined as the periodic (sinusoidal) strain that is applied. In the dynamic sollicitation at constant frequency (ω), there are two important parameters: maximum amplitude (σ_m or γ_m) and phase angle (δ). The phase angle is null for an elastic solid and equal to $\pi/2$ for a viscous liquid. The response of a viscoelastic

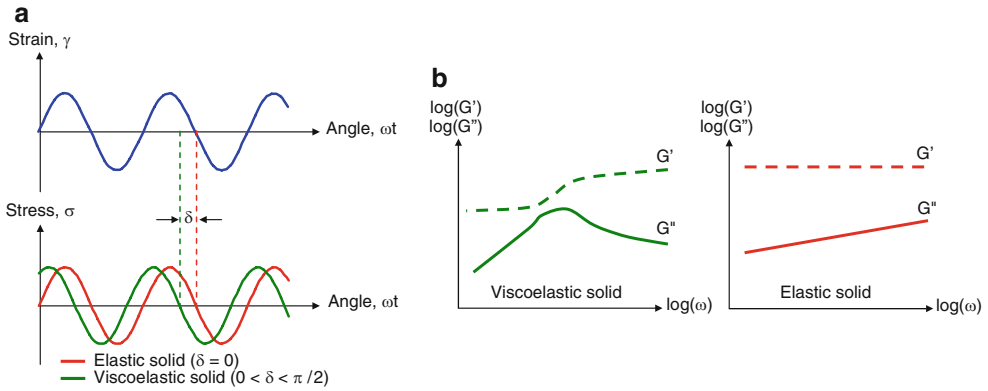


Fig. 1. (a) Typical stress response for different materials during oscillatory measurements. (b) Typical behavior of the storage modulus (G') and loss modulus (G'') as a function of frequency during dynamic mechanical testing.

material (liquid or solid) depends heavily on the solicitation frequency. In this case, the phase angle is $0 < \delta < \pi/2$. If the strain is defined as a complex oscillatory function of time with maximum amplitude and frequency, then

$$\gamma^* = \gamma_m \exp(i\omega t) \quad (1)$$

The measured response in this case is defined as:

$$\sigma^* = \sigma_m \exp(i\omega t + \delta) \quad (2)$$

A standard notation for sinusoidal tests is the complex dynamic modulus (G^*), defined as the ratio of the complex stress (σ^*) to the applied complex strain (γ^*):

$$G^* = \frac{\sigma^*}{\gamma^*} \quad (3)$$

Substituting (1) and (2) into (3), we can then write:

$$G^* = \frac{\sigma_m}{\gamma_m} \exp(i\delta) = \frac{\sigma_m}{\gamma_m} \cos \delta + i \frac{\sigma_m}{\gamma_m} \sin \delta = G' + iG'' \quad (4)$$

Here, G' is the real component (elastic or storage modulus) and G'' is the imaginary component (viscous or loss modulus).

The storage modulus G' provides information regarding the elasticity or energy stored in the material during deformation, whereas the loss modulus G'' describes the viscous character or energy dissipated as heat. The ratio between G'' and G' is expressed by the dissipation factor or loss tangent ($\tan \delta = G''/G'$), where δ is the phase angle. The loss tangent is a measure of the ratio of energy lost against energy stored in a cyclic deformation [7].

In general, the behavior of the storage modulus (G') and loss modulus (G'') as a function of frequency (ω) are predicted in Fig. 1b. The elastic solid is characterized by a storage modulus (G'), which is frequency independent and a loss modulus (G''), which decreases with decreasing frequency. Logically, G'' should not exist. In practice, we always measure a G'' , which is often

50, 100, or more times less than G' . On the other hand, a viscoelastic solid shows a plateau with a constant G' in the low frequency zone and G'' is dependent on frequency [7].

Cartilage Morphology, Properties and Diseases

Articular cartilage is a specialized connective tissue located on the surface of long bones facing the synovial fluid. Healthy articular cartilage appears bright white and slightly translucent and is called “hyaline,” because it has a high refractive index due to its high proteoglycan (PG) content, which is able to absorb large quantities of water. The main role of the articular cartilage is to absorb, transmit, and distribute the constraints to the subchondral bone. It also allows bones to slide against each other. The articular cartilage is considered stable in comparison to growth plate cartilage, which is transitory. Furthermore, unlike the cartilage growth plate, articular cartilage has a particularity – it is resistant to vascular invasion, to mineralization, and to replacement by bone [8]. The articular cartilage is not vascularized and not innervated. Its nutrition comes by diffusion from synovial fluid, a process that also removes waste. The synovial fluid is composed of water and nutrients such as electrolytes, small molecules, glucose, and metabolic waste from the renewal of the matrix as oxygen and carbon dioxide. The nutritional intake of chondrocytes occurs through two successive diffusion systems, first through the synovial membrane and then through the cartilage matrix. The diffusion of nutrients depends on the size, shape and charge of molecules, and the concentration of PG in the cartilage. The concentration of PGs plays a key role in the nutrient distribution. The load setting on a joint leads to a compression of the cartilage that expels waste into the synovial fluid. The discharge from the joint causes a return of fluid in the cartilage thus enabling nutrients to enter. The Extracellular matrix (ECM) of articular cartilage forms a molecular sieve that selects molecules able to diffuse into the cartilage. Consequently, the elements of a molecular mass greater than that of hemoglobin (69 kDa) generally cannot be taken up.

Composition of Articular Cartilage

Articular cartilage is composed of 70–80% of water retained in the form of a stable macromolecular gels. The Extracellular matrix (ECM) and chondrocytes represent 20–30% of the articular cartilage [9]. The ECM is composed of collagen and collagenous proteins, but not primarily a network of collagen fibers II, IX, and XI, and the PG represented are aggrecan.

Chondrocyte

Chondrocyte is the only cell type of the articular cartilage. Articular chondrocytes have a round or polygonal morphology, but it can also have a flattened or discoid morphology depending on its location within the articular cartilage. Because of the synthesis of PGs, on the one hand, which requires processing large amounts of glucose and glucosamine, and, the lack of vascularization of the articular cartilage, on the other hand, the major metabolic pathway of chondrocytes is the anaerobic glycolysis [10]. The metabolism of chondrocytes is permanently influenced by the physicochemical conditions prevailing in the pericellular space. Indeed, the cyclical forces applied to the cartilage influence the pericellular space and the shape of chondrocytes. The result is a modification of the cytoskeletal actin filaments, which may alter the expression of certain genes. Therefore, there is a direct link between the physical and chemical conditions surrounding the chondrocyte and its metabolic activity [11]. Chondrocytes are responsible for the synthesis, the maintenance, and the renewal of the ECM.

Thus, chondrocytes produce the components of the ECM like collagens and PGs. They also synthesize enzymes able to degrade the ECM as metalloproteinases [12] or hyaluronidase [13]. Finally, chondrocytes are the source of many cytokines and growth factors important in the regulation of anabolic and catabolic processes of cartilage. Many cytokines, vitamins, hormones, or growth factors influence chondrocytic phenotype. For example, insulin, TGF- β (transforming growth factor β), IGF (insulin like growth factor), BMP (bone morphogenetic protein), and ascorbic acid all play a role in chondrogenic differentiation or in maintaining the chondrocytic phenotype.

The extracellular matrix (ECM) of articular cartilage consists of a network of collagen fibers embedded in a gels composed of PGs and water. The ECM of cartilage is mainly composed of fibers of collagen type II, IX, and XI, which are embedded in the PG as aggrecan. The ECM also contains noncollagenous proteins, such as, COMP (cartilage oligomeric matrix protein) or CMP (cartilage matrix protein) and small PGs. The collagens are the most abundant proteins in the human body. Collagen fibers are also the main source of tension forces in animal tissue. There are currently 27 known different types of collagens [14]. The fibril network of articular cartilage is a copolymer of collagen II, IX, and XI. Other types of collagen, such as collagen I, III, VI, X, XIII, and XIV are found in small quantities [15].

The PGs represent 22–28% of the dry weight of adult articular cartilage. These are macromolecules whose molecular weight is between 6,104 and 4,106 Da. The PGs are glycoproteins consisting of a protein that is axially connected to one or more very long chain polysaccharide acids called glycosaminoglycans (GAG). The GAG structure is based on repeating disaccharides: one of the sugars is either an N-acetylglucosamine (GlcNAc) or an N-acetylgalactosamine (GalNAc), and the other sugars are acid sugars, like glucuronic acid or iduronic acid or galactose [16]. The articular cartilage has five different types of GAGs: four sulfated GAGs – chondroitin sulfate (CS), the dermatan sulfate (DS), the keratan sulfate (KS), and heparin sulfate (HS) and a nonsulfated GAG – the hyaluronic acid (HA).

Aggrecan is the major PG of the articular cartilage; it represents 90% of cartilage PG. It is a large molecular aggregate containing more than one hundred CS and KS chains covalently linked to an axial protein [17]. In cartilage, aggrecan is associated with hyaluronic acid and a small glycoprotein liaison or link protein to form large aggregates [16]. The PGs in high concentrations create a high osmotic pressure, which keeps the water in the articular cartilage [18]. Hyaluronic acid (HA) is synthesized in the form of a long chain branched polymer and is negatively charged. It is composed of repeating disaccharides of glucuronic acid and N-acetylglucosamine with alternate β 1-4 and β 1-3 bonding. The synthesis of HA is different from that of PG, since it is not sulfated after synthesis [19]. The HA has remarkable hydrodynamic characteristics; it causes a highly viscous environment that is capable of holding large quantities of water. Thus it plays an important role in homeostasis and tissue integrity [19]. HA interacts with PGs in articular cartilage, as well as with other molecules important for the assembly of the ECM [20]. HA, due to its lubricating properties, is used in intra-articular injection for the treatment of pain associated with osteoarthritis [21].

Histological Organization of Articular Cartilage

The composition and histological organization of articular cartilage varies with age depending on its position relative to the articular surface [22]. Indeed, chondrocytes as well as collagen, PGs, and other proteins are organized in a defined order that is distinguished as four zones in the articular cartilage (Fig. 2). The superficial zone in contact with the synovial fluid is the sliding surface of the cartilage and accounts for 5–10% of the thickness of cartilage.

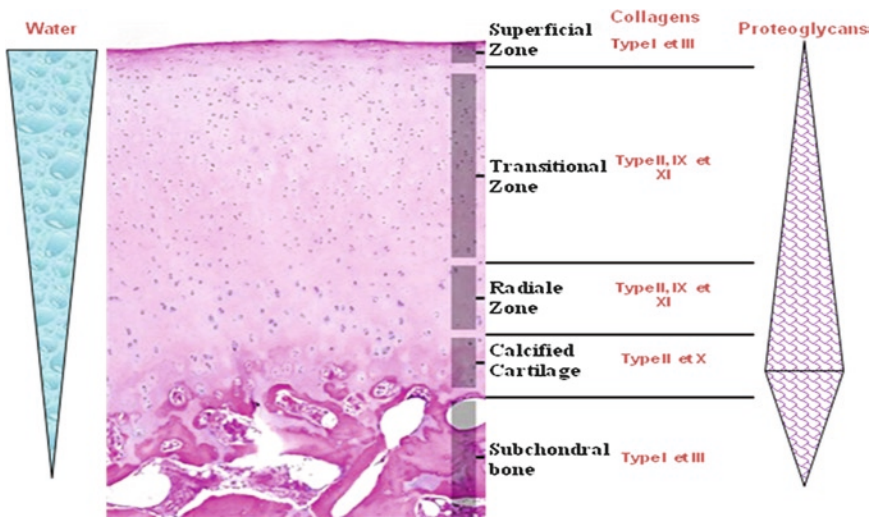


Fig. 2. Histological organization of articular cartilage.

This surface area can be divided into two sublayers: The first layer of an acellular matrix contains fine fibrils of collagen I, II, and III and low-PGs. In a deeper layer, the chondrocytes are flat, ellipsoidal, and oriented parallel to the articular surface. In this zone, the chondrocytes synthesize small collagen fibers 30 nm in diameter. These collagen fibers are arranged parallel to the articular surface. Chondrocytes in this zone synthesize lubricin. However, these chondrocytes synthesize less PG than other regions. In this area, the chondroitin sulfate (CS) chains predominate compared with the keratin sulfate (KS) chains that form an impermeable barrier to the diffusion of hormones and nutrients but permeable to water and oxygen. The orientation of collagen fibers and a stronger collagen-PG association enables the superficial zone to protect the underlying cartilage from tearing or shear forces generated during joint stroke [23].

The transition zone occupies 40–50% of the thickness of articular cartilage. In this zone, chondrocytes are round or oval and larger than those of the superficial layer. They are anachically arranged in the ECM. Chondrocytes of the transition zone are metabolically active in the synthesis of PGs and collagen. These collagens are type II, IX, and XI in thick fibers of 30–80 nm in diameter. The fibers obliquely intersect and form a nonoriented network less dense than in the superficial layer. The radial layer occupies about 30–40% of the thickness of the articular cartilage. The name is based on the radial orientation of the cells and collagen fibers that make up this layer. The morphology of the chondrocytes is spherical and arranged in columns perpendicular to the articular surface. The PG content is important, while the water content is the lowest of all in the articular cartilage. These collagen fibers, also composed of collagen II, IX, and XI, are the thickest (~100 nm in diameter). These collagen fibers are oriented vertically relative to the articular surface, which provides the cartilage resistance to compressive forces.

The calcified layer is the surface layer and represents only 5–10% of the cartilage thickness. This layer separates the articular cartilage and the subchondral bone. The arrangement of proteins in the ECM in this area is very close to that observed in the radial zone. Chondrocytes are in limited number, hypertrophic and synthesize type X collagen in addition

to collagen II and XI. A biological carbonated apatite is deposited on collagen fibers that penetrate directly into the bone epiphysis to anchor the cartilage. The calcified cartilage layer is separated from nonmineralized cartilage layers by a dense line called the tidemark. This tidemark is rich in collagen fibers and contains hyaluronic acid, but it appears not to contain GAG [24].

Extracellular Matrix (ECM)

The ECM exhibits differences that depend on the distance of the chondrocytes embedded in a chondron. Thus, the ECM areas can be classified into distinct regions called pericellular matrix and interterritorial matrix. The pericellular area is a region circumscribed around the chondrocyte. The association of pericellular matrix and chondrocyte is a microanatomical entity called “chondron” [25]. The pericellular matrix contains all the constituents of the other areas of the ECM, such as collagen type II, IX, XI, aggrecan and fibromodulin, in normal cartilage. This area is distinguished by the presence of type VI collagen. This area also has high levels of sulfated PG, as well as high aggrecan, hyaluronic acid, and link protein concentrations [26]. In fact, this area may regulate the biomechanical and biochemical microenvironment of chondrocyte [27]. It was assumed that the “chondron” serves as a transducer of mechanical signals [28].

In the territorial matrix envelope, the pericellular matrix of chondrocytes is either isolated, organized into blocks, or arranged in columns, as in the radial zone. Collagen fibers are thicker in this area and form packages, which appear to be directly adhered to the pericellular matrix. Collagen fibers form a fibrillar cage around cells and provide mechanical protection for the chondrocytes. These fibers also contain a lot of PG that are rich in CS chains. The interterritorial matrix provides the mechanical properties to the articular cartilage. Collagen fibers of this interterritorial matrix shift from a tangential orientation in the superficial zone to a radial orientation in the radial zone. The interterritorial matrix is the broader part of cartilage matrix and contains PG rich in KS chains and the thickest collagen fibers.

Pathology of Articular Cartilage

Trauma: Articular cartilage lesions are due to repetitive impact trauma or progressive mechanical degeneration due to a specific activity. These lesions are the cause of many disabling symptoms such as pain and functional disturbance of the affected joint. The articular cartilage lesions can be classified according to their depth. The ICRS (International Cartilage Repair Society) established a classification of cartilage lesions to standardize the description of focal lesions of cartilage (Fig. 3).

A grade 0 lesion corresponds to normal healthy cartilage. Grade 1, where the cartilage is almost considered normal, may be divided into two; grade 1A, where the articular surface has a soft appearance and contains fibrillar element, and grade 1B, where the articular surface has cracks or surface tears. A grade 2 is considered as abnormal and has a deeper injury than grade 1, but its depth is less than 50% of the articular cartilage thickness. In a grade 3A, the depth of the cartilage is more than 50% of the articular cartilage thickness, but does not extend to the calcified layer. Grade 3B reaches the calcified layer, and grade 3C reaches the subchondral bone without crossing through. Grade 3D is similar to grade 3C but has bulges on the surface of cartilage. Finally, a grade 4 lesion extends up to cross through the subchondral bone. Other cartilage lesions classifications exist, but the ICRS classification is one of the most relevant.

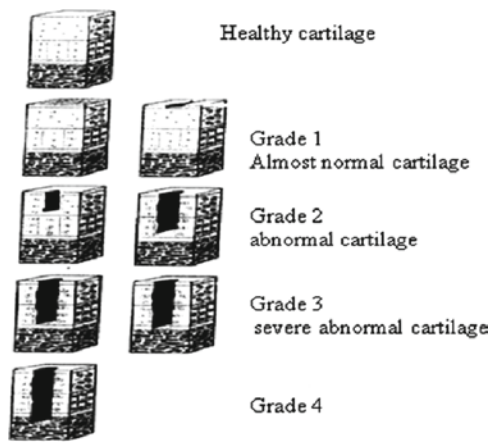


Fig. 3. International cartilage repair society classification of articular cartilage lesions.

Osteoarthritis: Among the many degenerative diseases of articular cartilage, osteoarthritis is the most common rheumatological disorder. It is the second leading cause of disability after cardiovascular diseases [29]. Rheumatoid arthritis, juvenile arthritis, and ankylosing spondylitis are inflammatory disorders, and so are not part of the prime targets of tissue engineering because of the inflammatory processes underlying these pathologies. Osteoarthritis is now the leading cause of morbidity in all of the developed countries. In 1995, the estimated number of cases in the United States was 20 million. The aging of the U.S. population will increase that number to over 50 million by 2020 [30]. According to WHO, 10% of the population over 60 suffer from osteoarthritis, 80% have limited movements, and 25% are unable to perform their daily activities. Osteoarthritis is the most common cause of long-term disability among those over 65 [31].

Two types of osteoarthritis can be distinguished: the primary or idiopathic osteoarthritis, which has no known cause, and secondary osteoarthritis that is caused by traumatic injury, heredity, inflammation, or metabolic disorders [32]. A typical symptom of osteoarthritis is a gradual increase of pain and stiffness in and around the joint, combined with function impairment of the articulation [33]. Different joints may be affected by osteoarthritis: the hip, the cervical and lumbar vertebrae, the first metatarsophalangeal joint of the feet, distal and the proximal interphalangeal joints, the first carpo-metacarpal joint of the hand, and the knee joint. However, idiopathic osteoarthritis rarely reaches the shoulder articulation, elbow, or ankle. It affects preferentially the hand, foot, knee, or hip [34]. Osteoarthritis is the result of a degeneration of the joint, a process that involves a progressive loss of articular cartilage accompanied by attempted repair of articular cartilage, a remodeling and sclerosis of the subchondral-bone, and the formation of osteophytes [35, 36].

Cartilage Repair

Spontaneous Cartilage Repair: The lack of vascularization of the articular cartilage prevents the development of an inflammatory response; this lack severely limits spontaneous repair. Only lesions penetrating the subchondral bone, that is vascularized, are able to trigger the repair process [37, 38]. A grade 1 lesion, where the articular surface remains intact,

is visible only at the macromolecular level and corresponds to a decrease in the PG content of the cartilage. This decrease in PG reduces the resistance of articular cartilage and increases its permeability. How to repair these types of lesions is not clearly established. The hypothesis on the possible repair of the grade 1 lesions depends on several conditions: the loss of PG must not exceed that which is being produced by the chondrocytes, the network of collagen fibrils must remain intact, and the number of chondrocytes able to respond to these lesions must be sufficient [39]. However, this hypothesis needs to be validated to determine the extent to which these grade 1 lesions can progress.

The grade 2 and 3 lesions, which interrupt the articular cartilage surface, give rise to the proliferation of chondrocytes and an increase matrix molecules synthesis. However, this newly formed matrix does not fill the defect and soon after the trauma, the increase in cell activity and proliferation ceases [36]. The defect becomes permanent, which alters the mechanical function of the joint and increases the risk of cartilage degeneration. Since this injury does not reach the subchondral bone, where it would have cellular contact, it cannot be repaired spontaneously.

In a grade 4 injury, the cartilage lesion passes through the subchondral bone and, therefore, reaches the bone marrow, triggering a stream of cells and blood into the defect. In 2 days, a blood clot is created that fills the defect [40]. The inflammation phase then takes place, which is characterized by vasodilatation and increased permeability of the vessels membrane of the subchondral bone, which initiates the process of transudation and exudation. This leads to the formation of a dense network of fibrin containing inflammatory cells and stem cells able to differentiate into reparative cells. In the case of cartilage damage passing through the subchondral bone, the mesenchymal cells from the bone marrow reshape the blood clot and participate in the repair process [41]. The final phase of this spontaneous process is the reparation phase. Blood vessels, under the influence of angiogenic factors, invade the network of fibrin and fibroblasts to produce a fibrous repair tissue that then becomes scar tissue [42]. In the following months, the articular area forms a repair tissue intermediate between the hyaline cartilage and fibrocartilage [41, 43]. However, this repair tissue has inferior mechanical properties with less PG, collagen II, and other biochemical markers of articular cartilage than for normal articular cartilage. After 1 year, this repair tissue often shows signs of deterioration, such as, fibrillation, fragmentation, and irregularities, which promote degeneration [40].

The current data indicates that traumatic articular cartilage lesions do not repair when they affect the cartilaginous area of the joint. In deeper lesions affecting the subchondral bone, the body attempts to repair the damage through the formation of a fibrocartilaginous repair tissue remaining transient. Lesions of articular cartilage often change toward larger lesions like osteoarthritis lesions. Consequently, using cell-free scaffolds for cartilage repair is not possible. The data strongly indicates the necessity for the development of innovative therapeutic approaches for the treatment of bone and cartilage. Tissue engineering that combines cell biology and biomaterial engineering to design and maturation of various tissues, could open new therapeutic modes for cartilage-applied regeneration.

Cartilage Regeneration

Tissue Engineering (TE)

Injury or loss of organs or tissues can cause structural and metabolic changes resulting in significant morbidity or even death [44]. To treat the loss of tissue or organs, current

therapy consists of implanting a prosthesis to replace, within limits, structure and function to the injured body. Tissue engineering combines the principles of engineering and life sciences to develop biological substitute tissue to restore, maintain, or improve tissue functions [45]. The principle of tissue engineering is to use a biocompatible matrix seeded with appropriate cells and/or loaded with biologically active molecules to promote differentiation and cell maturation [46]. Two approaches have been developed; the first approach is to manufacture in vitro a fully functional tissue before implantation, and the second approach is to implant a scaffold with immature cells cultivated in vitro and allowed to mature in vivo [47].

Articular cartilage is considered to be a good candidate for tissue engineering, as it requires less metabolic involvement due to low cellularity and avascular matrix. [48]. Three components are important in cartilage tissue engineering; matrices, cells, and morphogenic factors. A major research aim is the development of matrices that can meet the specific requirements for engineering cartilage tissue. To determine the ideal cell source, current research is oriented toward optimizing culture conditions to stimulate chondrogenesis in vitro and in vivo by using a bioreactor. Recent developments in molecular biology and gene therapy are providing newer and better approaches to genetically engineered articular cartilage.

Cell Origins

Chondrocytes: Adult chondrocytes, able to form an ECM, have been isolated from different sources, as well as cells of choice for articular cartilage tissue engineering [49, 50]. However, chondrocytes derived from elastic cartilage (ear), do not have the mechanical properties of hyaline cartilage (joint, nasal septum). An in vitro and in vivo study [50] revealed that chondrocytes from different anatomical sites form tissue that has the characteristics of the tissue origin. Consequently, chondrocytes from a hyaline cartilage source should be used for articular cartilage repair applications. A comparison of the hyaline chondrocytes from nasal and rib chondrocytes are superior as articular chondrocytes in terms of the amount of cartilage formed in subcutaneous sites. However, there are significant limitations to the use of chondrocytes, whatever their origin, due to the instability of the phenotype in the monolayer culture. Indeed, chondrocytes grown in monolayer lose their phenotype, which results in loss of expression of chondrocytes phenotypic markers as collagen II and aggrecan primarily, but also the SZP (superficial zone protein) [51]. This loss of chondrocytes phenotype is the orientation of cells toward a fibroblastic phenotype. The acquisition of the fibroblast phenotype is characterized by an increased expression of type I collagen and the adoption of the characteristic spindle shape of fibroblasts. This process of dedifferentiation is still reversible and when dedifferentiated chondrocytes are placed in a 3D construct, they recover their differentiated phenotype [52–54].

Studies have shown that chondrocytes isolated from osteoarthritis cartilage undergo metabolic changes, such as the disruption of the balance between anabolism and catabolism, which may cause an alteration to cellular response [55]. These chondrocytes retrieve a type II collagen expression and produce PG similar to that of normal chondrocytes. This suggests that osteoarthritic chondrocytes may be a source of chondrocytes for cartilage tissue engineering. Despite this positive data, osteoarthritic joints often lose articular cartilage, which limits the amount of tissue available.

Mesenchymal Stem Cells: Mesenchymal stem cells (MSC) are pluripotent cells characterized by their capacity to proliferate and differentiate. Indeed, the MSCs are capable of a self renewal and to move toward a chondrocytic, adipocytic, osteoblastic, neurogenic, and myogenic phenotype [56, 57]. The discovery of these cells has led to new therapeutic

strategies, partly due to their ease of access. Bone marrow is the most widely used source of MSC, but MSC have been isolated from other tissues, such as muscles [58], adipose tissue [59, 60], periosteal or perichondral tissue [61]. Furthermore, the pluripotentiality of MSC isolated from bone marrow, adipose tissue [62], muscle, and the synovium has been demonstrated [61]. These MSC may be of major interest for tissue engineering as they do not seem to possess molecule histocompatibility complex (MHC) class II responsible for immune rejection. It is now well established that the MSCs have immunomodulatory properties. MSCs are able to inhibit the function of mature T cells as a result of their activation by nonspecific antigen. They are also able to reduce the memory and naive T cells response. They can also prolong the graft survival with a bad histocompatibility and, therefore, reduce the reaction of graft against the host [63]. Thus MSC could potentially be used as an allogeneic [64] source of cells for cartilage tissue engineering.

Unlike autologous chondrocytes, MSC can be easily manipulated to become chondrocytes [65]. However, chondrogenic differentiation of MSC in 3D culture often leads to hypertrophy of chondrocytes and ECM mineralization [66, 67]. The MSCs in these growing conditions appear to have an endochondral type of differentiation leading to early hypertrophy that is reflected by the expression of collagen X, the MMP13 and alkaline phosphatase and the mineralization of the ECM. Therefore, chondrogenic differentiation of MSC should be checked before their use in cartilage repair to prevent any risk of neofomed tissue mineralization [67, 68].

Scaffolds

Scaffolds represent one of the key components for tissue engineering. The applications range from the substitution of a periosteal flap in the autologous chondrocytes implantation treatment to a drug delivery device that could enhance tissue regeneration and reduce the osteoarthritis related inflammatory processes. The scaffold can be associated with cells in a bioreactor before implantation [69] and provide a 3D environment that is desirable for the production of cartilaginous tissue [70]. Ideally the scaffold should: (1) have directed and controlled degradation, (2) promote cell viability, differentiation, and ECM production, (3) allow for the diffusion of nutrients and waste products, (4) adhere and integrate with the surrounding native cartilage, (5) span and assume the size of the defect, and (6) provide mechanical integrity depending on the defect location. The more common scaffolds used for cartilage are based on hydrophilic polymers in the form of hydrogels, sponges, or meshes.

Currently, regenerative medicine is moving toward using less and less invasive surgical techniques with the objective of reducing morbidity and the duration of hospitalization. This quest for minimally invasive surgery has motivated the development of injectable matrices for bone and cartilage tissue engineering. Once implanted, these injectable matrices must also be able to set, acquire the desired shape, and present mechanical properties in relation to the tissue to be repaired or replaced. Polymers with high viscosity in water can be used to make hydrogels via physical, ionic, or covalent cross-linking. In this case, hydrogels are used to make actual macromolecular networks comparable to the extracellular matrix (ECM).

Hydrogels Polymers (FIGURE 4)

Hydrogels are very valuable scaffolds for 3D culture of cells due to their biomimetic nature. Natural materials are advantageous in that they contain information that facilitates cell

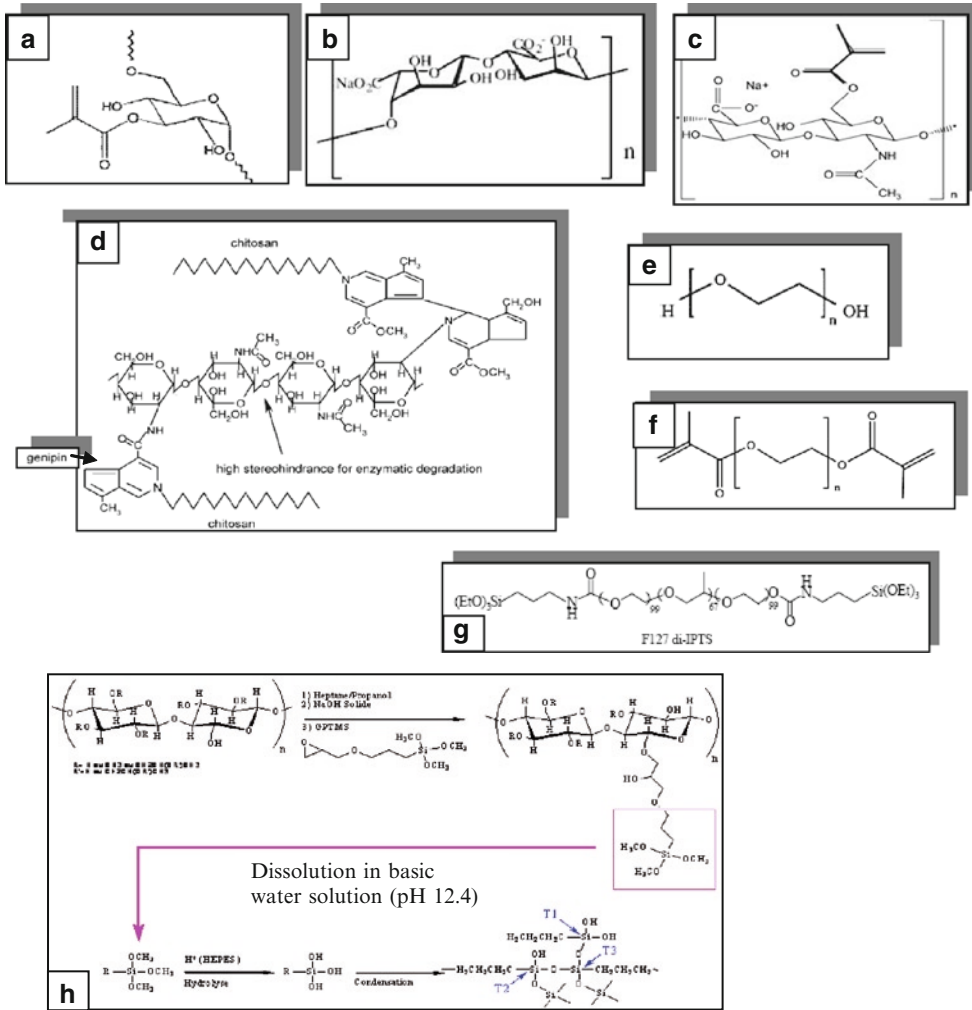


Fig. 4. Chemical structure of the polymers commonly used in cartilage tissue engineering. (a) Methacrylated Poly-dextrane from [91] (b) Sodium alginate from [86] (c) Methacrylated hyaluronic acid from [76] (d) Chitosan cross linking with genipin from Mi [115] (e) Poly(ethylene oxide) (PEO) or poly(ethylene glycol) (PEG) and (f) Dime-thacrylated poly(ethylene oxide) (PEODM) from [85]. (g) Silated PEO–PPO–PEO triblocks from Sosnik [108] (h) pH sensitive HPMC-si crosslinking.

attachment or maintenance of differentiated function. On the other hand, synthetic polymers allow precise control over molecular weight, degradation time, hydrophobicity, and other properties, but they may not interact with cells in a desired manner [45]. Macroporous biodegradable polymers (sponges) have been used for tissue engineering [71, 72]; however, uniform cell seeding and culturing within these macroporous polymers remain difficult due to limited penetration of the cells and diffusion of nutrients. Furthermore, these bulk macroporous polymers are not suitable for percutaneous surgery. Another approach is to mix cells with a viscous aqueous solution made of a hydrophilic polymer; this is a mixture of cells and polymer that can be injected in the surgical site. The polymer is then crosslinked and set in situ.

For cartilage tissue engineering, the ability to withstand the shear and compressive forces at the joint surface is very important.

Uncellularized hydrogels. For intervertebral discs, in the early stage of degenerative disc disease or traumatic herniations, the treatment may involve replacing the *nucleus pulposus* and preserving the *annulus fibrosus*. One solution is to use methacrylate based copolymers without cells to substitute the *nucleus pulposus* in terms of mechanical properties.

Hyaluronate-based hydrogels were prepared by using a double chemical modification and then simultaneously grafted alkyl hydrophobic groups on the backbone and chemically crosslinking the polymer chains. This double process forms hydrogels with shear-thinning properties due to the hydrophobic interactions between the alkyl groups, as well as a sufficient structural stability due to the chemical crosslinking. Optimization of the reaction parameters made it possible to prepare injectable hydrogels crosslinked both physically and chemically, with improved rheological properties compared to those of only physically crosslinked gels obtained from amphiphilic derivatives.

Cellularized hydrogels by cell encapsulation. The greatest challenges is to implant and maintain live cells that produce new cartilage tissue with appropriate physiological and functional extra cellular matrix. Photopolymerization of substituted poly(ethylene oxide) has been used to transform encapsulated chondrocyte cells in a liquid polymer solution to form a gels [73]. This process forms gels rapidly under physiological temperature with minimal heat production, as well as, in controlled time and space [74]. The hydrogels are stable and mechanically strong, because the polymer networks are held together by the covalent crosslinks.

Successful cell encapsulation requires a uniform cell suspension and mild photopolymerizing conditions; low concentrations of photoinitiator and low-intensity UV light [75]. To initiate polymerization, the photoinitiators are carefully dose regulated as they can effect cytotoxicity of the cartilage cells [75]. Free radicals can directly react with cellular components, such as membranes, proteins and DNA, thereby, inducing cellular damage or indirectly by forming reactive oxygen species (ROS) [76]. For example, using 2-hydroxy-1-[4-(2-hydroxyethoxy)phenyl]-2-methyl-1-propanone as the photoinitiator, multipotent stromal cells (MSC) [76] were affected in monolayer conditions but not in 3D hydrogels, such as methacrylate derivatized hyaluronic acid and methacrylated hyperbranched polyglycerol hydrogels.

Barbucci et al. use the thixotropic behavior of crosslinked hydrogels that became fluid under mechanical stimulus; after the stimulus is removed the hydrogels resumes the original consistency. To entrap cells inside the reticulated hydrogels, the hydrogels is placed inside a syringe and subjected to a mechanical stimulus by the piston movement until it became liquid. This is injected into a Petri dish containing 200 μL of cell suspension (5×10^3 cells). The hydrogels and the cell suspension are then drawn back into the syringe and deposited into the Petri dish. The ensuing gels traps the cells in the network. Another method that used by the same team involved freeze drying the hydrogels to form a porous solid that then took up cells that were in the swelling medium of the hydrogels [77].

Biopolymers. Macromolecules, also called biopolymers, come from biological sources and are used in tissue engineering of cartilage. Two types of biopolymers are used to make hydrogels: proteins such as collagens [78] and polysaccharides such as alginates [79], hyaluronic acid, [80] and chitin. The hydrogels made of collagens lead to notable cellular reactions with a high production of metalloproteases. Using fibrin hydrogels, a high reduction in volume was observed after implantation [70]. Collagens are visco-elastic and exhibit good cell and tissue compatibility [81]. The most readily available forms are injectable collagen

gels as suspensions of collagen fibers and nonfibrillar, viscous solutions in aqueous media. The collagen network easily retains cells by physical entrapment. Collagen gels are also used as scaffolds in tissue engineering [82]. To overcome microorganism transmission and immunological reactions with biomaterials from other patients or animal species, autologous injectable hydrogels made of autologous plasma [83] is used with chondrocytes. This system is similar to fibrin hydrogels glue [84] without risk of contamination.

Alginates, obtained from seaweed as a liquid, were one of the first polysaccharides used for cartilage tissue engineering [85, 86]. With cells inside, the viscous phase can be injected and crosslinked with calcium to prevent migration from the defect before the reticulation. Specialists in this area of cartilage regeneration are Vacanti et al. [87], Leone, and Barbucci for hydrogels based on polysaccharides [88], such as, alginates and carboxymethyl celluloses modified by amino or phosphate groups. All of these polymers are important as cartilage tissue engineering materials.

Dextran is a naturally occurring bacterial polysaccharide, which consists primarily of α -1,6-linked D-glucopyranose residues with a small percent of α -1,2-, α -1,3-, and α -1,4-linked side chains [89]. Polydextran based hydrogels are biocompatible in vitro [90] and in vivo [91], but reticulated dextran based macromolecules do not allow cell encapsulation. However, haluronan can be photopolymerized (HYAFF® 120) to form excellent biocompatible material for tissue engineering [92]. Chitosan, derived from chitin, is an amphiphilic copolymer in which the relative proportion of acetylated and deacetylated residues plays an important role in the balance between hydrophilic and hydrophobic interactions. It is well known for its good biocompatibility.

Synthetic polymers. Due to possible antigenicity complications and inadequate supply of natural polymers with consistent composition, investigators have turned to the development of synthetic polymers. Many synthetic polymers form hydrogels, such as poly(vinyl alcohol), poly(ethylene glycol) (PEO), and copolymer of poly(ethylene oxide) and poly(propylene oxide) (PPO).

Poly(vinyl alcohol), PVA, is a nontoxic and nonimmunogenic material. The hydroxyl side groups on PVA make it hydrophilic with a semicrystalline structure via intramolecular hydrogen bonding. However, PVA hydrogels lack the strength and toughness to serve as a cartilage substitute material. To resolve this shortcoming, an interpenetrating network with polyacrylamide as a load-bearing cartilage substitute was developed as a microporous hydrogels substitute for cartilage without cells [93]. Hubble et al. prepared degradable PEG- based hydrogels using enzymes and functionalized hydrogels [94].

Physically crosslinked hydrogels. Many polysaccharides, in aqueous solutions, form hydrogels due to intermolecular reversible hydrophobic interactions, leading to a 3D network [95, 96]. These hydrogels have shear-thinning properties and can be injected to promote chondrocyte proliferation and cartilage repair. However, the gels are only physically crosslinked and progressively lose their 3D structure when they are in contact with aqueous fluids. The polymers used for this type of hydrogels undergo reversible thermal gelation (RTG) and produce low viscosity aqueous solutions at ambient temperatures, that create a gels at higher temperatures. Most are temperature-sensitive hydrogels that have a low critical solution temperature (LCST) below which, they swell in water and other fluids. Above this temperature, they will deswell or repel the fluids. Poly(ethylene oxide)-(PEO)-poly(propylene oxide), PEO-PPO-PEO triblocks are one of the most important RTG-displaying materials (the PEO₉₉-PPO₆₇-PEO₉₉ triblock is known as Pluronic F127). These physically cross-linked hydrogels are not stable and dissolve in culture mediums. Cohn added crosslinking agents, such as methacrylate and silane groups, to improve the mechanical behavior of these

systems [97]. Subsequently, agarose, a low gelling temperature polysaccharide, was used as a 3D culture for cartilage cells for human intervertebral disc cells [98].

Ionic hydrogels. The ionic hydrogels, such as alginates, are frequently used for 3D cultures and cartilage tissue engineering. Alginic acid (or alginate), is a viscous gum that is abundant in the cell walls of brown algae. It is a linear copolymer with homopolymer blocks of (1-4)-linked β -D-mannuronate (M) and its C-5 epimer, α -L-guluronate (G), is covalently linked in different sequences. The monomers can reside in homopolymer blocks of consecutive G-residues (G-blocks), consecutive M-residues (M-blocks), alternating M and G-residues (MG-blocks), or randomly organized blocks. Gelation occurs in the presence of divalent cations, such as calcium, which ionically crosslinks the polyguluronate carboxylate groups in the alginate. The gentle gelling property of these gels has led to their use as cell transplantation vehicles for new tissue growth and has been used in 3D chondrocyte cultures.

The number of human articular chondrocytes cells remained nearly constant with no proliferation from day 1 to 26 in in vitro experiments performed alone with 1.2 and 2.4% alginate gels [99]. In contrast, in vivo experiments with suspensions of chondrocytes in 2% alginate that were gelled by mixing with CaSO_4 (0.2 g/mL) and injected into the dorsal aspect of nude mice have survived for up to 30 weeks. Analysis of the implanted constructs indicated progressive cartilage formation with time [100].

Covalent hydrogels. Covalent crosslinking to make hydrogels is usually done ex vivo. The covalent reticulated hydrogels obtained is only by surface association with cells or as biomaterial to fill a defect. A different strategy involves using a biomechanical competent hydrogels with no degradation under biological conditions called a “hydrogels patch.” In another method, the cells are mixed in the polymer solution before injection, and crosslinking occurs inside the matrix with cells being entrapped within the polymer network. For this strategy, the crosslinking must be performed in water under physiological conditions without toxic reacting agents. These hydrogels are known as “live hydrogels.”

In Situ Crosslinkable Hydrogels

For many clinical uses, injectable in situ crosslinkable hydrogels are preferred because they can be: (a) formed into desired shapes at the site of injury, (b) positioned in complex areas and then crosslinked to conform to the required dimensions, (c) the polymer mixture adheres to the tissue during gels formation, which strengthens the tissue–hydrogels interface, and (d) in situ injection or laparoscopic placement minimizes the invasive procedures [101].

A polymeric cartilage tissue named oligo(poly(ethylene glycol) fumarate) (OPF) was engineered as a nonphoto crosslinkable PEG based injectable hydrogels that enabled cell encapsulation. The macromer is crosslinked through the fumarate unsaturated double bond in situ with a radical initiator to form a hydrogels without the need for ultraviolet light. The fumarate ester bonds is hydrolytically cleavable, thus providing a degradable hydrogels [102].

Another strategy for self-setting hydrogels is to use pH changes that cause covalent links to form between macromolecules. For example, modifications to the pH of self assembled peptide hydrogels is a simple way to encapsulate cells in a 3D culture. Polysaccharides have been functionalized to perform a self-setting hydrogels with cells entrapped inside its network; a strategy developed in this laboratory [103, 104]. The self-hardening principle of the hydroxypropylmethylcellulose-silated (HPMC-Si) hydrogels is based on the silanes grafted by an epoxy function along the HPMC chains (HPMC-Si) [105]. The silane used in this approach is 3-glycidoxypropyltrimethoxysilane (GPTMS). The grafted silane percentage on HPMC is determined from silicon content. Dissolution of HPMC-Si takes place in a strong

basic medium (NaOH at pH 13.2), which leads to silane ionization into sodium silanolate ($-\text{SiO}-\text{Na}^+$). The limiting pH of the sodium silanolate stabilization is ~ 12.1 – 12.2 , below which sodium silanolate transform into silanols ($-\text{SiOH}$). The ions undergo condensation reactions, forming a 3D network of the HPMC-Si chains. The synthesis of silated polysaccharides was described in 1990, by Turczyn et al. [103]. This hydrogels was then utilized in this laboratory for bioapplications and has great potential for articular tissue engineering with different cells origins [2, 54, 106, 107].

Cohn [97, 108] developed strategies, based on heat-sensitive physical hydrogels, to make a copolymer $\text{PEO}_{99}-\text{PPO}_{67}-\text{PEO}_{99}$ called Pluronic F127. These micellar constructions are made with at least 20% polymer, but their properties are very weak and break in culture media. Subsequently, Cohn silanized the macromeres to create covalent crosslinks with $\text{R}-\text{Si}-\text{OH}$.

Polymer Associations

To improve the bioactivity or biological reactivity of hydrophilic macromolecules, specific macromolecules were developed to enhance the adhesion, degradation, ECM production, and/or differentiation of mesenchymal stem cells. Polysaccharides and protein IPNs of a hydrogels series, based on methacrylate and aldehyde-bifunctionalized dextran and gelatin, was synthesized and characterized [109]. The methacrylate groups were UV crosslinked, and the aldehyde groups enabled the incorporation of attached gelatin.

Several hydrogels for cartilage tissue were engineered based on photopolymerized PEG and chondroitin sulfate CS to enhance the mesenchymal stem cells differentiation toward chondrocyte phenotype [110–112]. Other biopolymers, such as hyaluronic acid and/or type I collagens were grafted onto photopolymerized PEG to form different matrix microenvironments [112]. The CS-based hydrogels showed the strongest response in terms of gene expression and matrix accumulation for both chondrocytes harvested from superficial and deep zones of the articular cartilage, while the HA and type I collagen-based hydrogels demonstrated zone-dependent cellular responses.

Physical and Mechanical Behavior

Currently, surgical integration of tissue is generally carried out using sutures and/or applying a tissue adhesive [113]. There are several adhesives used clinically, including derivatives of cyanoacrylates (Superglue), glutaraldehyde–albumin (Bioglue), and fibrin glue (Tisseal, Tissucoll). Although these adhesives are effective, the biocompatibility is poor and bonding strength is inadequate. Biomacromolecules were functionalized with aldehyde groups as a primer to form bridges for the hydrogels hybrid constructs with host tissue proteins. This bonding primer improved the hydrogel–cartilage interface strength from less than 6 kPa in uniaxial tensile or horizontal shear to 45 kPa. Wang et al. demonstrated the importance of hydrogels bonding in a chondral defect of rabbit and goat models to maintain the tissue engineered construct in the implanted site [113].

Another important fundamental material behavior is the mechanical strength under load bearing conditions. The best material behavior is the one closest to that of cartilage itself. Cartilage has a complex inhomogeneous organization with depth dependent shear G values from 70 to 650 kPa [114]. The depth-dependent shear modulus profile of healthy articular cartilage indicates that the compliant region just below the superficial zone may act as an internal slip or energy dissipation mechanism, helping to maintain cartilage integrity over years of wear.

Table 1. Physical and chemical characterizations of different hydrogels used in cartilage tissue engineering

Hydrogels	Reticulating agent and process	Crosslinking mode	Dynamic elastic modulus: (kPa)	Cells encapsulation within hydrogels	References
Atelocollagen-type II	mTGase	Enzyme cross linking	G' : 0.5–1.2	Yes	[78]
Hyaluronic acid	TEG-diOTs	Physically and covalent before use	0.01	No	[116]
IPN methacrylate and aldehyde-bifunctionalized dextran and gelatin		UV and aldehyde chemical reaction	E' : 10–15	Yes	[109]
Odex/CEC	Oxidized dextran (Odex)	In situ crosslinkable	G' : 0.1–1	Yes	[117]
Si-HPMC	Alkoxy-Silane	Covalent in situ crosslinkable	G' : 0,4	Yes	[7]
Cross linked alginic acid	1,3 Diamino propane	covalent	G' : 7	Yes	[88]
Cross linked Hyaluronic acid	1,3 Diamino propane	covalent	G' : 1.8–2	Yes	[88]
PEODM	HPK	UV	E' : 1		[74]
OPF	Ammonium persulfate/ascorbic acid		E_t : 10–80	Yes	[102]
Pluronic F127 PEO ₉₉ -PPO ₆₇ -PEO ₉₉		Physically crosslinked	G' : 22	Yes	[97]
Pluronic F127-DIPTS PEO ₉₉ -PPO ₆₇ -PEO ₉₉	Ethoxysilane	In situ crosslinkable	G' : 30–40		[97, 108]
Pluronic F127 DMA PEO ₉₉ -PPO ₆₇ -PEO ₉₉	Dimethyl methacrylate	Physically and covalently crosslinked	G' : 70		[97]
HEMA/4IEMA	2,2' Azobis (isobutyronitrile) (AIBN)	Radical copolymerization	G' : 100–1,000		[118]
HYAFF 11 sponge	HA benzyl ester		G' : 90–300	Yes	[80]
Dextran-tyramine conjugates	H ₂ O ₂ /horseradish peroxidase (HRP)	Enzymatic crosslinking	G' : 4–41 kPa		[119]
Articular cartilage			G' : 400		[74]
Intervertebral disk (<i>nucleus pulposus</i>)			E' : 10.000 11.3		

G' shear modulus; E' stiffness modulus; E_t tensile modulus

Compressive strain decreases G just below the superficial zone implies that axial compression should improve resistance to wear. Engineered tissue has to mimic this spatial and mechanical organization to satisfy the biomechanical strength. Listed in Table 1 are the different macromolecules and crosslinking methods proposed for the biomechanical behavior of the different hydrogels constructs. The best tissue engineering strategy is to have hydrogels constructs with mechanical properties nearest to that of the tissue with a high level of biocompatibility and tissues replacement rates to allow a quick functional tissue substitution.

Summary

The development of tissue engineering, which is a technique based on the association of cells with biomaterials for the *ex vivo* growth of repair tissue needs technical breakthroughs and investment. Beside the importance of stem cell investigations, one of the key points is nonpathogenic and biomimetic 3D scaffolds suitable for cells culture and tissue production. Tissue engineering is an expensive technology, and there is a need to reduce the cost in order to make it affordable. Efforts must be made on cell culturing and harvesting technologies as well as on the nature of the biomaterials. Hydrogels for biomaterials is a highly competitive field of research, and there is a push to make creative 3D scaffolds for tissue engineering. The number of publications has increased from 200 to 800 references in Pubmed database between 2000 and 2009. Numerous hydrogels have been prepared, but none entirely satisfy the applications. The polymers used to form these hydrogels are both natural in origin (i.e., hyaluronic acid, alginate, chitosan, chondroitin sulfate, collagen, fibrin adhesive and cellulose ether) and synthetic in origin (i.e., poly(lactide-co-glycolic acid), poly(ethylene glycol), poly(vinyl alcohol), and poly(propylene fumarate). The advantages and disadvantages of these polymers are multiple; the synthetic materials are more consistent and cheaper but more toxic prone than the natural ones, which in turn, could be pathogenic, such as the hyaluronic acid from animal origins. Three-dimensional matrices that contain up to 90% water that can maintain and allow cells to proliferate entrapped within are currently rare. Due to their high water content, these matrices have a high biocompatibility level for cartilage tissue engineering. However, their biomechanical strength is not adapted enough for articular cartilage. Overcoming this limitation is the challenge for future hydrogels developments. Thus, there is a large research avenue open for developing new constructs and hydrogels designs for address the needs associated with cell therapy for cartilage regeneration.

References

1. Brittberg M, Lindahl A, Nilsson A, Ohlsson C, Isaksson O, Peterson L (1994) Treatment of deep cartilage defects in the knee with autologous chondrocyte transplantation. *N Engl J Med* 331(14):889–895
2. Vinatier C, Guicheux J, Daculsi G, Layrolle P, Weiss P (2006) Cartilage and bone tissue engineering using hydrogels. *Biomed Mater Eng* 16:107–113
3. Causa F, Netti PA, Ambrosio L (2007) A multi-functional scaffold for tissue regeneration: the need to engineer a tissue analogue. *Biomaterials* 28(34):5093–5099
4. Drury JL, Mooney DJ (2003) Hydrogels for tissue engineering: scaffold design variables and applications. *Biomaterials* 24(24):4337–4351
5. Hwang NS, Varghese S, Elisseeff J (2008) Controlled differentiation of stem cells. *Adv Drug Deliv Rev* 60(2):199–214
6. Orwin EJ, Borene ML, Hubel A (2003) Biomechanical and optical characteristics of a corneal stromal equivalent. *J Biomech Eng* 125(4):439–444

7. Fatimi A, Tassin JF, Quillard S, Axelos MA, Weiss P (2008) The rheological properties of silylated hydroxypropylmethylcellulose tissue engineering matrices. *Biomaterials* 29(5):533–543
8. Lories RJ, Luyten FP (2005) Bone morphogenetic protein signaling in joint homeostasis and disease. *Cytokine Growth Factor Rev* 16(3):287–298
9. Aigner T, Stove J (2003) Collagens—major component of the physiological cartilage matrix, major target of cartilage degeneration, major tool in cartilage repair. *Adv Drug Deliv Rev* 55(12):1569–1593
10. Muir H (1970) The intracellular matrix in the environment of connective tissue cells. *Clin Sci* 38(2):8P
11. Sommarin Y, Larsson T, Heinegard D (1989) Chondrocyte-matrix interactions. Attachment to proteins isolated from cartilage. *Exp Cell Res* 184(1):181–192
12. Shlopov BV, Lie WR, Mainardi CL, Cole AA, Chubinskaya S, Hasty KA (1997) Osteoarthritic lesions: involvement of three different collagenases. *Arthritis Rheum* 40(11):2065–2074
13. Flannery CR, Little CB, Hughes CE, Caterson B (1998) Expression and activity of articular cartilage hyaluronidases. *Biochem Biophys Res Commun* 251(3):824–829
14. Canty EG, Kadler KE (2005) Procollagen trafficking, processing and fibrillogenesis. *J Cell Sci* 118(Pt 7): 1341–1353
15. Eyre D (2002) Collagen of articular cartilage. *Arthritis Res* 4(1):30–35
16. Dudhia J (2005) Aggrecan, aging and assembly in articular cartilage. *Cell Mol Life Sci* 62(19–20):2241–2256
17. Rogers BA, Murphy CL, Cannon SR, Briggs TW (2006) Topographical variation in glycosaminoglycan content in human articular cartilage. *J Bone Joint Surg Br* 88(12):1670–1674
18. Kiani C, Chen L, Wu YJ, Yee AJ, Yang BB (2002) Structure and function of aggrecan. *Cell Res* 12(1):19–32
19. Toole BP (2004) Hyaluronan: from extracellular glue to pericellular cue. *Nat Rev Cancer* 4(7):528–539
20. Toole BP (2001) Hyaluronan in morphogenesis. *Semin Cell Dev Biol* 12(2):79–87
21. Moreland LW (2003) Intra-articular hyaluronan (hyaluronic acid) and hylans for the treatment of osteoarthritis: mechanisms of action. *Arthritis Res Ther* 5(2):54–67
22. Gardner DL (1994) Problems and paradigms in joint pathology. *J Anat* 184(Pt 3):465–476
23. Roth V, Mow VC (1980) The intrinsic tensile behavior of the matrix of bovine articular cartilage and its variation with age. *J Bone Joint Surg Am* 62(7):1102–1117
24. Lyons TJ, Stoddart RW, McClure SF, McClure J (2005) The tidemark of the chondro-osseous junction of the normal human knee joint. *J Mol Histol* 36(3):207–215
25. Poole CA, Flint MH, Beaumont BW (1988) Chondrons extracted from canine tibial cartilage: preliminary report on their isolation and structure. *J Orthop Res* 6(3):408–419
26. Poole CA (1997) Articular cartilage chondrons: form, function and failure. *J Anat* 191(Pt 1):1–13
27. Guilak F, Jones WR, Ting-Beall HP, Lee GM (1999) The deformation behavior and mechanical properties of chondrocytes in articular cartilage. *Osteoarthr Cartil* 7(1):59–70
28. Youn I, Choi JB, Cao L, Setton LA, Guilak F (2006) Zonal variations in the three-dimensional morphology of the chondron measured in situ using confocal microscopy. *Osteoarthr Cartil* 14(9):889–897
29. Labos M (2004) Place du traitement non pharmacologique dans la prise en charge de la gonarthrose chez 60 patients. Université Paris VI-Pierre et Marie Curie-U.F.R de Saint Antoine
30. Lawrence RC, Helmick CG, Arnett FC, Deyo RA, Felson DT, Giannini EH, Heyse SP, Hirsch R, Hochberg MC, Hunder GG, Liang MH, Pillemer SR, Steen VD, Wolfe F (1998) Estimates of the prevalence of arthritis and selected musculoskeletal disorders in the United States. *Arthritis Rheum* 41(5):778–799
31. Felson DT, Zhang Y, Hannan MT, Naimark A, Weissman BN, Aliabadi P, Levy D (1995) The incidence and natural history of knee osteoarthritis in the elderly. The Framingham Osteoarthritis Study. *Arthritis Rheum* 38(10): 1500–1505
32. Ge Z, Hu Y, Heng BC, Yang Z, Ouyang H, Lee EH, Cao T (2006) Osteoarthritis and therapy. *Arthritis Rheum* 55(3):493–500
33. Glass GG (2006) Osteoarthritis. *Dis Mon* 52(9):343–362
34. Felson DT (2004) An update on the pathogenesis and epidemiology of osteoarthritis. *Radiol Clin North Am* 42(1): 1–9, v
35. Buckwalter JA, Martin J (1995) Degenerative joint disease. *Clin Symp* 47(2):1–32
36. Buckwalter JA (1998) Articular cartilage: injuries and potential for healing. *J Orthop Sports Phys Ther* 28(4): 192–202
37. Buckwalter JA (2002) Articular cartilage injuries. *Clin Orthop* 402:21–37
38. Buckwalter JA, Mankin HJ (1998) Articular cartilage: degeneration and osteoarthritis, repair, regeneration, and transplantation. *Instr Course Lect* 47:487–504
39. Buckwalter JA, Brown TD (2004) Joint injury, repair, and remodeling: roles in post-traumatic osteoarthritis. *Clin Orthop Relat Res* 423:7–16

40. Jackson DW, Lalor PA, Aberman HM, Simon TM, Jackson DW, Lalor PA, Aberman HM, Simon TM (2001) Spontaneous repair of full-thickness defects of articular cartilage in a goat model. A preliminary study. *J Bone Joint Surg Am* 83-A(1):53–64
41. Shapiro F, Koide S, Glimcher MJ (1993) Cell origin and differentiation in the repair of full-thickness defects of articular cartilage. *J Bone Joint Surg Am* 75(4):532–553
42. Tynni A, Karlsson J (2000) Biological treatment of joint cartilage damage. *Scand J Med Sci Sports* 10(5):249–265
43. Mankin HJ (1982) The response of articular cartilage to mechanical injury. *J Bone Joint Surg Am* 64(3):460–466
44. Elisseeff J (2004) Injectable cartilage tissue engineering. *Expert Opin Biol Ther* 4(12):1849–1859
45. Langer R, Vacanti JP (1993) Tissue engineering. *Science* 260(5110):920–926
46. Tuli R, Li WJ, Tuan RS (2003) Current state of cartilage tissue engineering. *Arthritis Res Ther* 5(5):235–238
47. Chen FH, Rousche KT, Tuan RS (2006) Technology Insight: adult stem cells in cartilage regeneration and tissue engineering. *Nat Clin Pract Rheumatol* 2(7):373–382
48. Ateshian GA (2007) Artificial cartilage: weaving in three dimensions. *Nat Mater* 6(2):89–90
49. Kafienah W, Jakob M, Demarteau O, Frazer A, Barker MD, Martin I, Hollander AP (2002) Three-dimensional tissue engineering of hyaline cartilage: comparison of adult nasal and articular chondrocytes. *Tissue Eng* 8(5):817–826
50. Isogai N, Kusuhara H, Ikada Y, Ohtani H, Jacquet R, Hillyer J, Lowder E, Landis WJ (2006) Comparison of different chondrocytes for use in tissue engineering of cartilage model structures. *Tissue Eng* 12(4):691–703
51. Darling EM, Athanasiou KA (2005) Rapid phenotypic changes in passaged articular chondrocyte subpopulations. *J Orthop Res* 23(2):425–432
52. Domm C, Schunke M, Christesen K, Kurz B (2002) Redifferentiation of dedifferentiated bovine articular chondrocytes in alginate culture under low oxygen tension. *Osteoarthr Cartil* 10(1):13–22
53. Malda J, van Blitterswijk CA, Grojec M, Martens DE, Tramper J, Riesle J (2003) Expansion of bovine chondrocytes on microcarriers enhances redifferentiation. *Tissue Eng* 9(5):939–948
54. Vinatier C, Magne D, Weiss P, Trojani C, Rochet N, Carle G, Vignes-Colombeix C, Chadjichristos C, Galera P, Daculsi G, Guicheux J (2005) A silanized hydroxypropyl methylcellulose hydrogel for the three dimensional culture of chondrocytes. *Biomaterials* 26:6643–6651
55. Fukui N, Purple CR, Sandell LJ (2001) Cell biology of osteoarthritis: the chondrocyte's response to injury. *Curr Rheumatol Rep* 3(6):496–505
56. Caplan AI, Bruder SP (2001) Mesenchymal stem cells: building blocks for molecular medicine in the 21st century. *Trends Mol Med* 7(6):259–264
57. Pittenger MF, Mackay AM, Beck SC, Jaiswal RK, Douglas R, Mosca JD, Moorman MA, Simonetti DW, Craig S, Marshak DR (1999) Multilineage potential of adult human mesenchymal stem cells. *Science* 284(5411):143–147
58. Huard J, Cao B, Qu-Petersen Z (2003) Muscle-derived stem cells: potential for muscle regeneration. *Birth Defects Res C Embryo Today* 69(3):230–237
59. Gimble J, Guilak F (2003) Adipose-derived adult stem cells: isolation, characterization, and differentiation potential. *Cytotherapy* 5(5):362–369
60. Zuk PA, Zhu M, Ashjian P, De Ugarte DA, Huang JI, Mizuno H, Alfonso ZC, Fraser JK, Benhaim P, Hedrick MH (2002) Human adipose tissue is a source of multipotent stem cells. *Mol Biol Cell* 13(12):4279–4295
61. De Bari C, Dell'Accio F, Luyten FP (2001) Human periosteum-derived cells maintain phenotypic stability and chondrogenic potential throughout expansion regardless of donor age. *Arthritis Rheum* 44(1):85–95
62. Zuk PA, Zhu M, Mizuno H, Huang J, Futrell JW, Katz AJ, Benhaim P, Lorenz HP, Hedrick MH (2001) Multilineage cells from human adipose tissue: implications for cell-based therapies. *Tissue Eng* 7(2):211–228
63. Krampera M, Pasini A, Pizzolo G, Cosmi L, Romagnani S, Annunziato F (2006) Regenerative and immunomodulatory potential of mesenchymal stem cells. *Curr Opin Pharmacol* 6(4):435–441
64. Devine SM, Peter S, Martin BJ, Barry F, McIntosh KR (2001) Mesenchymal stem cells: stealth and suppression. *Cancer J* 7(Suppl 2):S76–S82
65. Tuan RS (2006) Stemming cartilage degeneration: adult mesenchymal stem cells as a cell source for articular cartilage tissue engineering. *Arthritis Rheum* 54(10):3075–3078
66. Nelea V, Luo L, Demers CN, Antoniou J, Petit A, Lerouge S, Wertheimer MR, Mwale F (2005) Selective inhibition of type X collagen expression in human mesenchymal stem cell differentiation on polymer substrates surface-modified by glow discharge plasma. *J Biomed Mater Res A* 75(1):216–223
67. Pelttari K, Winter A, Steck E, Goetzke K, Hennig T, Ochs BG, Aigner T, Richter W (2006) Premature induction of hypertrophy during in vitro chondrogenesis of human mesenchymal stem cells correlates with calcification and vascular invasion after ectopic transplantation in SCID mice. *Arthritis Rheum* 54(10):3254–3266

68. Hanada K, Solchaga LA, Caplan AI, Hering TM, Goldberg VM, Yoo JU, Johnstone B (2001) BMP-2 induction and TGF-beta 1 modulation of rat periosteal cell chondrogenesis. *J Cell Biochem* 81(2):284–294
69. Nestic D, Whiteside R, Brittberg M, Wendt D, Martin I, Mainil-Varlet P (2006) Cartilage tissue engineering for degenerative joint disease. *Adv Drug Deliv Rev* 58(2):300–322
70. Chung C, Burdick JA (2008) Engineering cartilage tissue. *Adv Drug Deliv Rev* 60(2):243–262
71. Hacker M, Tessmar J, Neubauer M, Blaimer A, Blunk T, Gopferich A, Schulz MB (2003) Towards biomimetic scaffolds: anhydrous scaffold fabrication from biodegradable amine-reactive diblock copolymers. *Biomaterials* 24(24):4459–4473
72. Jung Y, Park MS, Lee JW, Kim YH, Kim S-H, Kim SH (2008) Cartilage regeneration with highly-elastic three-dimensional scaffolds prepared from biodegradable poly(l-lactide-co-[var epsilon]-caprolactone). *Biomaterials* 29(35):4630–4636
73. Nguyen KT, West JL (2002) Photopolymerizable hydrogels for tissue engineering applications. *Biomaterials* 23(22):4307–4314
74. Elisseeff J, McIntosh W, Anseth K, Riley S, Ragan P, Langer R (2000) Photoencapsulation of chondrocytes in poly(ethylene oxide)-based semi-interpenetrating networks. *J Biomed Mater Res* 51(2):164–171
75. Elisseeff J, Anseth K, Sims D, McIntosh W, Randolph M, Langer R (1999) Transdermal photopolymerization for minimally invasive implantation. *Proc Natl Acad Sci U S A* 96(6):3104–3107
76. Fedorovich NE, Oudshoorn MH, van Geemen D, Hennink WE, Alblas J, Dhert WJA (2009) The effect of photopolymerization on stem cells embedded in hydrogels. *Biomaterials* 30(3):344–353
77. Barbucci R, Leone G, Lamponi S (2006) Thixotropy property of hydrogels to evaluate the cell growing on the inside of the material bulk (Amber effect). *J Biomed Mater Res B Appl Biomater* 76(1):33–40
78. Halloran DO, Grad S, Stoddart M, Dockery P, Alini M, Pandit AS (2008) An injectable cross-linked scaffold for nucleus pulposus regeneration. *Biomaterials* 29(4):438–447
79. Alsberg E, Anderson KW, Albeiruti A, Rowley JA, Mooney DJ (2002) Engineering growing tissues. *Proc Natl Acad Sci U S A* 99(19):12025–12030
80. Borzacchiello A, Mayol L, Ramires PA, Pastorello A, Bartolo CD, Ambrosio L, Milella E (2007) Structural and rheological characterization of hyaluronic acid-based scaffolds for adipose tissue engineering. *Biomaterials* 28(30):4399–4408
81. Wallace DG, Rosenblatt J (2003) Collagen gel systems for sustained delivery and tissue engineering. *Adv Drug Deliv Rev* 55(12):1631–1649
82. Battista S, Guarnieri D, Borselli C, Zeppetelli S, Borzacchiello A, Mayol L, Gerbasio D, Keene DR, Ambrosio L, Netti PA (2005) The effect of matrix composition of 3D constructs on embryonic stem cell differentiation. *Biomaterials* 26(31):6194–6207
83. Bryan N, Rhodes NP, Hunt JA (2009) Derivation and performance of an entirely autologous injectable hydrogel delivery system for cell-based therapies. *Biomaterials* 30(2):180–188
84. Vinatier C, Gauthier O, Masson M, Malard O, Moreau A, Fella BH, Bilban M, Spaethe R, Daculsi G, Guicheux J (2008) Nasal chondrocytes and fibrin sealant for cartilage tissue engineering. *J Biomed Mater Res A* 89(1):176–185
85. Temenoff JS, Mikos AG (2000) Injectable biodegradable materials for orthopedic tissue engineering. *Biomaterials* 21(23):2405–2412
86. Rowley JA, Madlambayan G, Mooney DJ (1999) Alginate hydrogels as synthetic extracellular matrix materials. *Biomaterials* 20(1):45–53
87. Paige KT, Cima LG, Yaremchuk MJ, Vacanti JP, Vacanti CA (1995) Injectable cartilage. *Plast Reconstr Surg* 96(6):1390–1398
88. Leone G, Delfini M, Di Cocco ME, Borioni A, Barbucci R (2008) The applicability of an amidated polysaccharide hydrogel as a cartilage substitute: structural and rheological characterization. *Carbohydr Res* 343(2):317–327
89. Weng L, Romanov A, Rooney J, Chen W (2008) Non-cytotoxic, in situ gelable hydrogels composed of N-carboxyethyl chitosan and oxidized dextran. *Biomaterials* 29(29):3905–3913
90. De Groot CJ, Van Luyn MJA, Van Dijk-Wolthuis WNE, Cadee JA, Plantinga JA, Otter WD, Hennink WE (2001) In vitro biocompatibility of biodegradable dextran-based hydrogels tested with human fibroblasts. *Biomaterials* 22(11):1197–1203
91. Cadee JA, van Luyn MJ, Brouwer LA, Plantinga JA, van Wachem PB, de Groot CJ, den Otter W, Hennink WE (2000) In vivo biocompatibility of dextran-based hydrogels. *J Biomed Mater Res* 50(3):397–404
92. Revell PA, Damien E, Di Silvio L, Gurav N, Longinotti C, Ambrosio L (2007) Tissue engineered intervertebral disc repair in the pig using injectable polymers. *J Mater Sci Mater Med* 18(2):303–308
93. Adelow C, Segura T, Hubbell JA, Frey P (2008) The effect of enzymatically degradable poly(ethylene glycol) hydrogels on smooth muscle cell phenotype. *Biomaterials* 29(3):314–326

94. Raeber GP, Lutolf MP, Hubbell JA (2007) Mechanisms of 3-D migration and matrix remodeling of fibroblasts within artificial ECMs. *Acta Biomater* 3(5):615–629
95. Jeong B, Kim SW, Bae YH (2002) Thermosensitive sol-gel reversible hydrogels. *Adv Drug Deliv Rev* 54(1):37–51
96. Tirelli N, Lutolf MP, Napoli A, Hubbell JA (2002) Poly(ethylene glycol) block copolymers. *Rev Mol Biotechnol* 90(1):3–15
97. Cohn D, Sosnik A, Garty S (2005) Smart hydrogels for in situ generated implants. *Biomacromolecules* 6(3):1168–1175
98. Gruber HE, Fisher EC Jr, Desai B, Stasky AA, Hoelscher G, Hanley EN Jr (1997) Human intervertebral disc cells from the annulus: three-dimensional culture in agarose or alginate and responsiveness to TGF-beta1. *Exp Cell Res* 235(1):13–21
99. Perka C, Spitzer RS, Lindenhayn K, Sittinger M, Schultz O (2000) Matrix-mixed culture: new methodology for chondrocyte culture and preparation of cartilage transplants. *J Biomed Mater Res* 49(3):305–311
100. Chang SC, Rowley JA, Tobias G, Genes NG, Roy AK, Mooney DJ, Vacanti CA, Bonassar LJ (2001) Injection molding of chondrocyte/alginate constructs in the shape of facial implants. *J Biomed Mater Res* 55(4):503–511
101. Zheng Shu X, Liu Y, Palumbo FS, Luo Y, Prestwich GD (2004) In situ crosslinkable hyaluronan hydrogels for tissue engineering. *Biomaterials* 25(7–8):1339–1348
102. Temenoff JS, Athanasiou KA, LeBaron RG, Mikos AG (2002) Effect of poly(ethylene glycol) molecular weight on tensile and swelling properties of oligo(poly(ethylene glycol) fumarate) hydrogels for cartilage tissue engineering. *J Biomed Mater Res* 59(3):429–437
103. Turczyn R, Weiss P, Lapkowski M, Daculsi G (2000) In situ self hardening bioactive composite for bone and dental surgery. *J Biomater Sci Polym Ed* 11(2):217–223
104. Bourges X, Weiss P, Coudreuse A, Daculsi G, Legeay G (2002) General properties of silylated hydroxyethyl cellulose for potential biomedical applications. *Biopolymers* 63(4):232–238
105. Bourges X, Weiss P, Daculsi G, Legeay G (2002) Synthesis and general properties of silylated-hydroxypropyl methylcellulose in prospect of biomedical use. *Adv Colloid Interface Sci* 99(3):215–228
106. Vinatier C, Magne D, Moreau A, Gauthier O, Malard O, Vignes-Colombeix C, Daculsi G, Weiss P, Guicheux J (2007) Engineering cartilage with human nasal chondrocytes and a silylated hydroxypropyl methylcellulose hydrogel. *J Biomed Mater Res A* 80(1):66–74
107. Vinatier C, Gauthier O, Fatimi A, Merceron C, Masson M, Moreau A, Moreau F, Fellah B, Weiss P, Guicheux J (2009) An injectable cellulose-based hydrogel for the transfer of autologous nasal chondrocytes in articular cartilage defects. *Biotechnol Bioeng* 102(4):1259–1267
108. Sosnik A, Cohn D (2004) Ethoxysilane-capped PEO-PPO-PEO triblocks: a new family of reverse thermo-responsive polymers. *Biomaterials* 25(14):2851–2858
109. Liu Y, Chan-Park MB (2009) Hydrogel based on interpenetrating polymer networks of dextran and gelatin for vascular tissue engineering. *Biomaterials* 30(2):196–207
110. Sharma B, Williams CG, Khan M, Manson P, Elisseeff JH (2007) In vivo chondrogenesis of mesenchymal stem cells in a photopolymerized hydrogel. *Plast Reconstr Surg* 119(1):112–120
111. Varghese S, Hwang NS, Canver AC, Theprungsirikul P, Lin DW, Elisseeff J (2008) Chondroitin sulfate based niches for chondrogenic differentiation of mesenchymal stem cells. *Matrix Biol* 27(1):12–21
112. Hwang NS, Varghese S, Lee HJ, Theprungsirikul P, Canver A, Sharma B, Elisseeff J (2007) Response of zonal chondrocytes to extracellular matrix-hydrogels. *FEBS Lett* 581(22):4172–4178
113. Wang DA, Varghese S, Sharma B, Strehin I, Fermanian S, Gorham J, Fairbrother DH, Cascio B, Elisseeff JH (2007) Multifunctional chondroitin sulphate for cartilage tissue-biomaterial integration. *Nature Mater* 6(5):385–392
114. Buckley MR, Gleghorn JP, Bonassar LJ, Cohen I (2008) Mapping the depth dependence of shear properties in articular cartilage. *J Biomech* 41(11):2430–2437
115. Mi FL, Tan YC, Liang HF, Sung HW (2002) In vivo biocompatibility and degradability of a novel injectable-chitosan-based implant. *Biomaterials* 23(1):181–191
116. Huin-Amargier C, Marchal P, Payan E, Netter P, Dellacherie E (2006) New physically and chemically cross-linked hyaluronate (HA)-based hydrogels for cartilage repair. *J Biomed Mater Res A* 76(2):416–424
117. Weng L, Chen X, Chen W (2007) Rheological characterization of in situ crosslinkable hydrogels formulated from oxidized dextran and N-carboxyethyl chitosan. *Biomacromolecules* 8(4):1109–1115
118. Boelen EJH, van Hooy-Corstjens CSJ, Bulstra SK, van Ooij A, van Rhijn LW, Koole LH (2005) Intrinsically radiopaque hydrogels for nucleus pulposus replacement. *Biomaterials* 26(33):6674–6683
119. Jin R, Hiemstra C, Zhong Z, Feijen J (2007) Enzyme-mediated fast in situ formation of hydrogels from dextran-tyramine conjugates. *Biomaterials* 28(18):2791–2800

Gelatin-Based Hydrogels for Controlled Cell Assembly

Xiaohong Wang, Yongnian Yan, and Renji Zhang

Abstract Controlled cell assembly technique is a new research area in complex organ development technologies. Gelatin-based hydrogels, such as gelatin, gelatin/alginate, gelatin/chitosan, gelatin/fibrinogen, gelatin/hyaluronan, and gelatin/alginate/fibrinogen, have played an important role in the rapid fabrication of tissue or organs with well-defined structures and functions. Cryoprotectants, such as dimethylsulfoxide (DMSO) and glycerol, can be easily incorporated into the system for long-term conservation of the cell containing constructs. Hepatocytes, chondrocytes, cardiac myocytes, and adipose-derived stromal cells (ADSCs) are used to show function of the assembled cells. ADSCs can be controlled to differentiate into different targeted cell types according to their positions within the orderly pre-designed three-dimensional (3D) constructs. A multicellular model for the metabolic syndrome was established along with the development of the double-syringe deposition system which lead to a hybrid cell/hydrogels construct with a vascular-like network fabricated using a digital model. The preliminary results indicate that the double-syringe assembly technique is a powerful tool for fabricating complex constructs with special intrinsic/extrinsic structures, and has the potential to be widely used in regenerative medicine and drug screening.

Introduction

Although organ failure patients can be treated effectively by transplantations, these procedures are limited by donor organ availability, high costs, and the lifelong use of immunosuppressants [1]. The recent development of controlled cell assembly is a milestone in complex organ manufacturing techniques. This process requires a highly accurate three-dimensional (3D) micropositioning system with a pressure-controlled syringe to deposit cell/hydrogels structures with a lateral resolution of 10 μm (Fig. 1). Combined with the multinozzle organ manufacturing techniques novel therapeutic procedures are possible for failed organs. With the multinozzle cell assembling techniques, it is possible we were able to directly deposit different cells and hydrogels and/or other important chemical components into specific sites to form 3D living organ analogies in vitro or in vivo to mimic the respective organs at the right time, in the right position, in the right amount, and in different bioenvironments [2–10].

Hydrogels are natural or synthetic polymeric materials that typically have a dry mass between 1 and 20% that swells in water while maintaining a distinct 3D network structure by virtue of specific crosslinks [11]. Currently, several natural hydrogels, such as gelatin, chitosan, hyaluronan, alginate, fibrinogen, are being used for organ regeneration since they facilitate cell attachment and differentiation [12, 13].

X. Wang, Y. Yan, and R. Zhang • Key Laboratory for Advanced Materials Processing Technology, Ministry of Education & Center of Organ Manufacturing, Department of Mechanical Engineering, Tsinghua University, Beijing 100084, People's Republic of China • Institute of Life Science and Medicine, Tsinghua University, Beijing 100084, People's Republic of China
e-mail: wangxiaohong@tsinghua.edu.cn

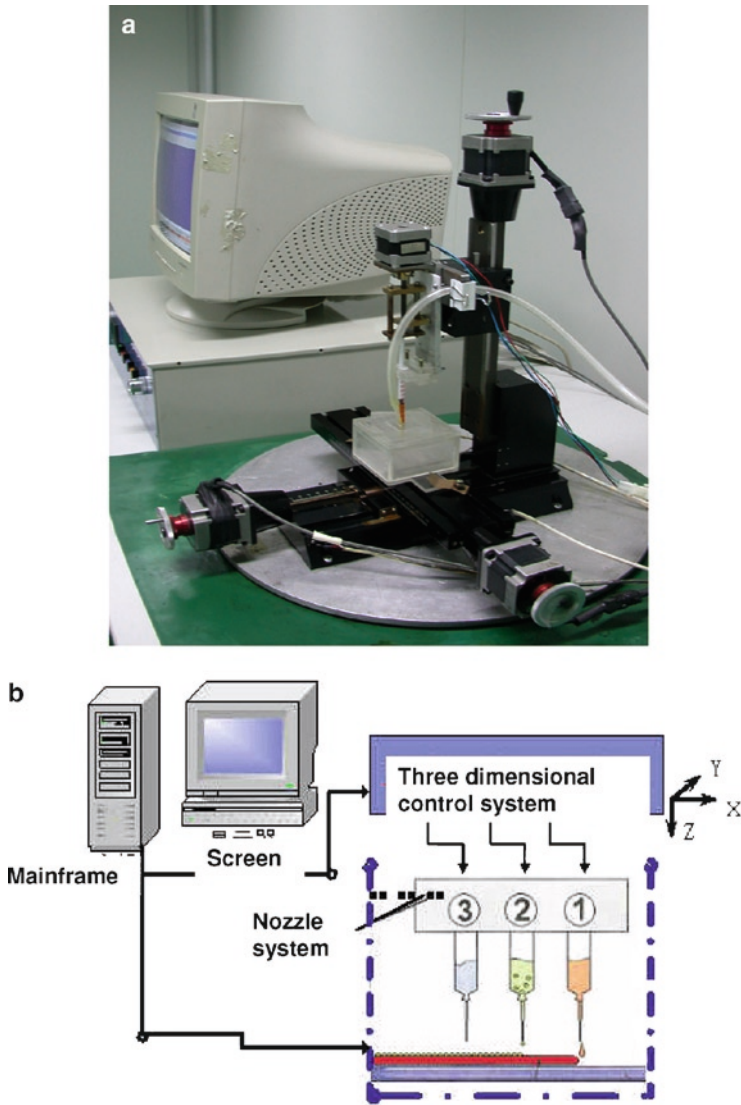


Fig. 1. A cell assembling machine with a cell assembling system.

Gelatin is a denatured, biodegradable polypeptide derived from the controlled partial hydrolysis of collagen, which is widely found in nature and is the major constituent of skin, bones, and connective tissue. After being chemically or physically crosslinked [14], gelatin can be used for medical purposes, including wound dressings, plasma volume expanders, and drug delivery systems [15]. Chitosan, a positively charged amino polysaccharide (poly-1, 4 D-glucoamine), derived from chitin by deacetylation, is known for its numerous and unique biological properties during wound healing. When mixed with positively charged chitosan, negatively charged gelatin ionically interacts with chitosan to form a polyionic complex. Hyaluronic acid (HA) is another major constituent of the extracellular matrix (ECM) in the human body. It can bind other large glycosaminoglycans (GAGs) and proteoglycans through specific HA-protein interactions [16]. Alginate is a collective term for a family of polysaccharides obtained from brown algae and is

widely used for many medical applications [17]. Fibrin is a haemostatic wound dressing material that can be made in the form of a sponge, film, powder, and sheet [18, 19]. All of these natural polymers have been used to produce biocompatible and biodegradable hydrogels that acts as temporary replacements for medical regeneration [20, 21].

The combination of gelatin and other natural polymers made it possible to fabricate 3D constructs with rapid prototyping techniques. In the controlled cell assembly process, a series of gelatin-based hydrogels, such as gelatin, gelatin/chitosan, gelatin/hyaluronan, gelatin/alginate, gelatin/fibrinogen, and gelatin/alginate/fibrinogen, is used to obtain the necessary space and stabilizing factors for seeding various cells (Figs. 2–6) [2–10]. The cells were deposited in a sol–gel that is deposited onto a substrate surface layer by layer in a chamber at $\sim 10^{\circ}\text{C}$ and the sol then is transformation into a hydrogels. The use of the natural gelatin-based hydrogels is clearly a distinct advantage for direct cell assembly technique in fabricating tissue analogs [2–10]. Besides providing cells with nutrients, the hydrogels also play an important role in supporting the whole structure. The special thermoresponsive property of gelatin allows extruded mixtures to be shaped at environmental temperatures below 20°C . However, the gels states of the gelatin-based hydrogels cannot be maintained when the structures are transferred to a 37°C environment. Consequently, after the cell-laden hydrogels are deposited

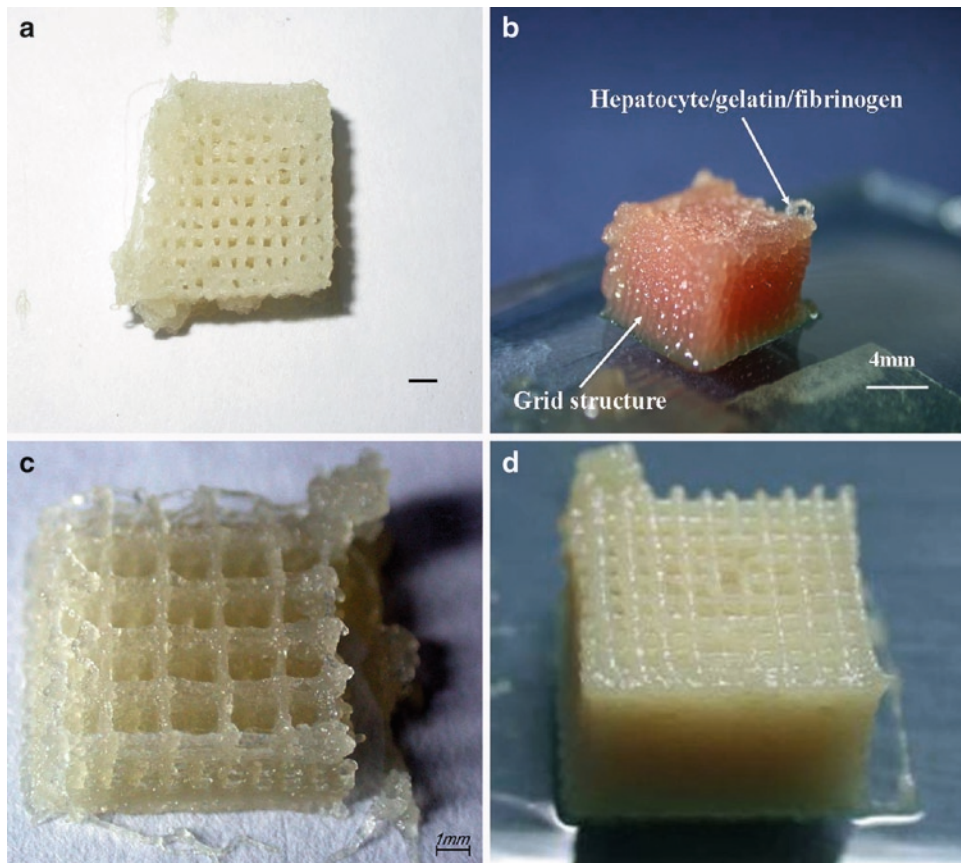


Fig. 2. Some cell/hydrogels constructs with open channels made by the cell assembling machine: (a) one 3D hepatocyte/gelatin construct. Scale bar indicates $700\ \mu\text{m}$; (b) a 3D hepatocyte/gelatin/fibrinogen construct; (c) a 3D hepatocyte/gelatin/chitosan construct; (d) a 3D hepatocyte/gelatin/alginate construct.

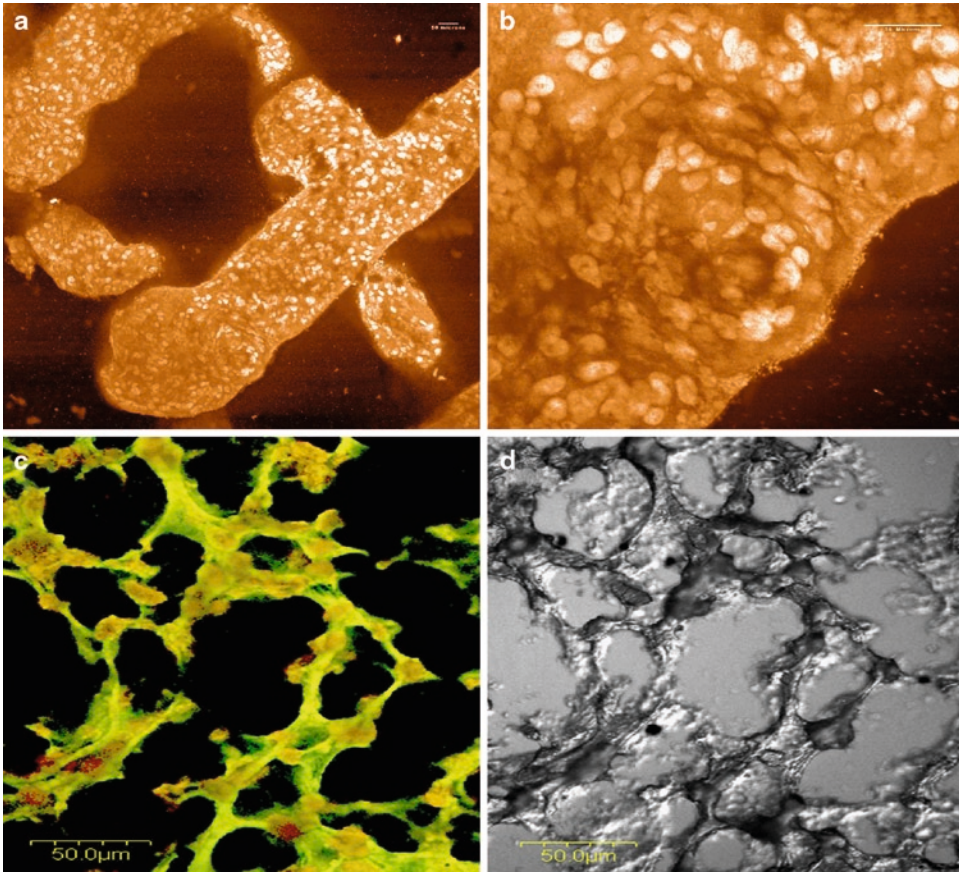


Fig. 3. Hepatocytes in the gelatin/chitosan 3D structures after 6 days of culture: (a) LSCM observation (PI staining); (b) the magnification of (a); (c) PI staining and FITC-conjugation; (d) a black control of (c).

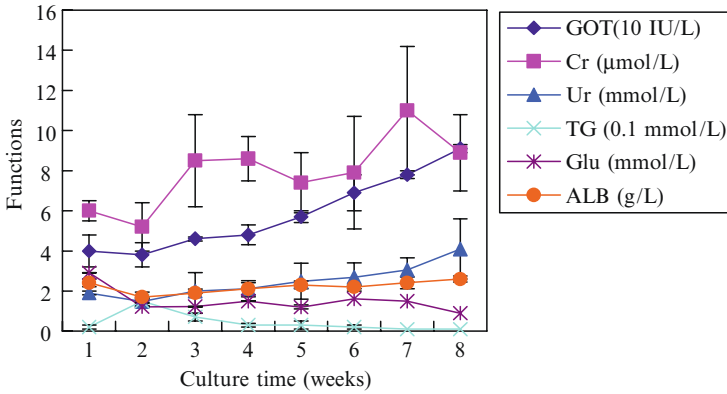


Fig. 4. Glutamate-oxaloacetate transaminase (GOT), albumin (ALB), urea (Ur), glucose (Glu), creatinine (Cr), and triglyceride (TG) secreted by hepatocytes in the 3D gelatin/chitosan constructs after different culture time.

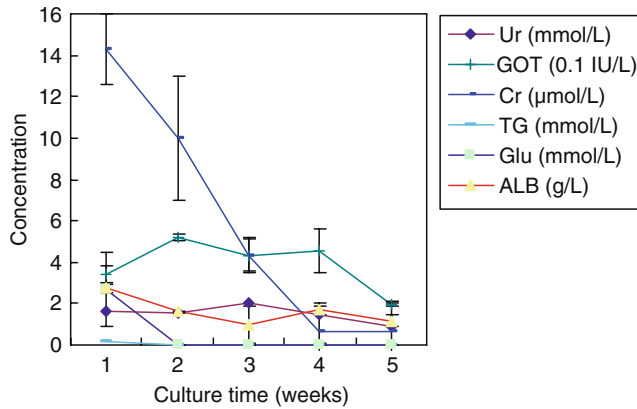


Fig. 5. Glutamate-oxaloacetate transaminase (GOT), albumin (ALB), urea (Ur), glucose (Glu), creatinine (Cr), and triglyceride (TG) secreted by hepatocytes in the 3D gelatin constructs after different culture time. Data represent means \pm SD ($n=3$).

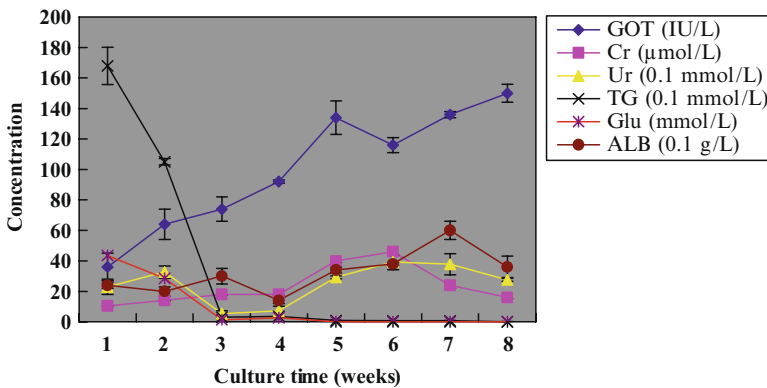


Fig. 6. Glutamate-oxaloacetate transaminase (GOT), albumin (ALB), urea (Ur), glucose (Glu), creatinine (Cr), and triglyceride (TG) secreted by hepatocytes in the 3D gelatin/alginate constructs after different culture time.

the constructs have to be crosslinked or polymerized to yield a defined shape and stable 3D structure. To stabilize the structure, different crosslinkers are used. For example, glutaraldehyde solution is used to crosslink the gelatin molecules, and CaCl_2 solution is used to stabilize the hydrogels structures containing alginate molecules. Due to the special properties, fibrinogen, a soluble plasma glycoprotein, is polymerized to fibrin. During this process, the polymer chains are covalently tethered to form a fibrous network that immobilizes the cells in the hydrogels system.

By stabilizing the cell/hydrogels construct, a biomimetic 3D cell survival microenvironment is created. This construct can be used to address biological, mechanical, and architectural needs to promote functional tissue. The gelatin-based hydrogels networks provide a stable support for 3D constructs during the fabrication stage. During the post culture period, the gelatin-based hydrogels serves as an extracellular matrix to mimic the microenvironment in native tissue. Adipose-derived stem cells (ADSCs) can be controlled to differentiate into different targeted cell types according to their positions within the orderly pre-designed 3D structure (Fig. 7). In a double-syringe deposition manufacturing system, a cell/hydrogels

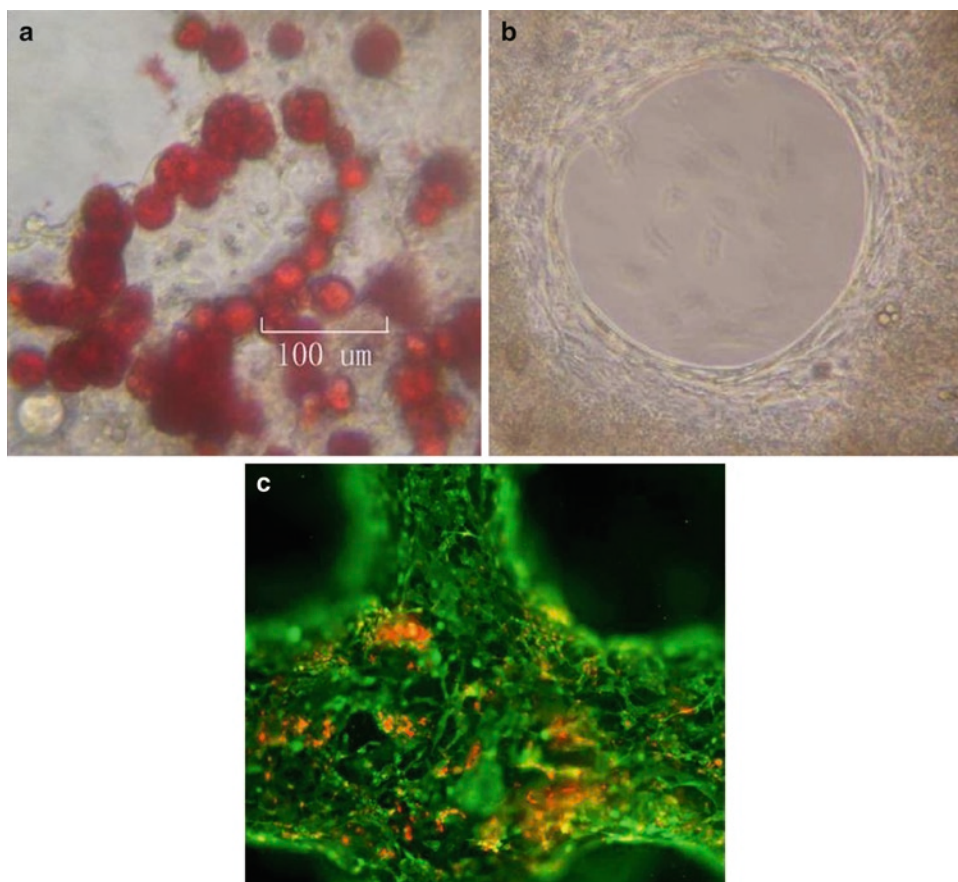


Fig. 7. ADSCs in the gelatin/alginate/fibrinogen construct. (a) ADSCs grew and proliferated into aggregates in the hydrogels; (b) ADSCs were induced into endothelial like cells on the walls of the channel; (c) immunostaining of the 3D structure using mAbs for CD31+ cells in green and PI staining the nuclear in red.

mixture can be placed into different regions or compartments (Figs. 8 and 9) [22, 23]. The gelatin-based hydrogels constructs provide the communication and organization support for cell assembly and set the basis for the formation of a 3D tissue or organ in vitro.

Gelatin-Based Hydrogels for the Controlled Hepatocyte Assembly

Hepatocytes are notoriously difficult to maintain their phenotype during in vitro culture. In one of our previous studies [24], we found that a small change in the cell survival matrix constitution significantly affects hepatocyte behavior within the structure. Hepatocytes can be arranged as rods, cords, or other shapes that exhibit special polarization on an ammonia-treated collagen/chitosan (1:1) membrane.

Consequently, the choice of hydrogels plays a major role in influencing cell shapes and gene expressions that relate to cell growth and the preservation of native phenotypes. It is very difficult to attain a compatible microbioenvironment to mimic an in vivo organ, whereby the cells support one another via cell–cell interactions, supplemented by small amounts of extracellular matrices (ECMs) secreted by the cells [25]. It is well known that the

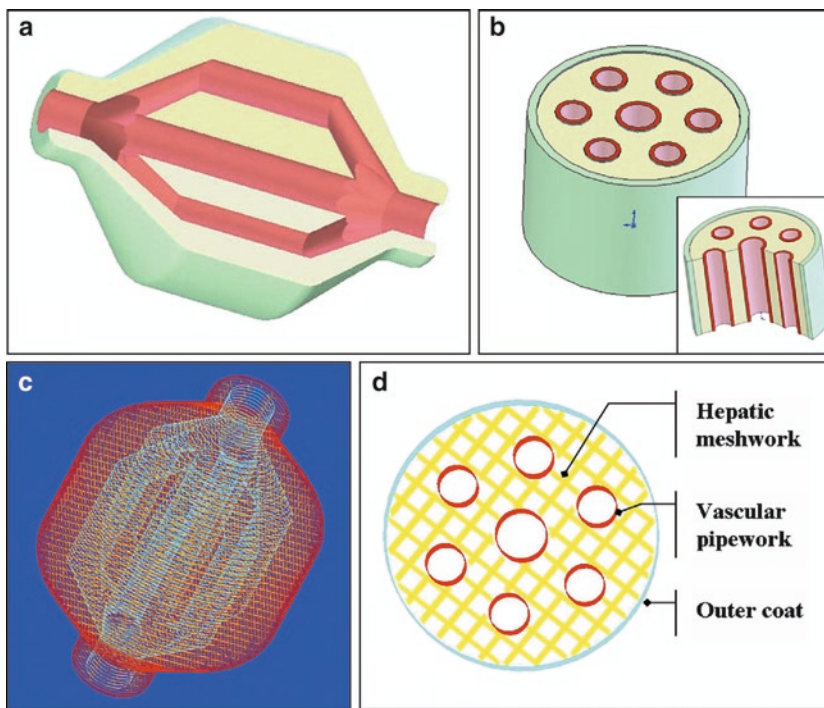


Fig. 8. Illustration of the digital models of the hybrid construct (the *red tubelines* denote the vascular network, while the *yellow* part was expected to form hepatic tissues): (a) a cutaway view of the full model with branched network and one-way inlet and outlet for dynamic perfusion culture; (b) the middle part of (a); (c) a CLI result of (a); (d) one CLI layer of (b).

success of bioartificial organs ultimately depends on the stability of the cell phenotype and its regulation by microenvironment cues [26].

Typically, as shown in Fig. 1, the first generation of a cell/hydrogels deposition system, developed in the Center of Organ Manufacturing, at Tsinghua University, consisted of a syringe with a 20 μm stainless steel capillary needle as the tip. The outer diameter of tip is 0.5 mm with an inner diameter of 0.3 mm. The tip has a flat end and is gently tapered with emery paper. The fluid of cell/matrix in the tip syringe is maintained at 0.25 μm per pulse, at 5 psi and 20 mL for volume, thus creating a driving force to deliver cell/matrix from the syringe to a poly(vinyl chloride) board. Hepatocytes embedded in the gelatin-based hydrogels are coextruded through a syringe with a needle tip onto a glass surface. These constructs are built layer by layer, by delivering the cellular containing matrices onto a stationary stage by applying pressure to a XYZ motor drive syringe. The 3D outcome of this process is a 100% interconnected porous construct, with defined architecture and can be built with a customized pattern. After deposition, more than 98% of the embedded hepatic cells remain viable.

The gelatin-based natural hydrogels, such as gelatin, gelatin/chitosan, gelatin/alginate, gelatin/hyaluronan, gelatin/fibrinogen, and gelatin/alginate/fibrinogen, are used in cell assembly as cell-loading support matrices and make the deposition processes easier. When hepatocytes are mixed with the hydrogels and deposited into special grid structures, with go-through pore-like channels under the computer control, hepatocytes are embedded in the hydrogels (Figs. 2–6) [2–10]. The hydrogels provide a highly hydrated microenvironment that allows nutrient diffusion, which supplies the necessary biochemical, cellular, and physical stimuli

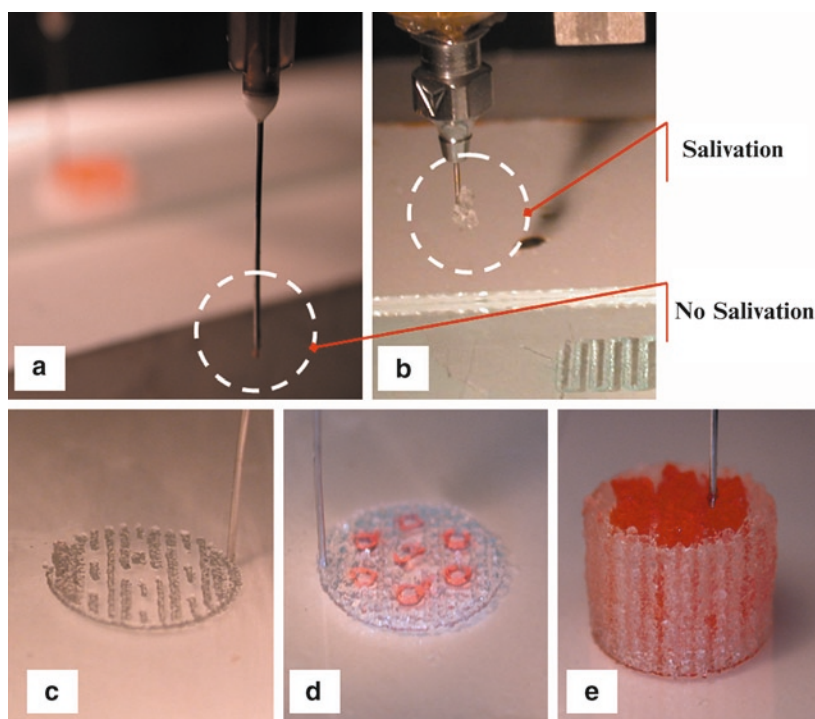


Fig. 9. Demonstration of an improved cell assembling controlling system and fabricating process with two syringes (the red part was made of ADSC/gelatin/alginate/fibrinogen in DMEM/F12, while the white part was made of hepatocyte/gelatin/alginate/chitosan in PBS): (a) no salivation with the improved method in the processing intervals; (b) salivation occurred with an old controlling method; (c–e) the layer-by-layer fabrication process.

influencing cellular processes, such as migration, proliferation, and differentiation [27]. Otherwise, the hepatocytes die when they are 20–30 μm away from a blood supply [28].

The gelatin composite was chosen as the basic cell assembly matrix based on its special sol–gel transformation properties. The other polymers, such as chitosan, alginate, hyaluronan, and fibrinogen, are added with the expectation that they would influence different cell types to deposit into predesigned locations and to reorganize into functional 3D aggregates for in vitro culture or in vivo implantation. It is found that different polymer additives incorporated in the gelatin hydrogels resulted in different behavior by the hepatocyte [2–10]. For example, hepatocytes in the gelatin/chitosan hydrogels aggregate to form vortex like structures [3]. Due to the instability of the gelatin-based hydrogels at room temperature and normal cell culture at 37°C, chemical crosslinkers, such as glutaraldehyde, sodium tripolyphosphate (TPP), CaCl_2 , or thrombin, are employed to stabilize the constructs.

In general, glutaraldehyde is a toxic but an effective crosslinking agent. It is commonly used to harden gelatin by crosslinking the amino groups of proteins [29]. At certain concentrations, the crosslinking time of glutaraldehyde is directly related to structure stability. An increase in crosslinking time from 1 s to 5 min increases the stability of the 3D structures significantly. Longer crosslinking time produces rigid structures in which hepatocytes die, while less crosslinking time results in less stable structures. Hepatocytes on the outside of the extruded cell/hydrogels filaments also often die during the crosslinking process [2, 3]. Subsequently, a glutaraldehyde concentration of 2.5% and a crosslinking time of 5 s were selected [2, 3]. Under these conditions,

a hydrogels that is soft and yet can be handled without losing its integrity was developed. The hydrogels state remained stable for more than 2 months. After the outside of the hydrogels was crosslinked, the hepatocytes were embedded in the gelatin macromolecules ensuring a relatively homogeneous distribution of cells in the grid. During the *in vitro* culture period, some of the interconnected gelatin molecules distributed in the inner parts of the structure, and the uncross-linked material gradually dissolved at 37°C. Unlike the traditional 2D cell culture systems, the hepatocyte activity in the 3D structures is controlled by the crosslinked hydrogels networks, the soluble signals in the culture medium, as well as by cell–cell interactions. These 3D structures provide the hepatocytes with a microenvironment that more closely mimic those in the liver.

The 3D construct containing hepatocytes in a gelatin/chitosan hydrogels is formed by crosslinking with 3% TPP solution for 5 min, and then with 0.25% glutaraldehyde solution for 5 sec, respectively. If the construct is only crosslinked with TPP, a progressive loss of structure occurs after 2 weeks in culture. Apparently, the TPP in the crosslinked chitosan molecules is depleted with time and the gelatin/chitosan hydrogen is degraded by enzymes. When the concentration of TPP in the culture medium is far less than that in the crosslinked chitosan molecules, some of the TPP dissolves in the medium leading to the disassembled forms. Theoretically, the gelatin in the hydrogels should biodegrade much faster than chitosan, since hepatocytes produce enzymes that can biodegrade collagen as well as gelatin. Thus the hepatocytes are able to enzymatically digest the gelatin/chitosan hydrogels formed with TPP. Therefore, to further stabilize the structures, the cell-loaded architectures need to be treated with glutaraldehyde to provide a longer lasting hepatocyte survival environment during the *in vitro* culture period (Fig. 3). These structures remain intact until the cell aggregates are large enough to break the grid walls.

Similar results were obtained with the hepatocyte containing gelatin/alginate constructs [2]. After the calcium alginate hydrogels is formed, the gelatin molecules are irreversibly embedded in the calcium alginate molecules and the hepatocytes are then immobilized in the mixture. After setting, the hydrogels state remains for more than 2 weeks before the constructs appear to break down. The hydrogels structures decompose due to the loss of calcium ions in the cross-linked alginate molecules and the degradation of the gelatin/alginate hydrogen by enzymes.

In another approach, biodegradable fibrin was introduced into the gelatin-based cell system to stabilize the 3D cellular structures. Fibrin is a good haemostatic and wound dressing material that can be made in the form of sponges, films, powders, and sheets [19, 30]. During the fibrinogen gelation process, the protease thrombin cleaves the dimeric fibrinogen molecules at two symmetric sites. Once the fibrinogen is cleaved, a self assembly step takes place in which the fibrinogen monomers come together to form a noncovalently crosslinked polymer gels via the proteolytic exposure of binding sites [31]. A gelatin/fibrin hydrogels was chosen as the cell assembly matrix using a 1:1(v/v) ratio which exhibited the greatest elasticity modulus and compressive strength, and a thrombin solution (100 IU/mL) was used to polymerize the fibrinogen.

In contrast to glutaraldehyde crosslinked materials, this polymerization is reversible and can be disrupted by aprotinin, which gives the material its good processability. Furthermore, this kind of biomaterial has shown to be extremely biocompatible *in vivo* [32] and can be biodegraded in aqueous media by enzymolysis. To prevent polymerization of the fibrinogen within the delivery syringe, *in situ* preparation of the solution is recommended. After deposition, the constructs are gently bathed in cold thrombin solution and placed in a 4°C incubator for further stabilization.

There are several factors that contribute to the long survival and improved performance of hepatocytes. First, a stable 3D spatial microenvironment that mimics the liver is required. Unlike monolayer cell culture systems, the cells are enveloped by the gelatin-based hydrogels or by other cells. Second, a supply of nutrients and oxygen and expel metabolic wastes and carbon dioxide is required. Third, the hydrogels must protect the cells from harm, such as the

glutaraldehyde crosslinker and culture polluted media, for example, cells die immediately when contacted directly with glutaraldehyde or after the 3D matrices break down. Fourth, the gelatin-based hydrogels can be biodegraded by the enzymes secreted by the living cells and provide space for cells to aggregate within the crosslinked membranes. Hence, the environment created must allow the cells to thrive in a 3D culture over a long time period. The crosslinked hydrogels structure provides a semi-permeable network that allows nutrient and waste infiltration, oxygen exchange, and cellular communication to occur.

In the human liver, hepatocytes are connected to each other laterally to form plate-like structures lined with three predominant types of nonparenchymal cells (NPCs) on the basal surfaces, creating sinusoids for blood flow. Organ manufacturing constructs that effectively duplicate natural organ functions must also maintain organ organization features, particularly the integration of multiple cell types that preserve distinct, integrated phenotypes. In particular, the need for angiogenesis or an established vasculature bed is evident by the success of the endothelial cells in the structures close to the culture medium.

Recently a double-syringe cell assembling technique was developed in the Center of Organ Manufacturing at Tsinghua University (Figs. 8 and 9) [22, 23]. This technique can layer two different cells simultaneously to create 3D constructs that can reproduce functions of a large population of two different cell types. The gelatin-based hydrogels are also used to provide structural stability, nutrients, and space for cell growth and aggregation. Both hepatocytes and endothelial cells were loaded in a stable structure. It is found that endothelial cells seeded on the bottom of pores are able to survive preferentially within the gelatin/chitosan channels. Regardless of the spheroids formed in the matrices, endothelial cells next to the hepatocytes undergo proliferation during the first several days (Fig. 9). The grid structures allow both the hepatocytes and endothelial cells access to nutrient and waste exchange as well as provide more surface area for endothelial cells to spread, coalesce, and elongate to form vessel-like structures throughout the channels. In addition, this technique offers many new opportunities for the design of the matrix components, the complex architectures, and for the study of the collaborations of cells, matrices as well as growth factors at different levels to meet special clinical demands.

It is expected that with the development of multisyringe systems, more different cells and extracellular matrices could be delivered simultaneously to the connective positions or with relative accuracy into the 3D structures that mimic their respective position in organs. Thus creating a suitable environment for cell–gels and cell–cell interactions and bring about self-organization of cells or cell aggregates into metastable tissue structures with desired shapes. The multisyringe deposition system holds the promise to eventually make a human liver with whole spectrum of functions.

Establishing a Multicellular Model by 3D Cell Assembly for Metabolic Syndrome

Presently, one of the major obstacles to engineering thicker and complex tissues *in vitro* is the need to vascularize the tissue to maintain cell viability during tissue growth and structural organization. Currently, *in vitro* 3D tissue formation within a hydrogels, typically by embedding cells or cell spheroids, is limited by the slow spontaneous aggregation of cells with poorly controlled size and shape [33, 34]. The self-assembly by proliferating cells to form functional tissues below a certain density is restricted in most hydrogels because the polymer chains themselves are able to entrap cells and inhibit cell migration. Whether cells can organize within a 3D hydrogels depends on many of the characteristics of the hydrogels that influence the mass ratio of cells to hydrogels [35].

Engineered adipose tissue can be used in plastic surgery and reconstructive surgery to augment soft tissue lost due to mastectomy or lumpectomy [36, 37]. Adipose-tissue engineering with collagen scaffolds combined with human preadipocytes was recently reported [38, 39]. Patrick et al. formed adipose tissue in the rat subcutis using a porous poly(lactide-co-glycolide) scaffold preseeded with autologously isolated preadipocytes [40, 41]. ADSCs are multipotent cells found in adipose tissue and are receiving more and more attention [42].

Metabolic syndrome (MS) is a cluster of growing epidemic diseases including obesity, diabetes, hypertension, and atherosclerosis [43]. It is difficult to use the traditional techniques to develop multifunctional drugs for the metabolic syndrome (MS). Therefore, it is necessary to establish an *in vitro* model that addresses the more complex features of the disease.

Cell-assembly technology is a remarkable new invention developed specifically to establish multicellular models for metabolic syndrome. A software package was used to fabricate a complex structure model with orderly channels. A gelatin/alginate/fibrinogen hydrogels was used for assembling the ADSCs as a stream of drops in 3D positions that mimic the respective positions a living organ. In the 3D construct, the ADSCs control differentiation into different targeted cell types according to their positions within the orderly predesigned 3D structure. After differentiation, the ADSCs, pancreatic islets were deposited at designated locations and constituted adipoinular axes with adipocytes. Oil red O staining confirmed that the ADSCs in the structure differentiated into adipocytes with a spherical shape while immuno-staining tests confirmed that endothelial growth factor (EGF) induced ADSCs on the walls of the channels that differentiated into mature endothelial cells and formed tubular structures throughout the engineered 3D structures. Endothelin-1 and nitric oxide release rules by the endothelial cells were coincident with that *in vivo*. In contrast, after preculturing with EGF, the ADSCs under the channel walls were more sensitive to differentiation into adipocytes than the cells on the walls. The reasons could be: (1) the EGF concentration under the walls of the channels was lower than that on the surface of the channels due to a diffusion gradient; (2) the mechanical properties of the surface of the channels induced the ADSCs to differentiate into endothelial cells more easily; (3) once differentiated into mature endothelial cells, the ADSCs lost all other differentiation potentials. This approach has the prospect of establishing an *in vitro* energy metabolic system with orderly endothelial vessel networks as well as in vascularized adipose-tissue engineering (Figs. 10 and 11) [8, 9].

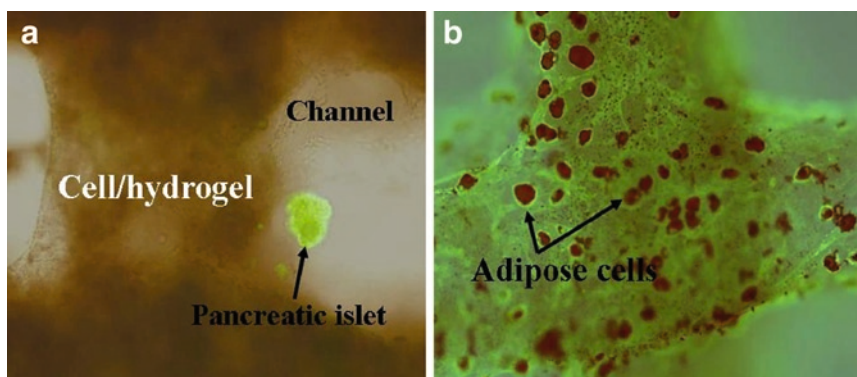


Fig. 10. A multicellular model for drug screening: (a) a pancreatic islet was implanted in the channel of the ADSC/gelatin/alginate/fibrinogen construct; (b) ADSCs on the walls of the channel were induced into endothelial cells while ADSCs in the hydrogels were induced into adipose cells.

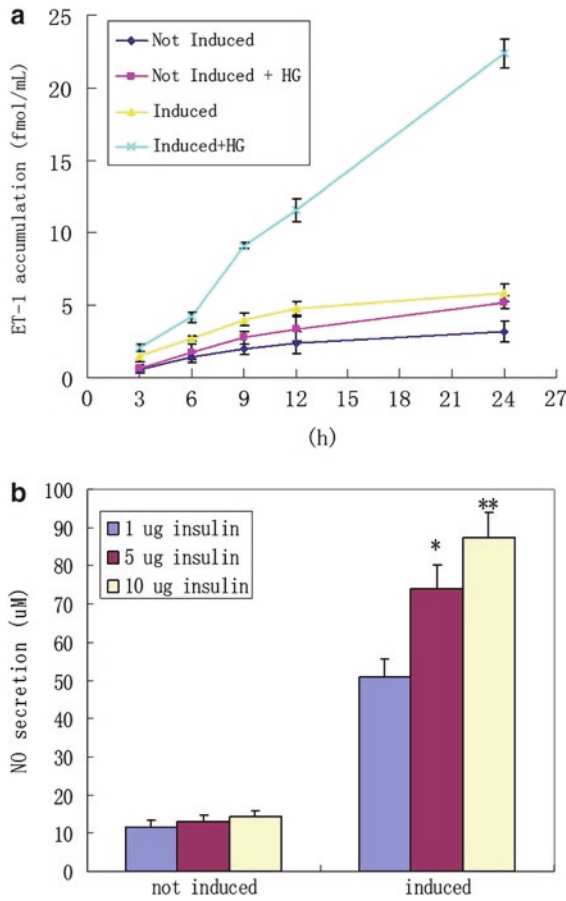


Fig. 11. Endothelin-1 and NO secretion of the endothelial cells in the 3D structures. At the 13th day, the structure was cultured with DMEM containing 25 mM glucose, (a) ET-1 secretion kinetics of the endothelial cells were measured for 24 h, ET-1 concentrations in the culture media were measured by ELISA kit. Data are mean \pm SD, $n=3$. (b) The media were harvested at the 15th day. NO concentrations in the culture media were detected using NO Detection kit. Data are mean \pm SD, $n=6$. * $p<0.01$, vs. 1 μ g insulin-treated group; ** $p<0.01$, vs. 5 μ g insulin-treated group.

Cryopreservation of 3D Constructs Based on Controlled Cell Assembly

The development of tissue engineering and organ manufacturing requires effective cryopreservation technology for the cells in the 3D constructs. Cryopreservation technology plays an important role in conserving 3D constructs containing cells. Besides preserving the characteristics of the construct, it can also save resources, such as cell culture space, culture vessels, and culture medium.

The cryopreservation of 3D constructs that contain cells is different from the direct cryopreservation of single-cell suspension as there are complex connections between cells and materials in the 3D construct. Kang and coworkers analyzed the different responses between the fibroblasts exposed to low temperatures in monolayer cultures and 3D cultures [44]. They found that after recovering from the low temperatures, the cells in the 3D collagen scaffold

secreted more fiber proteins and growth factors. The functional expression of the stress protein in the 3D structure was denser than those in monolayer and suspension cultures. These results indicate that the cryopreservation may bring extra benefits for the cells in 3D constructs. After the cryopreservation process, the 3D construct adapted to the pathological environment and promoted better wound healing and tissue repair [44].

With the advantages of the 3D controlled cell assembly technique, a new cryopreservation method for the 3D construct was developed. Various cryoprotectants, such as dimethylsulfoxide (DMSO), glycerol, and dextran-40, can be directly incorporated into the cell/hydrogels system and undergo a freezing/thawing process after assembly. The cells contained in the 3D construct can be preserved below -80°C for more than 1 week. After the construct

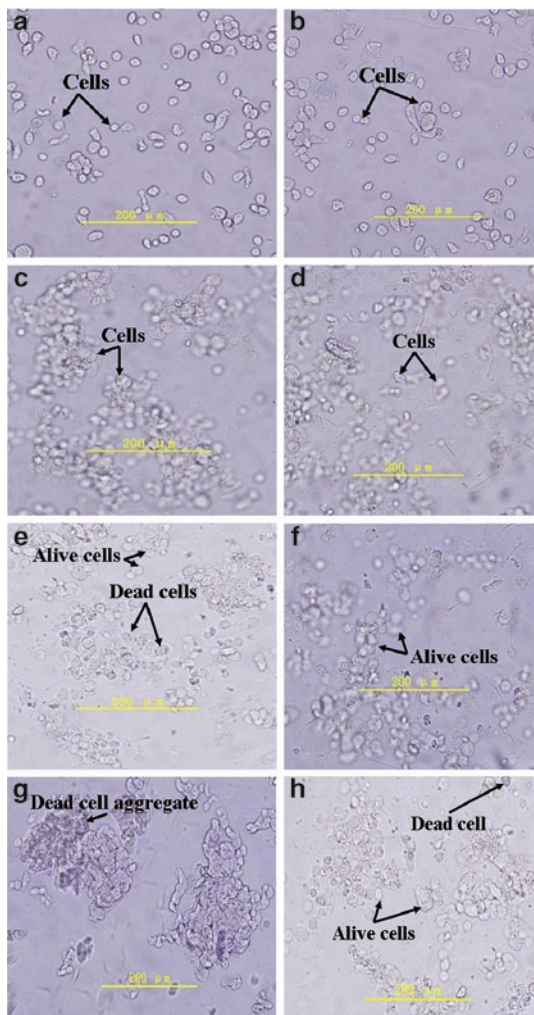


Fig. 12. Trypan Blue staining before and after cryopreservation: (a) ADSCs in gelatin/alginate/fibrinogen suspension without DMSO; (b) ADSCs in gelatin/alginate/fibrinogen suspension with 10% DMSO; (c) ADSCs in gelatin/alginate/fibrinogen hydrogels without DMSO before assembling; (d) ADSCs in gelatin/alginate/fibrinogen hydrogels with 10% DMSO before assembling; (e) ADSCs in gelatin/alginate/fibrinogen hydrogels without DMSO after assembling; (f) ADSCs in gelatin/alginate/fibrinogen hydrogels with 10% DMSO after assembling; (g) ADSCs in gelatin/alginate/fibrin hydrogels without DMSO after thawing; (h) ADSCs in gelatin/alginate/fibrin hydrogels with 10% DMSO after thawing.

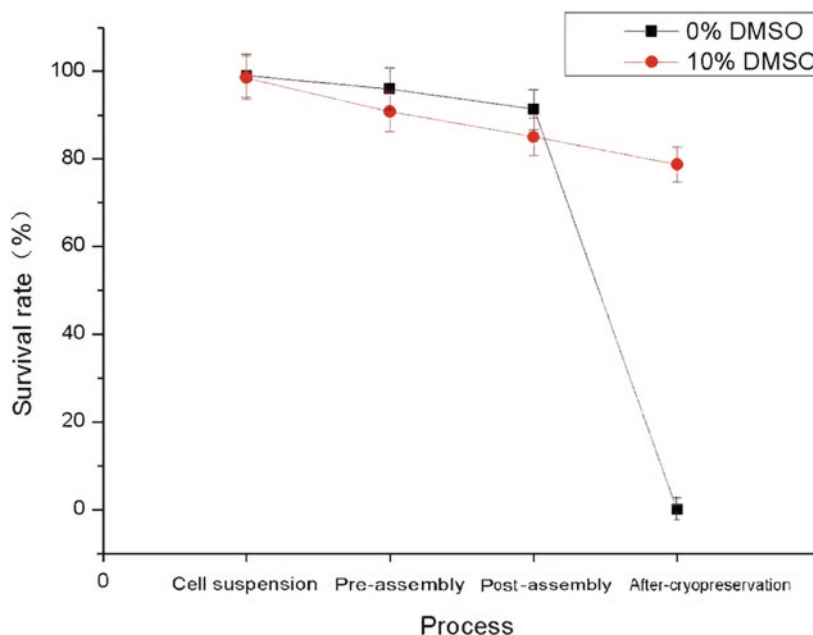


Fig. 13. Cell survival rate before and after cryopreservation.

undergoes a thawing process, cell viability and proliferation ability were regained. DMSO plays an important role in the cell survive processes. A cell viability of $78.7 \pm 3.94\%$ in the gelatin/alginate/fibrin hydrogels with 10% DMSO was obtained, which is much greater than that without the DMSO. This technique can potentially be used in other complex organ manufacturing areas (Figs. 12 and 13) [45].

Natural hydrogels, like gelatin, fibrin, and alginate, are commonly applied as cell-entrapping materials because of their outstanding biocompatibility and mild gelling conditions [46]. Fibrin gels is made by mixing two blood coagulation components, fibrinogen and thrombin [47]. These hydrogels also have protective effects on the cells during the freezing/thawing processes. The incorporation of the cryoprotectant, DMSO, in the gelatin/alginate/fibrinogen hydrogels has greatly improved the cell survival abilities during the assembly and freezing/thawing processes.

Summary

During the controlled cell assembly processes, cells are mixed with the gelatin-based hydrogels and placed into predesigned structures. The embedded cells remain viable and perform biological functions as long as the 3D structures are retained. The gelatin-based hydrogels protect the cells from harmful attacks, such as the glutaraldehyde crosslinker, keep the structural stable, and provide mass exchange networks. During the in vitro culture period, the hydrogels can be eventually digested by enzymes secreted by living cells or existing in the culture medium and provide more space for the cells to aggregate and communicate. With the double-syringe deposition system, two different cell types can be fabricated into a single construct. ADSCs in the 3D construct can be controlled to differentiate into specific cell

types. The gelatin-based hydrogels used with cell assembly technology have the potential for high-throughput production of artificial human tissues and organs and high-throughput drug screening systems.

References

1. Keefe EB (2001) Liver transplantation: current status and novel approaches to liver replacement. *Gastroenterology* 120(3):749–762
2. Yan YN, Wang XH, Xiong Z, Liu HX, Liu F, Lin F, Wu RD, Zhang RJ, Lu QP (2005) Direct construction of a three-dimensional structure with cells and hydrogel. *J Bioact Compat Polym* 20(3):259–269
3. Yan YN, Wang XH, Pan YQ, Liu HX, Cheng J, Xiong Z, Lin F, Wu RD, Zhang J, Lu QP (2005) Fabrication of viable tissue-engineered constructs with 3D cell-assembly technique. *Biomaterials* 26:5864–5871
4. Wang XH, Yan YN, Pan YQ, Xiong Z, Liu HX, Cheng J, Liu F, Lin F, Wu RD, Zhang RJ, Lu QP (2006) Generation of three-dimensional hepatocyte/gelatin structures with rapid prototyping system. *Tissue Eng* 12:83–90
5. Xu W, Wang XH, Yan YN, Zheng W, Xiong Z, Lin F, Wu RD, Zhang RJ (2007) Rapid prototyping three-dimensional cell/gelatin/fibrinogen constructs for medical regeneration. *J Bioact Compat Polym* 22(4):363–377
6. Yao R, Zhang RJ, Wang XH (2009) Design and evaluation of a cell microencapsulating device for cell assembly technology. *J Bioact Compat Polym* 24(S1):48–62
7. Yao R, Zhang RJ, Yan YN, Wang XH (2009) In vitro angiogenesis of three-dimensional tissue engineered adipose tissues. *J Bioact Compat Polym* 24:5–24
8. Xu ME, Yan YN, Liu HX, Yao R, Wang XH (2009) Control adipose-derived stromal cells differentiation into adipose and endothelial cells in a 3-D structure established by cell-assembly technique. *J Bioact Compat Polym* 24(S1):31–47
9. Xu ME, Yan YN, Liu HX, Yao R, Wang XH (2008) Establishing a multicellular model by three-dimensional cell-assembly technique for metabolic syndrome. *Nature Precedings*, Posted 8 Jan 2008
10. Wang XH, Yan YN, Zhang RJ (2007) Rapid prototyping as a tool for manufacturing bioartificial livers. *Trends Biotechnol* 25:505–513
11. Hoffman AS (2002) Hydrogels for biomedical applications. *Adv Drug Deliv Rev* 54:3
12. Heimbach D, Lutermaier A, Burke J, Cram A, Hunt J, Jordan M, McManus M, Solem L, Warden G, Zawacki B (1998) Artificial dermis for major burn: a multi-center clinical trial. *Ann Surg* 208:313–320
13. Chen WY, Abatangelo G (1999) Functions of hyaluronan in wound repair. *Wound Repair Regen* 7:79–89
14. Veis A (1964) The macromolecular chemistry of gelatin. Academic, New York
15. Schacht EH, Nobels M, Vansteenkiste S, Demeester J, Franssen J, Lemahieu A (1993) Cross-linkage of gelatin by dextran dialdehyde. *Polym Gels Netw* 1:213–224
16. Landers R, Hübner U, Schmelzeisen R, Mülhaupt R (2002) Rapid prototyping of scaffolds derived from thermoreversible hydrogels and tailored for application in tissue engineering. *Biomaterials* 23:4437–4447
17. Govan JR, Fyfe JA, Jarman TR (1981) Isolation of alginate-producing mutants of *Pseudomonas fluorescens*, *Pseudomonas putida* and *Pseudomonas mendocina*. *J Gen Microbiol* 125(1):217–220
18. Bergel S (1909) On the functions of fibrins. *Dtsch Med Wochenschr* 35:633
19. Ferry JD, Morrison PR (1946) Fibrin film and other products from human plasma. *Ind Eng Chem* 38:1217–1221
20. Sastry TP, Rose C, Gomathinayagam S, Ganga R (1998) Chemically modified fibrin-gelatin composites: preparation and characterization. *J Appl Polym Sci* 68:1109–1115
21. John P, Courts A (1977) The science and technology of gelatin. In: Ward AG, Courts A (eds) Academic Press, New York, p 138
22. Li SJ, Xiong Z, Wang XH, Yan YN, Liu HX, Zhang RJ (2009) Direct fabrication of a hybrid cell/hydrogel construct via a double-nozzle assembling technology. *J Bioact Compat Polym* 24:249–264
23. Li SJ, Yan YN, Xiong Z, Weng CY, Zhang RJ, Wang XH (2009) Gradient hydrogel construct based on an improved cell assembling system. *J Bioact Compat Polym* 24(S1):84–99
24. Wang X, Yan Y, Xiong Z, Lin F, Wu R, Zhang R, Lu Q (2005) Preparation and evaluation of ammonia treated collagen/chitosan matrices for liver tissue engineering. *J Biomed Mater Res- Part B, Appl Biomater* 75(1):91–98
25. Ong SM, Zhang C, Toh YC, Kim SH, Foo HL, Tan CH, van Noort D, Park S, Yu H (2008) A gel-free 3D microfluidic cell culture system. *Biomaterials* 29:3237–3244

26. Colette S, Ranucci AK, Surendra PB, Prabhas VM (2000) Control of hepatocyte function on collagen foams: sizing matrix pores toward selective induction of 2-D and 3-D cellular morphogenesis. *Biomaterials* 21:783–793
27. Fedorovich NE, Alblas J, de Vijn JR, Hennisnk WE, Verbout AJ, Dhert WJA (2007) Hydrogels as extracellular matrices for skeletal tissue engineering: state-of-the-art and novel application in organ printing. *Tissue Eng* 13:1905–1925
28. Kim SS, Sundback CA, Kaihara S, Benvenuto MS, Kim B, Mooney DJ, Vacanti JP (2000) Dynamic seeding and in vitro culture of hepatocytes in a flow perfusion system. *Tissue Eng* 6(1):39–44
29. Richards FM, Knowles JR (1968) Glutaraldehyde as a protein crosslinking agent. *J Mol Biol* 37:231–233
30. Bergel S (1909) On the functions of fibrins. *Dtsch Med Wochenschr* 35:633, Cited in Mihaly Gerendas. *Fibrin products as aids in hemostasis and wound healing*. In: Koloman Laki. *Fibrinogen*. New York: Marcel Dekker Inc.; 1968. pp 277–316
31. Schense JC, Hubbell JA (1999) Crosslinking exogenous bifunctional peptides into fibrin gels with factor XIIIa. *Bioconjugate Chem* 10(1):75–81
32. Bruns H, Kneser U, Holzhueter S, Roth B, Kluth J, Kaufmann PM, Kluth D, Fiegel HC (2005) Injectable liver: a novel approach using fibrin gel as a matrix for culture and intrahepatic transplantation of hepatocytes. *Tissue Eng* 11:1718–1726
33. Bryant SJ, Anseth KS (2002) Hydrogel properties influence ECM production by chondrocytes photoencapsulated in poly(ethylene glycol) hydrogels. *J Biomed Mater Res* 59:63–72
34. Kelm JM, Timmins NE, Brown CJ, Fussenegger M, Nielsen LK (2003) Method for generation of homogeneous multicellular tumor spheroids applicable to a wide variety of cell types. *Biotechnol Bioeng* 83:173–180
35. Tan W, Desa TA (2003) Microfluidic patterning of cells in extracellular matrix biopolymers: effects of channel size, cell type, and matrix composition on pattern integrity. *Tissue Eng* 9:255–267
36. Cho SW, Song KW, Rhie JW, Park MH, Choi CY, Kim BS (2007) Engineered adipose tissue formation enhanced by basic fibroblast growth factor and a mechanically stable environment. *Cell Transplant* 16(4):421–434
37. Griffith LG, Naughton G (2002) Tissue engineering – current challenges and expanding opportunities. *Science* 295:1009–1014
38. Patrick CW Jr (2000) Adipose tissue engineering: the future of breast and soft tissue reconstruction following tumor resection. *Semin Sur Oncol* 19:302–311
39. Patrick CW Jr, Chauvin PB, Hobbey J, Reece GP (1999) Preadipocytes seeded PLGA scaffolds for adipose tissue engineering. *Tissue Eng* 5:139–151
40. von Heimburg D, Zachariah S, Heschel I, Kuehling H, Schoof H, Hafemann B, Pallua N (2001) Human preadipocytes seeded on freeze-dried collagen scaffolds investigated in vitro and in vivo. *Biomaterials* 22:429–438
41. von Heimburg D, Zachariah S, Low A, Pallua N (2001) Influence of different biodegradable carriers on the in vivo behavior of human adipose precursor cells. *Plast Reconstr Surg* 108:411–420
42. Zuk PA et al (2001) Multilineage cells from human adipose tissue: implications for cell-based therapies. *Tissue Eng* 7:211–228
43. Despres JP, Lemieux I (2006) Abdominal obesity and metabolic syndrome. *Nature* 444:881–887
44. Liu K, Yang YJ, Mansbridge J (2000) Comparison of the stress response to cryopreservation in monolayer and three-dimensional human fibroblast cultures: stress proteins, MAP kinases, and growth factor gene expression. *Tissue Eng* 6(5):539–554
45. Sui SC, Wang XH, Liu PY, Yan YN, Zhang RJ (2009) Cryopreservation of 3D constructs based on a controlled cell assembling technology. *J Bioact Compat Polym* 24(5):5–19
46. Lee J, Cuddihy MJ, Kotov NA (2008) Three-dimensional cell culture matrices: state of the art. *Tissue Eng: Part B* 14(1):61–86
47. Blomback B, Bark N (2004) Fibrinopeptides and fibrin gel structure. *Biophys Chem* 112:147–151

Double Network Hydrogels as Tough, Durable Tissue Substitutes

Takayuki Murosaki and Jian Ping Gong

Abstract Hydrogels are soft and wet materials with a wide range of biomedical applications to make tissue due to their unique properties, such as phase-transition, chemo-mechanical behavior, stimuli-responsiveness, and low surface friction. However, most hydrogels are mechanically too weak to be used practically in load-bearing applications. Double Network (DN) hydrogels are composed of both rigid and soft hydrogels networks, and are expected to perform better under mechanical loads. The DN gels exhibit a 0.1–1 MPa elastic modulus, 60 MPa compressive fracture stress, 3,000% of tensile strain, and 2,500 J/m² of fracture energy. These soft and wet gels materials with high mechanical strength, low surface friction, and high deterioration-resistance properties are good candidates as load-bearing tissue substitutes, such as auricular cartilage.

Introduction

Hydrogels are soft and wet polymer networks swollen with large amounts of water [1]. Technically, the human body is largely made of gels; for example, blood vessels, muscles, articular cartilages, and organs are hydrogels with water content up to 50–90%.

Therefore, hydrogels compositions are good candidates for biocompatible biomaterials or biomedical materials, such as artificial muscles and artificial cartilage. However, most of hydrogels are not qualified for biological applications like the cartilage of the joints, due to the lack of mechanical strength.

Recently, new hydrogels, Double Network Gels, with good mechanical performance have been developed [2]. These gels consist of two interpenetrated polymer networks, one made of highly crosslinked rigid polymers and the other made of loosely crosslinked flexible polymers and known as a “double network (DN) gels.” The DN gels, containing about 90 wt% water, possess both hardness (elastic modulus of 0.3 MPa) and toughness (fracture stress of ~10 MPa).

The current research in the development of hydrogels with tough mechanical strength, low frictional coefficient, and wear-resisting properties as substitutes for biological tissues, such as artificial articular cartilage, is very encouraging. Robust gels made of biocompatible polymers and DN gels are now a reality.

T. Murosaki and J.P. Gong • Faculty of Advanced Life Science, Hokkaido University, Sapporo 060-0810, Japan
e-mail: gong@mail.sci.hokudai.ac.jp

Robust Gels with High Elasticity

DN Gels from Synthetic Polymers

The DN gels is synthesized via a two-step network formation: the first step is to form a rigid highly crosslinked gels, and the second is to form a loosely crosslinked network with the first gels. An optimal combination is poly(2-acrylamido-2-methylpropane sulfonic acid) (PAMPS) gels as the first network and poly(acrylamide) (PAAm) gels as the second network (*N,N'*-methylenebis (acrylamide) (MBAA) as a crosslinking agent for both networks) [2].

A comparison of the behavior of the PAMPS gels (a), and the PAMPS/PAAm DN gels (b) prepared by the optimized conditions under compression is shown in Fig. 1. The S–S curves for the PAMPS/PAAm, the PAMPS, and the PAAm gels are profiled in Fig. 2. The DN gels holds up to a stress of 17.2 MPa, with a vertical strain λ of 92%. On the other hand, the PAMS gels and PAA gels break at stresses of 0.4 MPa ($\lambda=41\%$) and 0.8 MPa ($\lambda=84\%$), respectively.

Tough DN gels are obtained only when i) the gels consists of polyelectrolyte as the first network and neutral polymer as the second network, ii) the molar ratio of the first to the second component is very specific and, iii) the first component is tightly crosslinked and the second one is more linear and loosely crosslinked (Fig. 3). Both the concentration and the molecular

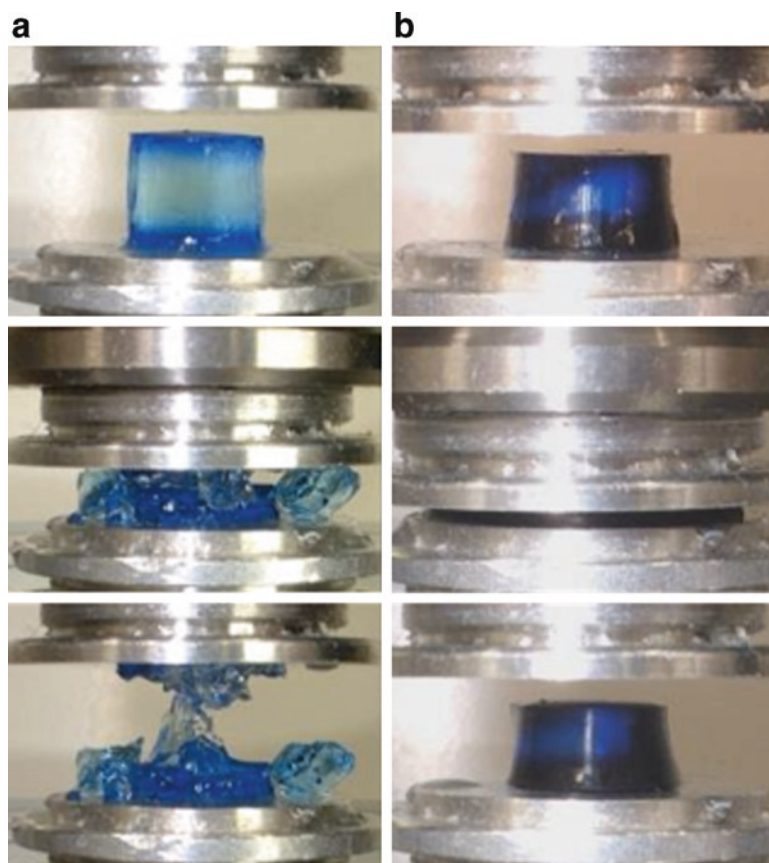


Fig. 1. PAMPS (a) and PAMPS/PAAm DN gels (b) under compression test. Crosslinker to monomer ratio: 4 mol% for PAMPS, 0.1 mol% for PAAm. Reproduced with permission from the literature [2].

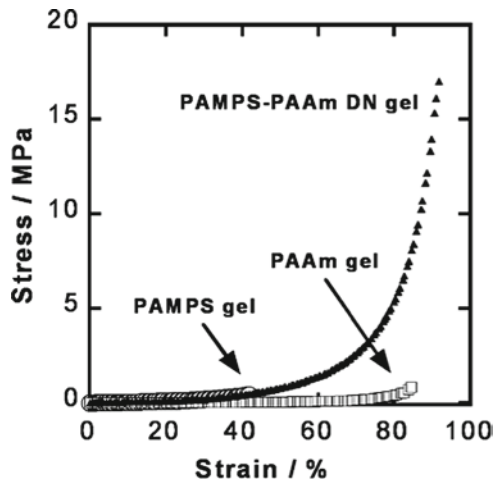


Fig. 2. Stress–strain curves for the PAMPS/PAAm DN gels, PAMPS gels, and PAAm gels. Crosslinker to monomer ratio: 4 mol% for PAMPS, 0.1 mol% for PAAm. Reproduced with permission from the literature [2].

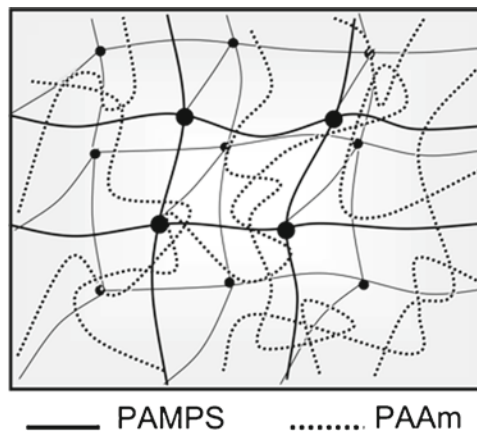


Fig. 3. Illustration of the structure of DN gels. PAMPS network is tightly crosslinked and PAAm is in linear state or is loosely crosslinked. Reproduced with permission from the literature [2].

weight (M_w) of the second linear polymer are important parameters related to the mechanical strength of DN gels. The relationship between the average molecular weight of PAAm and the mechanical strength of DN gels can be seen in Fig. 4. When the M_w is lower than 10^6 , the DN gels are as fragile as PAMPS single network gels, showing a $\sigma \approx 0.1$ MPa and a fracture energy G less than 1 J/m². When $M_w > 10^6$; however, the strength of the DN gels dramatically increases is maximized at a M_w of 3×10^6 , with values as high as $\sigma \approx 20$ MPa and $G \approx 10^3$ J/m² [3]. Since the PAAm linear chains having a molecular weight of $M_w > 10^6$ are much larger than the average mesh size of the first network, the prominent molecular weight effect of the PAAm cannot be explained in terms of the chain sliding mechanism in the PAMPS network.

The DN gels possess both hardness and toughness. Adjusting compositions of the first and second networks of the gels can independently control these two qualities for practical applications.

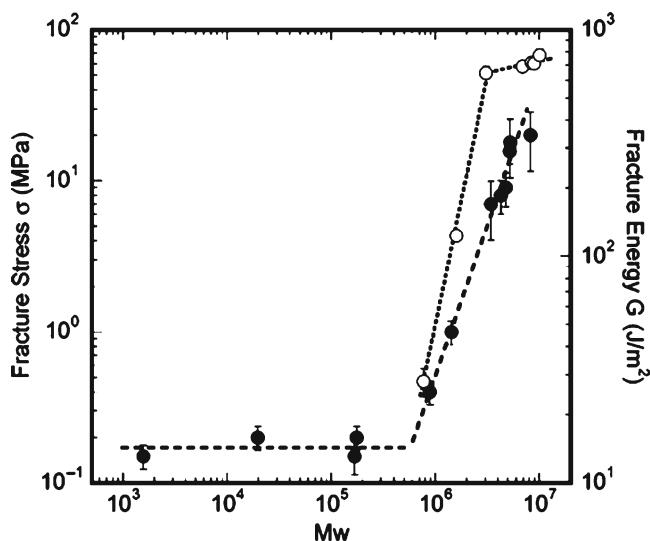


Fig. 4. Relationship between the average molecular weight of PAAm, the compressive fracture stress (*filled circle*), and fracture energy (*open circle*) of the DN gels. The dashed lines are guides for eyes. Reproduced with permission from the literature [3].

Necking Phenomenon of DN Gels

The molecular weight of the polymer forming the second network is important for mechanical strength of DN Gels. We modified the first network structure, by reducing the crosslinker concentration or by adopting γ -ray radiation for the crosslinking, that produced the necking phenomenon in the DN gels [4]. This necking phenomenon, during elongation of the gels, formed constricted zones in the sample that grew with further elongation. This necking phenomenon is the first observed in gels systems as other tough DN gels do not exhibit this phenomenon.

The necking deformation process in a DN Gels is shown in Fig. 5; images (a–e) represent the correspondence between the images and the respective data points. At the early stage of the elongation, the stress monotonically increases with the extension; at this stage, the sample is uniformly elongated as shown in a and b. When the stress reaches the critical value σ_c (σ_c is about 0.21 MPa, indicating very little dependence on the elongation velocity), the necked regions appear around the upper and lower clamps (clamps are not shown in images c–e). Upon further elongation, the necked regions expand into the un-necked region located in the middle part of the sample, while the elongation stress barely increases (c and d). After the un-necked region disappears, the sample is uniformly stretched again (e), which corresponds to the stress reincrease seen in the loading curve. The necking propagation usually starts at the extension of 2–3 and finishes at 7–8 respectively. The necking DN gels remarkably softens after the necking: the Young's modulus of the softened gels, E_s , is ~ 0.015 MPa, which is much smaller than the gels modulus before necking, $E_h \approx 0.1$ MPa. The softened gels can sustain an extraordinarily large extension (>10 times the initial length) before breaking.

Based on these findings, a model for the necking propagation was proposed (Fig. 6). The PAMPS SN gels are considered to be quite brittle and breaks into small pieces with small deformations. It seems that during the necking deformation, that the first PAMPS network fragments into small clusters and that the clusters play a role crosslinking of the long

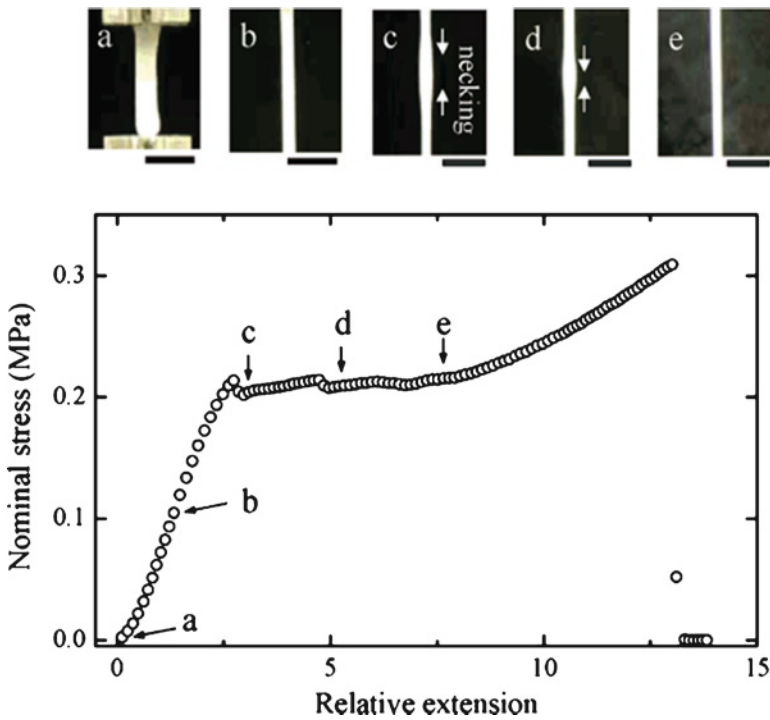


Fig. 5. Loading curve of PAMPS/PAAm DN gels obtained by necking phenomenon under uniaxial elongation at an elongation velocity of 500 mm/min, and pictures that demonstrate how the necking makes progress. The insert letters represent the correspondence between the pictures and the arrowed data points. Scale bars show 10 mm, and the width of the undeformed gels in picture a corresponds to the thickness of the sample (4 mm). In pictures c and d, the upper and lower parts (*necked regions*) of the gels are slightly narrowing compared with the middle part (*un-necked region*). The necked regions grow up with the extension of the sample. Reproduced with permission from the literature [4].

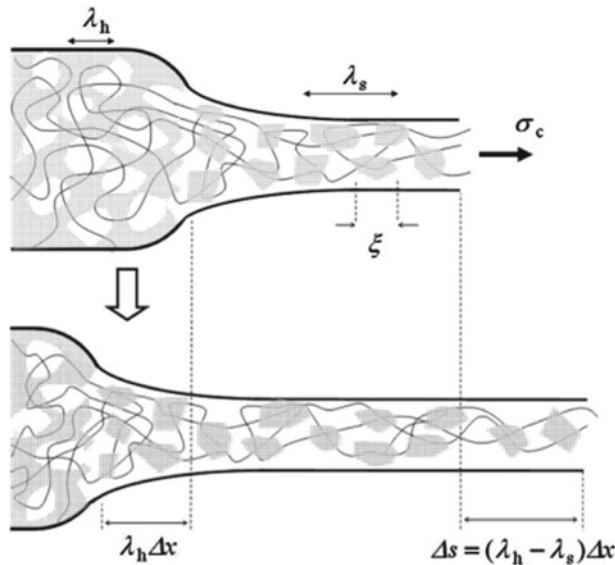


Fig. 6. Illustrations of the necking propagation and a model of the network structure of the softened DN gels after the necking. The mesh and the curves represent the first (PAMPS) and the second (PAAm) networks, respectively. Reproduced with permission from the literature [4].

PAAm chains since the crosslink density of the second network is so slight that the PAAm SN gels alone behaves as a sticky sol rather than a gels. Thus, the “molecular weight between crosslinks” allows chain sliding in response to deformation. The capability of chain sliding is in common with the so-called topological gels, known as ductile and tough hydrogels that were developed concurrently with the rigid and tough DN gels. When a PAMPS cluster is deformed and suffers a larger stress than the others, the stress inequality can be corrected by redivision. Due to these effects, the resultant network structures have fewer mechanical defects. The superior mechanical properties of the softened gels are attributed to these structural features.

In contrast to the DN gels that possess both hardness and toughness, the new necking DN gels show superior extensibility with nearly complete recovery. This is meaningful for biomedical engineering applications and for studying the fundamental physics of polymer networks.

Local Damage Zone Model for the Toughening Mechanism of DN Gels

A theoretical model for the toughening mechanism of DN gels, based on necking phenomena, assumes that, at the highly stretched region in front of the “crack tip,” the material first yields and is transformed into a very soft material with intrinsic fracture energy G_0 and the “crack tip” passes through the softened (damaged) zone (Fig. 7) [5, 6]. When considering the energy balance of fracture mechanics, a scaling level expressions were proposed, in which the effective fracture energy G , is expressed in terms of the yielding stress σ_c , the size of the softened zone h , the intrinsic fracture energy G_0 , and the strain where the necking ends, ϵ_c [6].

$$G = G_0 + \sigma_c \epsilon_c h$$

The value of G can be estimated from the numerical data of the necking gels to predict the size of the necking zone.

Robust Gels from Bacterial Cellulose

The development of hydrogels with good mechanical properties would provide a wide range of applications in industry, such as fuel cell membranes, load-bearing water absorbents, separation membranes, printing, optical devices, low friction gels machines as well as in the biomechanical fields, such as artificial cartilages, tendons, blood vessels, and other bio-tissues.

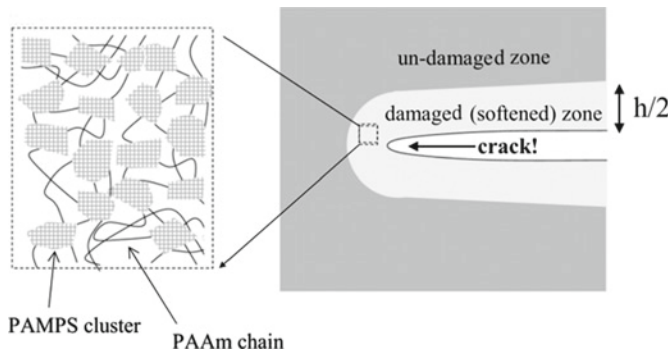


Fig. 7. Local damage zone model for explaining the extraordinary fracture energy of DN gels. Reproduced with permission from the literature [6].

To realize these biomedical applications, biocompatible polymers are paramount. Hydrogels derived from natural polymers frequently demonstrate adequate biocompatibility and are widely used in tissue engineering approaches but generally lack toughness [7]. In designing tough DN gels in this area, some progresses has been made by combining bacterial cellulose (BC) and gelatin [8].

BC is an extracellular cellulose, produced by *Acetobacter* bacteria that consists of a hydrophobic ultra-fine fiber network stacked in a stratified structure [9]. Scanning electron microscopy (SEM) images show that BC gels has alternating dense and sparse cellulose layers with a period of 10 μm , which contribute to its anisotropic mechanical properties. It has a high tensile modulus (2.9 MPa) along the fiber-layer direction but a low compressive modulus (0.007 MPa), perpendicular to the stratified direction. Due to its poor water-retaining ability, water is easily removed from the BC gels network, although an “as-prepared” BC containing 90% water there is no enhanced recovery in swelling because of hydrogen-bond formation between cellulose fibers.

Gelatin is a polypeptide derived from extracellular collagen matrix. Gelatin gels can retain water and recovers from repeated compression. Due to its poor mechanical strength, a gelatin gels is easily fragmented under modest compressions of ~ 0.12 MPa. By using the DN gels method, strong and biocompatible gels, consisting of BC and gelatin, were developed with high mechanical strength [8].

A BC/gelatin DN gels was synthesized by immersing a BC substrate into gelatin solution (30 wt%); then the gelatin was crosslinked with 1-ethyl-3-(3-dimethylaminopropyl) carbodiimide hydrochloride (EDC) (1 M). The wide-angle X-ray diffractions (WAXD) show that the BC crystal pattern is well maintained and SEM images exhibit homogeneous gelatin textures in the cellulose-poor layers in the BC/gelatin gels. The structure of BC/gelatin indicates that anisotropic mechanical strength of BC is maintained after combination with gelatin. Therefore, the mechanical strength against compression and elongation was performed perpendicular to and parallel to the stratified direction of BC/gelatin DN gels, respectively. Typical compressive and elongation stress–strain curves are shown in Fig. 8a, b, respectively. The BC/gelatin DN gels shows a compressive elastic modulus of 1.7 MPa (Fig. 8a), which is more than 240 times greater than that of BC gels (0.007 MPa) and 11 times greater than that of the gelatin gels (0.16 MPa).

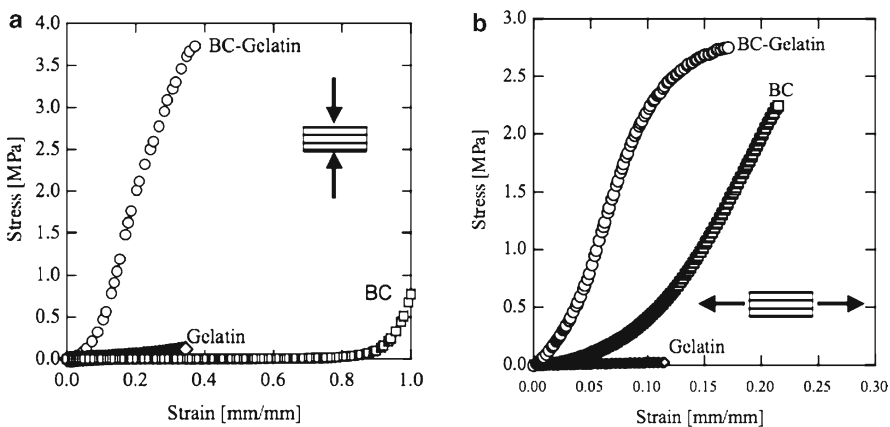


Fig. 8. Comparison of compressive (a) and elongational (b) stress–strain curves of BC-gelatin DN, gelatin, and BC gels. The compression and elongation were performed in perpendicular to and along with the stratified direction of BC and BC-gelatin DN gels, respectively. Concentration of gelatin in feed: 30 wt%. EDC concentration: 1 M. Reproduced with permission from the literature [8].

The fracture strength of BC/gelatin DN gels against compression in the vertical direction to the stratified structure was 3.7 MPa. The strength is in the range of an articular cartilage (1.9–14.4 MPa). This value is about 31 times higher than that of gelatin gels. Moreover, the BC/gelatin DN gels recovers well under repeated compression stress up to 30% strain. The elongation stress–strain curve (Fig. 8b) shows that BC/gelatin DN gels can sustain nearly 3 MPa elongation stress with 23 MPa elastic modulus, which is 112 times larger than that of gelatin gels.

Similar improvements in the mechanical strength were also observed for BC combined with polysaccharides, such as sodium alginate, gellan gum, and κ -carrageenan. For example, the compressive elastic modulus of BC- κ -Carrageenan DN gels is 0.12 MPa, and it is 17 and 13 times higher than that of individual BC and κ -carrageenan gels, respectively. In general, the mechanical properties of synthetic and natural gels can be effectively improved by the inducing double network structures. The composition of two different networks can be adjusted for different applications.

Sliding Friction of Gels

Some biological surfaces display fascinating low friction properties, for example, cartilages of animal joints have a friction coefficient in the range 0.001–0.03, remarkably low even for hydrodynamically lubricated journal bearings [10–16]. It is not well understood why the friction in the joint cartilages is so low even though the pressure between the bone surfaces reaches as high as 3–18 MPa and the sliding velocity is never greater than a few centimeters per second [10]. Under such conditions, the lubricating liquid layer cannot be sustained between two solid surfaces and the hydrodynamic lubrication does not work. Cartilage cells synthesize a complex extracellular matrix (ECM) and the weight bearing and lubrication properties of the cartilage are associated primarily with this matrix and its high water content (~75–80 wt%). The main macromolecular constituents of ECM are the proteoglycan, aggrecan, and the crosslinked networks of collagen fibrils [15, 16].

The tribological properties in the biological systems originate in the soft and wet nature of tissues and organs. Consequently, the role of solvated polymer networks existing in ECM as a *gels state* is critically important in the specific frictional behavior of the biological systems.

In the following section, the frictional behavior of various gels on solid substrates, and hydrogels with extremely low frictional property are introduced.

Frictional Behavior of Gels

Dependence on Load

The friction between solids obeys Amonton's law (1699);

$$F = \mu W,$$

which states that the frictional force F is linearly proportional to load W , and does not depend on apparent contact area A of two solid surfaces and sliding velocity v [17]. However, the gels friction does not simply obey this Amonton's law, and shows rich and complex features. Gels friction strongly depends on the properties of gels determined by its chemical structure, such as hydrophilicity, charge density, crosslinking density, water content, and elasticity [18, 19]; surface properties of opposing substrates, such as surface charges and hydrophobicity [19, 20]; and measurement conditions, such as normal load and sliding velocity [18–21].

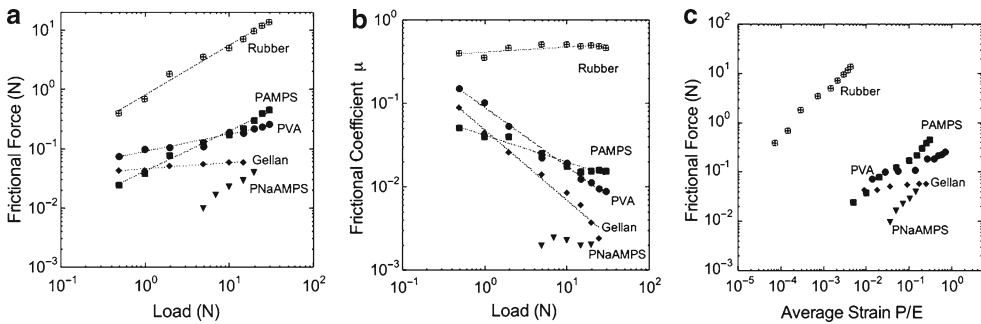


Fig. 9. Dependencies of frictional force F on load W (a), the frictional coefficient on load (b), and the frictional force on the average strain (c) for various kinds of hydrogels slid on glass substrate. Sliding velocity: 7 mm/min. Sample sizes for PVA, gellan, and rubber, 3×3 cm; PAMPS and PNaAMPS, 2×2 cm. Compressive modulus E : PVA, 0.014 MPa; gellan, 0.06 MPa; PAMPS, 0.25 MPa; PNaAMPS, 0.35 MPa; rubber, 7.5 MPa. Degree of swelling q : PVA, 17; gellan, 33; PAMPS, 21; PNaAMPS, 15. The measurement was performed by a tribometer in air. Reproduced with permission from the literature [19].

The friction behavior of hydrogels with different chemical structures such as poly(vinyl alcohol) (PVA), gellan, PAMPS, and its sodium salt PNaAMPS gels are shown in Fig. 9 [19]. These hydrogels were slid on a smooth glass surface at a sliding velocity of 7 mm/min, using a tribometer to determine the relation between a normal load and the frictional force (Fig. 9a). Relationship between frictional force (F) and normal load (W) obeys a power law, $F \propto W^\alpha$, where the scaling exponent α lies in a range of 0–1.0, depending on the chemical structure of the gels.

The frictional coefficient μ , which is defined as the ratio of the frictional force to applied load, is shown in Fig. 9b. The frictional coefficient μ of these gels, accordingly, shows unique load dependencies, which is quite different from those of solids. The corresponding μ s of PVA, gellan, and PAMPS gels decrease with an increase of load. On the other hand, the μ of the PNaAMPS gels is constant over the change of the load, similar to those of rubber, but its μ is as low as 0.002, two orders of magnitude lower than those of solids. PAMPS and PNaAMPS gels have different counter-ions, but they show a striking difference in frictional behavior on the glass surface. The frictional behavior of gels strongly depends on their chemical structure, and the frictional force of gels is two or three orders of magnitude lower than that of a rubber. The behavior can be continuously observed for several hours.

Some physically crosslinked gels show negative load dependences. When the average normal pressure exceeds a critical value, the frictional force of gellan and κ -carrageenan gels, both are physically crosslinked polysaccharide gels, show a pronounced negative load dependence. The observed specific phenomenon is attributed to the physical crosslinking nature of the polysaccharide gels. High normal pressure leads to losing and/or dissolving part of the crosslinks that brings about an increased viscous layer by the linear polymer at the friction interface, which would then serve as a good lubricator under the high load [21].

Sample Area Dependence

The linear dependence of friction on load established in solid friction,

$$F = \mu W$$

is explained in terms of the yielding mechanism; i.e., the solid surface is not molecularly flat and the real contact area between two surfaces increases with an increase of load due to yielding.

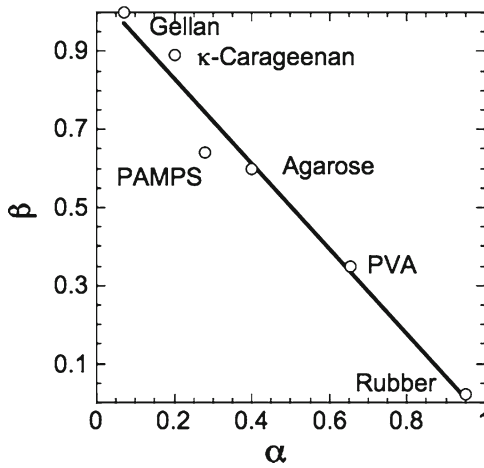


Fig. 10. Correlation between α and β , where α and β stand for the exponents in $F \propto W^\alpha A^\beta$. The α was measured at $A=9 \text{ cm}^2$; and the β was measured at $W=0.98 \text{ N}$. Sliding velocity: 180 mm/min. Degree of swelling: PVA, 20; gellan, 33; κ -carageenan, 33; agarose, 50; PAMPS, 17. The measurement was performed by a tribometer in air. Reproduced with permission from the literature [19].

Thus, the friction has no dependence on the apparent contact area of the two solid surfaces, and Amonton’s law holds [17].

To elucidate the feature of interface contact between the gels and the opposing plate, the frictional force of various kinds of gels was measured by varying the contact area of gels A under a constant load W [19]. It was found that the F also shows a power law with A , which can be denoted as $F \propto A^\beta$. Combining the results of F on W and A ;

$$F \propto W^\alpha A^\beta.$$

As shown in Fig. 10, a correlation between α and β was found as $\beta \approx 1 - \alpha$. Therefore,

$$F \propto AP^\alpha \tag{1}$$

where $P=W/A$ is the average normal pressure and $\alpha = 0 - 1$, depending on the chemical structure of the gels. This result demonstrates that the frictional force per unit area (frictional stress) is related with the normal pressure P , instead of the load W , by the power law. For solid friction, (1) is also valid, with $\alpha=1$.

With a typical elasticity ranging from 1 to 1,000 kPa, polymer gels are easily deformed due to the presence of the large amount of water. A small pressure is sufficient to cause a large deformation in a gels. This favors interfacial contact with the opposing surface. As shown in Fig. 9c, the average strains, $\lambda = P/E$, of gels under the experimental load range are more than several percent higher than that of rubber and much greater than that of solid and E is the compressive elastic modulus of the gels. Although the gels samples were measured under similar strain conditions, they showed quite different pressure dependence.

Substrate Effect

The frictional behavior of gels also depends on the opposing substrates. When the non-ionic PVA gels is allowed to slide on a tetrafluoroethylene (Teflon) plate, for example, the

behavior is the same as that on a glass surface. However, the behavior of strong anionic PAMPS gels on Teflon greatly changes and becomes similar to that of PVA on glass. When a pair of polyelectrolyte gels carrying the same charges, for example PNaAMPS gels with PNaAMPS gels, slide over each other, very low frictional force was observed [19]. On the other hand, when two polyelectrolyte gels carrying the opposite charges were slide over each other, the adhesion between the two gels was so high that the gels broke during the measurement [20]. The phenomenon indicates that the interfacial interaction between the gels surface and the opposing substrate is crucial in gels friction.

Extremely Low Friction Gels

Template Effect on Gels Surface Structure and Its Friction

The surface structure and, therefore, the friction of a gels are highly dependent on the substrate on which the gels is synthesized [22]. Such a substrate template effect is observed in a wide variety of hydrogels prepared from water-soluble vinyl monomers, such as the sodium salt of styrene sulfonate, acrylic acid, and acrylamide, on various hydrophobic substrates, such as Teflon, polyethylene, polypropylene, poly(vinyl chloride), and poly(methyl methacrylate) (PMMA) [22].

Hydrogels that are synthesized between two glass substrates have a mirror-like smooth surface. The same occurs when a hydrogels is synthesized on other hydrophilic substrates, such as mica and sapphire. However, for the same chemical structure, a hydrogels exhibits an eel-like slim surface when synthesized on hydrophobic substrates, such as Teflon and polystyrene (PS). The differences in the surface nature of the gels synthesized on different substrates are so obvious that they can be easily distinguished by touching with one's finger. When a hydrogels is synthesized between two plates, one hydrophobic and the other hydrophilic, heterogeneous gelation occurs [23]. After the equilibrated swelling in water, the gels exhibits a significant curvature as shown in Fig. 11, when the gels surface is formed on a Teflon surface it is always on the outside of the curvature and the side on the glass is the inside. The gels surface close to the Teflon has a higher swelling while the other one has a lower value. The gels has a gradient structure and the surface formed on Teflon (or other hydrophobic substrates) has a low crosslinking density with branched dangling polymer chains [24].

The frictional force and frictional coefficient of PAMPS gels synthesized on a glass plate and on a PS plate were measured against a glass plate in water by a rheometer (Fig. 12) [22]. The frictional stress of the gels prepared on PS substrate shows a lower value than that

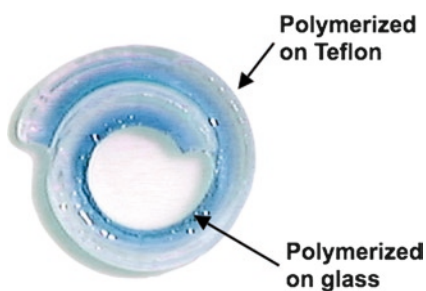


Fig. 11. Photograph of a colored water-swollen PAMPS gels prepared between a Teflon plate and a glass plate. Reproduced with permission from the literature [23].

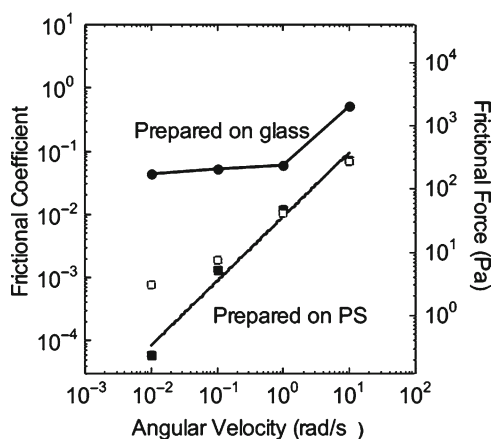


Fig. 12. Angular velocity dependencies of the frictional coefficient of PAMPS gels slid against a glass plate in water under a normal pressure of 4×10^3 Pa measured by a rheometer. (*filled circle*) prepared on glass, swelling degree, 21; (*filled square*) prepared on PS, swelling degree, 27; and (*open square*) containing linear polymer chains, Sample size, 1×1 cm, swelling degree, 15. Reproduced with permission from the literature [22].

prepared on the glass substrate. In the low velocity range in particular, the frictional stress of the gels prepared on PS substrate attains a value as low as 1 Pa, which is equivalent to the shear stress on the wall of blood vessels [25]. The frictional coefficient of the gels prepared on PS reaches 10^{-4} , which is at least two orders of magnitude lower than that of the gels synthesized on glass at the low velocity range. The reduction in friction is attributed to the presence of branched dangling chains on the gels surface prepared on the hydrophobic substrate, as revealed by the result for the PAMPS gels containing free linear PAMPS polymer chains prepared on the glass plate, which showed the similar low friction coefficients (Fig. 12). Therefore, extremely low friction hydrogels could have a wide range of applications in many fields where low friction is required.

Robust Hydrogels with Low Friction as Candidates for Artificial Cartilage

The design and production of hydrogels with a low surface friction and high mechanical strength are vitally important in the biomedical applications of hydrogels, such as contact lens, catheters, artificial articular cartilages, and artificial esophagus [26, 27]. Based on previous research, new soft and wet materials with both low friction and high strength were synthesized by introducing a weakly crosslinked PAMPS network (to form a triple-network, or TN gels) or a noncrosslinked linear polymer chain (to form a DN-L gels) as a third component in the optimal tough PAMPS/PAAm DN gels [28]. The TN and DN-L gels were synthesized by UV irradiation after immersing the DN gels in a large amount of a third solution of 1 M AMPS and 0.1 mol% 2-oxoglutaric acid with (TN) and without the presence of 0.1 mol% MBAA (DN-L). The mechanical properties of these gels are listed in Table 1. After adding crosslinked or linear PAMPS to the DN gels, the fracture strength of the TN- and DN-L gels and elasticity are higher than that of a DN gels (~ 2 MPa). In addition, the fracture strength of the DN-L increased remarkably because PAMPS linear chains effectively dissipate the fracture energy [2].

Shown in Fig. 13a, b are the frictional forces (F) and frictional coefficient (μ) of the three kinds of gels, respectively, as a function of normal pressure (P). The data based on

Table 1. Mechanical properties of DN (PAMPS/PAAm), TN (PAMPS/PAAm/PAMPS), and DN-L (PAMPS/PAAm/PAMPS-L) gels

Gels	Water content (wt%)	Elasticity (MPa)	Fracture stress δ_{\max} (MPa)	Fracture strain λ_{\max} (%)
DN	84.8	0.84	4.6	65
TN	82.5	2.0	4.8	57
DN-L	84.8	2.1	9.2	70

Reproduced with permission from the literature [28]

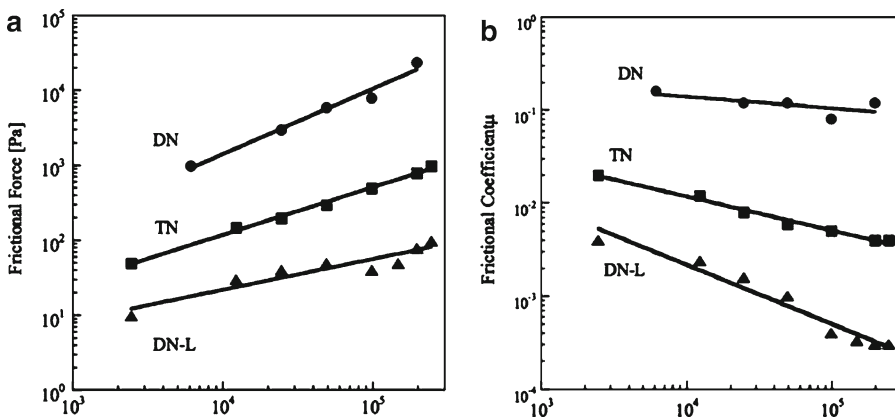


Fig. 13. Normal pressure dependence of frictional force (a) and frictional coefficient (b) of hydrogels against a glass plate in pure water. Sliding velocity: 1.7×10^{-3} m/s. Symbols denote DN (filled circle), TN (filled square), and DN-L (filled triangle) gels, respectively. Reproduced with permission from the literature [28].

sliding the gels on glass plate in water, clearly indicates that the frictional coefficient decreases in the order of $DN > TN > DN-L$, thus, introducing of PAMPS, in particular linear PAMPS as the third network component reduces the frictional coefficient of the gels.

The DN gels has a relatively large frictional coefficient ($\sim 10^{-1}$) since the second network, nonionic PAAm, dominates the surface of the DN gels, which is adsorptive to the glass substrate. However, when PAMPS network is added to the DN gels as the third component, the frictional coefficient of the TN decreases to $\sim 10^{-2}$; this is two orders of magnitude lower than the DN gels, since the surface of TN gels is dominated by PAMPS, resulting in repulsive interaction with the glass substrate and reducing frictional force. Furthermore, when linear PAMPS chains are introduced to the surface of the DN gels, the frictional coefficient is significantly reduced to $\sim 10^{-4}$, which is one to three orders of magnitude less than that of TN and DN gels, respectively. This demonstrates that the linear PAMPS chains on the gels surface reduce frictional force due to repulsive interactions with the glass substrate [25].

It should be emphasized that the lower friction coefficient of DN-L gels can be observed in the pressure range of 10^{-3} – 10^5 Pa, which is close to the pressure exerted on articular cartilage in synovial joints. These results demonstrate that the linear polyelectrolyte chains effectively retain lubrication even under extremely high normal pressures.

Wear Properties of Robust DN Gels

For the application of DN gels as artificial articular cartilage, it is critical to evaluate the wear properties, because articular joints are subjected to rapid shear forces in magnitude and millions of cycles over a lifetime. However, there are no established methods for evaluating the wear properties of a gels. The pin-on-flat wear testing that has been used to evaluate the wear property of ultra-high molecular weight polyethylene (UHMWPE), which is the only established rigid and hard biomaterial used in an artificial joint, was used to evaluate the wear properties of DN gels. Four kinds of DN gels, composed of synthetic or natural polymers, PAMPS/PAAm, PAMPS/poly (*N,N'*-dimethyl acrylamide) (PDMAAm), BC/PDMAAm, and BC/Gelatin, were evaluated [29].

Under one million friction cycles, which is equivalent to 50 km friction (50×10^6 mm), the maximum wear depth of the PAMPS/PAAm, PAMPS/PDMAAm, BC/PDMAAm, and BC/Gelatin gels was 9.5, 3.2, 7.8, and 1,302.4 μm , respectively. It is amazing that the maximum wear depth of PAMPS/PDMAAm DN gels is similar to the value of UHMWPE (3.33 μm). Although the maximum wear depth of PAMPS/PAAm DN gels and BC/PDMAAm DN gels was about 2–3 times higher than that of UHMWPE, these gels could bear the one million friction cycles. The results demonstrate that PAMPS/PAAm, PAMPS/PDMAAm, and BC/PDMAAm DN gels are resistant to wear to a greater degree than conventional hydrogels, and PAMPS/PDMAAm DN gels could potentially be used as replacement material for artificial cartilage. On the other hand, BC/Gelatin DN gels, which is composed of natural materials, had extremely poor wear properties compared with the other DN gels. The lower wear properties of BC/Gelatin DN gels are attributed to the relatively low water content, higher friction coefficient, and easy roughing by abrasion.

Biocompatibility of Robust DN Hydrogels

Overall, the DN hydrogels have excellent mechanical properties, high mechanical strength, low frictional coefficient, and high resistance to wear property. However, the substitute materials for biological tissues are required to be not only tough, but also resistant to biodegradation in the living body. Consequently, the biodegradation properties of the robust gels in the rabbit's subcutaneous was evaluated [30].

Evaluation of Robust Gels

PAMPS/PAAm, PAMPS/PDMAAm, BC/PDMAAm, and BC/Gelatin DN gels are composed of synthetic or natural polymers. Each DN gels was prepared as rectangular parallel-piped specimens ($10 \times 10 \times 5$ mm), and implanted into the subcutaneous space 8 cm below the surface. After 6 weeks, the four implanted gels specimens were carefully harvested from the subcutaneous tissue. In each rabbit, all of the skin incision healed without infections and the body weight did not change over a 6-week period. No signs of inflammation or infection, including redness of the skin, effusion and abscess, were observed at the implantation site. No obvious changes were found with PAMPS/PAAm and PAMPS/PDMAAm DN gels specimens (Fig. 14a, b). The surface of all the BC/PDMAAm DN specimens became rough, although they were smooth before implantation (Fig. 14c). All BC/gelatin DN gels specimens were mildly deformed and parts of these specimens were absorbed (Fig. 14d).

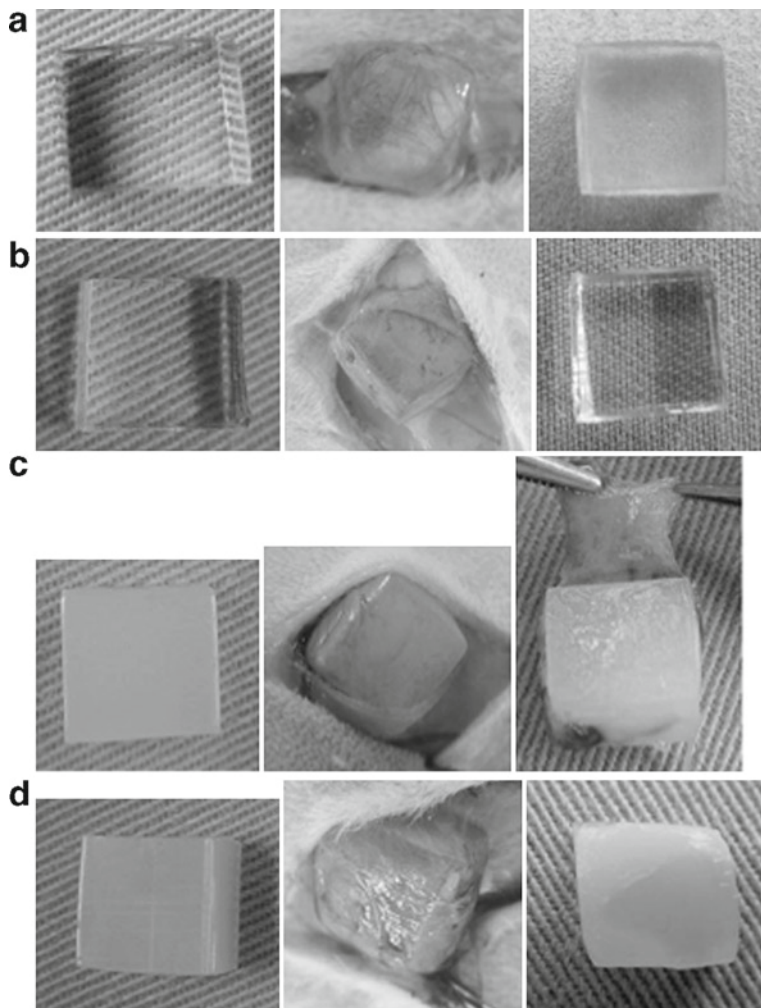


Fig. 14. Gross observations of each DN gels specimen before implantation (*Left*) and 6 weeks after implantation (immediately before harvest (*Center*) and after harvest (*Right*)). No obvious changes were found on PAMPS/PAAm (a), and PAMPS/PDMAAm (b) DN gels specimens. With BC/PDMAAm (c) DN gels, the surface of all specimens became rough, although it was smooth before implantation. Cellulose/gelatin (d) specimens were mildly deformed, and a part of the specimen was absorbed. Reproduced with permission from the literature [30].

Immediately after harvesting, changes in the mechanical properties and water content of each specimen due to implantation were investigated. The results are shown in Table 2; the ultimate stress in the compressive destruction test was determined from the peak of the stress–strain curve, and the tangent modulus was determined from the slope of the stress–strain curve in the range of 0–10% strain. For the PAMPS/PAAm DN gels, which is the strongest in the ultimate stress among the 4 DN gels, except for the tangent modulus and the water content, the mechanical parameters did not change after implantation. The DMAAm DN gels, which is highly resistant to wear in the pin-on-flat wear test, the ultimate stress and the tangent modulus were significantly increased with a significant reduction in the

Table 2. Changes in the mechanical properties and the water content of each DN gels due to implantation

Gels	PAMPS/PAAm	PAMPS/PDMAAm	BC/PDMAAm	BC/gelatin
<i>Tangent modulus (MPa)</i>				
Before	0.30 (0.05)	0.20 (0.01)	1.70 (0.70)	2.50 (1.10)
After	0.21 (0.02)	0.37 (0.04)	1.00 (0.60)	1.18 (1.10)
<i>P</i> -value	<i>P</i> =0.0002	<i>P</i> <0.0001	N.S.	N.S.
<i>Ultimate stress (MPa)</i>				
Before	11.40 (2.60)	3.10 (0.29)	1.90 (0.28)	4.30 (0.35)
After	10.02 (2.96)	5.40 (1.75)	2.17 (0.35)	1.98 (0.52)
<i>P</i> -value	N.S.	<i>P</i> =0.0194	N.S.	<i>P</i> <0.0001
<i>Strain at failure (mm/mm)</i>				
Before	0.83 (0.05)	0.73 (0.01)	0.37 (0.03)	0.33 (0.04)
After	0.88 (0.03)	0.76 (0.05)	0.40 (0.06)	0.40 (0.11)
<i>P</i> -value	N.S.	N.S.	N.S.	N.S.
<i>Water content (%)</i>				
Before	90.90 (0.30)	94.00 (0.00)	85.00 (0.71)	78.00 (2.30)
After	89.83 (0.90)	91.17 (0.75)	85.17 (0.75)	86.33 (0.75)
<i>P</i> -value	N.S.	<i>P</i> <0.0001	N.S.	<i>P</i> =0.0002

Before: specimens before implantation, After: specimens harvested 6 weeks after implantation. Reproduced with permission from the literature [30]

water content after implantation. In the Cellulose/PDMAAm DN gels, no significant changes in the mechanical properties or the water content were observed after implantation. The Cellulose/Gelatin DN gels, which had a relatively high tangent modulus compared with the other DN gels, the ultimate stress was dramatically reduced with a significant increase in the water content after implantation. Basically, the degradation properties of the 4 DN hydrogels within the living body are extremely different, depending on the properties of the polymers contained in each hydrogels. The characteristics of these materials need to be improved, not only to develop acceptable artificial cartilage, but also for other implants applications.

Summary

To design materials that are potentially useful as artificial cartilage, suitable viscoelasticity, high mechanical strength, durability to repeated stress, low friction, high resistance to wear, and resistance to biodegradation within the living body are required. It has been difficult to develop a gels material that satisfies even two of these requirements. However, current developments in the synthesis of mechanically stronger hydrogels using conventional gels concepts should open a new era of soft and wet materials as substitutes for articular cartilage and other tissues. These exceptional hydrogels would provide opportunities for wide industry applications, such as the fuel cell membranes, load-bearing water absorbents, separation membranes, printing, optical devices, and low friction gels machines.

References

1. Osada Y, Kajiwara K (2001) *Gels handbook*. Academic, New York
2. Gong JP, Katsuyama Y, Kurokawa T, Osada Y (2003) *Adv Mater* 15:1155
3. Tsukeshiba H, Huang M, Na Y-H, Kurokawa T, Kuwabara R, Tanaka Y, Furukawa H, Osada Y, Gong JP (2005) *J Phys Chem B* 109:16304
4. Na Y-H, Tanaka Y, Kawauchi Y, Furukawa H, Sumiyoshi T, Gong JP, Osada Y (2006) *Macromolecules* 39:4641
5. Brown HR (2007) *Macromolecules* 40:3815
6. Tanaka Y (2007) *Europhys Lett* 78:56005
7. Lee KY, Mooney DJ (2001) *Chem Rev* 10:1869
8. Nakayama A, Kakugo A, Gong JP, Osada Y, Takai M, Erata T, Kawano S (2004) *Adv Fun Mater* 14:1124
9. Klemm D, Schumann D, Udhardt U, Marsch S (2001) *Prog Polym Sci* 26:1561
10. McCutchen CW (1962) *Wear* 5:1
11. McCutchen CW (1978) *Lubrication of joints, the joints and synovial fluid*. Academic Press, New York
12. Dowson D, Unsworth A, Wright V (1970) *J Mech Eng Sci* 12:364
13. Ateshian GA, Wang HQ, Lai WM (1998) *J Tribol* 120:241
14. Hodge WA, Fijian RS, Carlson KL, Burgess RG, Harris WH, Mann RW (1986) *Proc Natl Acad Sci USA* 83:2879
15. Grodzinsky AJ (1985) *CRC Crit Rev Biomed Eng* 9:133
16. Buschmann MD, Grodzinsky AJ (1995) *J Biomech Eng* 117:179
17. Persson BNJ (1998) *Sliding friction: physical principles and applications*, 2nd edn, Nanoscience and technology series. Springer, Berlin
18. Gong JP, Higa M, Iwasaki Y, Katsuyama Y, Osada Y (1997) *J Phys Chem B* 101:5487
19. Gong JP, Iwasaki Y, Osada Y, Kurihara K, Hamai Y (1999) *J Phys Chem B* 103:6001
20. Gong JP, Kagata G, Osada Y (1999) *J Phys Chem B* 103:6007
21. Gong JP, Iwasaki Y, Osada Y (2000) *J Phys Chem B* 104:3423
22. Gong JP, Kurokawa T, Narita T, Kagata G, Osada Y, Nishimura G, Kinjo M (2001) *J Am Chem Soc* 123:5582
23. Kii A, Xu J, Gong JP, Osada Y, Zhang XM (2001) *J Phys Chem B* 105:4565
24. Narita T, Knaebel A, Munch J-P, Candau SJ, Gong JP, Osada Y (2001) *Macromolecules* 34:5725
25. Fung YC (1993) *Biomechanics: mechanical properties of living tissues*, 2nd edn. Springer, New York
26. Freeman ME, Furey MJ, Love BJ, Hampton JM (2000) *Wear* 241:129
27. Raviv U, Giasson S, Kampf N, Gohy JF, Jerome R, Klein J (2003) *Nature* 425:163
28. Kaneko D, Tada T, Kurokawa T, Gong JP, Osada Y (2005) *Adv Mater* 17:535
29. Yasuda K, Gong JP, Katsuyama Y, Nakayama A, Tanabe Y, Kondo E, Ueno M, Osada Y (2005) *Biomaterials* 26:4469
30. Azuma C, Yasuda K, Tanabe Y, Taniguro H, Kanaya F, Nakayama A, Chen YM, Gong JP, Osada Y (2007) *J Biomed Mater Res A* 81:373

Hydrogels Contact Lenses

Jiri Michalek, Radka Hobzova, Martin Pradny, and Miroslava Duskova

Abstract Contact lenses can be classified in a number of ways; however, the two main categories are hard and soft lenses, which are based on the material used for their manufacture. The soft lens category can be further divided into hydrophobic and hydrophilic subcategories. Consequently, the development of contact lens materials took three specific directions: hydrogels with high water content, rigid gas-permeable lenses with enhanced oxygen permeability, and surface modification of silicone elastomer lenses. These polymeric systems are expected to improve the water content of the contact lenses as well as the permeability to oxygen, which are crucial properties but controllable through the molecular design. Currently, the high water content hydrogels are being challenged by the silicone-hydrogels for the world market share.

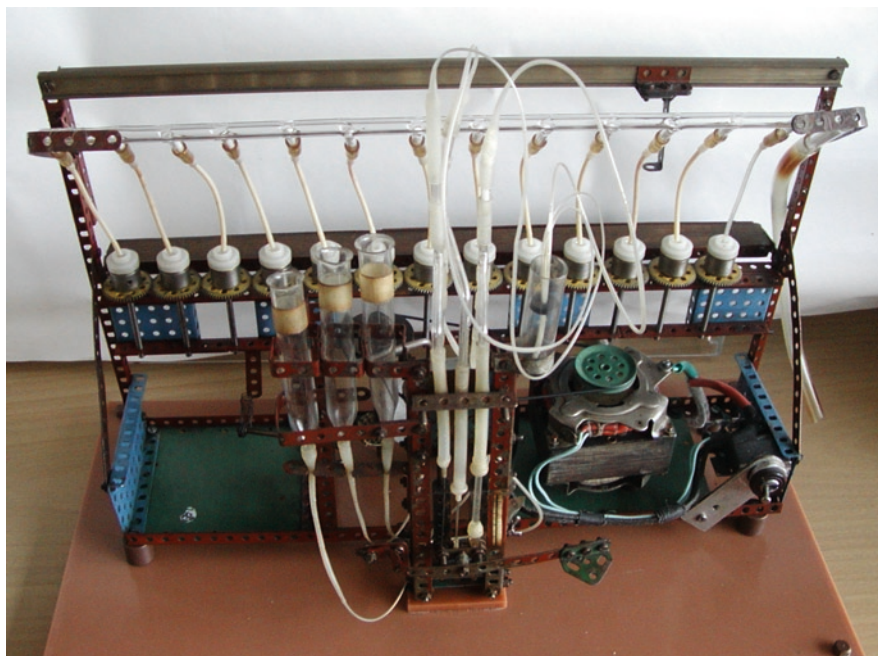
Introduction

In the literature on “hydrogels used in medicine,” one often sees the reference to Wichterle and Lim [1]. This fundamental work followed after the first Wichterle’s patent on hydrophilic methacrylates for biomedical applications. A key area, to the use of synthetic hydrogels for bioapplications, is for ophthalmology, especially contact lenses [1, 2]. Professor Wichterle made the first soft lenses using home-made equipment that he constructed from a popular Mechano metal toy set (Figs. 1–3).

Subsequently, he patented the spin-casting technology for processing polymerizing hydrogels into specific shapes. Several years later, he invented the lathe-cutting process for making lenses using dry hydrogels cylindrical rods. This was the beginning of the incredible hydrogels contact lens industry [3, 4]. While reviewing the literature on contact lenses, you find Wichterle’s invention of poly(2-hydroxyethyl methacrylate) [PHEMA or poly(HEMA)] lenses referenced many times [5].

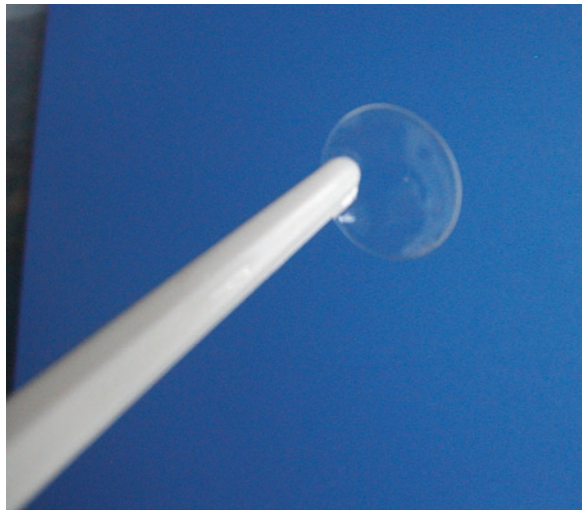
The first concept to alter the corneal power using an optical system that is placed directly on the cornea was described by Leonardo da Vinci in 1508 [6]; this consisted of immersing the eye in a bowl of water. The next generation of constructs was described by René Descartes (1636) and Thomas Young (1801); they used glass lens tubes filled with a fluid which were placed on the cornea [7] and the orbital rim [8]. In 1845, John Herschel proposed glass contact lens analogous to the modern lenses with the space between cornea and the lens sandwiched with animal gels. The first real contact lenses were actually prepared from glass using several different techniques to form scleral lenses; these were reported by Adolf Fick (Switzerland), Eugene Kalt (France), and August Müller (Germany) in the late 1880s [9, 10].

J. Michalek, R. Hobzova, M. Pradny, and M. Duskova • Institute of Macromolecular Chemistry, Academy of Sciences of the Czech Republic, Heyrovsky sq. 2 162 06, Prague 6, Czech Republic
e-mail: jiri@imc.cas.cz

Fig. 1. Prof. Otto Wichterle.**Fig. 2.** Contact lens machine – toy construction set Mechano.

The next significant advancement in contact lens development was the plastic scleral lenses (1936) made from poly(methyl methacrylate) (PMMA) using a lathe-cutting technique [11]. In 1948, Kevin Tuohy patented the PMMA corneal lens [12]. Since then, synthetic polymers are the only materials used for contact lens manufacture. At the end of 1960, poly(2-hydroxyethyl methacrylate) (PHEMA) lenses were developed by Professor Otto

Fig. 3. Contact lens.



Wichterle; this invention represents the most important step in contact lens development and the start of soft lenses era.

Contact lenses can be classified in a number of ways; however, two main categories, hard and soft lenses, based on the material used for their manufacture emerged. The soft category can be further divided into hydrophobic and hydrophilic subcategories [13].

The silicone elastomers were tested in 1965 for contact lens manufacture based on their high gas permeability (oxygen, carbon dioxide); however, poor clinical results were obtained. The hydrophobic nature of silicone elastomers gave poor wetting properties, and the development of surface deposits was observed in clinical tests. In the late 1970s, more trials were undertaken and several more compatibility complications appeared. The combination of high elasticity and resistance to water caused the lens to bind to the eye that lead to severe problems with the removal of the silicone lenses. Currently, these silicone lenses are used only for some special purposes (pediatric and aphakic fittings) in a limited extent [14].

In 1972, the hydrophilic soft hydrogels contact lenses were introduced to world market (12 years after their invention) by the Bausch & Lomb Company [4, 15]. Two years later, in 1974, the rigid gas-permeable lenses (RGP) were patented by Gaylord [16]. Since then, the development of contact lens materials took three directions: (1) hydrogels with high water content, (2) rigid gas-permeable lenses with enhanced oxygen permeability, and (3) surface modification of silicone elastomer lenses.

The next important achievements were the introduction of the first disposable lenses in 1988 and daily disposable lenses in 1994, which led to a reduction of possible complications as a result of contact lens wearing [17]. The last major historic advancement was made in 1999, when silicone-hydrogels materials were introduced on the market by Bausch & Lomb and Ciba Vision [18]. The importance of this enterprise may be compared with the Wichterle invention.

Although both types of soft contact lenses, conventional hydrogels and silicone hydrogels, are fitted on the client's eyes, the number of silicone-hydrogels lenses being worn is now rapidly increasing. Ten years after their introduction, they represent 50% of the new applications: the era of silicone-hydrogels contact lenses has begun.

Contact Lens Terminology

The contact lens is a small optical device placed directly on the cornea. It has two optical faces: inside (back) and outside (front). The shape of lenses can be described by various curves and their systems. Shown in Fig. 4 are two contact lenses: one with plus diopters and one with minus diopters and the basic shape parameters [19].

When contact lenses are placed directly on the cornea, they form a barrier to the natural physiological metabolism of the cornea, which is dependent on the transport of atmospheric oxygen to the eye surface. Because of this fact, the main development emphasis has been on the prevention of the hypoxic stress to cornea when covered by a contact lens. This meant using maximal oxygen permeability possible by the lens material. The rigid gas-permeable lenses have higher oxygen permeability than the hydrogels contact lenses, including those with high water content. However, hydrogels contact lenses, due to their many other benefits, developed a dominant position on the world market. They have good wettability of the contact surface area and thus cause minimal tissue irritation and low mechanical stress to the cornea, which are very important factors. Although the silicone elastomers exhibited high values of permeability for gases (O_2 , CO_2), they had several major drawbacks, such as their softness, hydrophobicity, and discouraging clinical results. Consequently, they never reached industrial scale production.

Mechanical stress to the cornea produces the same problems as the hypoxic stress, such as mitosis of the epithelial cells, elevated activity in proteases and glycosidases, corneal sensitivity, and changes in corneal hydration and transparency [20–24]. To reduce a contact lens’s influence on corneal metabolism, it is necessary to minimize the hypoxic and mechanical stress on the cornea caused by the lens. This can be achieved by meticulous choice of the contact material and adjustment of the lens shape.

Basically, the hydrogels contact lens materials successfully fulfill most of the requirements for physiological tolerance during wearing. They have only one major limitation, oxygen permeability. Since the solubility of oxygen in water is good, hypothetically, maximal oxygen permeability can be achieved by lenses prepared just from water. That is not only impossible, but, at the same time, the oxygen permeability achieved is still not sufficient for extended contact lens wear [25, 26].

Comfortable hydrogels contact lens demands a very subtle balance of material parameters, such as water content, mechanical properties (“modulus,” tensile strength, and elongation at break), oxygen permeability, surface wettability, optical properties, especially refractive index, and hydrolytic stability. In addition, the material has to be nontoxic and must withstand sterilization and disinfectants. Moreover, the lens material must have satisfactory biological tolerance for living tissue.

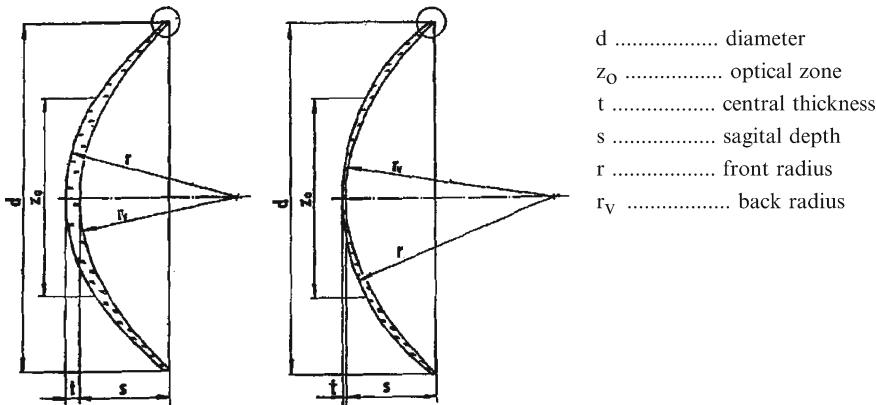


Fig. 4. Scheme of contact lenses for +diopters (left) and -diopters (right).

Materials Used for Hydrogels Contact Lenses

HEMA

The basic material for “standard” hydrogels contact lenses (38 wt% water, at swelling equilibrium) is the polymer from 2-hydroxyethyl methacrylate, better known as HEMA (*I*). Like all hydrophilic contact lenses, PHEMA lenses are formed by slightly crosslinking the polymer network using <1 mol% crosslinker in the monomer mixture. Typical ethylene dimethacrylate (EDMA) (*II*) is the crosslinker for PHEMA, which is widely used for methacrylate polymer networks. However, due to its hydrophobicity it can form hydrophobic associations during polymerization that cause heterogeneity in the network, and sometimes even these domains are visible. Therefore, in some cases, EDMA is replaced by triethylenglycol dimethacrylate (TEGDMA) (*III*), which is more polar and more hydrophilic (Table 1).

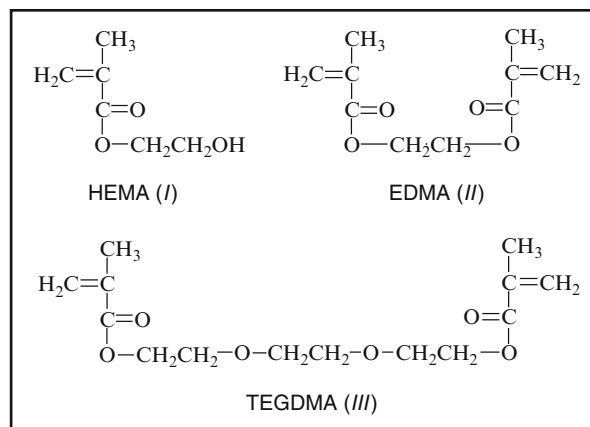
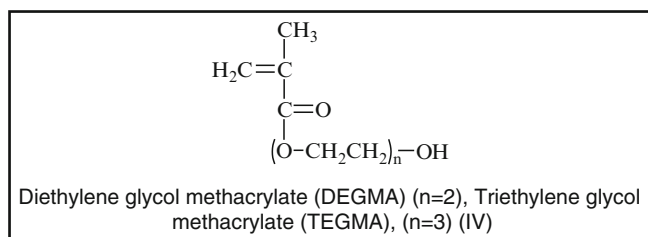


Table 1. Examples of PHEMA lenses [27–29]

Product name	Company	Material
Medalist 38	Bausch & Lomb	Polymacon
Optima 38	Bausch & Lomb	Polymacon
Frequency 38	CooperVision	Polymacon
Biomedics 38	Ocular Sciences	Polymacon

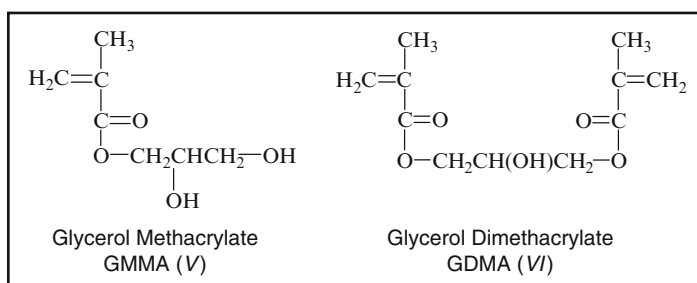
Other Glycol Methacrylates

To prepare nonionic hydrogels with higher hydrophilicity, the common HEMA monomer can be copolymerized with another monomer of high hydrophilicity to provide a polymer network with high water content, for example, the copolymerization of HEMA with diethylene glycol methacrylate (DEGMA) (*IV*, $n=2$) [30, 31] or triethylene glycol methacrylate (TEGMA) (*IV*, $n=3$). These copolymers were studied in the eighties by Wichterle and his coworkers at the Institute of Macromolecular Chemistry of the Czechoslovak Academy of Science, in Prague and tested industrially by the Okula Company in the Czech Republic [4]. Several users claimed that the HEMA-DEGMA lenses (55 wt% water) were the best lenses. However, their low reproducibility and rather poor mechanical properties stopped their use.



Dihydroxy Methacrylates

Increased water content in the swollen state of hydrogels was achieved by using dihydroxy methacrylates, such as glycerol methacrylate (GMMA) (V) as the comonomer. Typically, the crosslinker glycerol dimethacrylate (GDMA) (VI) is usually used. The contact lenses prepared from these materials exhibit water contents of 57–60 wt% and oxygen permeability $Dk=20$ Barrer (Table 2).



Methacrylic Acid

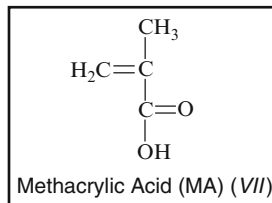
The most frequent comonomer used to increase the equilibrium water content in hydrogels is methacrylic acid (MA) (VII) and is found in many types of commercial contact lenses. Only a small amount of MA (1–3 wt%) is added to the monomer mixture to provide the highly swollen gels (55–85 wt% water). The activation of the polymer surfaces through carboxylic groups is a technique widely used for many polymer modifications. For example, to achieve an enhanced swelling effect, it is necessary to dissociate the MA carboxylic acid groups by converting them to the ionic sodium salt. The disadvantage of ionizing MA is the introduction of negative charges to the polymer matrix. In the swollen state, the material becomes pH sensitive as the carboxylic groups represent active sites on the polymer chains' protons, and the potential for absorption of proteins is supported by electrostatic forces (Table 3).

Table 2. Examples of glycerol methacrylate lenses [27–29]

Product name	Company	Material
Actisoft 60	Biocompatibles Hydron	Hioxifilcon-A
Laguna	Wilens	Hioxifilcon-A

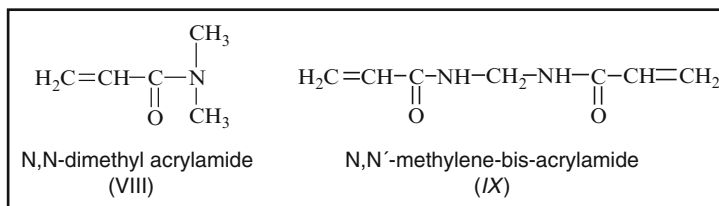
Table 3. Examples of lenses containing MA [27–29]

Product name	Company	Material
Frequency 55	CooperVision	Methafilcon A
Hydrasoft	CooperVision	Methafilcon A
D55	Wilens	Methafilcon A
Accusoft	Ophthalmos	Droxifilcon A
Acuvue	Vistakon J&J	Etafilcon A
Surevue	Vistakon J&J	Etafilcon A
Focus Monthly	CIBAVision	Vifilcon A
Softcon	CIBAVision	Vifilcon A
Ultraflex 55	Ocular Sciences	Ocufilecon D



Acrylamides

Acrylamide-based gels are an important class of hydrogels for their unique swelling properties. Generally, polyacrylamides (PAAm), due to their solubility in water, are used particularly as thickening, suspending, flocculating, and coagulating agents in wastewater treatment and papermaking. When crosslinked, PAAm forms highly swollen soft gels that are used for a number of biomedical purposes (i.e. superabsorbents). One of the advantages of PAAm is that the swelling is independent of the pH, compared to those containing methacrylic acid salt. For manufacturing PAAm contact lens, the monomer *N,N*-dimethyl acrylamide (VIII) is crosslinked with *N,N'*-methylene-bis-acrylamide (IX) (Table 4).

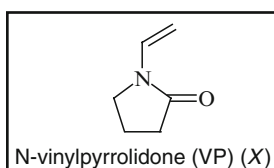
**Table 4.** Examples of PAAm lenses [27–29]

Product name	Company	Material
Gentle Touch	Wesley Jessen ^a	Netrafilcon A
Soft Mate II	Wesley Jessen	Bufilecon A
Hydrocurve II/3	Wesley Jessen	Bufilecon A

^aWesley Jessen company merged with 2000 with CIBA Vision

1-Vinyl-2-Pyrrolidone

A typical monomer for nonionic hydrogels with high water content is *N*-vinylpyrrolidone (1-vinyl-2-pyrrolidone, VP) (X). VP is used in a wide variety of biomedicine applications, pharmacy, and cosmetics. As a homopolymer, PVP exhibits poor mechanical properties. To improve the mechanical performance of VP-based hydrogels, while maintaining desirable optical transparency, VP was copolymerized with another monomer, such as HEMA or an alkyl methacrylate. The VP with methyl methacrylate copolymer is widely known under the commercial name of lidofilcon (Table 5).



FDA Contact Classification

The US Food and Drug Administration (FDA) classifies contact lens materials based on four specific norms: (a) those with water contents less than 50 wt%, (b) those with water contents greater than 50 wt%, (c) those that have nonionic moieties in the polymer chains or with an ionic component <0.2%, and (d) those that have charged moieties in the polymer chains with an ionic component >0.2%. These combinations form the four groups listed in Table 6.

Group I represents the types of PHEMA lenses and lenses based on HEMA copolymers that do not exceed group limits with respect to water content (0–50 wt%). Some of these are terpolymers of 2-hydroxyethyl methacrylate with 2-ethoxyethyl methacrylate (EOEMA) and less than 0.2% of methacrylic acid (HEMA-*co*-EOEMA-*co*-MA) or with *N*-vinylpyrrolidone and methyl methacrylate (HEMA-*co*-VP-*co*-MMA), or copolymer with partially hydrolyzed

Table 5. Several VP-based contact lenses [27–29]

Product name	Company	Material
Omniflex	Biocompatibles Hydron	Lidofilcon A
Procontact lensear	Biocompatibles Hydron	Omafilcon A
Medalist 66	Bausch & Lomb	Alphafilcon A
Softlens 66	Bausch & Lomb	Alphafilcon A
Permafex	Wesley Jessen ^a	Surfilcon A
Precision UV	Wesley Jessen	Vasurfilcon A

^aWesley Jessen company merged with 2000 with CIBA Vision

Table 6. FDA classification of contact lenses

FDA classification of contact lenses	Water content	
	0–50 wt%	50–99 wt%
Nonionic	Group I	Group II
Ionic	Group III	Group IV

polyvinyl acetate (HEMA-*co*-VAc-*co*-VA) or copolymer of glycidyl methacrylate with methyl methacrylate (GMA-*co*-MMA). The materials included in this group hold relatively low water content; they have low oxygen permeability and they are susceptible to protein deposits.

Group II is predominantly copolymers of 1-vinyl-2-pyrrolidone (VP) with various methacrylates and copolymers of acrylamides, poly(vinyl alcohol) (PVA), or poly(glycerol methacrylate) (GlyMA). This group of materials exhibits water content in the range of 60–74 wt%, with relatively high oxygen permeability (25–35 Barrer) and the susceptibility to lipid deposits.

Group III represents copolymers of HEMA with some alkyl methacrylate and a small amount of methacrylic acid (MA) as the sodium salt. These materials have a low water content, low oxygen permeability (less than 20 Barrer), and protein deposits are firmly bonded to the lens surface by electrostatic forces due to the presence of the negative charges on the ionized MA moieties.

Group IV includes predominantly copolymers of HEMA with a significant amount of MA in the sodium form, and in several cases terpolymers of HEMA, MA, and acrylamide or PVP or EOEMA are included. These materials have 55–58 wt% water contents, and the corresponding oxygen permeability is 20–23 Barrer. Similar to those in Group III, other benefits, such as water content, oxygen permeability, and the mechanical properties, make these lenses comfortable and widely used, especially as disposable lenses (interval replacement of 14–30 days), so that protein deposits are not a serious problem [28, 29].

Selected Types of Hydrogels Contact Lens Materials

One of the fundamental hydrogels materials for contact lenses is hydrogels made from 2-hydroxyethyl methacrylate or 1-vinyl-2-pyrrolidone, and both these hydrogels, typically, are manufactured as copolymers with methyl methacrylate (MMA), butyl methacrylate (BuMA), cyclohexyl methacrylate (CMA), 2-ethoxyethyl methacrylate (EOEMA), *N,N*-dimethyl acrylamide (DMAAm), diacetone acrylamide (DAAm), and methacrylic acid. Other types of interesting materials involved monomers, such as poly(vinyl alcohol), glycerol methacrylate, and glycidyl methacrylate. An overview of selected commercial materials used for contact lenses along with specifications of their principal compositions, water content, and oxygen permeability (Dk) parameters is listed in Table 7 [32].

Table 7. Selected commercial soft hydrophilic materials for contact lenses

Material	Principal composition	Water content (wt%)	Dk (Barrer)	FDA classification
Polymacon	HEMA	38	8	I
Droxifilcon A	HEMA, PVP, MA	47	15	III
Vifilcon A	HEMA, PVP, MA	55	20	IV
Methafilcon A	HEMA, MA	55	23	IV
Hioxifilcon A	GlyMA	57	20	II
Etafilcon A	HEMA, MA	58	28	IV
Tefilcon	VP, MMA	60	28	II
Alfilcon A	HEMA, VP	66	32	II
Nelfilcon A	PVA	69	26	II
Lidofilcon	VP, MMA	70	32	II
Vasurfilcon A	VP, MMA	74	38	II

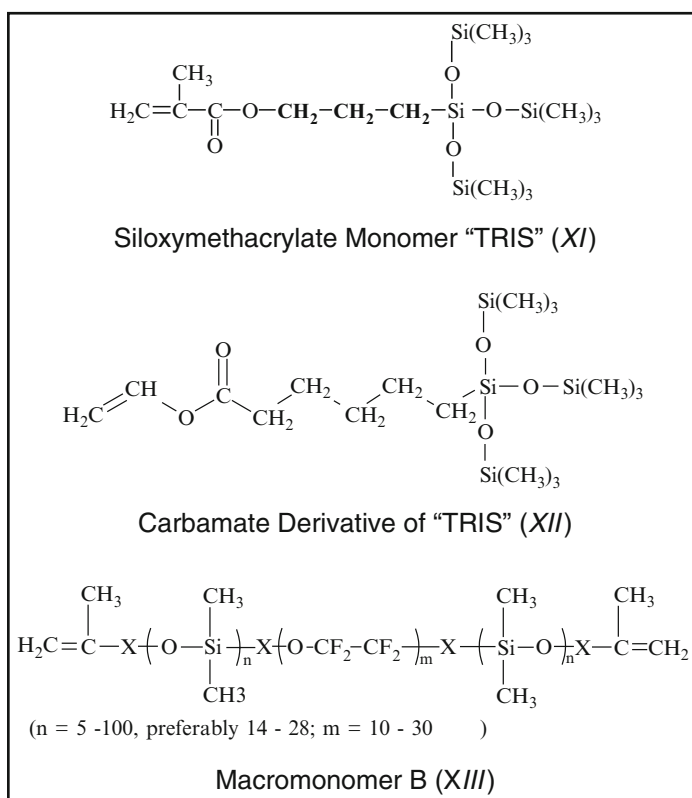
Silicone Hydrogels

Silicone hydrogels represent an independent group of contact lens materials, but a detailed discussion of these materials is beyond the scope of this article. However, they evolved from basic hydrogels, and moreover, they fulfill many of the requirements for lens material, such as significant swelling combined with high oxygen permeability. These were achieved by a unique co-continuous structure that interconnected hydrophilic chains with hydrophobic silicones in a homogenous optically and mechanically suitable composite.

The first silicone-hydrogels contact lenses were PureVision® (balafilcon A) introduced by Bausch & Lomb, and Focus Night & Day® (lotrafilcon A) introduced by CIBA Vision in 1999. Salient parameters of these first silicone-hydrogels lenses are shown in Table 8 [33].

Table 8. Salient parameters for silicone-hydrogel lenses PureVision® and Focus Night & Day®

Properties	Bausch & Lomb PureVision® Balafilcon A	CIBA Vision Focus Night & Day® Lotrafilcon A
Equilibrium water content	35 wt%	24 wt%
Oxygen permeability (Dk)	99×10^{-11} Barrer	140×10^{-11} Barrer
Oxygen transmissibility (Dk/t)(-3,0 D)	110×10^{-9} Barrer	175×10^{-9} Barrer
Young's modulus	1.1 MPa	1.2 MPa



High oxygen permeability is achieved with the siloxymethacrylate monomer commonly referred to as “TRIS” (XI) from the RGP materials. The methylene groups in the structure of TRIS represent the sites for hydrophilic modification. Material balafilcon A (PureVision® contact lenses) is based on polymer of vinyl carbamate derivative of TRIS (XII). Lotrafilcon A (Focus Night & Day®) is a copolymer of TRIS monomer (XI) with *N,N*-dimethyl acrylamide (VIII) and macromonomer B (XIII) [34].

Current Trends in Silicone-Hydrogels Lenses

The developments in silicone-hydrogels lenses have undergone considerable progress over the past 10 years. Several new types of contact lenses were made from these materials and introduced by CIBA Vision, Johnson & Johnson, and Cooper Vision. They are referred as silicone-hydrogels lenses of the second and third generation.

Research in silicone hydrogels materials has continued in order to increase the equilibrium water content; this led to a requisite reduction in the Young’s modulus, but also reduced permeability toward oxygen. High gas permeability of silicone materials is dependent on the nature of the matrix, the chain flexibility facilitating the diffusion of oxygen, and chemical structure of the chain that allows oxygen permeability. The gas transport mechanism in these materials is significantly different from conventional hydrogels, in which the transport of oxygen is ensured only by solubility of oxygen in the presence of water (i.e. the higher the water content, the higher the oxygen permeability) [35].

The current research trend, both for conventional and silicone-hydrogels, appears to be to reduce the drying by the lenses during normal wear. For this purpose, linear or branched hydrophilic polymer chains are being incorporated into the polymer structure in the form of an interpenetrated network. This means that the “wetting chains” are fixed only by physical bonds without any covalent attachments to the patterned hydrogels network.

Summary

The concept of attaching a lens directly to the cornea of a human eye emerged several centuries ago. However, it was not until the 1960s that the soft water-swelling synthetic macromolecular hydrogels were developed and processed into the specifically defined shapes and utility. These unique hydrogels materials became commercially successful as soft contact lenses. Several classes of these macromolecular systems proved to be particularly suitable for the contact lenses applications: the major ones are (a) the glycol methacrylates, above all, poly(2-hydroxyethyl methacrylate) (HEMA) and its copolymers with methacrylic acid, (b) the classic based on 1-vinyl-2-pyrrolidone (VP) and its copolymers with HEMA and alkyl methacrylates. In addition to these monomers and their copolymers is poly(vinyl alcohol) and its derivatives for contact lens systems. These polymeric systems are expected not only to improve the water content of the contact lenses but the permeability to oxygen, which are crucial properties that are controllable through the molecular design. Currently, the high water content hydrogels are being challenged by the silicone-based hydrogels.

References

1. Wichterle O, Lím D (1960) Hydrophilic gels for biological use. *Nature* 185:117
2. Wichterle O, Lím D (1961) Method for producing shaped articonact lenses from three-dimensional hydrophilic polymers. US Patent 2,976,576
3. Wichterle O, Lím D (1965) Cross-linked hydrophilic polymers and articonact lenses made therefrom. US Patent 3,220,960
4. Wichterle O (1992) The task: "Contact lenses". In: Dalrymple K (ed) *Recollection*. Impreso, Prague, pp 128–141
5. Efron N (2002) Historical perspective. In: *Contact lens practice*. Oxford: Butterworth-Heinemann, p. 9
6. Heitz RF, Enoch JM (1987) Leonardo da Vinci: an assessment on his discontact lensesosures on image formation in the eye. In: Fiorentini A, Guyton DL, Siegel IM (eds) *Advances in diagnostic visual optics*. Springer, New York, pp 19–26
7. Enoch JM (1956) Descartes' contact lens. *Am J Optom Arch Am Acad Optom* 33:77–85
8. Young T (1801) On the mechanism of the eye. *Philos Trans R Soc Lond Biol Sci* 91:23–88
9. Black CJ (1973) Contact lenses – an overview. In: *Symposium on contact lenses, Transactions of the New Orleans Academy of Ophthalmology*, C.V. Mosby, St. Louis, MO
10. Gould HL (1973) Therapeutic effect of flush-fitting scontact lenseseseral lenses and hydrogel bandage lenses. In: *Symposium on contact lenses, Transactions of the New Orleans Academy of Ophthalmology*, C.V. Mosby, St. Louis, MO
11. Feinbloom W (1936) A plastic contact lens. *Trans Am Acad Optom* 10:37–44
12. Braff SM (1983) The Max Schapero lecture: contact lens horizons. *Am J Optom Physiol Opt* 60:851–858
13. Refojo MF (1977) Contact lenses. In: Mark HF, Bikales NM (eds) *Encyclopedia of polymer science and technology*. Interscience, New York, pp 195–215
14. Brennan N, Coles C (2002) Continuous wear. In: Efron N (ed) *Contact lens practice*. Butterworth-Heinemann, Oxford, p 276
15. Wichterle O (1978) The beginning of the soft lens. In: Ruben M (ed) *Soft contact lenses: clinical and applied technology*. Baillière Tindall, London, pp 3–5
16. Gaylord NG (1974) Oxygen permeable contact lens composition methods and articonact lenses of manufacture (to Polycon Lab Inc.). US Patent 3,808,178
17. Nilsson S (1997) Ten years of disposable lenses – a review of benefits and risks. *Cont Lens Anterior Eye* 20:119–128
18. Tighe B, Brennan N, Coles C (1999) Silicone hydrogels – What are they and how should they be used in everyday practice? *Optician* 218(5726):31–32
19. Michálek J (2000) Materials for contact lenses for extended wearing (in Czech). In: *Proceedings of lectures, Czech society for contactologists, Prague*, pp 24–38
20. Čejková J (1996) Physiology of cornea and contact lenses (in Czech). In: *Proceedings of lectures, Czech society for contactologists, Prague*, pp 6–10
21. Čejková J, Lojda Z, Brůnová B, Vacík J, Michálek J (1988) Disturbances in the rabbit cornea after short-term and long-term wear of hydrogel contact lenses. Usefulness of histochemical methods. *Histochemistry* 89:91–97
22. Holden BA, Mertz GW (1984) Critical oxygen levels to avoid corneal edema for daily and extended wear contact lenses. *Invest Ophthalmol Vis Sci* 25:1161–1167
23. Tsubota K, Laing R (1992) Metabolic changes in the corneal epithelium resulting from hard contact lens wear. *Cornea* 11:121–126
24. Lin MC, Graham AD, Fusaro RE, Polse KA (2002) Impact of rigid gas-permeable contact lens extended wear on corneal epithelial barrier function. *Invest Ophthalmol Vis Sci* 43:1019–1024
25. Morgan PB, Efron N, Helland M et al (2001) Trends in international contact lens prescribing 2000. *Optician* 221(5799):26–32
26. Wilson G (2000) The epithelium in extended wear. In: Sweeney D (ed) *Silicone hydrogels: the rebirth of continuous wear contact lenses*. Butterworth-Heinemann, Oxford, pp 22–40
27. Efron N et al (1993) *The international contact lens year book*. WB Saunders, Philadelphia, PA
28. Tighe B (2002) Soft lens materials. In: Efron N (ed) *Contact lens practice*. Butterworth-Heinemann, Oxford, pp 75–76
29. FDA official websites: www.fda.gov

30. Čejková J, Lojda Z, Brůnová B, Vacík J, Michálek J (1989) A comparison of the compatibility of hydrophilic contact lenses from HEMA (37 H₂O) and HEMA-DEGMA (55, 65 H₂O) on the rabbit eye. I. Changes in the transparency of the cornea due to a disturbance in its hydration (in Czech). *Cesk Oftalmol* 6:401–407
31. Čejková J, Lojda Z, Brůnová B, Vacík J, Michálek J (1989) A comparison of the compatibility of hydrophilic contact lenses from HEMA (37 H₂O) and HEMA-DEGMA (55, 65 H₂O) on the rabbit eye. II. Changes in the transparency of the cornea due to deep degenerative processes (in Czech). *Cesk Oftalmol* 6:408–411
32. Stárková L, Michálek J (2006) Nowadays contact lenses on the Czech market (in Czech). XIII. Congress of the Czech contact lens society, Nymburk, Nov 2006
33. Tighe B (2000) Silicone hydrogel materials – how do they work? In: Sweeney D (ed) *Silicone hydrogels: the rebirth of continuous wear contact lenses*. Butterworth-Heinemann, Oxford, pp 1–21
34. Tighe B (2002) Soft lens materials. In: Efron N (ed) *Contact lens practice*. Butterworth-Heinemann, Oxford, pp 82–83
35. Koros WJ, Fleming GK (1993) Membrane-based gas separation. *J Memb Sci* 83:1–80

Part IV

Hydrogels With Unique Properties

Electroconductive Hydrogels

Ann M. Wilson, Gusphyl Justin, and Anthony Guiseppi-Elie

Abstract Methods for the synthesis of electroconductive hydrogels (ECH), as polymer blends and as polymer conetworks via chemical oxidation, electrochemical, or a combination of chemical oxidation followed by electrochemical synthesis techniques, are described. Specific examples are introduced to illustrate the preparation of ECHs synthesized from poly(HEMA)-based hydrogels and polyaniline or from poly(HEMA)-based hydrogels and polypyrrole. The key applications of ECHs, as biorecognition membranes for implantable biosensors, as electrostimulated drug eluting devices, and as the low interfacial impedance layer on neuronal prostheses, provide great new horizons for biodetection devices.

Introduction

Electroconductive hydrogels (ECH) are polymeric blends or conetworks that combine inherently conductive electroactive polymers (CEPs) with hydrated hydrogels. First described by Guiseppi-Elie [1–3] in 1995 and later by Wallace et al. [4] and Guiseppi-Elie et al. [5], these novel polymeric materials combine the unique and enduring properties of their constituents. For the hydrogels component this implies a high degree of hydration, swellability, in vitro and in vivo biocompatibility, and high diffusivity of small molecules. For the inherently CEP component this implies high electrical conductivity, ON–OFF electrical and optical switching and electrochemical redox properties. Both polymer constituents are stimuli-responsive materials, and each on its own is a viable candidate for sensory application. They share in common the potential for molecular engineering through copolymerization, crosslinking, and grafting to tune the final hybrid material's properties to targeted biologically relevant outcomes. They also share the fact that their syntheses are difficult to control and that the methods and conditions of synthesis significantly influence the final material properties via subtle contributions of multilength scale factors, such as trace impurities, conformation, nanostructure, and gross morphology. Since the early work of Guiseppi-Elie and Wallace, ECH have been the subject of expanding research [6].

ECHs belong to the general class of multifunctional smart materials conceptually illustrated in Fig. 1. As an emergent class, these materials seek to creatively combine the inherent properties of constituent materials to give rise to technologically relevant properties for devices and systems. For example, ECHs have been synthesized, characterized, and fashioned as a biorecognition membrane layer in various biosensors. In one instance, an ECH that was synthesized from a poly(HEMA)-based hydrogels and poly(aniline) was fashioned into a biosensor by the incorporation of recombinant cytochrome P450-2D6 [7]. This device was shown to be responsive to fluoxetine, the active ingredient in Prozac®. The poly(HEMA)-based poly(aniline) electroconductive hydrogels was subsequently fully characterized for its

A.M. Wilson and A. Guiseppi-Elie • ABTECH Scientific, Inc., Biotechnology Research Park,
800 East Leigh Street, Richmond, VA 23219, USA
e-mail: guiseppi@clemson.edu

G. Justin and A. Guiseppi-Elie • Center for Bioelectronics, Biosensors and Biochips (C3B),
Clemson University Advanced Materials Center, 100 Technology Drive, Anderson, SC 29625, USA



Fig. 1. Illustrated is the general concept of multifunctional smart materials that combine the properties of constituent materials to yield technologically relevant devices and systems of increasing complexity.

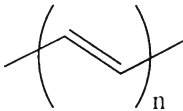
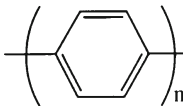
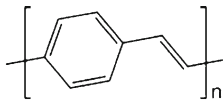
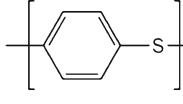
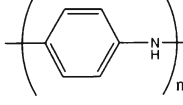
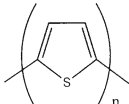
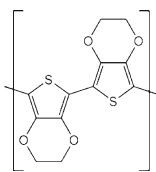
electrical, switching, and optical properties with demonstrated faster switching than its purely CEP counterpart [8]. In another instance, an ECH fashioned from poly(hydroxyethyl methacrylate) [poly(HEMA)] and polypyrrole (PPy) was investigated for its potential application to clinically important biomedical diagnostic biosensors by the incorporation of enzymes [9–12]. Among the various devices for which ECH polymers were investigated were neural prosthetic and recording devices (NPDs and NRDs) [13–15], electrostimulated drug release devices (ESRDs) [16–20], and implantable electrochemical biosensors [21–23]. Neuronal prosthetic devices and implantable biosensors benefit from a tissue-to-electrode interface that is compliant, conformal, with low interfacial impedance, and electrically diffuse [24–26]. The ESRDs benefit from high loading capacity and low voltage actuation. In all cases, these polymeric materials, which are both electronically and ionically conductive, provide a non-cytotoxic interface between the device and native living tissue or cell culture medium [27].

The background on hydrogels and inherently conductive polymers as well as the materials rationale for the cojoining of hydrogels with CEPs will be addressed. Details are provided on the methods and approaches for the synthesis of ECHs. The focuses will be on three applications of these novel materials; that of implantable electrochemical biosensors, ESRDs, and neuronal prosthetics.

Inherently Conductive Electroactive Polymers [28]

CEPs are a family of highly conjugated polymers possessing spatially extended π -bonding that confers unique electrical, electrochemical, and optical properties. These properties have been found useful in a number of current and emerging industrial applications. Within this family are polymers, such as polypyrrole (PPy), polyaniline (PAn), polythiophene (PTh), poly(phenylene) vinylene (PPv), and their copolymers and derivatives. Listed in Table 1 are

Table 1. Range of typical electrical conductivities of conductive electroactive polymers and their elementary repeating unit structures

Conductive electroactive polymers (CEP)	Elementary Repeating Unit Structure	Conductivity (S cm ⁻¹)
Polyacetylene (PA)		1,000
Poly(paraphenylene) (PP)		100–500
Poly(paraphenylene vinylene) (PPV)		3
Poly(paraphenylene sulfide) (PPS)		1–100
Polyaniline (PAn)		1–100
Polypyrrole (PPy)		40–100
Polythiophene (PTh)		10–100
Poly(3,4-ethylenedioxythiophene) (PEDOT)		10–100

several CEPs with their known conductivities. These polymers find applications as electrical conductors, nonlinear optical devices, polymeric light emitting diodes (LEDs), electrochromic windows, photoresists, antistatic coatings, chemical and biological sensors, electrodes of batteries, electromagnetic shielding materials, sensory elements in electronic noses, solar cells, microwave absorbing materials, optical modulators, valves in MEMS devices [29–32], and in nanoswitches.

CEPs display controllable switching of their electrical and optical properties. Moreover, because these properties may also be altered by changes in ambient variables, such as temperature, humidity, gas/vapor composition, medium ionic strength, pH, and the like, these materials are also regarded as stimuli responsive. The incorporation of CEPs as elements of

the structure of biosensors, molecular recognition devices that employ biomolecules (peptide sequences, enzymes, antibodies, oligonucleotides, aptamers), promises to improve the response time of these devices and their compatibility with advanced microfabrication and miniaturization technologies for incorporation into MEMS devices [33].

CEPs have been incorporated into biosensors for the detection of several tens of chemical species of biological or medical importance (enzyme substrates, antigens, ssDNA fragments, neurotransmitters, drug metabolites). Biosensors based on CEPs may operate as electrochemical, optical, or gravimetric detectors for measurements in discrete, low-volume samples and continuous flow systems for which biosensors with fast response times, high sensitivities, and detection limits in the μM range (for detection of enzyme substrates) and even several orders of magnitude lower (for detection of DNA) are required. For *in vivo* applications, biosensors have to meet additional biocompatibility specifications [34].

The chemistry of CEPs and the relative ease with which these materials may be synthesized and fashioned into functional devices make them compatible with many of the chemical processes found in microelectronics manufacturing. Polypyrroles can be synthesized under mildly oxidative conditions from aqueous media. One of the syntheses involves an oxidative wet chemical method using mild oxidants such as FeCl_3 , peroxy sulfate, or benzoyl peroxide. Hydrogen peroxide and potassium permanganate, while capable of initiating polymerization reactions, can also oxidatively degrade the resulting polymer, but with appropriate controls, these can be used to specifically introduce reactive functional groups. In another method, polypyrroles may be synthesized electrochemically from neutral to acidic media possessing an appropriate supporting electrolyte. Potentiostatic (chronoamperometry) oxidation is initiated at 0.65 V vs. Ag/AgCl, and some influence is exercised over the kinetics by the application of potentials up to 0.8 V vs. Ag/AgCl. True kinetic control is, however, achieved galvanostatically (chronopotentiometry) by the application of a constant current (typically 1 mA/cm²). Likewise, polyaniline may be synthesized under similar conditions, although formation of the highly conductive form requires the presence of acid ($\text{pH} \leq 4$). Electrochemical synthesis of polyaniline may also be initiated at 0.65 V vs. Ag/AgCl. Simple polythiophenes require a more extreme oxidation potential, and these monomers are generally not soluble in water. However, the attachment of simple functional groups, e.g., an alkyl sulfonate, to the monomer overcomes this limitation. The consequence of initiation and propagation of polymerization under oxidizing conditions is the simultaneous incorporation of dopant counter anions drawn from the environment into the CEP leading to formation of its conductive form.

The mild conditions used for polymerization are ideal for the simultaneous synthesis of the CEP and incorporation of biological molecules, such as enzymes, antibodies, nucleic acids, or even whole living cells. These conditions also support the incorporation of surfactant molecules and other polymers that may become entangled during the electrophoretic polymer deposition step. Such codeposition is facilitated by a net or partial negative charge on the dopant molecule. The organic, polymeric nature of the CEP, as opposed to the periodic nature of semiconductors and metals, produces favorable molecular level interactions between the host CEP and biological molecules. These interactions may be further enhanced by the inclusion of specific functionalities or moieties on the CEP backbone. Amongst these are reactive functional groups such as carboxylic acids and alcohols, which allow direct covalent bond formation between the CEP and biomolecule, pendant anion groups such as sulfonates that allow "internal doping," or peptide sequences that facilitate receptor-receptant interactions of whole cells. Such reactive functional groups may be introduced via copolymerization, achieved through the inclusion of functionalized monomers into the reaction mixtures. For example, pyrrole may be copolymerized with 4-(3-pyrrolyl)butyric

acid to introduce pendant acid functionality that does not adversely influence main chain conjugation and conductivity. An alternative approach is the postpolymerization modification via electrochemical overoxidation to convert PPy to OPPy, which becomes enriched in hydroxyl groups [35, 36].

The electronic, optical, and redox properties of CEPs may be exploited in a form of information transfer wherein the chemical potential energy of an analyte is converted into a proportionate electronic, optical, or electrochemical signal. In a sense, these polymers are transducer-active as they allow information about the concentration of an analyte to be conveyed electronically (impedance, conductance, capacitance, switching), optically (reflectivity, absorbance, shifts), or electrochemically (amperometrically, potentiometrically) via biomolecular recognition events to produce an analytical signal. These aspects of CEPs have been thoroughly presented in the *Handbook of Conductive Polymers* [6].

CEPs, while possessing many highly beneficial properties for bioapplications, do suffer some serious limitations. Among these are slow switching speeds in bioelectronic applications, the potential for unintended overoxidation leading to formation of reactive species, time–temperature drift of materials' properties, and questionable biocompatibility. The integration of CEPs with hydrogels promises to address these issues.

Hydrogels [37]

Polymer hydrogels are three-dimensional polymeric networks that are formed from highly hydrophilic monomers rendered water insoluble by electrostatic or covalent crosslinking; however, hydrogels can take up large amounts of water. The result is an elastic network with water effectively filling the interstitial space of the network. When immersed and equilibrated in aqueous medium, crosslinked hydrogels assume their final hydrated network structure, which brings into balance the forces arising from the solvation of the repeating units of the macromolecular chains that leads to an expansion of the network (the swelling force) and the counter balancing elastic force of the crosslinked structure (the retractive force) [38].

That water taken up by a hydrogels may be free or bound. Accordingly, the hydrogels can easily change its size and shape in response to environmental stimuli, and this is one of its intrinsic characteristics: effectively expelling or taking up free water. In so doing, hydrogels can also take up other monomeric, reactive, and potentially polymerizable species into their interstices, essentially occupying their void volume and interacting with chain segments or pendant moieties of the host hydrogels.

Hydrogels have emerged since the early 1950s as being of great importance in the biomaterials field [39]. Their unique soft elastomeric nature serves to minimize mechanical and frictional irritation to tissue, their low interfacial tension contributes to a reduction in protein adsorption and hence biofouling and cell adhesion, and their swelling capacity results in high permeabilities for low molecular weight drug molecules and metabolites [40]. These characteristics have allowed hydrogels to be used in biomedical applications that include biosensors, drug delivery systems, contact lenses, catheters, wound dressings, and tourniquets. Of particular interest is their use as matrices for the immobilization and stabilization of enzymes [41–45]. This interest has led to their parallel development as the biorecognition layer of potentiometric, conductometric, amperometric, and fiber-optic-based enzyme biosensors [46, 47]. Because of their high water content, hydrogels membrane layers and gels pads also find application as microbioreactors for the hosting and stabilization of biological molecules and for the conduct of biological reactions [48, 49]. Hence, hydrogels have been

used to host bioactive layers in several forms of enzyme-linked antibody biosensors and DNA biochips [50–54].

There are multiple reports involving hydrogels that document their biocompatibility [55], biodegradability [56], bioadhesion [57], dielectric relaxation [58], and mass transport properties [59]. The theoretical framework for the kinetics of the swelling of polymeric hydrogels has been well developed. The ionizable polymer hydrogels gives rise to important electrochemical swelling and deswelling characteristics, and this has been explained in terms of electrokinetic processes. Hence, an ionized hydrogels changes volume discontinuously as the solvent composition is continuously varied (i.e., a phase transition occurs). This phase transition is induced not only by a change in the solvent composition but may also be induced by a change in pH, ionic strength (salt concentration), temperature, and the application of an electric field. For example, a polyelectrolyte hydrogels when placed between a pair of electrodes deswells under an applied DC voltage with concomitant expulsion of water. This property is associated with the electrophoretic and electroosmotic transport of highly hydrated macromolecules and of their counterions. The shape change of hydrogels has also engendered applications as hydrogels actuators in bioMEMS devices and as artificial muscles due to the hydrogel's dramatic changes in physical dimensions caused by changes in the polarity of the electric field. These chemomechanical devices allow dynamic control of delivery of drug and other solute molecules across and from within hydrogels membranes.

Poly(HEMA)-based hydrogels are hydrolytically stable, may be engineered to possess similar water content and elastic moduli as body tissues, and exhibit good *in vitro* and *in vivo* biocompatibility [60, 61]. Consequently, these polymer hydrogels have emerged as one of the most widely researched, patented, and successfully commercialized biomedical polymers [62]. There are numerous studies that aim to modify the properties of p(HEMA). These studies aim to improve the mechanical properties [63], transport properties [64], temperature-responsive characteristics [65], and the degree of hydration [66, 67]. The degree of hydration and/or swelling is one of the important properties that allow for an understanding of the transport of small molecule solutes through the hydrogels matrix. However, hydration also influences the elastic modulus and surface properties, such as wettability – and consequently, protein adsorption – and is, thus, strongly correlated with *in vitro* and *in vivo* biocompatibility [68]. Apart from the poly(HEMA)-based hydrogels, other types of naturally occurring, synthetic, and hybrid hydrogels have been proposed and studied for the immobilization of biorecognition molecules and whole cells. Among these are agarose [69–71], alginates [72–74], polyvinyl alcohol [72], poly(acrylate) [75], collagen [75], albumin-PEG [76], and gelatin [71].

Poly(HEMA)-based hydrogels are generally synthesized via the free radical polymerization of acrylate and methacrylate monomers. The free radical initiator may be excited thermally or via UV light. Typically, the hydrogels matrices are prepared by mixing monomers, a crosslinker, prepolymer, distilled water, and ethylene glycol to obtain a homogenous solution with controlled viscosity and density to which the initiator is added. Varying the mole percentage composition and variety of monomers provides many unique copolymers. Controlling the mole percentage of the crosslinker relative to the reactive monomer allows control of the molecular weight between crosslinks and hence the void volume of the final hydrogels. Prepolymers of medium to high molecular weight may be added to control the viscosity of the cocktail.

The hydrogels cocktail may be spun onto electrodes and electronic devices, such as ion-sensitive field effect transistors (ISFETs) and surfaces of other materials, to produce adherent thin films with 1–10 μm thickness. To produce an adherent hydrogels thin film is a nontrivial matter, as the reversible swelling and deswelling leads to appreciable interfacial shear stress and its hydrophilic nature leads to interfacial accumulation of water, both of

which can lead to interfacial failure. Alternatively, the hydrogels cocktail may be freestanding, cast into a mold and deposited by any of the multiple coating processes, or prepared as microspheres via suspension or emulsion polymerization. UV polymerization is typically carried out at room temperature with brief exposures to the appropriate wavelength of light, generally with minimal increases in temperature, and with little or no compromise of biological activity.

Bioactive hydrogels reflect an emerging paradigm in the development of responsive [77], multifunctional [78] biorecognition membrane layers for implantable biosensors and deep brain stimulation devices. Bioactivity is derived from a combination of hydration levels, mechanical properties, surface chemistries, and micro-nanotopologies that render the hydrogels mimetic of the tissue bed within which it is to be implanted. The design and molecular engineering of bioactive hydrogels as the recognition membrane layer of biosensors requires that bioactive molecules, such as enzymes, their cofactors, redox mediators, and biomimetic moieties, be incorporated at biofunctionally relevant levels within the hydrogels [79]. Retaining these bioactive and/or functional entities, either by physical entrapment or covalent tethering, necessitates an understanding of the transport characteristic of these entities within the hydrogels matrix.

Electroconductive Hydrogels

The term electroconductive is a contraction of electroactive and conductive. An ECH describes a polymer that combines the properties of hydrogels and conductive systems and appears to have first originated with Gong et al. [80] who described a conductive charge transfer salt complex of 7,7,8,8-tetracyanoquinodimethane (TCNQ)-loaded hydrogels.

Since the first Guiseppi-Elie and Wallace papers, several studies on composites formed from CEP and hydrogels have been carried out. An electrically conductive composite material consisting of polyaniline nanoparticles dispersed in a polyvinyl pyrrolidone (PVP) hydrogels was prepared by water dispersion polymerization of aniline using PVP as a steric stabilizer, followed by γ -irradiation which induced crosslinking of the PVP component [81]. Moschou et al. [82] developed an artificial muscle material based on a hydrogels that was composed of acrylamide and acrylic acid that was doped with a polypyrrole/carbon black composite. Lira et al. [16] prepared polyaniline–polyacrylamide composites by electropolymerization of the conducting polymer inside an insulating hydrogels matrix of different pore sizes. The resulting new material was electroactive due to the polyaniline present inside the pores. These composites were applied to electrochemically controlled drug delivery devices.

The synthesis of a hydrogels composite in which polyaniline (linear) was entrapped within a crosslinked polyelectrolyte hydrogels, poly(2-acrylamido-2-methyl propane sulfonic acid) (PAMPS), was reported by Kumar and Gangopadhyay in 2005 [83]. The conducting polymer composites of PPy with poly(methyl methacrylate) were developed as materials for controlled delivery devices by Nikpour et al. [84]. The liquid porogen used was polypropylene glycol, while sodium chloride powder was used as the solid porogen. Koul et al. [85] reported on the synthesis of a polyaniline (acrylonitrile–butadiene–styrene) composite membrane as a sensor material for aqueous ammonia. The resistance change of the composite film upon exposure to different concentrations of aqueous ammonia showed its utility as a sensor material. Park and Park [86] investigated the electrical properties of the conducting composite poly(methyl methacrylate-*co*-pyrrolmethylstyrene)-*g*-polypyrrole (PMMAPMS-*g*-PPy). The PMMAPMS-*g*-PPy was synthesized by the electrochemical reaction of PMMAPMS and

pyrrole in the electrolyte solution containing lithium perchlorate and a mixture solvent of acetonitrile and dichloromethane.

Enzymes entrapped within polypyrrole (PPy) films, prepared by electropolymerization from aqueous solution, have been commonly used to prepare electrodes. For example, a glucose biosensor was developed based on GOx entrapment within a composite p(HEMA)/PPy hydrogels membrane [11]. A mixture of HEMA and tetraethylene glycol diacrylate (TEGDA) as a cross-linker and enzyme was deposited on the platinum electrode surface, and the polymerization of HEMA was performed by irradiating with UV under argon. Subsequently, the pyrrole monomer entrapped within the hydrogels network was electrochemically polymerized. An amperometric biosensor for cholesterol analysis was prepared by entrapping cholesterol oxidase (ChOx; E.C 1.1.3.6) into the p(HEMA)/PPy matrix [9]. The bioactive composites of polypyrrole containing p(HEMA) hydrogels were incorporated into an amperometric biosensor for clinically important analytes (galactose [87], glucose, and cholesterol). The biosensor showed excellent screening of physiological interferences, such as ascorbic acid, uric acid, and acetaminophen.

Synthesis of Electroconductive Hydrogels

ECHs are composites, blends, or conetworks of hydrogels and CEPs; for example, the hydrogels may be the continuous or dominant component within which the CEP is polymerized. Alternatively, the CEP may be the dominant or continuous phase and the hydrogels was polymerized within the CEP. The former is more commonly used. Polymer composites of inherently conductive polymers synthesized within other (host) polymers are not new. Early attempts to stabilize the environmentally labile optical and electrical properties of polyacetylene (CHx) were achieved by Ziegler–Natta catalytic synthesis of CHx within host polymers, such as polyethylene [88, 89].

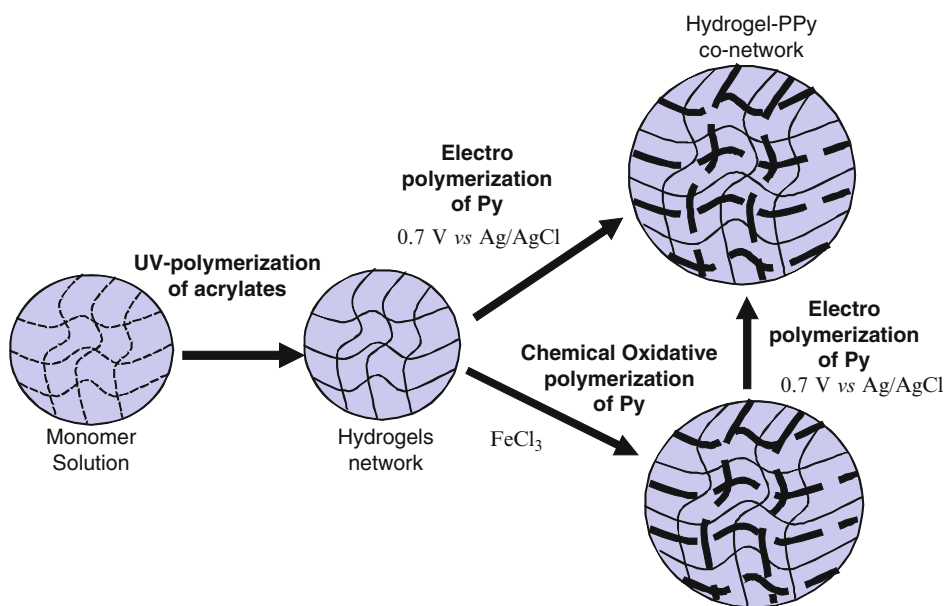


Fig. 2. Schematic of the generalized synthetic routes to electroconductive hydrogels.

Shown in Fig. 2 is a schematic illustration of the generalized synthetic routes to ECHs. The reactive monomer shown may be a combination of both hydrogels precursors and CEP precursors, which can be combined with photo or thermal free radical initiators into a single cocktail or prepolymer mixture. The cocktail may be cast into films, prepared as microspheres, spun as fibers, or spun-applied to electrodes and other solid-state electronic device substrates. Chemical oxidative polymerization does not require a substrate and can proceed when the hydrogels form (fiber, film, or microsphere) is immersed into a suitable solution containing the initializing oxidant, such as FeCl_3 or peroxy sulfate. Electrochemical polymerization requires that the hydrogels form be applied to a metallic or semiconducting electrode to which a suitable potential may be impressed relative to a reference electrode and the ensuing current supported by a counter electrode. In both cases, the bath solution may contain additional free monomer that may or may not be equilibrated with the electroactive monomer trapped within the hydrogels.

Listed in Table 2 are the monomer components used in a typical synthetic scheme for an ECH based on polypyrrole. The composition for three formulations are given in Table 2 which yield a prototypical TEGDA crosslinked poly(HEMA) hydrogels, a poly(HEMA)-based hydrogels of poly(HEMA-*co*-PEGMA-*co*-HMMA-*co*-SPMA)-PPy,

Table 2. Components and composition of the hydrogels cocktail for synthesis of an electroconductive hydrogels

Role	Compound in formulae	Mole (%)		
		Poly(HEMA)	Poly(HEMA)-PPy	Poly(HEMA)-P(Py- <i>co</i> -PyBA)
Monomer 1	2-Hydroxyethyl methacrylate (HEMA)	84.0	63.0	61.5
Monomer 2	<i>N</i> -[Tris(hydroxymethyl)methyl]acrylamide (HMMAm)	5.0	5.0	5.0
Pendant PEG	Poly(ethyleneglycol)(200) monomethacrylate (PEG200MMA)	5.0*	5.0*	5.0*
Crosslinker	Tetraethylene glycol diacrylate (TEGDA)	3.0	3.0	3.0
Dopant counter anion	3-Sulfopropyl methacrylate potassium salt (SPMA)	0	5.0	5.0
Prepolymer	Poly-(2-hydroxyethyl methacrylate) (pHEMA) 300,000	2.0*	2.0*	2.0*
Photoinitiator	2,2-Dimethoxy-2-phenylacetophenone (DMPA)	2.0	2.0	2.0
Electroactive monomer	Pyrrole (Py)	0	15.0	15.0
Electroactive monomer	4-(3-Pyrrolyl)butyric acid	0	0	1.5
Solvent	Water	20.0 wt%	20.0 wt%	20.0 wt%
Solvent	Ethylene glycol	20.0 wt%	20.0 wt%	20.0 wt%

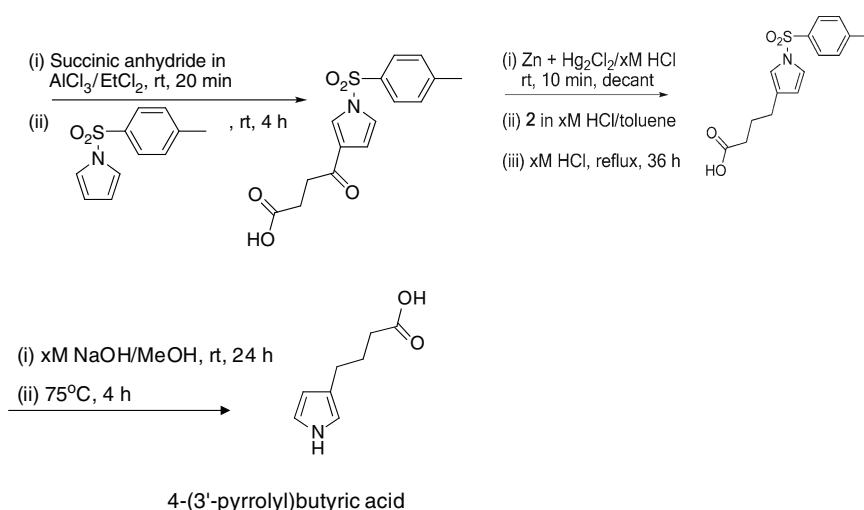
*Mole % calculated on the basis of the repeating unit molecular weight.

and a poly(HEMA)-based hydrogels of poly(HEMA-*co*-PEGMA-*co*-HMMA-*co*-SPMA)-P(Py-*co*-PyBA) where PyBA is 4-(3'-pyrrolyl)butyric acid.

These ECHs are based on 2-hydroxyethyl methacrylate (HEMA), a water-soluble monomer that can be UV-polymerized at low temperature (-20 to $+10^{\circ}\text{C}$) and may be readily copolymerized with other acrylate, methacrylate, and acrylamide monomers, e.g., poly(ethylene glycol) methacrylate (PEGMA) and *N*-[tris(hydroxymethyl)methyl]-acrylamide (HMMA) to yield hydrogels of varying physical and chemical properties [90]. The presence of PEGMA and HMMA confers the antiprotein fouling properties of the pendant polyethylene glycol (PEG) chains and the temperature-responsive properties of the acrylamide to the p(HEMA-*co*-PEGMA-*co*-HMMA) hydrogels [91, 92].

The polypyrrole component is synthesized by electropolymerization to yield a homopolymer of pyrrole or a copolymer of pyrrole and 4-(3'-pyrrolyl) butyric acid monomer that were physically entrapped within the p(HEMA)-based hydrogels while supplemented by pyrrole monomer that was in the bath solution [93]. In this system, the 3-sulfopropyl methacrylate potassium salt (SPMA) of the hydrogels component serves as the counter anion to the positively charged, oxidized form of the conductive electroactive polypyrrole. In Scheme 1, details for the synthesis of 4-(3'-pyrrolyl) butyric acid are illustrated. The 4-(3'-pyrrolyl) butyric acid (PyBA) of the conductive, electroactive component serves as a hydrophilic monomer that can potentially establish electrostatic interactions with the HMMA monomer of the hydrogels component. The molecular intimacy is designed into the two polymer systems so as to favor chemical compatibility and blend formation.

The necessary substrate surface modifications, derivatizations, and monomer casting to yield a poly(HEMA)-based PPy electroconductive hydrogels membrane are shown in Fig. 3. These adhered to an electrode surface via covalent tethering and multiple hydrogen bonding interactions with the PEG moieties. Because of the interfacial shear stress that accompanies repeated swelling and deswelling of the ECH, it is necessary to pay particular attention to the immobilization of the hydrogels onto electrode surfaces. This is particularly true for electrode structures and electronic devices that are heterogeneous, possessing exposed metal, semiconductor, and insulator surfaces. The results given in Fig. 3 are applicable to



Scheme 1. Synthesis and structure of 4-(3'-pyrrolyl) butyric acid.

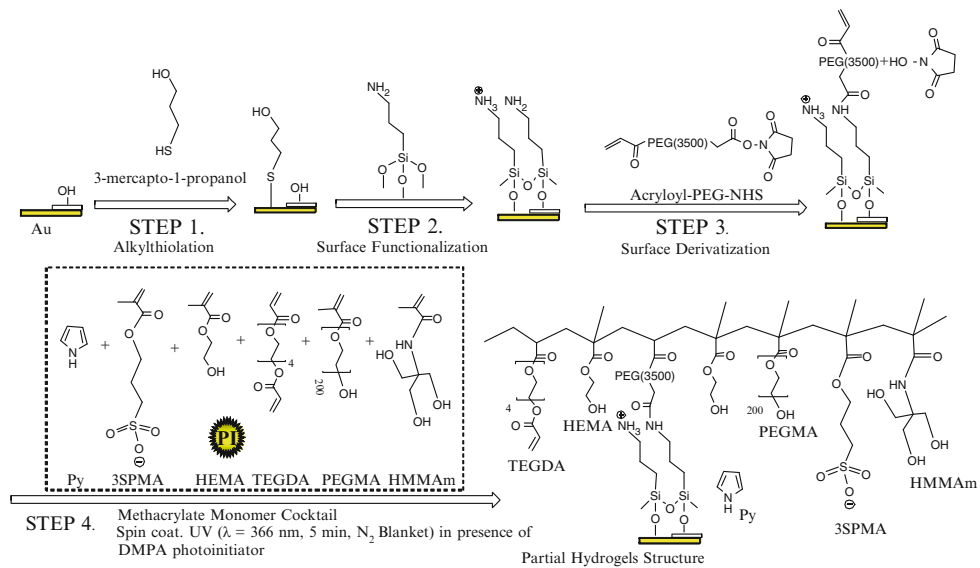


Fig. 3. Substrate surface modification, derivatization, and monomer casting to yield a poly(HEMA)-based PPy electroconductive hydrogels membrane that is adhered to an electrode surface via covalent tethering and multiple hydrogen bonding interactions with the PEG moieties.

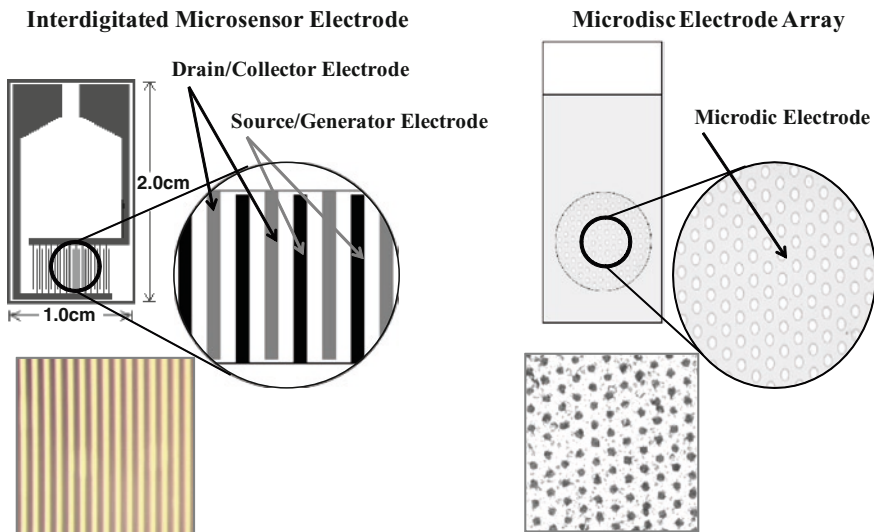


Fig. 4. *Left:* An interdigitated microsensor electrode (IME) showing 10- μ m fingered electrodes. *Right:* A microdisc electrode array (MDEA) showing individual 50- μ m-diameter microdiscs. Both shown are modified via coating with poly(HEMA)-based PPy electroconductive hydrogels.

a microfabricated interdigitated microsensor electrode (IME) or microdisc electrode array (MDEA), which consists of patterns of gold with critical dimensions of 1–20 μ m, revealed through photolithographically defined windows in an insulating Si₃N₄ layer [94–97]. A schematic

illustration of the structure of these devices is shown in Fig. 4; these are used in the development of electroconductive polymer sensor technology [98].

The IME and MDEA devices were cleaned by sequential ultrasonic washing in boiling trichloroethylene (3 min; 86.7°C), acetone (1 min; 56.2°C), and 2-propanol (1 min; 82.4°C) and then washed in room temperature deionized water. To remove the chemisorbed organic residues, the MDEA devices were treated for 10 min in the UV–ozone cleaner, washed by ultrasonication in 2-propanol, and then washed in room temperature deionized water. To remove residual organic/ionic contamination and to produce a uniform, reproducible layer of –OH groups on the surface of the Si₃N₄ (activation), the electrodes were immersed in a (5:1:1, v/v/v) 60°C solution of deionized H₂O:NH₄OH:H₂O₂ (RCA Clean), held for about 10 s, quenched in deionized water for 1 min, and then washed with running deionized water, followed by exposure to radiofrequency (RF) glow discharge plasma for 10 min within which humidified air was periodically allowed to bleed into the chamber. The gold surface of the cleaned and activated devices was chemically modified with 0.01 M 3-mercapto-1-propanol (in anhydrous ethanol) and stored at room temperature overnight to introduce pendant alkyl-hydroxy surface functionalities.

The pendant alkylhydroxy and surface –OH groups on the silicon nitride surface were subsequently functionalized by treatment with 3-(aminopropyl)trimethoxysilane (γ -APS; 0.01 M, in anhydrous toluene for 2 h) to introduce pendant alkylamino surface functionalities. The devices were cured at 40°C for 20 min, then 110°C for 20 min, and then 40°C for 20 min, for a total of 1 h. For the final functionalization and to establish a continuous path of covalent bonding between the device surfaces and the hydrogels layer the devices were incubated for 2 h in acryloyl(poly(ethylene glycol))-*N*-hydroxysuccinamide (Acryl-PEG-NHS, $M_w = 3,500$) solution (0.001 M) made up in 0.1 M HEPES (pH=8.5) – prepared under UV-filtered conditions.

Under UV-free conditions, the final hydrogels cocktail was sonicated, purged with nitrogen, and applied evenly to the surface of the Acryl-PEG functionalized devices using a spin coater. The mixture was immediately irradiated with UV light (366 nm, 2.3 W/cm², 5 min) in a UV crosslinker under an inert nitrogen atmosphere to effect polymerization of the hydrogels component. Finally, the electrodes with the base hydrogels were conditioned, and the unreacted monomer was extracted by sequential immersion in ethanol:deionized water mixtures (100% ethanol, 75:25; 50:50; 25:75; 100% deionized water; v/v) for a minimum of 1 h each. The electrodes with the pyrrole monomer containing hydrogels were immersed in a saturated pyrrole solution for subsequent electropolymerization of PPy or P(Py-*co*-PyBA). Illustrated in Fig. 5 is the hypothetical chemical structure of the UV-crosslinked hydrogels and its association with polypyrrole.

Shown in Fig. 6 are the substrate surface modifications, derivatizations, and monomer casting for a poly(HEMA)-based P(Py-*co*-PyBA) electroconductive hydrogels membrane that is adhered to an electrode surface via a covalent tethering and multiple hydrogen bonding interactions with the PEG moieties, while the hypothetical chemical structure of the UV-crosslinked hydrogels and its association with poly(Py-*co*-PyBA) are illustrated in Fig. 7.

The electropolymerization of Py is favored within the hydrogels milieu. As shown in Fig. 8, the chronopotentiograms are produced by galvanostatic (1 mA, fixed current) electropolymerization of Py at chemically modified and derivatized IME chips (IME*) to form IME*IPPy and IME*IGel-P(Py-*co*-PyBA) chips. To ensure adequate hydration of the hydrogels layer and to ensure equilibration of the pyrrole monomer and electrolytes between the solution and hydrogels phases, the devices were equilibrated in the electropolymerization bath of saturated pyrrole monomer (~0.4 M Py in 0.1 M Tris/0.1 M KCl, pH=6.1) for approximately 1 h prior to electropolymerization. The electrode potentials needed to support the kinetics at

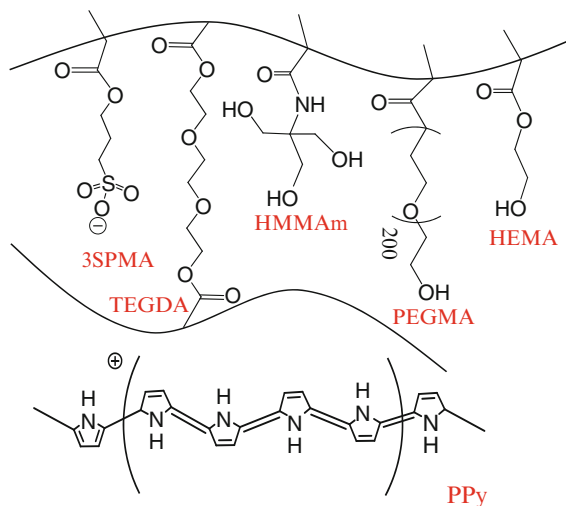


Fig. 5. An illustration of the molecular components of a poly(HEMA-*co*-PEGMA-*co*-HMMAm-*co*-SPMA)/PPy electroconductive hydrogels membrane. (Reproduced with permission).

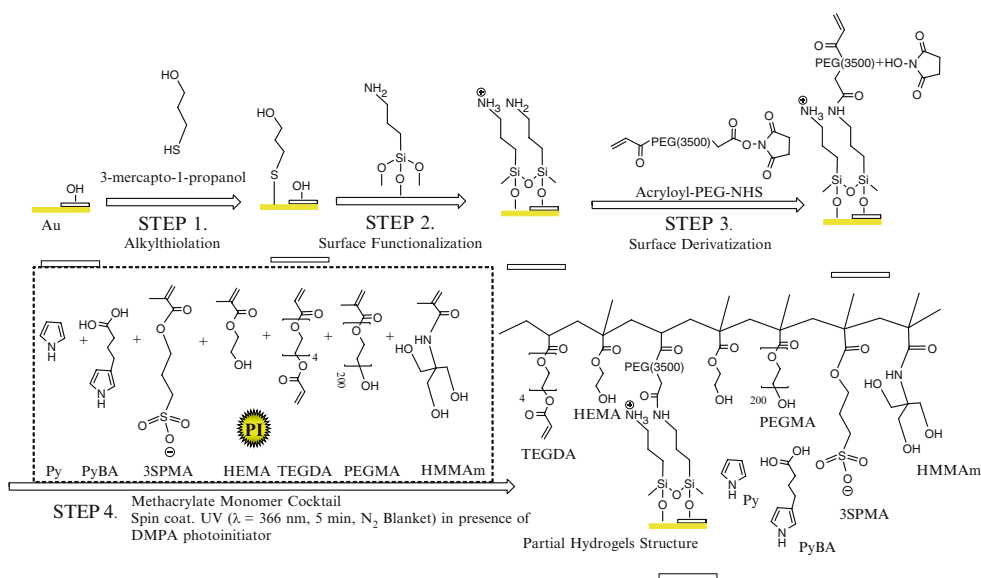


Fig. 6. Substrate surface modification, derivatization, and monomer casting to yield a poly(HEMA)-based P(Py-*co*-PyBA) electroconductive hydrogels membrane that is adhered to an electrode surface via covalent tethering and multiple hydrogen bonding interactions with the PEG moieties.

the uncoated and hydrogels-coated IMEs, separately, are shown in Fig. 8. For electropolymerizations occurring directly at the electrode there is a decrease in potential between 0.85 and 0.75 V within the first 25 s. Within this same time period the potential at the IME*Gel electrode falls more sharply from 0.80 to 0.68 V. The physical evidence also supports a more

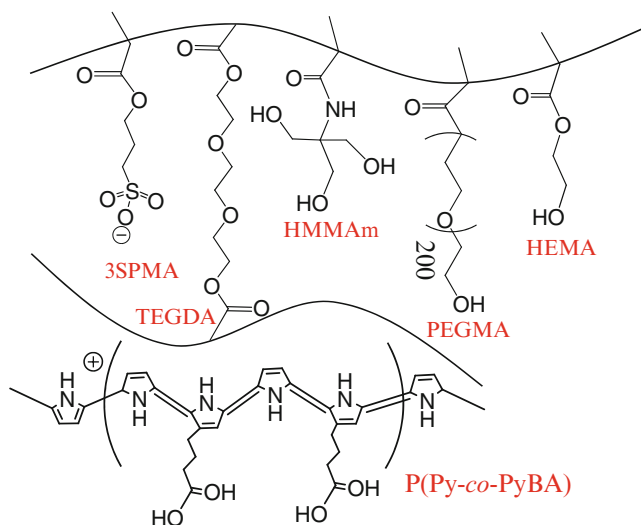


Fig. 7. An illustration of the molecular components of a poly(HEMA-co-PEGMA-co-HMMAm-co-SPMA)/P(Py-co-PyBA) electroconductive hydrogels membrane. (Reproduced with permission).

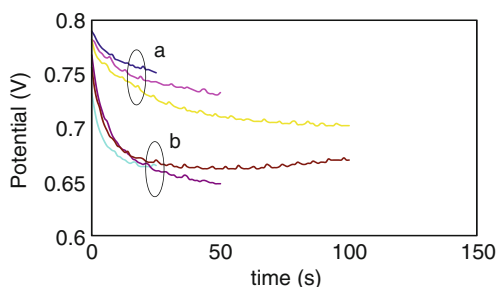


Fig. 8. Kinetics of galvanostatic electropolymerization of PPy onto (a) surface modified and derivatized Pt IMEs and (b) surface modified and derivatized Pt IMEs that were coated with hydrogels. Electropolymerization conditions were 0.4 M pyrrole, Tris buffer, pH 6, and 1 mA.

rapid and uniform electropolymerization of PPy within the hydrogels membrane. Several factors are at work in promoting more favorable kinetics: (1) the Py monomer may partition more favorably into the hydrogels resulting in a higher concentration, (2) the presence of the SPMA dopant anion on the hydrogels network, and (3) the presence of the PyBA within the hydrogels may favor both uniform and rapid electropolymerization.

The electrochemical impedance magnitude, $|Z|$, is shown in Fig. 9 as a function of frequency for a basic poly(HEMA) hydrogels membrane (column 3, Table 2), a pristine PPy membrane, and an electroconductive hydrogels poly(HEMA)-based P(Py-co-PyBA) (column 5, Table 2) that were prepared on an MDEA 050Au* device. These data confirm that poly(HEMA) hydrogels is an insulator with a purely capacitive response. However, the ECH shows similar interfacial impedance properties as the

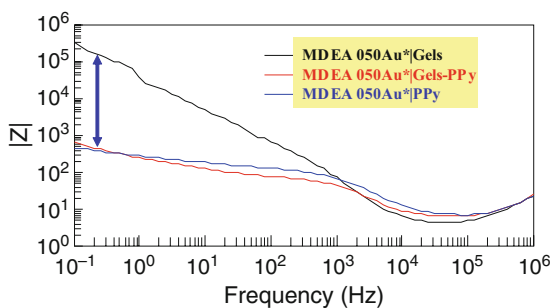


Fig. 9. Electrochemical impedance magnitude, $|Z|$, is plotted as a function of frequency for a hydrogels membrane. An electroconductive hydrogels and pristine PPy electropolymerized on an MDEA 050Au* device showed an equivalent reduction in interfacial impedance following electropolymerization of PPy, whether within the hydrogels membrane or directly onto the electrode device surface.

electropolymerized PPy, whether within the hydrogels membrane or directly onto the electrode device surface.

Summary

ECHs represent a unique outlook for combining inherently CEPs with hydrated hydrogels within an aqueous milieu with responsive properties that are compatible to biological molecules, such as peptide sequences, enzymes, antibodies, and DNA. The combination of hydrogels and inherently CEPs allows both materials to retain their unique responsive properties. In addition, the novel ECH engenders a new class of devices with low interfacial impedances suitable for neural prosthetic devices, such as deep brain stimulation electrodes, low-voltage actuation for electrically stimulated drug release devices, and potential for in vivo biocompatibility in implantable biosensors.

Acknowledgments

This work was supported by the US Department of Defense (DoDPRMRP) grant PR023081/DAMD17-03-1-0172, by the Consortium of the Clemson University Center for Bioelectronics, Biosensors and Biochips (C3B), and by ABTECH Scientific, Inc.

References

1. Guiseppi-Elie A, Sheppard NF Jr (1995) Conferring biospecificity to electroconductive polymer-based biosensor devices. In: ACS Northeast Regional Meeting (NERM), Rochester, NY, 22–25 October 1995
2. Guiseppi-Elie A, Wilson AM, Sujdak AR, Brown KE (1997) Electroconductive hydrogels: novel materials for the controlled electrorelease of bioactive peptides. *Polymer Prepr* 38(2):608
3. Guiseppi-Elie A, Sujdak A, Wilson AM (1997) Electroconductive hydrogels: electrical, electrochemical and impedance properties. In: Fall MRS Meeting Symposium J, Boston, 1–5 December 1997
4. Small CJ, Too CO, Wallace GG (1997) Responsive conducting polymer-hydrogel composites. *Polym Gels Netw* 5(3):251–265

5. Guiseppi-Elie A, Wilson AM, Sudjak AS (1998) Electroconductive gels for controlled electrorelease of bioactive peptides. In: ACS symposium series, vol 709. ACS Publications, Washington, DC, pp 185–202
6. Guiseppi-Elie A, Brahim S, Wilson A (2006) Biosensors based on electrically conducting polymers. In: Skotheim T, Reynolds JR (eds) Handbook of conducting polymers: conjugated polymer processing and applications, 3rd edn. Marcel Dekker, New York, pp 435–479
7. Iwuoha EI, Wilson A, Howel M, Mathebe NGR, Montane-Jaime K, Narinesingh D, Guiseppi-Elie A (2004) Cytochrome P450_{2D6} (CYP2D6) bioelectrode for fluoxetine. *Anal Lett* 37(5):943–956
8. Owino JHO, Arotiba OA, Baker PGL, Guiseppi-Elie A, Iwuoha EI (2008) Synthesis and characterization of poly (2-hydroxyethyl methacrylate)-polyaniline based hydrogels composites. *React Funct Polym* 68(8): 1239–1244
9. Brahim S, Narinesingh D, Guiseppi-Elie A (2001) Amperometric determination of cholesterol in serum using a cholesterol oxidase biosensor with a polypyrrole / hydrogel membrane. *Anal Chim Acta* 448:27–36
10. Guiseppi-Elie A, Brahim S, Narinesingh D (2001) Composite hydrogels containing polypyrrole as support membranes for amperometric enzyme biosensors. *J Macromol Sci Pure Appl Chem A38(12):1575–1591*
11. Brahim S, Narinesingh D, Guiseppi-Elie A (2002) Polypyrrole-hydrogel composites for the construction of clinically important biosensors. *Biosens Bioelectron* 17(1–2):53–59
12. Brahim S, Narinesingh D, Guiseppi-Elie A (2002) Interferent suppression using a novel polypyrrole-containing hydrogel in amperometric enzyme biosensors. *Electroanalysis* 14(9):627–633
13. Kim D-H, Abidian M, Martin DC (2004) Conducting polymers grown in hydrogel scaffolds coated on neural prosthetic devices. *J Biomed Mater Res A* 71A(4):577–585
14. Cui X, Lee VA, Raphael Y, Wiler JA, Hetke JF, Anderson DJ, Martin DC (2001) Surface modification of neural recording electrodes with conducting polymer/biomolecule blends. *J Biomed Mater Res* 56(2):261–272
15. Green RA, Lovell NH, Wallace GG, Poole-Warren LA (2008) Conducting polymers for neural interfaces: challenges in developing an effective long-term implant. *Biomaterials* 29(24–25):3393–3399
16. Lira LM, Cordoba de Torresi SI (2005) Conducting polymer-hydrogel composites for electrochemical release devices. *Electrochem Commun* 7:717–723
17. Murdan S (2003) Electro-responsive drug delivery from hydrogels. *J Control Release* 92(1–2):1–17
18. Wellinghoff ST, Baker CK (1991) Electrochemical drug release and article. US Patent 4,994,023
19. Pernaut J-M, Reynolds JR (2000) Use of conducting electroactive polymers for drug delivery and sensing of bioactive molecules. A redox chemistry approach. *J Phys Chem B* 104(17):4080–4090
20. George PM, LaVan DA, Burdick JA, Chen CY, Liang E, Langer R (2006) Electrically controlled drug delivery from biotin-doped conductive polypyrrole. *Adv Mater* 18(5):577–581
21. Guiseppi-Elie A, Brahim S, Slaughter G, Ward K (2005) Design of a subcutaneous implantable biochip for monitoring of glucose and lactate. *IEEE Sens J* 5(3):345–355
22. Brahim S, Narinesingh D, Guiseppi-Elie A (2002) Bio-smart hydrogels: co-joined molecular recognition and signal transduction in biosensor fabrication and drug delivery. *Biosens Bioelectron* 17(11–12):973–981
23. Brahim S, Narinesingh D, Guiseppi-Elie A (2002) Bio-smart materials: kinetics of immobilized enzymes in p(HEMA)/p(Pyrrole) hydrogels in amperometric biosensors. *Macromol Symp* 186:63–73
24. George PM, Lyckman AW, LaVan DA, Hegde A, Leung Y, Avasare R, Testa C, Alexander PM, Langer R, Sur M (2005) Fabrication and biocompatibility of polypyrrole implants suitable for neural prosthetics. *Biomaterials* 26(17): 3511–3519
25. Guimard N, Gomez N, Schmidt CE (2007) Conducting polymers in biomedical applications. *Prog Polym Sci* 32:876–892
26. Ateh DD, Navasaria HA, Vadgama P (2006) Polypyrrole-based conducting polymers and interactions with biological tissues. *J R Soc Interface* 3(11):741–752
27. Fonner JM, Forciniti L, Nguyen H, Byrne JD, Kou Y-F, Syeda-Nawaz J, Schmidt CE (2008) Biocompatibility implications of polypyrrole synthesis techniques. *Biomed Mater* 3:034124
28. Skotheim T, Reynolds JR (2007) Handbook of conducting polymers: conjugated polymer processing and applications, 3rd edn. Taylor and Francis, New York
29. Kumar D, Sharma RC (1998) Advances in conductive polymers. *Eur Polym J* 34:1053–1060
30. Jia W, Tchoudakov R, Segal E, Narkis M, Siegmann A (2003) Electrically conductive composites based on epoxy resin containing polyaniline-DBSA- and polyaniline-DBSA-coated glass fibers. *J Appl Polym Sci* 91(2):1329–1334
31. Trojanowicz M (2003) Application of conducting polymers in chemical analysis. *Microchim Acta* 143(2–3): 75–91
32. Ogurtsov NA, Pud AA, Kamarchik P, Shapoval GS (2004) Corrosion inhibition of aluminum alloy in chloride mediums by undoped and doped forms of polyaniline. *Synth Met* 143:43–47

33. Malhotra BD, Chaubey A, Singh SP (2006) Prospects of conducting polymers in biosensors. *Anal Chim Acta* 578: 59–74
34. Sadik OA (1999) Bioaffinity sensors based on conducting polymers: a short review. *Electroanalysis* 11(12): 839–844
35. Jaramillo A, Spurlock LD, Young V, Brajter-Toth A (1999) XPS characterization of nanosized overoxidized polypyrrole films on graphite electrodes. *Analyst* 124:1215–1221
36. Wanekaya A, Sadik OA (2002) Electrochemical detection of lead using overoxidized polypyrrole films. *J Electroanal Chem* 537(1–2):135–143
37. Lin CC, Metters AT (2006) Hydrogels in controlled release formulations: network design and mathematical modeling. *Adv Drug Deliv Rev* 58(12–13):1379–1408
38. Trigo R, Blanco M, Huerta P, Olmo R, Teijon J (1993) L-Ascorbic acid release from poly(2-hydroxyethyl methacrylate) hydrogels. *Polym Bull* 31:577–584
39. Ulijn RV, Bib N, Jayawarna V, Thornton PD, Todd SJ, Mart R, Smith AM, Gough JE (2007) Bioresponsive hydrogels. *Mater Today* 10(4):40–48
40. Li H, Wang DQ, Liu BL, Gao LZ (2004) Synthesis of a novel gelatin-carbon nanotubes hybrid hydrogel. *Colloids Surf B Biointerfaces* 33:85–88
41. Jimenez C, Bartrol J, de Rooij NF, Koudelka-Hep M (1997) Use of photopolymerizable membranes based on polyacrylamide hydrogels for enzymatic microsensor construction. *Anal Chim Acta* 351(1–3):169–176
42. Arica MY, Bayramoglu G (2004) Polyethyleneimine-grafted poly(hydroxyethyl methacrylate-co-glycidyl methacrylate) membranes for reversible glucose oxidase immobilization. *Biochem Eng J* 20(1):73–77
43. Arica MY, Bayramoglu G (2004) Reversible immobilization of tyrosinase onto polyethyleneimine-grafted and Cu(II) chelated poly(HEMA-co-GMA) reactive membranes. *J Mol Catal B Enzym* 27(4–6):255–265
44. Doretti L, Gattolin P, Burla A, Ferrara D, Lora S, Palma G (1998) Covalently immobilized choline oxidase and cholinesterases on a methacrylate copolymer for disposable membrane biosensors. *Appl Biochem Biotechnol* 74(1):1–12
45. Schulz B, Riedel A, Abel PU (1999) Influence of polymerization parameters and entrapment in poly(hydroxyethyl methacrylate) on activity and stability of GOD. *J Mol Catal B Enzym* 7(1–4):85–91
46. Sheppard NF Jr, Lesho MJ, McNally P, Francomacaro AS (1995) Microfabricated conductimetric pH sensor. *Sens Actuators B Chem* 28(2):95–102
47. Li L, Walt DR (1995) Dual-analyte fiber-optic sensor for the simultaneous and continuous measurement of glucose and oxygen. *Anal Chem* 67(20):3746–3752
48. Thornton P, McConnell G, Ulijn RV (2005) Enzyme-responsive polymer hydrogel beads. *Chem Commun* 47: 5913–5915
49. Ulijn RV (2006) Enzyme-responsive materials: a new class of smart biomaterials. *J Mater Chem* 16:2217–2225
50. Pellissier M, Zigah D, Barrière F, Hapiot P (2008) Optimized preparation and scanning electrochemical microscopy analysis in feedback mode of glucose oxidase layers grafted onto conducting carbon surfaces. *Langmuir* 24(16): 9089–9095
51. Pekel N, Salih B, Guven O (2005) Enhancement of stability of glucose oxidase by immobilization onto metal ion-chelated poly(N-vinyl imidazole) hydrogels. *J Biomater Sci Polym Ed* 16(2):253–266
52. Kim D-N, Lee W, Koh W-G (2008) Micropatterning of proteins on the surface of three-dimensional poly(ethylene glycol) hydrogel microstructures. *Anal Chim Acta* 609(1):59–65
53. Soto C, Patterson C, Charles P, Martin B, Spector M (2005) Immobilization and hybridization of DNA in a sugar polyacrylate hydrogel. *Biotechnol Bioeng* 92(7):934–942
54. Rubina AY, Pankov SV, Dementieva EI, Penkov DN, Butygin AV, Vasiliskov VA, Chudinov AV, Mikheikin AL, Mikhailovich VM, Mirzabekov AD (2004) Hydrogel drop microchips with immobilized DNA: properties and methods for large-scale production. *Anal Biochem* 325(1):92–106
55. Luo Y, Kirker KR, Prestwich GD (2000) Crosslinked hyaluronic acid hydrogel films: new biomaterials for drug delivery. *J Control Release* 69(1):169–184
56. Poon YF, Cao Y, Zhu Y, Judeh ZM, Chan-Park MB (2009) Addition of beta-malic acid-containing poly(ethylene glycol) dimethacrylate to from biodegradable and biocompatible hydrogels. *Biomacromolecules* 10(8):2043–2052
57. Peppas NA, Sahlin JJ (1996) Hydrogels as mucoadhesive and bioadhesive materials: a review. *Biomaterials* 17(16): 1553–1561
58. Kyritsis A, Pissis P, Grammatikakis J (1995) Dielectric relaxation spectroscopy in poly(hydroxyethyl acrylates)/ water hydrogels. *J Polym Sci B Polym Phys* 33(12):1737–1750
59. Pishko MV, Revzin A, Simonian AL (2002) Mass transfer in amperometric biosensors based on nanocomposite thin films of redox polymers and oxidoreductases. *Sensors* 2(3):79–90

60. Abraham S, Brahim S, Ishihara K, Guiseppi-Elie A (2005) Molecularly engineered p(HEMA)-based hydrogels for implant biochip biocompatibility. *Biomaterials* 26:4767–4778
61. Kabra B, Gehrke S, Hwang S, Ritschel W (1991) Modification of the dynamic swelling behavior of poly(2-hydroxyethyl methacrylate) in water. *J Appl Polym Sci* 42(9):2409–2416
62. Alfrey T Jr, Gurnee E, Lloyd W (1966) Diffusion in glassy polymers. *J Polym Sci C* 12(1):249–261
63. Mack E, Okano T, Kim S, Peppas N (1988) *Hydrogels in medicine and pharmacy polymers*, vol II. CRC Press, Boca Raton
64. Elvira C, Mano J, San Román J, Reis R (2002) Starch-based biodegradable hydrogels with potential biomedical applications as drug delivery systems. *Biomaterials* 23(9):1955–1966
65. Flory P, Rehner J (1943) Statistical mechanics of crosslinked polymer networks II. *J Phys Chem* 11:521–526
66. Brahim S, Narinesingh D, Guiseppi-Elie A (2003) Release characteristics of novel pH-sensitive p(HEMA-DMAEMA) hydrogels containing 3-(Trimethoxy-silyl) propyl methacrylate. *Biomacromolecules* 4(5):1224–1231
67. Gayet J, Fortier G (1996) High water content BSA-PEG hydrogel for controlled release device: evaluation of the drug release properties. *J Control Release* 38(2–3):177–184
68. Falk B, Garramone S, Shivkumar S (2004) Diffusion coefficient of paracetamol in a chitosan hydrogel. *Mater Lett* 58(26):3261–3265
69. Luo Y, Shoichet MS (2004) Light-activated immobilization of biomolecules to agarose hydrogels for controlled cellular response. *Biomacromolecules* 5(6):2315–2323
70. Cao X, Shoichet MS (2002) Photoimmobilization of biomolecules within a 3-dimensional hydrogel matrix. *J Biomater Sci Polym Ed* 13(6):623–636
71. Spargo BJ, Cliff RO, Rollwagen FM, Rudolph AS (1995) Controlled release of transforming growth factor-Beta from lipid-based microcylinders. *J Microencapsul* 12(3):247–254
72. Fine T, Leskinen P, Isobe T, Shiraiishi H, Morita M, Marks RS, Virta M (2006) Luminescent yeast cells entrapped in hydrogels for estrogenic endocrine disrupting chemical biodetection. *Biosens Bioelectron* 21(12):2263–2269
73. Braschler T, Johann R, Heule M, Metref L, Renaud P (2005) Gentle cell trapping and release on a microfluidic chip by in situ alginate hydrogel formation. *Lab Chip* 5(5):553–559
74. Kong HJ, Smith MK, Mooney DJ (2003) Designing alginate hydrogels to maintain viability of immobilized cells. *Biomaterials* 24(22):4023–4029
75. O'Connor SM, Andreadis JD, Shaffer KM, Ma W, Pancrazio JJ, Stenger DA (2000) Immobilization of neural cells in three-dimensional matrices for biosensor applications. *Biosens Bioelectron* 14(10–11):871–881
76. Jean-Francois J, D'Urso EM, Fortier G (1997) Immobilization of L-asparaginase into a biocompatible poly(ethylene glycol)-albumin hydrogel: evaluation of performance in vivo. *Biotechnol Appl Biochem* 26(3):203–212
77. Park K, Shalaby W, Park H (1993) *Biodegradable hydrogels for drug delivery*. Technomic Publishing Co., Basel
78. Klomp G, Hashiguchi H, Ursell P, Takeda Y, Taguchi T, Dobelle W (1983) Macroporous hydrogel membranes for a hybrid artificial pancreas. II. Biocompatibility. *J Biomed Mater Res* 17(5):865–871
79. Guiseppi-Elie A, Brahim S, Narinesingh D (2002) A chemically synthesized artificial pancreas: release of insulin from glucose-responsive hydrogels. *Adv Mater* 14(10):743–746
80. Gong JP, Kawakami I, Sergeev VG, Osada Y (1991) Electroconductive organogel. 3. Preparation and properties of a charge-transfer complex gel in an organic solvent. *Macromolecules* 24:5246–5250
81. Dispenza C, Fiandaca G, Presti CL, Piazza S, Spadaro G (2007) Electrical properties of gamma-crosslinked hydrogels incorporating organic conducting polymers. *Radiat Phys Chem* 76(8–9):1371–1375
82. Moschou E, Madou MJ, Bachas LG, Daunert S (2006) Voltage-switchable artificial muscles actuating at near neutral pH. *Sens Actuators B Chem* 115(1):379–383
83. Kumar S, Gangopadhyay R (2005) Conducting polymer gel: formation of a novel semi-IPN from polyaniline and crosslinked poly(2-acrylamido-2-methyl propanesulphonic acid). *Polymer* 46(9):2993–3000
84. Nikpour M, Chaouk H, Mau A, Chung DJ, Wallace G (1999) Porous conducting membranes based on polypyrrole-PMMA composites. *Synth Met* 99(2):121–126
85. Koul S, Chandra R, Dhawan SK (2001) Conducting polyaniline composite: a reusable sensor material for aqueous ammonia. *Sens Actuators B Chem* 75(3):151–159
86. Park YH, Park SB (2002) Preparation and electroactivity of poly(methylmethacrylate-co-pyrrolylmethylstyrene)-g-polypyrrole. *Synth Met* 128(2):229–234
87. Brahim S, Maharajh D, Narinesingh D, Guiseppi-Elie A (2002) Characterization of a galactose biosensor using a novel polypyrrole-hydrogel composite membrane. *Anal Lett* 35(5):797–812
88. Galvin ME, Wnek GE (1985) Characterization of polyacetylene/low density polyethylene composites prepared by in situ polymerization. *J Polym Sci Polym Chem Ed* 21(9):2727–2737

89. Galvin ME, Wnek GE (1985) Towards the synthesis of electroactive block copolymers via anionic-to-Ziegler-Natta transformation reactions. *Polym Bull* 13(2):109–114
90. Brahim S, Narinesingh D, Guiseppi-Elie A (2003) Synthesis and hydration properties of pH-sensitive, p(HEMA)-based hydrogels containing 3-(trimethoxysilyl)propyl methacrylate. *Biomacromolecules* 4(3):497–503
91. Lee W, Lin W (2002) Preparation and gel properties of poly[hydroxyethylmethacrylate-co-poly(ethylene glycol) methacrylate] copolymeric hydrogels by photopolymerization. *J Polym Res* 9(1):23–29
92. Sun Y, Gombotz W, Hoffman A (1986) Synthesis and characterization of non-fouling polymer surfaces: I. Radiation grafting of hydroxyethyl methacrylate and polyethylene glycol methacrylate onto silastic film. *J Bioact Compat Polym* 1(3):316
93. Brahim S, Guiseppi-Elie A (2005) Electroconductive hydrogels: electrical and electrochemical properties of polypyrrole-poly(HEMA) composites. *Electroanalysis* 17(7):556–570
94. Justin G, Abdur Rahman AR, Guiseppi-Elie A (2009) Bioactive hydrogel layers on microdisc electrode arrays: cyclic voltammetry experiments and simulations. *Electroanalysis* 21(10):1125–1134
95. Justin G, Finley S, Abdur Rahman AR, Guiseppi-Elie A (2009) Biomimetic hydrogels for biosensor implant biocompatibility: electrochemical characterization using micro-disc electrode arrays (MDEAs). *Biomed Microdevices* 11(1):103–115
96. Abdur Rahman AR, Justin G, Guiseppi-Elie A (2009) Bioactive hydrogel layers on microdisc electrode arrays: impedimetric characterization and equivalent circuit modeling. *Electroanalysis* 21(10):1125–1134
97. Abdur Rahman AR, Justin G, Guiseppi-Elie A (2009) Towards an implantable biochip for glucose and lactate monitoring using micro-disc electrode arrays (MDEAs). *Biomed Microdevices* 11(1):75–85
98. Guiseppi-Elie A (1998) Chemical and biological sensor devices having electroactive polymer thin films attached to microfabricated devices and possessing immobilized indicator moieties. US Patent 5,766,934, 16 June 1998

Self-assembled Nanogel Engineering

Nobuyuki Morimoto and Kazunari Akiyoshi

Abstract Functional nanogels have been designed by the self-assembly of various associating polymers. In particular, cholesterol-bearing polysaccharides form physically crosslinked nanogels by self-assembly in water. The nanogels trap proteins mainly by hydrophobic interaction and show chaperon-like activity. They are useful as polymeric nanocarriers especially in protein delivery. Macrogels with well-defined nanostructures were obtained by self-assembly and chemical crosslinking of these nanogels as building blocks.

Introduction

Polymer nanogels are hydrogels nanoparticles that possess three-dimensional network structures consisting of crosslinked hydrophilic polymers. They can also be formed into nano biomaterials and a variety of nanogels have been reported [1, 2]. Based on their crosslinking, they are either chemically crosslinked nanogels, crosslinked via covalent bonds, or physically crosslinked nanogels that are crosslinked via noncovalent bonds, such as hydrogen bonds, ionic bonds, and hydrophobic interactions.

A new method to form physically crosslinked nanogels was developed via self-assembly of partly hydrophobized polymers. These nanogels are able to interact not only with hydrophobic drugs but also with proteins, nucleic acids, and liposomes to form new hybrid nano complexes. They are useful as nanocarriers and/or biotechnological materials. New hydrogels, by crosslinking of functional substituted group nanogels, have been designed. Functional polysaccharide hydrogels materials are currently being made by self-assembled nanogel engineering for biomedical applications.

Self-Assembled Polysaccharide Nanogels

Pullulan, a linear homopolymer of glucopyranose linked by $\alpha(1 \rightarrow 4)$ and $\alpha(1 \rightarrow 6)$ bonds in a 2:1 ratio, bearing a small number of cholesteryl groups (cholesteryl pullulan (CHP), Fig. 1) forms stable nanoparticles in water [3]. The CHP nanoparticles range in size from 20 to 30 nm. with excellent size monodispersity. They behave like hydrated nanogels with cholesteryl nano domains that act as physical crosslinking points [4]. The size, density, and number of crosslinking domains within the nanoparticles are regulated by the number and the structure of the hydrophobic groups. These CHP nanogels undergo hierarchical

N. Morimoto • Department of Materials Processing, Graduate School of Engineering, Tohoku University, 6-6-02 Aramaki-aza Aoba, Aoba-ku, Sendai 980-8579, Japan

K. Akiyoshi • Institute of Biomaterials and Bioengineering, Tokyo Medical and Dental University, 2-3-10 Kanda-surugadai, Chiyoda-ku, Tokyo 101-0062, Japan
e-mail: akiyoshi.org@tmd.ac.jp

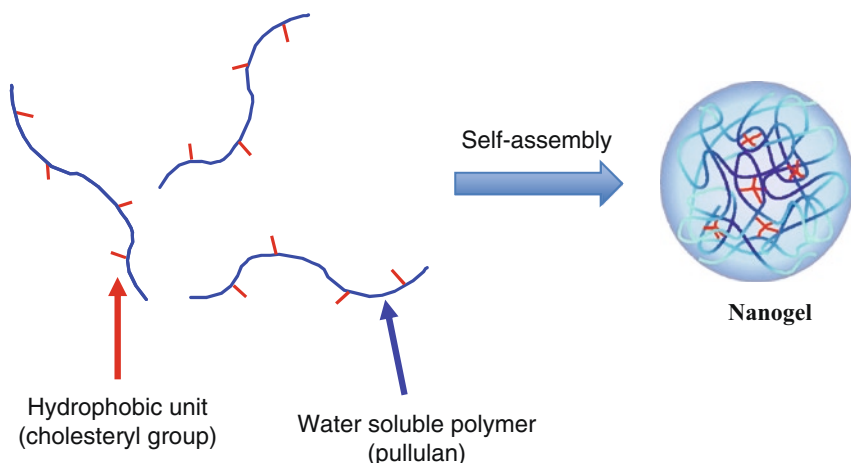


Fig. 1. Schematic representation of self-assembled nanogel of associating polymer.

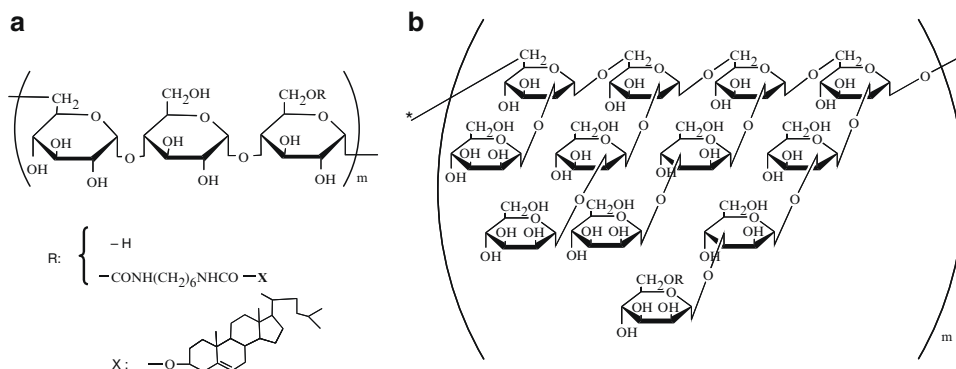


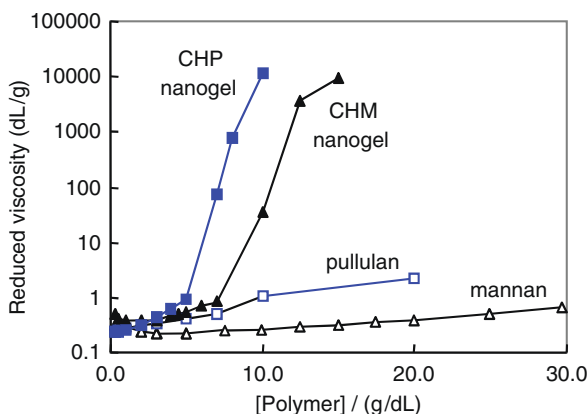
Fig. 2. Chemical structure of (a) CHP and (b) CHM. Reproduced with permission from reference 8.

self-assembly, to form macroscopic gels in semidilute solutions [5]. The impact of the hydrophobic structures and the degree of substitution on the physicochemical properties of the resulting nanoparticles were investigated in detail for a number of polysaccharides, leading to design rules with respect to the hydrophobes [6, 7].

The solution properties of cholesteryl derivatives of mannan, a polymer of mannose, is a highly branched polysaccharide with $\alpha(1 \rightarrow 2)$ - and $\alpha(1 \rightarrow 3)$ -linked mono-, di-, and trimannopyranose side chains with phosphodiester-linked side chains (2.6 phosphorus in 100 mannopyranose units) attached to the backbone of $\alpha(1 \rightarrow 6)$ -linked mannopyranoses (Fig. 2) [8]. Listed in Table 1 are the main structural characteristics of the self-assembled nanogels of CHP and cholesteryl mannan (CHM) with similar molecular weights ($M_w = 5 \times 10^4$) and degree of cholesteryl substitution (one per 100 sugar units). The aggregation number of CHM (7.5) is smaller than that of CHP (11.0) and the hydrodynamic radius of CHM nanogels is ~ 1.7 times larger than that of CHP nanogels. The density of these CHM nanogels is less than that of CHP nanogels and the aggregation number of the cholesteryl moieties (N_{ch}) in CHM nanogels (~ 8.8) is about twice than that of the CHP nanogels (~ 4.4).

Table 1. Physical properties of nanogels

Sample	M_w	M_w/M_n	R_H (nm)	$N_{\text{polysaccharides}}$	Φ_H (g/mL)	N_{ch}	n_{domain}
CHM nanogel	4.1×10^5	1.09	7.5	19.5	0.02	8.8 ± 0.4	2.9
CHP nanogel	6.2×10^5	1.03	11	11.6	0.16	4.4 ± 0.5	9

**Fig. 3.** The reduced viscosity of the aqueous solution of mannan, pullulan, CHM, and CHP. Reproduced with permission from reference 8.

In the semi-dilute regime, CHM nanogels form a macrogel network for concentrations higher than 12.5% w/w, whereas CHP nanogels only undergo macrogelation above a threshold concentration of 8.0% w/w, as revealed by viscosity measurements (Fig. 3). A comparative study of the two types of nanogels revealed that the structure and level of hydration of the polysaccharide chain significantly affected the microscopic structure of the self-aggregates and the microviscosity of the hydrophobic domain within the nanogels. This is attributed to differences in the mobility of the CHM cholesteryl groups which are predominantly linked to short oligomannopyranose branches, whereas in CHP they are linked to the polymer main chain. A schematic representation of the self-assembly of CHM and CHP nanogels is given in Fig. 4.

The self-assembling method enables the formation of novel physically crosslinked nanogels is being widely applied to various hydrophobized polysaccharides and other water-soluble polymers. For example, the synthesized cholesterol-bearing poly(L-lysine) (CHPLL) [9]. Similar to a hydrophobized polysaccharide, CHPLL polymers form a nanogel with relatively monodispersed nanoparticles with approximately 40 nm diameters. A new nanogel with α -helix structure may be induced by folding of the poly(L-lysine) chain during the self-assembly of the cholesterol groups.

Stimuli-Responsive Self-Assembled Nanogels

The driving forces for the formation of the CHP nanogel are the hydrophobic interaction and van der Waal interactions. Other interactions, such as electrostatic interactions and hydrogen bonding may occur as well. Stimuli-responsive molecules are also possible

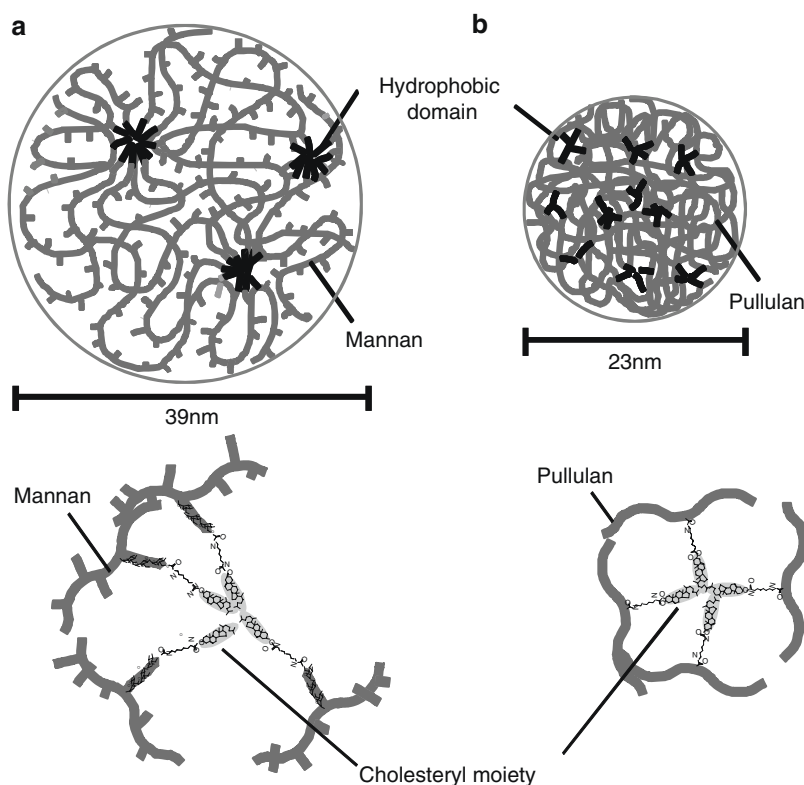


Fig. 4. Schematic illustration of (a) CHM nanogel and (b) CHP nanogel. Reproduced with permission from reference 8.

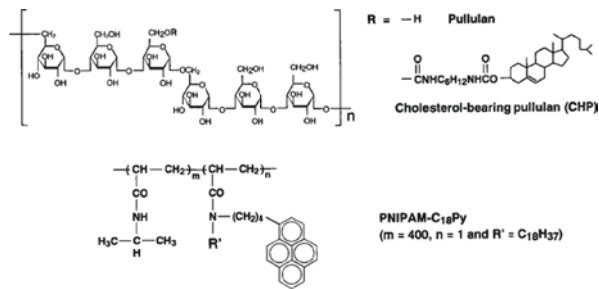
instead of hydrophobic molecules. The various stimuli-responsive nanogels obtained by the self-assembly of functionally associated polymers are outlined below.

Thermoresponsive Nanogels

A hydrophobized thermoresponsive polymer composed of poly(*N*-isopropyl acrylamide) (PNIPAM) partly substituted with alkyl chains (A-PNIPAM) has been prepared [10]. A mixture of two types of hydrophobized polymers, such as CHP and A-PNIPAM, form a hybrid-type nanogel (~40 nm) with hydrophobic physical crosslinking points (Fig. 5a). The assembly and dissociation between the nanogel components occurs by heat-induced controllable responsive properties of PNIPAM.

Another CHP–PNIPAM hybrid hydrogels was synthesized by introducing PNIPAM chains directly onto the CHP nanogel [11]. First, the polymerizable CHP was prepared by the introduction of a methacryloyl group into CHP (CHPMA). The NIPAM monomer was mixed with the nanogel of CHPMA followed by radical polymerization in a dilute aqueous solution. The formation of the CHP–PNIPAM hybrid nanogel is shown in Fig. 5b. The nanogel is able to undergo repeated swelling and shrinking in response to hydration and dehydration of the PNIPAM chain near the phase transition temperature (~32°C). At temperatures 10–15°C higher

a Self-assembly of two hydrophobized polymers



b Copolymerization between polymerizable nanogels and N-isopropylacrylamide

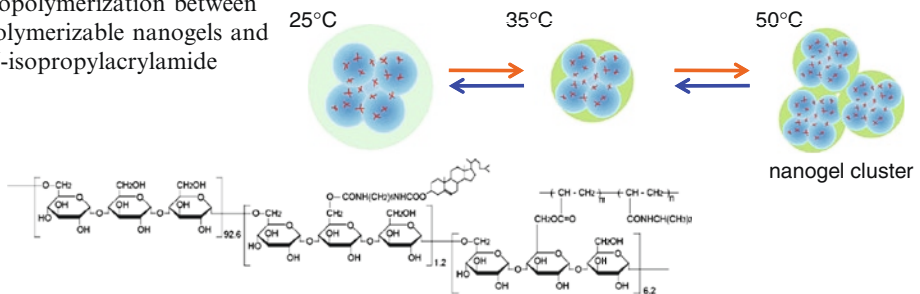


Fig. 5. Thermoresponsive hybrid nanogels.

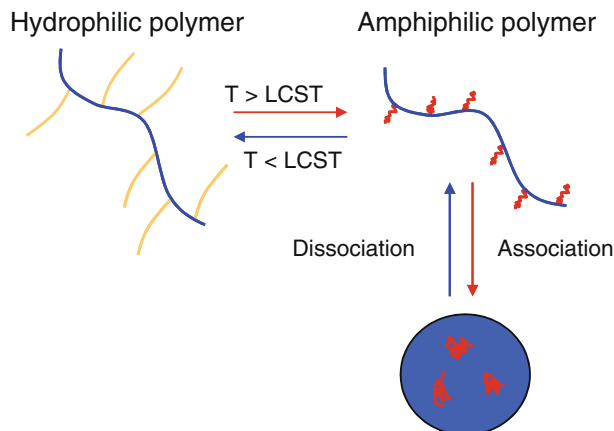


Fig. 6. Pullulan–PNIPAM hybrid nanogels. Reproduced with permission from reference 12.

than the phase transition temperature, the nanogels assemble to form nanogel aggregates that were relatively uniform in size (100–300 nm, depending on the temperature of incubation) and resembled grape-like clusters.

Dual Stimuli (Heat-Redox)-Responsive Nanogels

A new associating polymer was made, in which amphiphilic polymer chains, PNIPAM (Fig. 6) [12] or poly(2-isopropyl-2-oxazoline) [13] were grafted onto pullulan. A redox-responsive associating polymer containing a thiol group on the terminus of the

PNIPAM chain was developed, that forms a disulfide bond after the nanogel formation [14]. Specifically, a small quantity (1–3%) of a chain transfer agent capable of reversible addition-fragmentation chain transfer (RAFT) polymerization with pullulan, NIPAM and a water-soluble initiator were added to perform RAFT polymerization in water. It was possible to control the thermoresponsive temperature of the molecules between 35 and 50°C by adjusting the molecular weight of the PNIPAM. When the molecular weight of PNIPAM side chain was 2,500 or longer and the pullulan–PNIPAM solution was heated above LCST, monodisperse nanogels (25–30 nm) were formed (Fig. 6). The formation of the nanogel was controlled reversibly (by heating and cooling) based on the hydrophilic-to-hydrophobic transition of PNIPAM side chains with temperature.

The characteristic feature of this RAFT polymerization is the easy conversion of a thiol at the terminus of PNIPAM [15]. An assembly of PNIPAM chain with a thiol group on the terminus provided nanogels that were chemically crosslinked via a disulfide bond after formation of the nanogel at a temperature above the LCST. Even after cooling the temperature to lower than the LCST, the structure of the nanogel was maintained as a swollen hydrophilic nanogel. In the presence of a reducing agent, the nanogel can be reduced to the thiol group. Thus a dual-responsive nanogel with both heat- and redox reaction-responsive properties was developed.

Photoresponsive Nanogels

To prepare a photoresponsive nanogel, a spiropyran-bearing pullulan (SpP) as a hydrophobic group can be synthesized by substituting pullulan with a spiropyran molecule which changes polarity in response to light and heat (Fig. 7) [14]. The SpP formed ~75 nm nanogels in water. The assembly was controlled by changing the amphiphilicity of the spiropyran molecule in response to photo-irradiation or heat. Refolding of the chemically denatured proteins after dilution of the protein solution was facilitated by photo-irradiation. SpP nanogels acted as a novel photoresponsive artificial molecular chaperone.

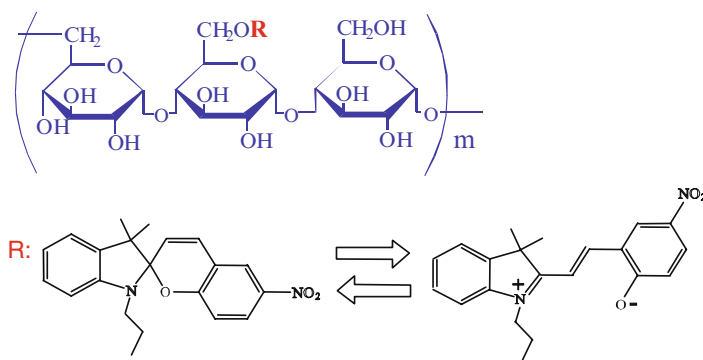


Fig. 7. Chemical structure of spiropyran-bearing pullulan (SpP).

Biomedical Applications of Polysaccharide Nanogels

Physically crosslinked nanogels are different from conventional chemically crosslinked nanogels in their dynamic properties. For instance, the cholesterol-substituted pullulan (CHP) polysaccharide nanogels selectively trap proteins in a hydrophobic interaction, to form nanogel–protein complexes [15, 16]. The dynamic properties of the network were controlled by changing the structure of the hydrophobic group. By host–guest interaction between cholesterol-substituted pullulan and cyclodextrin, the formation and dissociation of nanogels can be reversibly controlled. Using this property, an artificial molecular chaperone can be prepared with controlled uptake and release of denatured proteins [17–19]. This molecular chaperone function is an important development for protein delivery systems.

Many bioactive proteins, such as cytokines, are promising therapeutic agents. However, it is clinically difficult to use most proteins as effective drugs because of their very low stability and pleiotropic actions *in vivo*. To overcome these difficulties, polymer hydrogels are being used to deliver appropriate amounts of excipients, such as growth factors, to target sites in a desired time scale [20–22]. There still remain problems with trapping unstable proteins without denaturation in hydrogels and to control the release of these proteins. To address this issue, for example, we have developed polysaccharide nanogels as protein and peptide delivery systems [23–29].

The induction of a specific immune response against tumor cells is an achievable goal as immune therapy for cancer. For example, a nanogel/oncoprotein complex vaccine was made of CHP complexed with HER2 soluble protein nanogels. In the mouse model, efficient CD8⁺ and CD4⁺ T cell responses that produce high titers of antibodies against HER2 protein were elicited [24, 25]. Clinical trials demonstrated that vaccination with the CHP–HER2 induced HER2-specific CD8⁺ and/or CD4⁺ T cell immune responses [26, 27]. Vaccines made with CHP–NY-ESO-1 against esophageal cancer patients also showed significant tumor suppression [28]. A polysaccharide nanogel delivery system for cytokine, such as recombinant murine IL-12 (rmIL-12) was also developed [29]. For a valid cytokine immunotherapy of malignancies, a suitable delivery system that ensures slow-release of cytokines is required, because of the short half-life *in vivo* and severe systemic toxic effects. After subcutaneous injection into mice, the CHP/rmIL-12 complex and CHP–PEG/rmIL-12 complex led to a prolonged elevation in IL-12 concentration in the sera [30]. Repetitive administrations of the CHP/rmIL-12, but not rmIL-12 alone, induced dramatic growth retardation of pre-established subcutaneous fibrosarcoma without causing serious toxic effects.

To improve the efficiency of nanogel uptake into cells, a cationic group was introduced into the CHP nanogels. Ethylenediamine was added into the CHP nanogel as (CHP–NH₂) and modified to form positively charged nanogels ~30 nm. The CHP–NH₂ nanogels interacted with a variety of proteins and were able to retain the same diameter and positive charge after complex formation [31]. For example, the enzyme activity of β-galactosidase was retained after forming a complex with the CHP–NH₂ nanogel and taken up into HeLa cells. The CHP–NH₂ nanogel–protein complex had lower toxicity and could be efficiently delivered into various cell types even in the presence of serum [31]. Importantly, the introduction efficiency was superior to that of commercially available protein carriers. In order to improve the rate of protein transfer to the cytosol and to modify its ability to carry nucleic acids, such as pDNA and RNAi, libraries of cationic CHP nanogels were constructed with a variety of cationic groups and analyzed for efficiency [32].

Organic–inorganic hybrid nanomaterials for biomedical application were also prepared using polysaccharide nanogels. The CHP and CHM nanogels were used as templates for mineralization of calcium phosphate [33, 34] and apatite [35]. In addition, CHP nanogels–quantum dot complex nanoparticles are being used as bioimaging agents [36, 37].

When a CHP-NH₂ nanogel was mixed with quantum dot-labeled proteins, such as protein A or IgG, complex nanoparticles (~40 nm) were obtained. The complexes were effectively internalized in a variety of cells. The quantum dot-nanogel complexes are being investigated as cell trackers for regenerative medicine [38].

Design and Function of Nanogel-Based Hydrogels Materials

The structure of crosslinking points and the control of the network nanostructure of hydrogels are still major challenges [39]. For conventional bulk hydrogels, it is relatively difficult to determine the structure at the molecular and nanometer levels. In contrast, nanogels offer simple microstructural analyses and intermolecular interactions with proteins or other molecules and readily evaluated. In order to further utilize the properties of nanogels as bulk hydrogels biomaterials, we are developing technologies that utilize nanogels as building blocks to create novel functional hydrogels that are structurally controlled at the nano-level. When CHP nanogels were prepared at semi-dilute concentration (30 mg/mL or higher), they lost fluidity and behaved as hydrogels [5]. From electron microscope observations, the nanogel structure was maintained after macrogel formation; this implied that these hydrogels are nanogel aggregates.

Hybrid gels Crosslinked by Polymerizable Nanogels

Six polymerizable methacryloyl groups per 100 glucose units were introduced into the CHP to form CHPMA nanogels from 4–5 macromolecules with particle diameters of ~30 nm. Approximately 170 polymerizable groups were calculated to be present in a CHPMA nanogel. CHPMA nanogels-crosslinked PMPC hydrogels (CM gels) were obtained by copolymerization of the CHPMA nanogel and 2-methacryloyloxyethyl phosphorylcholine (MPC) under semi-dilute solution conditions (Fig. 8) [40]. Freeze-fracture TEM observations of the CM gels revealed that the nanogels retained their form and were dispersed evenly within

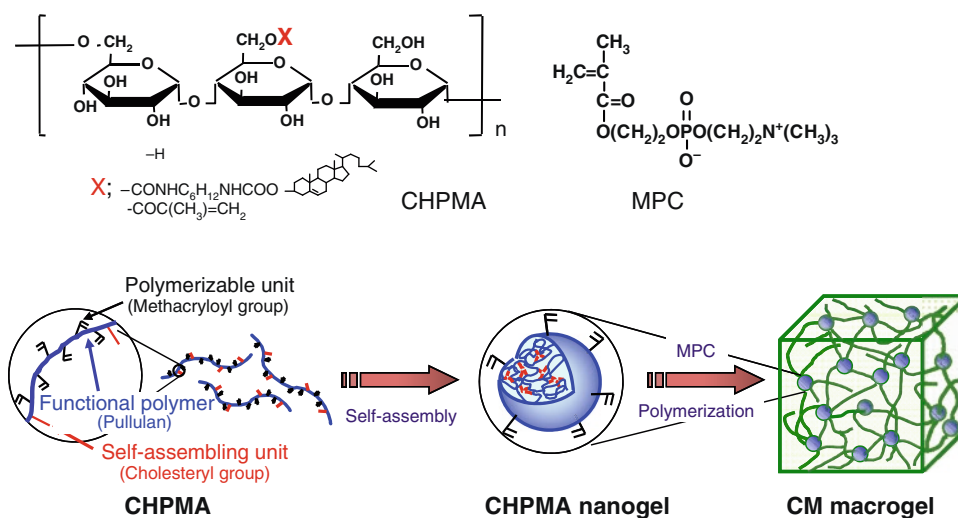


Fig. 8. Schematic illustration of CM macrogel preparation. Reproduced with permission from reference 40.

the hydrogels. The hydrogels is a nanomatrix gels consisting of nanogels as building blocks. Immersion of the CM gels into a solution of FITC-labeled insulin resulted in a spontaneous uptake of 20 times greater than that of the external solution. Furthermore, the addition of cyclodextrin resulted in dissociation of the nanogel physical crosslinks within the CM gels, with subsequent release of the encapsulated insulin. Since the uptake and release of proteins was controllable, the CM gels functioned like an immobilized artificial molecular chaperone [40].

Compared to conventional homogeneous nanogel chaperones, solubilized proteins, by chemical denaturing agents, were efficiently taken up by these hydrogels and the denaturing agent was completely removed by washing with buffer without needing separation from the nanogels. Effective refolding efficiency of various proteins was demonstrated, and is being applied as a regeneration system for inclusion bodies.

Rapid Shrinking Hydrogels Using Nanogel Crosslinker

CHPMA nanogel and the thermoresponsive NIPAM were copolymerized to produce a PNIPAM hydrogels crosslinked by CHPMA nanogels (CN gels). When the hydrogels was transferred from cold water to a hot water bath above LCST, the CN gels rapidly shrank [41]. Compared to the conventional PNIPAM hydrogels by a bifunctional monomer, the shrinking rate of CN gels, determined by half-volume time, was 3,400 times faster. Freeze-fracture TEM images of this gels prepared below or above LCST showed that the distance between nanogels dispersed inside the CN gels was less, above LCST. This indicated that the hydrophilic nano domain of the nanogel formed a path for water release during the shrinking process, thereby, contributing to the rapid shrinking. CN gels are responsive to cyclodextrin and because it is a multifunctional hydrogels with a nano domain, it could be applicable as a stimuli-responsive drug reservoir.

Biodegradable Nanogel-Crosslinked Hydrogels and Application in Regenerative Medicine

Current designs of biodegradable hydrogels are taking advantage of the interactions of nanogels with hydrophobic drugs and proteins. To form these hydrogels, a gelsation method was developed that utilized the Michael addition reaction between acryloyl- and thiol groups [42]. By mixing a nanogel solution of acryloyl group-modified CHP with an aqueous solution of a 4-armed poly(ethyleneglycol) (PEG) with a thiol group at the terminus followed by incubation at 37°C for 1 h, a transparent CHP-PEG hydrogels was obtained (Fig. 9). Electron microscope images showed a nanogel crosslinked gels in which the nanogels were evenly distributed. Hydrolysis of the ester bond connecting the nanogel and the PEG chain resulted in degradation of the hydrogels. This gels could be used as a delivery system in which the nanogel is released by hydrogels degradation.

CHP-PEG hydrogels are useful as controlled-release carriers in regenerative medicine. By allowing the acryloyl group-modified CHP nanogel to absorb prostaglandin E2 (PGE2), a PGE2 encapsulated CHP-PEG hydrogels was prepared [42]. After implanting the gels in the calvaria of mice, new bone formation was confirmed after 4 weeks. The level of new growth was substantially greater than that in a system in which 20 single doses of PGE2 were administered. Furthermore, the CHP-PEG hydrogels system exhibited no side effects, such as increase in the cancellous bone and femur bone formation was facilitated specifically at

6. Akiyoshi K, Sunamoto J (1996) Supramolecular assembly of hydrophobized polysaccharide. *Supramol Sci* 3:157–163
7. Morimoto N, Nomura SM, Miyazawa N et al (2006) Nanogel engineered designs for polymeric drug delivery. In: Svenson S (ed) *Polymeric drug delivery volume ii – polymeric matrices and drug particle engineering*, ACS Symposium Series 924. American Chemical Society, Washington, DC
8. Akiyama E, Morimoto N, Kujawa P et al (2007) Self-assembled nanogels of cholesteryl-modified polysaccharides: effect of the polysaccharide structure on their association characteristics in the dilute and semi-dilute regimes. *Biomacromolecules* 8:2366–2373
9. Akiyoshi K, Ueminami A, Kurumada S et al (2000) Self-association of cholesteryl-bearing poly(L-lysine) in water and control of its secondary structure by host-guest interaction with cyclodextrin. *Macromolecules* 33:6752–6756
10. Akiyoshi K, Kang E-C, Kurumada S et al (2000) Controlled association of amphiphilic polymers in water: thermosensitive nanoparticles formed by self-assembly of hydrophobically modified pullulans and poly(*N*-isopropylacrylamides). *Macromolecules* 33:3244–3249
11. Morimoto N, Winnik FM, Akiyoshi K (2007) Botryoidal assembly of cholesteryl-pullulan/poly(*N*-isopropylacrylamide) nanogels. *Langmuir* 23:217–223
12. Morimoto N, Qiu XP, Winnik FM et al (2008) Dual stimuli-responsive nanogels by self-assembly of polysaccharides lightly grafted with thiol-terminated poly(*N*-isopropylacrylamide) chains. *Macromolecules* 41:5985–5987
13. Morimoto N, Obeid R, Yamane S et al (2009) Composite nanomaterials by self-assembly and controlled crystallization of poly(2-isopropyl-2-oxazoline)-grafted polysaccharide. *Soft Matter* 5:1597–1600
14. Hirakura T, Nomura Y, Aoyama Y et al (2004) Photoresponsive nanogels formed by the self-assembly of spiro-pyrane-bearing pullulan that act as artificial molecular chaperones. *Biomacromolecules* 5:1804–1809
15. Nishikawa T, Akiyoshi K, Sunamoto J (1994) Supramolecular assembly between nanoparticles of hydrophobized polysaccharide and soluble protein complexation between the self-aggregate of cholesterol-bearing pullulan and alpha-chymotrypsin. *Macromolecules* 27:7654–7659
16. Nishikawa T, Akiyoshi K, Sunamoto J (1996) Macromolecular complexation between bovine serum albumin and self-assembled hydrogel nanoparticle of hydrophobized polysaccharides. *J Am Chem Soc* 118:6110–6115
17. Akiyoshi K, Sasaki Y, Sunamoto J (1999) Molecular chaperone-like activity of hydrogel nanoparticles of hydrophobized pullulan: thermal stabilization with refolding of carbonic anhydrase B. *Bioconj Chem* 10:321–324
18. Nomura Y, Ikeda M, Yamaguchi N et al (2003) Protein refolding assisted by self-assembled nanogels as novel artificial molecular chaperone. *FEBS Lett* 553:271–276
19. Nomura Y, Sasaki Y, Takagi M et al (2005) Thermoresponsive controlled association of protein with a dynamic nanogel of hydrophobized polysaccharide and cyclodextrin: heat shock protein-like activity of artificial molecular chaperone. *Biomacromolecules* 6:447–452
20. Kopecek J (2002) Swell gels. *Nature* 417:388–390
21. Hoffman AS (2002) Hydrogels for biomedical applications. *Adv Drug Deliv Rev* 54:3–12
22. Byrne ME, Park K, Peppas NA (2002) Molecular imprinting within hydrogels. *Adv Drug Deliv Rev* 54:149–161
23. Akiyoshi K, Kobayashi S, Shichibe S et al (1998) Self-assembled hydrogel nanoparticle of cholesterol-bearing pullulan as a carrier of protein drugs: complexation and stabilization of insulin. *J Control Release* 54:313–320
24. Gu X-G, Schmitt M, Hiasa A et al (1998) A novel hydrophobized polysaccharide/oncoprotein complex vaccine induces in vitro and in vivo cellular and humoral immune responses against HER2 expressing murine sarcoma. *Cancer Res* 58:3385–3390
25. Ikuta Y, Katayama N, Wang L et al (2002) Presentation of a major histocompatibility complex class 1-binding peptide by monocyte-derived dendritic cells incorporating hydrophobized polysaccharide-truncated HER2 protein complex: implications for a polyvalent immuno-cell therapy. *Blood* 99:3717–3724
26. Kitano S, Kageyama S, Nagata Y et al (2006) Induction of HER2-specific T Cell immune responses in patients vaccinated with truncated HER2 A. *Clin Cancer Res* 2:7397–7405
27. Kageyama S, Kitano S, Hirayama M et al (2008) Humoral immune responses in patients vaccinated with HER2 protein complexed with cholesteryl pullulan nanogel (CHP-HER2). *Cancer Sci* 99:601–607
28. Uenaka A, Wada H, Isobe M et al (2007) T cell immunomonitoring and tumor responses in patients immunized with a complex of cholesterol-bearing hydrophobized pullulan (CHP) and NY-ESO-1 protein. *Cancer Immun* 7:9–20
29. Alles N, Soysa NS, Mian AH et al (2009) Polysaccharide nanogel delivery of a TNF- α and RANKL antagonist peptide allows systemic prevention of bone loss. *Eur J Pharm Sci* 37:83–88
30. Shimizu T, Kishida T, Hasegawa U et al (2008) Nanogel DDS enables sustained release of a cytokine for tumor immunotherapy. *Biochem Biophys Res Commun* 367:330–335

31. Ayame H, Morimoto N, Akiyoshi K (2008) Self-assembled cationic nanogels for intracellular protein delivery system. *Bioconj Chem* 19:882–890
32. Morimoto N, Tamada J, Sawada S et al (2009) Interaction of self-assembled cationic nanogels with oligo-dna and function as artificial nucleic acid chaperone. *Chem Lett* 38:496–497
33. Sugawara A, Yamane S, Akiyoshi K (2006) Nanogel-templated mineralization: polymer-calcium phosphate hybrid nanomaterials. *Macromol Rapid Commun* 27:441–446
34. Yamane S, Sugawara A, Sasaki Y et al (2009) Nanogel-calcium phosphate hybrid nanoparticles with negative or positive charges for potential biomedical applications. *Bull Chem Soc Jpn* 82:416–418
35. Yamane S, Sugawara A, Watanabe A et al (2009) Hybrid nanoapatite by polysaccharide nanogel-templated mineralization. *J Bioact Compat Polym* 24:129–150
36. Hasegawa U, Nomura SM, Kaul CS et al (2005) Nanogel-quantum dot hybrid nanoparticles for live cell imaging. *Biochem Biophys Res Commun* 331:917–921
37. Toita S, Hasegawa U, Koga H et al (2008) Protein-conjugated QD effectively delivered into living cells by a cationic nanogel. *J Nanosci Nanotechnol* 8:1–7
38. Fukui T, Kobayashi H, Hasegawa U et al (2007) Intracellular delivery of nanogel-quantum dot hybrid nanoparticles into human periodontal ligament cells. *Drug Metab Lett* 1:131–135
39. Hennink WE, van Nostrum CF (2002) Novel crosslinking methods to design hydrogels. *Adv Drug Deliv Rev* 54:13–36
40. Morimoto N, Endo T, Iwasaki Y et al (2005) Design of hybrid hydrogels with self-assembled nanogels as cross-linkers: interaction with proteins and chaperone-like activity. *Biomacromolecules* 6:1829–1834
41. Morimoto N, Ohki T, Kurita K et al (2008) Thermo-responsive hydrogels with nanodomains: rapid shrinking of nanogel-crosslinking hydrogel of poly (*N*-isopropyl acrylamide). *Macromol Rapid Commun* 29:672–676
42. Kato N, Hasegawa U, Morimoto N et al (2007) Nanogel-based delivery system enhances PGE₂ effects on bone formation. *J Cell Biochem* 101:1063–1070
43. Hayashi C, Hasegawa U, Saita Y et al (2009) Osteoblastic bone formation is induced by using nanogel-crosslinking hydrogel as novel scaffold for bone growth factor. *J Cell Phys* 220:1–7

Engineered High Swelling Hydrogels

Hossein Omidian and Kinam Park

Abstract High swelling hydrogels (HSHs) are materials with the ability to swell to a large size in an aqueous medium. The swelling feature and mechanical properties of the HSH polymers depend on many factors. Therefore, the HSH properties can be engineered to tailor a hydrogels for a specific application. This chapter begins with the HSH anatomy and its engineering aspects, and continues with the purity of hydrogels and the sources of impurities in HSH polymers. The characterization of HSH polymers includes swelling determination, mechanical properties, and analytical issues, which will be discussed with a focus on both practical and theoretical aspects. Since final hydrogels properties are closely related to the level of its stability, this aspect is discussed by explaining the sources of instability, which potentially threaten the hydrogels properties. The chapter ends with two important groups of hydrogels that have been suggested and engineered for specific applications in pharmaceutical area.

Introduction

Hydrogels are hydrophilic materials that display gelling properties in the presence of an aqueous medium. Depending on the hydrophilicity, crosslink density, ion content, temperature, ionic strength of the swelling medium, and other factors, the hydrogels swelling may range from a few percent to a few thousand times its dry weight. Hydrogels have applications established in hygiene (baby diapers, feminine incontinent products), agriculture (water-retaining agents, soil-conditioning agents), biomedical (contact lenses), pharmaceutical (controlled release matrices), and are rapidly moving into more advanced applications in pharmaceutical (gastric retention and diet aid) and biomedical (scaffolding and tissue culture, tissue expander) industries, in which properties other than swelling are equivalently important.

Hydrogels are classified as ionic, nonionic, and hydrophobically modified. Ionic hydrogels offer superior swelling properties in distilled water. Anionic polymers, such as poly(acrylic acid), poly(sodium acrylate) and poly(potassium acrylate), as well as anionic hydrocolloids, such as sodium alginate offer improved swelling in high pH swelling medium. Low pH solutions provide a better swelling medium for synthetic and hydrocolloidal cationic polymers, such as poly(diallyldimethyl ammonium) chloride and chitosan. For nonionic polymers, the only driving force for the swelling is the polymer-solvent interaction. As interaction increases, so does the swelling. Polymers, such as polyacrylamide, poly(hydroxyethyl methacrylate), and poly(*N*-vinyl pyrrolidone) are not sensitive to the pH but to the type of solvent and the composition of the swelling medium. The hydrophobically modified hydrogels are intended for temperature-sensitive applications where the hydrogels swells and shrinks in response to the temperature change of the swelling medium. Polymers such as poly(NIPAAm),

H. Omidian • College of Pharmacy, Nova Southeastern University, Fort Lauderdale, FL, USA
e-mail: omidian@nova.edu

K. Park • Departments of Biomedical Engineering and Pharmaceutics,
Purdue University, West Lafayette, IN, USA

block copolymers of ethylene oxide and propylene oxide, and methyl cellulose are examples of thermosensitive hydrogels.

Stimuli-sensitive hydrogels that react to changes in pH, temperature, solvent composition, and active ingredients (glucose or antigens) are generally used as sensors or biosensors, actuators, valves, and pumps [1–3]. Food packaging is currently benefiting from the high swelling feature of the hydrogels pad inside the food product. The pad absorbs blood and other fluids, which keeps the product more dry and stable while minimizing the fluid leakage from the packaging.

Engineered Hydrogels

The most demanding properties for high swelling hydrogels (HSHs) are swelling (capacity and rate) and mechanical properties. Nevertheless, the requirements, such as safety and toxicity are also important for specific applications especially in the pharmaceutical and biomedical areas. HSHs swell to a large size at a reasonable rate that is suitable for many specific applications. For example, superporous hydrogels offer large as well as fast swelling kinetics. Shown in Fig. 1 is a very porous HSH that can reach its maximum swelling capacity in just a minute.

The first step in achieving high swelling properties is to generate a structure with a high affinity for water or other aqueous medium. Water affinity is provided by hydrophilicity, chain flexibility, and structural modification (porosity). Structurally, functional groups, such as carboxyl, amide, and hydroxyl that readily form hydrogen bonds, and monovalent ions, such as sodium, potassium, and ammonium are important factors. These groups thermodynamically favor the dissolution process and hence the swelling of the polymer in water. In addition, the inherent electrostatic and osmotic forces also entropically favor the dissolution process. The infinite dissolution of a hydrosol polymer can be controlled by adding crosslinks to the polymer structure, which change the hydrosol to a hydrogels. Depending on the number and types of functional groups, ion types and ion content as well as the crosslink density, the hydrogels can absorb water from a few percent to several thousand times its weight. For example, hydroxyethyl methacrylate, which is used in hard contact lenses is regarded as a low-swelling hydrogels. On the other hand, poly(sodium acrylate) is regarded as a very high swelling (superabsorbent) hydrogels. Although hydrogels candidates should be hydrophilic in structure, these include those classified as nonionic and ionic hydrogels while amphoteric and zwitterionic hydrogels are not very common. Depending on their source, the hydrogels may alternatively be classified as either synthetic or natural-based. Most

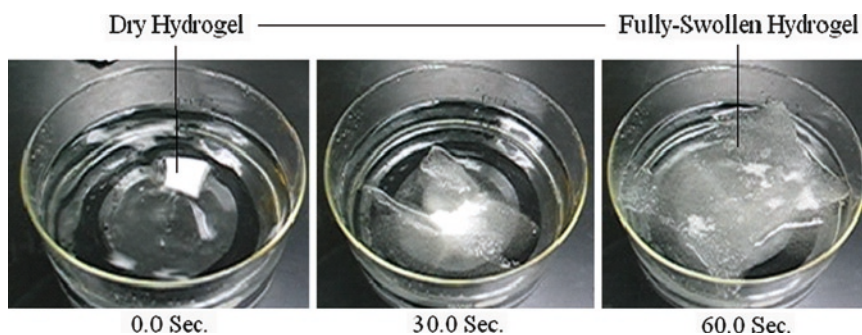


Fig. 1. Swelling capacity and rate of a very porous high swelling hydrogels.

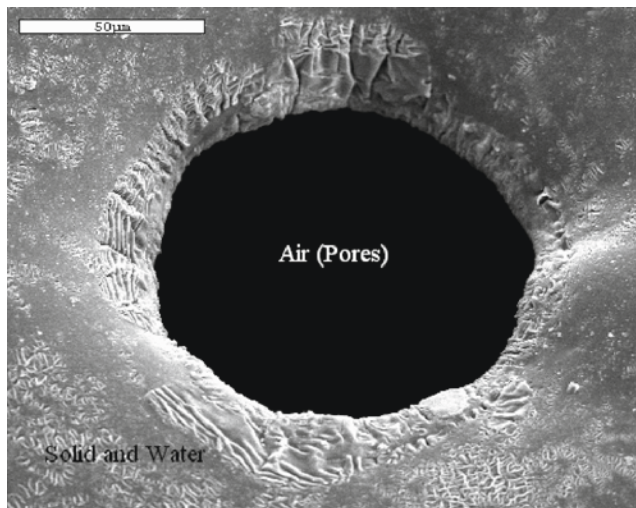


Fig. 2. Anatomy of a hydrogels composite.

HSHs are synthetic, while the natural-based hydrogels are usually modified with water-soluble monomers through a chemical grafting process. Despite the fact that functional groups and ions determine the hydrophilic lipophilic balance (HLB) of a hydrogels polymer, the amount and type of crosslinker critically affect the swelling properties. For a hydrogels with a given HLB value, fewer crosslinker results in increased swelling. The addition of more crosslinks offsets the driving forces for the swelling, and the hydrogels eventually disintegrates at very high crosslinker concentration. This feature has been utilized in making superdisintegrants, which are used to disintegrate tablet and capsule pharmaceutical dosage forms.

In the dried state, most HSHs are a composite of a solid hydrogels, water, and air (pores) as shown in Fig. 2. While the solid part of the composite controls the swelling forces and pressure, the other two phases significantly improve the swelling kinetics. To design hydrogels for a specific application, these three elements need to be carefully considered.

The solid element of each HSH product is composed of a crosslinked hydrophilic polymer. Degree of crosslinking and polymer hydrophilicity are the most important determinants of the swelling properties. Swelling improves in hydrogels with low crosslink density, high hydrophilicity, and high molecular weight. Nonionic hydrogels have low to medium pH-independent swelling, less swelling dependency on salt, and good mechanical properties. On the other hand, anionic and cationic monomers are used to prepare hydrogels with high swelling at high and low pH, respectively. Swelling dependence on ionic strength, inferior mechanical properties, and brittleness in dry and swollen states are characteristics of the ionic gels.

Swelling is improved with bifunctional crosslinkers as opposed to tri or more functional crosslinkers. As crosslinking and functionality increases, the hydrogels becomes more stiff and rigid. One way to make stronger hydrogels with less brittleness is to crosslink the surface of the hydrogels.

Since initiators affect the final hydrogels properties, their selection should be based on the pH, initiator half-life, toxicity, temperature, and solubility. High initiator concentration favors the swelling but increases the initiator impurities. It promotes rapid polymerization and reduces the crosslinking efficiency by generating short polymer chains. An oil-soluble crosslinker provides higher swelling due to its lower efficiency in the aqueous medium.

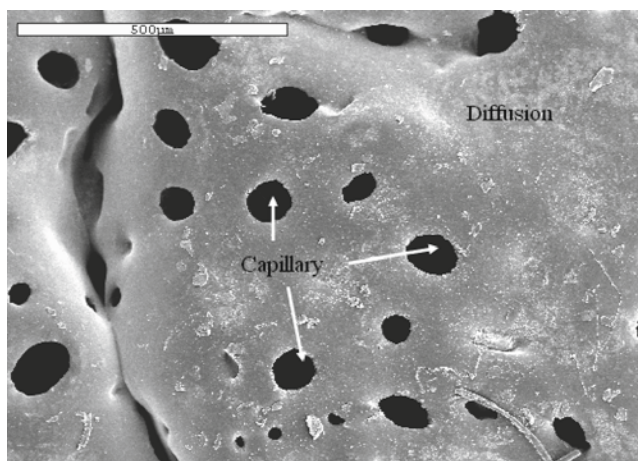


Fig. 3. Hydrogels with diffusional and capillary forces of water transport.

The type and amounts of the monomer, crosslinker, and initiator is critical in preparing a HSH. HSHs with tailor-made properties can be achieved by changing the polymerization method, such as, solution or reverse dispersion polymerizations. For example, an inverse suspension polymerization can be utilized to prepare particulate HSHs with narrow or wide particle size distributions [4, 5]. Higher molecular weight polymers provide better hydrogels swelling and mechanical properties. High molecular weight polymers also reduce the amount of crosslinker by increasing the efficiency of the crosslinking process.

The water component in the composite is bound water that comes from the synthesis step. Generally, the amount of the bound water is about 1–5% and cannot be removed during the drying process; however, the water can be minimized by freeze drying the hydrogels. Water can affect the composite properties positively by plasticizing the polymer, which expedites the initial swelling or diffusion process. A negative effect of water is that it reduces the molecular interactions between the polymer chains and the rigidity of the composite. Water can also facilitate hydrolysis and oxidation reactions during hydrogels storage.

The air component in the composite facilitates the diffusion of external materials into the polymer structure by reducing the intermolecular interactions between the polymer chains. As shown, with highly porous superabsorbent hydrogels in Fig. 3, the interconnected pores provide a rapid diffusion by increasing the capillary action of the transport process. Pores are important for purification or any other processes for which a faster mass transport (such as drying) is desired. The air adversely affects the hydrogels mechanical properties by decreasing the intermolecular interactions. Physical and chemical stability of a hydrogels decreases at higher pore concentration. Pores can lose their structural integrity during storage depending on the water content of the hydrogels, the storage temperature, and the relative humidity of the storage environment. Pores are also responsible for degradative oxidation and hydrolysis reactions.

While the swelling capacity of hydrogels is the sole function of the solid content of the composite, the mechanical properties are a function of all elements – solid, liquid, and gas. The solid part provides mechanical property; the liquid and the gaseous parts of the composite weaken the properties by reducing the intermolecular interaction of the polymer chains which are the only source for the mechanical strength. Many approaches, as listed in Table 1,

Table 1. Approaches to improve mechanical properties of hydrogels

Nanocomposite hydrogels of acrylamide, dimethyl acrylamide, and <i>N</i> -isopropyl acrylamide prepared in an aqueous clay solution via free radical polymerization at room temperature; higher modulus hydrogels obtained by increasing the hydrophobic content of the structure.	[20]
Epichlorohydrin-crosslinked poly(vinyl alcohol) annealed at higher temperature offers high mechanical properties while maintaining high swelling.	[21]
Hydrogels blends made of water soluble polymers of poly(vinyl alcohol–vinyl acetate) and poly(vinyl pyrrolidone) treated with glutaraldehyde.	[22]
Low water content poly(vinyl alcohol) hydrogels prepared by crystallization of the PVA in dimethylsulfoxide/water solution; improved mechanical properties after annealing the polymer at higher temperatures.	[23]
Improve mechanical properties of thermosensitive poly(<i>N</i> -isopropyl acrylamide) hydrogels by grafting the poly(NIPAAm) onto a nonwoven polypropylene.	[24]
Increase mechanical properties of acrylamide hydrogels containing hydroxyapatite via addition of itaconic acid; acid enhances the degree of polymerization by which mechanical property is expected to increase.	[25]
Modify properties of poly(vinyl alcohol) hydrogels by mixing the polymer with a mixture of hydrophilic and hydrophobic monomers of 2-hydroxyethyl methacrylate and methyl methacrylate utilizing ionizing radiation.	[26]
A delivery platform for growth factors based on epichlorohydrin-crosslinked dextran.	[27]
Hydrogels with tunable mechanical and drug release properties by copolymerizing hydroxyethyl methacrylate with a methacrylate-derivative of beta-cyclodextrin; specially suggested for a medicated soft contact lens.	[28]
Poly(vinyl alcohol) hydrogels with improved thermal stability and swelling by adding sodium alginate followed by electron beam irradiation.	[29]
Improve mechanical properties of poly(2-hydroxyethyl methacrylate) by incorporating hydrophobic polycaprolactone.	[30]
Fast swelling and mechanically stable superabsorbent hydrogels based on gum arabic chemically modified with glycidyl methacrylate, acrylic acid, and acrylamide.	[31]
Hydrogels with elastic properties made by crosslinking bovine serum albumin and activated poly(ethylene glycol).	[32]
Effect of crosslink density on particle size of the poly(methacrylic acid) hydrogels prepared in bulk and mechanically ground to different particle sizes; average particle size decreases with increased crosslink density; lower crosslink density provides wider particle size distribution.	[33]
Hydrogels with long term stability based on carboxymethyl starch (from potato) cross-linked with mono- and dichloroacetic acid.	[34]
A composite hydrogels material consisting of a silicone rubber matrix in which particles of a lightly crosslinked polyacrylamide hydrogels are dispersed.	[35]
Glyoxal-crosslinked hydrogels interpenetrated with poly(ethylene glycol) offers elastic properties compared to a crosslinked chitosan.	[36]
Hydrogels based on collagen and modified hyaluronic acid (crosslinked with poly(ethylene glycol diglycidyl ether)) intended as wound dressing material.	[37]
Modify swelling and mechanical properties of amphiphilic urethane acrylate hydrogels by varying the molecular weight of the soft segments and the type of diisocyanate.	[38]
Crosslinked poly(vinyl alcohol-vinyl pyrrolidone) hydrogels with barrier properties prepared via free radical solution polymerization using potassium persulfate; barrier properties against common microbes.	[39]
Chitosan poly(acrylic acid) interpenetrating networks prepared by UV irradiation offering good mechanical properties due to interchain complexation of the amino (chitosan) and carboxyl (acrylic acid) groups.	[40]

(continued)

Table 1. (continued)

Amphiphilic semi IPN hydrogels made by grafting acrylic acid onto cationic starch in mild aqueous medium of poly(dimethyldiallylammonium chloride); offers high compressive strength in their swollen state.	[41]
Modified photocrosslinkable hydroxypropyl chitosan as a porous scaffold.	[42]
Monitoring chemical crosslinking of hydrogels by means of ultrasonic wave propagation and low frequency dynamic mechanical analysis; correlate ultrasonic behavior to the degree of crosslinking.	[43]
Improve mechanical properties of poly(<i>N</i> -vinyl pyrrolidone) by grafting the polymer onto a nonwoven polypropylene grafted with methyl methacrylate.	[44]
Interpenetrating hydrogels of gelatin and poly(<i>N</i> -vinyl pyrrolidone) prepared in aqueous solution using potassium persulfate and glutaraldehyde offers high compression strength.	[45]
Stimuli-sensitive semi IPN of sodium carboxymethyl cellulose and poly(<i>N</i> -isopropyl acrylamide) loaded with inorganic clay offers high tensile strength and high deformation.	[46]
Improve mechanical properties of ionotropically gelled chitosan (using tripolyphosphate) with the addition of clay or cassava starch granules.	[47]
Crosslinker-free preparation of polyacrylamide hydrogels in the clay suspension; clay behaves as crosslinker.	[48]
Prepare strong hydrogels by dispersing montmorillonite clay into aqueous monomer solution	[49]
A polyacrylamide nanocomposite loaded with bentonite clay; study the effect of cationic surfactant (cetylpyridinium chloride).	[50]
Free radical polymerization of monomers with different hydrophilicity (Acrylamide, <i>N</i> , <i>N</i> -dimethylacrylamide, <i>N</i> -isopropylacrylamide) in clay dispersion; the extent of clay-polymer interaction dictates the level of improved mechanical properties (NIPAAm and DMAAm do better than acrylamide).	[20]
Interpenetrating networks of acrylic acid and poly(ethylene glycol) with pH-sensitive mechanical properties.	[51, 52]
Interpenetrating networks of bacterial cellulose with gelatin, sodium alginate, gellan gum, or iota-carrageenan with high mechanical strengths.	[53]
Correlation between swelling/ mechanical properties of hydrogels and the solvent composition during synthesis.	[54]
Poly(<i>N</i> -vinyl pyrrolidone) based hydrogels modified with kappa- and iota carrageenans; prepared by gamma irradiation of the ingredients in air at ambient temperature; display mechanical stability and pH-responsive swelling properties.	[55]
Semi-IPNs of poly(<i>N</i> -vinyl pyrrolidone) and beta-chitosan crosslinked with glutaraldehyde.	[56]
Interpenetrating hydrogels networks of crosslinked polyacrylamide and gelatin crosslinked via UV irradiation; suggested for cold or hot packs.	[57]
Use of polyacrylonitrile fibers with good swelling and shrinking properties as microactuator.	[58]
Semi IPN hydrogels networks of chitosan and chitosan-carbon nanotube with good mechanical properties prepared via prefreezing and sequential freeze drying using glutaraldehyde as crosslinker.	[59]
Thermosensitive hydrogels based on chitosan and poly(vinyl alcohol) loaded with sodium bicarbonate; liquid at low temperature but gels under physiological conditions.	[60]
Poly(vinyl alcohol) hydrogels prepared by quenching PVA solutions in water or in aqueous dimethylsulfoxide; change in hydrogels properties by changing DMSO concentration, initial PVA concentration, and quench temperature; high DMSO and PVA concentration improve the mechanical properties.	[61]
Branched copolymers of poly(NIPAAm) and poly(ethylene glycol) as in situ forming replacement for the nucleus pulposus of the intervertebral disc; gels elasticity dependent on the PEG block molecular weight and PEG content.	[62]

(continued)

Table 1. (continued)

pH- sensitive carboxymethyl cellulose hydrogels prepared by ionizing radiation of highly concentrated CMC solutions.	[63]
Nanocomposite hydrogels of hydroxyapatite-poly(vinyl alcohol) as artificial cornea fringe with interconnected porous structure, good swelling, and mechanical properties.	[64]
Semi interpenetrating nanocomposite prepared by grafting acrylic acid onto starch in an aqueous dispersion containing cationic polyacrylamide/ bentonite; high swelling and mechanical properties.	[65]
Irradiated carboxymethyl chitin in aqueous solution offers a pH sensitive hydrogels with good swelling and excellent mechanical properties.	[66]
Photo-crosslinkable dendritic polymers with stable integrity and mechanical properties as hydrogels scaffold for cartilage repair; hydrogels is based on tri-block copolymer consisting of a poly(ethylene glycol) core and methacrylated poly(glycerol succinic acid) dendrimer terminal blocks.	[67]
Genetically engineered elastin-like polypeptides of Val-Pro-Gly-X-Gly repeats, crosslinked with tris-succinimidyl aminotriacetate after expression in <i>E. coli</i> and purification.	[68]
Polycaprolactone diol, polyethylene glycol (both as soft segments), lysine diisocyanate (hard segment), and 2-hydroxyethyl methacrylate polymerized under UV irradiation to a degradable light-curable elastic polyurethane hydrogels.	[69]
<i>N</i> -isopropylacrylamide grafted onto thin porous polypropylene films using irradiation to improve its mechanical properties.	[70]
HEMA used to enhance mechanical properties of thermosensitive hydrogels based on poly(<i>N</i> -isopropylacrylamide) and methacrylic acid or poly(NIPAAm) and acrylic acid; while NIPAAm offers thermosensitivity, the methacrylic or acrylic acid part offers pH sensitivity, and HEMA enhances the mechanical property and integrity of the terpolymer hydrogels.	[71]
Utilize chemical crosslinking and ionotropic gelation to prepare elastic high swelling hydrogels of acrylamide and calcium-treated alginate.	[72]
Introduce different approaches to increase mechanical properties of superporous hydrogels.	[73]
Tailoring mechanical properties of superporous hydrogels through ion equilibration.	[11]
Superporous hydrogels for applications in very harsh swelling medium; pH-independent swelling and mechanical properties.	[12]
Superporous hydrogels of glycol/chitosan/PVOH with improved mechanical properties by multiple cycles of freeze-thawing and drying.	[74]
Acidified poly(acrylamide-co-acrylic acid) superporous hydrogels with improved mechanical properties.	[75]
Improve mechanical properties by increasing monomer concentration during the hydrogels synthesis.	[76]
Crosslinking poly(vinyl alcohol) using epichlorohydrin, followed by drying at high temperature of 90°C; improved mechanical properties due to formation of microcrystalline domain.	[21]
Photoreactive gelatin using 3,3,4,4'-benzophenone tetracarboxylic dianhydride and 2-hydroxyethyl methacrylate with swelling properties upon irradiation; potential use as protective wound dressings and hemostatic absorbents for less invasive surgeries.	[77]
A fast swelling and mechanically stable superabsorbent hydrogels based on modified gum arabic, glycidyl methacrylate, acrylic acid, and acrylamide.	[31]
Crosslinked plasticized poly(<i>N</i> -vinyl-2-pyrrolidone) prepared using an electron beam irradiation in the form of a composite with agar and poly(ethylene glycol); a hydrogels membrane containing 10% PVP, 1–3% agar, and PEG irradiated at 25 KGy dose found to be elastic, transparent, flexible, sterile, and impermeable to bacteria.	[78]
A hydrogels blend based on poly(vinyl pyrrolidone) and poly(vinyl methyl ether) prepared using electron beam irradiation and gamma irradiation of their aqueous solutions; bio-compatible and temperature sensitive.	[79]

(continued)

Table 1. (continued)

Gamma irradiation of an aqueous solution of poly(vinyl pyrrolidone) along with agar and poly(ethylene glycol) using a Cobalt-60 source at room temperature; an elastic, transparent, and flexible film impermeable to bacteria.	[80]
Poly(sodium L-glutamate) to modify elastic properties of PVOH hydrogels; blending the concentrated aqueous solutions of the two polymers, followed by high pressure thermal treatment; glutamate improves the hydrogels elastic modulus via interaction with PVOH chains.	[81]
Studying swelling and elastic properties of gelatin gels.	[82]
Effect of a tetrafunctional (N,N'-methylenebisacrylamide) and an octafunctional crosslinker (glyoxal bis(diallyl acetal) in preparation of thermosensitive hydrogels based on isopropylacrylamide and acrylic acid.	[83]
Poly[1-(3-sulfopropyl)-2-vinyl-pyridinium-betaine] synthesized to high conversion by free radical polymerization of the zwitterionic monomer and methylenebisacrylamide crosslinker in solution; improved elastic modulus with increase in crosslinker concentration.	[84]

have been used to improve the hydrogels mechanical properties by changing the hydrogels structure (types and concentrations of monomer, crosslinker), hydrogels synthesis (reaction conditions, initiator type and concentration, adding other excipients), and hydrogels processing (treatment and various drying techniques).

Purity of HSHs

The most important considerations, in any purification process, are to maintain the polymer properties (swelling and mechanical), to avoid additional unwanted impurities, to avoid polymer degradation, and cost effectiveness. To reduce the level of residual monomers inside the hydrogels, chemical and physical methods are used. With the former, an additive (a second monomer or a catalyst) is added at the end of the reaction to react with the unreacted monomers. Increasing the temperature and vacuum may also reduce the monomer level. For the latter, electron beam radiation, ultraviolet radiation, monomer stripping followed by ozonation as well as distillation followed by supercritical devolatilization have been employed [6].

Impurities in a HSH product can be classified into three groups: synthesis impurities, washing impurities, and drying impurities. The synthetic impurities are from the synthesis step and trapped inside the hydrogels network structure are usually called primary impurities. These impurities are rinsed out of the network using washing solutions composed of water and alcohol at different concentrations. Reducing the size of the hydrogels (if applicable) significantly improves the efficacy of the washing step. Although concentration of the primary impurities can be reduced down to an acceptable level for most applications, the water and alcohol should also be removed from the hydrogels. To remove the water, the hydrogels can be placed in different aqueous solutions containing various concentrations of alcohol. The alcohol is then removed by utilizing an efficient drying process, such as, forced oven drying at low temperature of $\sim 40^{\circ}\text{C}$. Another category of impurities originate during the storage of hydrogels as a result of hydrogels interaction with the environmental factors such as moisture, oxygen, ozone, excipients, etc. Shown in Fig. 4 are the different steps needed to purify a HSH using water alcohol mixtures.

The flexibility of the hydrogels during the washing and drying steps is still a critical factor in purification. Increased flexibility causes the polymer chain to move faster and easier

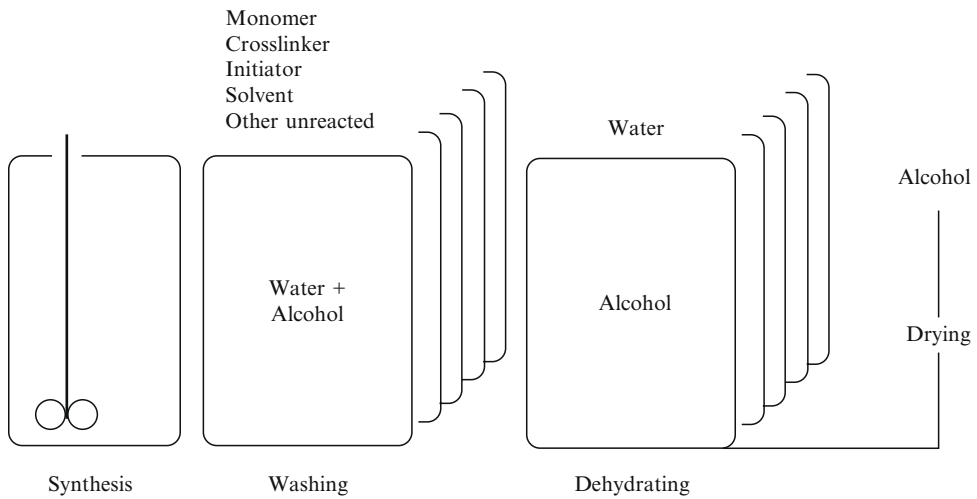


Fig. 4. An example of a very effective purification process for high swelling hydrogels.

making the monomer removal by diffusion more efficient. Flexibility is achieved using higher temperatures. A low glass transition monomer during the synthesis provides internal plasticity to the polymer, which in turn would make the purification process more effective. For example, a low concentration of an acrylate ester monomer can be added during the synthesis of highly swelling poly(acrylic acid) hydrogels [7].

The heterogeneity of the hydrogels is especially critical for porous hydrogels as highly heterogeneous pore morphology may result in higher impurity levels in the product. It has been shown that the impurity level of SPH products can be reduced by improving the way that sodium bicarbonate is dispersed in the reacting medium [7]. Another aspect is the particle size and its distribution, which is especially important for hydrogels prepared by inverse suspension techniques. Usually, the particle size may vary in the range of 100 μm to 1mm with the average size of 250–300 μm . The larger particles have smaller surface areas and require more washing than the smaller particles. For superporous hydrogels, the hydrogels homogeneity is highly dependent on the pore distribution throughout the hydrogels. Apparently, the more porous areas of the hydrogels absorb washing solution faster and hence the impurities are removed faster. Therefore, washing may work better and becomes more effective for the more porous than the less porous areas of the hydrogels.

A washing with water or water-alcohol mixtures requires the hydrogels to be stable in the swollen state in that specific solution. Very low or high swelling may cause a less efficient purification and a loss of hydrogels integrity. To optimize the size of the swollen hydrogels for the washing step, the swelling transition of the hydrogels in the mixed solvent and nonsolvent should be determined. Swelling transition occurs at lower alcohol concentrations with more hydrophilic hydrogels.

Another purification process is to induce cycles of hydrogels shrinking and swelling in the washing solutions. Two solutions with different nonsolvent concentrations (below and above the transition point concentrations) can be used to induce the swelling and shrinking of the hydrogels. If the hydrogels is strong enough in the swollen state, the physical techniques, such as rubbing, filtration, and centrifugation, can also be utilized to reduce impurities [7].

Hydrogels Characterization

Determination of swelling: Swelling is a thermodynamic process in a way that hydrogels has to reach its maximum or equilibrium capacity in the swelling medium. It is also a kinetic process due to the fact that the swelling is time dependent and many factors may affect how fast a hydrogels can swell in the swelling medium. Although swelling can be measured at any conditions, for qualitative or quantitative purposes, the most reliable method of measuring swelling is to mimic the real swelling conditions. If the hydrogels during service is expected to face high temperature, mechanical load, chemical stress, light, or salts, these factors have to be included in the swelling evaluations.

Generally, swelling data is collected by saturating the hydrogels in the swelling medium (distilled water, saline, simulated gastric fluid, buffers, simulated intestinal fluid, or blood), and measuring the amounts of fluid absorbed at specific time intervals until maximum capacity is reached. The most common and straightforward way of swelling evaluation is conducted under no load conditions and is called free swelling. A reliable free swelling measurement requires the hydrogels particles to be completely separated, so that the whole hydrogels mass is equally exposed to the swelling medium. Particles are dispersed under moderate to vigorous agitation into the swelling medium and are left to reach maximum or equilibrium swelling capacity. The swollen particles are filtered using a sieve and then weighed. For solid poreless hydrogels, the method is appropriate but the reliability is diminished with hydrogels porosity. The free swelling data for porous hydrogels have higher error bars because the pores act as temporary reservoirs for water, which give rise to higher swelling readings. In these cases, the hydrogels is centrifuged to remove the interstitial water between the particles and within the pores. The centrifugal force has to be adjusted to assure complete removal of the unbound water and to avoid hydrogels breakdown.

Although free swelling is driven by an entropically favored dissolution of the polymer in the swelling medium, it can also be enhanced by the generation of electrostatic and osmotic forces. However, the swelling, or the so called controlled dissolution process, is limited due to the negative elastic forces imposed by the crosslinks. If the hydrogels is expected to serve in a physically loaded environment, its swelling capacity has to be measured under a given load. For some applications, swelling, either free or loaded, is measured by dimension. The result can also be extended to volume and the equilibrium swelling can be expressed as either dimensional increase or volume increase. Loaded swelling capacity can also be measured by using a texture analyzer [8].

Swelling model: A parallel assembly of a spring (elastic) and a dashpot (viscous), as shown in Fig. 5, is used to predict three important features in water absorption process of the HSH polymers [9]. The spring and the dashpot represent the expansion and relaxation forces within the hydrogels. When the assembly is loaded under a fixed stress (σ), the whole system deforms to a constant deformation of ϵ . If the elastic and viscous elements of the system are represented by E (spring modulus) and η (fluid viscosity), the equilibrium deformation (maximum swelling capacity), the initial rate of deformation, and the retardation time (time to reach 63% of the equilibrium deformation) would be represented by σ/E , σ/η , and η/E , respectively. The equilibrium swelling is determined by the expansion forces of the hydrogels, and the initial rate of expansion is determined by the relaxation of the polymer chains. The retardation time, or deviation from an elastic behavior is a function of both expansion forces and relaxation barriers [9]. The swelling behavior of hydrogels is very consistent with the deformation behavior of the Voigt element under a constant load (Fig. 6).

At a fixed relaxation to expansion ratio (fixed retardation time), the swelling capacity of a given hydrogels can be increased by decreasing the number of crosslinks (Fig. 7). The

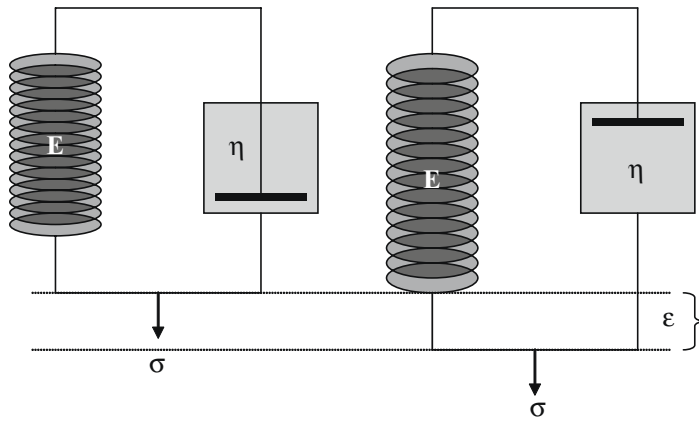


Fig. 5. A Voigt assembly.

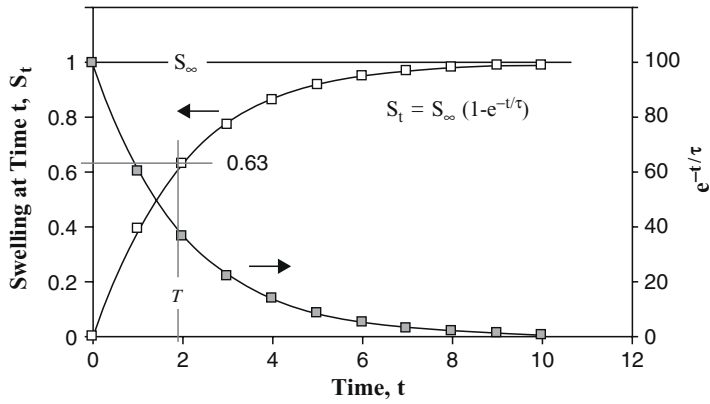


Fig. 6. Theoretical swelling or deformation based on a Voigt model.

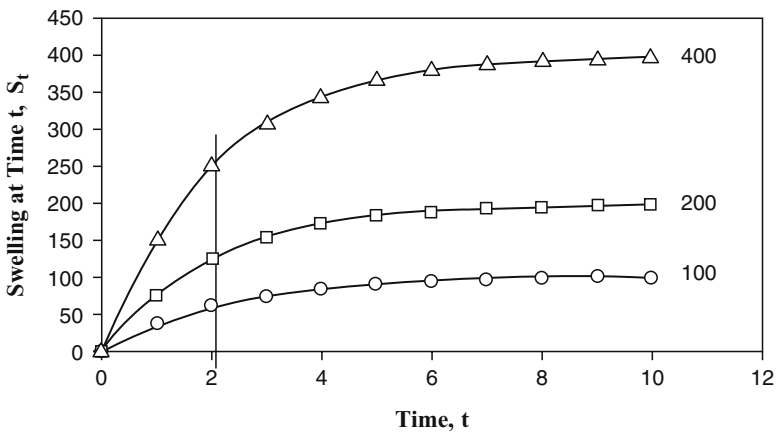


Fig. 7. Swelling kinetics at constant retardation time but various expansion forces.

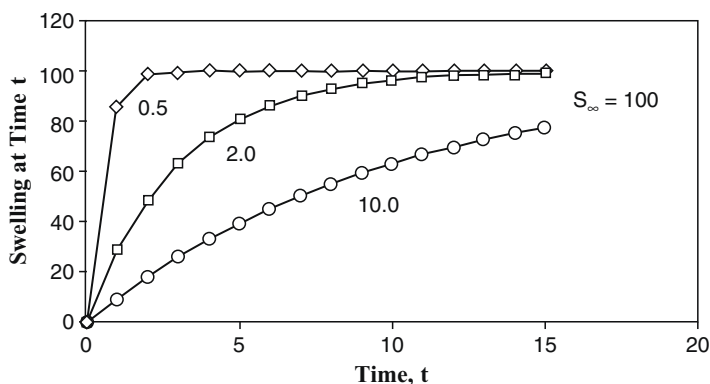


Fig. 8. Swelling kinetics at constant expansion forces but different retardation times.

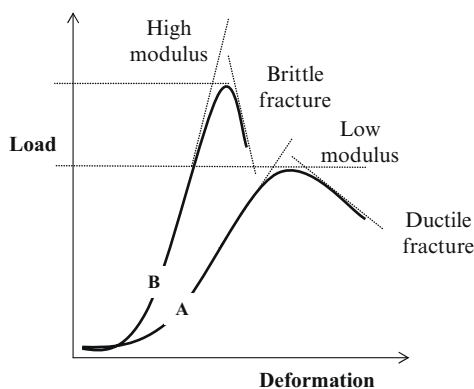


Fig. 9. A typical mechanogram of a hydrogels obtained from of a mechanical tester.

swelling rate of a hydrogels is dependent on the barrier imposed by the relaxation of the polymer chains as shown in Fig. 8. At a given ionic content and functional group concentration, the expansion forces within the hydrogels are solely determined by the crosslink density, which is a measure of the elastic forces. This inversely affects the retardation time. As crosslink density of a hydrogels (the elastic forces) increases, the time to reach 63% of the equilibrium capacity decreases. An increase in porosity imposes a similar effect by lowering the intermolecular interaction between the polymer chains.

Mechanical properties: Similar to swelling, the mechanical properties of the hydrogels have to be determined under close to real conditions such as temperature, pressure, static or dynamic loading, saline, and so on and so forth. This is particularly important for applications with high demand properties. For example, a swellable platform has been suggested to prolong the retention of an active ingredient in the stomach [10–12]. The platform is expected to swell to a large size in less than 10 minutes and hold the active for hours while maintaining its own integrity in the harsh stomach conditions. The platform during its service for this application faces a very low pH environment, strong contraction and expansion forces, food, hot or cold beverages, salt, as well as other factors. The platform should have the ability to be degraded after its service is done. This application requires the hydrogels to maintain its mechanical integrity for some time. The static and dynamic mechanical properties of hydrogels can be simply measured by a mechanical tester or texture analyzer. Under static conditions (one time loading), the equipment provides

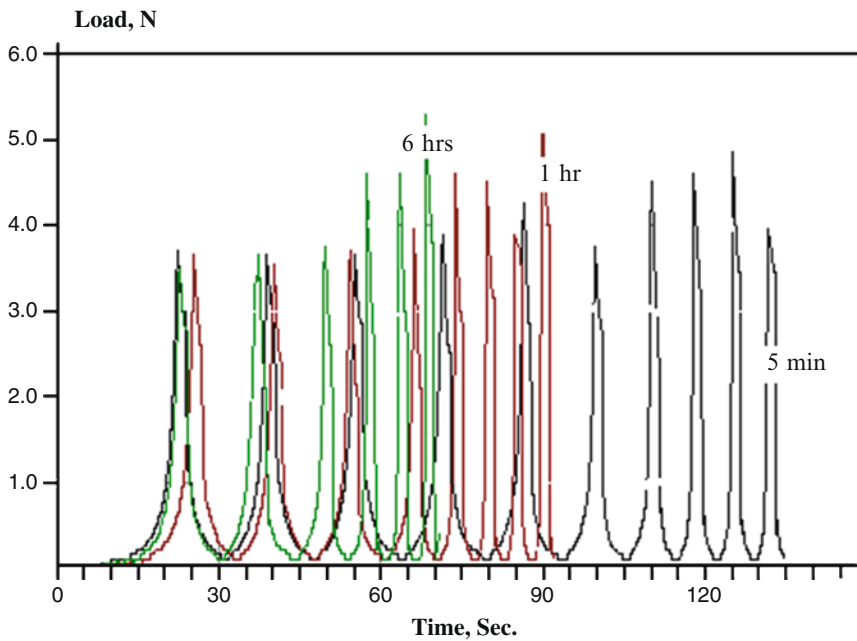


Fig. 10. A hydrogels under fatigue study.

three important data: failure point, modulus, and mode of fracture or failure (Fig. 9). With a lower breaking point and an extended deformation, a lower modulus swollen polymer “A” would fail under a ductile behavior. A higher modulus swollen polymer “B” with a higher breaking point and a limited deformation would display a brittle fracture mechanism. The fatigue properties of the swollen hydrogels can be evaluated under dynamic loading. The number of loading/unloading cycles that a swollen hydrogels can resist before it fails is an indication of hydrogels durability. The dynamic mechanical properties of an acrylate–chitosan hydrogels hybrid after swelling in 0.1 N HCl after 5 minutes, 1 and 6 hours in the acidic swelling medium is shown in Fig. 10. A variable dynamic load of 1–3.5 N was applied, and the swollen hydrogels started losing its integrity following a long retention in the acidic swelling medium. A unique mechanical tester has been designed with the ability to determine contraction and expansion forces based on a “water hammer” theory [13, 14]. The equipment generates mixed forces of compression, tension, bending, and twisting, and the test hydrogels receives almost the same amount of force throughout its body. The hydrogels will eventually lose its integrity and start failing at the weakest spot, which will be the starting point for the craze and crack formation and disintegration of the whole platform. The equipment measures the total amount of energy, which is adequate to break the hydrogels.

Porosity: Pores within the structure of HSHs are generally intended for faster swelling kinetics. In this regard, the pore characteristics such as pore size and its distribution as well as pore shape are instrumental. While the former affects the swelling kinetics, the latter provides anisotropy to the swelling behavior [15]. Porosity of the porous HSH polymers can be studied and evaluated by different techniques, such as, scanning electron microscopy [16, 17], mercury porosimetry [18], liquid intrusion [19], and image analysis. In mercury porosimetry, differential pressure on mercury and the intrusion volume of mercury are measured. The data are used to calculate volume, diameter, volume distribution, and surface area of the pores. The pore size data can be correlated to the overall porosity of the hydrogels. Using liquid extrusion techniques, a given amount of the hydrogels is placed in the test cell and is saturated with water up

to its maximum swelling capacity. Pressurized air is then used to extrude all the water by gradual increase in air pressure. Data on differential gas pressure and volume of the extruded liquid are used to calculate volume, volume distribution, and the surface area of the pores.

Analytical issues: The two most common pieces of equipment for determining the residual monomers and other unreacted impurities are HPLC and Gas Chromatography. Monomers, such as acrylic acid or potassium acrylate, as well as crosslinkers, such as poly(ethylene glycol) diacrylate, can be monitored using gradient elution high performance liquid chromatography. An aqueous phosphoric acid or acetonitrile solution is generally used as the mobile phase. The hydrogels particles have to be extracted with an efficient and reliable solution for a given time. The supernatant fluid left after the centrifugation is then analyzed. The initiator residues, liquid monomers, hydroquinone stabilizer, ethanol (dehydrant) as well as acids can be monitored using gas chromatography techniques. Although selecting the analytical equipment and mobile phases are important considerations, the extraction process remains the most challenging analytical step. The rule of thumb is: *“the faster the swelling is, the more impurities would be extracted over a given time period”*. Therefore, the same analytical method should not be used to characterize a poreless and a porous hydrogels. The same applies to porous hydrogels with different pore contents. Porosity facilitates the extraction process as it does with the swelling. Apparently, a successful analytical method needs to be modified for a less porous or poreless hydrogels. The modification may include selecting more efficient extracting solutions, extraction at a higher temperature, or for a longer time period.

Hydrogels Stability

A HSH is attractive for applications where high swelling is the most desirable property. This requires that the swelling capability of the hydrogels remain stable over the storage period (stable shelf life) and application period. There are many examples where a hydrogels may lose its specified swelling capacity and rate as well as its mechanical or even adhesion properties. A summary of instability sources in HSHs that eventually affect the final hydrogels properties is given in Table 2.

The stability study would be realistic if the hydrogels stability is tested under real service conditions. The hydrogels may lose its structure, may have its functional group reacted with another excipient, or lose its pores and pore morphology (shape and size); all these have to be considered for a stability study. Generally, the stability study would involve looking at the appearance of the hydrogels (color, stain, crack, pore size, and shape), the swelling properties (capacity and rate), and the extractable chemicals (any impurities which might be generated during the stability period). Since most hydrogels contain certain amounts

Table 2. Instability sources in high swelling hydrogels

Moisture	Causes hydrolysis; catalyzes oxidation; suppress pores; loss of compressibility; difficult handling; increased contamination.
Temperature	Suppress pores; loss of compressibility; expedites degradative reactions.
Light	Chromophore containing hydrogels may degrade photolytically.
Excipients	Hydrogels structure may interact with other excipients if formulated into a dosage form like a tablet; significant effect in the presence of ions.
Oxygen	Oxidation; reaction with the hydrogels and unreacted monomers; color change.
Packaging	Reaction of hydrogels or its reactive components with packaging material; severe reaction between aldehyde-containing or ion-containing hydrogels with gelatin.

of water in their dry state, there would be a risk of unwanted physical and chemical reactions. In view of the fact that the hydrogels medium is wet (1–5% water content), it may catalyze other reactions, such as oxidation. Hydrogels interaction with the service excipients such as stomach acid, food, beverages, and its housing material (capsule) needs to be included in the stability study.

Engineered HSH Polymers

Two major pharmaceutical applications for the HSHs are gastric retention and diet aid. A gastric retention platform is intended to prolong retention of an active pharmaceutical in the gastric medium. A diet aid is intended to fill the stomach volume in order to induce a sense of fullness or satiety. The hydrogels swells to a very large size, which potentially activate the stretch and mechano-receptors of the stomach providing a sense of fullness. For both applications, the service environment is the dynamic stomach, where that has very harsh conditions, such as low pH, contraction/expansion forces, food effect, salt, temperature, static and dynamic loading, subject to subject variability, as well as other factors. In general, hydrogels for these applications swell very fast in the stomach medium and should remain stable during their service. Normally, the hydrogels should take less than 10 min to reach the maximum swelling capacity. This assures that water taken with the hydrogels with the half-life of about 25 min is absorbed by the hydrogels before it is emptied from the stomach. For the gastric retention and diet applications, the hydrogels size should be designed based on the pylorus size and the stomach size, respectively. This means a potential hydrogels for these applications should occupy a volume of $\sim 30 \text{ cm}^3$ and $\sim 400 \text{ cm}^3$, respectively as shown in Fig. 11. The gastro retentive and diet platforms are expected to be administered as single and multiple doses, respectively.

The most important consideration for both applications is the rate of gastric emptying. Since protein, carbohydrate, fat, and water contents of the foods are different, the food effect on gastric emptying varies. The higher caloric foods have longer retention, solids have longer retention than liquids, and beverages, including water, potentially promote gastric emptying. Indigestible fibers and larger objects usually prolong retention. To minimize variability of the stomach motility between the human subjects, food (even a low caloric one) needs to be taken with the hydrogels platform; otherwise, the platform could leave the subjects' stomach in a few minutes to a few hours. The oral dosage of the platform should be taken in encapsulated form to minimize the risk of esophagus obstruction. The platform design should be simple and cost effective to be commercially attractive. Moreover, the platform should have minimal effect on the drug release unless the platform itself is intended for controlled delivery of the

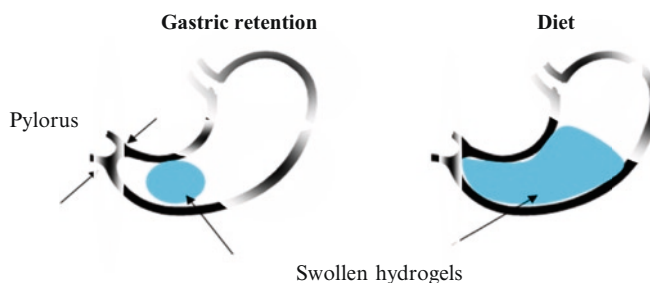


Fig. 11. Hydrogels for gastric retention and diet aid applications.

Table 3. Recent research on porous high swelling hydrogels

Copolymerization of acrylic acid (AAc) and gelatinized maize starch in aqueous medium using gamma-irradiation, followed by neutralization with alkali solution; higher the dose, higher the gels content; FTIR, TGA, and SEM used for characterization; copolymers have better thermal stability than individual polymers; respective swelling of nonhydrolyzed and hydrolyzed copolymer of 200 and 350 g/g in DW.	[16]
Preparation and characterization of superabsorbent hydrogels obtained by radiation induced crosslinking of polyacrylamide (PAAm), poly(acrylic acid) (PAAc), poly(vinyl alcohol) (PVA), and potassium polyacrylate (PAAcK) for agriculture use; porosity obtained using ammonium carbonate.	[85]
Crosslinked CMC-NIPAAm hydrogels prepared using electron beam irradiation; gels content increases with dose and AAm content; porous polymers obtained by adding ammonium carbonate during irradiation; suggested for personal care industry.	[86]
Superabsorbent based on methacrylic acid-partially neutralized acrylic acid prepared in reverse suspension.	[87]
Recent progresses in the development and applications of smart polymeric gels, especially in the context of biomedical devices; improve stimuli-sensitiveness by engineering pores inside the hydrogels.	[88]
Making porous superabsorbent to improve swelling kinetics; adding superdisintegrant to increase mechanical properties; evaluate gastric retention properties in dogs both in fasted and fed states; using hard gelatin capsule for oral administration.	[10]
Synthesis of hydrogels with fast swelling and superabsorbent properties; various vinyl monomers polymerized in the presence of progens; dehydration to preserve pores; wetting agents to accelerate swelling.	[89]
Synthesis of SPH with 100 μm pore size based on acrylamide and NIPAAm; thermo-sensitive in the range of 10–65°C at NIPAAm ratio of 9/1.	[90]
SPH composites for oral administration of drugs with narrow absorption window; stable porous structure with improved mechanical properties.	[91]
Temperature-sensitive poly(<i>N</i> -isopropylacrylamide) hydrogels with large pore size and fast response prepared via polymerization in aqueous sodium chloride solutions at different concentrations; very high swelling at temperatures < LCST, exhibit much faster response rates at temperatures > LCST.	[92]
Acrylamide-based superporous hydrogels composite (SPHC) with hydroxyapatite (HA) prepared by solution polymerization; proof of HA inclusion by FTIR and EDAX; HA improves the compressive strength; cytocompatible and suggested for bone tissue engineering.	[93]
Using SPH and SPH composites to enhance the transport of <i>N</i> -alpha-benzoyl-arginine ethyl ester (BAEE) and fluorescein isothiocyanate-dextran 4400 (FD4) across porcine intestinal epithelium.	[94]
Investigate mechanism of opening of tight junctions in Caco-2 cell monolayers using superporous hydrogels (SPH) and SPH composite (SPHC) polymers as permeation enhancers for peptide drug delivery.	[95]
Solid NMR for structural characterization of SPHs; conventional SPHs have more pores and higher swelling ratio and weaker mechanical properties compared to SPH composites.	[96]
Effect of SPH and SPH composite as permeation enhancers for peptide drug delivery on Caco-2 cell monolayers; study cytotoxicity using trypan blue test, MTT assay, and propidium iodide staining.	[97]
Gastric retention study of SPH composites in man using scintigraphy; SPHs labeled with Tc-99 and administered orally in an enteric-coated gelatin capsule.	[98]

- Peroral peptide drug delivery systems based on SPH and SPH composite; release of the peptide drugs busserelin, octreotide, and insulin from SPH and SPHC polymers and the developed delivery systems; stability of the peptides during the release and the integrity of insulin in the polymeric matrix of SPHC. [99]
- Develop protein and peptide delivery system for peroral administration. [100]
- Improve intestinal absorption of insulin in healthy pigs using SPH and SPH composites. [101]
- Enhance peroral octreotide absorption using SPH and SPH composites. [102]
- pH sensitive SPHs based on acrylamide and acrylic acid. [103]
- Study of internal and surface pore morphology and their effect on SPH swelling; internal pores were found influential. [18]
- Study of the effect of compression on SPH products; anisotropic compression and swelling properties. [104]
- HEMA-based SPHs for use as support in cell cultivation. [105]
- Fast swelling highly porous superabsorbent hydrogels via solution polymerization of concentrated neutralized acrylic acid; use of double progens of sodium bicarbonate and acetone; use of water and oil-soluble crosslinkers. [106, 107]
- A cost-effective approach to enhance gels strength of the superabsorbent hydrogels; conduct solution polymerization in the presence of kaolin; FTIR confirms graft of acrylic chains onto kaolin surface; superior mechanical at the expense of swelling properties; better thermal stability as confirmed with DSC and TGA; change in thermal transition confirms chemical interaction of acrylic chains and kaolin. [108]
- Porous hydrogels composite with very high swelling and enhanced kinetics through simultaneous polymerization and foaming; compare oven-drying and methanol as nonsolvent; methanol was found more effective than acetone to preserve pores. [109]
- Increased rate of response in NIPAAm-based thermosensitive hydrogels by adding nanosize silica particles followed by extraction using HF. [110]
- Effect of acidification on swelling and mechanical properties of acrylic acid-acrylamide SPH polymers. [75]
- Synthesis of comb-type macroporous hydrogels to improve rate of response (swelling and shrinkage); NIPAAm grafted onto surface or into the bulk of a pH-responsive alginate. [111]
- Synthesis of porous thermosensitive hydrogels based on NIPAAm, and hydrophobic monomers using emulsion technique utilizing calcium carbonate or PEG 8000 as progen. [112]
- Crosslinking acrylamide-acrylic acid hydrogels with diacrylate of glycerol with improved mechanical properties compared to using methylene bisacrylamide. [113]
- Macroporous superabsorbent of acrylamide and sodium methacrylate by solution polymerization in the presence of glucose solution. [114]
- L-18 Taguchi matrix to examine the influence of formulation ingredients on gels properties during the synthesis of polyacrylamide hydrogels. [115]
- Review of the formulation, characterization, properties, and application of superporous hydrogels. [116]
- Use of polysaccharides in the preparation of elastic superporous hydrogels. [72]
- Design gastric retention devices based on chitosan and glycol chitosan. [117]
- Improve transport of desmopressin across the intestinal mucosa using superporous hydrogels. [118]

(continued)

Table 3. (continued)

Combine photocrosslinking and foaming reactions to prepare peptide-activated PEG-based hydrogels with interconnected pores for tissue engineering application.	[119]
Porous NIPAAm-based hydrogels by free radical polymerization of monomer and crosslinker in the presence of silica particles followed by acid extraction.	[120]
Synthesis of superporous hydrogels based on poly(vinyl alcohol) and poly(vinyl pyrrolidone) using double emulsion technique; possess porosity (for tissue integration) and good mechanical properties (compatible with the healthy tissue); hydrogels emulsions crosslinked physically by freeze thawing.	[121]
New superporous hydrogels composites based on aqueous carbopol solution for transmucosal drug delivery.	[17]
Carbopol-containing SPHs with fast and high swelling properties via free radical polymerization; study biocompatibility and cytotoxicity; suggested as a safe and effective carrier for peroral delivery of peptides and proteins.	[122]
A two step polymerization to prepare a fully interpenetrated network based on acrylamide.	[123]
Synthesis of acrylamide-based SPH composite containing hydroxyapatite via solution polymerization; lower swelling capacity but better mechanical property (compressive strength); suggested as a suitable scaffold for bone tissue engineering.	[124]
Stimuli-sensitive organic/inorganic nanocomposite hydrogels by introducing fibrillar attapulgite into poly(2-hydroxyethyl methacrylate-co-poly(ethylene glycol) methyl ether methacrylate-co-methacrylic acid) network with greater swelling capacity, much faster response rate and superior tensile mechanical properties compared to conventional chemical crosslinking.	[125]
Use of acrylic-based SPHs as disintegrant in fast-dissolving tablets.	[126]
Semi-IPN superporous hydrogels based on sulfopropyl acrylate and linear polymers; suggested for gastric retention application.	[127]
Synthesis and use of a fully interpenetrating porous network of acrylic acid-acrylamide-carboxymethyl chitosan for oral delivery of insulin.	[128–130]
Incorporating sodium alginate to improve mechanical properties of superporous hydrogels via making interpenetrating polymer networks.	[131]
A mechanical tester based on water-hammer concept to measure mechanical and fatigue properties of highly swelling porous hydrogels.	[13, 14, 132]
Dynamic mechanical and anisotropic swelling properties of porous high swelling hydrogels.	[133, 134]
Pre-clinical studies for SPH safety and toxicity.	[135]
Studies on the retention of SPHs in swine stomach.	[136]

drug. Finally, a proper animal model should be selected for the proof of principle studies. Since dogs and pigs are not appropriate models, the proof of efficacy of hydrogels for the gastric retention and diet applications requires a pilot study in man. Recent research on highly porous HSHs, with the focus on drug delivery applications, is summarized in Table 3. These hydrogels were studied as controlled release platform, as disintegrant for oral dosage forms and as a gastro retentive matrix.

Summary

Engineering application as opposed to a general application implies an engineered material to possess specific features for a given application. Due to their composite structure, HSHs can be engineered for pharmaceutical and biomedical applications, where unique swelling and mechanical properties as well as stability, safety, nontoxicity, durability, and other factors are equivalently desirable. These materials are relatively young, and much more research is needed to establish them in such high demanding areas. These applications require the material to not only function properly but also to be safe, stable, nontoxic, and durability. Therefore, parallel research should be attempted in order to invent cost-effective, environment friendly, and feasible manufacturing methods, to design reliable analytical methods for their characterization, to study their long-term properties, and to evaluate their biocompatibility and drug compatibility.

References

1. Gerlach G et al (2005) Chemical and pH sensors based on the swelling behavior of hydrogels. *Sens Actuators B Chem* 111:555–561
2. Gunther M et al (2005) Piezoresistive chemical sensors based on hydrogels. *Tm-Technisches Messen* 72(2):93–102
3. Kuckling D et al (2003) Photo cross-linkable poly(*N*-isopropylacrylamide) copolymers III: micro-fabricated temperature responsive hydrogels. *Polymer* 44(16):4455–4462
4. Askari F et al (1993) Synthesis and characterization of acrylic-based superabsorbents. *J Appl Polym Sci* 50: 1851–1855
5. Omidian H et al (1999) Modified acrylic-based superabsorbent polymers (dependence on particle size and salinity). *Polymer* 40:1753–1761
6. Araujo PHH et al (2002) Techniques for reducing residual monomer content in polymers: a review. *Polym Eng Sci* 42(7):1442
7. Omidian H et al (2008) Very pure superporous hydrogels having outstanding swelling properties. US Patent Application 20080206339, Abbott Laboratories
8. Han W, Omidian H, Rocca JG (2005) Dynamic swelling of superporous hydrogels under compression. American Association of Pharmaceutical Scientists, Tennessee, USA
9. Omidian H et al (1998) A model for the swelling of superabsorbent polymers. *Polymer* 39(26):6697–6704
10. Chen J et al (2000) Gastric retention properties of superporous hydrogel composites. *J Control Release* 64(1–3): 39–51
11. Omidian H, Rocca JG (2006) Formation of strong superporous hydrogels. US Patent 7,056,957, Kos Pharmaceuticals, USA
12. Omidian H, Rocca JG (2008) Superporous hydrogels for heavy duty applications. US Patent Application 20080089940, Abbott Laboratories
13. Gavrilas C, Omidian H, Rocca JG (2005) A novel simulator to evaluate fatigue properties of superporous hydrogels. Presented at the 8th US-Japan Symposium on Drug Delivery Systems, Hawaii, USA
14. Gavrilas C, Omidian H, Rocca JG (2005) A novel gastric simulator. The 32nd annual meeting of the Controlled Release Society, Miami, FL, USA
15. Omidian H, Park K (2008) Swelling agents and devices in oral drug delivery. *J Drug Deliv Sci Technol* 18(2):83–93

16. Abd El-Mohdy HL, Hegazy ESA, Abd El-Rehim HA (2006) Characterization of starch/acrylic acid super-absorbent hydrogels prepared by ionizing radiation. *J Macromol Sci Part A-Pure Appl Chem* 43(7):1051–1063
17. Tang C et al (2005) New superporous hydrogels composites based on aqueous Carbopol((R)) solution (SPHCs): synthesis, characterization and in vitro bioadhesive force studies. *Eur Polym J* 41(3):557–562
18. Gemeinhart RA, Park H, Park K (2000) Pore structure of superporous hydrogels. *Polym Adv Technol* 11(8–12): 617–625
19. Partap S et al (2007) Preparation and characterization of controlled porosity alginate hydrogels made via a simultaneous micelle templating and internal gelation process. *J Mater Sci* 42(10):3502–3507
20. Abdurrahmanoglu S, Can V, Okay O (2008) Equilibrium swelling behavior and elastic properties of polymer-clay nanocomposite hydrogels. *J Appl Polym Sci* 109(6):3714–3724
21. Bo J (1992) Study on PVA hydrogels cross-linked by epichlorohydrin. *J Appl Polym Sci* 46(5):783–786
22. Cauich-Rodriguez JV, Deb S, Smith R (1996) Characterization of hydrogel blends of poly(vinyl pyrrolidone) and poly(vinyl alcohol vinyl acetate). *J Mater Sci Mater Med* 7(5):269–272
23. Cha WI et al (1996) Mechanical and wear properties of poly(vinyl alcohol) hydrogels. *Macromol Symp* 109:115–126
24. Chen KS et al (2003) Surface grafting polymerization and crosslinking of thermosensitive NIPAAm hydrogels onto plasma pretreated substrates and drug delivery properties. *Thermec'2003* 426–434(Pts 1-5):3267–3271
25. Chen KS et al (2003) Preparation and characterization of hydroxyapatite powder/poly(acrylamide/itaconic acid) composite hydrogel. *Thermec'2003* 426–432(Pts 1–5):2101–2106
26. Darwis D et al (2002) Characterization of poly(vinyl alcohol) hydrogel for prosthetic intervertebral disc nucleus. *Radiat Phys Chem* 63(3–6):539–542
27. Dogan AK, Gumusderelioglu M, Aksoz E (2005) Controlled release of EGF and bFGF from dextran hydrogels in vitro and in vivo. *J Biomed Mater Res Part B-Appl Biomater* 74B(1):504–510
28. dos Santos JFR et al (2008) Poly(hydroxyethyl methacrylate-co-methacrylated-beta-cyclodextrin) hydrogels: synthesis, cytocompatibility, mechanical properties and drug loading/release properties. *Acta Biomater* 4(3):745–755
29. El-Din HMN, Abd Alla SG, El-Naggar AWM (2007) Swelling, thermal and mechanical properties of poly(vinylalcohol)/sodium alginate hydrogels synthesized by electron beam irradiation. *J Macromol Sci Part A-Pure Appl Chem* 44(3):291–297
30. Eschbach FO, Huang SJ (1994) Hydrophilic–hydrophobic interpenetrating polymer networks and semiinterpenetrating polymer networks. *Interpenetrating Polym Netw* 239:205–219
31. Favaro SL et al (2008) Superabsorbent hydrogel composed of covalently crosslinked gum arabic with fast swelling dynamics. *J Appl Polym Sci* 107(3):1500–1506
32. Gayet JC, He P, Fortier G (1998) Bioartificial polymeric material: poly(ethylene glycol) crosslinked with albumin II: mechanical and thermal properties. *J Bioact Compat Polym* 13(3):179–197
33. Griffin JM, Robb I, Bismarck A (2007) Preparation and characterization of surfactant-free stimuli-sensitive microgel dispersions. *J Appl Polym Sci* 104(3):1912–1919
34. Hess C et al (2007) Influence of soluble polymer residues in crosslinked carboxymethyl starch on some physical properties of its hydrogels. *Starch-Starke* 59:423–429
35. Hron P et al (1997) Silicone rubber hydrogel composites as polymeric biomaterials: 9. Composites containing powdery polyacrylamide hydrogel. *Biomaterials* 18(15):1069–1073
36. Khalid MN et al (1999) Swelling properties and mechanical characterization of a semi-interpenetrating chitosan/polyethylene oxide network – comparison with a chitosan reference gel. *STP Pharma Sci* 9(4):359–364
37. Kim JK et al (2007) Preparation and properties of collagen/modified hyaluronic acid hydrogel for biomedical application. *J Nanosci Nanotechnol* 7(11):3852–3856
38. Kim JW, Suh KD (1998) Amphiphilic urethane acrylate hydrogels having heterophasic gel structure: swelling behaviors and mechanical properties. *Colloid Polym Sci* 276(4):342–348
39. Lakouraj MM, Tajbakhsh M, Mokhtary M (2005) Synthesis and swelling characterization of cross-linked PVP/PVA hydrogels. *Iran Polym J* 14(12):1022–1030
40. Lee JW et al (1999) Synthesis and characteristics of interpenetrating polymer network hydrogel composed of chitosan and poly(acrylic acid). *J Appl Polym Sci* 73(1):113–120
41. Li X et al (2008) The swelling behaviors and network parameters of cationic starch-g-acrylic acid/poly(dimethylallylammonium chloride) semi-interpenetrating polymer networks hydrogels. *J Appl Polym Sci* 110(3): 1828–1836
42. Ling K et al (2008) Effects of substitution degree of photoreactive groups on the properties of UV-fabricated chitosan scaffold. *J Biomed Mater Res Part A* 87A(1):52–61
43. Lionetto F, Sannino A, Maffezzoli A (2005) Ultrasonic monitoring of the network formation in superabsorbent cellulose based hydrogels. *Polymer* 46(6):1796–1803

44. Lopergolo LC, Lugao AB, Catalaini LH (2002) Development of a poly(*N*-vinyl-2-pyrrolidone)/poly (ethylene glycol) hydrogel membrane reinforced with methyl methacrylate-grafted polypropylene fibers for possible use as wound dressing. *J Appl Polym Sci* 86(3):662–666
45. Lopes CMA, Felisberti MI (2003) Mechanical behaviour and biocompatibility of poly(1-vinyl-2-pyrrolidone)–gelatin IPN hydrogels. *Biomaterials* 24(7):1279–1284
46. Ma JH et al (2007) Preparation and characterization of sodium carboxymethylcellulose/poly(*N*-isopropylacrylamide)/clay semi-IPN nanocomposite hydrogels. *Eur Polym J* 43(6):2221–2228
47. Sangeetha K, Abraham TE (2008) Investigation on the development of sturdy bioactive hydrogel beads. *J Appl Polym Sci* 107(5):2899–2908
48. Xiong LJ et al (2008) Polymer-laponite nanocomposite hydrogels with super-elongation. *Prog Chem* 20(4):464–468
49. Xu K et al (2007) Study on the synthesis and performance of hydrogels with ionic monomers and montmorillonite. *Appl Clay Sci* 38(1–2):139–145
50. Starodoubtsev SG, Ryabova AA, Dembo AT, Dembo KA, Aliev II, Wasserman AM, Khokhlov AR (2002) Composite gels of polyacrylamide with incorporated bentonite. Interaction with cationic surfactants, ESR and SAXS study. *Macromolecules* 35(16):6362–6369
51. Myung D et al (2007) Biomimetic strain hardening in interpenetrating polymer network hydrogels. *Polymer* 48:5376–5387
52. Myung D et al (2008) Progress in the development of interpenetrating polymer network hydrogels. *Polym Adv Technol* 19(6):647–657
53. Nakayama A et al (2004) High mechanical strength double-network hydrogel with bacterial cellulose. *Adv Funct Mater* 14(11):1124–1128
54. Ravi N et al (2002) Characterization of the network properties of poly(ethylene glycol)–acrylate hydrogels prepared by variations in the ethanol-water solvent composition during crosslinking copolymerization. *J Polym Sci Part B-Polym Phys* 40(23):2677–2684
55. Rellve L et al (1999) Radiation-modified hydrogel based on poly(*N*-vinyl-2-pyrrolidone) and carrageenan. *Angew Makromol Chem* 273:63–68
56. Risbud MV, Bhat SV (2001) Properties of poly(vinyl pyrrolidone)/beta-chitosan hydrogel membranes and their biocompatibility evaluation by haemorheological method. *J Mater Sci Mater Med* 12(1):75–79
57. Shin HS et al (1998) Synthesis and properties of polyacrylamide–gelatin interpenetrating polymer networks. *Polym-Korea* 22(5):683–690
58. Solari M (1994) Evaluation of the mechanical-properties of a hydrogel fiber in the development of a polymeric actuator. *J Intell Mater Syst Struct* 5(3):295–304
59. Tang JC et al (2008) Mechanical property and pH sensitivity of chitosan-carbon nanotube/chitosan semi-interpenetrating hydrogel. *Acta Chim Sin* 66(5):541–544
60. Tang YF et al (2007) Rheological characterisation of a novel thermosensitive chitosan/poly(vinyl alcohol) blend hydrogel. *Carbohydr Polym* 67(4):491–499
61. Trieu H, Qutubuddin S (1995) Poly(vinyl alcohol) hydrogels: 2. Effects of processing parameters on structure and properties. *Polymer* 36(13):2531–2539
62. Vernengo J et al (2008) Evaluation of novel injectable hydrogels for nucleus pulposus replacement. *J Biomed Mater Res Part B-Appl Biomater* 84B(1):64–69
63. Wach RA et al (2003) Radiation crosslinking of carboxymethylcellulose of various degree of substitution at high concentration in aqueous solutions of natural pH. *Radiat Phys Chem* 68(5):771–779
64. Xu FL et al (2008) Porous nano-hydroxyapatite/poly(vinyl alcohol) composite hydrogel as artificial cornea fringe: characterization and evaluation in vitro. *J Biomater Sci Polym Ed* 19(4):431–439
65. Xu SM, Zhang SF, Yang JZ (2008) An amphoteric semi-IPN nanocomposite hydrogels based on intercalation of cationic polyacrylamide into bentonite. *Materials Lett* 62(24):3999–4002
66. Zhao L et al (2003) Radiation synthesis and characteristic of the hydrogels based on carboxymethylated chitin derivatives. *Carbohydr Polym* 51(2):169–175
67. Sontjens SHM et al (2006) Biodendrimer-based hydrogel scaffolds for cartilage tissue repair. *Biomacromolecules* 7(1):310–316
68. Trabbic-Carlson K, Setton LA, Chilkoti A (2003) Swelling and mechanical behaviors of chemically cross-linked hydrogels of elastin-like polypeptides. *Biomacromolecules* 4(3):572–580
69. Zhang CH, Zhang N, Wen XJ (2007) Synthesis and characterization of biocompatible, degradable, light-curable, polyurethane-based elastic hydrogels. *J Biomed Mater Res Part A* 82A(3):637–650
70. Wu MH et al (1999) Preparation of thermosensitive hydrogel (PP-g-NIPAAm) with one-off switching for controlled release of drugs. *Radiat Phys Chem* 56(3):341–346
71. Vakkalanka SK, Brazel CS, Peppas NA (1996) Temperature- and pH-sensitive terpolymers for modulated delivery of streptokinase. *J Biomater Sci Polym Ed* 8(2):119–129

72. Omidian H, Rocca JG, Park K (2006) Elastic, superporous hydrogel hybrids of polyacrylamide and sodium alginate. *Macromol Biosci* 6(9):703–710
73. Omidian H et al (2005) Hydrogels having enhanced elasticity and mechanical strength properties. US Patent 6,960,617, Purdue Research Foundation, United States
74. Park K, Kim DJ (2006) Swelling and mechanical properties of glycol chitosan/poly (vinyl alcohol) IPN-type superporous hydrogels. *J Biomed Mater Res Part A* 78A(4):662–667
75. Kim DJ, Seo K, Park K (2004) Polymer composition and acidification effects on the swelling and mechanical properties of poly (acrylamide-co-acrylic acid) superporous hydrogels. *J Biomater Sci Polym Ed* 15(2):189–199
76. Baker JP et al (1994) Effect of initial total monomer concentration on the swelling behavior of cationic acrylamide-based hydrogels. *Macromolecules* 27(6):1446–1454
77. Ding FC, Hsu SH, Chiang WY (2008) Synthesis of a new photoreactive gelatin with BTDA and HEMA derivatives. *J Appl Polym Sci* 109(1):589–596
78. Foroutan H, Khodabakhsh M, Rabbani M (2007) Investigation of synthesis of PVP hydrogel by irradiation. *Iran J Radiat Res* 5(3):131–136
79. Gottlieb R, Schmidt T, Arndt KF (2005) Synthesis of temperature-sensitive hydrogel blends by high-energy irradiation. *Nucl Instrum Methods Phys Res* 236:371–376
80. Hilmy N, Darwis D, Hardiningsih L (1993) Poly(*N*-vinylpyrrolidone) hydrogels: 2. hydrogel composites as wound dressing for tropical environment. *Radiat Phys Chem* 42(4-6):911–914
81. Nagura M, Nishimura H, Ohkoshi Y (1991) Structure of the highly elastic and high water-content hydrogels obtained from poly(vinyl alcohol) poly(sodium L-glutamate) water-system. *Kobunshi Ronbunshu* 48(8):517–523
82. Yang XJ et al (1997) Swelling behaviour and elastic properties of gelatin gels. *Polym Int* 44(4):448–452
83. Xue W, Champ S, Huglin MB (2001) Network and swelling parameters of chemically crosslinked thermoreversible hydrogels. *Polymer* 42(8):3665–3669
84. Xue W, Huglin MB, Liao B (2007) Network and thermodynamic properties of hydrogels of poly[1-(3-sulfopropyl)-2-vinyl-pyridinium-betaine]. *Eur Polym J* 43:4355–4370
85. Abd El-Rehim HA, Hegazy ESA, Abd El-Mohdy HL (2004) Radiation synthesis of hydrogels to enhance sandy soils water retention and increase plant performance. *J Appl Polym Sci* 93(3):1360–1371
86. Abd El-Rehim HA, Hegazy ESA, Diaa DA (2006) Characterization of super-absorbent material based on carboxymethylcellulose sodium salt prepared by electron beam irradiation. *J Macromol Sci-Pure Appl Chem* A43(1):101–113
87. Bajpai SK, Bajpai M, Sharma L (2007) Inverse suspension polymerization of poly(methacrylic acid-co-partially neutralized acrylic acid) superabsorbent hydrogels: synthesis and water uptake behavior. *Des Monomer Polym* 10(2):181–192
88. Chaterji S, Kwon IK, Park K (2007) Smart polymeric gels: redefining the limits of biomedical devices. *Prog Polym Sci* 32:1083–1122
89. Chen J, Park H, Park K (1999) Synthesis of superporous hydrogels: hydrogels with fast swelling and superabsorbent properties. *J Biomed Mater Res* 44(1):53–62
90. Chen J, Park K (1999) Superporous hydrogels: fast responsive hydrogel systems. *J Macromol Sci-Pure Appl Chem* A36(7–8):917–930
91. Chen J, Park K (2000) Synthesis and characterization of superporous hydrogel composites. *J Control Release* 65(1–2):73–82
92. Cheng SX, Zhang JT, Zhuo RX (2003) Macroporous poly(*N*-isopropylacrylamide) hydrogels with fast response rates and improved protein release properties. *J Biomed Mater Res Part A* 67A(1):96–103
93. Demirtas TT, Karakecili AG, Gumusderelioglu M (2008) Hydroxyapatite containing superporous hydrogel composites: synthesis and in-vitro characterization. *J Mater Sci Mater Med* 19(2):729–735
94. Dorkoosh FA et al (2002) Evaluation of superporous hydrogel (SPH) and SPH composite in porcine intestine ex-vivo: assessment of drug transport, morphology effect, and mechanical fixation to intestinal wall. *Eur J Pharm Biopharm* 53(2):161–166
95. Dorkoosh FA et al (2004) Transport of octreotide and evaluation of mechanism of opening the paracellular tight junctions using superporous hydrogels polymers in Caco-2 cell monolayers. *J Pharm Sci* 93(3):743–752
96. Dorkoosh FA et al (2000) Preparation and NMR characterization of superporous hydrogel (SPH) and SPH composites. *Polymer* 41(23):8213–8220
97. Dorkoosh FA et al (2002) Effects of superporous hydrogels on paracellular drug permeability and cytotoxicity studies in Caco-2 cell monolayers. *Int J Pharm* 241(1):35–45
98. Dorkoosh FA et al (2004) Feasibility study on the retention of superporous hydrogel composite polymer in the intestinal tract of man using scintigraphy. *J Control Release* 99(2):199–206
99. Dorkoosh FA et al (2002) Peroral delivery systems based on superporous hydrogel polymers: release characteristics for the peptide drugs buserelin, octreotide and insulin. *Eur J Pharm Sci* 15(5):433–439

100. Dorkoosh FA et al (2001) Development and characterization of a novel peroral peptide drug delivery system. *J Control Release* 71(3):307–318
101. Dorkoosh FA et al (2002) Intestinal absorption of human insulin in pigs using delivery systems based on superporous hydrogel polymers. *Int J Pharm* 247(1–2):47–55
102. Dorkoosh FA et al (2002) Peroral absorption of octreotide in pigs formulated in delivery systems on the basis of superporous hydrogel polymers. *Pharm Res* 19(10):1532–1536
103. Gemeinhart RA et al (2000) pH-sensitivity of fast responsive superporous hydrogels. *J Biomater Sci Polym Ed* 11(12):1371–1380
104. Gemeinhart RA, Park H, Park K (2001) Effect of compression on fast swelling of poly(acrylamide-co-acrylic acid) superporous hydrogels. *J Biomed Mater Res* 55(1):54–62
105. Horak D et al (2008) Superporous poly(2-hydroxyethyl methacrylate) based scaffolds: preparation and characterization. *Polymer* 49(8):2046–2054
106. Kabiri K et al (2003) Synthesis of fast-swelling superabsorbent hydrogels: effect of crosslinker type and concentration on porosity and absorption rate. *Eur Polym J* 39(7):1341–1348
107. Kabiri K, Omidian H, Zohuriaan-Mehr MJ (2003) Novel approach to highly porous superabsorbent hydrogels: synergistic effect of porogens on porosity and swelling rate. *Polym Int* 52(7):1158–1164
108. Kabiri K, Zohuriaan-Mehr MJ (2003) Superabsorbent hydrogel composites. *Polym Adv Technol* 14(6):438–444
109. Kabiri K, Zohuriaan-Mehr MJ (2004) Porous superabsorbent hydrogel composites: synthesis, morphology and swelling rate. *Macromol Mater Eng* 289(7):653–661
110. Kaneko T, Asoh TA, Akashi M (2005) Ultrarapid molecular release from poly(*N*-isopropylacrylamide) hydrogels perforated using silica nanoparticle networks. *Macromol Chem Phys* 206(5):566–574
111. Kim JH et al (2002) Rapid temperature/pH response of porous alginate-g-poly(*N*-isopropylacrylamide) hydrogels. *Polymer* 43(26):7549–7558
112. Lee WF, Yeh YC (2006) Effect of porosity and hydrophobic monomer on the fast swelling–deswelling behaviors for the porous thermoreversible copolymeric hydrogels. *J Appl Polym Sci* 100(4):3152–3160
113. Lopez-Ureta L et al (2008) Synthesis and characterization of acrylamide/acrylic acid hydrogels crosslinked using a novel diacrylate of glycerol to produce multistructured materials. *J Polym Sci Part A-Polym Chem* 46(8):2667–2679
114. Mohan YM, Murthy PSK, Raju KM (2006) Preparation and swelling behavior of macroporous poly(acrylamide-co-sodium methacrylate) superabsorbent hydrogels. *J Appl Polym Sci* 101(5):3202–3214
115. Omidian H, Park K (2002) Experimental design for the synthesis of polyacrylamide superporous hydrogels. *J Bioact Compat Polym* 17(6):433–450
116. Omidian H, Park K, Rocca JG (2007) Recent developments in superporous hydrogels. *J Pharm Pharmacol* 59(3):317–327
117. Park H, Park K, Kim D (2006) Preparation and swelling behavior of chitosan-based superporous hydrogels for gastric retention application. *J Biomed Mater Res Part A* 76A(1):144–150
118. Polnok A et al (2004) In vitro evaluation of intestinal absorption of desmopressin using drug-delivery systems based on superporous hydrogels. *Int J Pharm* 269(2):303–310
119. Sannino A et al (2006) Synthesis and characterization of macroporous poly(ethylene glycol)-based hydrogels for tissue engineering application. *J Biomed Mater Res Part A* 79A(2):229–236
120. Serizawa T et al (2002) Thermoresponsive properties of porous poly(*N*-isopropylacrylamide) hydrogels prepared in the presence of nanosized silica particles and subsequent acid treatment. *J Polym Sci Part A-Polym Chem* 40(23):4228–4235
121. Spiller KL et al (2008) Superporous hydrogels for cartilage repair: evaluation of the morphological and mechanical properties. *Acta Biomater* 4(1):17–25
122. Tang C et al (2007) Swelling behavior and biocompatibility of carbopol-containing superporous hydrogel composites. *J Appl Polym Sci* 104(5):2785–2791
123. Tang QW et al (2008) A high mechanical strength hydrogel from polyacrylamide/polyacrylamide with interpenetrating network structure by two-steps synthesis method. *E-Polymers* 21:1–6
124. Tolga Demirtas T, Karakecili AG, Gumusderelioglu M (2008) Hydroxyapatite containing superporous hydrogel composites: synthesis and in-vitro characterization. *J Mater Sci Mater Med* 19(2):729–735
125. Xiang YQ, Peng ZQ, Chen DJ (2006) A new polymer/clay nano-composite hydrogel with improved response rate and tensile mechanical properties. *Eur Polym J* 42(9):2125–2132
126. Yang SC et al (2004) Application of poly(acrylic acid) superporous hydrogel microparticles as a super-disintegrant in fast-disintegrating tablets. *J Pharm Pharmacol* 56(4):429–436
127. Yang SC, Park K, Rocca JG (2004) Semi-interpenetrating polymer network superporous hydrogels based on poly(3-sulfopropyl acrylate, potassium salt) and poly(vinyl alcohol): synthesis and characterization. *J Bioact Compat Polym* 19(2):81–100

128. Yin LC et al (2008) Beneficial properties for insulin absorption using superporous hydrogel containing interpenetrating polymer network as oral delivery vehicles. *Int J Pharm* 350(1–2):220–229
129. Yin LC et al (2007) Superporous hydrogels containing poly(acrylic acid-co-acrylamide)/O-carboxymethyl chitosan interpenetrating polymer networks. *Biomaterials* 28(6):1258–1266
130. Yin LC et al (2008) Polymer–protein interaction, water retention, and biocompatibility of a stimuli-sensitive superporous hydrogel containing interpenetrating polymer networks. *J Appl Polym Sci* 108(2):1238–1248
131. Yin LC et al (2007) Synthesis, characterization, mechanical properties and biocompatibility of interpenetrating polymer network-super-porous hydrogel containing sodium alginate. *Polym Int* 56:1563–1571
132. Gavrilas C, Omidian H, Rocca JG (2005) Dynamic mechanical properties of superporous hydrogels. In 8th US-Japan symposium on drug delivery systems, Hawaii, USA
133. Li G, Omidian H, Rocca JG (2004) Anisotropic properties of superporous hydrogel hybrids intended for gastric retention. American Association of Pharmaceutical Scientists, Baltimore, USA
134. Li G, Omidian H, Rocca JG (2005) Acrylate–chitosan superporous hydrogel hybrids. The 32nd annual meeting of the Controlled Release Society, Miami, USA
135. Townsend R, Rocca JG, Omidian H (2005) Safety and toxicity studies of a novel gastroretentive platform administered orally in a swine emesis model. The 32nd annual meeting of the Controlled Release Society, Miami, USA
136. Han W, Omidian H, Rocca JG (2004) Evaluation of gastroretentive superporous hydrogel platforms using swine model. The 31st annual meeting of the Controlled Release Society, Honolulu, USA

Superabsorbent Hydrogels

Grigoriy Mun, Ibragim Suleimenov, Kinam Park, and Hossein Omidian

Abstract Superabsorbent hydrogels have unique swelling features that are highly attractive for biomedical, pharmaceutical, and industrial applications. The swelling capacity of many hydrogels, however, is very sensitive to the pH and ionic strength of the solution. Acids and bases, as well as salts (monovalent, multivalent) can significantly affect the solution properties of these polymers. Therefore, it is essential to understand the swelling phenomena of hydrogels, such as the forces responsible for the swelling and swelling barriers. Since the swelling rate of hydrogels is basically required for most applications, detailed information with respect to the swelling kinetics in hydrogels is important as well as the theoretical aspects of swelling mechanisms, especially in solutions containing salts.

Introduction

Hydrogels are hydrophilic macromolecules crosslinked by one or more mediators, as shown in Fig. 1. Macromolecular chains forming these networks acquire coil conformations in their dry state, but are significantly expanded to a large size once they are exposed to water or other aqueous medium. The main property of a hydrogels is to absorb and to retain water for a long time. For superabsorbent hydrogels, the increase in volume could be as high as 10,000 g of water per gram of the dry material. This feature has been attractive enough to introduce superabsorbents into areas where the absorption of water or aqueous solutions is of prime importance. Superabsorbent products are mostly used in hygiene products (baby diapers and incontinence pads), as well as in agriculture and horticulture industries, where they moisten and condition the soil.

Since the swelling is the most important property for these applications, many hydrogels polymers are generally made of ionic monomers. These polymers usually have pendant sodium or potassium ions, such as sodium acrylate, potassium acrylate. The ionic entities readily dissociate in water and generate electrostatic forces (Fig. 2).

Polyelectrolyte hydrogels can be synthesized by crosslinking polyacids, polysalts, or polybases. Although hydrogels based on sulfonic acids and derivatives of vinyl ether of monoethanol amine and other amines are well described in the literature, hydrogels based on acrylic acid derivatives are more widely studied and produced [1]. High water absorbent hydrogels used in sanitary towels, diapers, and other medical and hygienic goods are crosslinked networks of acrylic acid and sodium acrylate copolymers.

G. Mun • Department of Chemical Physics and Macromolecular Chemistry, Kazakh National University, Almaty, Republic of Kazakhstan

I. Suleimenov • Almaty Institute of Power Engineering and Telecommunications, Almaty, Republic of Kazakhstan

K. Park • Departments of Biomedical Engineering and Pharmaceutics, Purdue University, West Lafayette, IN, USA

H. Omidian • College of Pharmacy, Nova Southeastern University, Fort Lauderdale, FL, USA
e-mail: omidian@nova.edu

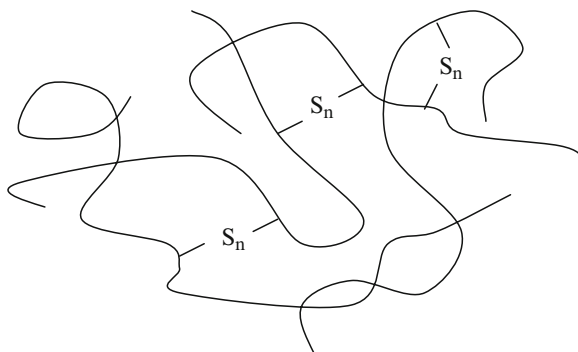


Fig. 1. A crosslinked polymer network.

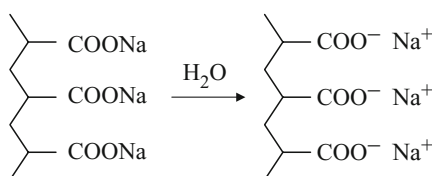


Fig. 2. Dissociation of sodium polyacrylate.

Hydrogels Swelling

Although superabsorbent hydrogels theoretically absorb only water, in practice, they absorb physiological solutions, such as blood and saline. For agricultural and horticultural uses, the hydrogel is intended to absorb solutions containing water along with fertilizers and other nutritional entities. The degree to which a specific hydrogel can swell in an aqueous medium essentially depends on the presence and chemical nature of the solutes [2, 3]. In general, the swelling degree of polyelectrolyte hydrogels strongly depends on the presence of low molecular weight salts, acids, and bases in the solution. For example, ions, of any type, are able to screen their own charges in the network, which significantly reduces the swelling of the electrolyte-based (ionic) swellable hydrogels. Different acrylic-based hydrogels can swell in aqueous solutions containing low molecular weight salts including sodium thiosulfate, potassium hexacyanoferrate, and sodium sulfate as shown in Fig. 3 [4]. Based on the data obtained for poly(acrylic acid) and acrylic acid-co-sodium acrylate copolymer, the swelling behavior is dependent on the average salt concentration inside the gels and in the surrounding solution. When a dry hydrogel is placed into saline solution (an aqueous salt solution), a concentration redistribution effect occurs. This happens due to the difference in salt concentration in the vicinity of the gels area and in the remainder of the gels-solution system. Therefore, the salt concentration needs to be averaged in order to obtain a realistic picture of the system [4, 5].

As shown in Fig. 3, for an ionic hydrogels, the maximum swelling occurs in pure water. The swelling capacity of the gels then decreases as salt is added and then reaches a plateau. This behavior is due to the effect of salt on electrostatic interactions which are the major driving force for the ionic hydrogels swelling. However, the known swelling theories for polyelectrolyte networks do not satisfactorily explain all aspects of the gels-solution systems [6]. Polyelectrolyte hydrogels including those based on acrylamido-2-methyl propane sulfonic

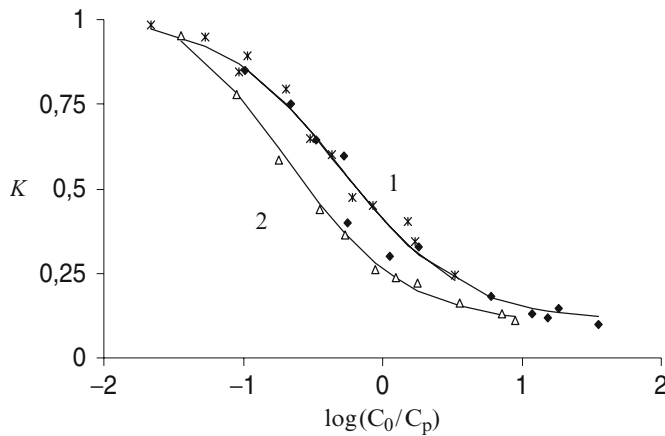


Fig. 3. Change in swelling ratio K with salt concentration of sodium thiosulfate (*asterisk*), potassium hexacyanoferrate (*filled diamond*) and sodium sulfate (*triangle*), 1 Poly(acrylic acid), 2 Neutralized poly(acrylic acid) (a copolymer hydrogels containing 75% sodium acrylate and 25% acrylic acid residues).

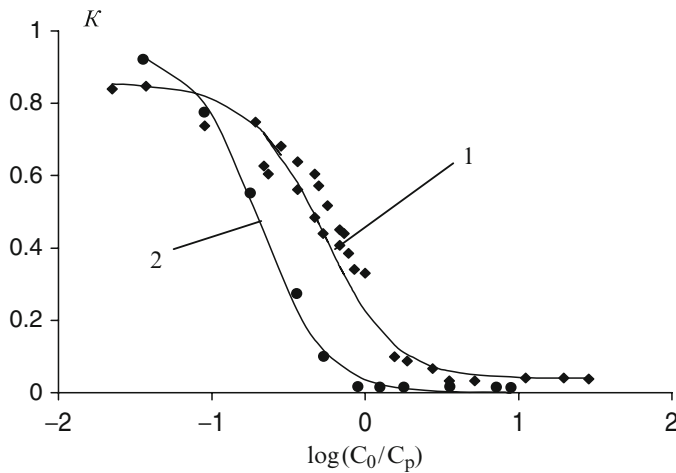


Fig. 4. Swelling ratio K versus acid and salt concentration for a polyacrylic gels; (1) HCl; (2) CuSO₄.

acid and dimethyl acrylamide display similar swelling behavior as poly(acrylic acid) in solutions containing potassium chloride, sodium chloride, potassium sulfate, and sodium sulfate [7]. Similar swelling behavior is observed for poly(acrylic acid) in highly acidic solutions or containing polyvalent cations (Fig. 4) [5].

For some hydrophilic gels, the gels swelling continues to rise even at high salt concentrations. Although not as pronounced, the swelling values with only a few grams of water per gram of the hydrogels are directly related to the uncharged networks that do not associate with water. For these networks, the swelling profile is not sensitive to the ions in the swelling medium. Essentially, the swelling capacity of a polyelectrolyte hydrogels at a given crosslink density depends on the charge density of the network and the degree to which electrostatic forces are suppressed. For hydrogels based on weak carbonic acids, such as

poly(acrylic acid), the most influential factor is the degree of dissociation of the ionic groups – the greater the dissociation, the larger the swelling degree. The degree of dissociation of weak carbonic acids is about 10%, but the salt of a weak acid and a strong base (sodium polyacrylate) dissociate to a greater extent. Thus, pure poly(acrylic acid) and sodium polyacrylate display swelling capacity in the range of 200–300 g/g and 500–700 g/g, respectively.

Although charge density of the network is associated with the charge concentration within the hydrogels and the swelling medium, the network density or crosslink density is solely related to the chemical structure of the gels. The crosslinking density can be controlled by changing the ratio of the crosslinker to monomer. The greater the ratio is, greater the density. Highly crosslinked systems swell less but are mechanically stronger and retain their shape in the swollen form.

The hydrogels swelling is a delicate balance between swelling and elastic forces. A hydrogels containing hydrophilic functional groups and ions can generate strong interactions with the swelling medium, which causes hydrogels expansion. On the other hand, crosslinks prevent infinite expansion of the network by generating elastic forces. Therefore, a crosslinked hydrogels in water may experience expansion and contraction depending on the magnitude of each individual force. The nature of the contraction forces is similar to that of rubber, i.e., the elasticity of a macromolecular “ball” entropically tends to be the most probable conformation of a coagulated ball. With a high crosslink density, the chain length between the network junctions of a hydrogels is relatively short. As such, the swelling degree of these networks is small because of their restricted ability to swell.

The chain length between the two successive crosslinks determines whether the network is a hydrogels or an ionite. If the length corresponds to a polymer size, the network is called a hydrogels with a very high swelling capacity. On the other hand, if the length corresponds to an oligomer size, the network is an ionite with limited or no swelling. The swelling degree of an ionite network is usually a few percent of the initial volume. For instance, a crosslinked natural rubber network can be formed by curing natural rubber with specific amounts of sulfur. At very high sulfur contents as high as 30–40%, the usually soft and stretchable natural rubber is transformed to a very rigid and brittle product with almost no swelling in hydrocarbon solvents. On the other hand, at sulfur level of less than 1%, the rubber displays elastic properties (like a rubber band) with good swelling in a hydrocarbon solvent. Rubbers crosslinked at low and high crosslinker concentrations resemble hydrogels and ionites, respectively. The hydrogels crosslink density can also be increased sharply if the swelling medium contains metal ions that form insoluble products by reacting with the polymer network. For example, sodium polyacrylate hydrogels react with multivalent cations, such as calcium and iron. This results in an increased crosslink density in the hydrogels network which causes the swollen polymer to precipitate in the swelling medium with little or no water absorption.

Mechanism of hydrogels Swelling

The swelling of a polyelectrolyte has been interpreted with reference to linear macromolecules [8]. The theory is based on the repulsion of charges that are hardly connected to the backbone of the macromolecule. Some researchers indicate that the increased rigidity of a macromolecular chain is due to the electrostatic repulsion of charges of dissociated groups. According to the literature, it is likely that the chain inflexibility leads to a growth of the Kuhn segment and to increase the statistical coil size, i.e., swelling. However, there is another

interpretation of the swelling process called the “osmotic effect”. Dissociation of ionic functional groups in a gels results in the appearance of mobile low molecular weight ions or counter ions. However, the mobility of the counter ions is restricted as they cannot leave the gels. If they leave, the gels system will assume a nonzero electrostatic charge, with the ability to attract counter ions. Therefore, the hydrogels surface can be considered as a membrane, permeable to water but not to mobile ions. The membrane allows the liquid to pass in order to balance the ion concentration outside and inside the gels. As ion concentration increases, more osmotic pressure is built up in the membrane.

Interactions other than osmotic may favor or disfavor the swelling process. Hydrophilic interactions that are nonelectrostatic may promote swelling. This can be seen in uncharged networks, such as polyacrylamide and poly(vinyl alcohol). Excessive hydrogen bonding in a poly(vinyl alcohol) polymer may decrease its swelling capacity. On the other hand, hydrophobic interactions produce a compact macromolecular structure and swelling capacity decreases. Overall, swelling in hydrogels can be caused by osmosis, hydrogen bonding, hydrophobic association, as well as chain aggregation. Depending on the structure of the macromolecule, the individual contributions would be different. Thus, the swelling mechanism based on the “osmotic” point of view relies on an analogy between a separating membrane and the hydrogels surface. Modern literature now presents corresponding thermodynamic calculations to determine the hydrogels swelling capacity at given conditions.

The theory of the hydrogels swelling is based on the direct analysis of the distribution of low molecular weight ions [9]. The electrostatic interactions do not allow the low molecular weight ions to leave the hydrogels mass; otherwise the hydrogels cannot maintain neutrality. However, a small portion of ions do leave the hydrogels surface due to “chaotic” thermal motion. Dynamic equilibrium takes place near the surface under which the diffusion flow is balanced by flow due to electrostatic attraction of low molecular weight ions into the area with noncompensated network charge. This dynamic equilibrium results in the appearance of a double electric layer near the hydrogels surface (Fig. 5). First layer is a solution rich in mobile ions near the hydrogels surface and the second layer is essentially noncompensated for the network charge. The second layer does not allow the low molecular weight ions to move very far from the gels surface, which cause stretching forces. Calculations of the electrostatic component of the swelling pressure for homogeneous gels based on an osmotic and double layer models give similar results [9].

The two models start to show their differences when the surface effects of the hydrogels are taken into account. These effects are functional in a broad range of hydrogels systems as they are responsible for very high swelling degrees of gels, in particular for the gels based on weak carbonic acids.

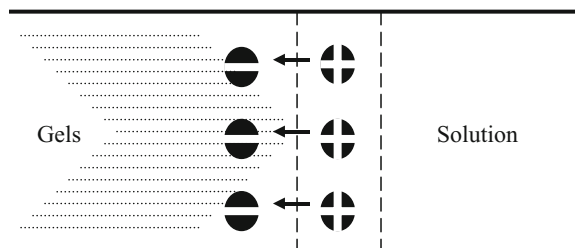
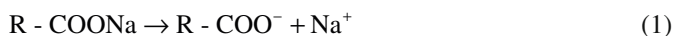


Fig. 5. Double electric layer in swelling hydrogels.

The Effect of Neutralization and Acidity on the Swelling Capacity of Polycarbonic Acids

Ionization can at best be seen when a salt form of a given gels is studied. At equilibrium, the following reactions determine the overall charge density of the network:



Salts (sodium acrylate) of a weak acid (acrylic acid) and a strong base (sodium hydroxide) can be considered as completely dissociated (1). However, ionized groups formed in this reaction are able to combine with hydrogen ions (2), which are formed in the process of water ionization. As a result, a significant portion of the network functional groups based on sodium acrylate is deionized, and the medium inside of the gels becomes alkaline. This accounts for the large swelling capacity of the hydrogels based on sodium acrylate and acrylic acid copolymer. For example, a poly(acrylic acid-co-sodium acrylate) hydrogels shows peak swelling at [PAA]:[PAANa] molar ratio of about 25:75. The swelling peak does not appear at 100% neutralization due to the excessive concentration of counter ions. Therefore, superabsorbents used in hygiene products are 75% neutralized poly(acrylic acid). Shifting of the equilibrium in (2) influences the behavior of pure polyacid hydrogels. As mentioned above, the membrane separating the gels and the solution phases (surface layer of the gels) may have a complicated structure. In particular, the hydrogen ions formed by the dissociation of the R-COOH groups can move in the solution due to thermal motion. In turn, the equilibrium shifts toward more ionization. This could increase the charge density of the network within the surface layers of the hydrogels than the inner layers. Based on (4), the equilibrium ionization reaction of polyacids depends on the total concentration of the R-COOH and R-COO⁻ groups, i.e., on the network charge density *N*.



The degree of association or β calculated based on the dissociation constant of acrylic acid is shown in Fig. 6.

It can be seen that β -values decrease with an increase in network crosslinking density at a given acid-to-salt ratio. This is the basis of mechanical regulators of the medium acidity described by Suleimenov [10]. The mechanical effect by such regulators changes the total density of the ionized and nonionized carboxylic groups and leads to the acidity change across the gels and in the neighboring solution. The Donnan equilibrium explains what essentially drives a hydrogels to absorb aqueous solutions.

Donnan's Equilibrium and Potential in a hydrogels Solution System

Donnan ratios were initially determined by the theory of membrane equilibriums, and later found to be applicable in the theory of ionites and hydrogels. According to the osmotic model of polyelectrolyte hydrogels, the swelling pressure is based on the difference between the total concentrations of mobile ions outside and inside of the hydrogels. In fact, salts or any

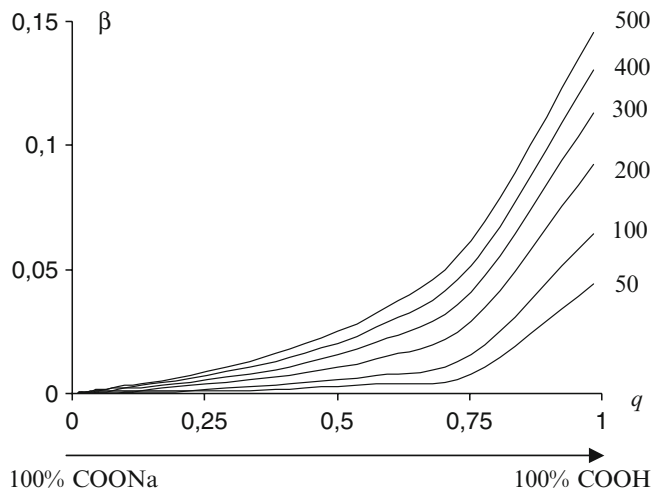


Fig. 6. Calculated degree of association of COOH groups, β , at different swelling ratios.

other low molecular weight electrolytes are able to penetrate into the hydrogels mass. According to this model, the difference in the total ion concentrations and the degree to which ions can travel between the phases determines the actual swelling of the hydrogels. A correlation between the concentrations of mobile ions inside and outside of the hydrogels can be determined from Donnan ratios. To explain the model, the simplest case would be a network based on sodium polyacrylate in a solution containing sodium chloride. Since functional groups are completely dissociated, ions tend to leave the gels under the influence of thermal motion. As a result, an electrostatic field develops in order to recover the ions. More accurately, the field can direct a flow of the low molecular weight ions from the solution to the gels. An equilibrium is established when both diffusion and directed components equilibrate each other. The electrostatic field resembles a barrier for low molecular weight ions that hold them inside of the gels. The appearance of the field of a double electric layer leads to a potential difference between the gels and surrounding solution, i.e., Donnan potential. It seems that the field can develop only in the immediate proximity of the gels surface because ions near the surface are the only ones that can leave the gels. In other words, a double electric layer is formed within the boundary of the gels and the solution. Behavior of the electrostatic field, E , and potential of double layer φ is shown in Fig. 7. The double layer forms a potential well inside of the gels, which contains the low molecular weight ions and does not allow them to travel into the surrounding solution. Small extension of the double layer field allows determining its general characteristic – the potential difference between the gels and the solution, Donnan potential, without detailed analysis of the motion equations of the ions.

The dispersion of the charged particles obeys Boltzman’s distribution and the corresponding equations for the positive and negative ions are as follows:

$$n^- = n_0^- \exp(+q_0\varphi / kT) \tag{5}$$

$$n^+ = n_0^+ \exp(-q_0\varphi / kT) \tag{6}$$

where n^- and n^+ are the concentrations of the mobile negative and positive ions in the combined hydrogels solution system, and n_0^- and n_0^+ are multipliers showing ion concentrations

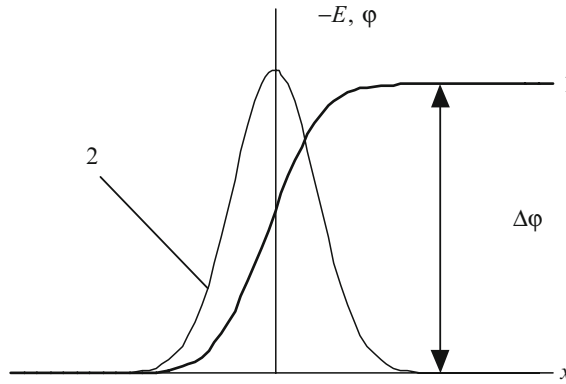


Fig. 7. Electrostatic field, E , and potential of the double layer φ .

at zero potential. Due to the electric neutrality, the total concentration of positive ions is equal to the concentration of negative ions far from the hydrogels surface, where the Donnan potential can be found. The potential may be counted from an arbitrary point in the depth of the solution and thus, $n_0^- = n_s^-$, $n_0^+ = n_s^+$ (concentrations of the mobile ions marked by an index s). The following equality would be in progress due to the electric neutrality of the solution:

$$n_s^+ = n_s^- \quad (7)$$

Concentration of positive (n_g^+) and negative (n_g^-) ions in the hydrogels volume is expressed by concentration of mobile ions in the depth of the solution and the corresponding value of the Donnan potential $\Delta\varphi_0$ from (5) and (6). Therefore:

$$n_g^- = n_s^- \exp(+q_0 \Delta\varphi_0 / kT) \quad (8)$$

$$n_g^+ = n_s^+ \exp(-q_0 \Delta\varphi_0 / kT) \quad (9)$$

The well known Donnan ratio, where the difference of potentials between phases does not enter into the equation, can be easily obtained by multiplying the (8) and (9):

$$n_g^+ n_g^- = n_s^+ n_s^- \quad (10)$$

Concentrations of the mobile ions inside the hydrogels are bound with each other by factor of electrical neutrality of the sample:

$$n_g^+ = N_0 + n_g^- \quad (11)$$

where N_0 is the concentration of dissociated functional groups inside the network. The concentration of mobile negative charged ions inside the network (n_g^-) is consistent with the concentration of salt C_g , entered into the hydrogels, i.e., $C_g = n_g^-$. Therefore, the unknown concentrations of both ions inside and outside the hydrogels can be determined if (7), (10), and (11) are sustained. This means that any of the unknowns can be considered as external parameter for the system and all others are dependent. The external parameter can be expressed by average concentration of salt in the system [4, 5], which is specified at particular experimental conditions. The concentration of the salt outside the gels, $C_s = n_s^+ = n_s^-$, is considered as an external parameter. Single equation which correlates the concentrations of salt

inside and outside the hydrogels can be obtained by solving (7), (10), and (11), followed by simple transformations:

$$C_g (C_g + N_0) = C_s^2 \tag{12}$$

When divided by C_s^2 , it can be seen that the ratio of salt concentration in different sides of the hydrogels surface, $\beta = C_g / C_s$, is defined by a single directing parameter, $[y = (N_0 / C_s) \ll 1]$, as shown in the (13).

$$\beta(\beta + y) = 1 \tag{13}$$

Despite its simplicity, the expression (13) is quite important. A useful correlation can be made between the logarithm of concentration ratio β and Donnan potential if the logarithm of the ratio (13) is known.

$$\Delta\varphi_0 = -\frac{kT}{q_0} \ln \beta \tag{14}$$

Donnan potential can be expressed by solving (13):

$$\Delta\varphi_0 = -\frac{kT}{q_0} \ln \left(\frac{\sqrt{y^2 + 4} - y}{2} \right) \tag{15}$$

Donnan potential from directing parameter in absolute values (volts) at temperature of 25°C is presented in Fig. 8. It can be seen that at high concentrations of salt $[y = (N_0 / C_s) \ll 1]$, the Donnan potential is characterized by millivolt units or less. This value reaches to the tenth of a volt only, when y value is about 100.

Nevertheless, since dissociation of water has not been considered in this equation, this consideration is inapplicable when the concentration of salt decreases further. In other words, this factor defines a limit value of the Donnan potential similar to that of distilled water. Therefore, Donnan potential is characterized by noticeable values. Moreover, it should be emphasized that voltrop defined by this potential is in fact concentrated in a very narrow area, i.e., in double layers. These layers could be developed on the hydrogels surface and achieve a very high value. Nevertheless, these results are corresponded to the situations, where the concentration of salt inside the gels is used as an external parameter. In reality, this value is dependent in part on the swelling capacity of the hydrogels, which is also dependent on the

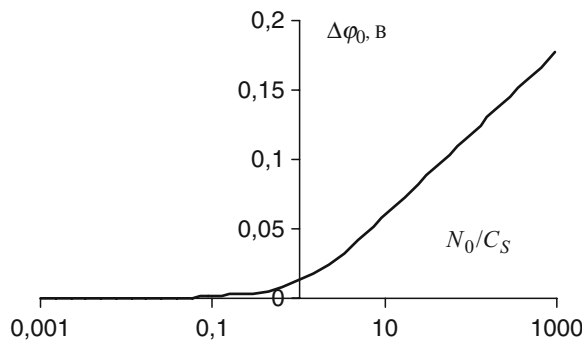


Fig. 8. Donnan potential and salt concentration.

concentration redistribution of salt. The difference between total concentrations of mobile ions inside and outside of the hydrogels decreases as salt concentration in the solution increases. This would eventually lower the osmotic pressure of the hydrogels.

Effect of Concentration Redistribution

The existence of a nonzero Donnan potential implies that, the effect of concentration redistribution takes place in a hydrogels [4, 5]. This effect is opposed to the sorption, where concentration of the absorbed component in the solution decreases due to chemical interaction. For instance, when a dry polyacrylate hydrogels is placed in a solution of sodium acrylate (concentration C_0), the hydrogels due to swelling occupies a volume of V_g out of the total volume (V_0), which is occupied by the gels and the solution. As a result, the concentration of salt inside and outside the hydrogels would change. To describe such a system, it has to be noted that the transition region of the electric double layer is negligible compared to the size of the gels itself. To describe this system, the following equations are required:

1. Equation of Donnan balance for counter ions and co-ions.

$$[Na^+]_g = \alpha [Na^+]_s \quad (16)$$

$$[A^-]_g = \alpha^{-1} [A^-]_s \quad (17)$$

where $\alpha = \exp\left(\frac{e\Delta\phi}{kT}\right) > 1$ is the multiplier found by conditions of electrostatic equations, $\Delta\phi_0$ is the difference of Donnan potential between the hydrogels and the solution, and indices g and s are, respectively, used for the area inside of the hydrogels and the solution.

2. Conditions of electro-neutrality of the medium inside and outside of the hydrogels far from the hydrogels boundary or double layer:

$$[A^-]_g = [Na^+]_s \quad (18)$$

$$N_0 + [A^-]_g = [Na^+]_s \quad (19)$$

where N_0 is the concentration of functional groups (carboxylate groups COO^-) inside the hydrogels, calculated based on the volume that hydrogels occupies (total number of dissociated functional groups related to the hydrogels volume).

3. Equation of material balance for anions

$$w[A^-]_g + (1-w)[A^-]_s = C_0 \quad (20)$$

where $w = V_g / V_0$ is the inclusion volume fraction of hydrogels in the system, V_g is the hydrogels volume, and V_0 is the volume of the hydrogels solution system.

Equation (19) could not be used because the concentration of salt inside the gels is unknown and considered as a directing parameter. The condition of Donnan equilibrium can be obtained by multiplying (16) and (17), and using (18) and (19):

$$[A^-]_g ([A^-]_g + N_0) = [A^-]_s^2 \quad (21)$$

Average concentration of polymer in the system is defined as $C_p = m_p / (M V_0)$, where M is the molar mass of the polymer, and m_p is the polymer mass. Analogical expression is also right for concentration of functional groups inside the hydrogels, $N_0 = m_p / (M V_g)$. Therefore, the index n can be found as:

$$w = \frac{C_p}{N_0} = \frac{1}{n} \tag{22}$$

Expression (20) can easily be transformed to the following equation using (22):

$$C + (n-1)C' = nC_0 \tag{23}$$

where, $C = [A^-]_g$ and $C' = [A^-]_s$ (expressed in mol/l) are equilibrium concentrations of salt inside the hydrogels and solution, respectively.

Assuming $x = C / C_p$, $y = C' / C_p$, and $z = C_0 / C_p$, (21) and (23) can be rewritten using normalized concentrations as:

$$\begin{cases} (x+n)x = y^2 \\ x + y(n-1) = nz \end{cases} \tag{24}$$

This system is transformed to a single square equation based on normalized salt concentrations $y = C' / C_p$ by substituting, $x = nz - y(n-1)$.

$$y^2 (n-2) - y(1+2z)(n-1) + nz(z+1) = 0 \tag{25}$$

The equation (25) can be solved as follows:

$$y = \frac{(n-1)(1+2z) - \sqrt{4z(z+1) + (n-1)^2}}{2(n-2)} \tag{26}$$

The sign of the square root is based on the condition that $y \rightarrow z$ has to take place at unlimited increase of the initial salt concentration in the system ($z \rightarrow \infty$). Therefore the equilibrium concentrations of salt C' / C_p in the hydrogels solution system, which is formed due to interaction of gels with electrolyte solution, are analytically dependent on known parameters of the system including the initial salt concentration C_0 , average concentration of polymer in system C_p , and inverse inclusion volume fraction of hydrogels in system V_0 / V_g . Figure 9 shows

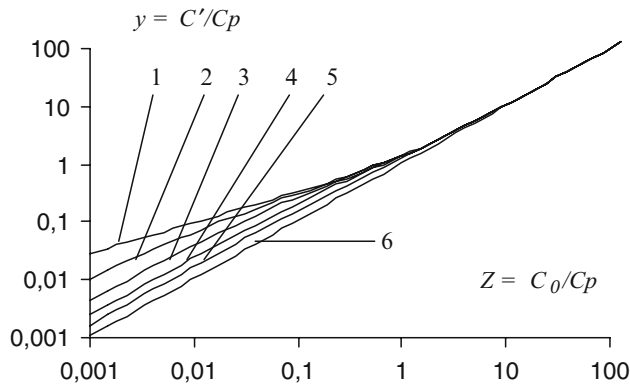


Fig. 9. Normalized salt concentration in a hydrogels and relative value of average salt concentration in a hydrogels solution system.

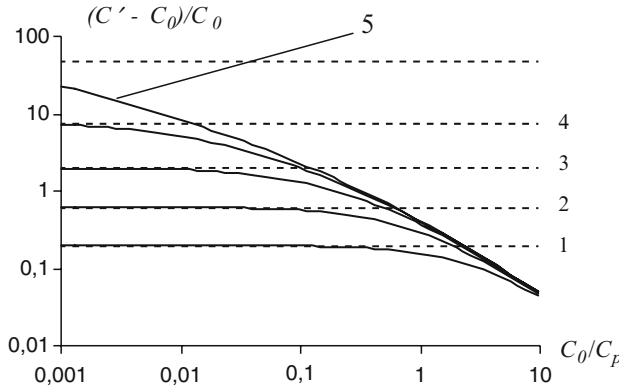


Fig. 10. Concentration redistribution and normalized salt concentration.

the normalized salt concentrations for “ $n = V_0/V_g$ ” values of 1.01, 1.1, 1.3, 1.7, 2.5, and 20 that are, respectively, assigned to the graphs 1–6. The bisector on the graph corresponds to a condition, where the concentration redistribution does not exist, i.e., $C' = C_0$.

Based on Fig. 9, that part of the hydrogels volume affects the character of the concentration redistribution in the given system. Values of $n = V_0/V_g$ close to unity correspond to a case where the hydrogels occupies almost all the volume of the system. In such cases, the enrichment of solution by adding more solvents is generally effective. As shown in graph 6 of Fig. 9 (where hydrogels-to-solvent ratio is 1/20), the hydrogels has no influence on the values of concentration in the solution if it’s only a small fraction of the whole system. There are data and experiments to confirm this claim [11]. It is also seen from the figure that noticeable redistribution of concentrations takes place when the salt concentration in the system is less than the concentration of the polymer, i.e., when normalized concentration $z = C_0/C_p$ is less than unity. Shown in Fig. 10 is the dependency of $\frac{C' - C_0}{C_0}$ to the normalized salt concentrations.

The concentrations $y = C'/C_p$ calculated using (26) for “ $n = V_0/V_g$ ” values of 1.02, 1.13, 1.5, 2.6, and 6 as, respectively, shown in the graphs 1–5.

For extreme situations where salt becomes completely concentrated in the solution (if salt does not penetrate into the gels), volume of the solution becomes $V_0 - V_g$, and the condition of complete concentration of salt in solution can be expressed as:

$$(V_0 - V_g) C' = V_0 C_0 \tag{27}$$

From which:

$$C' = \frac{V_0}{V_0 - V_g} C_0 = \frac{n}{n - 1} C_0 \tag{28}$$

or:

$$\frac{C' - C_0}{C_0} = \frac{1}{n - 1} \tag{29}$$

Extreme values corresponded to different values of parameter n are shown in Fig. 10 (dotted lines). It is seen that salt does not penetrate into the hydrogels at small enough concentrations in the given system. This fact has been a basis for a number of practical applications of hydrogels [11], which are mentioned in the following section.

Kinetics of Hydrogels Swelling

The use of hydrogels as superabsorbent is often limited by kinetic factors. The swelling degree of superabsorbent hydrogels is uniquely high as they offer almost a tenfold increase in their dimension in water. It is reasonable that during the swelling process, the surface layers of the hydrogels swell first due to the direct contact with water. Diffusion of water through the swollen layers restricts the swelling rate of the hydrogels at the later stages. Using simple experiments (Fig. 11), the diffusion of water through a hydrogels the process can be measured. A sample of hydrogels (e.g., sodium polyacrylate) is placed in the middle of the tube (1). Since the hydrogels dimension in its swollen state is larger than the tube diameter, the hydrogels is spontaneously affixed inside the tube due to its own swelling. The space above the hydrogels (2) is filled with water; and the rate of water flow into the empty section of the tube (3) is monitored. Approximately 20 mL of water flows from the upper part into the lower part of the tube during an hour of experiment. Apparently, this value depends on many factors including the crosslink density of the hydrogels and composition.

The most direct way to increase the hydrogels swelling rate is to increase the contact area of the hydrogels with water. This can be achieved in two ways – grinding the hydrogels particles (widely used for the superabsorbent in hygiene and agricultural products) or by making monolithic superporous hydrogels [12–14]. Increased surface area in superporous hydrogels is similar to that of activated carbon or other fast-acting porous sorbents. Superporous hydrogels are recognized as substances with all the advantages of monolithic hydrogels.

Structure of a single granule of a swollen hydrogels, with a collapsed core and a swollen shell, is schematically shown in Fig. 12. For the inner core to swell, the water must travel

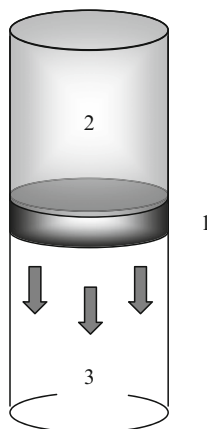


Fig. 11. Experiment to measure the rate of water diffusion through a swollen hydrogels.

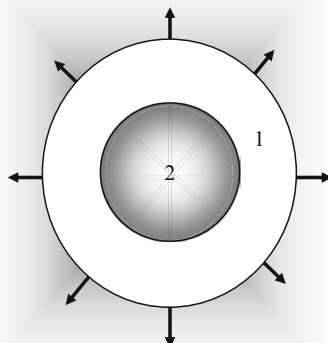


Fig. 12. Core-shell structure of a swelling hydrogels; (1) swollen shell and (2) solid core.

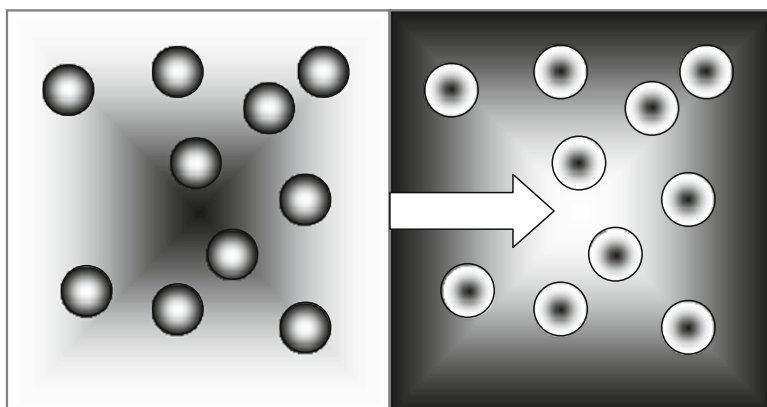


Fig. 13. Movement of the front of a chemical reagent through a matrix filled with inhibitor.

though a swollen gels to reach the core. Therefore, the rate of swelling would be dependent on how fast water can diffuse through a swollen hydrogels layer.

Depending on many factors including molecular structure, porosity, and molecular weight, the swelling process is controlled by both diffusion and relaxation processes [15].

“Stefan’s tasks” have been introduced into the modern physical chemistry. Historically, one task has been to describe the underlying theory of the frost permeation to the ground. Similar to hydrogels, there is a moving boundary between the frosted and thawed phases, which varies with time. Likewise, another task describes the penetration of reagents through a polymer matrix filled with an inhibitor. Such matrices have been developed to fight corrosion in chemical reactors. Similarly, a boundary exists between the area where a chemical reaction has taken place and the area where the unreacted inhibitor is located. The boundary is moving as the reagent gradually penetrates through the filled matrix (Fig. 13).

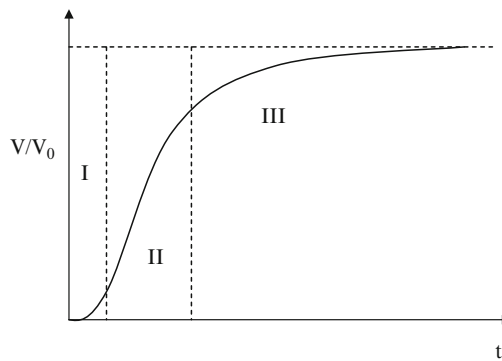


Fig. 14. Typical kinetics of swelling in hydrogels.

Generally, the rate of a chemical reaction between a reagent and an inhibitor is quite fast. Therefore, the overall rate is limited by the rate of diffusion of reagent through the polymer. The swelling of a typical hydrogels from the dry condition, shown in Fig. 14, is also considered to be a Stefan's task. In such a process, there is a time-dependent moving boundary between three different entities, i.e., dry hydrogels, partially swollen hydrogels, and fully swollen hydrogels. The boundary can move faster or slower depending on many factors including monomers, initiators, crosslinkers, reaction time, reaction temperature, particle size, pore size, pore size distribution, and molecular weight. Such boundaries move quite fast in superporous hydrogels regardless of the synthetic factors, as pores inside the hydrogels structure open another effective path for the water to diffuse. On the other hand, the boundaries would move very slowly over time in nonporous hydrogels, as the rate of swelling is solely controlled by the diffusion of water.

As shown in Fig. 14, three stages can be distinguished on the swelling graph. First, the dry layer of the hydrogels in contact with water becomes wet (phase I). Since the glass transition temperature of a dry superabsorbent hydrogels is well above the room temperature, it takes time for water to plasticize the molecules of the solid hydrogels. As soon as the first signs of plasticization appears, water starts to diffuse into the hydrogels mass very quickly as shown with marked increase in swelling rate (phase II). Finally, the equilibrium swelling capacity is reached followed by a complete relaxation of the polymer chains, which is generally a very slow process (phase III).

Most swelling data in the literature include phases II and III. In other words, the swelling of a dry hydrogels begins with a diffusion-controlled process followed by a relaxation process. This is valid for most of the superabsorbents studied in the literature as they are in granular form and very hydrophilic. Both features favor a fast diffusion process as it is the case with solid porous polymers. The first phase is generally characterized in nonporous hydrogels with a lower hydrophilic lipophilic balance. The Stefan's task can provide a better description of the second phase as shown in (30), where the size of the hydrogels particle is also included into the equation [16]:

$$l(t) = \sqrt{2D\alpha t + l^2(0)} \quad (30)$$

This observation is in good agreement with the solution of another Stefan's tasks, where the displacement of the boundary is also proportional to the square root of time. The powerful

theory of elasticity and nonequilibrium thermodynamics has been used to describe the kinetics of the hydrogels swelling [17]. These studies have been more focused on the third phase of the swelling process, where there is a boundary between the compact nonswollen core and the swollen shell. Once the solid core disappears, the kinetics of the swelling can be determined by the following equation:

$$l(t) = l_{\max} - A \exp(-Bt) \quad (31)$$

the constants A and B are experimental factors.

Summary

Absorbent hydrogels are characterized by two main features, equilibrium swelling and swelling rate. Polyelectrolyte hydrogels are good candidates for absorbing neutral aqueous solutions with no to very low ionic strength. On the other hand, nonelectrolyte hydrogels can be good sorbents for acidic or salt-containing media. Two methods have been practiced to improve the swelling rate of hydrogels; (a) size reduction of the hydrogels and (b) introduction of superporosity into the hydrogels structure. Although synthetic electrolyte and nonelectrolyte hydrogels are being used in a variety of applications, research is moving toward more biocompatible and environment friendly natural polymer alternatives, such as those based on cellulose or chitin. Due to their unique swelling features, superabsorbent hydrogels could be employed as intelligent materials. With their high swelling capacity and ability to respond to the electric field, these hydrogels could potentially be used in printers and TV screens. Although most super water absorbent polymers are used as disposable absorbent materials, there are few applications (such as in agriculture and horticulture, medical devices), where the absorbent is required to perform numerous cycles of absorption and desorption. Porous hydrogels including superporous hydrogels as well as thermo-responsive hydrogels have found very specific applications, where properties other than swelling capacity and rate are desirable. Self-assembled or self-organized hydrogels as well as those based on natural polymers (biohydrogels) could influence more advanced applications of hydrogels.

References

1. Askari F et al (1993) Synthesis and characterization of acrylic-based superabsorbents. *J Appl Polym Sci* 50:1851–1855
2. Omidian H et al (1999) Modified acrylic-based superabsorbent polymers (dependence on particle size and salinity). *Polymer* 40:1753–1761
3. Phillipova O (2000) Responsive polymer gels. *Polymer Sci* 42(2):208–228
4. Budtova TV et al (1993) Concentration redistribution of low molecular weight salts of metals in the presence of strongly swelling polyelectrolyte hydrogels. *Polymer* 34:5154–5156
5. Budtova TV et al (1995) Redistribution of the low molecular mass acid between polyelectrolyte hydrogel and solution. *Polymer Sci A37*:646–650
6. Buchholz FL, Peppas NA (1994) Superabsorbent polymers: science and technology. American Chemical Society, Symposium Series, Washington DC
7. Xinxing L, Zhen T, Ou H (1995) Swelling equilibria of hydrogels with sulfonate groups in water and in aqueous salt solutions. *Macromolecules* 28:3813–3817
8. Katchalsky A, Lifson S (1953) The electrostatic free energy of polyelectrolyte solutions. Randomly linked macromolecules. *J Polymer Sci* 11(5):409–423

9. Budtova TV et al (1995) A diffusion approach to the description of swelling of polyelectrolyte hydrogels. *Polymer Science* (official translation of *Vysokomolek. Soed.*), A37, 10
10. Suleimenov IE et al (2007) Problems of physical chemistry of polyelectrolytes (in Russian). Almaty
11. Budtova TV, Suleimenov IE (1995) Physical principles of using polyelectrolyte hydrogels for purifying and enrichment technologies. *J Appl Polym Sci* 57:1653–1658
12. Omidian H, Rocca JG, Park K (2005) Advances in superporous hydrogels. *J Control Release* 102(1):3–12
13. Omidian H, Park K (2008) Swelling agents and devices in oral drug delivery. *J Drug Deliv Sci Technol* 18(2): 83–93
14. Omidian H, Park K, Rocca JG (2007) Recent developments in superporous hydrogels. *J Pharm Pharmacol* 59(3): 317–327
15. Omidian H et al (1998) A model for the swelling of superabsorbent polymers. *Polymer* 39(26):6697–6704
16. Budtova TV, Suleimenov IE, Becturov EA (2002) Swelling kinetics of highly swelling hydrogels under the coexistence of two phases. *Polymer Sci* 44:1010–1015
17. Komori T, Sakamoto R (1989) Colloid: On Tanaka-Fillmore's kinetics swelling of gels. *Polymer Sci* 267:179–183

Name Index

- Aamer, K.A., 159
Abatangelo, G., 269
Abbasi, A., 15
Abd Alla, S.G., 355
Abd El-Mohdy, H.L., 363, 366
Abd ElRehim, H.A., 363, 366
Abdur Rahman, A.R., 329
Abdurrahmanoglu, S., 355, 356
Abe, K., 23, 24
Abel, P.U., 323
Aberman, H.M., 255
Abidian, M., 320
Abraham, S., 324
Abraham, T.E., 356
Abramson, H.A., 138
Acton, S.T., 187
Adachi, E., 23
Adamson, A.W., 9
Adams, S.B.J., 240
Adelow, C., 260
Aeschlimann, D., 207, 216
Agarwal, A.K., 57
Agasti, S.S., 100
Aghajani, V., 15
Agnely, F., 182
Agrawal, M., 115
Agrawal, S.K., 159
Aguilar, M.R., 147–154
Aharoni, A., 191
Ahmad, S., 228
Ahmed, T.A.E., 215
Ahn, J.S., 127
Ahn, K-M., 220
Ahn, Y.K., 189
Aida, T., 18
Aigner, T., 250, 257
Akahoshi, T., 77, 78
Akala, E.O., 72
Akashi, M., 367
Akashi, R., 18
Akiyama, E., 340
Akiyama, M., 29
Akiyama, Y., 23
Akiyoshi, K., 87, 339–342, 344, 345
Aksoz, E., 355
Akutsu, T., 23, 24
Albeirutti, A., 259
Albin, G.W., 67
Alblas, F.N.E., 229, 236
Alblas, J., 258, 259, 276
Alexander, P.M., 320
Alexandridis, P., 157, 182
Alexeev, V.L., 47
Alfonso, Z.C., 257
Alfrey, T. Jr., 324
Aliabadi, P., 254
Aliev, I.I., 356
Alini, M., 259, 263
Allemann, E., 158
Alles, N., 345
Almany, L., 219
Almeida, J.P., 124
Almgren, M., 124
Alsberg, E., 207, 259
Aluru, N.R., 51
AlvarezLorenzosa, C., 179
Amalvy, J.L., 111
Ambrosio, L., 229–236, 247, 259, 260, 263
Amemiya, T., 32
Amidon, G., 157
Amiji, M.M., 138, 181
Amiya, T., 65
Am, J., 77
Amntea, M.A., 95
Anderson, D.J., 320
Anderson, K.W., 259
Andersson, L.I., 19
Ando, M., 21, 23
Andrä, W., 189
Andreadis, J.D., 324
An, K., 185
Annaka, M., 65
Annunziato, F., 257
Anseth, K.S., 158, 159, 205, 206, 219, 220, 259, 263, 278
Antonietti, M., 112
Antoniou, J., 257
Aoki, H., 52
Aoki, S., 35
Aoki, T., 20, 68, 157
Aoshima, S., 124
Aoyagi, T., 20, 25, 28, 125

- Aoyama, Y., 344
 Aqil, A., 189
 Arakawa, H., 36
 Arata, H.F., 52
 Araujo, P.H.H., 358
 Aravind, A., 193
 Argüelles-Monal, W., 153
 Arica, M.Y., 323
 Armes, S.P.J., 54, 72, 88, 91, 111, 112, 138
 Arndt, K.F., 357
 Arneja, A., 236
 Arnett, F.C., 254
 Arnoczky, S.P., 232
 Arnon, R., 95
 Arotiba, O.A., 320
 Arthur, J.A., 219
 Arumugam, P., 100
 Asaka, K., 18
 Asami, N., 19, 57, 74–76
 Asami, T., 242
 Asanuma, H., 19
 Aschkenasy, C., 51
 Asher, S.A., 18, 20, 47
 Ashjian, P., 257
 Askari, F., 354, 375
 Asoh, T.A., 367
 Ateh, D.D., 320
 Ateshian, G.A., 256, 292
 Atfi, A., 220
 Athanasiou, K.A., 217, 256, 261, 263
 Attwood, D., 124
 Au, A., 211
 Audebert, R., 135
 Avasare, R., 320
 Avichechter, D., 95
 Axelos, M.A., 249, 250, 263
 Ayame, H., 345
 Ayano, E., 21, 23
 Azuma, C., 298–300
- Bachas, L.G., 54, 81, 325
 Baek, K.H., 55
 Baer, A., 228, 233, 234
 Bae, S.J., 133
 Bae, Y.H., 65, 96, 124, 125, 127–129, 132–137,
 150, 151, 159, 163, 167, 179, 183, 212, 260
 Bahadur, D., 114, 116
 Bajpai, M., 366
 Bajpai, S.K., 182, 366
 Ba, J.W., 181
 Bakalova, R., 187, 188
 Baker, C.K., 320
 Baker, J.P., 357
 Baker, P.G.L., 320
- Balakrishnan, B., 207, 216
 Baldini, N., 235
 Ballauff, M., 114
 Bansal, V., 184
 Bao, Q., 234
 Barakat, I., 159
 Barbucci, R., 259, 260, 263
 Bareggi, R., 102
 Barker, M.D., 256
 Bark, N., 282
 Barreiro-Iglesias, R., 181
 Barriere, F., 324
 Barron, A.E., 211
 Barry, F., 257
 Bartolo, C.D., 259, 263
 Bartrol, J., 50, 323
 Bashir, R., 47, 48
 Baskin, J.M., 209
 Bassetti, M.J., 51
 Bassler, N., 190
 Bassoullet, M.T., 183
 Basu, P., 184
 Batrakova, E.V., 87
 Battista, S., 260
 Baudys, M., 131
 Bauer, J.M., 28, 54, 56, 98
 Bayramoglu, G., 323
 Bazile, D., 183
 Beaumont, B.W., 253
 Beck, L.R., 158
 Beck, S.C., 256
 Becturov, E.A., 389
 Beebe, D.J., 28, 30, 51, 54–57
 Beernink, R., 215
 Behm, C.Z., 187
 Behraves, E., 217
 Bekeradjian, R., 191
 Belleville, P., 185
 Bellomo, E.G., 151
 Bender, R.J., 159, 205, 220
 Bendszus, M., 187
 Benhaim, P., 257
 Beniash, E., 54
 Ben-Moshe, M., 47
 Benvenuto, M.S., 276
 Benya, P.D., 220
 Bergel, S., 271, 277
 Bergmann, N.M., 77
 Berkowski, K.L., 54, 72
 Bertozzi, C.R., 209
 Besseling, N.A.M., 124
 Betre, H., 215
 Bey, E., 192
 Bhandari, K.H., 182

- Bhatia, S.N., 190
Bhatia, S.R., 159, 212
Bhat, S.V., 356
Bhattarai, N., 179, 216
Bianco-Peled, H., 215, 219
Bibi, N., 47, 54, 57
Bib, N., 323
Bilban, M., 260
Billingham, N.C., 91, 138
Birnbaum, J.C., 132
Bismarck, A., 355
Bivens, K.A., 235
Black, C.J., 303
Blaimer, A., 257, 258
Blaker, J.J., 239, 240
Blanchette, J.O., 55
Blanco, M., 323
Blesa, M.A., 185
Bloch, S.H., 192
Blomback, B., 282
Blum, H.E., 97
Blunk, T., 257, 258
Boelen, E.J.H., 263
Boettcher, C., 158
Bogdabova, A., 95
Bogdanov, A. Jr., 95, 185
Bo, J., 355, 357
Bonassar, L.J., 236, 261, 262
Bontha, S., 87
Boppart, S.A., 191
Borden, M.A., 187, 192
Borene, M.L., 248
Borgogna, M., 216
Borioni, A., 260, 263
Borselli, C., 260
Borzacchiello, A., 259, 260, 263
Bourges, X., 261
Bowman, C.N., 158
Bowyer, A., 179
Brad, P.B., 193
Braff, S.M., 304
Brahim, S., 319, 320, 323–326, 328
Brajter-Toth, A., 323
Brannigan, M., 191
Braschler, T., 324
Braun, K., 29, 240
Brazel, C.S., 15, 65, 357
Brechtbiel, M.W., 90
Bredley, M., 112
Breedveld, V., 151, 212, 213
Brennan, N., 305
Breuer, C.K., 22
Breuls, R.G.M., 205
Briggs, T.W., 251
Brittberg, M., 247, 257
Brizzolara, D., 159
Brochu, S., 159
Bromberg, L., 87, 151
Brøndsted, H., 72
Bronich, T.K., 87
Brouwer, L.A., 258, 260
Brown, C.J., 278
Brown, H.R., 290
Browning, T.W., 54, 81
Brown, K.E., 319
Brownlee, M., 69
Brown, T.D., 255
Brown, W., 124, 157
Bruchez, M.P. Jr., 187, 191
Bruder, S.P., 256
Brugger, B., 111
Bruns, D.E., 124
Bruns, H., 277
Brůnová, B., 306, 307
Bryan, N., 260
Bryant, S.J., 159, 205, 206, 219, 220, 278
Buchholz, F.L., 376, 386
Buckley, M.R., 262
Buckwalter, J.A., 232, 254, 255
Budtova, T.V., 376, 377, 379, 382, 384, 386, 387, 389
Bulmus, E.V., 157
Bulpitt, P., 207, 216
Bulstra, S.K., 263
Buma, P., 240
Bunya, M., 19, 68, 69
Buonocore, G.G., 15
Burdick, J.A., 205, 206, 216, 220, 257, 259, 320
Bures, P., 234
Burger, M., 32
Burgess, R.G., 292
Burghardt, W.R., 125
Burke, J., 269
Burla, A., 323
Burnes, P.N., 187
Burnham, J.C., 72
Burns, P.N., 191
Burtles, S., 104
Buschmann, M.D., 240, 292
Butnariu-Ephrat, M., 240
Butterfield, D.E., 183
Bütün, V., 88, 91, 138
Butygin, A.V., 324
Buurma, N.J., 183
Byrne, J.D., 320
Byrne, M.E., 77, 345
Cadee, J.A., 258, 260
Cai, S., 153

- Caldwell, K.D., 182
 Calve, S., 230
 Campoccia, D., 228, 233, 237
 Canavan, H.E., 183
 Candau, S.J., 295
 Cannon, S.R., 251
 Cantow, H.J., 159
 Canty, E.G., 251
 Can, V., 355, 356
 Canver, A.C., 262
 Cao, B., 257
 Cao, L., 253
 Cao, T., 254
 Cao, X., 324
 Cao, Y., 22, 324
 Caplan, A.I., 239, 256, 257
 Cappello, J., 216
 Caravan, P., 90
 Carle, G., 256, 262
 Carlson, K.L., 292
 Carnahan, M.A., 209
 Carpenter, J.E., 187
 Carredano, E., 23
 Cartier, S., 67
 Carvalho, R., 207, 216
 Cascio, B., 262
 Casolaro, M., 21
 Cassanas, G., 171
 Cassidy, J.J., 104, 228, 233, 234
 Castelletto, V., 125
 Catalaini, L.H., 356
 Cataldi, A., 102
 Caterson, B., 251
 CauichRodriguez, J.V., 355
 Causa, F., 230, 233–237, 247
 Cavalieri, F., 208, 209
 Čejková, J., 306, 307
 Cellesi, F., 214
 Cerami, A., 69
 Cerankowski L.D., 124
 Cerrai, P., 158
 Chadjichristos, C., 256, 262
 Chae, B.-S., 80, 81, 219
 Champ, S., 358
 Chanagul, A., 185
 Chancellor, M., 129
 Chandra, R., 325
 Chang, C.J., 15
 Chang, G.T., 131, 159
 Chang, S.C., 261
 Chang, Y.M., 189
 Chan-Park, M.B., 262, 263, 324
 Chansakul, T., 218, 219
 Chan, W.C.W., 187, 190
 Chaouk, H., 325
 Chaput, C., 124, 216
 Charinpanitkul, T., 185
 Char, K., 129
 Charles, P., 324
 Chaterji, S., 366
 Chatterjee, A.N., 51
 Chaubey, A., 322
 Chaudhary, M., 184
 Chauvin, P.B., 279
 Chau, Y., 219
 Cha, W.I., 355
 Cheah, C.M., 236
 Chen, A.H., 116, 181
 Chen, B.H., 179
 Chen, C-S., 209
 Chen, C.Y., 181, 320
 Chen, D., 116, 131
 Chen, D.J., 368
 Chen, D.P., 158
 Chen, D.W., 159
 Chen, F., 181
 Chen, F.H., 256
 Chen, F.M., 181
 Chen, G., 28, 65
 Cheng, I., 83
 Cheng, J., 269, 271, 275, 276
 Cheng, S.X., 366
 Cheng, S.Y., 60
 Cheng, X., 183
 Cheng, Y.L., 124, 125, 183
 Chenite, A., 124, 216
 Chen, J.H., 99, 125, 362, 366
 Chen, K.S., 355
 Chen, L.W., 14, 125, 251
 Chen, P., 14
 Chen, Q.Z., 53, 99, 239, 240
 Chen, S.Y., 191
 Chen, W., 260, 263
 Chen, W.Y., 269
 Chen, X.S., 135, 263
 Chen, Y., 187, 189
 Chen, Y.H., 28, 53
 Chen, Y.M., 298–300
 Cheung, A.C.Y., 219
 Chia, H.S., 185
 Chiang, W.Y., 357
 Chiari, C., 239
 Chibante, P., 108
 Chiessi, E., 208, 209
 Chilkoti, A., 211, 215, 357
 Cho, C.S., 180
 Choi, C.Y., 279
 Choi, H.K., 180

- Choi, J.B., 253
 Choi, S., 131
 Choi, S.H., 159, 211
 Choi, S.W., 128, 159, 213
 Choi, S.Y., 128, 159
 Choi, Y.H., 182
 Choi, Y.K., 128, 129, 183
 Cho, J.H., 181
 Choo, E.S.G., 185
 Cho, S.W., 279
 Cho, T.H., 204, 206, 211
 Chowdhury, S.M., 157
 Christen, E.H., 82
 Christesen, K., 256
 Christiansen, J., 187
 Christopoulos, T.K., 74
 Chua, C.K., 236
 Chubinskaya, S., 251
 Chu, C.C., 206, 216
 Chuchi, S., 116
 Chudinov, A.V., 324
 Chu, M., 14
 Chung, C.K., 182, 205, 216, 257, 259
 Chung, D.J., 325
 Chung, H.J., 161, 181, 206, 214
 Chung, J.E., 183, 211, 216
 Chung, Y-I., 220
 Chung, Y.M., 132
 Chun, M.K., 180
 Ciapetti, G., 235
 Cima, L.G., 260
 Clague, M.J., 88, 95
 Cliff, R.O., 324
 Cobain, E., 159
 Cocco, L., 102
 Cohen, I., 262
 Cohen, R.E., 47
 Cohn, D., 126, 127, 158, 233, 234, 258, 260, 262, 263
 Colbern, G.T., 95
 Cole, A.A., 251
 Cole, B.B., 209, 214
 Coles, C., 305
 Colette, S., 275
 Colfen, H., 112
 Collett, J.H., 124
 Colosia, A.D., 99
 Concheiro, A., 181
 Concheiroa, A., 179
 Connor, E.E., 184
 Conroy, S., 190
 Constantinidis, I., 60
 Cook, J.L., 239
 Cordoba de Torresi, S.I., 320, 325
 Cornejo-Bravo, J., 153
 Cornelio, L., 209
 Coronilla, R., 181
 Corrigan, O., 153
 Cosgrove, D., 187
 Cosmi, L., 257
 Costerton, J.W., 51
 Cotton, G.J., 209
 Coudreuse, A., 261
 Courts, A., 271
 Coutinho, C.A., 116
 Couvrer, P., 51
 Coviello, T., 216
 Cowsar, D.R., 158
 Craig, S., 256
 Cram, A., 269
 Crampton, H., 152
 Cravatt, B.F., 209
 Crescenzi, V., 125, 209
 Cristino, S., 231
 Critchfield, F.H., 124
 Cruikshank, G.A., 54, 55
 Crum, L., 51
 Cuddihy, M.J., 282
 Cui, W., 90
 Cui, X., 320
 Culp, W., 192
 Cummins, S.S., 187
 Cunningham, B.W., 234
 Cutler, E.C., 100
 Cuyper, M.D., 185
 Czeisler, C., 54
 Czerwonka, L.A., 236
 Daculsi, G., 247, 256, 260–262
 Dadsetan, M., 217
 Dai, H., 53
 Dalmont, H., 111
 Damien, E., 260
 D'Amore, A., 230, 233
 D'andrea, P., 241
 Dangas, G., 191
 Darcy, D., 187
 Dare, E.V., 215
 Darling, E.M., 256
 Darwis, D., 355, 358
 Dasari, R., 19, 77
 Daunert, S., 54, 81, 325
 Davidenko, N., 153
 Davies, L.C., 14
 Davis-Arehart, K.A., 206, 219
 Davis, P.A., 234
 Davis, S., 185
 Day, A.F., 124

- Dayananda, K., 137, 140, 179
 Dayton, P.A., 187, 191, 192
 De Bari, C., 257
 de Boer, D., 180
 Deb, S., 355
 Dee, K., 230
 De Groot, C.J., 258, 260
 De Groot, J.H., 239
 Deguchi, S., 339
 De Jaeghere, F., 158
 de Jong, S.J., 159, 211, 242
 Delfini, M., 260, 263
 Dell'Accio, F., 257
 Dellacherie, E., 181, 263
 Delsanti, M., 109
 Demarteau, O., 256
 Dembo, A.T., 356
 Dembo, K.A., 356
 Demeester, J., 159, 242, 270
 Dementieva, E.I., 324
 Demers, C.N., 257
 Demirtas, T.T., 366
 Deng, X.M., 158
 Deng, Y., 157, 183
 Denis, D., 182
 Dennis, J.E., 237
 Dennis, R., 230
 den Otter, W., 258, 260
 Deo, S.K., 54, 81
 Derfus, A.M., 190
 de Rooij, N.F., 50, 323
 DeRossi, D., 65
 Desai, B., 261
 De Santis, R., 230–235
 Desa, T.A., 278
 Désert, S., 109
 De, S.K., 51
 De Smedt, S.C., 159, 211, 242
 Desnoyers, S., 98
 De Sousa, D.A., 181
 Despres, J.P., 279
 De Ugarte, D.A., 257
 Devadoss, C., 28, 54, 56
 de Vijn, J.R., 276
 Devine, S.M., 257
 De Wijn, J.R.J., 229, 236
 Deyo, R.A., 254
 Dhawan, S.K., 325
 Dhert, W.J.A., 258, 259, 276
 Diaa, D.A., 366
 Diamandis, E.P., 74
 Di Cocco, M.E., 260, 263
 Diederichs, K., 159
 Dietz, H., 83
 Dijkstra, P.J., 125, 131, 211
 Dikovsky, D., 215, 219
 Di Martino, A., 216
 DiMeo, C., 209
 Dimitrov, I., 125
 Ding, F.C., 357
 Ding, J.H., 131, 191, 206
 DiPersio, L., 152
 Di Silvio, L., 260
 Dispenza, C., 325
 Djojoseburoto, M., 97
 Dobbelle, W., 325
 Dockery, P., 259, 263
 Dogan, A.K., 355
 Doherty, P., 228, 233, 237
 Domb, A., 158
 Domingo, C., 185
 Domm, C., 256
 Donati, I., 216
 Dong, L.-C., 57, 65
 Doretti, L., 323
 Dorkoosh, F.A., 366, 367
 Dorotka, R., 239
 dos Santos, J.F.R., 355
 Douglas, R., 256
 Downes, S., 215
 Dowson, D., 292
 Doyle, F.J. III., 50, 56, 58, 67
 Drumheller, P., 153
 Drumright, R., 339
 Drury, J.L., 203, 247
 D'souza, A.J.M., 180
 Dubovik, A.S., 179
 Dubrovskii, S.A., 14
 Dudhia, J., 251
 Dufes, C., 181
 Dumortier, G., 182
 Duncan, R., 57, 95, 104, 147, 148
 Dunn, S.E., 183
 Durand, A., 181
 Durand, K.L., 159, 205, 220
 D'Urso, E.M., 324
 Dusek, K., 65
 Dutta, J., 185
 Dutza, S., 189
 Du, Z., 203, 205
 Earnshaw, W.C., 98
 Eastoe, J., 185
 Ebara, M., 25
 Eby, J.K., 53
 Eckert, F., 114, 116
 Eddington, D.T., 28, 51, 54–56
 Edgar, T.F., 58

- Edmond, M., 179
Efron, N., 303, 306–310
Ehrbar, M., 82
Ehrick, J.D., 54, 81
Eilles, C., 98
Elbert, D., 153
El-Din, H.M.N., 355
Elisseeff, J.H., 206, 236, 248, 255, 259, 262, 263
Elizondo, G., 185
Ellegala, D.B., 187
Ellison, J.J., 90
El-Mohdy, H.L.A., 14
El-Naggar, A.W.M., 355
El-Rehim, H.A.A., 14
El Salmawi, K.M., 14
Elvira, C., 324
Enami, S., 151
Endo, T., 111, 346, 347
Endres, M., 220
Engbers, C.M., 95, 184
Engbers, G.H.M., 215
Engler, A.J., 205
Enoch, J.M., 303
Enoki, T., 19, 77
Epstein, I.R., 30
Erata, T., 291
Erik, B., 190
Eschbach, F.O., 355
Eslamian, M., 15
Espartero, J.L., 158
Euliss, L.E., 185
Eyre, D., 251
Ezaki, K., 180

Fain, H., 192
Fairbrother, D.H., 262
Fait, E., 103
Falamarzian, M., 180
Falcieri, E., 102
Falk, B., 324
Fang, J.E., 53
Fan, X.D., 179
Fan, X.H., 158
Farmer, T.G., 58
Fatimi, A., 249, 250, 262, 263
Fava, D., 116
Favaro, S.L., 355, 357
Fedorovich, N.E., 214, 258, 259, 276
Feher, J., 18
Feijen, J., 125, 131, 158, 183, 263
Feil, H., 125, 183
Feinbloom, W., 304
Feld, M.S., 19, 77
Felisberti, M.I., 356

Fellah, B.H., 260, 262
Felson, D.T., 254
Feringa, B.L., 55
Fermanian, S., 262
Fernandes, C.M., 181
Fernandez, B.A., 111
Fernández, M., 153
Ferrara, D., 323
Ferraro, N.F., 22
Ferreira, L., 207, 216
Ferry, J.D., 271, 277
Fiandaca, G., 325
Fiegel, H.C., 277
Field, R.J., 32
Fields, G.B., 81
Fijian, R.S., 292
Filipcei, G., 18
Fillmore, D.J., 65, 107
Fine, T., 324
Finley, S., 329
Fiorini, M., 237
Firestone, B.A., 180
Firpo, M.A., 206, 208
Fisher, E.C. Jr., 261
Flannery, C.R., 251
Fleagle, J.T., 95
Fleischmann-Mundt, B., 97
Fleming, G.K., 313
Flint, M.H., 253
Flory, P., 324
Focella, T.M., 188
Fokin, V.V., 209
Folmer, Y., 97
Fong, Y.C., 185
Fonner, J.M., 320
Foo, H.L., 274
Forcada, J., 108
Forciniti, L., 320
Foroutan, H., 357
Fortier, G., 324, 355
Fox, D.B., 239
Fraier, D., 104
Francis Suh, J.K., 216
Francolini, I., 51
Francomacaro, A.S., 323
Fransen, J., 270
Franssen, O., 180, 181
Fraser, J.K., 257
Fraser, J.R., 216
Frazer, A., 256
Frechet, J.M., 96
Freeman, M.E., 296
Freemont, T.J., 111, 114
Freier, T., 158

- Frey, P., 260
Frick, B., 111
Frigerio, E., 104
Fritzinger, B., 57
Fuegy, P.W., 206, 208
Fu, F.H., 231
Fujimoto, K., 108, 111, 340, 346
Fujimoto, T., 109
Fujita, H., 52
Fujiura, K., 151
Fujiwara, T., 157–173
Fu, K., 206
Fukui, N., 256
Fukui, T., 346
Fukushima, S., 95, 96
Fukushima, T., 18
Fulda, C., 97
Funakoshi, T., 231
Fung, Y.C., 230, 296, 297
Furey, M.J., 296
Furst, E.M., 80, 81
Furukawa, H., 287–289
Furukawa, M., 65
Fusaro, R.E., 306
Fussenegger, M., 82, 215, 278
Futrell, J.W., 257
Fyfe, J.A., 271
- Gaharwar, A.K., 114, 116
Galera, P., 256, 262
Gallaher, C.M., 181
Gallardo, A., 153
Gallea, S., 220
Galvin, M.E., 326
Ganga, R., 271
Gangopadhyay, R., 325
Gan, J., 116
Gan, L.H., 127, 151, 182
Gao, C., 215
Gao, J., 18, 109, 237
Gao, L.Z., 323
Gao, M., 191
Gao, Z., 192
Garcia, A.J., 205
Garcia, C.A., 217
García, L., 147–154
Gardner, D.L., 251
Garg, S., 55
Garnett, M.C., 183
Garramone, S., 324
Garreau, H., 158
Garty, S., 260, 262, 263
Gast, A.P., 88
Gattolin, P., 323
- Gaumann, A., 103
Gaur, U., 181
Gauthier, O., 260, 262
Gavrilas, C., 363, 368
Gayet, J.C., 324, 355
Gaylord, N.G., 305
Gehrke, N., 112
Gehrke, S.H., 109, 324
Gemeinhart, R.A., 363, 367, 368
Genes, N.G., 261
Gentleman, E., 230
George, P.M., 320
Gerbasio, D., 260
Gerlach, G., 352
Gershon, B., 233, 234
Gerweck, L.E., 88, 90
Ge, Z., 233, 254
Ghandehari, H., 72, 216
Ghasemzadeh, H., 15
Ghosh, P.C., 181
Ghosh, R.N., 88, 95
Ghzaoui, A.E., 128
Giacomelli, L., 125
Giannini, E.H., 254
Giasson, S., 296
Gibbons, D.F., 231
Gil, E.S., 124
Gillies, E.R., 96
Gimble, J., 257
Gin, P., 187
Glass, G.G., 254
Gleeson, J.M., 69
Gleghorn, J.P., 262
Glimcher, M.J., 255
Gloria, A., 234, 235
Gluzband, Y.A., 240
Go, D.H., 181
Goetzke, K., 257
Goh, J.C.H., 230, 233
Goh, S.H., 134
Gohy, J.F., 138, 296
Goldbart, R., 51, 57
Goldberg, V.M., 237, 257
Gole, A., 184
Gomathinayagam, S., 271
Gombotz, W., 328
Gomella, L.G., 187
Gomez, N., 320
Gonen-Wadmany, M., 219
Gong, J.P., 27, 285–289, 291–300, 325
Gong, Y., 191, 205–207
Goodman, D., 239
Gopferich, A.M., 220, 257, 258
Goraltchouk, A., 158

- Gordon, A.N., 95
Gore, M.E., 95
Gorham, J., 262
Gottlieb, R., 357
Gough, J.E., 47, 54, 57, 215, 323
Gould, H.L., 303
Govan, J.R., 271
Grad, S., 259, 263
Graham, A.D., 306
Graham, D.J., 183
Graham, N.B., 158
Grammatikakis, J., 324
Grancharov, S.G., 185
Grandolfo, P., 241
Grant, G.T., 182
Grassi, F., 231
Greco, M., 235
Green, L.G., 209
Green, R.A., 320
Gref, R., 158, 159
Greisch, J.F., 189
Griffin, J.M., 355
Griffith, L.G., 73, 211, 236, 279
Griffith, M., 215
Grigolo, B., 237
Grimm, D., 98
Grimm, J., 188
Grinberg, N.V., 124
Grodzinsky, A.J., 240, 292
Grojec, M., 256
Grosberg, A.Y., 19, 77
Grossiord, J.L., 182
Gruber, H.E., 261
Gruenberg, J., 88, 95
Guan, Y., 53
Guarino, V., 233, 236, 237
Guarnieri, D., 260
Gueroui, Z., 99
Guicheux, J., 247, 256, 260, 262
Guilak, F., 215, 253, 257
Guilherme, M.R., 14
Guillet, J.E., 109
Guillet, J.J., 183
Guillot, S., 109
Guimard, N., 320
Guiseppe-Elie, A., 319–333
Gumusderelioglu, M., 355, 366, 368
Gunning, A.P., 157
Gunn, J., 179, 216
Gunther, M., 352
Guo, G., 191
Gupta, A.K., 47, 48
Gupta, D., 153
Gupta, K.M., 9
Gupta, N., 209
Gupta, P., 55
Gupta, S., 115
Gupta, V.K., 116
Gurav, N., 260
Gurnee, E., 324
Guthrie, D., 95
Gutowska, A., 131, 132, 212
Guven, O., 324
Gu, X-G., 345
Hacker, M., 257, 258
Hafemann, B., 279
Hafkemeyer, P., 97
Haider, M., 216
Hainfeld, J.F., 188
Hain, J., 116
Ha, J., 211
Halbesma, G.J., 205
Hales, K.D., 212
Hall, H., 54
Halloran, D.O., 259, 263
Halpern, E.J., 187
Hamachi, I., 52
Hamaguchi, T., 95
Hamai, Y., 292–295
Hamm, B., 185
Hammond, P.T., 47
Hampton, J.M., 296
Hanada, K., 257
Han, B.R., 128, 132
Han, C.K., 124
Han, D.K., 128
Hanley, E.N. Jr., 261
Hannan, M.T., 254
Hannington, J.P., 185
Han, S.H., 241
Hans-Juergen, A., 116
Hanson, N.A., 215
Hantzschel, N., 114
Han, W., 360, 368
Hao, J., 151
Hao, Q., 133
Hao, T.N., 159
Hapiot, P., 324
Haq, I., 183
Harada, A., 96, 99
Haraguchi, K., 28, 30
Hara, Y., 32, 33, 36, 39, 41
Harden, J.L., 81
Hardiningsih, L., 358
Hardman, R.A., 191
Harimoto, M., 23, 24
Harrinauth, R.K., 116

- Harrington, D.A., 54
 Harris, W.H., 292
 Harsh, D.C., 109
 Hartgerink, J.D., 54
 Hasegawa, M., 25
 Hasegawa, U., 87, 345–347
 Hasegawa, Y., 23
 Hashiguchi, H., 325
 Hashi, J., 72
 Hashimoto, S., 32, 33, 35, 41
 Hassan, C.M., 67, 180
 Hasty, K.A., 251
 Hasuda, H., 36
 Hatton, T.A., 87, 157, 182
 Haveman, J., 88, 90
 Hawiger, J., 99
 Hayashi, C., 347
 Hayashida, Y., 23
 Hayashi, H., 88, 95, 100
 Hayashi, S., 18
 Hayashi, T., 158, 215
 Hay, D.N.T., 183
 Healy, K.E., 125
 He, C.L., 123–141, 179, 212
 Hedrick, M.H., 257
 Hegazy, E.S.A., 14, 363, 366
 Hegde, A., 320
 Heijkants, R.G., 239
 Heimbach, D., 269
 Heinegard, D., 250
 Heitz, R.F., 303
 He, J., 213, 214
 Hejazi, R., 181
 Helland, M., 306
 Heller, A., 47, 48
 Heller, J., 57
 Helmick, C.G., 254
 Heng, B.C., 254
 Hennig, T., 257
 Hennik, W.E., 124
 Hennink, W.E., 89, 207, 212, 216, 258–260, 346
 Hennisnk, W.E., 276
 Henry, S.M., 205
 He, P., 355
 Hergta, R., 189
 Hering, T.M., 257
 Herold, C.B., 124
 Hersh, E., 191
 Heschel, I., 279
 Heskings, M., 109, 183
 Hess, C., 355
 Hesslink, R. Jr., 181
 Hetke, J.F., 320
 Heule, M., 324
 He, X., 219
 Heymer, A., 230
 Heyse, S.P., 254
 Hiasa, A., 345
 Hideto, T., 211
 Hiemstra, C., 160, 161, 206, 208, 209, 211, 214, 216, 263
 Higa, M., 292
 Higham, P.A., 234
 Higuchi, H., 191
 Higuchi, T., 157
 Hilborn, J., 209
 Hilditch, T.E., 104
 Hillier, J., 184
 Hillyer, J., 256
 Hilmy, N., 358
 Hilt, J.Z., 47, 48
 Hiltner, A., 228, 233, 234
 Hincke, M., 215
 Hinman, A.D., 206
 Hirai, D., 182
 Hirai, M., 18
 Hirai, T., 18
 Hirakura, T., 344
 Hirasawa, H., 35
 Hirayama, F., 213
 Hirayama, M., 345
 Hirokawa, Y., 65
 Hirooka, A., 241
 Hirose, M., 23, 24, 26, 183
 Hirose, Y., 65
 Hirsch, R., 254
 Hisatome, T., 206
 Hobley, J., 279
 Hobling, W., 215
 Ho, B.S., 112
 Hochberg, M.C., 254
 Hodge, W.A., 292
 Hoelscher, G., 261
 Hoemann, C.D., 216
 Hoffman, A.S., 19, 53, 65, 70, 71, 123, 135, 229, 234, 269, 328, 345
 Hoffmann, H., 157
 Holden, B.A., 306
 Hollander, A.P., 256
 Holland, T.A., 211, 215
 Hollister, S.J., 236
 Holmberg, D.L., 69
 Holmes, C.C., 181
 Holmes, J.D., 185
 Holmes, M., 241
 Holte, Ø., 182
 Holtz, J.H., 18, 20, 47
 Holtz, J.S.W., 18

- Holzhüter, S., 277
 Holzwarth, J.F., 157
 Homming, G.N., 240
 Hong, S.P., 190
 Hong, Y., 205–207, 216
 Hoogsteen, W., 160
 Horak, D., 367
 Horbett, T.A., 21, 49, 67
 Hori, H., 18, 51, 65
 Horii, F., 159
 Hori, K., 159
 Ho, R.J.Y., 104
 Horne, R.A., 124
 Hoshikawa, A., 215
 Hoshino, F., 88, 109
 Hostetler, M.J., 100
 Hou, J., 112
 Hou, Q.P., 179
 Hourdet, D., 135
 Hovgaard, L., 72
 Howel, M., 319
 Hristova, K., 99
 Hron, P., 355
 Hsu, S.H., 357
 Hua, F.J., 134
 Huang, H., 188
 Huang, J.I., 257
 Huang, K.L., 189
 Huang, L., 129, 130, 159
 Huang, M., 287, 288
 Huang, S.J., 234, 355
 Huard, J., 159, 257
 Hua, Y., 53
 Hubbell, J.A., 54, 81, 153, 157, 205, 206, 208,
 209, 211, 214, 219, 227, 228, 260 277
 Hubel, A., 248
 Hu, B.H., 73, 219
 Hübner, U., 270
 Hu, D.S.G., 158
 Hudson, S.M., 124
 Huerta, P., 323
 Huesker, M., 97
 Hughes, C.E., 251
 Huglin, M.B., 358
 Huh, K.M., 72, 134
 Huin-Amargier, C., 263
 Hui, P.W., 242
 Hukins, D.W.L., 233, 234
 Hunder, G.G., 254
 Hunt, J.A., 260, 269
 Husein, M., 185
 Hussain, S.M., 185
 Hutmacher, D.W., 220
 Hu, Y., 254
 Huynh, D.P., 137, 139, 140
 Hu, Z.B., 18, 28, 109, 117
 Hvidt, S., 157
 Hwang, M.J., 133
 Hwang, N.S., 248, 262
 Hwang, S., 324
 Hwang, Y., 185
 Hyon, S.H., 159
 Hyun, H., 133
 Iannace, S., 229, 230, 234
 Ibrahim, S.M., 14
 Ibusuki, S., 205
 Ichijo, H., 31
 Ichikawa, H., 234
 Ifkovits, J.L., 206
 Iijima, M., 88, 95, 100, 159
 Ikada, Y., 159, 256
 Ikai, A., 36
 Ikeda, I., 157
 Ikeda, M., 52, 345
 Iko, Y., 52
 Ikuta, Y., 345
 Illum, L., 183
 Imanishi, Y., 21, 28
 Imaz, A., 108
 Inamoto, T., 206
 Indovina, P.L., 103
 Inoue, T., 65
 Irie, M., 51, 65
 Irie, T., 213
 Irvine, D.J., 47
 Isaacs, S.R., 100
 Isaksson, O., 247
 Ishihara, K., 21, 67, 158, 324
 Ishii, T., 100
 Ishikawa, I., 25
 Ishimaru, N., 67
 Ishizuka, K., 52
 Isobe, M., 345
 Isobe, T., 324
 Isogai, N., 256
 Isoi, Y., 23, 24
 Itaka, K., 88
 Ito, K., 27, 29
 Ito, S., 36, 52, 107
 Ito, T., 95
 Ito, Y., 21, 28, 32, 36
 Iwasaki, N., 231
 Iwasaki, Y., 292–295, 346, 347
 Iwuoha, E.I., 319, 320
 Jabbari, E., 217, 219
 Jackson, D.W., 255

- Jack, Z.S., 187
 Jacobsen, L.O., 183
 Jacobs, H., 65
 Jacquet, R., 256
 Jain, R.K., 95
 Jain, T.K., 189, 191
 Jaiswal, R.K., 256
 Jakob, M., 256
 James, E., 109
 Jamshidi, K., 159
 Janevik, E., 152
 Jang, E., 52
 Jansen, H.W., 239
 Jaramillo, A., 323
 Jarman, T.R., 271
 Jaszcz, K., 206
 Jayakrishnan, A., 207, 216
 Jayawarna, V., 47, 54, 57, 323
 Jean-Francois, J., 324
 Jedlinski, Z., 158
 Jena, A.K., 9
 Jeong, B., 127–129, 131, 132, 134, 150, 151, 159, 163, 167, 183, 212, 260
 Jeong, J.H., 159
 Jeong, S.Y., 134
 Jeong, Y., 133
 Jeon, S-H., 220
 Jerome, R., 296
 Jia, L., 133
 Jiang, H., 52, 57
 Jiang, Y.R., 189
 Jiang, Z., 151
 Jian, Y.C., 53
 Jia, W., 321
 Jia, X., 205, 216
 Jige, M., 19, 78–80
 Jikihara, A., 70, 71
 Jiménez, C., 50, 323
 Jimin, R., 190
 Jin, H.J., 55
 Jin, J.I., 124
 Jin, M., 228
 Jinno, D., 182
 Jin, R., 211, 216, 263
 Jiya, T.U., 205
 Jo, B.H., 28, 54, 56
 Johann, R., 324
 John, C., 179
 John, G., 54, 55
 John, P., 271
 Johnson, C.S., 209
 Johnson, J.A., 209
 Johnstone, B., 257
 Johnston, K.P., 185
 Jolivet, J.P., 185
 Jones, C.D., 108
 Jones, W.R., 253
 Joniau, M., 185
 Joo, M.K., 133, 134
 Jordan, M., 269
 Jorgensen, E.B., 157
 Jo, S., 131, 206, 217
 Judeh, Z.M., 324
 Junger, O., 52
 Jung, P.J., 209
 Jung, Y.G., 55, 258
 Jun, H.W., 54
 Juntanon, K., 180
 Justin, G., 329
 Kabanov, A.V., 87
 Kabiri, K., 367
 Kabra, B., 324
 Kadler, K.E., 251
 Kafienah, W., 256
 Kagata, G., 292, 295, 296
 Kageyama, S., 345
 Kaihara, S., 276
 Kajiwara, K., 65, 108, 157, 285
 Kakinoki, S., 153
 Kakizone, T., 95
 Kakugo, A., 291
 Kamada, H., 180
 Kamarchik, P., 321
 Kamath, K.R., 205
 Kamijo, Y., 108
 Kampf, N., 296
 Kanaya, F., 298–300
 Kanazawa, H., 21, 23
 Kanda, T., 183
 Kaneko, D., 296, 297
 Kaneko, T., 65, 367
 Kaneko, Y., 28, 183
 Kaneshima, D., 116
 Kang, E-C., 342
 Kang, H., 83
 Kang, J.D., 15, 231
 Kang, S.W., 134
 Kannan, R., 152
 Kanzaki, Y., 65
 Kaplan, D.L., 211
 Karakecili, A.G., 366, 368
 Karikusa, F., 23
 Karlsson, J., 255
 Karmalkar, R.N., 50, 51
 Karp, J.F., 54, 55
 Karp, J.M., 190
 Kashiwase, Y., 21

- Kasko, A.M., 209, 214
 Kataoka, K., 18–20, 68, 69, 88, 95, 96, 99, 132
 Kataoka, S., 108
 Katayama, N., 345
 Katchalsky, A., 378
 Kathryn, H., 179
 Kato, K., 65
 Kato, N., 347
 Katono, H., 65
 Kato, T., 111
 Katsuyama, Y., 27, 285–287, 292, 296, 298
 Katz, A.J., 257
 Kaufmann, P.M., 277
 Kaufmann, S.H., 98
 Kaul, C.S., 345
 Kawaguchi, A., 159
 Kawaguchi, H., 88, 107–117
 Kawakami, I., 325
 Kawakami, K., 211, 216
 Kawano, S., 291
 Kawasaki, K., 216
 Kawauchi, Y., 288, 289
 Kawguchi, H., 114, 117
 Kaye, S.B., 104
 Kayes, J.B., 182
 Kazanskii, K.S., 14
 Kedar, R.P., 187
 Keeffe, E.B., 269
 Keene, D.R., 260
 Keifer, P.A., 87
 Keil, K., 124
 Kelm, J.M., 278
 Kempe, R., 114
 Kennedy, A., 192
 Kenworthy, A.K., 99
 Kessler, J.A., 54
 Khademhosseini, A., 235
 Khalid, M.N., 355
 Khang, G., 133
 Khan, M., 262
 Khattak, S.F., 212
 Kheirolomoom, A., 191
 Khodabakhsh, M., 357
 Khokhlov, A.R., 356
 Kiani, C., 251
 Kibbey, M.R., 132
 Kielty, C.M., 237
 Kii, A., 295
 Kiick, K.L., 80, 81
 Kikuchi, A., 20–26, 28, 65, 68, 183, 236
 Kikunaga, Y., 124
 Kim, B.S., 137, 276, 279
 Kim, C., 134
 Kim, D., 183, 367
 Kim, D-H., 320
 Kim, D.J., 357, 367
 Kim, D.K., 184, 188
 Kim, D-N., 324
 Kim, D.W., 183
 Kim, E.H., 189
 Kim, H., 47
 Kim, I.S., 204, 206, 211
 Kim, I-Y., 216
 Kim, J., 131, 204, 206, 211
 Kim, J.C., 183
 Kim, J.H., 47, 52, 61, 77, 136, 137, 180, 367
 Kim, J.K., 355
 Kim, J-M., 213
 Kim, J.O., 180
 Kim, J.W., 355
 Kim, K., 137
 Kimmel, E., 191
 Kim, M.H., 183
 Kim, M.R., 214
 Kim, M.S., 133, 139
 Kim, R.S., 191, 192
 Kim, S., 150, 151, 324
 Kim, S.C., 128, 183
 Kim, S-H., 258
 Kim, S.H., 133, 181, 206, 216, 258, 274
 Kim, S.J., 52
 Kim, S.K., 133
 Kim, S.S., 276
 Kim, S.W., 19, 65, 69, 123, 128–131, 135, 159, 183, 212, 260
 Kim, T., 183, 209
 Kimura, 160
 Kimura, J., 95
 Kimura, S., 211
 Kimura, T., 241
 Kimura, Y., 157–173
 Kim, W., 56
 Kim, Y., 134
 Kim, Y.H., 133, 258
 Kim, Y.I., 182
 Kim, Y.J., 68, 131, 159
 Kim, Y.M., 56
 Kinjo, M., 295, 296
 Kipshidze, N.N., 191
 Kirchner, C., 187
 Kirker, K.R., 324
 Kirsten, N.H., 179
 Kiser, R.F., 20
 Kishida, T., 345
 Kisiday, J., 228
 Kissel, T., 152, 158
 Kister, G., 171
 Kitagawa, T., 95

- Kitano, S., 345
 Kitaoka, K., 215
 Kitchens, C., 185
 Kleinen, J., 112
 Klein, J., 296
 Klemm, D., 291
 Klibanov, A.L., 187
 Klomp, G., 325
 Klouda, L., 212, 217
 Klumb, L.A., 49
 Kluth, D., 277
 Kluth, J., 277
 Knaebel, A., 295
 Knag, Y.S., 185
 Kneser, U., 277
 Knowles, J.R., 276
 Kobayashi, E., 124
 Kobayashi, H., 90, 346
 Kobayashi, J., 21
 Kobayashi, M., 21, 67
 Kobayashi, S., 211, 345
 Koch, A., 220
 Koch, S., 182
 Kodibagkar, V.D., 90
 Kofuji, K., 182
 Kofuji, K.E., 182
 Koga, H., 345
 Koga, S., 32
 Koh, J.J., 131
 Kohori, F., 125
 Koh, W-G., 324
 Koide, S., 255
 Koike, H., 95
 Koizumi, S., 125
 Kokufuta, E., 18, 31, 35, 69
 Kolhe, P., 152
 Koller, U., 239
 Komatsu, H., 52
 Komiyama, M., 19
 Komori, T., 390
 Komura, A., 18
 Kondo, E., 298
 Kondo, M., 95
 Kondo, T., 111
 Kon, E., 239
 Konerding, M.A., 103
 Kong, H.J., 324
 Konno, C., 23, 26
 Konno, T., 95
 Kono, K., 21
 Kontinen, Y.T., 237
 Koole, L.H., 263
 Koot, H.W.J., 240
 Kopecek, J., 72, 76, 81, 97, 212, 213, 228, 242, 345
 Kopeckova, P., 67, 72, 97, 212
 Kopeček, J., 212, 213
 Koros, W.J., 313
 Korpanty, G., 191
 Kosaka, A., 18
 Kosnik, P., 230
 Kost, J., 21, 51, 57
 Kotani, Y., 234
 Kotov, N.A., 282
 Koudelka-Hep, M., 50, 323
 Koul, S., 325
 Kouvrokoglou, S., 179
 Kou, Y-F., 320
 Kovarova, J., 158
 Koyama, Y., 68
 Kraft, C.T., 100
 Krampera, M., 257
 Kreibig, U., 184
 Kreisersaunders, I., 158
 Kressler, J., 182
 Krestin, G.P., 185
 Kretschmann, O., 213
 Kricheldorf, H.R., 158
 Krijgsveld, J., 215
 Krishnan, R.S., 217
 Krupinski, E., 187
 Kubies, D., 158
 Kubo, A., 68
 Kubuka, S., 97
 Kuckling, D., 352
 Kudara, S., 187
 Kuebler, S.M., 29
 Kühling, H., 279
 Kuhnel, F., 97
 Kuijpers, A.J., 215
 Kujawa, P., 340
 Kulkarni, M.G., 50, 51
 Kumacheva, E., 112
 Kumar, D., 321
 Kumar, G.S., 72
 Kumar, S., 116, 185, 325
 Kumashiro, T., 55
 Kungwachakun, D., 51
 Kuo, C.K., 204, 216
 Kurata, T., 69
 Kurcok, P., 158
 Kurihara, K., 292–295
 Kurisawa, M., 72, 73, 211, 216
 Kurita, K., 347
 Kuroda, K., 77, 340, 346
 Kurokawa, T., 27, 285–288, 295–297
 Kurumada, S., 341, 342
 Kurz, B., 228, 256
 Kushida, A., 23

- Kusuhara, H., 256
 Kuwabara, R., 287, 288
 Kwok C., 51
 Kwon, G., 95
 Kwon, I.C., 134
 Kwon, I.K., 125, 366
 Kwon, K.W., 129
 Kwon, O.H., 23, 26, 183
 Kyritsis, A., 324
- Labhasetwar, V., 87
 Labos, M., 254
 Lacave, A., 95
 Laing, R., 306
 Lai, W.M., 241, 292
 Lakouraj, M.M., 355
 Lallemand, F., 220
 Lator, P.A., 255
 Lamponi, S., 259
 Landers, R., 270
 Landis, W.J., 256
 Lando, G., 127
 Laney, M.W., 179
 Langer, K.J., 51
 Langer, R., 22, 52, 138, 203, 235, 240, 256, 258,
 259, 263, 320
 Langevin, D., 109
 Langrana, N.A., 83
 Lankford, M., 187
 Lapkowski, M., 261, 262
 LaPlaca, M.C., 205
 Larsson, T., 250
 Lauer-Fields, J.L., 81, 205, 208, 219
 Lauffer, R.B., 90
 Laukkanen, A., 125
 Laurent, T.C., 216
 LaVan, D.A., 320
 Lawrence, R.C., 254
 Layrolle, P., 247, 262
 Lazebnik, Y.A., 98
 Leach, J.B., 235
 LeBaron, R.G., 261, 263
 Lebaron, R.G., 217
 Lechaire, J.P., 185
 Lee, A.S., 88
 Lee, B.H., 214
 Lee, C.M., 95
 Lee, D.S., 123–141, 150, 151, 159, 163, 167, 169,
 183, 212, 214
 Lee, E.H., 188, 254
 Lee, G.M., 253
 Lee, H., 52, 219
 Lee, H.J., 218, 219, 262
 Lee, H.R., 188
- Lee, H.S., 189
 Lee, H.T., 130
 Lee, H.Y., 183, 189
 Lee, J., 134, 282
 Lee, J.B., 214
 Lee, J.H., 182, 184, 188
 Lee, J.K., 52
 Lee, J-S., 218, 219
 Lee, J.W., 134, 258, 355
 Lee, K.M., 132, 212
 Lee, K.Y., 207, 215, 291
 Lee, L.Y., 191
 Lee, M.R., 55
 Lee, M.R., 127
 Leenslag, J.W., 239
 Lee, P.Y., 129, 130, 159
 Lee, S.B., 124, 183
 Lee, S.C., 134
 Lee, S.D., 52
 Lee, S.H., 56, 189
 Lee, S.J., 71, 132
 Lee, T.R., 52, 61, 100
 Lee, V.A., 320
 Lee, W.F., 324, 328, 367
 Lee, Y.H., 161, 214
 Légaré, A., 216
 Legeay, G., 261
 Leite, S.M., 236
 Lele, B.S., 180
 Lemahieu, A., 270
 Lemieux, I., 279
 Lendlein, A., 52
 Leobandung, W., 234
 Leonard, M., 181
 Leone, G., 259, 260, 263
 Leong, K.-F., 203, 205, 236
 Leong-Poi, H., 187, 191
 Lepisto, M., 77
 Lerouge, S., 257
 Leroux, J.C., 123, 180, 182, 212
 Lesho, M.J., 323
 Leskinen, P., 324
 Lessard, D.G., 180
 Leung, P.C., 242
 Leung, Y., 320
 Lev, E.B., 179
 Levesque, S.G., 216, 219
 Levy, A., 126
 Levy, D., 254
 Lewis, A.L., 54, 72
 Lewis, D.H., 158
 Ley, K.F., 187
 Liang, B., 113, 116
 Liang, E., 320

- Liang, H.F., 182, 258
Liang, J., 191
Liang, M.H., 254
Liang, R., 14
Lian, T., 104
Liao, B., 358
Li, B., 187
Libchaber, A., 99
Li, C., 112, 183
Licea-Claverie, A., 153
Li, C.M., 54, 72
Li, D.X., 182
Liedl, T., 83, 187
Lie, W.R., 251
Li, F., 128, 134
Lifson, S., 378
Li, G.Y., 189, 368
Li, H., 99, 323
Li, J.T., 134, 152, 182, 214
Li, L.B., 153, 160, 185, 211, 323
Lim, 248
Li, M., 191
Lima, E.G., 241
Lim, D.W., 159, 203, 211, 215, 229, 303
Lim, R.M., 216
Lim, Y.M., 183
Lin, C.C., 323
Lindahl, A., 247
Lin, D.C., 83
Lindenbaum, S., 157
Lindenhayn, K., 237, 261
Lindner, J.R., 187
Lindner, P., 117
Lin, D.W., 262
Lin, F., 269, 271, 274–277
Ling, K., 356
Lin, H.H., 124, 125, 183
Lin, H.L., 180
Linker, R.A., 187
Lin, M.C., 306
Lin, S., 153
Lin, W., 328
Lin, X.Z., 158
Lin, Y.H., 182
Lionetto, F., 356
Lira, L.M., 320, 325
Li, R.H., 216
Li, S., 128, 134
Li, S.J., 274, 278
Li, S.M., 158, 160, 173
Little, C.B., 251
Liu, B.L., 323
Liu, F., 269, 271, 275–277
Liu, G., 116
Liu, H., 83
Liu, H.J., 158
Liu, H.X., 269, 271, 274–279
Liu, J., 153
Liu, K., 280, 281
Liu, M.Z., 14
Liu, P.Y., 282
Liu, Q.F., 125, 182
Liu, R.H., 28, 54, 56
Liu, S.C., 112, 181, 183
Liu, W., 191
Liu, X.-Y., 99, 182
Liu, Y., 153, 208, 216, 261–263
Liu, Y.C., 228
Liu, Y.F., 180
Liu, Y.Y., 179
Livesay, G., 230
Li, W.J., 204, 256
Li, X.H., 158, 214, 356
Li, Y., 111
Li, Y.F., 14, 28, 65
Li, Y.X., 158
Li, Z.H., 129, 130, 159
Lloyd, W., 324
Loebis, A.E., 181
Loethen, S., 213
Lohmeijer, B.G.G., 138
Loh, X.J., 134, 152
Lojda, Z., 306, 307
Longinotti, C., 260
Lopergolo, L.C., 356
Lopes, C.M.A., 356
Lopez, C.E., 111
Lopez-Ureta, L., 367
Lopina, S., 152
Lora, S., 323
Lorenz, H.P., 257
Lories, R.J., 250
Lou, J., 237
Love, B.J., 296
Lovell, N.H., 320
Low, A., 279
Lowder, E., 256
Lugao, A.B., 356
Luginbuehl, V., 220
Lugo-Medina, E., 153
Lukaszczyk, J., 206
Lu, L., 205
Lum, A.F.H., 191, 192
Lu, M.G., 125
Lum, L., 236
Luo, K.Q., 83
Luo, L., 180, 257
Luo, N., 206, 219

- Luo, S., 99
Luo, W., 14
Luo, Y., 219, 261, 324
Lu, Q.P., 269, 271, 274–277
Luterman, A., 269
Lutolf, M.P., 81, 205, 208, 209, 211, 219, 228, 260
Lu, X.H., 18, 109
Luyten, F.P., 250, 257
Lu, Z.-R., 76
Lyckman, A.W., 320
Lynn, D.M., 138
Lyon, L.A., 47, 77, 108, 114, 117, 339
Lyons, T.J., 253
- Machida, Y., 216
Mackay, A.M., 256
Mack, E.J., 19, 69, 324
Madlambayan, G., 258, 260
Madou, M.J., 54, 81, 325
Madsen, J., 54, 72
Maeda, H., 87, 95
Maeda, M., 83, 242
Maeda, N., 23
Maeda, S., 32, 33, 35, 41
Maeda, T., 183
Maeda, Y., 157
Maekawa, Y.M., 125
Maffezzoli, A., 356
Ma, G-H., 216
Magne, D., 256, 262
Maharajh, D., 326
Maia, J., 207, 216
Mainardi, C.L., 251
Mainil-Varlet, P., 257
Ma, J.H., 113, 116, 356
Majima, T., 231
Makino, K., 19, 69, 111
Ma, L., 215
Malafaya, P.B., 205, 215
Malard, O., 260, 262
Malaviya, P., 239
Malda, J., 256
Malhotra, B.D., 322
Malkoch, M., 209
Mamada, A., 51
Mankin, H.J., 254, 255
Mann, B.K., 208, 209, 216
Mann, R.W., 292
Mann, S., 185
Manns, M., 97
Mano, J., 324
Manolova, N., 158
Mansbridge, J., 280, 281
Manson, P., 262
- Mansur, H.S., 180
Manuel Perez, J., 188
Mao, Z., 206, 215, 216
Ma, P.X., 22, 216
Marcacci, M., 239
Marchal, P., 263
Marchand, K.E., 185
Marder, S.R., 29
Marecos, E.M., 95
Marianecchi, C., 216
Markland, P., 135
Marks, R.S., 324
Marletta, G., 235
Marom, G., 233, 234
Marotta, D., 99
Marquez, M., 117
Marsch, S., 291
Marshak, D.R., 256
Marsich, E., 216
Martens, D.E., 256
Martens, P.J., 205, 206, 220
Martin, B.J., 257, 324
Martin, C., 95
Martin, D.C., 320
Martinek, V., 240
Martínez-Chapa, S.O., 56, 58–60
Martinez, M.B., 158
Martin, I., 256, 257
Martin, J., 254
Martins-Dias, S., 14
Mart, R.J., 47, 54, 57, 73, 74, 323
Maruyama, A., 65
Masada, I., 180
Masahiko, O., 127
Masamune, S., 19, 77
Masci, G., 125
Mashelkar, R.A., 50, 51
Mashkevich, A.Y., 124
Mason, M.N., 158, 206
Mason, R.P., 90
Massart, R., 185
Massia, S.P., 181
Masson, M., 260, 262
Masuda, F., 14
Matelli, A.M., 102
Mathebe, N.G.R., 319
Matricardi, P., 216
Matsuda, A., 18
Matsuda, H., 95
Matsuda, T., 125, 215, 242
Matsui, K., 67
Matsumoto, A., 20, 69
Matsumoto, J., 158
Matsumoto, S., 52

- Matsumura, Y., 87, 95
 Matsuo, Y., 72
 Matsushima, Y., 21
 Matthew, H.W.T., 216, 228
 Matyas, J.R., 232
 Mau, A., 325
 Mauck, R.L., 204, 241
 Ma, W., 324
 Mawad, D., 206
 Ma, X.C., 131, 159
 Maxfield, F.R., 88, 95
 Mayer, J.E., 22
 Mayol, L., 259, 260, 263
 McCallan, J., 191
 McClure, J., 253
 McClure, S.F., 253
 McConnell, G., 73, 323
 McCready, V.R., 187
 McCullen, G.M., 234
 McCutchen, C.W., 292
 McGrath, J., 114, 117
 McGrath, K.P., 81
 McHale, M.K., 211, 215
 McIntosh, K.R., 257
 McIntosh, W., 206, 259, 263
 McLemore, R., 214
 McLeod, M.C., 185
 McIntosh, T.J., 99
 McManus, M., 269
 McMurry, T.J., 90
 McNally, P., 323
 McNeill, M.E., 158
 McPherson, G.K., 231
 Meierhaack, J., 158
 Meinhart, J., 215
 Mei, Y., 114
 Mendenhall, H.V., 231
 Mendes, D.G., 240
 Merceron, C., 262
 Mertz, G.W., 306
 Mesa, J., 216
 Messersmith, P.B., 73, 211, 219
 Mestdagh, M.M., 182
 Metref, L., 324
 Metters, A.T., 81, 158, 208, 323
 Metzger, P., 187
 Meyer, D.E., 215
 Mian, A.H., 345
 Miao, Y.J., 216
 Michailidou, V., 111
 Michálek, J., 306, 307, 311
 Mi, F.L., 258
 Mikhailovich, V.M., 324
 Mikheeva, L.M., 124
 Mikheikin, A.L., 324
 Mikos, A.G., 179, 206, 212, 217, 236, 258, 260, 261, 263
 Milella, E., 259, 263
 Miller, S.R., 67
 Miller, T.E., 181
 Minamitake, Y., 159
 Mingyong, H., 187
 Miqin, Z., 190
 Mirzabekov, A.D., 324
 Misra, E., 152
 Mitra, S., 181
 Miura, T., 22
 Mi, Y., 83
 Miyagawa, N., 88
 Miyajima, N., 114
 Miyamoto, M., 162, 165
 Miyamoto, S., 159
 Miyao, M., 206
 Miyasaka, M., 95
 Miyata, T., 19, 57, 65–84, 242
 Miyuchi, M., 213
 Miyazaki, H., 19, 68, 69
 Miyazawa, N., 340
 Mizuno, H., 257
 Mladenovska, K., 152
 Modzelewski, R.A., 187
 Mohan, Y.M., 367
 Mokari, T., 191
 Mokhtary, M., 355
 Molina, I., 158
 Mollica, F., 230–235
 Moneghini, M., 180
 Montane-Jaime, K., 319
 Montero, P., 182
 Mooney, D.J., 203, 207, 215, 236, 240, 247, 258–261, 276, 291, 324
 Moon, H-S., 216
 Moon, J.Y., 189
 Moore, J.S., 28, 54, 56, 72
 Moorman, M.A., 256
 Moosbauer, J., 98
 Morales, M.A., 189, 191
 Morales-Menéndez, R., 58
 Moreau, A., 260, 262
 Moreau, F., 262
 Moreland, L.W., 251
 Moret, E.E., 89
 Morgan, M.T., 216
 Morgan, P.B., 306
 Moriguchi, N., 339
 Morimoto, N., 87, 340, 342, 343, 345–347
 Morishita, K., 125
 Morita, M., 324

- Morita, Y., 108
Moriyasu, F., 95
Moronne, M., 187
Morris, E.R., 182
Morrison, P.R., 271, 277
Morrison, R., 104
Mortensen, K., 126
Mortisen, D.J., 205
Mosbach, K., 19, 77
Mosca, J.D., 256
Moschou, E., 325
Moscona, A., 103
Moss, J.M., 216
Motokawa, R., 125
Mourad, P., 51
Mow, V.C., 241, 252
Mueller-Schulte, D., 114, 116
Mühlebach, A., 180
Muir, H., 250
Muir, T.W., 209
Mukawa, T., 19
Mukherjee, S., 88, 95
Mukose, T., 160, 163–169, 173
Muller, A.H.E., 125
Müller, B., 180
Muller, R.H., 19, 183
Munch, J-P., 295
Munion, J., 181
Munro, C.H., 18
Muradali, D., 187
Murai, T., 95
Murakami, Y., 83, 159, 242
Murase, Y., 35
Murata, Y., 68, 182
Murdan, S., 320
Murphy, C.L., 251
Murphy, W.H., 216
Murray, L.S., 104
Murray, R.W., 100
Murray, T., 104
Murthy, P.S.K., 367
Musch, J., 117
Mwale, F., 257
Mwamuka, J., 184
Myrvold, R., 182
Myung, D., 356

Nagahama, K., 151
Nagahara, S., 242
Nagai, S., 23
Nagao, Y., 68
Nagasaki, Y., 87–104, 159
Nagata, Y., 157, 345
Nagorski, H., 14

Nagura, M., 358
Nahmias, Y., 236
Naimark, A., 254
Naito, M., 95
Nakada, Y., 158
Nakamae, K., 65, 66, 70, 71
Nakaminami, T., 19, 78–80
Nakamura, S., 28
Nakamura, T., 88, 99, 158
Nakanishi, T., 95
Nakano, J., 160, 163, 165–169, 173
Nakayama, A., 291, 298–300, 356
Nakayama, D., 18, 77, 78
Nakayama, G., 57
Nakayama, Y., 215
Nakazawa, Y., 108
Na, K.M., 128, 206
Namba, T., 15
Nam, Y.S., 236
Nandkumar, M.A., 23
Napoli, A., 260
Narine, K., 205
Narinesingh, D., 319, 320, 324–326, 328
Narita, T., 295, 296
Narkis, M., 321
Nasongkla, N., 192
Nassif, N., 112
Naughton, G., 236, 279
Nauman, E.A., 242
Navasaria, H.A., 320
Nayak, S., 47, 77, 339
Na, Y-H., 287–289
Neckers, D.C., 72
Needham, D., 20, 99
Negishi, Y., 191
Nelea, V., 257
Nemoto, H., 18
Neradovic, D., 183
Nesic, D., 257
Netter, P., 263
Netti, P.A., 229–237, 247, 260
Nettles, D.L., 215, 216
Neubauer, M., 257, 258
Neuwelt, E.A., 185
Newa, M., 182
Newman, M.S., 95
Nguyen, H., 320
Nguyen, K.T., 206, 259
Nguyen, M.K., 139, 140
Niamlang, S., 180
Nicolais, L., 230–235, 242
Niece, K.L., 54
Nielsen, L.K., 278
Nie, S., 187

- Ni, H., 111
 Nikoleta, T., 185
 Nikpour, M., 325
 Nilsson, A., 247
 Nilsson, S., 305
 Ning, W., 129, 159
 Ni, P., 112
 Nishida, K., 23
 Nishikawa, T., 344, 345
 Nishimura, G., 295, 296
 Nishimura, H., 358
 Nishimura, T., 21, 23
 Nishino, T., 65
 Nishio, Y., 180
 Nishio, I., 65
 Niu, G., 214
 Ni, X., 214
 Niyibizi, C., 216
 Nizuka, T., 65
 Nobels, M., 270
 Noble, M., 51
 Nogawa, M., 32
 Noji, H., 52
 Nomura, S.M., 340, 345
 Nomura, Y., 344, 345
 Norased, N., 190
 Norris, P., 51
 Noth, U., 230
 Novais, J.M., 14
 Nowak, A.P., 151, 212
 Nozaki, Y., 99
 Nuopponen, M., 125
 Nuttelman, C.R., 205, 206
 Nykanen, A., 125

 Obaidat, A.A., 71
 Obeid, R., 343
 O'Brien, P., 187
 O'Brien, S., 185
 Ochi, M., 216
 Ochs, B.G., 257
 O'Connor, S.M., 324
 Oda, H., 124
 Odell, R.A., 206
 Ogata, N., 20, 65, 68
 Oguro, K., 18
 Ogurtsov, N.A., 321
 Ogushi, Y., 211
 Ohba, H., 187, 188
 Oh, H., 134
 Oh, J.K., 339
 Ohki, T., 347
 Ohkoshi, Y., 358
 Oh, K.S., 191, 192

 Ohlsson, C., 247
 Ohmori, T., 32
 Ohshima, H., 111
 Ohtani, H., 256
 Ohtsuka, Y., 88, 108, 109
 Oh, Y.K., 182
 Oishi, M., 87–104
 Okada, T., 159
 Okada, Y., 21, 23
 Okamoto, A., 216
 Okano, K., 95
 Okano, T., 19–41, 65, 68, 69, 95, 159, 236, 324
 Okay, O., 355, 356
 Okihara, T., 159
 Okumura, Y., 27
 Okuzaki, H., 18, 51, 65
 Olmo, R., 323
 Olsen, G.B., 69
 Olson, E.J., 231
 Omelyanenko, V., 97
 Omidian, H., 1–15, 354, 357, 359, 360, 362, 363, 367, 368, 376, 387, 388
 Ong, S.M., 274
 Ong, S.R., 215
 Onishi, H., 36, 216
 Onodera, S., 31
 Ono, K., 216
 Onsøyen, E., 182
 Ooya, T., 55, 72
 Ormrod, D.J., 181
 Orwin, E.J., 248
 Osada, Y., 18, 20, 27, 29, 51, 65, 285–289, 291–300, 325
 Ossipov, D.A., 209
 Oss-Ronen, L., 219
 Otero, T.C., 239
 Otter, W.D., 260
 Oudshoorn, M.H., 258, 259
 Ou, H., 377, 387
 Ouwerx, C., 182
 Ouyang, H., 230, 254
 Owens, D.E., 50, 53
 Owino, J.H.O., 320
 Oya, T., 19, 77
 Ozbas, B., 212
 Ozdemir, A., 183

 Packhaeuser, C., 152
 Pai, C.M., 69
 Paige, K.T., 22, 260
 Pakstis, L.M., 151, 212
 Palla, C.S., 80, 81
 Pallua, N., 279
 Palma, G., 323

- Palumbo, F.S., 208, 216, 261
Pancrazio, J.J., 324
Pandit, A.S., 259, 263
Panitch, A., 214, 239
Pankov, S.V., 324
Pan, Y.Q., 269, 271, 275, 276
Paoletti, M., 241
Papadaki, M.G., 179
Parag, V., 193
Paramonov, S.E., 54
Park, D.K., 179
Park, E.K., 183
Parker, R.S., 58, 67
Park, H., 136, 137, 206, 211, 215, 217, 325, 363, 366–368
Parkin, D.E., 95
Park, J., 185
Park, J.K., 180
Park, J.S., 100
Park, K., 1–15, 71, 77, 123, 205, 325, 345, 357, 363, 366–368, 387
Park, K.D., 181
Park, K.H., 134, 206
Park, M.H., 279
Park, M.J., 129, 132
Park, M.S., 258
Park, S., 274
Park, S.B., 325
Park, S.J., 184, 188
Park, S.Y., 128, 132, 135
Park, T.G., 53, 159, 161, 206, 211, 214, 219, 236
Park, Y.D., 206, 208, 209
Park, Y.H., 325
Parras, P., 125
Partap, S., 363
Pasini, A., 257
Pastorello, A., 259, 263
Patel, D., 189
Patrick, C.W. Jr., 235, 279
Patterson, C., 324
Payan, E., 263
Payne, R.G., 217
Pedersen, J.S., 126
Peer, D., 190
Pekel, N., 324
Pellissier, M., 324
Pelton, R.H., 108, 183
Pelttari, K., 257
Peng, Z.Q., 368
Peniche, C., 153
Penkov, D.N., 324
Pennings, A.J., 160
Peppas, L.B., 65
Peppas, N.A., 15, 45–62, 65, 67, 77, 180, 234, 324, 345, 357, 376, 386
Peracchia, M.T., 159
Peretti, G.M., 240
Perez, C., 158, 159
Pérez-Mateos, M., 182
Pérez, P., 153
Perka, C., 237, 261
Pernaut, J-M., 320
Perry, J.W., 29
Persson, B.N.J., 292, 294
Peter, S., 257
Peterson, L., 247
Peterson, W.D., 228
Petherick, P., 95
Petit, A., 257
Petka, W.A., 81
Peyramaure, S., 184
Pharisa, C., 180
Philippova, O.E., 135
Phillipova, O., 376
Piazza, S., 325
Pi, B.S., 137, 139, 140
Pich, A., 114–116
Pieper, J.S., 215
Pileni, M.P., 125
Pillemer, S.R., 254
Pinna, N., 112
Pinprayoon, O., 111
Pishko, M.V., 324
Pissis, P., 324
Pitt, C.G., 158
Pittenger, M.F., 256
Pizzolo, G., 257
Plantinga, J.A., 258, 260
Plunkett, K.N., 54, 72
Podual, K., 50, 56, 58
Poehlein, G.W., 88
Poirier, G.G., 98
Pojman, J.A., 30
Polnok, A., 367
Polotsky, A., 211
Polse, K.A., 306
Poole, C.A., 253
Poole-Warren, L.A., 320
Pool, M.D., 158
Poon, Y.F., 324
Porter, T.R., 191, 192
Postema, A.R., 160
Pourjavadi, A., 15
Pourjavadi, H., 390
Prabhas, V.M., 275
Prasad, H.R.Y., 14
Pratoomsot, C., 159

- Premnath, V., 50, 51
 Presti, C.L., 325
 Prestwich, G.D., 208, 209, 216, 261, 324
 Price, C., 157
 Prigent, P., 184
 Princivalle, F., 180
 Proch, S., 114
 Prud'homme, C., 183
 Prudhomme, R.E., 159
 Pud, A.A., 321
 Puelacher, W.C., 22, 240
 Puleo, C., 236
 Purple, C.R., 256
 Putnam, D., 158, 159
- Qao, M.X., 159
 Qiao, M.X., 131, 159
 Qin, H., 53
 Qiu, H., 189
 Qiu, X.P., 343
 Qiu, Y., 123
 Quellec, P., 158
 Quillard, S., 249, 250, 263
 Quinten Ruh, P., 217
 Qu-Petersen, Z., 257
 Qutubuddin, S., 356
- Rabbani, M., 357
 Rabin, O., 188
 Rabolt, J.F., 185
 Radice, M., 228, 233, 237
 Raeber, G.P., 81, 205, 208, 211, 219, 260
 Ragan, P., 259, 263
 Raicki, R., 152
 Rainaldi, G., 103
 Raju, K.M., 367
 Ramay, H.R., 179, 216
 Ramires, P.A., 259, 263
 Randolph, M.A., 205, 216, 259
 Ranger, M., 180
 Ranucci, A.K., 275
 Raphael, Y., 320
 Rapoport, N., 182, 192
 Rashkov, I., 158
 Rassing, J., 124
 Rathi, R., 130, 151
 Ratner, B.D., 21, 51, 67
 Ravi, N., 356
 Raviv, U., 296
 Rawlins, D.A., 182
 Raymond, S., 190
 Raynal, I., 184
 Reber, N., 125
 Reddy, M.K., 87
- Reece, G.P., 279
 Rees, D.A., 157, 182
 Refojo, M.F., 305
 Rehner, J., 324
 Reinhardt, M., 187
 Reinhold, H.S., 88, 90
 Reis, R.L., 205, 215, 324
 Relleve, L., 356
 Renaud, P., 324
 Ren, J., 192
 Revell, P.A., 229, 230, 234, 260
 Revzin, A., 324
 Reynolds, J.R., 320
 Rezwani, K., 239, 240
 Rhie, J.W., 279
 Rhodes, N.P., 260
 Rice, M.A., 159
 Richards, F.M., 276
 Richtering, W., 111, 112, 114, 116, 117
 Richter, W., 257
 Ricker, N.L., 67
 Rickert, P.G., 183
 Riedel, A., 323
 Riesle, J., 256
 Riley, C.M., 206, 208
 Riley, S., 259, 263
 Rim, S.J., 191
 Ringsdorf, H., 157
 Risbud, M.V., 216, 356
 Risbud, S., 185
 Ritschel, W., 324
 Robb, I., 355
 Robb, S.A., 214
 Roberts, A., 236
 Roberts, B., 185
 Roberts, S.C., 212
 Robinson, D., 240
 Rocca, J.G., 15, 357, 360, 362, 363, 367, 368, 387
 Rochet, N., 256, 262
 Rodil, E., 185
 Rodriguez Clemente, R., 185
 Rogers, B.A., 251
 Rogers, W.J., 184
 Rohde, M.F., 99
 Rollwagen, F.M., 324
 Romagnani, S., 257
 Román, J.S., 147–154
 Romanov, A., 260
 Ronca, D., 230, 233, 234
 Ron, E., 151
 Rooney, J., 260
 Rose, C., 271
 Rose, M.G., 182
 Rosenberg, M., 187

- Rosenblatt, J., 259
Rosenzweig, Z., 187
Roseti, L., 237
Roskos, K., 57
Rostovtsev, V.V., 209
Rotello, V.M., 100
Roth, B., 277
Roth, V., 252
Rousche, K.T., 256
Rousseau, D., 15
Rouzes, C., 181
Rovelyn, T., 185
Rowley, J.A., 258–261
Roy, A.K., 261
Rubina, A.Y., 324
Rubio-Retama, J., 115
Rubio, R.J., 111
Rudolph, A.S., 324
Rudolph, K.L., 97
Ruel-Gariepy, E., 123, 182, 212
Rujiravanit, R., 180
Ryabova, A.A., 356
Rychak, J.J., 187
Rypacek, F., 158
- Sabatini, G., 230
Sadahira, C.M., 180
Sadik, O.A., 322, 323
Saffran, M., 72
Sahlin, J.J., 324
Sahoo, S.K., 189, 191
Saita, Y., 347
Saito, H., 153
Saito, T., 237
Saito, Y., 216
Sakai, H., 23
Sakai, K., 19–21, 25, 28, 65, 125
Sakai, S., 211, 216
Sakai, T., 32, 34, 36, 38, 41
Sakamaoto, C., 21, 23
Sakamoto, R., 390
Sakiyama, T., 19, 77
Sakurai, K., 158
Sakurai, Y., 19–21, 23, 26, 28, 65, 68, 69, 95
Sakura, T., 88
Salerno, A., 236
Salgado, A.J., 220
Salih, B., 324
Salinas, C.N., 209, 214
Salley, S.O., 228
Sambanis, A., 60
Sanabria-DeLong, N., 159
Sanborn, T.J., 211
Sanchez, A., 158, 159
Sanchez-Chávez, I.Y., 45–62
Sandell, L.J., 256
Sander, E.A., 241, 242
Sangeetha, K., 356
Sannino, A., 15, 242, 356, 368
San Roman, J., 324
Santavirta, S., 237
Santini, M.T., 103
Sanui, K., 20, 65, 68, 157
Sarakinos, G., 236
Sardinha, H., 159
Sarhan, A., 77
Sarkar, N., 124
Sarracino, F., 230–235
Sasaki, M., 88
Sasaki, S., 32
Sasaki, Y., 345
Saslavski, O., 51
Sastry, T.P., 271
Sato, J., 151
Sato, T., 109
Saunders, B.R., 111, 114
Savariar, C., 72
Savarino, L., 235
Save, M., 112
Sawada, S., 345
Sawasaki, Y., 23
Sawa, T., 95
Schacht, E.H., 270
Schätzlein, A.G., 181
Schechter, B., 95
Schense, J.C., 277
Schield, H.G., 107
Schild, H.G., 124
Schillen, K., 124
Schloo, B., 22
Schmaljohann, D., 135
Schmidt, C.E., 235, 320
Schmidt, T., 357
Schmitt, M., 345
Schmoekel, H.G., 81, 205, 208, 219
Schneider, M., 97
Schneider, S., 117
Schoenberger, J., 98
Schoenmakers, R., 82, 153
Scholes, G.D., 116
Schoof, H., 279
Schowen, R.L., 180
Schrinner, M., 114
Schultz, O., 261
Schulz, B., 323
Schulz, M.B., 257, 258
Schumann, D., 291
Schunke, M., 256

- Schupp, K., 230
 Schuurmans-Nieuwenbroek, M.M.E., 89
 Schwinger, C., 182
 Scotchford, C.A., 215
 Seal, B.L., 214, 239
 Sechriest, V.F., 216
 Seetharaman, K., 88, 90
 Segal, E., 321
 Segura, T., 260
 Seifert, S., 183
 Seki, T., 34, 38
 Seliktar, D., 215, 219
 Selligren, B., 77
 Seminoff, L.A., 69
 Sen, S., 205
 Seo, K.S., 133, 357, 367
 Seo, S.-J., 216
 Sergeyev, V.G., 325
 Serizawa, T., 368
 Sertchook, H., 191
 Setomaru, T., 23, 24
 Setton, L.A., 211, 215, 253, 357
 Seydel, T., 111
 Sfika, V., 152
 Shaffer, C.B., 124
 Shaffer, J.D., 220
 Shaffer, K.M., 324
 Shah, A., 65
 Shah, N.M., 158
 Shah, P.S., 185
 Shah, S.S., 158
 Shalaby, W., 325
 Shapiro, F., 255
 Shapoval, G.S., 321
 Sharma, B., 220, 262
 Sharma, L., 366
 Sharma, R.C., 321
 Shea, K., 77
 Shelton, J.C., 229, 230, 234
 Shen, D., 53
 Shen, L., 116
 Sheppard, N.F. Jr., 319, 323
 Sher, A., 242
 Shibuta, Y., 35
 Shichibe, S., 345
 Shih, C., 130, 151
 Shiino, D., 68, 69
 Shikinami, Y., 234
 Shimamura, K., 180
 Shimizu, T., 23, 24, 183, 345
 Shimko, D.A., 241
 Shimko, V.F., 241
 Shim, M.S., 130, 151, 183
 Shimomura, T., 15
 Shim, W.S., 130, 135–137
 Shim, Y.H., 183
 Shin, H.S., 206, 217, 356
 Shin, I., 55
 Shinohara, I., 67
 Shinohara, J., 21
 Shinohara, S., 34
 Shinohara, Y., 23
 Shinoka, T., 22
 Shiraiishi, H., 324
 Shiroyanagi, Y., 23
 Shirshova, N., 112
 Shive, M.S., 217
 Shivkumar, S., 324
 Shlopov, B.V., 251
 Shlyakhtenko, L.S., 87
 Shohet, R.V., 191
 Shoichet, M.S., 153, 158, 216, 219, 324
 Shon, J., 128
 Shon, Y.-S., 100
 Shortencarier, M.J., 192
 Shtilman, M.I., 180
 Shubhra, S., 182
 Shukla, R., 184
 Shung, A.K., 217
 Shu, X.Z., 153, 228
 Siegel, R.A., 65, 180
 Siegmann, A., 321
 Siegwart, D.J., 339
 Silva, G.A., 54, 205, 215
 Simanek, E., 152
 Simmel, F., 83
 Simmons, K.L., 132
 Simonetti, D.W., 256
 Simon, F., 115
 Simonian, A.L., 324
 Simon, T.M., 255
 Sims, D., 259
 Singh, A., 211
 Singh, M.J., 21
 Singh, N., 77
 Singh, R., 185
 Singh, S.P., 322
 Sittinger, M., 216, 261
 Skotheim, T., 320
 Slatkin, D.N., 188
 Slaughter, B.V., 53
 Slaughter, G., 320
 Small, C.J., 319
 Smidsrod, O., 182
 Smiga, M., 206
 Smith, A.M., 47, 54, 57, 323
 Smith, K.A., 191
 Smith, M.K., 324

- Smith, R., 355
Smit, T.H., 205
Sofia, S.J., 211
Soga, O., 124, 183
Sohn, Y.S., 133, 134
Solari, M., 356
Solchaga, L.A., 237, 257
Solem, L., 269
Sommarin, Y., 250
Song, B.H., 158
Song, H., 205–207
Song, I.B., 133
Song, J., 187, 191
Song, K.W., 279
Song, L., 214
Song, S.C., 124
Sontjens, S.H.M., 357
Sosnik, A., 126, 127, 258, 260,
262, 263
Sota, H., 23
Soto, C., 324
Souza, A.N., 180
Soysa, N.S., 345
Spadaro, G., 325
Spaethe, R., 260
Spargo, B.J., 324
Spector, M., 324
Speers, A.E., 209
Sperinde, J.J., 73, 211
Sperling, L.H., 12
Spiller, K.L., 368
Spitzer, R.S., 237, 261
Spohr, R., 125
Spurlock, L.D., 323
Srivastava, P., 14
Stabenfeldt, S.E., 205
Staks, T., 185
Stamm, M., 111, 115
Stark, D.D., 185
Stark, J., 181
Stárková, L., 311
Starodoubtsev, S.G., 356
Stasky, A.A., 261
Stayton, P.S., 135
Steck, E., 257
Steenbergen, V.M.J., 89
Steen, V.D., 254
Stefflova, K., 99
Steinbuechel, A., 158
Stellacci, F., 29
Stenekes, R.J.H., 181
Stenger, D.A., 324
Stevenson, P.C., 184
Stewart, J.E., 180
Stewart, P.S., 51
Stewart, R.J., 81, 212, 242
Stieger, S.M., 187
Stile, R.A., 125
Stoddart, M., 259, 263
Stoddart, R.W., 253
Stolnik, S., 183
Stoodley, P., 51
Stove, J., 250
Strehin, I., 262
Strohalm, J., 242
Stuart, M.C.A., 55
Stupp, S.I., 54
Suc, B., 180
Sudjak, A.S., 319
Sugawara, A., 87, 345
Suggs, L.J., 217
Sugimoto, M., 206
Suh, J.M., 127, 133
Suh, K.D., 355
Sui, S.C., 282
Sujdak, A.R., 319
Suleimenov, I.E., 380, 386, 387, 389
Sumitani, S., 88, 90
Sumiyoshi, T., 288, 289
Summers, M., 185
Sunamoto, J., 340, 344–346
Sundback, C.A., 276
Sung, H.W., 258
Sun, H.H., 181
Sun, J., 216
Sunkara, H.B., 18
Sun, L-g., 213, 214
Sun, S.-T., 65
Sun, Y., 328
Surendra, P.B., 275
Sur, M., 320
Suslick, K.S., 191
Sutherland, R.M., 103
Su, W., 95
Suwa, K., 124
Suwa, S., 95
Suzaki, R., 191
Su, Z-G., 216
Suzuki, A., 52, 65
Suzuki, D., 38, 111, 114, 116, 117
Suzuki, M., 95
Swadeshmukul, S., 185
Sweeney, H.L., 205
Swift, G., 15
Swislow, G., 65
Syeda-Nawaz, J., 320
Szabo, D., 18
Szatkowski, J.P., 217

- Tabata, K.V., 52
 Tabata, O., 32, 35
 Tabata, Y., 77, 78, 206, 215
 Tada, T., 296, 297
 Taguchi, T., 153, 325
 Tait, C.J., 124
 Tajbakhsh, M., 355
 Tajima, H., 339
 Takagi, M., 345
 Takahashi, C., 23, 24
 Takahashi, T., 31
 Takai, M., 291
 Takai, N., 21
 Takalkar, A.M., 187
 Takaoka, K., 159
 Takeda, Y., 325
 Takehisa, T., 28
 Takei, K., 32
 Takei, Y.G., 20, 157
 Takeoka, Y., 18, 19, 34, 38, 77
 Takeuchi, T., 19
 Takizawa, T., 191
 Talsma, H., 125, 181
 Tamada, J., 345
 Tam, J.P., 99
 Tam, K.C., 112, 127, 151, 182
 Tamura, A., 88, 90
 Tanabe, Y., 298–300
 Tanahashi, K., 217
 Tanaka, K., 19, 77
 Tanaka, M., 31
 Tanaka, T., 17–19, 51, 52, 65, 69, 77, 95, 107
 Tanaka, Y., 287–290
 Tan, B.H., 112
 Tan, C.H., 274
 Tanel, R.E., 22
 Tanford, C., 99
 Tang, C., 363, 368
 Tang, F.Q., 116
 Tang, J.C., 356
 Tang, M., 179
 Tang, Q.W., 368
 Tang, T., 125, 237
 Tang, Y.F., 53, 99, 113, 116, 356
 Taniguro, H., 298–300
 Tanioka, H., 159
 Tan, J.P.K., 112
 Tan, J.S., 183
 Tano, Y., 23
 Tan, T.W., 15
 Tan, W., 83, 278
 Tan, Y.C., 258
 Tarret, M., 185
 Tartis, M.S., 191
 Tassin, J.F., 249, 250, 263
 Tateyama, S., 35
 Tator, C., 153
 Tauer, K., 112
 Taupitz, M., 185
 Taylor L.D., 124
 Tchoudakov, R., 321
 Teijon, J., 323
 Temenoff, J.S., 206, 211, 215, 217, 258, 260, 261, 263
 Templeton, A.C., 100
 Teng, D., 112
 Teraoka, I., 169
 Tessmar, J.K., 220, 257, 258
 Testa, C., 320
 Tetley, L., 181
 Tew, G.N., 159
 Thambyah, A., 230
 Theprungsirikul, P., 262
 Thompson, D.H., 213
 Thornberry, N.A., 98
 Thornton, P.D., 47, 54, 57, 73, 74, 323
 Thorsen, A.J., 236
 Thoson, A.H., 104
 Tienen, T.G., 239
 Tighe, B.J., 127, 305, 307–313
 Timmins, N.E., 278
 Timmons, S., 99
 Ting-Beall, H.P., 253
 Tirelli, N., 81, 206, 214, 260
 Tirrell, D.A., 81
 Tobias, G., 261
 Todd, S.J., 47, 54, 57, 323
 Toh, Y.C., 274
 Toita, S., 345
 Tokita, Y., 216
 Tolga Demirtas, T., 368
 Toma, H., 23
 Toneguzzi, S., 231
 Too, C.O., 319
 Toole, B.P., 251
 Topp, E.M., 180
 Topp, M.D.C., 125
 Torchilin, V.P., 180
 Torgerson, T.R., 99
 Tortora, M., 208, 209
 Totani, K., 29
 Toublan, F.J.J., 191
 Tower, T.T., 236
 Townsend, R., 368
 Trabbic-Carlson, K., 357
 Traitel, T., 51, 57
 Tramper, J., 256
 Tricoli, M., 158

- Trieu, H., 356
 Trigo, R., 323
 Trojani, C., 256, 262
 Trojanowicz, M., 321
 Tronc, E., 185
 Trubetskoy, V.S., 180
 Trzebicka, B., 125
 Tse, A.S., 18
 Tsitsilians, C., 152
 Tsubota, K., 306
 Tsuda, Y., 26
 Tsuji, H., 159
 Tsuji, M., 159
 Tsuji, S., 108, 109, 111
 Tsukeshiba, H., 287, 288
 Tsukioka, Y., 95
 Tsuruta, T., 158
 Tsutsui, H., 18
 Tsutsumi, Y., 180
 Tuan, R.S., 256, 257
 Tuli, R., 256
 Tuncel, A., 183
 Turczyn, R., 261, 262
 Turkevich, J., 184
 Turner, N.J., 237
 Twelves, C., 104
 Tyagi, P., 129
 Tyyni, A., 255
- Uchida, K., 28, 65, 183
 Uchio, Y., 216
 Udhardt, U., 291
 Ueblacker, P., 240
 Uekama, K., 213
 Ueminami, A., 341
 Uenaka, A., 345
 Ueno, M., 298
 Ueno-Nishio, S., 65
 Ueno, S., 52
 Uetsuka, H., 36
 Ulbrich, K., 242
 Ulbricht, W., 157
 Ulijn, R.V., 47, 54, 57, 72–74, 323
 Umezu, M., 23, 24, 26
 Ungar, E.C., 192
 Unger, E.C., 187, 191
 Uno, T., 100
 Unsworth, A., 292
 Upton, J., 22
 Uragami, T., 19, 57, 66, 74–76, 78–80, 242
 Urakawa, H., 108
 Ursell, P., 325
 Utsumi, M., 23, 26
 Uyama, H., 211
- Vacanti, C.A., 22, 260, 261
 Vacanti, J.P., 22, 203, 256, 258, 260, 276
 Vacík, J., 306, 307
 Vadgama, P., 320
 Vadnere, M., 157
 Vail, T.P., 216
 Vakkalanka, S.K., 357
 Valckenborgh, D.V., 205
 Valenzuela, R.G., 205
 van Blitterswijk, C.A., 256
 van Bommel, K.J.C., 55
 Van Damme, M-PI., 216
 vandeManakker, F., 213
 VanderAa, L.J., 208, 209, 216
 Vanderhooft, J.L., 208, 209, 216
 vanderPot, M., 213
 Van de Wetering, P., 153
 Van Dijk-Wolthuis, W.N.E., 181, 260
 van Eerdenbrugh, B., 159, 211
 van Esch, J., 55
 van Geemen, D., 214, 258, 259
 van Hooy-Corstjens, C.S.J., 263
 van Luyn, M.J.A., 258, 260
 van Mathieu, S., 182
 Vannan, M., 191
 van Noort, D., 274
 van Nostrum, C.F., 124, 159, 183, 207, 211, 212, 346
 van Ooij, A., 263
 van oojen, R.D., 180
 van Rhijn, L.W., 263
 van Steenberghe, M.J., 124
 Vansteenkiste, S., 270
 Van Tomme, S.R., 161, 216
 van Wachem, P.B., 258, 260
 Varghese, S., 220, 248, 262
 Varshney, S.K., 138
 Vasey, P.A., 104
 Vasiliskov, V.A., 324
 Veis, A., 270
 Velings, N., 182
 Vemula, P.K., 54, 55
 Venzmer, J., 157
 Vera, J., 185
 Verbout, A.J., 276
 Verma, K.K., 14
 Vermani, K., 55
 Vermonden, T., 124, 213, 214
 Vernengo, J., 356
 Vert, M., 134, 158, 160, 171, 173
 Vestberg, R., 209
 Veth, R.P., 239
 Vignes-Colombeix, C., 256, 262
 Vinatier, C., 247, 256, 260, 262
 Vincent, B., 112

- Vinogradov, A.M., 51
 Vinogradov, S.V., 87
 Virta, M., 324
 Vlatakis, G., 19
 Voinovich, D., 180
 Volland, C., 158
 Vollmer, M., 184
 von Elverfeldt, D., 190
 von Heimburg, D., 279
 von zur Muhlena, C., 190
 Voycheck, C.L., 183

 Wach, R.A., 357
 Wada, H., 345
 Wada, Y., 124
 Wahls, M.W.C., 159, 211, 242
 Wakitani, S., 241
 Walach, W., 158
 Walker, M.G., 237
 Wallace, D.G., 259
 Wallace, G.G., 319, 320, 325
 Walsh, C.J., 239
 Walt, D.R., 323
 Wanekaya, A., 323
 Wang, A.Q., 15
 Wang, C.H., 28, 81, 191, 212, 242
 Wang, D., 124, 191, 216
 Wang, D.A., 220, 262
 Wang, D.Q., 323
 Wang, G.Q., 19, 77, 117
 Wang, H.Q., 206, 216, 292
 Wang, J.M., 129, 159
 Wang, L., 345
 Wang, L.F., 179
 Wang, L.Q., 131, 132
 Wang, M., 116
 Wang, P., 116
 Wang, S.C., 179
 Wang, W.B., 15
 Wang, X.H., 112, 269, 271, 274–279, 282
 Wang, Y.X., 185
 Wang, Z.C., 112, 209
 Wanka, G., 157
 Wanless, E.J., 111
 Warden, G., 269
 Ward, J.H., 58
 Ward, K., 320
 Wasserman, A.M., 356
 Watanabe, A., 345
 Watanabe, H., 23
 Watanabe, K., 23
 Watanabe, M., 18, 34, 77, 78
 Watanabe, T.M., 29, 191
 Wathier, M., 209

 Watrin, A., 206
 Weaver, J.V.M., 112
 Weber, F.E., 81
 Weber, W., 82
 Wei, B., 83
 Wei, H., 183, 213, 214
 Weinand, C., 240
 Weissleder, R., 95, 185
 Weissman, B.N., 254
 Weissman, J.M., 18
 Weiss, P., 247, 249, 250, 256, 261–263
 Weller, G.E.R., 187
 Wellinghoff, S.T., 320
 Wendt, D., 257
 Weng, C.Y., 274, 278
 Weng, L., 260, 263
 Wenk, E., 220
 Wenseleers, W., 29
 Wen, X.J., 357
 Wertheimer, M.R., 257
 Westby, M.J., 88
 West, J.L., 51, 157, 206, 259
 Wetering, V.P., 89
 Wever, O.D., 205
 White, M.L., 216
 Whiteside, R., 257
 Wichterle, 248
 Wichterle, O., 203, 229, 303, 305, 307
 Wike-Hooley, J.L., 88, 90
 Wiler, J.A., 320
 Williams, C.G., 220, 262
 Williams, F., 72
 Wilson, A.M., 319, 323
 Wilson, D.E., 69
 Wilson, G., 20, 306
 Wilson, P., 104
 Wilson, S.R., 187, 191
 Windisch, C.F., 132
 Winnik, F.M., 157, 342, 343
 Winnik, M.A., 114, 116
 Winter, A., 257
 Wintersteiner, O., 138
 Wirsta, M.D., 151
 Wirth, T., 97
 Wirtz, D., 81
 Wissink, M.J.B., 215
 Wnek, G.E., 326
 Woerly, S., 228
 Wolf, A., 125
 Wolfe, F., 254
 Woller, N., 97
 Won, C.Y., 206, 216
 Wong, D.L., 14
 Wong, J.E., 114, 116

- Wong, M.K.K., 187, 215
Wood, K.M., 55
Woodle, M.C., 184
Working, P.K., 95
Wright, S.C., 95
Wright, S.L., 180
Wright, V., 292
Wu, C., 109, 116
Wu, G., 180
Wu, J., 216
Wulff, G., 77
Wu, M.H., 357
Wu, R.D., 269, 271, 274–277
Wu, X., 59, 60
Wu, Y.J., 99, 251
Wyllie, A.H., 98
Wyslouzil, B.E., 236
- Xiang, Y.Q., 368
Xian, W.H., 180
Xiaohu, G., 187
Xie, W.H., 158
Xing, D., 99
Xinxing, L., 377, 387
Xiong, L.J., 356
Xiong, X.Y., 127, 151, 182
Xiong, Z., 269, 271, 274–278
Xu, C., 189, 212, 213
Xue, W., 358
Xu, F.L., 357
Xu, J., 53, 183, 295
Xu, K., 356
Xu, M.E., 269, 271, 275, 276, 279
Xu, S.M., 112, 357
Xu, W., 182, 269, 271, 275, 276
Xu, X.D., 209
Xu, X.L., 237
- Yakushiji, T., 20
Yallapu, M.M., 87
Yamada, A., 180
Yamada, N., 23
Yamada, Y., 108
Yamaguchi, N., 80, 81, 219, 345
Yamaguchi, S., 52
Yamaguchi, T., 31, 32, 36
Yamamoto, K., 21, 23
Yamamoto, N., 72
Yamamoto, Y., 180
Yamanaka, H., 23
Yamane, S., 87, 343, 345
Yamaoka, T., 157–173
Yamato, M., 23–26, 183
Yamauchi, A., 65
- Yamazaki, Y., 23
Yanada, S., 206
Yang, B.B., 251
Yang, F., 220, 233, 236
Yang, H., 83, 152
Yang, J.Z., 133, 212, 228, 357
Yang, S., 203, 205
Yang, S.C., 368
Yang, S.L., 158
Yang, X.J., 188, 189, 191, 358
Yang, Y.J., 280, 281
Yang, Y.Y., 211, 216
Yang, Z., 135, 254
Yan, Y.N., 269, 271, 274–279, 282
Yao, R., 269, 271, 275, 276, 279
Yaremchuk, M.J., 260
Yasin, M., 127
Yasuda, K., 298–300
Yasunaga, Y., 206
Yaszemski, M.J., 217
Yee, A.J., 251
Yeh, J., 187
Yeh, P.-Y., 72
Yeh, Y.C., 367
Ye, J., 183
Yi, J.B., 185
Yilmaz, Y., 19, 77
Yin, L.C., 368
Yin, X.C., 135
Yokoyama, F., 180
Yokoyama, M., 68, 95, 159
Yonekura, Y., 183
Yong, C.S., 182
Yoo, J.S., 135–137, 139
Yoo, J.U., 257
Yoon, J.J., 206, 214
Yoshida, R., 19–41, 65, 69, 116, 183
Yoshizako, K., 23
You, C.-C., 100
Younes, H., 158
Young, S., 215
Young, T., 303
Young, V., 323
Youn, I., 253
You, Y., 151
Yuan, F., 181
Yuan, M.L., 158
Yuan, R., 189
Yu, F.T., 180
Yu, G.E., 157
Yuguchi, Y., 108
Yu, H., 274
Yui, N., 55, 72, 73
Yu, J.-X., 90

- Yuk, S.H., 182, 191, 192
 Yu, L., 131, 159
 Yu, M.D., 180
 Yu, Q., 28, 54, 56
 Yura, H., 216
 Yurke, B., 83
 Yu, S.Y., 185
 Yu, T.L., 180
 Yuwono, V., 54
 Yu, Y.B., 212

 Zabrocki, K., 77
 Zachariah, S., 279
 Zafeiropoulos, N.E., 115
 Zahran, A.H., 14
 Zaikin, A.N., 30
 Zalipsky, S., 184
 Zareie, H.M., 157
 Zawacki, B., 269
 Zeman, A.D., 87
 Zender, L., 97
 Zentner, G.M., 130, 151
 Zeppetelli, S., 260
 Zhabotinsky, A.M., 30
 Zha, L., 113, 116
 Zhang, C.H., 274, 357
 Zhang, F., 114
 Zhang, H., 131, 159, 191, 214
 Zhang, J.T., 112, 183, 269, 271, 275, 276, 366
 Zhang, K., 59, 60
 Zhang, L., 80, 81, 99, 219
 Zhang, N., 357
 Zhang, P., 125
 Zhang, Q., 113, 116
 Zhang, R.J., 179, 269, 271, 274–278, 282
 Zhang, S.F., 357
 Zhang, W., 180

 Zhang, X., 112
 Zhang, X.M., 295
 Zhang, X.Z., 183
 Zhang, Y.Q., 18, 69, 135, 191, 254
 Zhang, Z.R., 181
 Zhao, C.W., 135
 Zhao, L., 357
 Zhao, X., 116
 Zhao, Y.M., 15, 181
 Zhelev, Z., 187, 188
 Zheng, G., 99
 Zheng Shu, X., 208, 216, 261
 Zheng, W., 269, 271, 275, 276
 Zheng, Y.A., 15, 28
 Zhen, T., 377, 387
 Zhong, Z.Y., 131, 160, 161, 206, 208, 209, 211,
 214, 216, 263
 Zhou, J., 117
 Zhou, S., 109
 Zhou, W., 161, 206, 214
 Zhou, Y., 183
 Zhuang, Y.F., 125
 Zhu, K.J., 158
 Zhu, M., 257
 Zhuo, R.X., 366
 Zhu, W., 206
 Zhu, X., 205
 Zhu, Y., 324
 Zhu, Z.Q., 125
 Zigah, D., 324
 Zisch, A.H., 81, 208, 219
 Zohuriaan-Mehr, M.J., 367
 Zourob, M., 54
 Zrinyi, M., 18
 Zuk, P.A., 257, 279
 Zund, G., 22
 Zygorakis, K., 217

Subject Index

- Acetobacter* bacteria, 291
- Acrylamide-based gels, 309
- Adipose-derived stem cells (ADSCs), 273, 274, 279, 281
- α -fetoprotein (AFP), 78
- AFP. *See* α -fetoprotein
- AFP-imprinted hydrogel, 78–79
- Agrecan, 251
- Agricultural hydrogels, 13–14
- Albumin (ALB), 218, 271–273
- Alginates, 182, 216, 260, 270–271
- Amonton's law, 292
- Ampholytic hydrogels, 5
- Angiogenic factors, 255
- Annulus fibrosus, 259
- Anterior cruciate ligament (ACL), 232–233
- Articular cartilage tissue engineering
 - cartilage regeneration
 - cell origins, 256–257
 - less metabolic involvement, 256
 - scaffolds, 257
 - characterization, hydrogels, 248
 - chondrocyte, 250–251
 - composition, 250
 - ECM, 253
 - histological organization
 - calcified layer, 252–253
 - collagen fibers, 252
 - non-mineralized cartilage layers, 253
 - superficial zone, 251
 - transition zone, 252
 - hydrogel polymers
 - biopolymer, 259–260
 - cellularized hydrogels, cell encapsulation, 259
 - chemical structure, 257, 258
 - covalent hydrogels, 261
 - ionic hydrogels, 261
 - physically crosslinked hydrogels, 260–261
 - synthetics polymers, 260
 - uncellularized hydrogel, 259
 - in situ crosslinkable hydrogels, 261–262
 - morphology, properties and diseases, 250
 - pathology
 - osteoarthritis, 254
 - trauma, 253, 254
 - physical and mechanical behavior, 262–264
 - polymer associations, 262
 - spontaneous cartilage repair, 254–255
 - viscoelastic behavioral theory, 248–250
- Asp-Glu-Val-Asp (DEVD) peptide, 98. *See also* Stimuli-responsive PEGylated smart nanogels
- Avidin, 189
- Bacterial cellulose (BC)
 - BC/gelatin DN gels, 291–292
 - BC-*t*-Carrageenan DN gels, 292
 - definition, 291
 - elongation stress–strain curve, 291, 292
 - hydrogel development, 290
- Belousov–Zhabotinsky (BZ) reaction, 32
- Biochemical markers, 255
- Biodegradable hydrogels
 - chemically bonded hydrogels, 153
 - hydrogen bonded hydrogels, 153
 - hydrophobic interactions hydrogels
 - cyclodextrins (CDs), 152
 - DDS, 152
 - dendritic structures, 151
 - reverse thermal gelation, 150
 - sol–gel transition, 150, 151
 - synthetic block copolypeptides, 151
 - ionic interaction hydrogels, 152–153
 - physical hydrogels, 149–150
 - polymer therapeutics, 147–148
 - preparation, natural/synthetic polymers, 149
 - supramolecular structures, 147
 - synthesis, drug delivery, 148, 149
- Biodegradable nanogel-crosslinked hydrogels, 347–348
- Biomimetic micro-/nano-actuator design
 - lithography microfabrication, 37
 - microgel beads monolayer fabrication, 39–41
 - nano-oscillator, 38
 - self-flocculating/dispersing oscillation, 38–40
 - self-oscillating gel array, 37
 - self-walking gels, 34–37
- Biomimetic scaffolds, 217
- Biomolecule-responsive hydrogel
 - cell-responsive sol–gel transition system, 81–82

- Biomolecule-responsive hydrogel (*Continued*)
 dimeric heparin-binding growth factor (VEGF), 80–81
 DNA-responsive hydrogels, 83
 drug-responsive hydrogels, 82–83
 glucose-responsive hydrogels
 glucose oxidase, 66–67
 lectin, 69–71
 phenylboronic acid, 67–69
 heparin-modified star polymer crosslinking, 80–81
 molecularly imprinted hydrogels
 AFP-imprinted hydrogels, 78–79
 schematics, 77
 swelling ratio changes, 79–80
 temperature-responsive hydrogels, 77
 properties and types, 65–66
 protein-responsive hydrogels
 antigen-responsive hydrogels, 74–77
 enzyme-responsive hydrogels, 72–74
 Biopolymers, 259–260
 Biot number, 49
 Boltzman's distribution, 381
- κ -Carrageenan gels, 293
 Cell-adhesive peptides immobilization, 26–28
 Cell assembling machine, 270
 Cell–cell interactions, 278
 Cell-entrapping material, 282
 Cell/hydrogel deposition system, 270, 275
 Cell-responsive sol–gel transition system, 81–82
 Cell-sheet engineering
 cell harvesting, 25
 intelligent surface
 cell-adhesive peptides immobilization, 26–28
 micropatterned surfaces, 28–29
 PIPAAm-grafted surfaces, 25
 scaffolds, 24
 temperature-responsive culture dishes, 24
 tissue reconstruction, 25–26
 CEPs. *See* Conductive electroactive polymers
 Chemical and physical crosslinks, 3–4, 214
 Chemical peptide ligation, 209
 Chitosan, 181, 216
 Cholesterol substituted pullan (CHP), 339–342, 345–348
 Chondrocytes, 220, 250–252, 256
 Chondron, 253
 Click chemistry reaction, 207–210
 Collagen, 215
 Collagen meniscus implants (CMI), 239
 Composite properties, hydrogels, 8
 Concentration redistribution effects, 384–387
 Conductive electroactive polymers (CEPs)
 chemistry of, 322
 conductivities, 321
 electronic, optical and redox properties, 323
 Crosslinked polymers, 1
 Crosslinking functional groups
 chemical peptide ligation, 209
 click chemistry reaction, 207–210
 Michael addition reaction, 208–209
 Schiff-base formation, 207–208
 Cyclodextrin (CD), 152, 213, 347
- Desorption process, 11
 Deswelling process, 11
 Dextran, 72, 73, 180–181, 216, 260
 Dihydroxy methacrylates, 308
 Dimethylsulfoxide (DMSO), 281
 Dispersion polymerization, 3
 Disposable lenses, 305, 311
 DNA-responsive hydrogel, 83
 Donnan's equilibrium and potential
 Boltzman's distribution, 381
 electric neutrality, 382
 osmotic model, 380
 salt concentration, 383, 384
 Double network (DN) hydrogels
 frictional behavior
 load dependence, 292–293
 sample area dependence, 293–294
 substrate effect, 294–295
 interpenetrated polymer networks, 285
 low friction gels
 artificial cartilage, 296–297
 template effect, gel surface structure, 295–296
 robust gels, high elasticity
 bacterial cellulose, 290–292
 biocompatibility, 298–300
 local damage zone model, 290
 necking phenomenon, 288–290
 synthetic polymer, 286–288
 wear properties, 298
 sliding friction, 292
 Double-syringe cell assembling technique, 278
 Doxorubicin (DOX), 192
 antitumor activity, 88, 97
 conjugated dextran, 181
 endosomal/lysosomal release, 95
 fluorescence microscopy, 97–98
 fluorescence spectra, 96
 loading of, 95–96
 release, 98, 132
 schematics, 95
 time and pH-dependent profiles, 96

- Drug delivery systems
 alginate, 182
 chitosan hydrogels, 181
 dextran hydrogels, 180–181
 fluorescence dyes, 185–186
 gold nanoparticles, 184
 iron oxide nanoparticles/polymer composite systems, 189–190
 magnetic nanoparticles, 184–185
 microbubble/polymer composite systems, 191
 microbubbles, 187
 molecular imaging capability, 191–193
 molecular probe/polymer composite systems, 187–189
 molecular probes, imaging, 184
 PEG and copolymers, 183
 pluronic, 182–183
 PNIPAM, 183, 185
 PVA, 180
 quantum dot/polymer composite systems, 190, 191
 quantum dots, 187, 188
 swelling transition, 182
 therapeutic agents and diagnostic imaging probe, 179, 180
- Drug-responsive hydrogels, 82–83
- Dual stimuli-responsive nanogels, 343–344
- Ductile hydrogels, 290
- ECM. *See* Extracellular matrix
- EDC hydrochloride. *See* 1-Ethyl-3-(3-dimethylaminopropyl) carbodiimide hydrochloride
- Electroconductive hydrogels (ECHs)
 bioactive hydrogels, 325
 biomedical applications, 323
 CEPs
 chemistry of, 322
 conductivities, 321
 electronic, optical and redox properties, 323
 degree of hydration, 319, 324
 electrochemical impedance magnitude, 332–333
 galvanostatic electropolymerization, 332
 interdigitated microsensor electrode (IME), 328, 329
 poly(HEMA)-based hydrogels, 324
 polymer hydrogels, 323, 324
 radiofrequency (RF), 330
 substrate surface modifications, 329
 synthesis of
 chemical oxidative polymerization, 326, 327
 electrochemical polymerization, 327
 PMMAPMS-g-PPy synthesis, 325
 polypyrrole, 320, 321, 326–328, 330
 7,7,8,8-tetracyanoquinodimethane (TCNQ), 325
- Electrolytic crosslinking, 4
- Electro-stimulated drug release devices (ESRDs), 320
- Enantiomeric PLA-PEG linear block copolymers
 ABA triblock copolymers
 gelation mechanism, enantiomeric mixture, 165, 166
 micellar solutions, 163, 164
 sol–gel transition, 163–164
 stereocomplex formation, 164–165
 storage modulus, 166–167
 WAXS measurement, 164–166
 AB-diblock copolymers
 bimodal size distribution, 171
 gelation mechanism, 170
 gel–sol transition, 167, 168
 helix formation, 171
 micellar solutions, 168–169
 phase diagram, 168, 169
 WAXS profiles, 169–170
 BAB triblock copolymers, 167–168
 copolymer synthesis and gel formation, 158, 163
 properties and applications, 172, 173
 stereocomplexed micellar hydrogel, 162
- Enantiomeric PLAs stereocomplexation
 crystal formation, homopolymer, 159, 160
 dextran-graft-oligo (LA) system, 159
 gelation mechanism, 159–161
 protein, 161
 WAXS and rheological analyses, 160
- Energy metabolic system, 279
- Engineered hydrogels
 anatomy, 353
 degree of crosslinking, 353
 diet aid applications, 365
 diffusional and capillary forces, 354
 dissolution process, 352, 360
 gastric retention platform, 365
 higher molecular weight polymers, 354
 mechanical properties, 354–358
 research on porous, 366–368
 swelling capacity, 352, 354
- Enzymatic reactions, 210–211
- Enzyme cofactor feedback system, 57
- 1-Ethyl-3-(3-dimethylaminopropyl) carbodiimide (EDC) hydrochloride, 291
- Ethylene dimethacrylate (EDMA) lens, 307
- Extracellular matrix (ECM), 24, 251, 253, 292

- FDA contact classification, 310–311
- Feedback control system
- basic functional elements, 45–46
 - feedforward and cascade system, 60–62
 - hydrogel-based actuator
 - chemically controlled system, 53–54
 - electronically controlled system, 51
 - magnetically and ultrasonically controlled systems, 51
 - photo-controlled system, 51–53
 - protein-responsive and controlled system, 54–55
 - thermally controlled system, 53
 - hydrogel-based sensor
 - enzyme activity preservation, 50
 - enzyme secondary substrate limitation, 48–50
 - mechanical and electric transduction, 47, 48
 - optical transduction, 47
 - self-regulated system
 - enzyme cofactor feedback system, 57
 - glucose concentration feedback system, 58–60
 - pH feedback system, 55–56
 - protein concentration feedback system, 57
 - temperature feedback system, 57
- Feedforward and cascade system, 60–62
- Fibrin, 271, 277, 282
- Fibrin gels, 215
- Fluorescein isothiocyanate (FITC), 185, 186
- Fluorescein isothiocyanate (FITC)-labeled
- DEVD peptide, 13, 99. *See also*
 - Stimuli-responsive PEGylated smart nanogels
- Focus Night & Day®, 312, 313
- Free swelling, 360
- Freezing/thawing process, 281–282
- Gadolinium, 185
- Gelatin based hydrogels
- biodegradable polypeptide, 270
 - biomimetic 3D cell survival
 - microenvironment, 273
 - cell assembling machine, 269–271
 - cell-laden hydrogels, 271
 - chitosan, 270
 - controlled hepatocyte assembly
 - calcium alginate molecules, 277
 - cell-loading support matrices, 275
 - cell survival matrix constitution, 274
 - crosslinked hydrogel networks, 277
 - endothelial cells, 278
 - fibrin, 277
 - glutaraldehyde, 276–278
 - motor drive syringe, 275
 - non-parenchymal cells (NPCs), 278
 - phenotypes preservation, 278
 - sol–gel transformation, 276
 - TPP, 276–277
 - 3D constructs cryopreservation
 - cell survival rate, 282
 - single-cell suspension, 280
 - trypan blue staining, 281, 282
 - digital models, 274, 275
 - double-syringe deposition manufacturing system, 274, 276
 - hepatocytes, 271–274
 - multicellular model establishment
 - adipose-tissue engineering, 279
 - drug screening, 279
 - 3D structures, 279, 280
 - polymer chains, 273
 - synthetic polymeric materials, 269
- Gellan gels, 293
- Glucose (Glu), 271–273
- Glucose concentration feedback system, 58–60
- Glucose-responsive hydrogel
- glucose oxidase
 - insulin release system, 67
 - pH-responsive hydrogel, 66–67
 - schematics, 66
- lectin
- copolymerization preparation, 70–71
 - poly(2-glucosyloxyethyl methacrylate) (PGEMA)–concanavalin A (Con.A) complex, 70–71
 - saccharide-responsive hydrogel preparation, 69–70
 - swelling ratio vs. time, 70
- phenylboronic acid
- glucose recognition function, 68–69
 - preparation of, 67–68
 - temperature dependence vs. swelling curve, 68–69
- Glutamate-oxaloacetate transaminase (GOT), 271–273
- Glycerol dimethacrylate (GDMA) lens, 308
- Glycidyl methacrylate (GMA), 114, 115
- Glycidyl methacrylate dextran (Dex-GMA), 181
- Glycosaminoglycans (GAG), 251
- Gold nanoparticles, 184
- Growth factors, hydrogel design, 205
- HEMA lens, 307–310
- Hepatocytes, 28, 29, 271–277
- High performance liquid chromatography, 364
- High swelling hydrogels (HSHs)
- engineered hydrogels

- anatomy, 353
- degree of crosslinking, 353
- diet aid applications, 365
- diffusional and capillary forces, 354
- dissolution process, 352, 360
- gastric retention platform, 365
- higher molecular weight polymers, 354
- mechanical properties, 354–358
- research on porous, 366–368
- swelling capacity, 352, 354
- hydrogel characterization
 - analytical issues, 364
 - mechanical properties, 362–363
 - porosity, 363–364
 - swelling determination, 360
 - swelling model, 360–362
- purity, 358–359
- stability, 364–365
- High-throughput drug screening systems, 283
- Horseradish peroxidase (HRP), 211
- HSHs. *See* High swelling hydrogels
- Humatrix[®], 130
- Hyaline, 250
- Hyaluronic acid (HA), 216, 251, 270
- Hydrogel-based actuator
 - chemically controlled system, 53–54
 - electronically controlled system, 51
 - magnetically and ultrasonically controlled systems, 51
 - photo-controlled system, 51–53
 - protein-responsive and controlled system, 54–55
 - thermally controlled system, 53
- Hydrogel-based sensor
 - enzyme activity preservation, 50
 - enzyme secondary substrate limitation
 - enzymatic hydrogel device configuration, 49
 - GO_x catalase reaction, 48–49
 - hydrogel membrane system, 49–50
 - mechanical and electric transduction, 47, 48
 - optical transduction, 47
- Hydrogel-cartilage integration, 221
- Hydrogel contact lenses
 - FDA contact classification, 310–311
 - hydrogel materials
 - silicone hydrogels (*see* Silicone hydrogel lens)
 - soft hydrophilic materials, 311
 - materials used
 - acrylamides, 309
 - dihydroxy methacrylates, 308
 - HEMA, 307–310
 - methacrylic acid, 308–309
 - 1-vinyl-2-pyrrolidone, 310–311
 - terminology, 306
- Hydrogel patch, 261
- Hydrogel swelling
 - acrylic-based hydrogels, 365, 366
 - degree of dissociation, 378
 - ionic hydrogel swelling, 376
 - kinetics of
 - chemical reaction rate, 389
 - diffusion and relaxation processes, 388
 - elasticity and nonequilibrium thermodynamics, 390
 - Stefan's task, 388, 389
 - swelling rate, 387–388
 - mechanism of, 378–379
 - swelling ratio *vs.* acid and salt concentration, 377
- Hydrophilic lyophobic balance (HLB), 353
- Hydrophilic polymers, 3–4
- Hydrosols, 3–4
- HydroThane[™] matrices, 231–232
- Hydroxypropyl cellulose (HPC), 109
- Inclusion complexation, 213
- Injectable hydrogels, 204
- In-situ gelling stimuli-sensitive PEG-based amphiphilic copolymer hydrogels
 - anionic weak polyelectrolytes
 - anti-tumor efficacy, 137
 - PCLA–PEG–PCLA triblock copolymer, 136
 - PEG/PCGA ratio, 138
 - sulfamethazine oligomers, 135
 - thermoreversible sol–gel–sol transition, 135, 137
 - cationic weak polyelectrolytes
 - cytotoxicity, 139
 - hydrophilic-hydrophobic transition, 138
 - insulin release, 140
 - multiblock copolymer aqueous solution, 141
 - pentablock copolymer hydrogels, 139
 - pH-sensitivity, 138
 - pH-and thermo-sensitive PEG-polyester amphiphilic copolymer hydrogels, 134–135
 - pluronic-based in situ forming hydrogels, 126–127
 - thermogelling PEG-based amphiphilic multi-block copolymers, 134
 - thermogelling PEG-PCL amphiphilic copolymers, 132–134
 - thermogelling PEG/PLGA amphiphilic block copolymers
 - aliphatic polyesters, 127
 - diffusion-controlled mechanism, 129
 - drug-loaded hydrogels, 128

- In-situ gelling stimuli-sensitive PEG-based amphiphilic copolymer hydrogels (*Continued*)
 gel-to-sol transition, 127
 in vitro drug release behavior, 129
 paclitaxel, 130–131
 phase-transition behaviour, 131
 PLGA-PEG-PLGA aqueous solution, 130
 soft sphere model, 128
 thermogelling PEG-PNIPAM block copolymers, 124–125
 thermogelling star-shaped and graft PEG/PLGA amphiphilic copolymers, 131–132
- Intelligent surfaces
 bio-separation, 22
 cell-adhesive peptides immobilization, 26–28
 cell-sheet engineering (*see* Cell-sheet engineering)
 micropatterned surfaces, 28–29
- Interdigitated microsensor electrode (IME), 328, 329
- International Cartilage Repair Society (ICRS), 253
- Interterritorial matrix, 253
- Intervertebral discs (IVDs)
 anisotropy, 234
 annulus fibrosus, 233, 234
 compression modulus and stress-strain curve, 235
 J-shaped stress-strain curves, 234, 235
 nucleus/annulus synthetic system, 234
 nucleus pulposus, 233
 structural design, 234
- Inverse dispersion polymerization, 3, 11
- Ion-sensitive field effect transistors (ISFETs), 324
- Iron oxide nanoparticles, 185
- IVDs. *See* Intervertebral discs
- Liquid extrusion technique, 9
- Load-deformation curve, 12
- Low critical solution temperature (LCST), 109, 110, 157
- Lower critical gelation temperature (LCGT), 126
- Macromolecules. *See* Biopolymers
- Mechano metal toy set lens, 303
- Mesenchymal stem cells (MSCs), 256–257
- Metabolic syndrome (MS), 279
- Methacrylic acid (MA) lens, 308–311
- Metronidazole, 181
- Michael addition reaction, 208–209
- Microstructural disorder, 237, 238
- Molecularly imprinted hydrogels
 AFP-imprinted hydrogels, 78–79
 schematics, 77
 swelling ratio changes, 79–80
 temperature-responsive hydrogel, 77
- Monolayer cell culture systems, 277
- Multiple hydrogel systems, 5–6
- Multi-porous hydrogel composites, 242
- Neural prosthetic devices (NPDs), 320
- N*-isopropylacrylamide (NIPA/NIPAM), 108, 112, 153
- Non-thrombogenic applications, 14
- Nucleus pulposus, 233, 259
- Orthopedic surgery, 237
- PAA. *See* Poly acrylic acid
- PAMPS network, 288, 289
- PEG. *See* Poly(ethylene glycol)
- Pericellular matrix, 253
- HEMA lenses, 304, 307, 310
- pH feedback system, 55–56
- Photoresponsive nanogels, 344
- pH-responsive hydrogels, 66–67
- pH-responsive PEGylated nanogels
 intracellular drug delivery system
 anticancer drug, 94–95
 DOX (*see* Doxorubicin)
 tumor-specific smart ¹⁹F MRI nanoprobe
 intensity, 91–93
 phantom, 94
 pH effects, 90–91, 93
 schematics, 90, 91
 synthesis, 90
 T₁ and T₂ relaxation times, 93–94
 V_{swelling}/V_{shrinking} ratio, 91, 92
- Plastic scleral lenses, 304
- Pluronic®, 151, 157
- Pluronic F127, 262
- Pluronic, 182–183
- PNIPAM. *See* Poly(*N*-isopropylacrylamide)
- Poloxamer 188, 182
- Poloxamer 407, 182
- Poloxamer®, 151, 157
- Poly(acrylamide) (PAAm) gel, 286
- Poly(2-acrylamido-2-methylpropanesulfonic acid) (PAMPS) gel, 286
- Poly acrylic acid (PAA), 376–378, 380
- Poly-b(1,4)-*D*-glucosamine. *See* Chitosan
- Poly(caprolactone) (PCL), 229
- Poly(3,4-ethylenedioxythiophene) (PEDOT) nanorods, 117
- Poly(ethylene glycol) (PEG), 87, 124, 150, 151, 183, 217. *See also* Stimuli-responsive PEGylated smart nanogels

- Poly(ethylene glycol)-SH (PEG-SH), 188
 Poly(glycolic acid) (PGA), 217
 Poly(2-hydroxyethyl-methacrylate) (PHEMA), 229
 Poly(lactic acid) (PLA), 217
 Poly(*N*-isopropylacrylamide) (PNIPAM), 183
 - block copolymers, 125
 - chemical structure, 124, 125
 - composite microgels, 114–115
 - microgels, 109
 - molecular structure, 185
 - negative and positive charge, 111
 - particles, 108
 - self-assemble, colloid crystals, 117
 Polysaccharide hydrogels
 - biomedical applications, 345–346
 - nanogel-based hydrogel materials
 - biodegradable nanogel-crosslinked hydrogels, 347–348
 - hybrid gels crosslink, 346–347
 - rapid shrinking hydrogels, 347
 Polystyrene (PS), 295
 Poly(vinyl alcohol) (PVA), 180, 260
 Poly(vinyl pyrrolidone) (PVP), 180
 Primaquine[®], 153
 Protein concentration feedback system, 57
 Protein-responsive and controlled system, 54–55
 Protein-responsive hydrogels
 - antigen-responsive hydrogels
 - antigen-antibody binding hydrogel network, 74–75
 - copolymerization preparation of, 74–75
 - microparticle fabrication, 77
 - reversible swelling/shrinking behavior, 75–76
 - enzyme-responsive hydrogels
 - colon microbial enzymes, 72
 - enzyme-triggered charge-induced polymer swelling, 73–74
 - interpenetrating polymer network (IPN) hydrogels, 72–73
 Proteoglycans (PG), 250–251
 Prozac[®], 319
 Pullulan, linear homopolymer, 339
 PureVision[®], 312, 313

 Radical polymerization, 206–207
 Rapid prototyping techniques, 271
 ReGel[®], 151
 Reticular endothelial system (RES), 184
 Reverse thermal gelation (RTG), 260
 Rheumatological disorder, 254
 Rigid gas-permeable lenses (RGP), 305, 306

 Salt leaching techniques, 237
 Scaffold design, tissue engineering and prosthesis
 - bio-mimetic materials, 228
 - properties
 - crosslinked PHEMA hydrogels, 229–230
 - IVDs, 233–235
 - mechanical and physical properties, 229
 - “permanent”/“chemical” gels, 229
 - PHEMA/PCL semi-IPNs, 229
 - tendons and ligaments, 230–233
 - tissue function replacement, 230
 - synthetic extracellular matrix (ECM) hydrogels, 228
 - tissue regeneration
 - bone replacement, 237, 238
 - cartilage, 240–242
 - hydrophilic nature, ECM, 236
 - load-bearing applications, 236
 - menisci, 239–240
 - porosity, 235
 - rate-controlled degradable materials, 236
 Scaffolds macromolecular engineering, 203
 Schiff-base formation, 207–208
 Self-assembled engineered nanogels
 - dual stimuli-responsive nanogels, 343–344
 - photoresponsive nanogels, 344
 - pullulan, linear homopolymer, 339
 - self-assembling method, 341
 - stimuli-responsive nanogels, 341–342
 - structural characteristics, 340
 - thermo-responsive nanogels, 342–343
 Self-assembly, 212–213
 Self-oscillating gels
 - Belousov–Zhabotinsky (BZ) reaction, 32
 - biomimetic micro-/nano-actuator design
 - (*see* Biomimetic micro-/nano-actuator design)
 - design, 32–33
 - miniature bulk gel, 33
 - oscillation period and amplitude control, 34
 - peristaltic motion, chemical wave propagation, 34, 35
 - self-beating motion, on-off regulation, 34
 Self-regulated system
 - enzyme cofactor feedback system, 57
 - glucose concentration feedback system, 58–60
 - diabetes applications, 58–59
 - injectable hydrogel microparticle system, 58
 - insulin delivery system, 59–60
 - pH feedback system, 55–56
 - protein concentration feedback system, 57
 - temperature feedback system, 57
 Self-walking gel, 34–37
 Semi-hydrophilic scaffolds, 240
 Silicone hydrogel lenses
 - current trends, 313

- Silicone hydrogel lenses (*Continued*)
 Focus Night & Day[®], 312, 313
 PureVision[®], 312, 313
 structure, 312
 TRIS, 312, 313
- Smart apoptosis nanoprobe
 activated caspase-3
 fluorescence-quenching, 98–99
 fluorescence spectra, 100–101
 relative fluorescence intensity, 101–102
 synthesis, 99–100
 HuH-7 cells incubation, staurosporine,
 102–104
 schematic illustration, 99
- Smart nanomedicine. *See* Stimuli-responsive
 PEGylated smart nanogels
- Sol–gel phase diagram, 182
- Sonoporation, 187
- Spin-casting technology, 303
- Stereocomplexation, 211–212
- Stimuli responsive hydrogels
 cell-sheet engineering (*see* Cell-sheet
 engineering)
 graft gel design, 30, 31
 information transmission and transformation
 molecular recognition function, 21
 optical function, 20
 shape memory function, 20
 intelligent surfaces
 bio-separation, 22
 cell-adhesive peptides immobilization,
 26–28
 micropatterned surfaces, 28–29
 mass transport function
 bio-separation, 22–24
 pulsatile drug release control, 21–22
 mechanical motion function, 20
 microfabrication, 30–31
 nanocomposite gel structure, 30
 self-oscillating gels
 Belousov–Zhabotinsky (BZ) reaction, 32
 biomimetic micro-/nano-actuator design
 (*see* Biomimetic micro-/nano-actuator
 design)
 design, 32–33
 miniature bulk gel, 33
 oscillation period and amplitude control, 34
 peristaltic motion, chemical wave propaga-
 tion, 34, 35
 self-beating motion, on-off regulation, 34
 topological gel, double network structure,
 29–30
- Stimuli-responsive nanogels, 341–342
- Stimuli-responsive PEGylated smart nanogels
 characteristics of, 87–88
 emulsion polymerization synthesis technique,
 88–89
 PEG tethered chain, 87
 pH effects, 88–90
 pH-responsive PEGylated nanogel
 intracellular drug delivery system, 94–98
 tumor specific smart ¹⁹F MRI nanoprobe,
 90–94
 smart apoptosis nanoprobe (*see* Smart
 apoptosis nanoprobe)
 zeta (ζ)-potentials of, 88–89
- Stimuli-sensitive microhydrogels
 assemblies and colloid crystals,
 thermosensitive microgels, 117
 metal nanoparticle/PNIPAM composite
 function, 114
 metal oxide nanoparticles/thermosensitive
 polymer composites
 magnetite nanoparticles, 114–115
 photoluminescent nanocrystals, 116
 titania nanoparticles, 116
 zinc oxide nanoparticles, 115–116
- PEDOT nanorods, 117
- physical properties, 107, 108
- preparation
 core particle surface modification, 108
 inorganic microgel composites, 112–114
 particle-forming polymerization, 108
 polymer molecule assembly, solution, 109
- stimuli responsiveness
 multistimuli-sensitivity, 112
 pH responsiveness, 111
 temperature dependent hydrophilicity–
 hydrophobicity, 111
 temperature responsiveness, 109, 110
 VPTT, 109–111
- Storage modulus, 249
- Structural characterization, 8–12
- Superabsorbent hydrogels, 14, 15
 concentration redistribution effects
 Donnan balance equation, 384
 material balance equation, 384
 normalized concentration, 385, 386
 polymer concentration, 385
 crosslinked polymer network, 375, 376
- Donnan's equilibrium and potential
 Boltzman's distribution, 381
 electric neutrality, 382
 osmotic model, 380
 salt concentration, 383, 384
 effect of neutralization and acidity, 380
- hydrogel swelling
 acrylic-based hydrogels, 365, 366

- chemical reaction rate, 389
- degree of dissociation, 378
- diffusion and relaxation processes, 388
- elasticity and nonequilibrium thermodynamics, 390
- ionic hydrogel swelling, 376
- mechanism of, 378–379
- Stefan's task, 388, 389
- swelling rate, 387–388
- swelling ratio vs. acid and salt concentration, 377
- neutralization and acidity effect, 380, 381
- sodium polyacrylate dissociation, 375, 376
- Surface plasmon resonance (SPR), 184
- Swelling capacity
 - ampholytic and cationic hydrogels, 5
 - engineered hydrogels, 352, 354
 - measurement, 4–5
 - mechanism, 6
 - osmosis, 6–8
- Synthetic extracellular matrix hydrogels, 228
- Synthetic factors, 2

- T1 and T2 relaxation processes, 184, 185
- Taxol®, 131
- Temperature-responsive hydrogel, 77
- Tendons and ligaments
 - ACL reconstruction, 233
 - artificial prostheses, 230
 - composite structure, 231
 - fibrous scaffolds, 230
 - filament winding technique, 231
 - knitted/braided design, 230–231
 - mechanical parameters, 232, 233
 - tensile stress–strain curves, 231, 232
- 7,7,8,8-Tetracyanoquinodimethane (TCNQ), 325
- Tetrafluoroethylene (Teflon) plate, 294
- Thermo-gelation, 212
- Thermo-responsive biodegradable hydrogels
 - enantiomeric PLA–PEG linear block copolymers
 - ABA triblock copolymers, 163–167
 - AB-diblock copolymers, 168–171
 - BAB triblock copolymers, 167–168
 - copolymer synthesis and gel formation, 158, 163
 - properties and applications, 172, 173
 - stereocomplexed micellar hydrogel, 162
 - enantiomeric PLAs stereocomplexation
 - crystal formation, homopolymer, 159, 160
 - dextran-graft-oligo (LA) system, 159
 - gelation mechanism, 159–161
 - protein, 161
 - WAXS and rheological analyses, 160
- micelles
 - BAB type triblock copolymer, 159
 - biomedical applications, 158
 - polymer structures and schematics, aqueous medium, 158
 - rheological properties, 159
 - tissue-adhesive hydrogels, 159
- Thermo-responsive nanogels, 342–343
- Thiele modulus, 49
- Tissue engineering (TE) applications
 - bone graft substitutes, 219–220
 - cartilage regeneration, 220–221
 - crosslinking methods
 - crosslinking functional groups, 207–210
 - enzymatic reactions, 210–211
 - inclusion complexation, 213
 - physical and chemical crosslinking, 214
 - radical polymerization, 206–207
 - self assembly, 212–213
 - stereocomplexation, 211–212
 - thermo-gelation, 212
 - hydrogel design
 - biocompatibility, 204–205
 - biodegradability, 205
 - biofunctionality, 205–206
 - naturally-derived hydrogels
 - polysaccharides, 216
 - protein-based polymers, 215–216
 - synthetic hydrogels
 - fumaric acids, 217
 - hybrid hydrogels, 217–219
 - PEG/PGA and PEG/PLA copolymers, 217
- Tissue function replacement, 230
- Tissue reconstruction, 25–26
- Tissue regeneration, 235–242
- Tough hydrogels, 290
- Transferrin, 181
- Transglutaminase (TG), 210–211
- Triethylenglycol dimethacrylate (TEGDMA), 307
- Triglyceride (TG), 271–273
- Tripolyphosphate (TPP), 277
- Tumor-specific smart ¹⁹F magnetic resonance imaging (MRI) nanoprobe
 - intensity, 91–93
 - phantom, 94
 - pH effects, 90–91, 93
 - schematics, 90, 91
 - synthesis, 90
 - T₁ and T₂ relaxation times, 93–94
 - V_{swelling}/V_{shrinking} ratio, 91, 92
- Ultra-higher molecular weight polyethylene (UHMWPE), 298
- Urea (Ur), 271–273

- N*-Vinylcaprolactam (VCL), 108
- 1-Vinyl-2-pyrrolidone, 310–311
- Viscoelasticity, 12–13
- Voigt model, 360, 361
- Volume phase transition temperature (VPTT),
109–111
- Water accommodation, osmosis, 6–8
- Wet-state stability, 11
- Wide-angle X-ray diffraction
(WAXD), 291
- Wide-angle X-ray scattering (WAXS),
163–165